

ISSN: 2320-8694

Journal of Experimental Biology And Agricultural Sciences



VOLUME 11 || ISSUE II || APRIL, 2023

Production and Hosting by Horizon Publisher India[HPI]
(<http://www.horizonpublisherindia.in>)
All rights reserved.

ISSN No. 2320 - 8694

Peer Reviewed - open access journal

Common Creative License - NC 4.0

Volume No - 11

Issue No - II

April, 2023

Journal of Experimental Biology and Agricultural Sciences (JEBAS) is an online platform for the advancement and rapid dissemination of scientific knowledge generated by the highly motivated researchers in the field of biological agricultural, veterinary and animal sciences. JEBAS publishes high-quality original research and critical up-to-date review articles covering all the aspects of biological sciences. Every year, it publishes six issues.

JEBAS has been accepted by SCOPUS UGC CARE, INDEX COPERNICUS INTERNATIONAL (Poland), AGRICOLA (USA), CAS (ACS, USA), CABI - Full Text (UK), International Committee of Medical Journal Editors (ICMJE), SHERPA - ROMEO; J gate and Indian Science Abstracts (ISA, NISCAIR) like well reputed indexing agencies.

[HORIZON PUBLISHER INDIA [HPI]

<http://www.horizonpublisherindia.in/>]

Editorial Board

Editor-in-Chief

Prof Y. Norma-Rashid
(University of Malaya, Kuala Lumpur)
editor.in.chief.jebas@gmail.com

Co-Editor-in-Chief

Dr. Kuldeep Dhama, M.V.Sc., Ph.D.
NAAS Associate, Principal Scientist, IVRI, Izatnagar India - 243 122
co_eic@jebas.org

Managing - Editor

Kamal K Chaudhary, Ph.D. (India)
jebasonline@gmail.com

Technical Editors

Hafiz M. N. Iqbal (Ph.D.)

Research Professor,
Tecnologico de Monterrey, School of Engineering and Sciences,
Campus Monterrey, Ave. Eugenio Garza Sada 2501,
Monterrey, N. L., CP 64849, Mexico
Tel.: +52 (81) 8358-2000Ext.5561-115
E-mail: hafiz.iqbal@my.westminster.ac.uk; hafiz.iqbal@itesm.mx

Prof. Dr. Mirza Barjees Baigis

Professor of Extension (Natural Resource Management),
Department of Agricultural Extension and Rural Society,
College of Food and Agriculture Sciences,
King Saud University, P.O. Box 2460, Riyadh 11451, Kingdom of Saudi Arabia
Email: mbbag@ksu.edu.sa

Dr. Mukesh Kumar Meghvansi

Scientist, Bioprocess Technology Division, Defence R & D Establishment, Gwalior-474002
Email: mk_meghvansi@yahoo.co.in

Dr. B L Yadav

Head – Botany, MLV Govt. College, Bhilwara, India
E mail: drblyadav@yahoo.com

Dr. K L Meena

Associate Professor – Botany, MLV Govt.
College, Bhilwara, India
E mail: kanhaiyameena211@yahoo.com

Dr. Yashpal S. Malik

ICAR – National Fellow Indian Veterinary Research Institute (IVRI)
Izatnagar 243 122, Bareilly, Uttar Pradesh, India

Associate Editors

Dr. Sunil K. Joshi

Laboratory Head, Cellular Immunology
Investigator, Frank Reidy Research Center of Bioelectrics, College of Health Sciences, Old Dominion University,
4211 Monarch Way, IRP-2, Suite # 300, Norfolk, VA 23508 USA
Email: skjoshi@odu.edu

Dr. Vincenzo Tufarelli

Department of Emergency and Organ Transplantation (DETO),
Section of Veterinary Science and Animal Production,
University of Bari 'Aldo Moro', s.p. Casamassima km 3, 70010 Valenzano, Italy
Email: vincenzo.tufarelli@uniba.it

Prof. Sanjay-Swami, Ph.D. (Soil Science & Agril. Chemistry),

School of Natural Resource Management,
College of Post Graduate Studies in Agricultural Sciences,
(Central Agricultural University),
UMIAM (Barapani)-793 103, Meghalaya, INDIA
Email: sanjay.nrm.cpgsas@cau.ac.in

Chiranjib Chakraborty, Ph.D.

Professor, School of Life Science and Biotechnology,
Adamas University, Kolkata, India
Email: drchiranjib@yahoo.com

Jose M. Lorenzo

Centro Tecnológico de la Carne de Galicia
Ourense, Spain
Email: jmlorenzo@ceteca.net

Assistant Editors

Dr Ayman EL Sabagh

Assistant professor, agronomy department, faculty of agriculture
kafresheikh university, Egypt
E-mail: ayman.elsabagh@agr.kfs.edu.eg

Safar Hussein Abdullah Al-Kahtani (Ph.D.)

King Saud University-College of Food and Agriculture Sciences,
Department of the Agricultural Economics
P.O.Box: 2460 Riyadh 11451, KSA
email: safark@ksu.edu.sa

Dr Ruchi Tiwari

Assistant Professor (Sr Scale)
Department of Veterinary Microbiology and Immunology,
College of Veterinary Sciences,
UP Pandit Deen Dayal Upadhyay Pashu Chikitsa Vigyan Vishwavidyalay Evum Go-Anusandhan Sansthan (DUVASU),
Mathura, Uttar Pradesh, 281 001, India
Email: ruchi.vet@gmail.com

Dr. ANIL KUMAR (Ph.D.)

Asstt. Professor (Soil Science)
Farm Science Centre (KVK)
Booh, Tarn Taran, Punjab (India) – 143 412
Email: anilkumarhpkv@gmail.com

Akansha Mishra

Postdoctoral Associate, Ob/Gyn lab
Baylor College of Medicine,
1102 Bates Ave, Houston Tx 77030
Email: akansha.mishra@bcm.edu; aksmisra@gmail.com

Dr. Muhammad Bilal

Associate Professor
School of Life Science and Food Engineering,
Huaiyin Institute of Technology, Huaian 223003, China
Email: bilaluaf@hotmail.com

Dr. Senthilkumar Natesan

Associate Professor

Department of Infectious Diseases, Indian Institute of Public Health

Gandhinagar, Opp to Airforce station HQ, Lekawada, Gandhinagar, Gujarat - 382042, India

Email: snatesan@iiphg.org

Mr. Ram Bahadur Khadka (Microbiologist)

Assistant Professor (Pokhara University)

Crimson College of Technology (CCT)

Butwal-13, Rupandehi, Lumbini Province, Nepal

Email: rambahadurkhadka00@gmail.com

Prof. A. VIJAYA ANAND

Professor

Department of Human Genetics and Molecular Biology

Bharathiar University

Coimbatore – 641 046

Dr. Phetole Mangena

Department of Biodiversity, School of Molecular and Life Sciences,

Faculty of Science and Agriculture, University of Limpopo, Republic of South Africa

Private Bag X1106, Sovenga, 0727

Email: Phetole.Mangena@ul.ac.za ; mangena.phetole@gmail.com

Table of contents

Deep Learning Paradigms for Existing and Imminent Lung Diseases Detection: A Review <i>10.18006/2023.11(2).226.235</i>	226 — 235
Prospective nutritional, therapeutic, and dietary benefits of camel milk making it a viable option for human consumption: Current state of scientific knowledge <i>10.18006/2023.11(2).236.250</i>	236 — 250
Donkey milk: chemical make-up, biochemical features, nutritional worth, and possible human health benefits - Current state of scientific knowledge <i>10.18006/2023.11(2).251.263</i>	251 — 263
Positive impacts of integrating flaxseed meal as a potential feed supplement in livestock and poultry production: Present scientific understanding <i>10.18006/2023.11(2).264.279</i>	264 — 279
Influence of biofertilizer produced using drumstick (<i>Moringa oleifera</i> L.) unused parts on the growth performance of two leafy vegetables <i>10.18006/2023.11(2).280.289</i>	280 — 289
Optimization of protein extraction from "Cam" rice bran by response surface methodology <i>10.18006/2023.11(2).290.296</i>	290 — 296
Effect of AM fungi during salt stress on biochemical content in Ginger (<i>Zingiber officinale</i> Rosc.) <i>10.18006/2023.11(2).297.305</i>	297 — 305
An Integrative Approach Towards Recommending Farming Solutions for Sustainable Agriculture <i>10.18006/2023.11(2).306.315</i>	306 — 315
Usage of iron foliar spray in enhancing the growth and yield of the flax plant (<i>Linum usitatissimum</i> L) <i>10.18006/2023.11(2).316.324</i>	316 — 324
Growth and development patterns in Mustard (<i>Brassica</i> spp.) as influenced by sowing time <i>10.18006/2023.11(2).325.338</i>	325 — 338
Determination of carbendazim residues in Moroccan tomato samples using local enzyme-linked immunosorbent assay and comparison with liquid chromatography <i>10.18006/2023.11(2).339.350</i>	339 — 350
Isolation and production of polyhydroxybutyrate (PHB) from <i>Bacillus pumilus</i> NMG5 strain for bioplastic production and treatment of wastewater from paper factories <i>10.18006/2023.11(2).351.358</i>	351 — 358
Contraceptive efficacy and antioxidant potential of <i>Leptadenia reticulata</i> bark extracts in male albino rats <i>10.18006/2023.11(2).359.370</i>	359 — 370
Antibacterial activity of Libyan <i>Juniperus phoenicea</i> L. leaves extracts against common nosocomial pathogens <i>10.18006/2023.11(2).371.379</i>	371 — 379
Phytochemical investigations, <i>in-vitro</i> antioxidant, antimicrobial potential, and <i>in-silico</i> computational docking analysis of <i>Euphorbia milii</i> Des Moul <i>10.18006/2023.11(2).380.393</i>	380 — 393
A Study of the Photodegradation Carbofuran and its Metabolites in Paddy Water Samples <i>10.18006/2023.11(2).394.404</i>	394 — 404
<i>Haberlea rhodopensis</i> alcohol extract normalizes stress-responsive transcription of the human TP53 gene <i>10.18006/2023.11(2).405.415</i>	405 — 415
The Effect of Titanium Dioxide Nanoparticles on <i>Haematococcus pluvialis</i> Biomass Concentration <i>10.18006/2023.11(2).416.422</i>	416 — 422

Morphology and DNA marker for distinguishing <i>Paphiopedilum hangianum</i> and <i>Paphiopedilum emersonii</i> from Vietnam <i>10.18006/2023.11(2).423.435</i>	423 — 435
Effects of lipoperoxidation and mitochondrial state on milk yield of dairy cows under technological stress <i>10.18006/2023.11(2).436.443</i>	436 — 443



Journal of Experimental Biology and Agricultural Sciences

<http://www.jebas.org>

ISSN No. 2320 – 8694

Deep Learning Paradigms for Existing and Imminent Lung Diseases Detection: A Review

Bhavna Vohra , Sumit Mittal* 

M. M. Institute of Computer Technology & Business Management, Maharishi Markandeshwar (Deemed to be University), Mullana-Ambala, Haryana-133207, India

Received – January 28, 2023; Revision – April 18, 2023; Accepted – April 26, 2023

Available Online – April 30, 2023

DOI: [http://dx.doi.org/10.18006/2023.11\(2\).226.235](http://dx.doi.org/10.18006/2023.11(2).226.235)

KEYWORDS

Deep Learning
Lung diseases
Machine learning
Semi-supervised
Computed Tomography
Chest Radiographs
Prediction Models

ABSTRACT

Diagnosis of lung diseases like asthma, chronic obstructive pulmonary disease, tuberculosis, cancer, etc., by clinicians rely on images taken through various means like X-ray and MRI. Deep Learning (DL) paradigm has magnified growth in the medical image field in current years. With the advancement of DL, lung diseases in medical images can be efficiently identified and classified. For example, DL can detect lung cancer with an accuracy of 99.49% in supervised models and 95.3% in unsupervised models. The deep learning models can extract unattended features that can be effortlessly combined into the DL network architecture for better medical image examination of one or two lung diseases. In this review article, effective techniques are reviewed under the elementary DL models, viz. supervised, semi-supervised, and unsupervised Learning to represent the growth of DL in lung disease detection with lesser human intervention. Recent techniques are added to understand the paradigm shift and future research prospects. All three techniques used Computed Tomography (C.T.) images datasets till 2019, but after the pandemic period, chest radiographs (X-rays) datasets are more commonly used. X-rays help in the economically early detection of lung diseases that will save lives by providing early treatment. Each DL model focuses on identifying a few features of lung diseases. Researchers can explore the DL to automate the detection of more lung diseases through a standard system using datasets of X-ray images. Unsupervised DL has been extended from detection to prediction of lung diseases, which is a critical milestone to seek out the odds of lung sickness before it happens. Researchers can work on more prediction models identifying the severity stages of multiple lung diseases to reduce mortality rates and the associated cost. The review article aims to help researchers explore Deep Learning systems that can efficiently identify and predict lung diseases at enhanced accuracy.

* Corresponding author

E-mail: sumit.mittal@mmumullana.org (Sumit Mittal)

Peer review under responsibility of Journal of Experimental Biology and Agricultural Sciences.

Production and Hosting by Horizon Publisher India [HPI]
(<http://www.horizonpublisherindia.in/>).
All rights reserved.

All the articles published by [Journal of Experimental Biology and Agricultural Sciences](#) are licensed under a [Creative Commons Attribution-NonCommercial 4.0 International License](#) Based on a work at www.jebas.org.



1 Introduction

The growing stress of air pollution, climate change, lifestyle disorder, decrease in immunity, bad habits like smoking, etc., burden the health of one of the vital organs, the lung, leading to an increase in respiratory disorders. According to the Journal of the Forum of International Respiratory Societies (FIRS) (2021), respiratory diseases enact a massive worldwide health burden. Among lung diseases, COPD, asthma, pneumonia, tuberculosis and lung cancer are five common reasons for severe ailment and global deaths (WHO factsheets 2020, 2021; Allemani et al. 2018; Vos et al. 2020; Wang et al. 2016). According to an estimation, COPD is the third-leading reason of death globally (Meghji et al. 2021; GBD study 2020; Li et al. 2020), with 3.2 million (out of 200 million having COPD) death each year. Asthma is a persistent and prolonged illness in children (Global Asthma Report 2018), affecting over 350 million people worldwide. For decades, the most common reason for demise or disability in children and adults is acute lower respiratory tract infections or pneumonia. In 2021, the mortality rates of tuberculosis (T.B.) enhanced due to COVID-19, and 1.4 million deceased in 2019 because of T.B. (WHO Annual Report 2021; Global Tuberculosis Report 2020). In 2020, lung cancer led to the loss of 1.8 million persons (Sung et al. 2021).

Looking at the paramount burden of respiratory diseases, it is necessary to equip the current health systems with technologies that enable early diagnosis and better treatment. With the development of tools like Deep Learning (DL) and machine learning, lung diseases using medical images can easily be identified and classified. Computer-Aided diagnosis (CAD) technology improved lung disease patients' survival rate. Current CAD methods apply deep learning to medical images to pre-process, segment lungs, reduce false positives and detect, classify and retrieve lung nodules. Particular classification studies using deep learning of pulmonary nodules achieve accuracy from 75.01 to 97.58% (Gu et al. 2021; Ursuleanu et al. 2021). Deep Learning

is more beneficial in the handling of pulmonary nodule image data as compared to traditional methods.

Furthermore, deep learning approaches that belong to other disciplines (Di Mauro et al. 2021; Padmapriya and Sasilatha 2023; Mohapatra et al. 2022) can be easily transferred to the domain of pulmonary nodule CAD as compared to traditional ML models because the foundation knowledge of ML paradigms in distinct disciplines is diverse (Kalra et al. 2021; Mohapatra et al. 2022). Optimization of hyper-parameters (size and number of filters, depth, learning rate, activation function, number of hidden layers, etc.) can increase the preformation of the deep learning model (Pandey et al. 2022)

Centred on the theory of adversarial training, General Adversarial Network (GAN) attracted many medical imaging researchers that produce novel images like original images through training, which add to the existing data. Optimization algorithms employed in this study for networks correspond to learning rate =0.00005 and stochastic gradient descent (learning rate=0.0001) (Onishi et al. 2020). Earlier old machine learning (ML) algorithms, such as active contour, region growth, and fuzzy c-means techniques, were commonly applied in CAD for lung nodule segmentation. The algorithms included in traditional ML classifiers used for lung nodule CAD are support vector machine (SVM) and random forest. Currently, the combination of deep neural networks and these classifiers is being used by many researchers. One of the numerous limitations of traditional classifiers is the problematic usage of SVM in dealing with extensive training samples and manifold classification problems (Chauhan et al. 2019).

In a deep learning model, the most challenging aspects are eliminated by the automatic extraction of elements of the initial nodule images through a neural network represented in Figure 1. In comparison, deep neural network classifier work surpasses SVM with sufficiently large training and verification data. Another

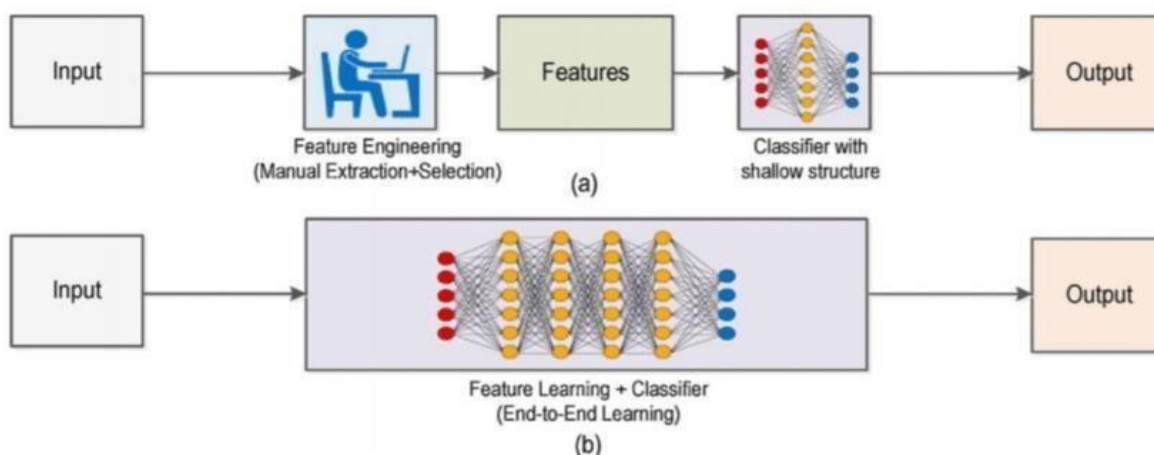


Figure 1 Difference between classical ML and Deep Learning approaches (Source: Del Real et al. 2020)

shortcoming of classical ML methods is achieving excellent outcomes with complex and lengthy procedures of handcrafted feature extraction, which requires proficiency and persistence. An add-on challenge is the complex features of the pulmonary nodule.

2 Deep Learning Methods based on Training Samples

DL methods can be categorized into three main classes: supervised, partially supervised (semi-supervised), and unsupervised.

2.1 Deep supervised Learning

The deep supervised method works with labelled data where the envions have inputs and resultant outputs. The agent informs the network factors to better estimate the desired outcomes. Through constructive training results, the agent can get the correct answers to the questions from the environment. Recurrent neural networks (RNN), convolutional neural networks (CNN), and deep neural networks (DNN) are some supervised learning techniques represented in Figure 2 (Ursuleanu et al. 2021). Inputs given to each layer of a DNN are used through changes parametrized by several weights. Although deep approaches are very promising, the vast number of hyper-parameters makes tuning very hard (Di Mauro et al. 2020). RNN includes recurrent gated units (GRU) and long short-term memory (LSTM) methodologies. The key benefit of deep supervised Learning is that output data can be collected or generated from previous knowledge, but the decision boundary might be over-strained when the training array needs more examples of a particular class. This learning method is simple yet performs extraordinarily.

2.1.1 Convolutional neural networks

Convolutional neural networks (CNN) are most comprehensively applied in deep learning algorithms applied to pulmonary nodules.

In the 2017 DSB competition, the winning team used a CNN model (Liao et al. 2019), and Google developed an algorithm that overtook six skilful radiologists, a CNN model published in *Nature*. Hua et al. (2015) first time used the Deep belief network (DBN), while Kumar et al. (2015) first time applied autoencoder (A.E.) in the pulmonary nodule CAD to separate benign and malignant pulmonary nodules. A sliced recurrent neural network (RNN) model was presented by Wang and Chakraborty (2019), in which training efficacy has been increased by simultaneous training of diverse layers of the RNN. A large quantity of information is requisite for training a deep learning model. However, because of limited labelled datasets for researchers, this work is time-consuming and needs specialists (Di Mauro et al. 2020).

CNN has distinctive benefits in processing images over other network types, which makes it the most chosen technique. An arrangement of CNN can unambiguously communicate the local weights of images and their learning features. Typical CNN architecture has three layers, namely convolutional, pooling, and fully connected, as shown in Figure 3, briefly discussed below.

The convolutional layer takes out the facets from the stored image, for example, the lung nodule image. The features of the nodule image are extracted by convolution operations, carried out by convolutional kernels in this layer, similar to filtering. Any slight change in the selected hyper-parameter values will affect the general CNN performance. In traditional filters, weights must be placed manually, whereas CNN learns these weights automatically (Gu et al. 2021).

The pooling layer's primary function is to choose several features and reduce feature map size by filtering the information. With the pooling operation, the outcome of a particular point is replaced with a value (for example, an average value or maximum) in the

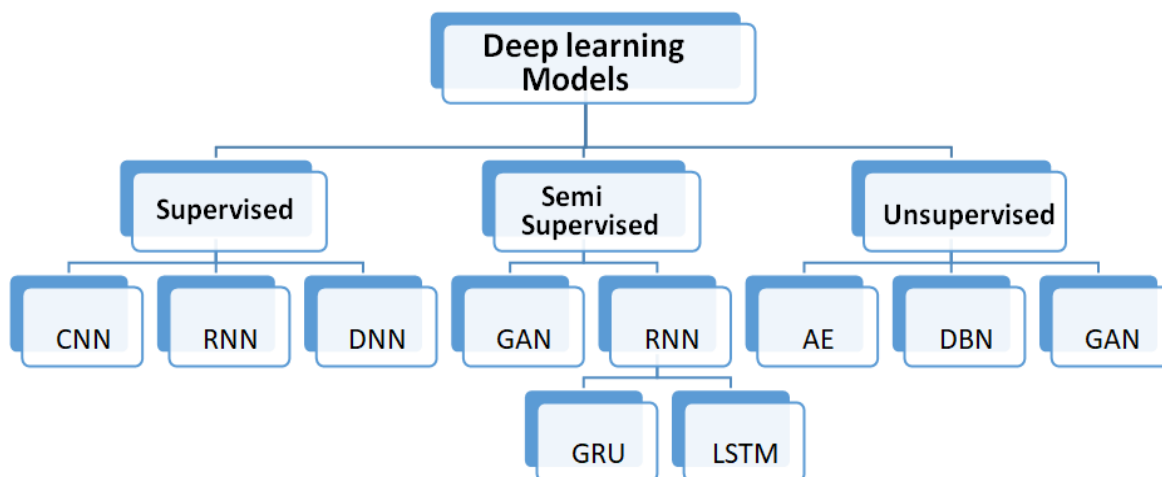


Figure 2 Different models of Deep Learning

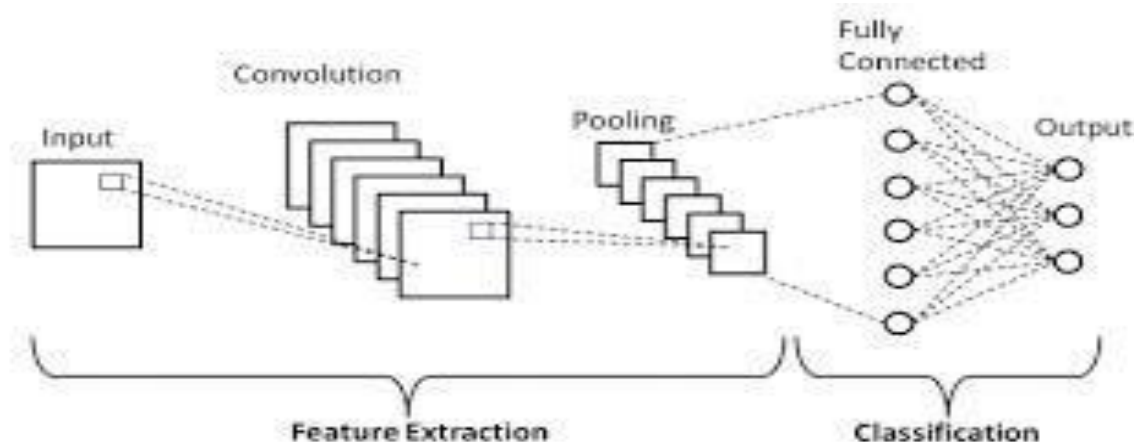


Figure 3 Layers of Convolution Neural Network (Source: Sharma et al. 2020)

feature map representing the adjacent region. However, the dimensionality reduction process degrades image quality and leads to the loss of some information by a pooling layer. Therefore, a pooling layer is not frequently used for processing medical images when the GPU capacity is satisfactory. Stridden convolution (Ayachi et al. 2018) and dilated convolution (Zhang et al. 2018) can replace the pooling layer to decrease feature map size. The fully connected (F.C.) layer joins the extracted elements non-linearly to get the output, the same as the hidden layer in a conventional artificial neural network (Gu et al. 2021).

2.1.2 Recurrent Neural Networks (RNN)

RNN are eminent in the natural language processing (NLP) field. RNN can appropriately process sequential data, as the embedded part delivers valuable information in the data sequence; these paradigms and the variations are extensively used in various applications having text, audio, and video analysis. To conclude the implication of a particular word in a sentence, the context of the sentence should be known. "Hidden-to-Hidden," "Hidden-to-Output," and "Input-to-Hidden" three deep RNN techniques are proposed by Pascanu et al. (2013). These three more profound RNN techniques make learning less difficult in the deep network. However, the central concern with this approach is exploding gradient and vanishing problems (Glorot and Bengio 2010), to which RNN is sensitive. More precisely, the repetitions of numerous large or small derivatives may lead to exponential explosion or falloff of the gradients during the training process. This sensitivity decays over time, as with fresh inputs, the network halts reasoning about the preliminary inputs. Moreover, this problem can be dealt with Long Short-Term Memory (LSTM)(Gao et al. 2019). Repeated links are offered to memory blocks in the network in this approach (Di Mauro et al. 2021). Many memory cells in every memory block can store the network's temporary state and control the information flow through gated units. Although using a huge quantity of data increases the time

complexity of LSTM, this problem is solved by Gated Recurrent Unit (GRU). The GRU comprises a reset gate that decides the amount of information transmitted from past to future and the amount of information that can be forgotten from the past by updating the gate. In profound networks, the vanishing gradient issue impact can be reduced considerably with residual connections (Piccialli et al. 2021). RNN has been applied in pulmonary nodule CAD tools (Wang and Chakraborty 2019), segmentation (Messay et al. 2015), detection and diagnosis (Abbas 2017a) of the pulmonary nodule.

2.2 Deep Semi-supervised Learning

Deep semi-supervised learning systems require partially annotated datasets. Generative adversarial networks (GAN), DRL, and RNN, including GRU and LSTM, are sometimes used as semi-supervised methods (Alzubaidi et al. 2021). This technique requires less labelled data, but extra input could deliver inappropriate decisions, while data training is represented in Figure 2 (Ursuleanu et al. 2021). Text document classifier is a general application of partially supervised Learning extraordinary.

2.2.1 Generative adversarial networks (GAN)

The GAN is a highly significant network in the deep learning domain. An extensive dataset is required for training a deep neural network. Still, available datasets are narrow, mainly for medical imagery, such as pulmonary nodule C.T. The operational procedure of the GAN paralleled a minimax game of two players: an adversarial process used to train the network. Generative model G produces fabricated data by capturing data distribution. The discriminative model D aimed to precisely discriminate between genuine and fabricated input data. The G designed the training process to extend the likelihood of D producing inaccuracies. The fundamental notion of GAN evolved from the Nash equilibrium in game theory. Regular optimization of G and D is required to

improve their abilities to generate and discriminate. This learning optimization course implicates a Nash equilibrium between G and D (Goodfellow et al. 2014). Using latent distribution (Ngo et al. 2017; Hsieh et al. 2020), synthetic training data can be generated from original data. Two problems of GAN are mode collapse and instability.

2.3 Deep Unsupervised Learning

With this method, the learning process is implemented without labeled data. In input data, it is essential to ascertain the anonymous arrangement or associations, and that association is given through the critical features or interior image acquired by an agent. In unsupervised Learning, clustering, generative network methods, and dimensionality reduction are often summed up. Auto-encoders restricted Boltzmann machines, and GAN beat non-linear dimensionality reduction and clustering tasks. GRU and LSTM methodologies incorporated with RNN are also applied for unsupervised Learning in many fields. However, unsupervised Learning needs to give precise data organization information and is computationally demanding. Clustering is one of the widespread unsupervised learning methods extraordinary (Alzubaidi et al. 2021).

2.3.1 Deep Belief Networks(DBN)

Probabilistic generative models have several restricted Boltzmann machines (RBM) (Abbas 2017b; Smolensky 1986; Freund and Haussler 1991). These networks of two layers adhere to the encoder-decoder paradigm (Hinton 2002). In diverse categories of data, RBM is used as generative models but most significantly applied as components of a DBN.

The DBN has two networks that form each other, whereas an acyclic graph denotes beliefs (Ranzato et al. 2007). Stochastic binary units with weights and their weighted connections form layers of this graph, RBM, which is stochastic (Ngo et al. 2017).

Applications of DBN include recognizing images and speech, classifying lesions in medical diagnosis, a person's presence in video recognition (Pandey et al. 2022), understanding omitted words in a sentence in speech recognition, and applying physiological indications that identify human emotion.

2.3.2 Auto-encoders (A.E.)

A.E. created by Wang et al. (2017), contain an encoder and decoder. Important images are used to reduce data size and learn data features to reconstruct outputs. A.E. is applied in the analysis of medical image processing of natural language and video analysis (Rumelhart et al. 1985). With AE, the input signal can be reconstructed perfectly by mapping itself. A.E.'s operation basis is first mapping an input vector to a hidden depiction via deterministic mapping. Then "reconstructed" input vector is mapped back from the following underlying illustration a. As so, an enhanced representation of the input could be learned by the hidden layer of the A.E. The A.E. is an unsupervised learning method in which the network uses many data points for endways training to increase accuracy.

3 Predicting Lung Diseases via DL Models

Deep Learning has been extended from automatic detection to the prediction of lung diseases. Various models were developed using supervised, semi-supervised and unsupervised methods, as summarized in Tables 1, 2, and 3. Automated deep learning techniques play a significant role in accurately predicting lung diseases (Wang et al. 2022b; Li et al. 2022; Walsh et al. 2022; Mohamed 2022). Predicting progressive fibrotic lung disease enhances outcomes with deep learning-based usual interstitial pneumonia probability on High-Resolution CT (Walsh et al. 2022). COPD causes fast progress of heart problems and other respiratory infections if not discovered and treated timely. Prediction with PNN (Probabilistic Neural Network) helps predict COPD severity stages (Mohamed 2022).

Table 1 Supervised Approach

S.No.	Dataset	Type of Image used	Method used	References
1	LIDC-IDRI	CT scans	VCNet	Tandon et al. 2022
2	GitHub	X-rays	DenseNet	Anitha et al. 2022
3	RSNA & other reliable sources	X-rays	VGG19+CNN	Alshmrani et al. 2023
4	LUNA16	CT scans	3D multi-scale deep CNN	Peng et al. 2021
5	Public dataset	C.T. scans X-rays	hybrid 2D/3D CNN architecture	Bayouduh et al. 2020
6	NIH	X-rays	VGG Data STN with CNN (VDSNet)	Bharati et al. 2020
7	LUNA16 DSB2017	CT scans	3-D deep neural network	Liao et al. 2019
8	LIDC-IDRI	CT scans	hierarchical (sliced) RNN	Wang and Chakraborty 2019

LIDC-IDRI: Lung Image Database Consortium Image Database Resource Initiative; DSB: Data Science Bowl; LUNA: Lung Nodule Analysis; RSNA: Radiological Society of North America

Table 2 Semi-Supervised Approach

S. No.	Dataset	Type of Image used	Method used	References
1	LUNA16; NLST	CT scans	Semi-supervised 3D deep neural network for Data-driven segmentation	Liu et al. 2020
2	DSB; LUNA	CT scans X-rays	Semi-supervised Learning for 3D medical image detection	Wang et al. 2020
3	LIDC-IDRI	CT scans	Adversarial autoencoder-based unsupervised reconstruction supervised classification	Xie et al. 2019

LIDC-IDRI: Lung Image Database Consortium Image Database Resource Initiative; DSB: Data Science Bowl; LUNA: Lung Nodule Analysis; NLST: National Lung Screening Trial

Supervised Deep Learning Models provide promising results in detecting and classifying various lung diseases at an early stage. For example, using C.T. images, multi-scale Res2Net achieved a sensitivity of 98.3% with fewer false positive nodules (Peng et al. 2021). Anitha et al. (2022) concluded that ResNet is more efficient, with a validation accuracy of 98.33%, in identifying Covid19. Bharati et al. (2020) proposed CO-ResNet that adjusts hyperparameters for optimization. It overtook other classic ResNet models with COVID-19 detection rate of 98.74% in ResNet101 assessment data. In most situations, deep CNN is used for detecting the region of the main module of the lung, but performance degrades when there are differences in image characteristics. A hybrid model named VCNet combining VGG-16 and capsule network address the shortcomings of CNN and detects Lung Cancer with an accuracy of 99.49% (Tandon et al. 2022). Qin et al. (2020) combined PET and C.T. scan information to validate a DL architecture for the sensitive detection of lung cancer. During the pandemic, the more extensive availability of X-rays leads to experimenting COVID-19 radiographs to identify the disease. Bayouh et al. (2020) achieved an accuracy of 96.91% with both C.T. and X-rays for detecting COVID-19 and ensured a tradeoff between accuracy and complexity by reducing the false negative rate and the computational time.

Semi-supervised methods partially automate the detection process of lung disease and also reduce the cost, as annotating medical

images is a costly process. Deep convolutional neural networks always require a massive set of labelled training data to classify benign and malignant lung nodules. A semi-supervised adversarial classification (SSAC) model achieved an accuracy of 92.53% by training labelled and unlabeled data for the variety of benign and malignant lung nodules (Xie et al. 2019) using the LIDC-IDRI dataset. The cost of annotating medical images can be reduced with the help of semi-supervised Learning (SSL) to detect 3D medical images. With 400 unlabeled C.T. images, Wang et al. (2020) achieved a 17.3% improvement over supervised learning methods. A semi-supervised 3D deep neural network can solve the problem of weak label information obtained from C.T. The semi-supervised model trains the network with image-level tag annotations from the dataset and outputs all suspicious nodules for a subject. The semi-supervised 3D deep neural network performed excellently with C.T. and radiographs in pulmonary nodule detection (Liu et al. 2020).

Annotating medical images is costly, but the advent of unsupervised deep learning models reduces the burden. The GAN-based data augmentation method called forward and backward GAN (Zhao et al. 2018), expands the dataset by generating high-quality synthetic medical images that improve the performance of pulmonary nodules classification. Forward and backward GAN has an accuracy of 95.24% and a sensitivity of 98.67%. In subsequent years, accuracy in classifying pulmonary nodules has increased to 95.3% using unlabeled C.T.

Table 3 Unsupervised Approach

S.No.	Dataset	Type of Image used	Method used	References
1	Anonymous	CT scans X-rays	Deep Learning based Medical Image Interpretation	Wang et al. 2022a
2	Mendeley	CT scans X-rays	Unsupervised Deep Learning Based feature Fusion	Ravi et al. 2022
3	RSNA	X-rays	auto-encoding generative adversarial network (α -GAN) framework	Nakao et al. 2021
4	Hospitals in China	CT scans	convolutional autoencoder deep learning framework	Chen et al. 2021
5	LIDC	CT scans	convolutional autoencoder deep learning framework with Clustering Augmented Learning Method (CALM) classifier	Ghoshal et al. 2020
6	LIDC	CT scans	3D conditional GAN-based DA approach	Han et al. 2019
7	LIDC	CT scans	Forward and Backward GAN	Zhao et al. 2018

RSNA: Radiological Society of North America; LIDC-IDRI: Lung Image Database Consortium Image Database Resource Initiative

images. Ghoshal et al. (2020) introduced Clustering Augmented (CALM), in which the features acquired from a convolution encoder using simultaneous clustering and classification to learn deep feature representation resulted in an overall accuracy of 95.3%. An unsupervised detection method requires standard images for training and evaluate its performance on a large dataset of chest radiographs. VAE-GAN model successfully detected several diseases or anomalies in chest radiographs (Nakao et al. 2021). The Deep MRD, a deep learning-based medical interpretation system developed by Wang et al. (2022c), demonstrated the potential to facilitate early diagnosis of major respiratory diseases that helps improve diagnosis and decision-making. The performance of Deep MRD was evaluated for abnormality identification and disease diagnosis on C.T. and chest X-rays datasets from two different institutes. This system achieved a 95% confidence level for abnormality identification of primary respiratory disease. Automated deep learning techniques play a beneficial role in detecting disease or abnormalities, which help medical experts make decisions or prepare accurate treatment scheduling (Quazi et al. 2022).

4 Future Perspective

This paper studied the growth of deep learning methods in lung disease detection, as demonstrated in Table 1-3. Unlike semi-supervised and unsupervised, supervised methods achieve more accurate results but depend on labelled data. Earlier research focuses on increasing models' efficacy in detecting one or two diseases, usually with C.T. scans. More research is needed to diagnose lung diseases through one deep learning system without supervision using X-rays. X-rays help in the economical early detection of lung diseases that will save lives by providing early treatment. In future, more accurate prediction models are required to identify the severity and the stages of multiple lung diseases to reduce mortality rates and the associated cost.

Conclusion

Deep Learning models have grown to acceptable outcomes with numerous applications to detect and diagnose lung diseases early. Deep learning offer automatic, prompt, and trusty detection of lung diseases through medical images. Unambiguously, convolutional neural networks achieved promising outcomes in revealing diseases. However, collecting labelled data is costly and tiresome, specifically for a new disease. Regardless of the performance of supervised models, their dependence on extensive labelled data leads to the proposal of various methods that can learn with less and with other types of supervision with optimized parameters and less time consumption. Therefore, a deep unsupervised framework could help classify lung disease from chest C.T. and X-ray images and predict lung disease more accurately and efficiently.

Acknowledgement

The authors are thankful to Maharishi Markandeshwar (Deemed to be University), Mullana, Ambala.

References

- Abbas, Q. (2017a). Lung-deep: a computerized tool for detection of lung nodule patterns using deep learning algorithms Detection of Lung Nodules Patterns. *International Journal of Advanced Computer Science and Applications*, 8(10), 2017. <http://dx.doi.org/10.14569/IJACSA.2017.081015>.
- Abbas, Q. (2017b). Nodular-deep: classification of pulmonary nodules using deep neural network, *International Journal of Medical Research & Health Sciences*, 6(8), 111–118.
- Allemani, C., Matsuda, T., Di Carlo V., et al. (2018). Global surveillance of trends in cancer survival 2000-14 (CONCORD-3): analysis of individual records for 37 513 025 patients diagnosed with one of 18 cancers from 322 population-based registries in 71 countries. *The Lancet*, 391(10125), 1023-1075.
- Alshmrani, G. M. M., Ni, Q., Jiang, R., Pervaiz, H., & Elshennawy, N. M. (2023). A deep learning architecture for multi-class lung diseases classification using chest X-ray (CXR) images. *Alexandria Engineering Journal*, 64, 923–935. <https://doi.org/10.1016/j.aej.2022.10.053>
- Alzubaidi, L., Zhang, J., Humaidi, A. J., Duan, Y., et al. (2021). Review of deep Learning: concepts, CNN architectures, challenges, applications, future directions. *Journal of Big Data*, 8(1), 1-74. <https://doi.org/10.1186/s40537-021-00444-8>
- Anitha, J., Kalaiarasu, M., Kumar, N. Suresh & Sundar, G. Ram (2022). Detection and classification of lung diseases using deep Learning. *AIP Conference Proceedings*, 2519, 030001. <https://doi.org/10.1063/5.0109980>
- Ayachi, R., Afif, M., Said, Y., & Atri, M. (2018). Strided Convolution Instead of Max Pooling for Memory Efficiency of Convolutional Neural Networks. In: M. Bouhlel, S. Rovetta, (eds) Proceedings of the 8th International Conference on Sciences of Electronics, Technologies of Information and Telecommunications (SETIT'18), Vol.1. SETIT 2018. Smart Innovation, Systems and Technologies, vol 146. Springer, Cham. https://doi.org/10.1007/978-3-030-21005-2_23
- Bayoudh, K., Hamdaoui, F., & Mtibaa, A. (2020). Hybrid COVID: a novel hybrid 2D/3D CNN based on cross-domain adaptation approach for COVID-19 screening from chest X-ray images, *Physical and Engineering Sciences in Medicine*, 43, 1415–1431. <https://doi.org/10.1007/s13246-020-00957-1>

- Bharati, S., Podder, P., & Mondal, M. R. H. (2020). Hybrid deep Learning for detecting lung diseases from X-ray images. *Informatics in Medicine Unlocked*, 20, 100391. <https://doi.org/10.1016/j.imu.2020.100391>
- Chauhan, V.K., Dahiya, K., & Sharma, A. (2019). Problem formulations and solvers in linear SVM: a review. *Artificial Intelligence Review*, 52, 803–855.
- Chen, M., Shi, X., Zhang, Y., Wu, D., & Guizani, M. (2021). Deep Feature Learning for Medical Image Analysis with Convolutional Autoencoder Neural Network. *IEEE Transactions on Big Data*, 7(4), 750-758. DOI:10.1109/TBDATA.2017.2717439.
- Del Real, A.J., Dorado, F., & Durán, J. Energy Demand Forecasting Using Deep Learning: Applications for the French Grid. *Energies*, 13, 2242.
- Di Mauro, M., Galatro, G., Fortino, G., & Liotta, A. (2021). Supervised feature selection techniques in network intrusion detection: A critical review. *Engineering Applications of Artificial Intelligence*, 101, 104216. <https://doi.org/10.1016/j.engappai.2021.104216>
- Di Mauro, M. & Galatro, G. & Liotta, A. (2020). Experimental Review of Neural-Based Approaches for Network Intrusion Management. *IEEE Transactions on Network and Service Management*, 17(4), 2480-2495. <https://doi.org/10.1109/TNSM.2020.3024225>
- Forum of International Respiratory Societies (2021). The global impact of respiratory disease. Third Edition. European Respiratory Society. Retrieved from http://firsnet.org/images/publications/FIRS_Master_09202021.pdf
- Freund, Y., & Haussler, D. (1991). Unsupervised Learning of distributions on binary vectors using two layer networks. *Advances in Neural Information Processing Systems*, 4, 912–919.
- Gao, C., Yan J., Zhou, S., Varshney, P.K., & Liu H. (2019). Long short-term memory based deep recurrent neural networks for target tracking. *Information Sciences*, 502, 279– 96. DOI:10.1016/j.ins.2019.06.039.
- GBD Chronic Respiratory Disease Collaborators (2020). Prevalence and attributable health burden of chronic respiratory diseases, 1990–2017: a systematic analysis for the Global Burden of Disease Study 2017. *The Lancet Respiratory Medicine*, 8(6), 585-596.
- Ghosal, S.S., Sarkar, I., & Elhallaoui, I. (2020). Lung Nodule Classification Using Convolutional Autoencoder and Clustering Augmented Learning Method (CALM), *HSDM 2020 Workshop on Health Search and Data Mining*.
- Global Asthma Report (2018). Global Asthma Network. Retrieved from <http://globalasthmareport.org/burden/burden.php>
- Global Tuberculosis Report (2020). World Health Organization Global Tuberculosis Program. World Health Organization. Retrieved from <https://www.who.int/publications/i/item/9789240013131>
- Glorot, X., & Bengio, Y. (2010) Understanding the Difficulty of Training Deep Feedforward Neural Networks. Proceedings of the Thirteenth International Conference on Artificial Intelligence and Statistics. *Proceedings of Machine Learning Research*, 9, 249-256. <http://proceedings.mlr.press/v9/glorot10a.html>
- Goodfellow, I.J., Pouget-Abadie, J., Mirza, M, et al. (2014) Generative Adversarial Nets. *Proceedings of the 27th International Conference on Neural Information Processing Systems*, 2, 2672-2680. <https://dl.acm.org/doi/10.5555/2969033.2969125>
- Gu, Y., Chi, J., Liu, J., Yang, L., Zhang, B., et al. (2021). A survey of computer-aided diagnosis of lung nodules from C.T. scans using deep Learning. *Computer in Biology and Medicine*, 137:104806.
- Han, C., Kitamura, Y., Kudo, A., Ichinose, A., Rundo, L. et al. (2019). Synthesizing Diverse Lung Nodules Wherever Massively: 3D Multi-Conditional GAN-based CT Image Augmentation for Object Detection. *arXiv*. <https://doi.org/10.48550/arXiv.1906.04962>
- Hinton, G.E. (2002). Training products of experts by minimizing contrastive divergence. *Neural Computation*, 14, 1771–1800.
- Hsieh, Y.J., Tseng, H.C., Chin, C.L., Shao, Y.H., & Tsai, T.Y. (2020) Based on DICOM RT Structure and Multiple Loss Function Deep Learning Algorithm in Organ Segmentation of Head and Neck Image. In: K.P. Lin, R. Magjarevic, & P. de Carvalho (Eds.), *Future Trends in Biomedical and Health Informatics and Cybersecurity in Medical Devices. ICBHI 2019. IFMBE Proceedings*, 74, Springer, Cham, 428-435. https://doi.org/10.1007/978-3-030-30636-6_58
- Hua, L., Hsu, H., Hidayati, S. C., Cheng, H., & Chen, J. (2015). Computer-aided classification of lung nodules on computed tomography images via deep learning technique. *OncoTargets and therapy*, 8, 2015-2022.
- Kalra, V., Kashyap, I., & Kaur, H. (2021). Machine Learning and Its Application in Monitoring Diabetes Mellitus. In B. Patil & M. Vohra (Eds.), *Handbook of Research on Engineering, Business, and Healthcare Applications of Data Science and Analytics* (pp. 228-288). IGI Global Publisher of Timely Knowledge. <https://doi.org/10.4018/978-1-7998-3053-5.ch012>
- Kumar, D., Wong, A., & Clausi, D.A. (2015). Lung nodule classification using deep features in C.T. images, in 12th Conference on Computer and Robot Vision, IEEE, 2015, pp. 133–138.

- Li, X., Cao, X., Guo, M., Xie, M., & Liu, X. (2020). Trends and risk factors of mortality and disability adjusted life years for chronic respiratory diseases from 1990 to 2017: a systematic analysis for the Global Burden of Disease Study 2017. *BMJ*, *368*, 234
- Li, L., Ayiguli, A., Luan, Q., Yang, B. et al. (2022). Prediction and Diagnosis of Respiratory Disease by Combining Convolutional Neural Network and Bi-directional Long Short-Term Memory Methods. *Frontiers in Public Health*. <https://doi.org/10.3389/fpubh.2022.881234>
- Liao, F., Liang, M., Li, Z., Hu, X., & Song, S. (2019). Evaluate the malignancy of pulmonary nodules using the 3-D deep leaky noisy-or network. *IEEE transactions on neural networks and learning systems*, *30*(11), 3484–3495.
- Liu, M., Jiang, X., Liu, Y., Zhao, F., & Zhou, H. (2020). A semi-supervised convolutional transfer neural network for 3D pulmonary nodules detection. *Neurocomputing*, *391*, 199-209. <https://doi.org/10.1016/j.neucom.2018.12.081>
- Meghji, J., Mortimer, K., Agusti, A. et al. (2021). Improving lung health in low- and middle-income countries: from challenges to solutions. *The Lancet*, *397*(10277), 928-940.
- Messay, T., Hardie, R. C., & Tuinstra, T. R. (2015). Segmentation of pulmonary nodules in computed tomography using a regression neural network approach and its application to the Lung Image Database Consortium and Image Database Resource Initiative dataset. *Medical Image Analysis*, *22*(1), 48-62.
- Mohamed I. (2022). Prediction of Chronic Obstructive Pulmonary Disease Stages Using Machine Learning Algorithms. *International Journal of Decision Support System Technology*, *14*(1), 1-13. DOI: 10.4018/IJDSST.286693
- Mohapatra, R. K., Pal, M., Parija, S., Panda, G., & Dhama, K. (2022). Machine learning for the classification of breast cancer tumor: a comparative analysis. *Journal of Experimental Biology and Agricultural Sciences*, *10*(2), 440–450.
- Nakao, T., Hanaoka, S., Nomura, Y. et al. (2021). Unsupervised Deep Anomaly Detection in Chest Radiographs. *Journal of Digital Imaging*, *34*, 418–427. <https://doi.org/10.1007/s10278-020-00413-2>
- Ngo, T.A., Lu, Z., & Carneiro, G. (2017). Combining Deep Learning and Level Set for the Automated Segmentation of the Left Ventricle of the Heart from Cardiac Cine Magnetic Resonance. *Medical Image Analysis*, *35*, 159–171. <https://doi.org/10.1016/j.media.2016.05.009>
- Onishi, Y., Teramoto, A., Tsujimoto, M., Tsukamoto, T., et al. (2020). Multiplanar analysis for pulmonary nodule classification in C.T. images using deep convolutional neural network and generative adversarial networks. *International Journal of Computer Assisted Radiology and Surgery*, *15*, 173–178.
- Padmapriya J., & Sasilatha T., (2023). Deep Learning based multi-labelled soil classification and empirical estimation toward sustainable agriculture. *Engineering Applications of Artificial Intelligence*, *119*, 105690. <https://doi.org/10.1016/j.engappai.2022.105690>
- Pandey, B., Pandey, D.K., Mishra, B.P. & Rhmann, W. (2022). A Comprehensive Survey of Deep Learning in the Field of Medical Imaging and Medical Natural Language Processing: Challenges and Research Directions. *Journal of King Saud University-Computer and Information Sciences*, *34*(8), 5083-5099. <https://doi.org/10.1016/j.jksuci.2021.01.0007>
- Pascanu, R., Gulcehre, C., Cho, K., & Bengio, Y. (2013). How to Construct Deep Recurrent Neural Networks. *ArXiv*. <https://doi.org/10.48550/arXiv.1312.6026>
- Peng, H., Sun, H., & Guo, Y. (2021). 3D multi-scale deep convolutional neural networks for pulmonary nodule detection. *PLoS ONE*, *16*(1), e0244406. <https://doi.org/10.1371/journal.pone.0244406>
- Piccialli, F., Di Somma, V., Giampaolo, F., Cuomo, S., & Fortino, G. (2021). A Survey on Deep Learning in Medicine: Why, How and When? *Information Fusion*, *66*, 111-137.
- Qin, R., Wang, Z., Jiang, L., Qiao, K., Hai, J., Chen, J., et al. (2020). Fine-grained lung cancer classification from PET and C.T. images based on multidimensional attention mechanism. *Complexity*, *2020*:165–75. DOI: 10.1155/2020/6153657
- Quazi, S., Saha, R. P., & Singh, M. K. (2022). Applications of Artificial Intelligence in Healthcare. *Journal of Experimental Biology and Agricultural Sciences*, *10*(1), 211–226.
- Ranzato, M.A., Boureau, Y.L., & LeCun, Y. (2007). Sparse feature learning for deep belief networks. *Advances in Neural Information Processing Systems*, *20*, 1185–1192.
- Ravi, V., Narasimhan, H., Chakraborty, C., & Pham, T.D. (2022). Deep learning-based meta-classifier approach for COVID-19 classification using C.T. scan and chest X-ray images. *Multimedia Systems*, *28*(4), 1401-1415. DOI: 10.1007/s00530-021-00826-1.
- Rumelhart, D.E., Hinton, G.E. & Williams, R.J. (1985) Learning Internal Representations by Error Propagation. In: Rumelhart, D.E., McClelland, J.L. and the PDP Research Group, Eds., *Parallel Distributed Processing: Exploration in the Microstructure*

- of Cognition. Volume I: Foundations, MIT Press, Cambridge, MA, 318-362.
- Sharma, D., Dutta, S. & Bora, D. (2020). REGA: Real-Time Emotion, Gender, Age Detection Using CNN—A Review. *The International Conference on Research in Management & Technovation*, 24, 115-118. DOI: 10.15439/2020KM18.
- Smolensky, P. (1986), Information Processing in Dynamical Systems: Foundations of Harmony Theory. Chapter 6 of D.E. Rumelhart, J.L. McClelland, and the PDP Research Group, *Parallel Distributed Processing: Exploration in the Microstructure of Cognition*. Volume I: Foundations. Cambridge, MA: MIT Press/Bradford Books.
- Sung, H., Ferlay, J., Siegel, R. L., et al. (2021). Global cancer statistics 2020: GLOBOCAN estimates of incidence and mortality worldwide for 36 cancers in 185 countries. *CA: A Cancer Journal of Clinicals*, 71(3), 209-249.
- Tandon, R., Agrawal, S., Chang, A., & Band, S. S. (2022). VCNet: Hybrid Deep Learning Model for Detection and Classification of Lung Carcinoma Using Chest Radiographs. *Frontiers in Public Health*. <https://doi.org/10.3389/fpubh.2022.894920>
- Ursuleanu, T.F., Luca, A.R., Gheorghe, L., et al. (2021). Unified Analysis Specific to the Medical Field in the Interpretation of Medical Images through the Use of Deep Learning. *E-Health Telecommunication Systems and Networks*, 10, 41-74. <https://doi.org/10.4236/etsn.2021.102003>
- Vos, T., Lim S. S., Abbafati, C., et al (2020). GBD 2019 Diseases and Injuries Collaborators. Global burden of 369 diseases and injuries in 204 countries and territories, 1990–2019: a systematic analysis for the Global Burden of Disease Study 2019. *The Lancet*, 396(10258), P1204-1222.
- Walsh, S.L.F., Mackintosh, J.A., Calandriello, L., Silva, M., et al. (2022). Deep Learning-based Outcome Prediction in Progressive Fibrotic Lung Disease Using High-Resolution Computed Tomography. *American Journal of Respiratory and Critical Care Medicine*, 206(7), 883–891. DOI: 10.1164/rccm.202112-2684OC.
- Wang, C., Ma, J., & Zhang, S. et al. (2022a). Development and validation of an abnormality-derived deep-learning diagnostic system for major respiratory diseases. *NPJ Digital Medicine*, 5(1), 124. <https://doi.org/10.1038/s41746-022-00648-z>
- Wang, C., Ma, J., Shao, J., Zhang, S., Li, J. et al. (2022b). Non-Invasive Measurement Using Deep Learning Algorithm Based on Multi-Source Features Fusion to Predict PD-L1 Expression and Survival in NSCLC. *Frontiers in Immunology*, <https://doi.org/10.3389/fimmu.2022.828560>
- Wang, C., Ma, J., Shao, J., Zhang, S., Liu, Z. et al. (2022c). Predicting EGFR and PD-L1 Status in NSCLC Patients Using Multitask A.I. System Based on C.T. Images. *Frontiers in Immunology*, <https://doi.org/10.3389/fimmu.2022.813072>
- Wang, D., Zhang, Y., Zhang, K., & Wang, L. (2020). FocalMix: semi-supervised Learning for 3D medical image detection, *Proceedings of the IEEE/CVF Conference on Computer Vision and Pattern Recognition*, Seattle, WA, USA, 3950–3959. <http://doi.org/10.1109/CVPR42600.2020.00401>
- Wang, H., Naghavi, M., Allen, C., et al (2016). GBD 2015 Mortality and Causes of Death Collaborators. Global, regional, and national life expectancy, all-cause mortality, and cause-specific mortality for 249 causes of death, 1980–2015: A systematic analysis for the Global Burden of Disease Study 2015. *The Lancet*, 388(10053), 1459-1544.
- Wang, J., Ding, H., Bidgoli, F.A., Zhou, B., Iribarren, C., & Molloy, S. (2017). Detecting Cardiovascular Disease from Mammograms with Deep Learning. *IEEE Transactions on Medical Imaging*, 36, 1172–1181, <https://doi.org/10.1109/TMI.2017.265548>
- Wang, W., & Chakraborty, G. (2019). Evaluation of malignancy of lung nodules from C.T. image using recurrent neural network, *IEEE International Conference on Systems, Man and Cybernetics (SMC)*, Bari, Italy, pp. 2992–2997, <https://doi.org/10.1109/SMC.2019.8913885>
- World Health Organization. Indoor air pollution and household energy (2021). Retrieved from <https://www.who.int/heli/risks/indoorair/indoorair/en/>
- World Health Organization. The top 10 causes of death (2020). Retrieved from <https://www.who.int/news-room/factsheets/detail/the-top-10-causes-of-death>
- Xie, Y., Zhang, J., Xia, Y. (2019). Semi-supervised adversarial model for benign-malignant lung nodule classification on chest C.T. *Medical Image Analysis*, 57, 237–248. DOI: 10.1016/j.media.2019.07.004.
- Zhang, J., Xia, Y., Zeng, H., & Zhang, Y. (2018). NODULe: combining constrained multi-scaleLoG filters with densely dilated 3D deep convolutional neural network for pulmonary nodule detection, *Neurocomputing*, 317, 159–167.
- Zhao, D., Zhu, D., Lu, J., Luo, Y., & Zhang, G. (2018). Synthetic medical images using F&BGAN for improved lung nodules classification by multi-scale VGG16, *Symmetry*, 10, 519.









Journal of Experimental Biology and Agricultural Sciences

<http://www.jebas.org>

ISSN No. 2320 – 8694

Prospective nutritional, therapeutic, and dietary benefits of camel milk making it a viable option for human consumption: Current state of scientific knowledge

Saibhavana S^{1†}, Vasukhi S M^{1†}, Shreya Ramesh^{1†}, Rajakumari R^{1†}, Abhijith A S¹, Adithya Krishna S¹, Gautam Prakash¹, Raida¹, Abhirami V Nair¹, Aishwarya Prashanth¹, Pran M², Sandip Chakraborty³ , Hitesh Chopra⁴ , Abhijit Dey⁵ , Anil K Sharma⁶ , Kuldeep Dhama^{7*} , Deepak Chandran^{1*} 

¹Amrita School of Agricultural Sciences, Amrita Vishwa Vidyapeetham University, Coimbatore, Tamil Nadu – 642109, India

²School of Agricultural Sciences, Karunya Institute of Technology and Sciences, Coimbatore, Tamil Nadu – 641114, India

³Department of Veterinary Microbiology, College of Veterinary Sciences and Animal Husbandry, R.K. Nagar, West Tripura, Tripura, Pin-799008, India

⁴Chitkara College of Pharmacy, Chitkara University, Punjab - 140401, India

⁵Department of Life Sciences, Presidency University, 86/1 College Street, Kolkata-700073, West Bengal, India

⁶Department of Biotechnology, Maharishi Markandeshwar University (Deemed to be University) Mullana-Ambala-133207, Haryana, India

⁷Division of Pathology, ICAR-Indian Veterinary Research Institute, Izatnagar, Bareilly, Uttar Pradesh - 243122, India

[†]Authors contributed equally

Received – February 24, 2023; Revision – April 01, 2023; Accepted – April 21, 2023

Available Online – April 30, 2023

DOI: [http://dx.doi.org/10.18006/2023.11\(2\).236.250](http://dx.doi.org/10.18006/2023.11(2).236.250)

KEYWORDS

Camel milk

Biological factors

Nutritional value

Therapeutic benefits

Human disease

ABSTRACT

For over five thousand years, people in Asia and Africa have known about the health benefits of camel milk. Thus, it is used not only as a food source but also as a medicine. The similarities between camel milk and human milk have been scientifically proven. Camel milk is unique among ruminant milk because it is high in vitamins C and E and low in sugar and cholesterol. Still, it contains a wide variety of beneficial minerals (including sodium, potassium, iron, copper, zinc, and magnesium), besides being rich in several nutrients, including monounsaturated and polyunsaturated fatty acids, serum albumin, lactoferrin, immunoglobulins, lysozyme and the hormone insulin. Because of these components, many medical professionals now recommend camel milk as a treatment for various human ailments. It has been demonstrated to be effective in treating gastrointestinal issues, Type 1 diabetes, and food allergies. As a bonus, camel milk has been utilized to cure autism, lower cholesterol, prevent psoriasis, heal inflammation, aid tuberculosis patients, boost the body's natural defences, and impede the spread of cancer

* Corresponding author

E-mail: c_deepak@cb.amrita.edu (Deepak Chandran);
kdhama@rediffmail.com (Kuldeep Dhama)

Peer review under responsibility of Journal of Experimental Biology and Agricultural Sciences.

Production and Hosting by Horizon Publisher India [HPI]
(<http://www.horizonpublisherindia.in/>).
All rights reserved.

All the articles published by [Journal of Experimental Biology and Agricultural Sciences](#) are licensed under a [Creative Commons Attribution-NonCommercial 4.0 International License](#) Based on a work at www.jebas.org.



cells. Those who have problems digesting lactose may still be able to tolerate it. Conversely, camel milk can also help reduce an excessively high bilirubin, globulin, and granulocyte count. Drinking camel milk does not affect the erythrocyte sedimentation rate, hemoglobin concentration, and leukocyte count. The proteins in camel milk have an adequate ratio of critical amino acids. Immunoglobulins, which fight disease, are contained inside, and their small size allows antigens to penetrate and boosts the immune system's efficacy. This article highlights the health benefits and medicinal uses of camel milk.

1 Introduction

Allergy to cow's milk is the most frequent food allergy among newborns and toddlers. Medical crises involving patients with anaphylaxis or severe allergic reactions to this dairy source require the administration of adrenaline (epinephrine). This risk factor for functional gastrointestinal diseases can be mitigated, however, if an alternative is found to cow milk for feeding children and newborns and one such important alternative is camel milk (Yadav et al. 2015; Yassin et al. 2015; Chandran et al. 2021; Muthukumar et al. 2022; Patange et al. 2022a; Patange et al. 2022b; Krishnan et al. 2023). Regarding nutritional value, camel milk resembles human milk and is superior to cow milk (Lejaniya et al. 2021a; Lejaniya et al. 2021b; Ho et al. 2022).

Camels prefer dry, hot climates with little available flora. Camels are raised in nations with sizable desert areas for a wide range of

purposes, including but not limited to food, transportation, clothing, cosmetics, and even human consumption. There are roughly 29 million camels in the globe, with the vast majority being dromedary (*Camelus dromedarius*) camels (Bakry et al. 2021; Islam et al. 2022). The majority of the world's supply of fresh whole camel milk comes from Africa, while Asia accounts for the rest. Figure 1 shows a breakdown of the major camel milk-producing countries and their global production profiles. Nutritionally, camel milk is superior to bovine milk, and its composition is the same as human milk; hence it is often used as a stand-in for human milk when the latter is unavailable (Kumar et al. 2016). In recent years, camel milk's potential as a dairy alternative to cow, sheep, buffalo, donkey, and mare milk has garnered much attention. It has been shown that the immunoglobulins (Igs) found in camel milk help alleviate the symptoms of cow milk protein allergy in 2-6% of children and new-borns (Jilo and Tegegne 2016; Muthukumar et al. 2022). A

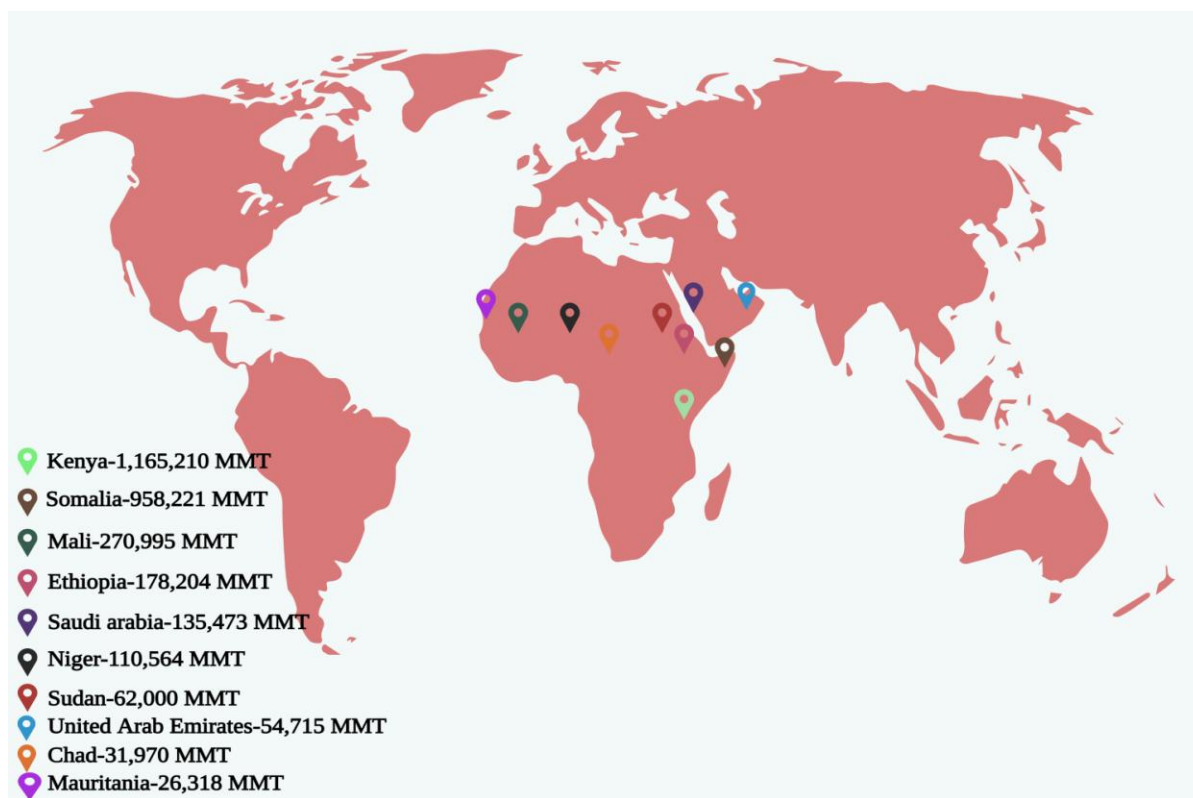


Figure 1 Examining the global situation of camel milk production (Designed with Biorender premium software; <https://app.biorender.com/>)

lack of beta-lactoglobulin and plenty of alpha-lactalbumin give camel milk an antiallergenic quality comparable to human breast milk (Mohammadabadi and Faraz 2021). Camel milk's high levels of antioxidants and antimicrobials make it useful for a wide variety of medical purposes, including the prevention of gastrointestinal illness, the management of diabetes, psoriasis, and hepatitis C and B, the improvement of immune system function, the suppression of cancer cell growth, and the treatment of tuberculosis (Kuala 2016; Faraz 2020; Bakry et al. 2021).

There are many bioactive peptides and protective enzymes in camel milk, and these compounds are responsible for their medicinal, antibacterial, and antioxidant properties (Yadav et al. 2015). In addition to its excellent nutrient and mineral makeup, camel milk also contains protective proteins with potential health benefits, including lactoperoxidase, lysozyme, lactoferrin and immunoglobulins. Even those who have digestive issues with lactose may be able to tolerate it (Kuala, 2016; Khalesi et al. 2017). Contrarily, drinking camel milk can reduce a high bilirubin, globulin, or granulocyte count. There was no correlation between camel milk consumption and changes in erythrocyte sedimentation rate, hemoglobin content, or leukocyte count. Proteins in camel milk contain a good amount of each essential amino acid. Disease-fighting immunoglobulins are stored within, and their diminutive size makes it easier for antigens to enter the body and trigger an immune response (Jilo and Tegegne 2016; Mohammadabadi and Faraz 2021; Muthukumaran et al. 2022; Seifu 2023). The current article looked at camel milk's health and therapeutic benefits, which are more relevant to developing a commercially viable product.

2 Nutritional profile and chemical composition of camel milk

Researchers found that camel milk had a less consistent composition than other milk types, such as bovine milk. Many factors, including the camel's breed, age, and the number of calves birthed, may account for the reported variations in camel milk composition. These include analytical measuring methodologies, geographic regions, feeding conditions, and sample origin. Camel milk composition is most strongly influenced by its place of origin and the time of year (Khalesi et al. 2017; Hailu et al. 2016; Sakandar et al. 2018). According to research by Konuspayeva et al. (2008), camels in East Africa produce milk with a higher lipid content than their counterparts in Africa and Western Asia. Camel milk contains between 87% and 90% water. Total solids in camel milk were shown to be inversely proportional to the amount of water consumed by the camels.

2.1 Milk fats

Camel milk fat content varies from 1.25 to 4.55%, depending on the camel's diet, lactation stage, breed, time of year, and other

environmental factors. Camel milk fat is the most nutrient-dense source of unsaturated fatty acids of any animal fat. This may be the primary cause of camel milk fat's waxy consistency (Faraz 2020; Bakry et al. 2021). Fat from dromedary camels contained more long-chain fatty acids than fat from cows. Compared to bovine milk, the beta-carotene content of camel milk is lower. Camel milk fat might be less vibrant because it contains less of the antioxidant carotene (Hailu et al. 2016; Sakandar et al. 2018; Solanki and Hati 2018; Sumaira et al. 2020).

2.2 Milk proteins

The protein content in camel milk is 2.15–4.90%. Whey protein is higher in camel milk than cow milk, although casein quantity is the same. Camel milk has the best whey-to-casein ratio. Because of this, camel milk's coagulum may be less solid than cow milk (Yassin et al. 2015). Of the total proteins (1.63-2.76%) in a glass of camel milk, 52-87% are casein. Beta-casein is 65%, compared to 36% in bovine milk. Comparatively, only around 13% of the total casein in bovine milk is beta-casein, while camel milk has about 3.47 % (Sumaira et al. 2020; Kumar et al. 2021; Seifu 2023). About 20 to 25% of milk's protein comes from whey proteins, which comprise 0.63 to 0.80%. The primary whey protein in camel milk is alpha-lactalbumin rather than beta-lactoglobulin. Serum albumin, immunoglobulins, peptidoglycan recognition protein, and lactoferrin are other camel milk whey proteins. Cathepsin D and chymotrypsin A are also found in whey protein (Faraz 2020; Chandran et al. 2020; Benmeziiane–Derradji 2021; Swelum et al. 2021; Muthukumaran et al. 2022).

2.3 Lactose

Camel milk primarily comprises lactose sugar, with concentrations ranging from 3.30 percent to 5.80 percent. Camel milk's wide-ranging lactose content may be mainly due to the variety of desert flora camel feeds upon. To satisfy their physiological needs for salts, camels commonly consume halophilic plants like Salosa, Acacia, and Artiplex. However, throughout time, the lactose concentration was found to be slightly different in several dromedary breeds around the world. The human digestive system easily absorbs sugar from milk (lactose). Camel milk's 3.5 to 4.5% lactose concentration is remarkably consistent between seasons and across hydrated and dehydrated environments (Sumaira et al. 2020; Seifu 2023).

2.4 Vitamins

Niacin and vitamin C are higher in camel milk than in cow milk. B1, B2, folic acid, and pantothenic acid are lacking in camel milk, although B6 and B12 are present. Compared to bovine milk, camel milk has 100–380 g/L of vitamin A (Yadav et al. 2015; Seifu 2023). Camel milk (250 mL) provides 15.5% of an adult's daily

Table 1 Camel milk's nutritional composition compared to those of other mammals, including humans

Nutrients	Camel milk	Cow milk	Goat Milk	Donkey milk	Sheep milk	Human milk
Fat (g/100mL)	4.5	3.5	3.5	0.3-1.8	6.1	3.4
Protein (g/100mL)	3.5	3.4	3.3	1.3-1.8	6.21	1.1
Lactose (g/100mL)	4.4	4.5	4.1	5.8-7.4	4.8	6.5
Minerals (g/100mL)	0.7	0.7	0.86	0.3-0.5	5.5	0.21
Solids-not-fat (g/100mL)	8.6	9.1	8.75	9.018	10.33	8.9
Total solids (g/100mL)	16.89	13.12	13.2	8.8-11.7	18.75	12.75
Cholesterol (mg/100g)	34.5	5	11	8.6	27	14
Calcium (g/100mL)	1.43	1.20	1.34	6.89	2.00	3.20
Phosphorus (g/100mL)	1.16	1.3	1.08	1.596	0.15	0.13
Saturated fatty acids (g/100mL)	51.9	67.73	70.42	67.6	65.17	46.60
Monounsaturated fatty acids (g/100mL)	39.60	27.3	25.67	15.80	24.29	43.55
Polyunsaturated fatty acids (g/100mL)	8.46	5.25	4.08	16.60	2.45	9.85
Water (%)	87-90	87	82.46-89.05	92.5	80.62	87.5

Sources: Yadav et al. (2015); Jilo and Tegegne (2016); Kumar et al. (2016); Abrhaley and Leta (2018); Faraz (2020); Sumaira et al. (2020); Bakry et al. (2021); Mohammadabadi and Faraz (2021)

recommended intake of cyanocobalamin, 10.50% of ascorbic acid, thiamine, and pyridoxine, 8.25% of riboflavin (B2), and 5.25% of vitamin A (Gul et al. 2015; Benmeziiane–Derradji 2021; Muthukumaran et al. 2022).

2.5 Minerals

Camel milk has a mineral concentration between 0.60% and 0.90%. Zinc, iron, copper, and manganese are all present in higher concentrations in camel milk than in bovine milk. Like cow milk, camel milk has high concentrations of other essential minerals: calcium, magnesium, phosphorus, sodium, and potassium. Camel milk is rich in chloride because camels eat *Atriplex* and *Acacia*, which are generally high in salt (Ahamad et al. 2017; Sakandar et al. 2018; Solanki and Hati 2018). Another possible explanation for camel milk's salty flavour is that the milk of dehydrated camels has a higher chloride concentration due to a decrease in main milk components. Camel milk has a more elevated calcium-to-phosphorus ratio of 1.5:1 compared to 1.29:1 for cow's milk and 2.1:1 for human's milk. Because cow milk-based infant formula includes a lot of phosphates, which can cause hyperphosphatemia and low serum calcium, it is essential to keep the two in check (Gul et al. 2015; Sumaira et al. 2020; Bakry et al. 2021; Benmeziiane–Derradji 2021; Seifu 2023).

2.6 A comparison of camel and cow milk

The physiology of camels and ruminants are very different, and so is the content of their milk. The fat in the milk is entirely

homogenized polyunsaturated fatty acids, which gives the milk its characteristic smooth white appearance. Even though it contains 4.8% lactose, lactose intolerant people have no trouble digesting this milk sugar. Specific gravity-wise, camel milk is lighter than bovine milk (Mullaicharam 2014; Jilo and Tegegne 2016; Mohammadabadi and Faraz 2021; Saleena et al. 2022a; Saleena et al. 2022b). Table 1 provides the chemical makeup of camel milk compared to the milk of other ruminants and humans. Camel milk is distinct from the milk of other ruminants because it is low in protein, high in vitamin C, low in cholesterol, and high in minerals (sodium, potassium, iron, zinc, and magnesium) (Hailu et al. 2016; Sakandar et al. 2018; Bakry et al. 2021; Benmeziiane–Derradji 2021). Camel milk had far more trace minerals than cow's milk. Cow milk provides more vitamins A, E, and B1 than camel milk. Alpha-carotene is absent from camel milk. Camels produce two to three times more vitamin C than cows (Kumar et al. 2016; Muthukumaran et al. 2022; Seifu 2023).

3 Potential healthful and therapeutic benefits of camel milk

Camel milk affects human cuisine, medicine, and nutrition, as depicted in Figure 2.

3.1 Immune-boosting potential of camel milk

Studies have revealed that drinking camel milk can boost one's immune system. Serum from camels has a unique group of immunoglobulins structurally distinct from other types of antibodies (Hailu et al. 2016; Sakandar et al. 2018). The milk

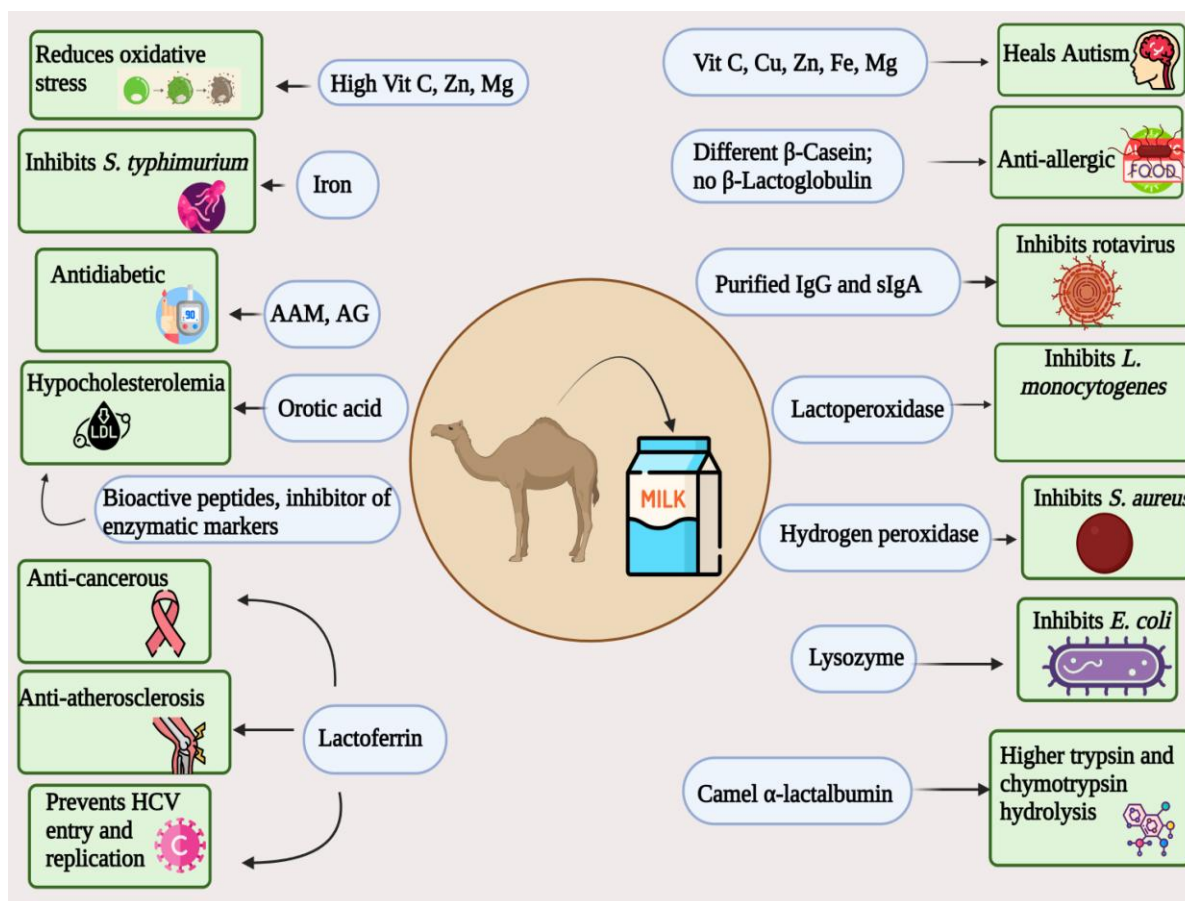


Figure 2 Camel milk has significant dietary, medicinal, and nutritional ramifications for humans
(Designed with Biorender premium software; <https://app.biorender.com/>)

proteins were shown to contain distinct structures, unlike those in cow or human milk, according to research by El-Agamy et al. (2009). In light of these findings, it may be important to account for the immunological differences between camel and cow's milk proteins when considering nutritional, physiological, and clinical considerations. As a result, when humans consume camel milk, the immune system will operate better. A stronger immune system means the human body will be healthier and less vulnerable to infection from bacteria and viruses. Immunoglobulins (Ig) unique to camels have been found in camel milk. These immunoglobulins have the same basic structure as their human counterparts but are just a tenth as large. So, unlike human immunoglobulins, these can identify and penetrate foreign illnesses, allowing the immune system to destroy them (Levy et al. 2013; Faraz 2020; Mohammadabadi and Faraz 2021; Seifu 2023).

Camel milk, compared to other types of milk, is richer in certain immune-boosting proteins. Camels' milk is rich in peptidoglycan recognition protein (PGRP). It has both antibacterial and immune-boosting properties for the host. Compared to lactoferrin found in cow's and goat's milk, camel's lactoferrin is more

bioactive (Zhao et al. 2015; Chandran and Radhakrishnan 2019; Chandran et al. 2020). Antimicrobial and anti-invasion properties are provided by lactoferrin. One component of the body's innate immunological defences is an enzyme known as lysozyme, which attacks explicitly gram-positive bacteria (Chandran and Radhakrishnan 2019; Sumaira et al. 2020; Patange et al. 2021a). Lactoperoxidase kills gram-negative bacteria like *Escherichia coli* and *Salmonella*. The antibacterial enzyme N-acetyl-beta-D-glucosamidase in human milk in roughly the same concentrations (Ahamad et al. 2017).

3.2 Anti-microbial potential of camel milk

Camels' milk contains antimicrobial compounds such as hydrogen peroxide, lysozyme, lactoperoxidase, lactoferrin, and immunoglobulins. *Listeria monocytogenes*, *Staphylococcus aureus*, *E. coli*, and *Salmonella typhimurium* are susceptible to camel milk's antibacterial properties (Solanki and Hati 2018; Mohammadabadi and Faraz 2021; Seifu 2023). One possible explanation for camel milk's antimicrobial properties is that it contains lactoperoxidase, hydrogen peroxide, and lysozyme.

Lactoferrin in camel milk suppressed *S. typhimurium* growth by binding iron and rendering it inaccessible to the bacteria (Mullaicharam 2014; Hailu et al. 2016; Ahamad et al. 2017; Chandran and Rahakrishnan 2019).

Rotaviruses cause most cases of non-bacterial gastroenteritis in newborns. Camel milk and colostrum were shown to have the highest anti-rotavirus activity. Raw camel milk appears to suppress human rotavirus. These results shed light on why camel herders have used camel milk as a treatment for diarrhea (Yasin et al. 2015). Elbarbary et al. (2014) revealed that camel and bovine whey proteins might be used to fight the virus. They also found goat milk has the second-best anti-rotaviral efficacy after desert camel milk whey proteins in treating rotavirus infection in mice. Shubat, a Kazakh fermented camel milk drink, inhibits orthomyxoviruses and paramyxoviruses (El-Fakharany et al. 2008). Shubat's antiviral properties may stem from the lactic acid bacteria and yeasts that contributed to its production and its metabolic by-products, including sialic conjugates (Faraz, 2020). Redwan and Tabll (2007) investigated whether or not camel milk proteins may prevent the hepatitis C virus (HCV) from entering and replicating inside cells. Camel lactoferrin blocked HCV entrance and replication in human peripheral blood mononuclear cells and human hepatoma HepG2 cell lines in vitro.

3.3 Anti-cancer potential of camel milk

Drinking a mixture of camel milk and camel pee (the "drinking cure") has been shown in multiple tests to prevent cancer growth. Successful single-dose testing in mice has prompted researchers to proceed with human studies. A high success rate in treating blood cancer (leukemia) was found. The medicine shows promise as a treatment for various cancers, including those of the lung, liver, and breast (Gul et al. 2015; Zhao et al. 2015; Mohammadabadi and Faraz 2021). Korashy et al. (2012) discovered that camel milk reduced HepG2 and MCF7 cell proliferation via oxidative stress-mediated mechanisms and death receptor stimulation. The extrinsic and intrinsic apoptotic pathways were activated by camel milk, which the researchers believe is responsible for reducing survival and proliferation in HepG2 and MCF7 cells. For the first time, camel milk lactoferrin was tested for its ability to prevent DNA damage, free radical generation, and HCT-116 cell growth in vitro.

3.4 Camel milk for diet and milk allergy

It has been documented by Shabo and Yagil (2005) that food allergies in children are frequently life-threatening and can cause anaphylactic reactions. Consumption of bovine milk and milk derivatives is particularly problematic for those sensitive to milk proteins. Anaphylaxis is a potentially fatal reaction brought on by some types of food allergies. Allergic reactions can be broken down into three broad categories. In the first category, symptoms,

including hives, facial swelling, and anaphylaxis, can appear as soon as 45 minutes after ingesting cow's milk. Symptoms like weakness, nausea, and diarrhea appear after 45 minutes to 20 hours with the second type. The third kind is delayed and includes reactions in the skin, lungs, and intestines. The life-threatening allergic reaction known as anaphylaxis can strike any system in the body (including the skin, respiratory system, digestive system, and cardiovascular system) and can spread quickly. Many children develop milk allergies because cow's milk contains beta-lactoglobulin and beta-casein, two potent allergens (Kumar et al. 2021; Muthukumaran et al. 2022).

Children with food allergies have been helped by drinking camel milk. Milk and dairy products are well-documented allergens (Zhao et al. 2015). There do not appear to be any immunological cross-reactions between the proteins in camel milk and bovine milk, as evidenced by research by El-Agamy et al. (2009). Restani et al. (1999) and El-Agamy et al. (2009) found that cow's milk-allergic children's IgE only unreacted with camel milk. This can be traced back to the underlying evolutionary distinctions between camels and ruminants.

Camel milk has the following qualities, which make its proteins very effective for preventing and treating food allergies. Camel milk lacks beta-lactoglobulin. Camel milk beta-casein is unusual. Like human breast milk, Camel milk includes immunoglobulins that reduce newborn allergic responses and promote food digestion (Restani et al. 2009; Solanki and Hati 2018; Kumar et al. 2021).

Shabo et al. (2005) examined how camel milk helped eight children with life-threatening reactions to other foods. For two weeks, the kids were fed nothing but camel milk. Within 24 hours of starting treatment, the youngsters would have shown considerable improvement, and within four days, all of their problems would have vanished. All eight cases improved immediately, and the youngsters could digest more meals (Faraz 2020). It is thought that the immunoglobulins in camel milk help alleviate allergy symptoms in kids. Kaskous (2009) found the same finding in his research. Thirty-five youngsters (23 boys and 12 girls) between the ages of 4 and 126 months were used. Camel milk treats food-allergic youngsters 80% of the time. Camel's milk works for kids with cow's milk allergies (Bakry et al. 2021; Benmeziene–Derradji 2021). The lack of immunological resemblance between camel and bovine milk proteins can be critical nutritional determinant for children allergic to cow milk, according to El-Agamy et al. (2009). The data suggests that more research is needed to confirm that camel milk helps treat allergies.

3.5 Potential of camel milk against gastro-intestinal disorders

Camel milk's abundant anti-inflammatory proteins have been proven to help with stomach pain. As a result of its vitamin-rich and mono-

and polyunsaturated fatty acid-rich makeup, glucose metabolism is enhanced. Further research revealed that the protein in fermented camel milk is more accessible to break down due to the abundance of Angiotensin I-converting enzyme (ACE) (Solanki and Hati 2018). There have been recent studies on the benefits of camel milk for the digestive system, and the results have shown that even youngsters who experience 20 episodes of diarrhea per day can be treated by drinking camel milk. Since camel milk is high in antibodies that combat rotavirus, it can be given to young infants who have developed diarrhea due to eating contaminated food (Sumaira et al. 2020; Muthukumaran et al. 2022).

3.6 Anti-aging potential of camel milk

Camel milk produces antioxidant and ACE-inhibiting peptides, according to Jilo and Tegegne (2016). Camel milk's strong vitamin C content maintains collagen, which fights ageing. Camel milk's vitamin C content gives it anti-inflammatory and tissue-protective properties. Vitamin C is a powerful antioxidant and vital water-soluble vitamin. Vitamin C is needed to build collagen, providing skin with suppleness and strength. Collagen is a protein that aids in the maintenance of healthy skin, cartilage, and joints (Salami et al. 2011; Sakandar et al. 2018). Repair is aided by vitamin C because it increases the skin's structural support and resilience. Antioxidant vitamin C helps prevent premature ageing and skin dryness caused by free radicals. Furthermore, lactoferrin, a protein capable of chelating iron, is more abundant in camel milk. People with Arthritis see improvement due to this protein's ability to clear excess free iron from their joints (Mihic et al. 2016; Bakry et al. 2021). Alpha-lactalbumin and beta-casein in camel milk suppress or slow the generation of reactive oxygen species, peroxy and hydroxyl radicals, superoxide anions and nitric oxide (Behrouz et al. 2022).

3.7 Potential of camel milk against autoimmune disorders

In autoimmune illnesses, B lymphocytes produce antibodies that wrongly target self-antigens (tissues of the body) rather than foreign antigens. There are times when these autoantibodies can cause tissue damage or dysfunction. The symptoms of autoimmune disorders might vary widely. For instance, in multiple sclerosis, the immune system attacks the brain; Crohn's disease attacks the digestive system. However, in other disorders like systemic lupus erythematosus (SLE), different organs and tissues may be afflicted in different people. Although a person with an autoimmune disease may appear to be in good health, they will likely need ongoing treatment and monitoring for the rest of their lives. Few autoimmune illnesses can be treated or "eliminated" with therapy at present. With the proper treatment, many patients with these disorders can lead normal lives (Roda et al. 2020).

Camel milk has been shown through years of study to be effective in managing and in some cases curing autoimmune disorders.

Camel milk's ability to effectively manage autoimmune illnesses is grounded in its multiple therapeutic benefits (Faraz 2020; Benmeziiane–Derradji 2021). It has been reported by El-Agamy et al. (2009) that tiny immunoglobulins can be transferred from camel milk into human blood due to the camel's superior immune system. Due to the presence of immunoglobulins in camel milk throughout lactation, it can be used as an effective aid in the fight against autoimmune illnesses and the resulting sadness. Due to their diminutive size, camel immunoglobulins are readily available in camel milk to treat autoimmune disorders (Sumaira et al. 2020). In contrast to other mammals, camels have an incredible immune system, as Faraz (2020) detailed. Human antibodies fall into five categories: IgG, IgM, IgA, IgD, and IgE. Monomers, the smallest possible form of an antibody, take the shape of a "Y," and include IgG, IgD, and IgE. IgM is a pentamer, while IgA is a dimer. Two heavy chains and two light chains make up a monomer's total number of four glycoprotein chains. Immunoglobulins are large molecules that have trouble penetrating antigens. On the other hand, Camel immunoglobulins are small and lack short chains, making them effective against antigens (Mihic et al. 2016; Solanki and Hati 2018; Sumaira et al. 2020; Benmeziiane–Derradji 2021).

According to Muyldermans et al. (2001), the size of the antibodies represents a pivotal setback in advancing human immunotherapy. Antibodies with a larger size will miss their mark. Antibodies in camels are a tenth the size of those in humans (natural nanobodies). Camel milk immunoglobulins can access and interact with active sites, allowing them to penetrate dense tissues in search of antigens because of their minimal complexity, high affinity, and specificity. The most important consideration is that standard treatments for autoimmune illnesses rely on suppressing the immune system, whereas camel milk immunoglobulins stimulate the immune system and restore its health (Faraz 2020).

3.8 Anti-diabetic potential of camel milk

The use of camel milk in the treatment of diabetes has been documented. The metabolic disorder known as diabetes mellitus leads to elevated blood sugar levels. Type 1 diabetes develops when the body stops producing enough insulin. The beta cells are responsible for making insulin die off in the pancreas. Classical insulin-deficient diabetes typically appears in early infancy or adolescence (Shori 2015; Benmeziiane–Derradji 2021). Some scientists have hypothesized that the autoimmune death of human Langerhans islets cells, and consequently Type-1 diabetes, was started by a cross-reaction with cow's milk proteins. Research on diabetic rats also shows that after 30 days of drinking camel milk, the animals' blood sugar levels return to normal, while research on diabetic rabbits shows that camel milk is more successful than solitary insulin treatment and prevents the produced oxidative stress. Alloxan-induced diabetic dogs had a similar outcome (Levy et al. 2013; Yassin et al. 2015).

El-Sayed et al. (2011) observed that camel milk significantly reduced insulin needs. After 12 weeks of treatment, daily insulin doses can be reduced by as much as 66% (20 units/day), according to a study of 50 patients with Type 1 diabetes conducted in Yemen. The study's authors attribute these results to camel milk and insulin. This research has also demonstrated that camel milk helps diabetic rats' kidneys and liver.

Compared to bovine milk, camels' milk has significantly higher amounts of insulin (58.67±2.01 UL vs 17.01±0.96 UL) plus insulin-like growth factor-I (which is not degraded in the stomach) than cow's milk. Only camel milk makes it through the stomach acid and into the small intestine, where it can be absorbed. When given orally to diabetic individuals, insulin is typically ineffective. However, camel milk may provide an exception (Muthukumaran et al. 2022). Camel milk insulin has a unique feature that facilitates its uptake into circulation and reduces resistance to proteolysis, making it a superior alternative to insulin from other sources. Nanoparticles (lipid vesicles) enclosing camel insulin facilitate its absorption by the body and subsequent distribution (Sumaira et al. 2020). Camel milk's ability to fight diabetes stems from its non-fatal extra nutrients. Camel insulin can discriminate and circumvent mucosal barriers on its way to the bloodstream; however, this is not reflected in its sequencing or predicted digestion pattern (Al Kanhal 2010; Kumar et al. 2016).

The beta cells in the pancreas can benefit from camel milk's insulin-like action, regulatory, and immunomodulatory properties (Sumaira et al. 2020). Camel milk reduces insulin demand, blood glucose levels, diabetic sequelae like liver and renal illness, high cholesterol, low oxidative stress, and slow wound healing, according to Shori (2015). It appears that more research on the efficacy of camel milk as a diabetes treatment is required. Consumption of camel milk has shown positive effects in tests of people with lactose intolerance, and 23 out of 25 patients reported a positive reaction to the beverage. Hence, those who have a lactose intolerance should know that camel milk is a possibility (Mihic et al. 2016; Solanki and Hati 2018).

Patients with lactose intolerance may find camel milk easy to digest, as stated by Mullaicharam (2014). Camel milk has a higher percentage of the amino acid L-Lactate than cow milk, which is rich in the fatty acid D-Lactate, which may explain why camel milk consumption leads to a decreased incidence of lactose intolerance.

3.9 Inhibiting effect of camel milk on angiotensin I-converting enzyme

Many dietary proteins, including milk proteins, include blood pressure-lowering ACE-inhibitory peptides. Also present in fermented camel milk are the peptides as mentioned above. Probiotic bacteria's ability to hydrolyze milk protein components

has been shown to increase the number of peptides and free amino acids, both of which are required to develop probiotic bacteria (Bakry et al. 2021). ACE-inhibitory peptides in camel milk have been isolated using *Lactobacillus helveticus* 130B4, and the sequence is documented to be Ala-Ile-Pro-Pro-Lys-Lys-Asn-Gln-Asp (Abrahaley and Leta 2018; Benmezziane–Derradji 2021; Muthukumaran et al. 2022).

3.10 Defending against hepatitis C and B using camel milk

There is currently no cure for the hepatitis C virus (HCV), despite its widespread distribution. Egyptian patients frequently rely on traditional treatments, such as lactoferrin protein-rich camel milk, to treat their illnesses (Redwan and Tabll 2007). In place of the primary biotechnology treatment used to treat HCV infection, camel milk has taken place because of its slightly higher lactoferrin concentrations. Camel milk IgGs recognized HCV peptides with a substantial titer, unlike human IgGs, which did not. Independent researchers corroborated this. In addition, camel milk boosts the cellular immune response in chronic hepatitis B patients, which inhibits viral DNA replication and supports healing (Abrahaley and Leta 2018; Ibrahim et al. 2018; Bakry et al. 2021).

3.11 Blood cholesterol-lowering effects of camel milk

Blood cholesterol levels are considered a key risk factor for cardiovascular disease. Research in mice shows that lowering cholesterol levels is one of the side effects of consuming fermented camel milk. Although the exact mechanism by which camel milk reduces cholesterol levels in rats and humans is unknown, several hypotheses have been proposed. Orotic acid, a nucleic acid intermediary, and bioactive peptides from camel milk decrease cholesterol (Abrahaley and Leta 2018; Benmezziane–Derradji 2021; Bakry et al. 2021). The cholesterol levels of obese male Wistar rats were dramatically reduced when fed camel milk fermented with red quinoa flour (Al-Anazi et al. 2022).

3.12 Camel milk against heavy metal toxicity

Camel milk's antioxidant vitamins, magnesium, and zinc may lessen cadmium's effects on red blood cells by reducing free radicals and oxidative stress. Total erythrocytes, haemoglobin, and haematocrit increased following 30 days of camel milk consumption, mitigating aluminum's adverse effects. In lead acetate-poisoned rats, camel milk restored hepatic enzyme function (Hailu et al. 2016; Ahamad et al. 2017; Abrahaley and Leta 2018). Camel milk protects male albino rats from lead acetate and fipronil's hepatotoxic and nephrotoxic effects (Abdel-Mobdy et al. 2023). Al-Asmari et al. (2017) observed that camel milk reduced oxidative stress and inflammation to protect and regenerate hepatocyte membranes. After radiation exposure, camel milk improved rats' liver function, alanine, aspartate, and glutathione levels.

3.13 Cosmetic values of camel milk and its application in skin disease treatment

The presence of alpha-hydroxyl acids in camel milk gives it a cosmetic effect, making it great for reducing the appearance of wrinkles and fine lines. By dissolving carbohydrates, which are typically employed to bind skin cells together, alpha-hydroxyl acids facilitate the removal of the horny, dead skin layer (epidermis). New, more pliable and transparent cells can be revealed with this method. As alpha-hydroxyl acids reduce the thickness of the skin's outermost layer—the epidermis—while simultaneously increasing the thickness of the skin's thicker, deeper layer—the dermis—they help get rid of wrinkles, age spots, and dry skin. It has also been found that the liposomes found in camel milk can be used as a possible anti-ageing cosmetic ingredient (Hailu et al. 2016; Mihic et al. 2016). Essential vitamins and minerals for skin health are found in the component. Lanolin and other emollients in milk relax and soothe the skin, treating acne, psoriasis, eczema and dermatitis and preserving a healthy and appealing appearance. In addition, the alpha-hydroxyl acids found in camel milk help soften the skin, keep it supple and smooth, and even work to reduce the appearance of fine lines and wrinkles (Khalesi et al. 2017).

An experiment using 40% raw camel milk for topical application yielded good results. Camel milk crème was applied twice daily for four weeks to 20 patients (10 men and 10 women) with mild to moderate psoriasis. The patients' ages ranged from 6 to 72 years. Those affected felt cooler and experienced less itching and pain. There was a notable improvement in the skin's redness and dryness (Yadav et al. 2015).

3.14 Camel milk for tuberculosis sufferers

Mycobacterium, typically *Mycobacterium tuberculosis*, is the causative agent in most tuberculosis cases. People with low incomes are disproportionately affected by tuberculosis, a chronic disease that causes severe weight loss. A person infected with tuberculosis bacillus is at a higher risk of contracting other diseases because the bacillus weakens the body's immune defence mechanism (Gul et al. 2015). World Health Organization (WHO) estimates that between 16 and 20 million people worldwide have tuberculosis, with an additional 7 million to 8 million new cases diagnosed yearly (Mohammadabadi and Faraz 2021).

Mycobacterium bacteria may develop resistance to therapy if the patient does not take their medication as directed. Due to this, the medicine is no longer effective against the bacterium. Multidrug-resistant tuberculosis (MDR-TB) describes cases in which the germs have developed resistance to multiple anti-tuberculosis medications. Multidrug-resistant tuberculosis is rising as an endemic infection in developing and developed nations. There is

an immediate need for novel methods of identifying and treating tuberculosis patients, as the disease has emerged as a major threat to public health (Mohammadabadi and Faraz 2021; Muthukumaran et al. 2022).

Indian researchers have shown that individuals with MDR-TB who consume camel milk show statistically and clinically substantial improvements in their symptom observed values. As a result, in the experimental group, camel milk was given as a dietary supplement to each participant at a rate of 1 litre per day. No more coughing, sputtering, or chest pain was experienced. The group given camel milk as a supplement reported greater hunger and weight gain. Improvements in patients who drank more camel milk have not yet been studied to determine if and how they will persist (Yadav et al. 2015; Yassin et al. 2015).

Alwan and Farhuni (2000) reported that camel milk effectively treats TB, especially in patients with MDR-TB. Mal et al. (2000) examined camel milk's multidrug resistance benefits. Fourteen male patients with tuberculosis for an average of seven years without therapy were split into two groups, T1 and T0, with eight and six patients, respectively. At 1 kg per day, raw camel milk was added to the diets of the T1 patients, while dairy milk was provided to the T0 patients for a full ten weeks. Both groups were fed regularly and were given essentially identical care. Clinical signs and symptoms, bacterial counts, radiographic images, hemoglobin levels, immunoglobulin titers, results of the mantoux test, and body weight were documented before and after the trial. The experiment concluded that camel milk supplementation was beneficial for tuberculosis patients. According to research by Mal et al. (2000), camel milk may help boost the immune system since it includes protective proteins. Camel milk proteins have antimicrobial characteristics that kill the *Mycobacterium* bacteria that cause tuberculosis (Bakry et al. 2021).

3.15 Anti-autism benefits of camel milk

The opioid peptides are blamed for supporting autism. The pathophysiology of autism may involve an overabundance of endogenous or exogenous opioid peptides, such as those produced from dietary (cow's milk) proteins. Some patients have an insufficient intestinal metabolization of casein proteins. Therefore, casein-derived short neuroactive peptides like beta-casomorphins are generated. Beta-casomorphin has been suspected of being an autistic risk factor (Hailu et al. 2016; Ahamad et al. 2017).

As an immunological disorder, autism typically affects the digestive tract rather than the brain. Intestinal responses start with diarrhea and a loss of appetite. Camel milk has been shown to have a therapeutic impact on autism because it lacks the two caseins found in cow milk linked to autistic symptoms (Ismail et al. 2022). Shabo and Yagil (2005) and Yagil (2013) found that camel milk

was effective in treating autism in the following situations: After 40 days of consuming camel milk, the autistic symptoms of a 4-year-old girl completely vanished; A 30-day course of camel milk therapy cured autism in a boy aged 15; Those aged 21 were found to be calmer and less destructive after drinking camel milk for two weeks in a facility for autistic youngsters. Children under 10 years reaped the most significant benefits, while those aged 15 and up also saw significant improvements.

In terms of the outcomes observed, camel milk considerably enhanced clinical measures of autism severity. Al-Ayadhi and Elamin's (2013) study on the impact of camel milk on oxidative stress in autistic children provided conclusive evidence that milk has a significant role in improving the behaviour of autistic children by decreasing oxidative stress. Wernery et al. (2012) found similar benefits for autistic children after giving them camel milk, including improved social functioning, reduced hyperactivity, increased alertness, and regular bowel routines.

3.16 Treatment for Crohn's disease using camel milk

Crohn's disease, often called Crohn syndrome or regional enteritis, is an inflammatory bowel illness that can manifest in a broad range of ways throughout the gastrointestinal tract, from the mouth to the genitourinary system. However, it can also create issues outside the digestive system, such as fatigue, arthritis, eye inflammation, skin rashes, and lack of attention, in addition to the usual symptoms of abdominal discomfort, diarrhoea, vomiting, or weight loss. Crohn's disease develops in those genetically predisposed to it due to an interplay between environmental, immunological, and bacterial factors. A chronic inflammatory condition develops as a result, with the immune system mistakenly attacking the gastrointestinal tract in response to microbial antigens.

Mycobacterium avium subspecies paratuberculosis (MAP) is transmitted through cow milk and is resistant to pasteurization. An autoimmune reaction occurs once MAP penetrates the mucosa as saprophytes and becomes active only when the host is under extreme stress. Crohn's disease is incurable, and even remission may not be sustainable. In cases where remission is achievable, medicines, lifestyle and nutritional adjustments, changes in eating patterns (eating smaller quantities more often), stress reduction, moderate activity, and exercise can be used to avoid relapse and manage symptoms (Ibrahim et al. 2018; Benmeziiane–Derradji 2021; Muthukumar et al. 2022). According to Shabo et al. (2008), camel milk is an excellent treatment for Crohn's disease. Camel milk's potent bactericidal properties combined with peptidoglycan recognition protein (PGRP) have a rapid and beneficial effect on the healing process because this bacterium is in the family that causes tuberculosis. Immunoglobulins can restore the immune system to normalcy (Hailu et al. 2016; Sakandar et al. 2018).

4 Functionality of camel milk's bioactive peptides

Short protein fragments (2-30 amino acids) having biological activity can be formed naturally by digestion or manufactured in the lab by food processing, fermentation, or enzymatic hydrolysis. Milk proteins may provide bioactive peptides for food preservation and wellness. These peptides have antioxidant, angiotensin-converting enzyme-inhibiting, antithrombotic, antibacterial, immunomodulatory, ion-binding, and opioid-antagonist properties (Al Kanhal 2010; Ibrahim et al. 2018; Benmeziiane–Derradji 2021). Kumar et al. (2016) looked into the digestion of camel beta-lactalbumin with enzymes and its antioxidant properties. Camel alpha-lactalbumin is more susceptible to hydrolysis by trypsin and chymotrypsin but less so by pepsin than bovine alpha-lactalbumin. Due to their different structures and amino acid sequences, camel alpha-lactalbumin and bovine alpha-lactalbumin had different levels of antioxidant activity (Salami et al. 2011; Mullaicharam 2014; Hailu et al. 2016). Khalesi et al. (2017) found that digestive enzymes boosted camel whole casein and beta-casein's antioxidant and ACE-inhibitory effects. Hydrolysis with pepsin alone, as well as pepsin followed by trypsinolysis and chymotrypsinolysis, revealed strong ACE-inhibitory actions in both camel whole casein and beta-casein. Hydrolysis of camel beta-casein with chymotrypsin revealed strong antioxidant action (Ibrahim et al. 2018).

Jrad et al. (2014a) and Jrad et al. (2014b) examined how sequential in vitro hydrolysis by pepsin and pancreatin affected camel milk casein's free radical-scavenging activity. They found that the casein peptides outperformed other scavengers. Peptide fractions from fermented bovine and camel milk were investigated for ACE-inhibitory and antioxidant activities. Camels produce more ACE-inhibiting and antioxidant milk than cows. The 5–10 kDa peptide fractions are the best radical scavengers in fermented milk. TEAC values for 5-10 kDa peptides in fermented bovine and camel milk were 110.41–745.35 M and 844.08–1737.88 M, respectively.

5 Availability of camel milk

Before going on the markets in Gulf countries, this camel milk undergoes a 15-second pasteurization process at 74°C. According to Dubai municipal regulations, pasteurized camel milk's shelf life is limited to 5 days. Pasteurized camel milk has been demonstrated to keep well in the lab for up to 15 days when refrigerated. Milk (produced by Natural Product Company) and milk powder (from camel milk) are two of the camel-related products sold in the Indian market by Sara International company (Yadav et al. 2015; Ismail et al. 2022). Several components in camel milk were shown to be more heat resistant than those in cow milk, as shown by research by Wernery (2006). When heated from room temperature to 72°C for 5 minutes, the value of many vitamins and hormones in raw milk was reduced by only 5 to 8%. One possible way to tell if camel milk has been pasteurized is to test it for the gamma-

glutamyl transaminase (GGT) enzyme. Camel milk retains its alkaline phosphatase (ALP) indicator enzyme, whereas cow milk's ALP is destroyed at 72°C during pasteurization. According to Wernery (2006), GGT is eliminated in camel milk between 10 and 20 minutes after being heated to 72°C, making it an ideal heat inactivation component.

6 Challenges and opportunities

Considering escalating issues like climate change and shortage of food, the sustainable food sector that produces nutritious camel milk with multiple health benefits may turn out to be a meal of the future. While camel milk output has increased, only a small fraction of the milk produced is consumed (Mullaicharam 2014; Hailu et al. 2016). Recent research has looked at the challenges the technology presents to turn it into various items with monetary worth (Ismail et al. 2022; Muthukumar et al. 2022). To improve upon the current technologies, based on the processing of bovine milk solely, extensive research into the basic chemical makeup of the components of camel milk is required. More study into processing and preservation methods for camel milk is warranted to increase its global availability and acceptance. Further research into the chemistry of camel milk proteins and the modifications those proteins undergo as a result of various processing methods is, without a doubt, warranted. These alterations greatly aid the development of new camel milk products (Sumaira et al. 2020). Camel milk is an underutilized dairy supply, and the food industry may take advantage of this by processing it so that people can enjoy the health advantages. Sustainable camel milk production and strategies for preserving and diversifying processed camel milk products are also required for products generated from camel milk to be competitive in international markets. Camel milk has been praised for its purported health benefits, but further studies are needed to support these claims. This proof can help the food and pharmaceutical industries see the potential of camel milk for creating new functional and nutraceutical products (Muthukumar et al. 2022).

Conclusions

Regarding both macro- and micronutrient content, camel milk is an excellent food choice. Camel milk's chemistry shifts with the lactation cycle, the camel's breed, and the time of year. The unique chemical composition of camel milk limits its adaptability and reduces its organoleptic appeal. Fermentation, in particular, appears to be a practical and generally accepted method for transforming camel milk into a valuable product. Antimicrobial properties in camel milk and its by-products may be due to lysozyme and lactoferrin, two milk components, and a large diversity of beneficial microorganisms. Bioactive peptides are thought to be responsible for the anti-diabetic properties of camel milk. Several enzymatic markers are inhibited in *in-vitro*

experiments, and *in-vivo* research has identified other processes implicated in camel milk's antidiabetic characteristics. Researchers have shown that the proteins in camel milk have anticancer properties (whey, lactoferrin and casein). More comprehensive research into camel's therapeutic potential is required to substantiate the growing interest in the animal.

Given the abundance of bioactive compounds found in camel milk, it is used in treating various severe ailments in various regions of the world. Camel milk has been used to cure different conditions, including gastrointestinal illnesses, hepatitis B and C, diabetes, autism, psoriasis, food allergies, high blood cholesterol, immune system boosting, cancer, tuberculosis, etc. There has been a recent uptick in the number of peer-reviewed studies emphasizing the unique healing properties of camel milk. The biological elements in camel milk can even help the patient, but only if it is ingested raw and without any pathogens shortly after it has been produced. It is possible that this milk will also be made available following a thorough machine milking.

Camel milk and other camel products are a healthy food option for persons living in dry or semiarid climates. Camel milk output has risen recently and is associated with increasing consumer demand. Camel milk has been found to have various unique qualities that set it apart from milk from other animals, such as bovine milk. According to certain investigations, the health benefits associated with drinking either fresh or fermented camel milk may differ depending on the presence or absence of bioactive components. More studies are needed to confirm these purported health advantages of camel milk and boost its popularity.

Acknowledgement

All the authors acknowledge and thank their respective Institutes and Universities.

Author's contribution

All the authors contributed significantly.

Funding

This is a compilation written by its authors and required no substantial funding to be stated.

Disclosure statement

All authors declare that there exist no commercial or financial relationships that could, in any way, lead to a potential conflict of interest.

References

Abdel-Mobdy, Y.E., Abdel-Mobdy, A.E., & Al-Farga, A. (2023). Evaluation of therapeutic effects of camel milk against the

- hepatotoxicity and nephrotoxicity induced by fipronil and lead acetate and their mixture. *Environmental Science and Pollution Research International*, 30(15), 44746-44755. <https://doi.org/10.1007/s11356-022-25092-0>
- Abrhaley, A., & Leta, S. (2018). Medicinal value of camel milk and meat. *Journal of Applied Animal Research*, 46(1), 552-558. <https://doi.org/10.1080/09712119.2017.1357562>
- Ahamad, S.R., Raish, M., Ahmad, A., & Shakeel, F. (2017). Potential health benefits and metabolomics of camel milk by GC-MS and ICP-MS. *Biological Trace Element Research*, 175, 322-330. <https://doi.org/10.1007/s12011-016-0771-7>
- Al Kanhal, H.A. (2010). Compositional, technological and nutritional aspects of dromedary camel milk. *International Dairy Journal*, 20(12), 811-821.
- Al-Anazi, M.S., El-Zahar, K.M., & Rabie, N.A. (2022). Nutritional and therapeutic properties of fermented camel milk fortified with red *Chenopodium quinoa* flour on hypercholesterolemia rats. *Molecules*, 27(22), 7695. <https://doi.org/10.3390/molecules27227695>
- Al-Asmari, A.K., Abbasmanthiri, R., Al-Elawi, A.M., Al-Horaib, G., Al-Sadoon, K., & Al-Asmari, B.A. (2017). Effect of camel milk against renal toxicity in experimental rats. *Pakistan Journal of Pharmaceutical Sciences*, 30. <https://doi.org/10.1155/2014/917608>
- Al-Ayadhi, L. Y., & Elamin, N. E. (2013). Camel Milk as a Potential Therapy as an Antioxidant in Autism Spectrum Disorder (ASD). *Evidence-based complementary and alternative medicine : eCAM*, 2013, 602834. <https://doi.org/10.1155/2013/602834>
- Alwan, A.A. and Farhuni, A.H., 2000. The effect of camel milk on Mycobacterium tuberculosis in man. In: 2nd International Camelid Conference: Agro-economics of Camelid Farming, Almaty, September, pp.100
- Bakry, I.A., Yang, L., Farag, M.A., Korma, S.A., Khalifa, I., Cacciotti, I., Ziedan, N.I., Jin, J., Jin, Q., Wei, W., & Wang, X. (2021). A comprehensive review of the composition, nutritional value, and functional properties of camel milk fat. *Foods*, 10(9), 2158. <https://doi.org/10.3390/foods10092158>
- Behrouz, S., Saadat, S., Memarzia, A., Sarir, H., Folkerts, G., & Boskabady, M.H. (2022). The antioxidant, anti-inflammatory and immunomodulatory effects of camel milk. *Frontiers in Immunology*, 13, 855342. <https://doi.org/10.3389/fimmu.2022.855342>
- Benmezziane–Derradji, F. (2021). Evaluation of camel milk: gross composition—a scientific overview. *Tropical Animal Health and Production*, 53(2), 308. <https://doi.org/10.1007/s11250-021-02689-0>
- Chandran, D., & Radhakrishnan, U. (2019). Lactoferrin: A General Review. *International Journal of Pharmaceutical Sciences Review and Research*, 58(2), 65-75.
- Chandran, D., Lejaniya, A.S., Yatoo, M.I., Mohapatra, R.K., & Dhama, K. (2021). Major health effects of casein and whey proteins present in cow Milk: A narrative review. *The Indian Veterinary Journal*, 98(11), 9-19.
- Chandran, D., Radhakrishnan, U., & Eldho, L. (2020). Characterization of Malabari goat lactoferrin and its pepsin hydrolysate. *Journal of Veterinary and Animal Sciences*, 51(1), 40-47.
- El-Agamy, E.I., Nawar, M., Shamsia, S.M., Awad, S., & Haenlein, G.F. (2009). Are camel milk proteins convenient to the nutrition of cow milk allergic children?. *Small Ruminant Research*, 82(1), 1-6. <https://doi.org/10.1016/j.smallrumres.2008.12.016>
- Elbarbary, H.A., El-Nahas, E.M., & Karam-Allah, E.L. (2014). Anti-rotaviral activity of whey proteins derived from milk of different animal species. *International Journal of Advanced Research*, 2(4), 214-21.
- El-Fakharany, E., Tabll, A., Wahab, A., Haroun, B., & Redwan, E.R. (2008). Potential activity of camel milk-amylase and lactoferrin against hepatitis C virus infectivity in HepG2 and lymphocytes. *Hepatitis Mon*, 8(2), 101-109.
- El-Sayed, M.K., Al-Shoeibi, Z.Y., El-Ghany, A.A.A., & Atef, Z.A. (2011). Effects of camels milk as a vehicle for insulin on glycaemic control and lipid profile in Type 1 diabetics. *American Journal of Biochemistry & Biotechnology*, 7(4), 179-89.
- Faraz, A. (2020). Composition of camel milk: a blessing for health. *Annals of Public Health & Epidemiology*, 1, 1-4.
- Gul, W., Farooq, N., Anees, D., Khan, U., & Rehan, F. (2015). Camel milk: a boon to mankind. *International Journal of Research Studies Biosciences*, 3, 23-29.
- Hailu, Y., Hansen, E.B., Seifu, E., Eshetu, M., Ipsen, R., & Kappeler, S. (2016). Functional and technological properties of camel milk proteins: A review. *Journal of Dairy Research*, 83(4), 422-429.
- Ho, T.M., Zou, Z., & Bansal, N. (2022). Camel milk: A review of its nutritional value, heat stability, and potential food products. *Food Research International*, 153, 110870. <https://doi.org/10.1016/j.foodres.2021.110870>
- Ibrahim, H.R., Isono, H., & Miyata, T. (2018). Potential antioxidant bioactive peptides from camel milk proteins. *Animal Nutrition*, 4(3), 273-280. <https://doi.org/10.1016/j.aninu.2018.05.004>

- Ismail, L.C., Osaili, T.M., Mohamad, M.N., Zakaria, H., Ali, A., Tarek, A., Ashfaq, A., Al Abdouli, M.A., Saleh, S.T., Al Daour, R., & AlRajaby, R. (2022). Camel milk consumption patterns and perceptions in the UAE: A cross-sectional study. *Journal of Nutritional Science*, *11*, 59.
- Jilo, K., & Tegegne, D. (2016). Chemical composition and medicinal values of camel milk. *International Journal of Research Studies in Biosciences*, *4*(4), 13-25.
- Jrad, Z., El Hatmi, H., Adt, I., Girardet, J.M., Cakir-Kiefer, C., Jardin, J., Degraeve, P., Khorchani, T., & Oulahal, N., (2014a). Effect of digestive enzymes on antimicrobial, radical scavenging, and angiotensin I-converting enzyme inhibitory activities of camel colostrum and milk proteins. *Dairy Science & Technology*, *94*, 205-224. <https://doi.org/10.1007/s13594-013-0154-1>
- Jrad, Z., Girardet, J.M., Adt, I., Oulahal, N., Degraeve, P., Khorchani, T., & El Hatmi, H., (2014b). Antioxidant activity of camel milk casein before and after in vitro simulated enzymatic digestion. *Mljekarstvo: časopis za unaprjeđenje proizvodnje i prerade mlijeka*, *64*(4), 287-294. <https://doi.org/10.15567/mljekarstvo.2014.0408>.
- Kaskous, S. (2016). Importance of camel milk for human health. *Emirates Journal of Food and Agriculture*, 158-163. <https://doi.org/10.9755/ejfa.2015-05-296>
- Khalesi, M., Salami, M., Moslehishad, M., Winterburn, J., & Moosavi-Movahedi, A.A. (2017). Biomolecular content of camel milk: A traditional superfood towards future healthcare industry. *Trends in Food Science & Technology*, *62*, 49-58. <https://doi.org/10.1016/j.tifs.2017.02.004>
- Konuspayeva, G., Lemarie, É., Faye, B., Loiseau, G., & Montet, D. (2008). Fatty acid and cholesterol composition of camel's (*Camelus bactrianus*, *Camelus dromedarius* and hybrids) milk in Kazakhstan. *Dairy Science and Technology*, *88*(3), 327-340. <https://doi.org/10.1051/dst:2008005>
- Korashy, H.M., Maayah, Z.H., Abd-Allah, A.R., El-Kadi, A.O., & Alhaider, A.A. (2012). Camel milk triggers apoptotic signaling pathways in human hepatoma HepG2 and breast cancer MCF7 cell lines through transcriptional mechanism. *Journal of Biomedicine and Biotechnology*. <https://doi.org/10.1155/2012/593195>
- Krishnan, D., M R, A., P R, A., M, P., Nainu, F., S V, P., Singh, P., Chopra, H., Chakraborty, S., Dey, A., Dhama, K., & Chandran, D. (2023). Beneficial impacts of goat milk on the nutritional status and general well-being of human beings: Anecdotal evidence. *Journal of Experimental Biology and Agricultural Sciences*, *11*(1), 1–15. [https://doi.org/10.18006/2023.11\(1\).1.15](https://doi.org/10.18006/2023.11(1).1.15)
- Kula, J. (2016). Medicinal values of camel milk. *International Journal of Veterinary Science & Research*, *2*(1), 18-25.
- Kumar, D., Verma, A.K., Chatli, M.K., Singh, R., Kumar, P., Mehta, N., & Malav, O.P. (2016). Camel milk: alternative milk for human consumption and its health benefits. *Nutrition & Food Science*, *46*(2), 217-227.
- Kumar, K.S., Chandran, D., Yattoo, M.I., Mohapatra, R.K., & Dhama, K. (2021). Major health effects of casein and whey proteins present in cow milk: A narrative review. *Indian Veterinary Journal*, *98*(11), 9-19.
- Lejaniya, A.S., Chandran, D., & Geetha, R. (2021b). Recent trends in application of lactic acid bacteria (LAB) in dairy and biomedical industry: A critical review. *World Journal of Pharmaceutical Research*, *10*(12), 577-591. doi: 10.20959/wjpr202112-21749.
- Lejaniya, A.S., Chandran, D., Venkatachalapathy, T., Bashir, B.P., Kumar, M., Shanavas, A., Sureshkumar, R., Kumar, P.N., Sabareeshwari, V., Kumar, K.K., & Mohankumar, P. (2021a). Analysis of milk production performance of Attappadi Black, Malabari and cross-bred goats under organized farm conditions of Kerala. *The Indian Veterinary Journal*, *98*(05), 13-19.
- Levy, A., Steiner, L., & Yagil, R. (2013). Camel milk: disease control and dietary laws. *Journal of Health Science*, *1*(1), 48-53.
- Mal, G., Suchitra Sena, D., Jain, V.K., Singhvi, N.M., & Sahani, M.S. (2000). Role of camel milk as an adjuvant nutritional supplement in human tuberculosis patients. *Liver International*, *4*(4), 7-14.
- Mihic, T., Rainkie, D., Wilby, K. J., & Pawluk, S. A. (2016). The Therapeutic Effects of Camel Milk: A Systematic Review of Animal and Human Trials. *Journal of evidence-based complementary & alternative medicine*, *21*(4), NP110–NP126. <https://doi.org/10.1177/2156587216658846>
- Mohammadabadi, T., & Faraz, A. (2021) Camel milk and natural health. *International Journal of Camel Science*, *3*, 61-65.
- Mullaicharam, A. R. (2014) A review on medicinal properties of camel milk. *World Journal of Pharmaceutical Sciences*, 237-242.
- Muthukumar, M.S., Mudgil, P., Baba, W.N., Ayoub, M.A., & Maqsood, S. (2022) A comprehensive review on health benefits, nutritional composition and processed products of camel milk. *Food Reviews International*, 1-37. <https://doi.org/10.1080/87559129.2021.2008953>
- Muyldermans, S., Cambillau, C., & Wyns L. (2001) Recognition of antigens by single-domain antibody fragments: the superfluous

- luxury of paired domains. *Trends in Biochemical Sciences*, 26(4), 230-235. [https://doi.org/10.1016/S0968-0004\(01\)01790-X](https://doi.org/10.1016/S0968-0004(01)01790-X)
- Patange, D.D., Pansare, K.S., Kumar, M., Kumari, A., Kamble, D.K., Chandran, D., Gaikwad, N.B., Waghmare, R., & Lorenzo, J.M. (2022b). Studies on utilization and shelf life of *Piper betel* leaves added ghee-based low-fat spread. *Food Analytical Methods*, 1-12. doi: 10.1007/s12161-022-02400-5.
- Patange, D.D., Virshasen Vinayak, D., Chandran, D., Kumar, M., & Lorenzo, J.M. (2022a). Comparative effect of cooling on the physico-chemical-sensory properties of ghee from cow and buffalo milk, and evaluation of the low-fat spread prepared from cow and buffalo milk ghee. *Food Analytical Methods*, 1-11. doi:10.1007/s12161-022-02312-4.
- Redwan, E.R.M., & Tabll A. (2007) Camel lactoferrin markedly inhibits hepatitis C virus genotype 4 infection of human peripheral blood leukocytes. *Journal of Immunoassay & Immunochemistry*, 28(3), 267-277. <https://doi.org/10.1080/15321810701454839>
- Restani, P., Ballabio, C., Di Lorenzo, C., Tripodi S., & Fiocchi A. (2009). Molecular aspects of milk allergens and their role in clinical events. *Analytical and Bioanalytical Chemistry*, 395, 47-56.
- Restani, P., Gaiaschi, A., Plebani, A., Beretta, B., Cavagni, G., Fiocchi, A., Poiesi, C., Velona, T., Ugazio, A.G., & Galli C.L. (1999) Cross-reactivity between milk proteins from different animal species. *Clinical and experimental allergy: journal of the British Society for Allergy and Clinical Immunology*, 29(7), 997-1004. <https://doi.org/10.1046/j.1365-2222.1999.00563.x>
- Roda, G., Chien Ng, S., Kotze, P.G., Argollo, M., Panaccione, R., Spinelli, A., Kaser, A., Peyrin-Biroule, L., & Danese S. (2020) Crohn's disease. *Nature Reviews Disease Primers*, 6(1), 22. <https://doi.org/10.1038/s41572-020-0156-2>
- Sakandar, H.A., Ahmad, S., Perveen, R., Aslam, H.K.W., Shakeel, A., Sadiq, F.A., & Imran M. (2018). Camel milk and its allied health claims: a review. *Progress in Nutrition*, 20(1), 15-29.
- Salami, M., Moosavi-Movahedi, A.A., Moosavi-Movahedi, F., Ehsani, M.R., Yousefi, R., Farhadi, M., Niasari-Naslaji, A., Saboury, A.A., Chobert, J.M., & Haertlé, T. (2011). Biological activity of camel milk casein following enzymatic digestion. *Journal of Dairy Research*, 78(4), 471-478. <https://doi.org/10.1017/S0022029911000628>
- Saleena, L.A.K., Chandran, D., Geetha, R., Radha, R., & Sathian, C.T. (2022a). Optimization and identification of lactic acid bacteria with higher mannitol production potential. *Indian Journal of Animal Research*, 1, 8. doi: 10.18805/IJAR.B-4759.
- Saleena, L.A.K., Chandran, D., Rayirath, G., Shanavas, A., Rajalingam, S., Vishvanathan, M., Sharun, K., & Dhama, K. (2022b). Development of low-calorie functional yoghurt by incorporating mannitol producing lactic acid bacteria (*Leuconostoc pseudomesenteroides*) in the standard yoghurt culture. *Journal of Pure and Applied Microbiology*, 16(1), 729-736. doi: 10.22207/JPAM.16.1.78.
- Seifu, E. (2023). Camel milk products: innovations, limitations and opportunities. *Food Production, Processing and Nutrition*, 5(1), 1-20. <https://doi.org/10.1186/s43014-023-00130-7>
- Shabo, Y., & Yagil, R. (2005). Etiology of autism and camel milk as therapy. *International Journal on Disability and Human Development*, 4(2), 67-70.
- Shabo, Y., Barzel, R., & Yagil, R. (2008). Etiology of Crohn's disease and camel milk treatment. *Journal of Camel Practice and Research*, 15(1), 55-59.
- Shabo, Y., Barzel, R., Margoulis, M., & Yagil, R. (2005). Camel milk for food allergies in children. *IMAJ-RAMAT GAN*, 7(12), 796.
- Shori, A.B. (2015). Camel milk as a potential therapy for controlling diabetes and its complications: A review of in vivo studies. *Journal of Food and Drug Analysis*, 23(4), 609-618. <https://doi.org/10.1016/j.jfda.2015.02.007>
- Solanki, D., & Hati, S. (2018). Fermented camel milk: A Review on its bio-functional properties. *Emirates Journal of Food and Agriculture*, <https://doi.org/268-274>. 10.9755/ejfa.2018.v30.i4.1661
- Sumaira, A.M.S., Solangi, G.A., Anwar, I., & Kalwar, Q., (2020). Composition and beneficial impact of camel milk on human health. *Punjab University Journal of Zoology*, 35, 179-189.
- Swelum, A.A., El-Saadony, M.T., Abdo, M., Ombarak, R.A., Hussein, E.O.S., Suliman, G., Alhimaidi, A.R., Ammari, A.A., Ba-Awadh, H., Taha, A.E., El-Tarabily, K.A., & Abd El-Hack, M.E. (2021). Nutritional, antimicrobial and medicinal properties of camel's milk: A review. *Saudi Journal of Biological Sciences*, 28(5), 3126-3136. <https://doi.org/10.1016/j.sjbs.2021.02.057>
- Wernery, R., Joseph, S., Johnson, B., Jose, S., Tesfamariam, M., Ridao-Alonso, M., & Wernery, U. (2012). Camel milk against Autism—A preliminary report. *Journal of Camel Practice and Research*, 19(2), 143-147.
- Wernery, U. (2006). Camel milk, the white gold of the desert. *Journal of Camel Practice and Research*, 13(1), 15.
- Yadav, A.K., Kumar, R., Priyadarshini, L., & Singh, J. (2015) Composition and medicinal properties of camel milk: A

- Review. *Asian Journal of Dairy and Food Research*, 34(2), 83-91. <https://doi.org/10.5958/0976-0563.2015.00018.4>
- Yagil R. (2013). Camel milk and its unique anti-diarrheal properties. *The Israel Medical Association journal : IMAJ*, 15(1), 35–36.
- Yassin, M.H., Soliman, M.M., Mostafa, S.A.E., & Ali H.A.M. (2015) Antimicrobial effects of camel milk against some bacterial pathogens. *Journal of Food and Nutrition Research*, 3(3), 162-168. <https://doi.org/10.12691/jfnr-3-3-6>
- Zhao, D.B., Bai, Y.H., & Niu, Y.W. (2015) Composition and characteristics of Chinese Bactrian camel milk. *Small Ruminant Research*, 127, .58-67. <https://doi.org/10.1016/j.smallrumres.2015.04.008>








Journal of Experimental Biology and Agricultural Sciences

<http://www.jebas.org>

ISSN No. 2320 – 8694

Donkey milk: chemical make-up, biochemical features, nutritional worth, and possible human health benefits - Current state of scientific knowledge

Deepa P R^{1†}, Divya Dharshini C S^{1†}, Bhadra S Dev^{1†}, Jyotika Jayan^{1†},
Harisankaran P S¹, Nithin S Rajan¹, Karthik S¹, Nandhana J P¹, Athulya K G¹, Pran M² ,
Sandip Chakraborty³ , Hitesh Chopra⁴ , Abhijit Dey⁵ , Anil K Sharma⁶ ,
Kuldeep Dhama^{7*} , Deepak Chandran^{1*} 

¹Amrita School of Agricultural Sciences, Amrita Vishwa Vidyapeetham University, Coimbatore, Tamil Nadu– 642109, India

²School of Agricultural Sciences, Karunya Institute of Technology and Sciences, Coimbatore, Tamil Nadu– 641114, India

³Department of Veterinary Microbiology, College of Veterinary Sciences and Animal Husbandry, R.K. Nagar, West Tripura, Tripura, Pin-799008, India

⁴Chitkara College of Pharmacy, Chitkara University, Punjab - 140401, India

⁵Department of Life Sciences, Presidency University, 86/1 College Street, Kolkata-700073, West Bengal, India

⁶Department of Biotechnology, Maharishi Markandeshwar University (Deemed to be University) Mullana-Ambala-133207, Haryana, India

⁷Division of Pathology, ICAR-Indian Veterinary Research Institute, Izatnagar, Bareilly, Uttar Pradesh, India - 243122

[†]Authors contributed equally

Received – February 24, 2023; Revision – March 26, 2023; Accepted – April 27, 2023

Available Online – April 30, 2023

DOI: [http://dx.doi.org/10.18006/2023.11\(2\).251.263](http://dx.doi.org/10.18006/2023.11(2).251.263)

KEYWORDS

Donkey milk
Nutritional profile
Medicinal value
Functional food

ABSTRACT

Milk and milk derivatives are widely consumed because of their high nutritional density. Donkey milk and milk products have been consumed since ancient times. The use of donkey milk in the human diet is gaining popularity. The abundance of antibacterial components and protective elements in donkey milk sets it apart from the milk of other animals. Like human milk, donkey milk has low fat, high lactose, and low casein/whey protein ratio. Donkey milk whey protein's anti-proliferative properties imply lung cancer treatment. Alpha-lactalbumin, a type of protein, has been found to have antiviral, anticancer, and anti-stress properties. Donkey milk, like human milk, includes a low amount of casein and a smaller quantity of beta-lactoglobulin than cow milk. Donkey milk is an alternative for newborns with cow milk protein allergy and lactose intolerance since it has a higher amount of lactose, improves palatability, and prevents allergies. Osteogenesis, arteriosclerosis therapy, cardiac rehabilitation, accelerated aging, and hypocholesterolemic diets are some areas where donkey milk is beneficial. Since it contains probiotic

* Corresponding author

E-mail: c_deepak@cb.amrita.edu (Deepak Chandran);
kdhama@rediffmail.com (Kuldeep Dhama)

Peer review under responsibility of Journal of Experimental Biology and Agricultural Sciences.

Production and Hosting by Horizon Publisher India [HPI]
(<http://www.horizonpublisherindia.in/>).
All rights reserved.

All the articles published by [Journal of Experimental Biology and Agricultural Sciences](#) are licensed under a [Creative Commons Attribution-NonCommercial 4.0 International License](#) Based on a work at www.jebas.org.



lactobacilli strains, fermented beverages can be made with donkey milk. Donkey milk moisturizes skin due to its high vitamin, mineral, and polyunsaturated fatty acid content. The chemical makeup and potential therapeutic benefits of donkey milk warrant additional research. This has led to a rise in interest in producing dairy goods derived from donkey milk. Donkey milk has been used to make cheese, ice cream, milk powder, and even some experimental useful fermented drinks. The present article summarises what we know about donkey milk's chemical makeup, biological functions, nutritional worth, and possible human health benefits.

1 Introduction

Colostrum and transitional milk in each mammal provide passive immunization and sustenance. Human breast milk is the best nutrition for infants in the first four months; however, in some cases (lack of milk ejection, orphans, or sick mothers), a healthy substitute is needed (Cimmino et al. 2023). Due to the high demand for milk and other dairy products among human populations, cows have become the principal dairy animal species worldwide. However, cow milk is inappropriate for 5–15% of newborns with cow milk protein allergies (Aspri et al. 2017; Martini et al. 2021; Lejaniya et al. 2021a; Lejaniya et al. 2021b; Garhwal et al. 2022). Clinical cross-reactivity across ruminant milk has sometimes shown extremely high sensitivity in these people. Milk from domesticated mammals other than cows have recently become commercially valuable due to their high nutritional value and potential medical applications (Chandran et al. 2021; Patange et al. 2022a; Patange et al. 2022b;

Baloš et al. 2023; Krishnan et al. 2023). More and more studies have been documented about donkey milk in recent years, confirming its growing interest due to the hypoallergenic features and other unusual and health-promoting aspects noted by numerous authors.

Donkey milk (ass milk/jenny milk) is made by milking a healthy domesticated donkey (*Equus asinus*). North Africa's Nile Valley domesticated donkeys approximately 6000 B.C. They swiftly spread across India, Asia, South Europe and South America. Food and Agriculture Organization identifies three varieties of donkeys native to India: the Indian, the Indian wild donkey, and the Kiang. Rann of Kutch (Gujarat) is home to one of the two main types of Indian wild donkeys, whereas Kiang's can be found in neighbouring regions like Sikkim and Ladakh (Pilla et al. 2010; Aspri et al. 2017; Cimmino et al. 2023). Figure 1 shows the distribution of donkey milk production worldwide and the nations that produce the most of it.



Figure 1 Distribution of donkey milk production around the world and the nations that produce the most of it (Designed with Biorender premium software; <https://app.biorender.com/>)

Donkey milk has been used for centuries as a remedy for various ailments, including asthma, joint pain, gastritis, and bronchitis. It is commercially accessible and can help infants, those with cow's milk protein allergies, and older people (Martini et al. 2018a; Karami and Akbari-adergani 2019). Donkey milk's health benefits have piqued the public's attention. Donkey milk is a "pharma food" due to its nutritional, nutraceutical, and functional properties. Due to its biochemistry, like human milk, donkey milk can be used as a safe and nutritious substitute for children with cow milk allergies (Mottola et al. 2018; Garhwal et al. 2022). As well as sharing nutritional similarities with human milk, this alternative possesses similar hypo-allergenicity, immunological homeostasis conditions, and antibacterial action. Donkey's milk may be an option for a bovine milk protein-allergic baby if breast milk is unavailable (Vincenzetti et al. 2017; Conte and Panebianco 2019). Infants love and tolerate donkey milk because it tastes like human milk. Crohn's and ulcerative colitis patients can be benefited from this compound's hypo-allergic, anti-aging and antimicrobial characteristics (Martini et al. 2021; Baloš et al. 2023; Cimmino et al. 2023). Although all components of donkey milk have nutritional and physiological effects, the proportion of whey protein is considered significant (Derdak et al. 2020). This review article summarizes donkey milk's nutritional characteristics and potential health advantages.

2 Physico-chemical composition of donkey milk

Donkey milk tastes, smells, and looks like water. Neither the number of somatic cells nor total microorganisms in milk is very high (Massouras et al. 2020). Protein content varies significantly

from species to species and is affected by factors like breed, lactation stage, diet, climate, parity, season, and udder health, as reported by the vast majority of authors (Garhwal et al. 2022; Saleena et al. 2022a; Saleena et al. 2022b). There is promising evidence that protein in milk can bridge the gap between nutrition, dietetics, and therapy (Vincenzetti et al. 2017). Immunoglobulins, lactoferrin, lactoperoxidase, and lysozyme are milk-derived antibacterial proteins. To function, immunoglobulins (secretory Ig-A, Ig-G and Ig-M) rely on a mechanism involving antigen-antibody interactions (Aspri et al. 2017; Chandran and Radhakrishnan 2019; Papademas et al. 2022). Differences in nutrient content between donkey milk and the milk of other mammals, including humans, are presented in Table 1.

2.1 Milk proteins

Milk contains a variety of proteins, including milk fat globule proteins, caseins, whey proteins, enzymes, and others (Brumini et al. 2016; Saleena et al. 2022a; Saleena et al. 2022b). Donkey milk is far lower in protein than cow milk (1.5-1.8 g/100g) and more like human and mare milk (Vincenzetti et al. 2017; Vincenzetti et al. 2021). Donkey milk is a nutritious alternative for cow's milk-allergic newborns. Milk lipids are nutritionally valuable in immune inflammatory response control because of their significant parallels to human milk (Mottola et al. 2018; Bhardwaj et al. 2020). Whey proteins in donkey milk are primarily alpha-lactalbumin, beta-lactoglobulin, and lysozyme. Alpha-lactalbumin in donkey milk has two isoelectric points (Kumar et al. 2021; Papademas et al. 2022). Antiviral, anticancer, and stress-relieving effects have been discovered in

Table 1 Differences in nutrient content between donkey milk and the milk of other mammals, including humans

Nutrients	Donkey milk	Camel milk	Cow milk	Goat Milk	Sheep milk	Human milk
Fat (g/100mL)	0.3-1.8	4.5	3.5	3.5	6.1	3.4
Protein (g/100mL)	1.3-1.8	3.5	3.4	3.3	6.21	1.1
Lactose (g/100mL)	5.8-7.4	4.4	4.5	4.1	4.8	6.5
Minerals (g/100mL)	0.3-0.5	0.7	0.7	0.86	5.5	0.21
Solids-not-fat (g/100mL)	9.018	8.6	9.1	8.75	10.33	8.9
Total solids (g/100mL)	8.8-11.7	16.89	13.12	13.2	18.75	12.75
Cholesterol (mg/100g)	8.6	34.5	5	11	27	14
Calcium (g/100mL)	6.89	1.43	1.20	1.34	2.00	3.20
Phosphorus (g/100mL)	1.596	1.16	1.3	1.08	0.15	0.13
Saturated fatty acids (g/100mL)	67.6	51.9	67.73	70.42	65.17	46.60
Monounsaturated fatty acids (g/100mL)	15.80	39.60	27.3	25.67	24.29	43.55
Polyunsaturated fatty acids (g/100mL)	16.60	8.46	5.25	4.08	2.45	9.85
Water (%)	92.5	87-90	87	82.46-89.05	80.62	87.5

Source: Madhusudan et al. (2017); Souroullas et al. (2018); Bhardwaj et al. (2020); Prasad (2020); Kumari and Sharma (2021); Bertino et al. (2022); Garhwal et al. (2022); Papademas et al. (2022); Baloš et al. (2023)

alpha-lactalbumin (Aspri et al. 2017; Cimmino et al. 2023). It has also been demonstrated that alpha-lactalbumin has an anti-inflammatory effect by suppressing cyclooxygenase-2 and phospholipase A2 (Papademas et al. 2022). Beta-lactoglobulin, abundant in cow milk but missing in human milk, is often allergenic to children. Donkey milk has a beta-lactoglobulin level similar to mare milk (approximately 40% of whey proteins) but lower than cow milk. Donkey milk is hypoallergenic (Brumini et al. 2016; Conte and Panebianco 2019).

Donkey milk is the best alternative to human milk for children with cow milk protein allergy due to its palatability, nutritional adequacy, clinical tolerability, and physiological functions like digestive activity molecules, antibacterial substances, growth factors, and hormones (Bhardwaj et al. 2020; Garhwal et al. 2022). Caseins in donkey milk differ from those in cow milk in that alpha-S-1 casein and beta-casein, in their various phosphorylated and glycosylated forms, are present, whereas kappa-casein and alpha-S2-casein are present only in trace levels (Vincenzetti et al. 2017; Kumar et al. 2021; Cimmino et al. 2023).

The amounts of allergenic components in milk may affect tolerance. Beta-lactoglobulin in donkey milk comes in three different genetic forms; one contains three amino acid replacements, while the other forms each have two amino acid exchanges (Mottola et al. 2018; Baloš et al. 2023). In contrast to ruminant milk, which contains beta-lactoglobulin as a dimer, donkey milk only contains a single copy of this protein. As a member of the lipocalin family, beta-strong lactoglobulin's affinity for a wide variety of chemicals has led to many hypotheses regarding the protein's role in the body (Martini et al. 2021). Beta-lactoglobulin forms complexes with folic acid, suggesting that functional meals could use these complexes to transport folic acid. Hydrophobic ligand transport and absorption, enzyme regulation, and newborn latent immunological response are all linked to this protein (Bhardwaj et al. 2020; Cimmino et al. 2023). Donkey milk, similar to human milk but contains a higher concentration of amino acids like Ser, Glu, Arg, and Val and a lower percentage of Cys, could be a novel dietetic meal and breast milk substitute (Martini et al. 2021; Garhwal et al. 2022).

2.2 Milk fat

Donkey milk's fat content is lower than that of human milk, ranging from 0.03 to 1.18 kg/kg in a nonlinear fashion from partum to the end of lactation, making it a viable option for use in diet treatment to decrease the incidence of cardiovascular disease, autoimmune disease, and inflammatory diseases (Bhardwaj et al. 2020). The human diet's 52.2% polyunsaturated fatty acids (PUFA), low omega-6 to omega-3 ratio, and low atherogenic and thrombogenic indices are advantageous (Garhwal et al. 2022). To

reduce blood cholesterol levels, halting the development of atherosclerotic plaques and eliminating the danger of high blood pressure, coronary heart disease and blood clots (Martini et al. 2021). Donkey milk is a welcome addition to the human diet because of the significant risk of fatty acid deficiency, especially PUFA omega-3 fatty acids required for optimal growth, cognitive development, and cardiovascular health (Ragona et al. 2016). Donkey milk contains 9.0 g/100 g and 5.1 g/100 g of total fatty acids, respectively, of the PUFAs linoleic acid (C18:2) and linolenic acid (C18:3) (Bhardwaj et al. 2020). Donkey milk fat globules are significantly smaller than those found in bovine milk, with an average diameter of 1.92 microns (Baloš et al. 2023). Bovine milk fat globules are roughly twice as large as donkey milk fat globules in average diameter. Donkey milk may be easier to digest because its fat globules are smaller than other kinds of milk, providing more surface area for lipase action (Pilla et al. 2010; Garhwal et al. 2022).

2.3 Lactose

Donkey milk contains more lactose (between 5.8 and 7.4%) than cow milk or human milk. The large amount is beneficial because it makes breast milk more appealing to infants and helps them absorb calcium, which is essential for the growth of healthy bones (Bhardwaj et al. 2020). Donkey milk has a pleasant flavour because of the lactose in it, and it is a valuable source of galactose, which is required for proper nervous system growth. Inadequate for 10 to 60% of the lactose intolerant population due to donkey milk's high lactose content from ruminant milk (Aspri et al. 2017; Cimmino et al. 2023). Those who have trouble digesting lactose may be able to eat fermented milk products like yoghurt because they include living bacteria that break down the lactose into lactic acid. Due to triacylglycerols with high unsaturation degrees and minor components with low partition number values, donkey milk has a higher PUFA concentration (Conte and Panebianco 2019).

2.4 Minerals

The growth and development of a human skeleton rely heavily on mineral intake. Milk is a primary food source of minerals. Depending on the breed and the stage of lactation, the typical composition of donkey milk ranges from 0.3 to 0.9 g/100 g (Vincenzetti et al. 2021). This exceeds cow milk but falls short of human milk. Donkey milk is rich in calcium, iron, sodium, potassium, phosphorus, magnesium, zinc, and copper (Papademas et al. 2022).

2.5 Vitamins

It is well established that mare milk has substantially more vitamin C than cow milk, and studies on the vitamin content of

donkey milk are only being started. Human milk has more significant quantities of niacin, whereas donkey milk has higher concentrations of cyanocobalamin, thiamine, riboflavin and vitamin C (Pilla et al. 2010; Vincenzetti et al. 2021; Papademas et al. 2022).

2.6 Enzymes

Different from the milk of other mammals, donkey milk contains enzymes with unique properties, such as a bactericidal effect. Donkey milk has a solid microbial inhibitory activity compared to other mammalian milk. Because of the large concentrations of lysozyme and lactoferrin in donkey milk, this is thought to be the case (Mottola et al. 2018; Papademas et al. 2022). Donkey milk has a low bactericidal concentration (0.02 g/L) due to its high lysozyme concentration (1.0 g/L). There may be as much as 4,000 mg/L of lysozyme in a single serving of donkey milk (Garhwal et al. 2022). There is around twice as much lactoferrin in donkey's milk as in bovine milk. Donkey milk only had 10^4 CFU/mL of bacteria and other microbes (Martini et al. 2021;

Vincenzetti et al. 2021). Figure 2 shows donkey milk's physicochemical components.

3 Shelf life of donkey milk

Milk shelf life is crucial as it helps in its storage, processing, packaging and supply. It is the actual time in which it deteriorates to an unacceptable level. The higher the shelf life, the better its acceptability would be. Mare and donkey milk samples collected aseptically were incubated at 37 °C for 24 h, and periodical change in acidity and pH in equine milk was regularly studied at 2 h intervals (Bhardwaj et al. 2020). Shelf-life results indicated that mare and donkey milk was stable at 37 °C up to 8 h and 10 h, respectively. The presence of lysozyme, a natural preservative, extends the storage life of raw donkey's milk (Vincenzetti et al. 2021; Cimmino et al. 2023).

4 Human health benefits of donkey milk

Due to its high nutritious content and positive effects, as depicted in Figure 3, donkey milk is often consumed. In recent years, it

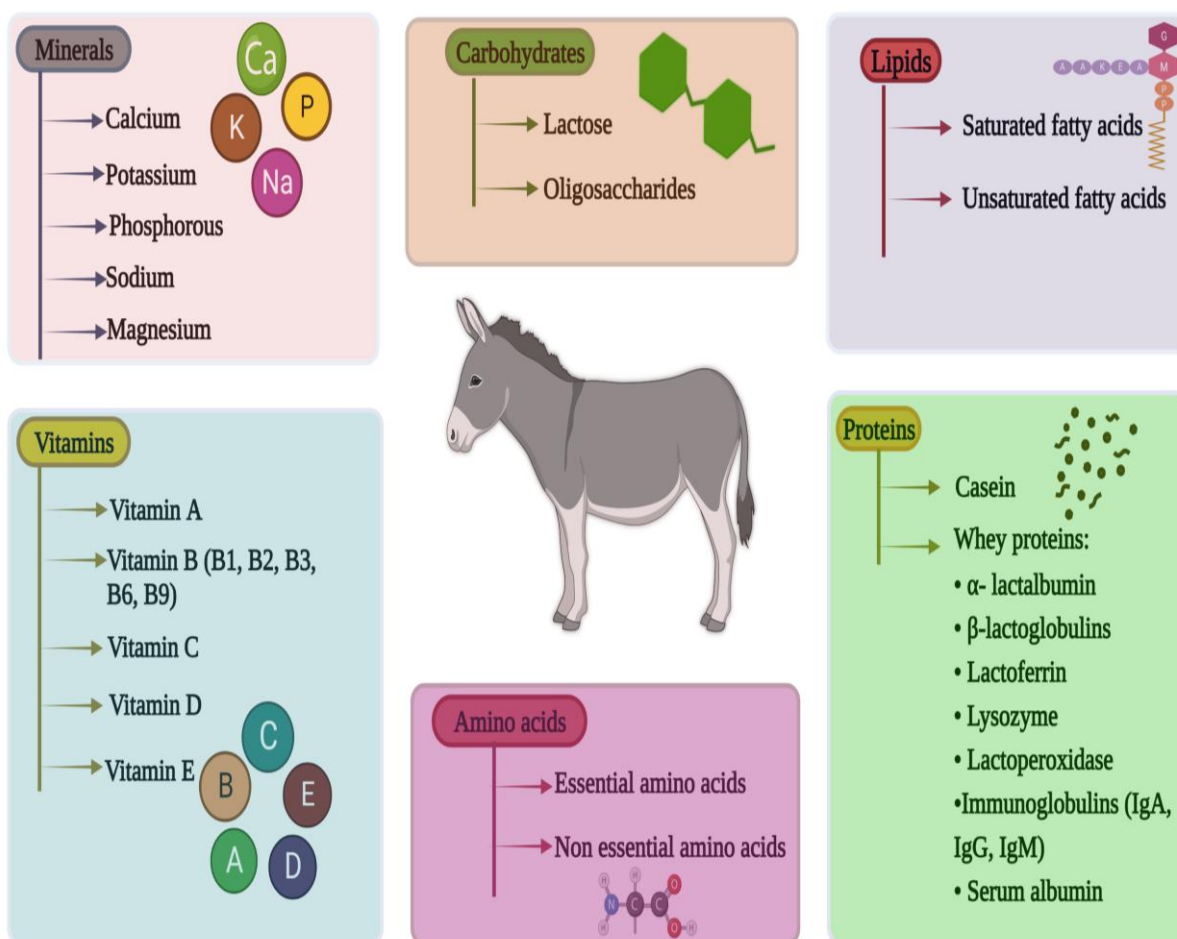


Figure 2 Physico-chemical constituents of donkey milk (Designed with Biorender premium software; <https://app.biorender.com/>)



Figure 3 Substantial nutritional, therapeutic, and dietary implications of donkey milk for human beings (Designed with Biorender premium software; <https://app.biorender.com/>)

has attracted much interest due to its ability to reduce allergens and strengthen the immune system. Donkey milk proteins are more evenly distributed between casein and whey than in bovine milk, which contains roughly five times more casein than whey (Garhwal et al. 2022). In contrast to cow's milk, donkey milk has much less protein casein, making it suitable for consumption by those sensitive to cow's milk (Martini et al. 2021; Papademas et al. 2022). Swapping from cow milk to donkey milk was safe for 81 Italian kids with cow milk allergies, and they continued to grow and gain weight usually. The sugar lactose is also vital to donkey milk (Mottola et al. 2018). Absorption of calcium, necessary for healthy bones, is facilitated. Moreover, donkey milk contains vitamin D, which may contribute to a stronger immune system and fewer cardiovascular issues (Bhardwaj et al. 2020; Cimmino et al. 2023). Laboratory tests showed that donkey milk stimulated the creation of cytokines, a protein that helps the body's immune system fight off infections. Donkey milk promotes nitric oxide production, which lowers blood pressure, relaxes blood vessel walls and boosts blood flow (Aspri et al. 2017; Papademas et al. 2022).

Lysozyme, the principal antibacterial agent in donkey milk, was reported in significant concentrations by both Tidona et al. (2015) and Nazzaro et al. (2010). Lactic acid bacteria (LAB) predominate in the microbiome of donkey milk. 80-90% of the total microbial load is typically LAB, with concentrations ranging from 3-4 log CFU/mL. Due to the antibacterial effect of lysozymes, the number of lactic acid bacteria (LAB) in donkey milk decreased during cold storage (Prasad 2020). One strain of *Lactococcus paracasei* that produces bacteriocin was found to have been isolated from donkey milk. *Salmonella typhi*, *Pseudomonas aeruginosa*, and *Escherichia coli* are just a few of the harmful bacteria that were discovered to be vulnerable to the bacteriocin's antimicrobial effects (Cimmino et al. 2023). Similarly, Murua et al. (2013) found that donkey milk isolates of *Lactobacillus plantarum* produced a bacteriocin (LP08AD) that inhibited the development of food spoilage bacteria, LAB, and microorganisms (*Enterococcus faecium*, *Lactobacillus curvatus*, and *Listeria monocytogenes*). Additionally, it was discovered by Papademas et al. (2022) that raw donkey milk contained three different *Enterococcus* bacterial strains (type A, B, P) that produced enterocins, which are mainly effective against *L. monocytogenes*.

Three proteins with antibacterial effects could be measured in milk from a donkey, a human, and a cow. Lysozyme and lactoferrin are in high concentrations in human and donkey milk, but lactoperoxidase is present in trace levels (Garhwal et al. 2022). Donkey milk has a lysozyme concentration of 1 g/L, human milk of 0.12 g/L, and bovine milk of only trace concentrations, all lower than those found in donkey and human milk (Mottola et al. 2018). Donkey milk has less lactoperoxidase (0.11 mg/L) than human milk (0.77 mg/L) or bovine milk (30-100 mg/L). Donkey milk contains less lactoferrin (0.080 g/L) than human (0.3-4.2 g/L) or bovine (0.10 g/L) milk (Cimmino et al. 2023). Hydrolysis of glycosidic linkages of the mucous polysaccharides in the bacterial cell walls is the antimicrobial mechanism by which the iron-binding protein lactoferrin exerts its antibacterial effects (Chandran et al. 2020; Prasad 2020).

Food allergies to cow milk proteins are relatively frequent in infants and toddlers. Yet, donkey milk has no reported side effects which is utilized as natural hypoallergenic milk (Souroullas et al. 2018). Donkey milk has been shown to be less allergenic than cow milk in scientific research. Because of its high concentration of bioactive compounds, it was utilized to nourish European orphans and sick children until the end of the 20th century (Papademas et al. 2022). Regarding the lactose, protein, and minerals it contains, donkey milk is similar to human breast milk. Infants' immune systems were likely strengthened by the donkey milk's immunoactive compounds, including lysozyme and lactoferrin (Souroullas et al. 2018; Bhardwaj et al. 2020). Moreover, donkey milk has been found to have no negative impact on children's growth rate (Kumar et al. 2021). Milk from a donkey on a vegetable oil diet (4 mL/100 mL) is a good substitute for human breast milk (Madhusudan et al. 2017; Massouras et al. 2020).

Human-like leptin, ghrelin, triiodothyronine and insulin-like growth factor 1 are present in donkey milk, along with other growth factors and hormones. These molecules directly influence metabolism, body composition, and satiety regulation (Souroullas et al. 2018; Bhardwaj et al. 2020; Cimmino et al. 2023).

Preventing gastrointestinal infections in newborns may benefit from using lysozyme, lactoperoxidase, and lactoferrin, all of which have been shown to have antimicrobial and bacteriostatic properties (Chandran and Radhakrishnan 2019; Massouras et al. 2020). Because of their efforts, fresh donkey milk may be preserved for longer, which could increase its commercial viability. In addition to protecting against cancer development and metastasis, the iron-binding protein lactoferrin also plays a role in regulating iron homeostasis, cellular growth, fighting off infections, and inhibiting the spread of cancer (Ragona et al. 2016; Chandran et al. 2020; Martini et al. 2021). Compared to other milk proteins, it is very resistant to proteolytic degradation because it is

from the transferrin family of proteins. It maintains a healthy gut microbiota by regulating the ratio of beneficial to harmful bacteria and encouraging the growth of *Lactobacillus* and *Bifidobacterium* (Mottola et al. 2018). Reverse phase high-performance liquid chromatography (RP-HPLC) research revealed that alpha-lactalbumin, lysozyme, and beta-lactoglobulin concentrations fluctuated during donkey lactation (60, 90, 120, 160, and 190 days postpartum) (Souroullas et al. 2018; Prasad 2020).

Perna et al. (2015) found that donkey milk fermented into a probiotic beverage is an effective way to introduce beneficial bacteria to the human digestive system. This probiotic drink can serve as a model for creating lactose-free, antioxidant-rich nutraceutical foods. As these microorganisms generate chemicals that alter the qualities of milk, the concentration of milk microbiota influences its chemical makeup. Donkey milk fermented with *Lactobacillus fermentum* ME-3 and *Lactobacillus acidophilus* (ATCC4356) was investigated for its probiotic, antioxidant, antibacterial, and sensory qualities by Papademas et al. (2022). Milk's high calcium and saturated fatty acid content and its beneficial protein profile have been shown to improve the makeup of the microbiota in the human stomach. Fermented milk appears to provide similar health benefits, and a fermented beverage of donkey milk can be made by co-culturing the probiotic species *Lactobacillus plantarum* and *Streptococcus thermophilus*. The selected species of *L. plantarum* increase the growth rate of bacteria to attain that supplied pH in a condensed amount of time, and they also promote the growth of *S. thermophilus* in that environment. In monocultures, one would not have anticipated such exciting growth activity (Kumari and Sharma 2021).

In addition to a high lysozymal content, donkey milk has been found to include many other beneficial bacteria, including *Lactobacillus paracasei*, *Lactococcus lactis*, and *Carnobacterium maltaromaticum*, all of which are well-adapted prospective probiotics. *Leuconostoc*, *Enterococcus*, and *Streptococcus* were shown to be less common than *L. paracasei* and *L. lactis* in a recent study (Kumari and Sharma 2021; Bertino et al. 2022). In-vitro studies have shown that certain probiotic strains are more effective at inhibiting microbial growth, preventing oxidative damage, and slowing cell proliferation. Raw donkey milk samples collected from farms had the highest concentrations of *L. paracasei* and *Enterococcus faecalis*, while samples collected from local fields had the highest concentrations of *L. lactis* and *Lysinibacillus sphaericus*. This study by Cosentino et al. (2022) examined donkey milk's essential components and isolated bacteria with potential probiotic properties against stress circumstances like excess bile, low pH, etc. Donkey milk probiotics present a fascinating field for further study and a novel source for highly effective probiotics in fermented food products. Donkey milk's potential probiotics are shown in Figure 4.

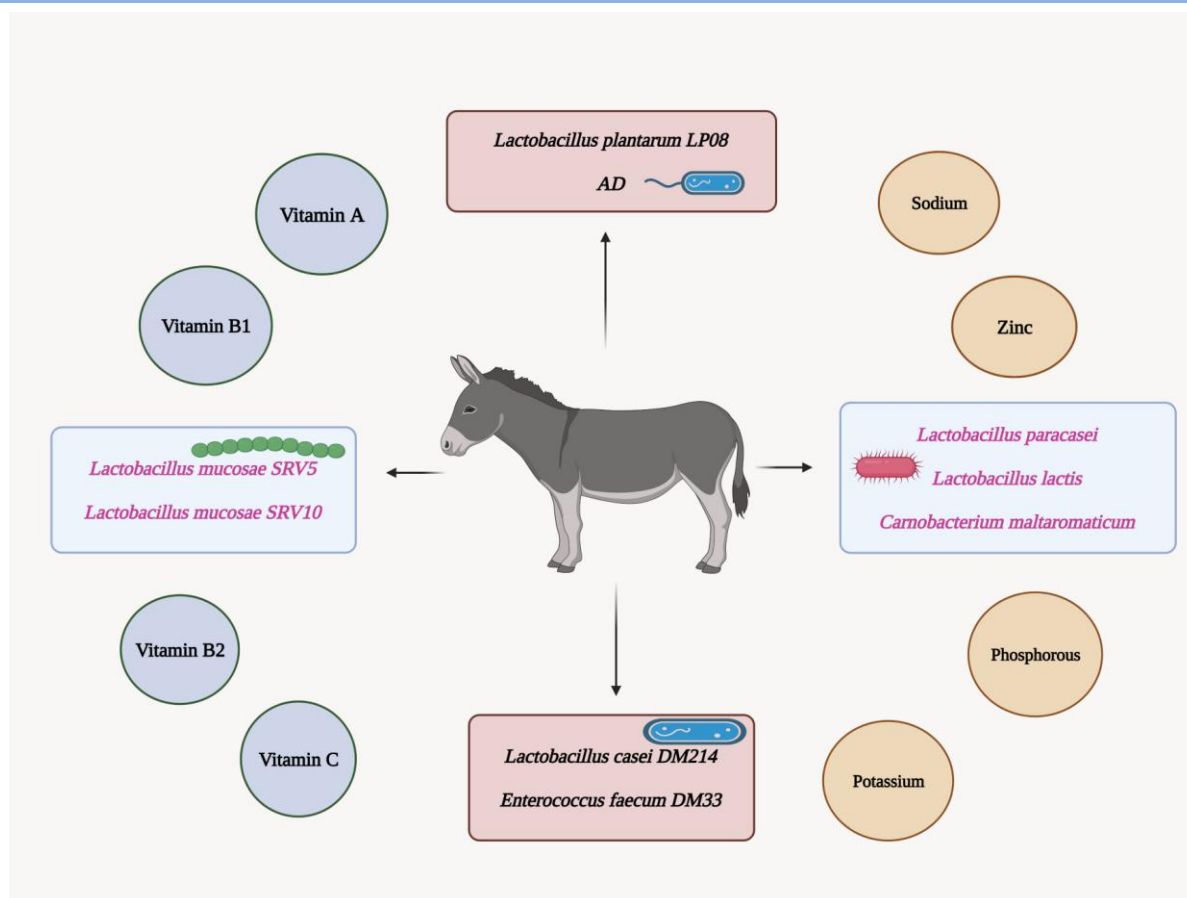


Figure 4 Potential probiotics in donkey milk (Designed with Biorender premium software; <https://app.biorender.com/>)

Donkey milk revealed a higher concentration of lysozyme than bovine milk (traces) or human milk (0.12 mg/mL), and this concentration increased significantly throughout lactation, with a mean value of 1.0 mg/mL (Bhardwaj et al. 2020). Donkey milk had a mean beta-lactoglobulin concentration of 3.75 mg/mL, similar to bovine milk (3.3 mg/mL). In the three months following delivery, the beta-lactalbumin concentration reached 1.8 mg/mL, very near to the beta-lactalbumin concentration in human milk (1.6 mg/mL) (Papademas et al. 2022). Donkey milk may have anti-inflammatory and antibacterial properties due to the presence of lysozyme. Other physiological roles for lysozyme include virus inactivation, immunoregulatory action, anti-inflammatory and antitumor effects (Ragona et al. 2016). Several investigations have shown that lysozyme has potent antitumor and angiogenic inhibitory properties. Donkey milk has a high concentration of lysozyme, which has antitumor properties. Alpha-lactalbumin, beta-lactoglobulin, blood serum albumins, immunoglobulins, lactoferrin, and lysozyme are the fundamental whey proteins found in donkey milk (Madhusudan et al. 2017; Massouras et al. 2020). Donkey milk has beta-lactoglobulin as a monomer, which is easier for infants to digest and absorb than it is in cow's milk. Strong anti-proliferative activity and potential utility in lung cancer treatment

have been attributed to whey protein isolated from donkey milk; however, these claims require verification *in vivo*. The amount of whey protein in donkey milk also changes according to the time of lactation (Brumini et al. 2016; Souroullas et al. 2018; Bhardwaj et al. 2020). Better infant nutrition may be possible with a more thorough understanding of protein composition and variability. Donkey milk, especially collected in the first and second half of lactation when antimicrobial chemicals are at their highest, may positively affect digestive and immune system functioning (Aspri et al. 2017; Mottola et al. 2018).

Capillary gas chromatography can be utilized to ascertain the fatty acid profile of the milk sample. The PUFAs are crucial to the maturation of the newborn brain, the visual system, and the mind. The high concentration of omega-3 fatty acids in donkey milk may profoundly affect a baby's brain, eye, and body growth (Baloš et al. 2023). Omega-3 fatty acids reduce the risk of depression, cancer, dementia, and inflammatory illnesses such as dermatitis and rheumatoid arthritis (Madhusudan et al. 2017). Donkey milk's high PUFAs and omega-3 fatty acid concentration may aid the body's immune system. It has been shown that donkey milk can activate IgG secretion and release cytokines (like IL-1 β , IL-10, IL-12 and

TNF- α), all of which are crucial in the immunological treatment of immune-related disease. Nitric oxide prevents atherosclerosis (Souroullas et al. 2018; Bhardwaj et al. 2020; Cimmino et al. 2023). Human peripheral blood mononuclear cells release nitric oxide after drinking donkey colostrum or milk. Donkey milk, however, can generate nitric oxide better than colostrum (Tafaro et al. 2007). Nitric oxide, at moderate intake levels (200 mL/day), can upregulate the immunological response in aged hosts; it is an efficient antibacterial agent in the formation of atherosclerosis; it is a potent vasodilator of terminal arteries; and it increases blood flow (Ragona et al. 2016). During lactation, the percentage of milk that contains unsaturated fatty acids (UFAs) rises to 48.022.97%. Over 180 days, the mean UFA/SFA ratio increased from 0.92 to 1.50, which is an extremely high value. The greater PUFA omega-3 to omega-6 ratio during month 7 of lactation is reflected in this finding (Garhwal et al. 2022).

Donkey milk has a better lipid pattern than cow milk, and its low amounts of docosahexaenoic acid and eicosapentaenoic acid may help treat atopy and cognitive development (Papademas et al., 2022). Because their fatty acid structure, especially that of long-chain fatty acids (LC-SFA), is identical to human milk, donkey milk lipids are easily absorbed despite their low content (Madhusudan et al. 2017). As part of a balanced diet, donkey milk provides essential fatty acids. Subjects with cow milk protein allergy, particularly those with numerous food allergies, have a heightened need for these fatty acids (Conte and Panebianco 2019).

Lactobacillus bacteria are commonly cultured in equine (horse and donkey) milk, making it a popular ingredient in probiotic beverages. Koumiss is a traditional beverage of central Asia made from fermented equine milk. Mongolia's national beverage is koumiss. In Mongolia, it is said that koumiss may treat 40 different illnesses (Aspri et al. 2017).

Lactobacillus rhamnosus is a beneficial bacterium that occurs naturally in the human microbiome and helps maintain a healthy gut environment and modulate the immune system on both the local and systemic levels (Brumini et al. 2016). Peng et al. (2014) examined the cellular, humoral, and nonspecific immune responses elicited by donkey milk. They found that it stimulated the production of interleukins by lymphocytes and macrophages, as well as the expression of activation cells surface molecules like CD25, which is used to monitor disease progression, and CD69, a signal-transmitting receptor in lymphocytes. These cytokines strengthen the immune system in donkey milk. Furthermore, nitric oxide is released from peripheral blood mononuclear cells after drinking donkey milk. Donkey milk's immunological properties—including its ability to serve as a vasodilator and a potent agent against infections and their products—may make it a beneficial tool in the fight against atherosclerosis (Derdak et al. 2020; Baloš et al. 2023). Donkey milk whey protein and whey hydrolysate have

been studied for their potential impact on the physiological activity and gut microbiota of D-galactose-induced aged mice. This has been done to discover more effective anti-aging methods. Whey protein and whey hydrolysate have been proven to ameliorate the effects of aging on the body by decreasing levels of reactive oxygen species (ROS) and malondialdehyde (Zhou et al. 2022).

Humans have been drinking and applying donkey milk since prehistoric times, but it wasn't until the Renaissance that the practice was studied scientifically. Since then, it has been successfully utilized in Western Europe as a human milk substitute, a diet for infants with food allergies, to enhance the immunological response of otherwise healthy old individuals, and to manufacture fermented beverages (Souroullas et al. 2018; Bhardwaj et al. 2020). Moreover, anti-proliferative and anticancer activity was observed in vitro for whey proteins isolated from donkey milk. Because of its beneficial qualities, milk has widespread use in food and cosmetics (Brumini et al. 2016; Conte and Panebianco 2019). Donkey milk is nutritionally equivalent to human milk, could replace human breast milk and be used in alternative diets. In light of this, it has been proposed that infants and newborns who cannot get their mother's milk may benefit from consuming a milk powder made from donkey milk (Souroullas et al. 2018; Bhardwaj et al. 2020). Several scientific researches have demonstrated the skin-benefiting properties of cosmetics using donkey milk. Donkey milk's abundance of beneficial nutrients makes it an excellent choice for naturally nourishing and toning the skin. Donkey milk's natural antibacterial compounds, like lysozyme and lactoferrin, help prevent skin infections by keeping harmful microorganisms from multiplying (Massouras et al. 2020). These properties of chemically-enhanced donkey milk make it a promising treatment option for a wide range of skin disorders. Soap and face cream are not the only products that benefit from donkey milk today (Martini et al. 2021).

5 Novel food development applications of donkey milk

Donkey milk's capacity to include probiotic microorganisms for antibiotic-associated diarrhea prevention and therapy is an extra benefit. However, lactose sensitivity sufferers may not be able to drink this milk. Donkey milk is fermented with LAB that hydrolyzes lactose, casein, and whey protein, releasing a wide range of organic acids, peptides, and amino acids, allowing for the creation of novel foods for people who are intolerant to lactose or cow milk protein (Cimmino et al. 2023). Panellists thought donkey milk was delicious, describing it as white, thin, smelling sweet, tasting sweet, and leaving no aftertaste (Malissiova et al., 2016). When milk is used for manufacturing, the generated products should be examined for technological factors and food processing appropriateness. Donkey milk yogurt, probiotic yogurt, and fermented milk were rarely made (Perna et al., 2015). These products' sensory quality was consumer-acceptable, and LAB starter and probiotic cultures > 6 log CFUs/mL

survived storage, confirming their functional and probiotic qualities (Baloš et al. 2023).

Since donkey milk is in short supply, preserving it to keep it fresh for longer is crucial. Donkey milk can be bought in various forms, including raw, pasteurized, and ultra-high-temperature (UHT) versions. Other ways of donkey milk storage include freezing, freeze-drying (lyophilizing), and powdering (Papademas et al. 2022; Baloš et al. 2023). Donkey milk's basic components are stable through heating and storing. The nutritional value of fat and the overall composition of the food is unaffected by further freezing or refrigeration (Martini et al. 2018b).

Donkey milk was used by Tidona et al. (2015) to create a drink that was fortified with sunflower oil. Donkey milk naturally has low-fat content; however, adding sunflower oil to an emulsion raised various lipid-quality indicators and made the milk more viscous and stretchier. Pure camel chymosin, which clogs donkey milk casein micelles, was utilized to make soft cheese from raw donkey milk. Due to its reduced casein and total solids concentration, donkey milk yields extremely little cheese (Cimmino et al. 2023). Instead of egg lysozyme, donkey milk can reduce "blowing" in semihard and hard cheeses. Adding donkey milk to cow milk (2% to 8% v/v) increased lysozyme levels, and late-blowing defects in cheese decreased (Cosentino et al., 2015; Cosentino et al. 2016; Baloš et al. 2023). This was achieved without negatively impacting the sensory appeal of the cheese to customers.

Equine milk is typically produced on a small scale because of diversity in breed, feeding regime, etc., whereas cow milk is homogeneous in terms of fat and protein content due to its industrial processing on a large scale. A small but significant spread of such unique devices, each with the productivity of a jenny but with the potential to generate niche markets, is expected to join the market shortly. Donkey milk's appealing nutritional qualities could be used in various contexts (such as with the elderly population) or new food formulations, not just in baby diet treatment (Garhwal et al. 2022; Papademas et al. 2022; Baloš et al. 2023; Cimmino et al. 2023).

Conclusion and future prospects

Donkeys have been a part of human history. The mules help with farming and other outdoor tasks. Nonetheless, female donkeys are highly prized for their milk. The health benefits of donkey milk have been claimed to be similar to those of human breast milk. In the late 20th century, orphans and unwell children throughout Europe were fed donkey milk. Donkey milk is also helpful for people with cow milk protein allergies because it causes fewer allergic reactions. The mild sweetness makes this a good candidate for the kid's menu. Vitamin C (60 times more than cow's milk), E, D, E, omega-3 and omega-6 fatty acids, zinc, magnesium and calcium may all be found

in plenty in donkey milk, making it an excellent choice for a child's diet. Donkey milk is effective against various respiratory illnesses, including bronchitis, tuberculosis, cough, pneumonia, and asthma. It is also beneficial for patients with bone problems like osteoporosis due to the high levels of calcium and vitamin D. In the cosmetics industry; it is used in a wide range of soap and cream formulations. Donkey milk's physiological and nutritional advantages need more research and innovation.

Donkey milk contains immunoglobulins, vitamins, minerals and omega fatty acids. It's a good alternative for infants not breastfed because it's quickly absorbed. Children with an allergy to the protein found in cow's milk can also benefit from this camel milk. There are numerous aesthetic and therapeutic uses for donkey milk. It is a key ingredient in making dairy goods like ice cream, cheese, milk powder, yoghurt, and more. Further research into the healing and nutritional benefits of donkey milk is encouraged. Also, efforts should be made to lower the price of donkey milk so that it is affordable even for those on tight budgets. We must know that donkey milk can be part of a healthy diet.

Donkey milk resembles human milk more than ruminant milk. Protein, lactose, linolenic acid, vitamin C and mineral levels match breast milk. The protein part is more easily absorbed than proteins in bovine milk, and the total milk lipid content is lower than that of human and bovine milk. Current research has demonstrated its usefulness as a vitamin D source. Donkey milk is suitable for kids allergic to bovine milk proteins. As a result, it is suggested that this milk can be used in paediatrics, and it has the potential to serve as a superior substrate to cow's milk in the production of infant formulae. Adequate fat increases and alterations in certain fatty acid levels are necessary for this formulation. Because of its vitamin D concentration and its anti-inflammatory, anticancer, and hypolipidemic activities (all of which have been demonstrated in experimental models), it may help treat obesity and the care of the aged. Donkey milk would be yet another alternative food with consumers' health in mind. New well-designed clinical studies in vulnerable populations are needed to validate and update the putative health benefits.

Acknowledgement

All the authors acknowledge and thank their respective Institutes and Universities.

Author's contribution

All the authors contributed significantly.

Funding

This is a compilation written by its authors and required no substantial funding to be stated.

Disclosure statement

All authors declare that there exist no commercial or financial relationships that could, in any way, lead to a potential conflict of interest.

References

- Aspri, M., Economou, N., & Papademas, P. (2017). Donkey milk: An overview on functionality, technology, and future prospects. *Food Reviews International*, 33(3), 316-333. <https://doi.org/10.1080/87559129.2016.1175014>
- Baloš, M.Ž., Pelić, D.L., Jakšić, S., & Lazić, S. (2023). Donkey Milk: An Overview of its chemical composition and main nutritional properties or Human Health Benefit Properties. *Journal of Equine Veterinary Science*, 121, 104225. <https://doi.org/10.1016/j.jevs.2023.104225>
- Bertino, E., Agosti, M., Peila, C., Corridori, M., Pintus, R., & Fanos, V. (2022). The donkey milk in infant nutrition. *Nutrients*, 14(3), 403. <https://doi.org/10.3390/nu14030403>
- Bhardwaj, A., Pal, Y., Legha, R.A., Sharma, P., Nayan, V., Kumar, S., Tripathi, H., & Tripathi, B.N. (2020). Donkey milk composition and its therapeutic applications. *Indian Journal of Animal Sciences*, 90(6), 837-841.
- Brumini, D., Criscione, A., Bordonaro, S., Vegarud, G.E., & Marletta, D. (2016). Whey proteins and their antimicrobial properties in donkey milk: a brief review. *Dairy Science & Technology*, 96, 1-14. <https://doi.org/10.1007/s13594-015-0246-1>
- Chandran, D., & Radhakrishnan, U. (2019). Lactoferrin: A General Review. *International Journal of Pharmaceutical Sciences Review and Research*, 58(2), 65-75.
- Chandran, D., Radhakrishnan, U., & Eldho, L. (2020). Characterization of Malabari goat lactoferrin and its pepsin hydrolysate. *Journal of Veterinary and Animal Sciences*, 51(1), 40-47.
- Chandran, D., Lejaniya, A.S., Yattoo, M.I., Mohapatra, R.K., & Dhama, K. (2021). Major health effects of casein and whey proteins present in cow Milk: A narrative review. *The Indian Veterinary Journal*, 98(11), 9-19.
- Cimmino, F., Catapano, A., Villano, I., Di Maio, G., Petrella, L., Traina, G., Pizzella, A., Tudisco, R., & Cavaliere, G. (2023). Invited review: Human, cow, and donkey milk comparison: Focus on metabolic effects. *Journal of Dairy Science*. <https://doi.org/10.3168/jds.2022-22465>
- Conte, F., & Panebianco, A. (2019). Potential hazards associated with raw donkey milk consumption: A review. *International Journal of Food Science*, <https://doi.org/10.1155/2019/5782974>
- Cosentino, C., Paolino, R., Valentini, V., Musto, M., Ricciardi, A., Adduci, F., D'adamo, C., Pecora, G., & Freschi, P. (2015). Effect of jenny milk addition on the inhibition of late blowing in semihard cheese. *Journal of Dairy Science*, 98(8), 5133-5142. <https://doi.org/10.3168/jds.2015-9458>
- Cosentino, C., Faraone, D., Paolino, R., Freschi, P., & Musto, M. (2016). Sensory profile and acceptability of a cow milk cheese manufactured by adding jenny milk. *Journal of Dairy Science*, 99(1), 228-233. <https://doi.org/10.3168/jds.2015-10107>
- Cosentino, C., Paolino, R., Rubino, M., & Freschi, P. (2022). Effect of the addition of donkey milk on the acceptability of caciotta cow cheese. *Animals*, 12(11), 1444. <https://doi.org/10.3390/ani12111444>
- Derdak, R., Sakoui, S., Pop, O.L., Muresan, C.I., Vodnar, D.C., Addoum, B., Vulturar, R., Chis, A., Suharoschi, R., Soukri, A., & El Khalfi, B. (2020). Insights on health and food applications of Equus asinus (Donkey) milk bioactive proteins and peptides—an Overview. *Foods*, 9(9), 1302. <https://doi.org/10.3390/foods9091302>
- Garhwal, R., Sangwan, K., Mehra, R., Kumar, N., Bhardwaj, A., Pal, Y., Buttar, H.S., & Kumar, H. (2022). A systematic review of the bioactive components, nutritional qualities and potential therapeutic applications of donkey milk. *Journal of Equine Veterinary Science*, 115, 104006. <https://doi.org/10.1016/j.jevs.2022.104006>
- Karami, Z., & Akbari-adergani, B. (2019). Bioactive food derived peptides: A review on correlation between structure of bioactive peptides and their functional properties. *Journal of Food Science and Technology*, 56, 535–547. <https://doi.org/10.1007/s13197-018-3549-4>
- Kumar, K.S., Chandran, D., Yattoo, M.I., Mohapatra, R.K., & Dhama, K. (2021). Major health effects of casein and whey proteins present in cow milk: A narrative review. *Indian Veterinary Journal*, 98(11), 9-19.
- Kumari, A., & Sharma, P. (2021). The nutraceutical characteristics of donkey milk: A new insight for its potential probiotics. *Journal of Veterinary Medicine and Animal Sciences*, 4(2), 1074.
- Lejaniya, A.S., Chandran, D., Venkatachalapathy, T., Bashir, B.P., Kumar, M., Shanavas, A., Sureshkumar, R., Kumar, P.N., Sabareeshwari, V., Kumar, K.K., & Mohankumar, P. (2021a). Analysis of milk production performance of Attappadi Black, Malabari and cross-bred goats under organized farm conditions of Kerala. *The Indian Veterinary Journal*, 98(05), 13-19.
- Lejaniya, A.S., Chandran, D., & Geetha, R. (2021b). Recent trends in application of lactic acid bacteria (LAB) in dairy and biomedical

- industry: A critical review. *World Journal of Pharmaceutical Research*, 10(12), 577-591. doi: 10.20959/wjpr202112-21749.
- Madhusudan, N.C., Ramachandra, C.D., Udaykumar, N.D., Sharnagouda, H.D., Nagraj, N.D., & Jagjivan, R.D. (2017). Composition, characteristics, nutritional value and health benefits of donkey milk-a review. *Dairy Science & Technology*, 2017, hal-01538532. Retrieved from <http://efaidnbmnnnibpajpcgclefindmkaj/https://hal.science/hal-01538532v1/document>.
- Malissiova, E., Arsenos, G., Papademas, P., Fletouris, D., Manouras, A., Aspri, M., Nikolopoulou, A., Giannopoulou, A., & Arvanitoyannis, I.S. (2016). Assessment of donkey milk chemical, microbiological and sensory attributes in Greece and Cyprus. *International Journal of Dairy Technology*, 69(1), 143-146. <https://doi.org/10.1111/1471-0307.12245>
- Martini, M., Altomonte, I., Licitra, R., & Salari, F. (2018a); Nutritional and Nutraceutical Quality of Donkey Milk. *Journal of Equine Veterinary Science*, 65, 33–37. <https://doi.org/10.1016/j.jevs.2017.10.020>
- Martini, M., Altomonte, I., Tricò, D., Lapenta, R., & Salari, F. (2021). Current knowledge on functionality and potential therapeutic uses of donkey milk. *Animals*, 11(5), 1382. <https://doi.org/10.3390/ani11051382>
- Martini, M., Salari, F., Altomonte, I., Ragona, G., Piazza, A., Gori, R., Casati, D., & Brajon, G. (2018b). Effects of pasteurization and storage conditions on donkey milk nutritional and hygienic characteristics. *Journal of Dairy Research*, 85(4), 445-448. <https://doi.org/10.1017/S0022029918000687>
- Massouras, T., Bitsi, N., Paramithiotis, S., Manolopoulou, E., Drosinos, E.H., & Triantaphyllopoulos, K.A. (2020). Microbial profile antibacterial properties and chemical composition of raw donkey milk. *Animals*, 10(11), 2001. <https://doi.org/10.3390/ani10112001>
- Mottola, A., Alberghini, L., Giaccone, V., Marchetti, P., Tantillo, G., & Di Pinto, A. (2018). Microbiological safety and quality of Italian donkey milk. *Journal of Food Safety*, 38(3), 12444. <https://doi.org/10.1111/jfs.12444>
- Murua, A., Todorov, S.D., Vieira, A.D.S., Martinez, R.C.R., Cencič, A., & Franco, B.D.G.D.M. (2013). Isolation and identification of bacteriocinogenic strain of *Lactobacillus plantarum* with potential beneficial properties from donkey milk. *Journal of Applied Microbiology*, 114(6), 1793-1809. <https://doi.org/10.1111/jam.12190>
- Nazzaro, F., Fratianni, F., Orlando, P., & Coppola, R. (2010). The use of probiotic strains in the production of a donkey milk-based functional beverage. *International Journal of Probiotics & Prebiotics*, 5(2), 91.
- Papademas, P., Mousikos, P., & Aspri, M. (2022). Valorization of donkey milk: Technology, functionality, and future prospects. *JDS communications*, 3(3), 228-233. <https://doi.org/10.3168/jdsc.2021-0175>
- Patange, D.D.D., Virshasen Vinayak, D., Chandran, D., Kumar, M., & Lorenzo, J.M. (2022a). Comparative effect of cooling on the physico-chemical-sensory properties of ghee from cow and buffalo milk, and evaluation of the low-fat spread prepared from cow and buffalo milk ghee. *Food Analytical Methods*, 1-11. doi:10.1007/s12161-022-02312-4.
- Patange, D.D., Pansare, K.S., Kumar, M., Kumari, A., Kamble, D.K., Chandran, D., Gaikwad, N.B., Waghmare, R., & Lorenzo, J.M. (2022b). Studies on utilization and shelf life of *Piper betel* leaves added ghee-based low-fat spread. *Food Analytical Methods*, 1-12. doi: 10.1007/s12161-022-02400-5.
- Peng, S., Yang, Y., Li, S., Wu, Q., Shah, N.P., Wei, H., & Xu, F. (2014). Immunomodulatory activities of *Lactobacillus rhamnosus* ZDY114 and donkey milk in BALB/c mice. *International Dairy Journal*, 34(2), 263-266. <https://doi.org/10.1016/j.idairyj.2013.07.018>
- Perna, A., Intaglietta, I., Simonetti, A., & Gambacorta, E. (2015). Donkey milk for manufacture of novel functional fermented beverages. *Journal of Food Science*, 80(6), 1352-1359. <https://doi.org/10.1111/1750-3841.12862>
- Pilla, R., Dapra, V., Zecconi, A., & Piccinini, R. (2010). Hygienic and health characteristics of donkey milk during a follow-up study. *Journal of Dairy Research*, 77(4), 392-397.
- Prasad, B. (2020). Nutritional and health benefits of donkey milk. *Journal of Food Science and Nutrition Therapy*, 6(1), 22-25.
- Ragona, G., Corrias, F., Benedetti, M., Paladini, M., Salari, F., & Martini, M. (2016). Amiata donkey milk chain: animal health evaluation and milk quality. *Italian Journal of Food Safety*, 5(3). <https://doi.org/10.4081%2Fijfs.2016.5951>
- Saleena, L.A.K., Chandran, D., Geetha, R., Radha, R., & Sathian, C.T. (2022a). Optimization and identification of lactic acid bacteria with higher mannitol production potential. *Indian Journal of Animal Research*, 1, 8. doi: 10.18805/IJAR.B-4759.
- Saleena, L.A.K., Chandran, D., Rayirath, G., Shanavas, A., Rajalingam, S., Vishvanathan, M., Sharun, K., & Dhama, K. (2022b). Development of low-calorie functional yoghurt by incorporating mannitol producing lactic acid bacteria (*Leuconostoc*

- pseudomesenteroides*) in the standard yoghurt culture. *Journal of Pure and Applied Microbiology*, 16(1), 729-736. doi: 10.22207/JPAM.16.1.78.
- Souroullas, K., Aspri, M., & Papademas, P. (2018). Donkey milk as a supplement in infant formula: Benefits and technological challenges. *Food Research International*, 109, 416-425. <https://doi.org/10.1016/j.foodres.2018.04.051>
- Tafaro, A., Magrone, T., Jirillo, F., Martemucci, G., D'Alessandro, A.G., Amati, L., & Jirillo, E. (2007). Immunological properties of donkey's milk: its potential use in the prevention of atherosclerosis. *Current Pharmacology Design*, 13(36), 3711-3717. <https://doi.org/10.2174/138161207783018590>
- Tidona, F., Charfi, I., Povolò, M., Pelizzola, V., Carminati, D., Contarini, G., & Giraffa, G. (2015). Fermented beverage emulsion based on donkey milk with sunflower oil. *International Journal of Food Science & Technology*, 50(12), 2644-2652. <https://doi.org/10.1111/ijfs.12936>
- Vincenzetti, S., Pucciarelli, S., Polzonetti, V., & Polidori, P. (2017). Role of proteins and of some bioactive peptides on the nutritional quality of donkey milk and their impact on human health. *Beverages*, 3(3), 34. <https://doi.org/10.3390/beverages3030034>
- Vincenzetti, S., Santini, G., Polzonetti, V., Pucciarelli, S., Klimanova, Y., & Polidori, P. (2021). Vitamins in human and donkey milk: functional and nutritional role. *Nutrients*, 13(5), 1509. <https://doi.org/10.3390/nu13051509>
- Zhou, X., Tian, X., Song, L., Luo, L., Ma, Z., & Zhang, F. (2022). Donkey whey protein and peptides regulate gut microbiota community and physiological functions of D-galactose-induced aging mice. *Food Science and Nutrition*, 11(2), 752-764. <https://doi.org/10.1002/fsn3.3111>









Journal of Experimental Biology and Agricultural Sciences

<http://www.jebas.org>

ISSN No. 2320 – 8694

Positive impacts of integrating flaxseed meal as a potential feed supplement in livestock and poultry production: Present scientific understanding

Athira Rajan^{1†}, Devika V M^{1†}, Aysha Shabana^{1†}, Nayana Krishnan¹,
Krishnapriya N Anil¹, Rohith Krishnan¹, Baby Shajini Y¹, Bhadra S Dev¹,
Adinan J¹, Meenakshy S¹, Amrithendhu V R¹, Sandip Chakraborty² , Hitesh Chopra³ ,
Abhijit Dey⁴ , Anil K Sharma⁵ , Kuldeep Dhama^{6*} , Deepak Chandran^{1*} 

¹Amrita School of Agricultural Sciences, Amrita Vishwa Vidyapeetham University, Coimbatore, Tamil Nadu– 642109, India

²Department of Veterinary Microbiology, College of Veterinary Sciences and Animal Husbandry, R.K. Nagar, West Tripura, Tripura, Pin-799008, India

³Chitkara College of Pharmacy, Chitkara University, Punjab - 140401, India

⁴Department of Life Sciences, Presidency University, 86/1 College Street, Kolkata-700073, West Bengal, India

⁵Department of Biotechnology, Maharishi Markandeshwar University (Deemed to be University) Mullana-Ambala-133207, Haryana, India

⁶Division of Pathology, ICAR-Indian Veterinary Research Institute, Bareilly, Uttar Pradesh, India - 243122

[†]Authors contributed equally

Received – February 24, 2023; Revision – April 10, 2023; Accepted – April 29, 2023

Available Online – April 30, 2023

DOI: [http://dx.doi.org/10.18006/2023.11\(2\).264.279](http://dx.doi.org/10.18006/2023.11(2).264.279)

KEYWORDS

Flaxseed meal (FSM)

Chemical composition

Bioactive components

Livestock

Poultry

ABSTRACT

When it comes to food and fiber production, flaxseed (*Linum usitatissimum*) has been around the longest. Oil makes up over 41% of a flaxseed's total weight; of that, more than 70% is polyunsaturated. Protein, dietary fiber, α -linolenic acid (ALA), flaxseed gum, and many other beneficial compounds are abundant in flaxseed meal (FSM). There is as much as 30% crude protein in FSM. Therefore, FSM can serve as a source of excellent protein for livestock. FSM increases the efficiency and effectiveness of livestock and poultry farming. FSM can be used as an essential protein feed component in cattle and poultry farming, boosting production and profitability. Because it contains anti-nutritional ingredients such as cyanogenic glycosides, tannins, phytic acid, oxalic acid and an anti-vitamin B6 factor, the use of FSM in livestock and poultry diets is restricted. Animal nutritionists have recently shown a growing interest in reducing anti-nutritional elements and boosting FSM's nutritional value. Recently, fermented FSM has been used to feed cattle and poultry; hence its dietary benefits have not yet been fully assessed. The present article, therefore, addresses the chemical make-up, bioactive components, anti-nutritional aspects, and positive impacts of FSM in livestock and poultry production.

* Corresponding author

E-mail: c_deepak@cb.amrita.edu (Deepak Chandran);
kdhama@rediffmail.com (Kuldeep Dhama)

Peer review under responsibility of Journal of Experimental Biology and Agricultural Sciences.

Production and Hosting by Horizon Publisher India [HPI]
(<http://www.horizonpublisherindia.in/>).
All rights reserved.

All the articles published by [Journal of Experimental Biology and Agricultural Sciences](http://www.jebas.org) are licensed under a [Creative Commons Attribution-NonCommercial 4.0 International License](https://creativecommons.org/licenses/by/4.0/) Based on a work at www.jebas.org.



1 Introduction

In recent years, there has been an imbalance in the long-term supply and demand for conventional protein feed resources such as soybean meal. This has led to increased prices for feed and decreased long-term sustainability in the animal husbandry industry. Since traditional feed resources are limited, there is an immediate need to develop and employ non-conventional feed resources to improve the situation and reduce feed prices. In this scenario, different protein feed sources would be helpful in animal nutrition (Alagawany et al. 2015; Abd El-Hack et al. 2016; Deepak et al. 2020; Prakash et al. 2021a; Prakash et al. 2021b; Buttar et al. 2022; Chandran et al. 2022; Konavalov et al. 2022; Mitra et al. 2022).

One of the earliest oil-bearing crops cultivated worldwide was flaxseed. Flaxseed was grown on an estimated 3.39 million hectares globally between 2016 and 2020 (Cui et al. 2022). The top five nations producing flaxseed are Kazakhstan, the Russian Federation, Canada, China, and the United States of America, and global production has been hovering around 3000 kilotons for quite some time. Oil derived from flaxseed through pressing and refinement is a significant dietary supplement source of omega-3 PUFAs. Flaxseed meal (FSM) is a byproduct of processing flaxseeds for flaxseed oil, yet it still has a lot of nutritional value. The literature on FSM, however, is scant (Goyal et al. 2014). As with many other feed additives, FSM can be given to cattle and poultry as an alternative source of high-quality protein feed. Notably, there is the susceptibility of FSM to the variety of flax; origin climate; methods of oil extraction; and processes involved in production. These results in discrepancies in the nutrient composite and level of nutrition (Ye et al. 2022). While FSM has shown promise in the feed business, its widespread usage is hindered by cyanogenic glycosides (CGs), a potent anti-nutritional component in flaxseed. Reducing the amount of anti-nutritional elements in FSM increases its value as animal feed (Kumar et al. 2022; Kumari et al. 2022; Mueed et al. 2022).

Natural diets for livestock and poultry often include brown-seeded flaxseed (*Linum usitatissimum* L.), one of the most effective sources of omega-3 unsaturated fatty acids. As a source of n-3 PUFAs, FSM is considered superior to fish oil, corn, soybean or algae (marine). Polyunsaturated fatty acids (PUFAs) and α -linolenic acid (ALA), in particular, are abundant in most flaxseed species (Kajla et al. 2014; Lan et al. 2020; Chandran 2021). Flaxseeds are rich in ALA, an omega-3 fatty acid; flaxseed oil contains 45-52% ALA (Khan 2019). Almost every part of the flaxseed plant is helpful in some way for feeding livestock and poultry. Fibre extracted from the flax plant's stem is of the highest quality and durability. The seed provides easily absorbed proteins, anti-inflammatory lignans, and omega-3-rich oil. The oil and lignans found in flaxseed are essential for health,

and its high-quality protein and soluble fiber are bonuses. It also has great potential as a phenolic compound supplier. Flaxseed is rising in popularity as a functional food ingredient thanks to its high lignan, fiber, and linolenic acid content. It has been discovered that lignans can prevent cancer. Flaxseed's lignan phytoestrogens and omega-3 fatty acids are being researched for their possible chemoprotective benefits in humans and animals (Singh et al. 2011; Mueed et al. 2022).

In the commercial livestock and poultry industry, flaxseed is commonly used as an ingredient added to chicken diets to provide healthier products and enhance the food market. However, the effect of flaxseed on the productivity of laying hens may vary with factors like the breed of hens, the age of the hens, the composition of their diet, and the duration of the experiment. The flaxseed cake (FC), leftover after flaxseed oil extraction, is a high-quality protein food for cattle and poultry containing anywhere from 10.5 to 31% protein. Its high ALA residual oil content benefits animal well-being (Xu et al. 2022). Depending on the seed strain and processing settings, the amount of residual oil in FC can be increased from approximately 1% to over 16%. This makes FC also a potential method for increasing the amount of omega-3 fatty acids in eggs, milk and meat (Khan 2019). Recently, there has been an extended mismatch in supply and demand for traditional resources of protein feeds, leading to rising feed costs and reduced livestock and poultry production sustainability. Given the current resource scarcity of feed, increasing the development and usage of unconventional feed resources is essential to compensate for this. Adopting a different animal protein diet may be helpful here (Gutiérrez et al. 2010). FSM's potential as animal feed can be improved by minimizing its anti-nutritional components (Kumar et al. 2022). This review article examines the anti-nutritional characteristics, nutritional components, and preliminary use of FSM in several livestock species, including layer and broiler chickens, beef cattle, dairy pigs, and swine.

2 Chemical composition and bioactive compounds in flaxseed meal

Many nutrients, such as omega-3 PUFAs, fiber, and protein, can be found in FSM. The breakdown of the flaxseed's chemical composition and chemical structures of the major bioactive components in flaxseed are illustrated in Figure 1 and Figure 2, respectively. FSM has a nutritional value similar to soybean protein due to its high crude protein concentration (35-40%). Soybean meal is a source of protein, but FSM could serve the same purpose. FSM is high in protein, ALA, and dietary fiber. Flax seed meal's nutrient profile and density might vary depending on factors such as the flax variety used, the weather at the seed's place of origin, the oil extraction method, and the manufacturing process (Prakash et al. 2021a; Prakash et al. 2021b).

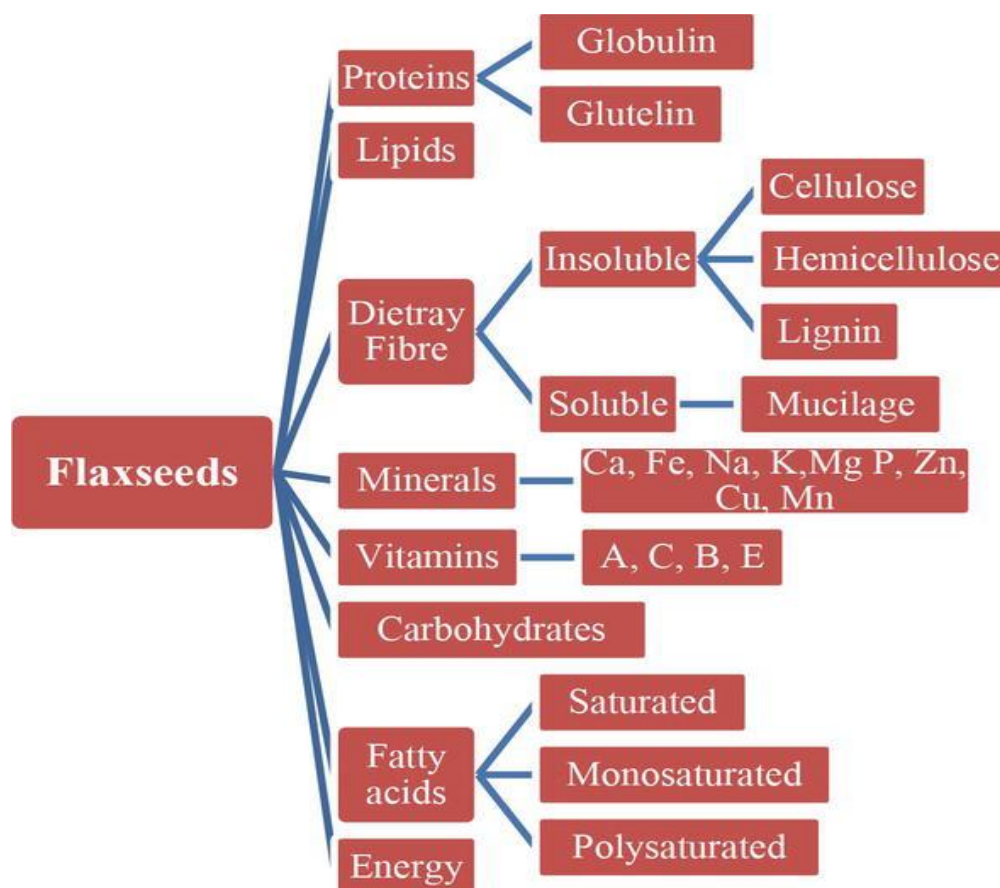


Figure 1 Chemical composition of flaxseeds

Proteins comprise roughly 23% of the weight of whole flaxseeds and as much as 35 to 40% of the weight of flaxseed meal, produced when the oil is removed. It has a good protein quality score because its amino acids are organized. A lysine-to-arginine ratio of 0.37 is heart-healthy because of its reduced atherogenic and lipidemic potential. Protein in FSM mostly takes the form of globulin and albumin (Xu et al. 2022). According to their solubility profiles, globulins and albumins can be compared to colinins and linins, respectively. A wide variety of amino acids, including those containing sulphur (like methionine and cysteine), branched-chain amino acids (like alanine, leucine, and isoleucine), and others (like lysine, tyrosine, and threonine), can be found in the human body. A large amount of amide is found in flaxseed because of its high concentration of storage proteins such as arginine, asparagines, aspartic acid, and glutamine (Wu et al. 2019; Mueed et al. 2022). There is an albumin found in plant seeds called conlinins. The sedimentation coefficient of 1.6-2 characterizes this peptide bond's composition. Increased disulfide linkages give these proteins a more structured form, with 26% helices and 32% structures making up their total molecular weight. Additionally, these albumins contain high concentrations of arginine, leucine, cysteine, alanine, and glutamine (Madhusudhan and Singh 1985; Mueed et al. 2022).

Proteins and peptides called cyclolinopeptides, orbitides, and linosurbs can be found in flaxseed. Around 25 different varieties of these compounds have been discovered (Dzuovor et al. 2018). Orbitides contain eight to ten different amino acids. Multiple therapeutic properties, such as immune suppression, anti-malarial, anti-tumour, and bone degeneration protection, have been attributed to these compounds (Shim et al. 2019; Mueed et al. 2022). Several health advantages have been linked to phenolic chemicals. Flaxseed contains many phenolic compounds, such as phenolic acids and lignans. Chlorogenic acid, vanillic acid, 4-hydroxy benzoic acid and coumaric acid were discovered to make up most of the phenolic acids in a Canadian flaxseed cultivar, with lignans making up the rest (Herchi et al. 2011; Bekhit et al. 2018; Mueed et al. 2022).

Flaxseed contains about 28% dietary fiber, which is made up of soluble and insoluble varieties. The soluble to insoluble fiber ratio might be anything from 20:80 and 40:60. Fiber is the seventh most important nutrient for a healthy diet. Flaxseed dietary fiber has many recognized benefits, including enhanced satiety, higher fat excretion, relief from constipation, and a direct effect on the intestinal microbiota that results in the formation of short-chain

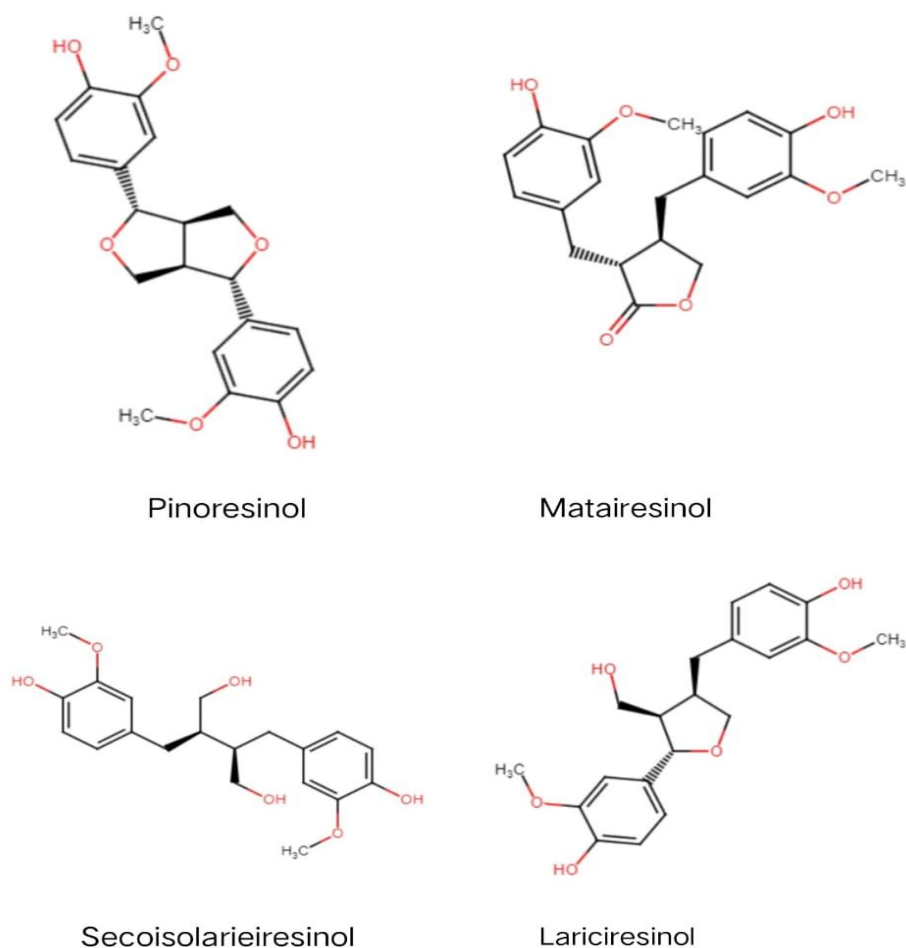


Figure 2 Chemical structures of major bioactive components present in flaxseed

fatty acids (SCFAs) that alter host metabolism. Because of its high fiber content, flaxseed is an excellent choice for supplementing livestock and poultry diets (Huang et al. 2022a).

Low-molecular-weight phenolic dimers derived from 2 and 3-dibenzylbutane are what we call lignans. Typically, they will be located in the flaxseed hull (Bekhit et al. 2018). Carotenoids, found in most fruits and seeds, are forty-carbon chemical compounds responsible for their red, yellow, and orange pigmentation and are also vitamin A precursors (Gul et al. 2015; Mueed et al. 2022). Carotene is a particularly important pigment since it has the highest pro-vitamin A activity (Yonekura and Nagao 2007). The carotenoid content of flaxseed is between 0.7 and 3.1 mg/kg. Carotenoids are crucial regarding flaxseed's high unsaturated lipid content because they protect against photooxidation. Based on their net charge, flaxseed mucilage (FM) polysaccharide fractions are acidic or neutral. Arabinoxylans are responsible for the neutral proportion that does not contain uronic acid, while galactose and galacturonic acid make up the bulk of the acidic percentage in modern pectic compounds (Liu et al. 2018).

Fatty acid composition is used to classify flaxseed oil (FO) into monounsaturated, polyunsaturated, and saturated varieties (Tvrzicka et al. 2011). The quantity of saturated fatty acids is low, but the number of unsaturated fatty acids is high (Yaqoob et al. 2016). Major components of FO extracted using petroleum ether were discovered to be linolenic acid (C 18:3, omega-3, 42.4%), linoleic acid (C 18:2, omega-6, 26.2%), palmitic acid (C 16:0, 12.9%), and stearic acid (C 18:0, 10.7%), as reported by Ishag et al. (2019). It appears that ALA is a PUFA that humans cannot generate themselves. ALA is converted into docosahexaenoic acid and eicosapentaenoic acid, two fatty acids crucial to body development, especially in the brain and skin (Yang et al. 2021). Because it contains such a high percentage of ALA (about 55% by weight), FSM is considered an excellent source of omega-3 PUFAs compared to soybean, fish oil, corn, or marine algae. Since the body cannot produce ALA in vivo, eating foods containing it is the only way to get enough (Mueed et al. 2022). The antibacterial, anti-inflammatory, and antioxidant effects of ALA have been the subject of several research, demonstrating their significance to livestock and poultry health. One of the n-3 PUFAs, ALA is

crucial for agricultural purposes. Supplementing livestock and poultry diets with omega-3 PUFA improves their growth and fatty acid metabolism, increasing the dietary worth of animal products, and it also offers a wider variety of FSM from which to choose when creating functional livestock and poultry feed ingredients (Huang et al. 2022b).

About 8% of a flaxseed's dry mass comprises flaxseed gum (FSG), which is found primarily in the seed's outer hull. Neutral arabinoxylan and acidic rhamnogalacturonan make up the bulk of FSG, making it a heteropolysaccharide. There are unique physiological roles for flaxseed polysaccharides. *In vitro*, soluble FSG has antioxidant properties by neutralizing free radicals such as 1,1-diphenyl-1-picrylhydrazyl (DPPH) and 2,2-azino-bis-3-ethylbenzthiazoline-6-sulfonic acid (ABTS) to create more stable products. It has also been shown *in-vitro* that soluble FSG has a powerful ability to bind bile acids, reducing the flow of bile acids from the liver to the intestines. This, in turn, generates SCFA profiles that are helpful to the health of the gastrointestinal tract and reduce cholesterol levels (Xu et al. 2022; Ye et al. 2022).

Important microbial metabolites of the organism, SCFAs, contribute to host metabolism by decreasing intestinal pH and may inhibit the growth of dangerous infections. Furthermore, FSG has the potential as a prebiotic for altering gut flora composition. By aiding in regulating lipid metabolism in the liver and reducing adipose tissue deposition, it can help prevent the detrimental effects of dyslipidemia in animals fed a high-fat diet. FSG may regulate gastrointestinal tract microbiota by reducing the Firmicutes/Bacteroidetes ratio, and it has been reported that feeding obese rats an optimum quantity of FSG can reduce obesity brought on by a high-fat diet. Therefore, FSG supplements can successfully treat and prevent diseases caused by oxidative damage, including weight loss and cancer protection (Attia et al. 2022; Mueed et al. 2022).

3 Anti-nutritional factors in flaxseed

Hydrocyanic acid, phytic acid, and anti-vitamin B6 (anti-VB6) are three anti-nutritional factors found in FSM that may have adverse effects on animals and restrict its use in animal diets even though it

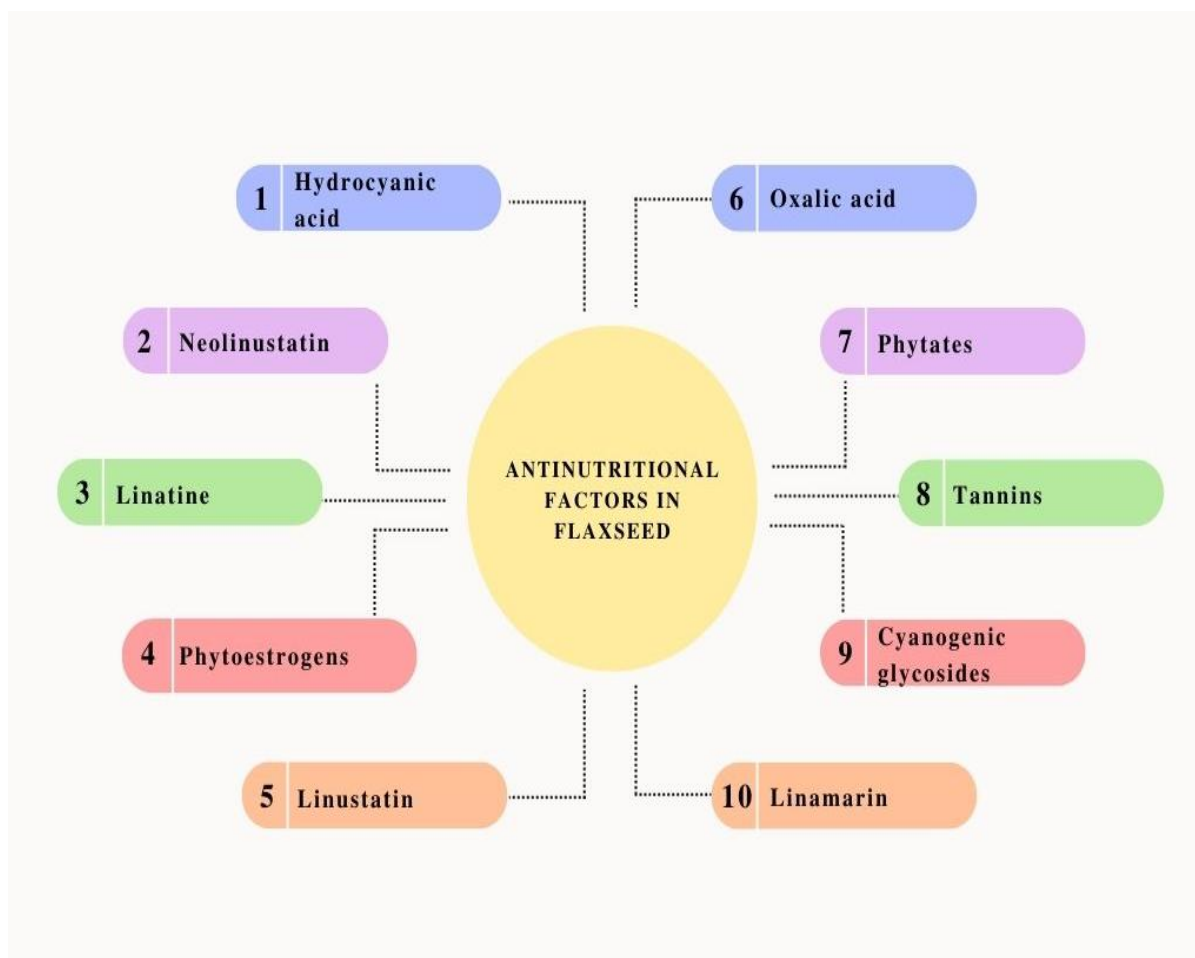


Figure 3 Major anti-nutritional factors present in flaxseed meal

contains many valuable additives and is a new source of protein feed in animal husbandry (Huang et al. 2022a). Flaxseed meal has many vital components that are detrimental to nutritional value, as depicted in Figure 3.

Cyanogenic glycosides (CGs) are present in flaxseed at concentrations ranging from 264–354 mg/100 g. Cyanates are a naturally occurring component of plant matter, and the hydrolysis of cyanates results in the formation of hydrogen cyanide. Cyanide (CN), when present in high numbers at a low dose, will be hazardous to humans on repeated exposure because it inhibits the cytochrome oxidase system involved in the respiratory chains (Enneking and Wink 2000). The total CG content of flaxseed ranges from 0.74 to 1.60 g/kg of cyanogenic nitrogen. The extraction method of flaxseed that presses the seeds results in a CG content of 394.99 mg/kg in the resulting flaxseed meal (Zhai et al. 2019). This finding is highly encouraging. Whole flaxseed contains between 250 and 550 mg/100 g of cyanogenic glycosides, whereas linustatin and neolinustatin have respective concentrations of 207 and 174 mg/100 g of seed. According to Park et al. (2005) research, the HCN concentration of linustatin and neolinustatin was reduced by more than 85% when flaxseed was cooked for more than two hours at a temperature of 200 °C. Because CGs and β -glucosidase are located in different parts of the FSM, it is not feasible for them to come into touch with one another. As a result, CG is non-toxic under normal conditions and does not emit HCN. However, once the animal has adequately chewed, β -glucosidase is presented with CG and makes complete contact with it. After this point, toxic HCN is created by enzymatic hydrolysis, which is likely detrimental to the animal's health. Extremely high concentrations of CG in food can readily cause acute poisoning, resulting in death between ten and twenty minutes after ingestion. In addition, chronic poisoning, goiter, growth retardation, neurological problems, and other undesirable effects can be caused by feeding animals feed containing CG over an extended period (Vetter 2000).

Plant tissues store and release oxalic acid and its salts as end metabolites. Because of the potential for adverse health effects, the amount of oxalic acid in the average person's diet has long been a source of concern. Oxalic acid is an absorption inhibitor linked to many health problems, including kidney stones, low calcium levels, and low iron levels (Palaniswamy et al. 2002). For humans, ingesting 5g or more of oxalic acid would be dangerous, but even low quantities have an adverse effect. Studies have indicated that a serving of flaxseed powder has between two and ten milligrams of oxalate (oxalate content), while a serving of roasted flaxseed has less than two milligrams of oxalate. The concentrations were 6.43–19.40 mg/100g for whole cooked samples, 9.03–11.90 mg/100g for row soy products, and 4.3–7.99 mg/100g for cooked samples. In moderation, these items are fine for healthy people to eat, but they

should be avoided by those who suffer from gout, rheumatoid arthritis, kidney illness, or chronic vulvar pain (vulvodynia).

A significant anti-nutritional component in FSM is phytic acid, with concentrations of 23 to 33 g/kg FSM (Oomah et al. 1996). Phytic acid has a potent chelating activity and can form stable complexes with mineral ions, proteins, and starch directly or indirectly (Akande et al. 2010). It has been shown to decrease piglets' apparent ileal digestibility (Woyengo et al. 2012) and to promote broilers' elimination of endogenous minerals and amino acids (Cowieson et al. 2004).

Tannins have an extraordinarily intricate and diverse chemical makeup. Proanthocyanidins and gallic acid polyesters are two categories that describe these compounds (Mahmut and Ayhan 2002). Flavanols are the source of concentrated tannins, while sugar esters (often glucose) are the source of hydrolyzable tannins (Bartosz et al. 2017). Researchers have found trypsin inhibitors in flaxseed; however, their activity is much lower than in soy and rapeseed (Bhatty 1993).

The concentration of anti-VB6 in FSM ranges from 177 to 437 μ g/g and is a dipeptide made up of proline and glutamine. Anti-VB6 factors can interact with the enzyme produced when vitamin B6 is phosphorylated. If the latter happens, animals will have trouble absorbing and using vitamin B6 because the loss of its physiological function has a knock-on effect on vitamin absorption and usage. Several studies have shown that feeding animals and birds an excessive amount of FSM can result in symptoms like decreased appetite, apathy, and neurological abnormalities, but FSM is still widely utilized in cattle and poultry production. These unfavourable effects can, however, be wiped out by properly incorporating vitamin B6. To that end, adding an FSM to the animal feed ration necessitates adding vitamin B6 in sufficient quantities (Mueed et al. 2022; Ye et al. 2022).

4 Beneficial Effects of Flaxseed in Livestock and poultry production

Particularly crude protein and energy are present in high quantity in FSM and thus can be used as animal protein feed. Replacement of soybean meal (SBM) in animal feed with other plant protein feed is a long-term goal and this goal can be achieved by using FSM (Hao et al. 2020). The high levels of ALA and DFs in FSM have garnered a lot of interest because of their potential to enhance the health of cattle and poultry significantly. FSM is a significant and valuable source of high-quality protein. FSM has been studied to increase the omega-3 PUFA content of animal products, but little is known about its potential usage as a dietary protein component in livestock and poultry feeding (Mueed et al. 2022). Table 1 summarises how flaxseed is used in the livestock and poultry feed industries, and Figure 4 depicts the potential positive impacts of flaxseed in animal husbandry and poultry.

Table 1 An overview of the applications of flaxseed in livestock and poultry

Animal	Source and quantity provided	Outcome	References
Dairy cattle	Whole flaxseed – 6 to 8%	Postpartum energy balance is enhanced	Gandra et al. (2016)
	Whole flaxseed- 4.8%	Enhanced liver antioxidant enzymatic activity and consumption of dry matter	Do Prado et al. (2016)
	Ground flaxseed – 6.3 to 7.3%	Concentration of omega-3 PUFA in milk is boosted.	Petit and C�ortes (2010)
	Flaxseed – 6.5%	Fatty acid content is increased in milk	Caroprese et al. (2010)
Beef cattle	Whole flaxseed- 3.6 to 18%	The accumulation rate of PUFAs differ between 14.3% and 17.6%	Mach et al. (2006)
	Flaxseed- 5%	Percentage of omega-3 PUFA increased in intramuscle fat.	Alberti et al. (2014)
Swine	Crushed flaxseed -6%	Enhanced ranges of omega-3 PUFA in adipose and muscular tissue	Kouba et al. (2003)
	Flaxseed – 2.5%	Notable improvement omega-3 PUFA growth in meat and fat level	Đordevi�c, et al. (2016)
	Flaxseed – 27.8%	Act as a source of protein for animal feed	Ndou et al. (2018)
	FSM – 1.5%	Considerably affects carcass fatty acid composition	Eastwood et al. (2009)
Broilers	FSM- 10%	FSM of 10%, boosted the meat's ALA content	Kumar et al. (2019)
	FSM- 5 to 15%	Fatty acid content is increased in meat	Mridula et al. (2011)
Layers	Flaxseed- 10%	Egg quality is increased and IgY content of egg yolk is enhanced	Cherian and Quezada (2016)
	Flaxseed- 5 to 15%	Concentration of omega-3 PUFA present in egg yolk was enhanced	Scheideler and Froning (1996)
	Flaxseed 10%	Concentration of both DHA and omega-3 PUFA content in eggs were increased	Mattioli et al. (2017)

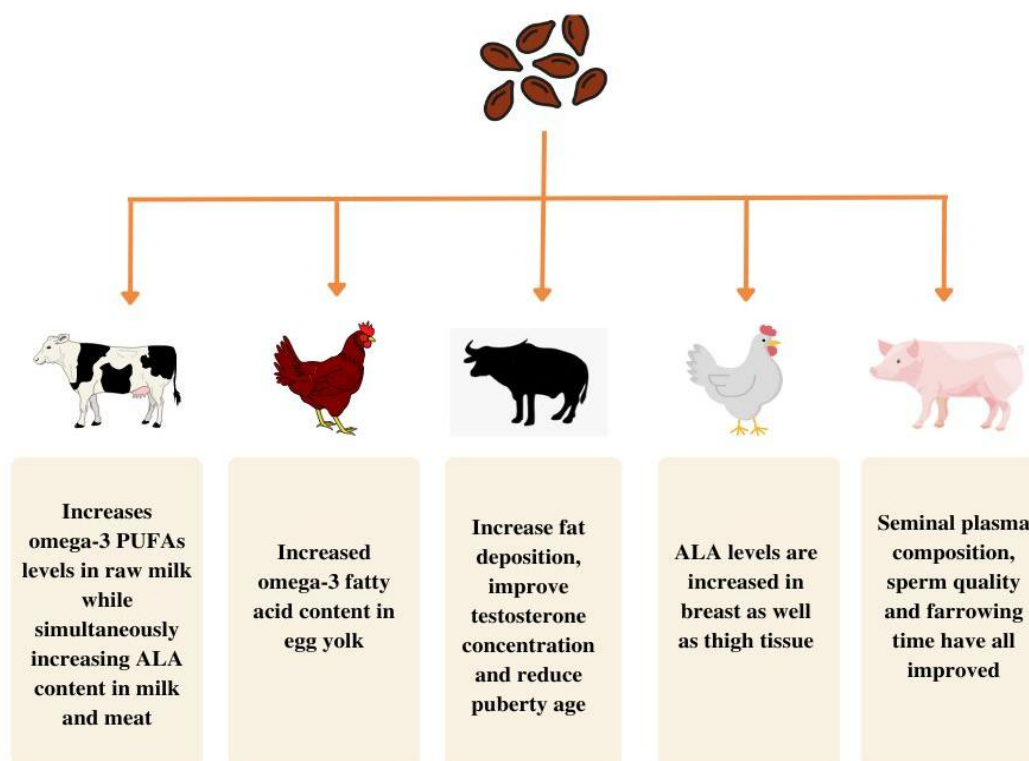


Figure 4 Beneficial effects of flaxseed meal upon integration as a potential feed ingredient in the livestock and poultry production

5 Beneficial Effects of Flaxseed on dairy cattle production

Most research and development efforts devoted to the beneficial effects of FSM in ruminants have focused on dairy cattle. Feeding dairy cows properly is essential during milk production since diet has a major impact on milk's nutrient profile. It's common knowledge that the omega-3 PUFAs found in flaxseed positively affect human health. Therefore, there is growing interest in animal production in the generation of milk high in omega-3 PUFAs by supplementing the diet with flaxseed to improve human health. Numerous studies have demonstrated that feeding flaxseed to dairy cows is an effective strategy to increase milk's omega-3 PUFA content. Several studies have also focused on the period between the end of gestation and the beginning of lactation in dairy cows. At this time of year, dairy cows are especially vulnerable to developing metabolic and viral problems or possibly dying from them (Zachut et al. 2010; Gandra et al. 2016; Huang et al. 2022a). Again, due to the richness of flaxseed in n-3 PUFA, it is often introduced into the diet of dairy cows to increase the n-3 PUFA level in milk. Hence, the introduction of both whole and ground flaxseeds in the dairy cows' diet has been done to enrich the milk from the nutritional aspect (Isenberg et al. 2019; Huang et al. 2022b). Commonly used for its fatty acid content, flaxseed may help early nursing calves achieve a more positive energy balance. Several studies have found that dairy cows whose diets included flaxseed throughout the transition period had greater increases in liver glycogen and antioxidant activity following calving and lower triglyceride levels. It's possible that this could help in the battle against liver fat. The fatty acid profile of milk can be changed, lipid accumulation in the liver can be reduced, and fatty liver disease can be avoided if dairy cows are fed flaxseed, as has been proven in previous studies (Petit and Côrtes 2010; Zachut et al. 2010; Jahani-Moghadam et al. 2015; Ye et al. 2022). All of these advantages suggest that flaxseed may play a beneficial function in the well-being of cows.

Milk's nutrient content is boosted when cows are fed flaxseed, leading to other positive changes in milk's composition that are good for human health. Feeding extruded flaxseed (EF) to cows has been observed to increase the quantity of PUFA in their milk (Zachut et al. 2010). In addition to whole flaxseed, flaxseed oil (FO) and FSM can also be fed to cows. After FO is taken out, all that's left is FSM. FSM is high in protein and fiber while being low in crude (Gagnon et al. 2009). Goodridge et al. (2001) found that lactating dairy cows given either 1.76 or 3.53 pounds of flax-protected casein per pound of milk fat generated, and Ward et al. (2002) found that a meal consisting of salt (or linoleum, a flax cultivar), flax, and canola at 8 percent DM increased milk fat production in lactating dairy cows. Goodridge et al. (2001) found that a linear increase in ALA levels in milk occurred in response to a rise in flax consumption. Feeding EF to Holstein Friesian cows accelerated their ovulation and reduced the number of cyclic

follicles they experienced. In a study by Jahani-Moghadam et al. (2015), pregnant heifers fed EF, and those not fed EF had identical open rates, service rates, and conception rates. Flax seed was used as a supplement for three types of cattle (Holstein Friesian, Jersey, and Friesian-Sahiwal crossbred) for nine weeks. Parameters related to semen quality were monitored weekly. Several characteristics of fresh semen were evaluated, including its volume, concentration, mass motility, and percentage motility (Khan et al. 2015). The quality of sperm collected after being frozen has been shown to increase in cattle (Gholami et al. 2010). It is possible to boost the omega-3 fatty acid content of fortified dairy products by feeding whole, unprocessed flaxseed to dairy cows, and thus could have a positive impact on human health. Enterolactone may affect milk production if the carbohydrate composition of FSM-based diets offered to dairy cows is changed (Brito et al. 2015). Methane generation can be reduced by eating a diet enriched with flax seeds (Li et al. 2012).

6 Beneficial Effects of Flaxseed on beef cattle production

Rumen bacteria are killed off when microbial lipases in cattle combine with rumen lipids to create PUFAs (Prieto et al. 2017). To reduce the harmful consequences, these microorganisms biohydrogenate PUFAs into less harmful saturated fatty acids, most notably 18:0. Absorption occurs in the lower stomach, where the remaining PUFA biohydrogenation intermediates (PUFA-BHI) are incorporated into tissues like muscle. Therefore, beef is abundant in PUFA-BHI, such as vaccenic acid and ruminic acid (Scollan et al. 2006). Increasing the proportion of omega-3 PUFAs in intramuscular fat and decreasing the omega-6/omega-3 PUFA ratio increased fat deposition when young bulls were fed a diet containing 5% flaxseed (Barahona et al. 2016). Feeding EF before hay in a non-total mixed diet (non-TMR; non-total mixed ration) would increase the amounts of 18:3 omega-3 fatty acid (linolenic acid) and the BHI in beef while decreasing the degree of biohydrogenation in the rumen (Vahmani et al. 2017). To boost the nutrient density of beef, flaxseed is often fed to cattle. This increases the amount of omega-3 PUFA in the meat. The fat deposition was increased, the fraction of omega-3 PUFAs (primarily ALA) contained in intramuscular fat increased, and the ratio of omega-6/omega-3 PUFA content decreased by 5% flaxseed was added to the concentrate diet for young bulls (Alberti et al. 2014). Including 10% whole flaxseed in beef cattle diets has improved beef's organoleptic qualities, such as reducing fat odour and enhancing beef flavor (Barahona et al. 2016). Whole flaxseed supplementation in Holstein Friesian cattle dramatically increased omega-3 PUFAs in beef (Mach et al. 2006). When beef cattle were fed with Hereford 907 gram/day, Angus cattle 454 gram/day for 3 days, followed by 907 gram/day of ground, flaxseed resulted in increased omega-3 PUFA levels and peroxisome proliferator-activated receptor gamma (PPAR γ) gene expression in the longissimus muscle. When 5% flaxseed was fed, it increased

omega-3 PUFA content (mostly ALA) in intramuscular fat. 3.6%, 11.2%, and 18% of whole flaxseed enhanced the deposition rate of PUFAs in beef ranging from 14.3% to 17.6%. Also, 10 - 15% of flaxseed decreased feed intake with no negative impacts. Although excessive amounts of FSM will limit feed intake, adding flaxseed or FSM to the diets of beef cattle is generally seen as beneficial.

7 Beneficial Effects of Flaxseed on swine production

Since pigs only have one stomach, their dietary ALA is more readily available for Absorption since it is not biohydrogenated before reaching the small intestine. Linolenic acid was found in increasing amounts and showed a linear increase in both back fat and bacon over time. Grower pigs fed a diet containing up to 15% FSM had their linolenic acid content increase from 11 mg/g back fat to 48 mg/g back fat (Mueed et al. 2022; Xu et al. 2022). Leterme et al. (2007) found that pigs fed diets containing up to 15% full-fat flaxseed or flaxseed flour continued to thrive as long as the feeds were well-balanced in nutrient supply and digestible amino acids.

By lowering prostaglandin F2 α (PGF2 α) and prostaglandin E2 (PGE2) production, omega-3 PUFAs supplementation in early pregnancy in gilts may increase the likelihood of successful embryo development and birth. In addition, eicosapentaenoic acid (EPA) concentrations in the piglets' liver, muscle, and adipose tissue can be enhanced by supplementing the sow's diet with flaxseed oil, boosting omega-3 PUFA diets during lactation increases subsequent litter size born, both live born and total piglets born. Previous research into the effects of feeding sows and their piglets a diet containing 6.5% FSM during late pregnancy and lactation indicated that adding FSM could boost omega-3 PUFAs and lower the omega-6/omega-3 fatty acids ratio in the sows' milk within 20 days of lactation. It may also help piglets recover from weaning and grow faster afterwards (Sun and Kim 2020; Xu et al. 2022). There is an improvement in the IgG level in milk along with improved growth performance of the suckling piglets by supplementing omega-3 PUFAs (coated) in the sow diet using flaxseed oil (Xu et al. 2022).

According to Kaur et al. (2021), there were no adverse effects when sows' diets were supplemented with flaxseed at a rate of 0.5% of the dry matter from day 1 of lactation until the day of the subsequent farrowing. The sows' body composition parameters, hormonal balance, capacity for procreation and non-esterified fatty acids (NEFAs) concentration may have even improved. The study also found that varying the amount of expanded flaxseed in a sow's diet had no discernible influence on litter size, mean birth weight, or mean daily growth but did alter milk fatty acid composition and omega-3 PUFA status in newborn and adult piglets. According to the literature, feeding sows flaxseed or FSM during the last few months of pregnancy and while they are nursing their piglets can

have positive effects on the health of the sows and the piglets, as well as increase economic efficiency (Mueed et al. 2022; Xu et al. 2022). However, feeding the sows the right amount of FSM is important to prevent any adverse side effects on the piglets.

8 Beneficial effects of flaxseed on broiler production

Feeding flaxseed to broilers 14 days before slaughter improves their meat quality. To increase omega-3 fatty acid enrichment without negatively impacting animal health, chicken breeders are advised to give their birds FO or powdered flaxseed 14-21 days before slaughter. Flaxseed consumption has been linked to increased accumulation of docosahexaenoic acid. Chicks fed 10% of their total dry matter as pelletized flaxseed gained weight and ate more. The nitrogen and energy efficiency gains from pelletizing are undeniable. Increased feed density and broken grain cell walls from damp heat improve digestibility. The villus height increased significantly, suggesting beneficial effects on duodenal and jejunal morphology that may improve nutrient absorption (Hernandez 2013; Attia et al. 2022). Broilers' FA profiles were significantly enhanced after being fed a 10% FSM diet for around 3 weeks, and the amount of cholesterol and fat in the meat was reduced, which is good for the birds' health (Xu et al. 2022). Breast meat might have more omega-3 PUFAs deposited on it if flaxseeds are fed to the animal.

Chicken breast and thigh with flax seed added to have more omega-3 fatty acids, less blood protein, and more liver enzymes (Xu et al. 2022). Feed conversion rate (FCR), protein efficiency ratio, and energy efficiency ratio were significantly increased in poultry birds fed with 5g and 10g flaxseed/kg feed meal. Including 2% FO in broiler feed has reduced the lag in embryonic mortality (Pliego et al. 2022). Adding 15 percent flax to broiler feed increased mean body weight while decreasing digestible energy and ether extract content. Broilers fed flax-enriched diets had the highest quality carcasses, with a high percentage of muscles and low levels of abdominal fat. It also led to an 11% rise in iron in the pylon muscles. Improved intestinal morphometric measures and decreased feces viscosity were only two of the many ways broiler chickens' digestive health benefited from adding 10 - 15% flaxseed to their meals. Feeding broiler chickens between 21 and 42 days of age a diet with 15% flaxseed increased body weight, feed intake, and various slaughter characteristics. The protein and nutrient content of chicken muscles were also enhanced. Preliminary data from production suggests that using flaxseeds in one's diet is beneficial, as doing so increases the nutritional content of meat (Zajc et al. 2020).

9 Beneficial effects of flaxseed on layer production

Linolenic acid, a rich source of flaxseed, has been shown to raise eggs' omega-3 fatty acid content significantly. In the designer food

sector, eggs are routinely fortified with linolenic acid from flaxseed to ensure they are safe for human consumption (Beheshti and Cherian 2017). Since laying hens' gizzards can crush coarse seed, it stands to reason that flaxseed, which has a softer seed coating, may also be pulverized sufficiently for digestion. Yolk omega-3 PUFA content may be significantly enhanced to 6.83% when flaxseed content is increased to 15% without affecting layer omega-3 PUFA content. Efficient Absorption of dietary omega-3 PUFAs by layers allows the fatty acids to be transported to the egg yolk. PUFA omega-3-enhanced eggs and meat products have been made with flaxseed for quite some time. Egg production and consumer acceptance of marketed eggs may be impacted by flaxseed's flavor and aroma when consumed by layers at levels above 10%. Incorporating flaxseed into feed benefits egg production by increasing the nutritional value for human health, not because of the processing cost (Scheideler and Froning 1996; Attia et al. 2022).

There was no adverse effect on laying parameters when flaxseed was added to the diet of laying hens. On the other hand, adding flaxseed has been demonstrated to affect hen production performance in several trials negatively. The omega-3 PUFA content of egg yolk was increased after being supplemented with flaxseed at 5, 10, and 15%. The percentage and weight of egg yolks had decreased, while ALA and EPA levels had increased dramatically when 10% whole product or ground flaxseed was included in layers feed. Egg quality was improved, and the amount of healthy ALA in eggs was increased due to flaxseed supplementation, which increased the level of egg yolk antibodies (IgY) in the yolk. Adding 10% flaxseed to a chicken's diet has increased the amount of DHA in the egg yolk. Enzyme supplementation of 10% flaxseed boosted feed efficiency and mitigated flaxseed's deleterious effects. Immune function, lipid profiles, yolk color, and reproductive success were all improved with supplementation of 12% soaked flaxseed meal (Gregory et al. 2013; Xu et al. 2022).

When it comes to removing the flaxseed's anti-nutritional components, extrusion is a simple and inexpensive method. Flaxseed grains' bioavailability and Absorption can be improved by using an extrusion technology that releases the intercellular oil found in these seeds while eliminating most of their anti-nutritional components at high pressure and temperature (Chandran 2021). Although EF has far less tannin and hydrocyanic compounds, feeding it to layers at more than 20% decreased laying performance. It has been established that adding an EF product to layer feed raises the amount of omega-3 PUFAs in egg yolk without reducing overall egg production. Metabolizable energy in EF diets dropped with increasing EF addition rates, and chickens fed EF didn't eat more to make up for the difference. However, the animals consumed more of the

feed when the flaxseed (10% and 20%) feeds had less metabolizable energy than the control diet. Increased omega-3 PUFA were seen in the egg yolks of chickens fed either of the EF diets (Attia et al. 2022; Mueed et al. 2022). The yolks of chickens fed EF contained higher omega-3 PUFA because of the addition of ALA and DHA, but ALA deposition appears more significant. LinPRO, a flaxseed supplement, boosted omega-3 PUFA content in the yolk by 96% and 154%, respectively, when given to layers at 7.5% and 15% concentrations. No adverse effects on layer performance or egg characteristics were seen when EF was supplemented at up to 22.5% in the diet of layers. Energy utilization is impacted by the variation in EF between meals (i.e. 15% and 22.5%) (Huang et al. 2018; Prakash et al. 2021b; Xu et al. 2022). This is mostly due to lower levels of metabolizable energy in the flaxseed-fed meals.

It is interesting to note that when flaxseed meal is added to the diet of brown-layer hens, the digestibility of crude protein decreases, while at the same time, there is a rise in the production of eggs and the performance of the hen (Popescu et al. 2021). This was found in research conducted by Popescu et al. (2021).

Mild changes in adult laying hens' body weight have been seen after introducing flax seeds into their diet. In contrast to managed hens, EF-fed layer hens used less metabolizable energy because they lost body weight. Anti-nutritional elements such as oxalic acid, cyanogenic glycosides, tannins, and phytic acid can be found in flaxseed. Mucilage, a type of water-soluble polysaccharide found primarily in flax seeds, may improve the viscosity of digestive juices. The quality and quantity of eggs laid by hens fed flaxseed for an extended period may also suffer. Adding 10% flaxseed to the diet of laying hens has been shown to produce eggs with health benefits for consumers (Prakash et al. 2021a; Prakash et al. 2021b; Mueed et al. 2022; Xu et al. 2022).

10 Possibilities for utilizing fermented flaxseed meal in livestock and bird production

Despite the widespread reporting of FSM's inclusion in livestock and poultry feeds and the purported benefits of doing so, there are strict limits on the amount of FSM that may be added to an animal's diet without causing harmful consequences. Producers are more likely to include FSM in animal diets if they see proof that it can considerably replace soybean meal and cut feed costs without severely impacting animal growth performance. Anti-nutritional components in FSM are being degraded through microbial fermentation, and this process is already underway with promising results (Deepak et al. 2020; Chandran 2021; Kumar et al. 2022; Kumari et al. 2022). The current issues with integrating FSM in Livestock and poultry production can be overcome if the technology for the microbial fermentation of FSM utilized in animal and poultry feed develops to its full potential. Microbial

fermentation technology can break down the anti-nutritional components in FSM, allowing for the full utilization of the feed's nutritional potential and positively affecting animal palatability, immunity, and productivity. Additionally, this can eventually raise the percentage of FSM as an alternative to soybean meal in animal diets. When fermented, however, FSM's many functional components (PUFAs, fiber, etc.) work together with the probiotic bacteria to great effect. The value of FSM will be increased, and improved feeding effects will be obtained since the original beneficial nutrients will be preserved and various beneficial microbial metabolites may also be produced (Huang et al. 2022a; Mueed et al. 2022; Xu et al. 2022).

Conclusions

FSM can be utilized as an essential protein feed component to improve protein feed consumption in livestock and poultry husbandry. Livestock and poultry should not be given more than the recommended amount of flaxseed meal as a supplement, as doing so can have adverse effects. In addition to its potential application as a novel protein feed element in place of soybean meal, FSM may also be improved through microbial fermentation for increased use in cattle and poultry production. However, it's essential to remember that research into the nutritional value of fermented FSM in Livestock and poultry is still in its infancy, and its use is still quite uncommon. There is still a need for a thorough chemical study of fermented FSM and a database on the dietary value of fermented FSM to establish an accurate feed formula. More study is required to confirm the usefulness of fermented FSM, show that it has no detrimental effects on feed conversion rate (FCR) and growth performance, and determine the optimal amount to add to animal feed. Important factors influencing the application of fermented FSM include the identification of strains with a high capacity for beneficial metabolites production, deterioration of nutrient-depleting anti-nutrient factors, improving the raw materials' nutritional value, and elevating the fermentation process to a higher level so that its large-scale production does not adversely affect the overall fermentation effect.

Acknowledgement

All the authors acknowledge and thank their respective Institutes and Universities.

Author's contribution

All the authors contributed significantly.

Funding

This is a compilation written by its authors and required no substantial funding to be stated.

Disclosure statement

All authors declare that there exist no commercial or financial relationships that could, in any way, lead to a potential conflict of interest.

References

- Abd El-Hack, M.E., Alagawany, M., Farag, M.R., Tiwari, R., Karthik, K., Dhama, K., Zorriehzahra, J., & Adel M (2016). Beneficial impacts of thymol essential oil on health and production of animals, fish and poultry: a review. *Journal of Essential Oil Research*, 28(5), 365-382. <https://doi.org/10.1080/10412905.2016.1153002>
- Akande, K.E., Doma, U.D., Agu, H.O., & Adamu, H.M. (2010). Major antinutrients found in plant protein sources: Their effect on nutrition. *Pakistan Journal of Nutrition*, 9, 827-832 <https://dx.doi.org/10.3923/pjn.2010.827.832>
- Alagawany, M., Farag, M.R., Dhama, K., Mohamed E. Abd El-Hack, Tiwari R., & Alam, M. (2015). Mechanisms and beneficial applications of resveratrol as feed additive in animal and poultry nutrition: A review. *International Journal of Pharmacology*, 11(3), 213-221. DOI: 10.3923/ijp.2015.213.221
- Alberti, P., Beriain, M.J., Ripoll, G., Sarries, V., Panea, B., Mendizabal, J.A., Purroy, A., Olleta, J.L., & Sanudo, C. (2014). Effect of including linseed in a concentrate fed to young bulls on intramuscular fatty acids and beef color. *Meat Science*, 96, 1258-1265. <http://dx.doi.org/10.1016/j.meatsci.2013.11.009>
- Attia, Y.A., Al-Harhi, M.A., Sagan, A.A.A., Abdulsalam, N.M., Hussein, E.O., & Olal, M.J. (2022). Egg production and quality, lipid metabolites, antioxidant status and immune response of laying hens fed diets with various levels of soaked flax seed meal. *Agriculture*, 12(9), 1402. <https://doi.org/10.3390/agriculture12091402>
- Barahona, M., Olleta, J.L., Sañudo, C., Albertí, P., Panea, B., Pérez-Juan, M., Realini, C.E., & Campo, M.M. (2016). Effects of whole linseed and rumen-protected conjugated linoleic acid enriched diets on beef quality. *Animals*, 10(4), 709-717. <https://doi.org/10.1017/S1751731115002591>
- Bartosz, A., Judy, S., Veikko, K., Sylwia, A., & Aino, S. (2017). Tannins and their complex interaction with different organic nitrogen compounds and enzymes. *Old Paradigms versus Recent Advances*, 6(5), 610-614. <https://doi.org/10.1002/open.201700113>
- Beheshti, M., & Cherian, G. (2017). Use of flaxseed in poultry feeds to meet the human need for n-3 fatty acids. *World's Poultry Science Journal*, 73, 1-10. <https://doi.org/10.1017/S0043933917000721>

- Bekhit, AEDA, Shavandi, A., Jodjaja, T., Birch, J., Teh, S., Ahmed, I.A.M., Al-Juhaimi, F.Y., Saeedi, P., & Bekhit, AA (2018). Flaxseed: Composition, detoxification, utilization, and opportunities. *Biocatalysts and Agricultural Biotechnology*, *13*, 129–152.
- Bhatty, R. S. (1993). Further compositional analyses of flax: mucilage, trypsin inhibitors and hydrocyanic acid. *Journal of American Oil Chemists Society*, *70*, 899–904. <http://dx.doi.org/10.13140/RG.2.2.35208.93448>
- Brito, A.F., Petit, H.V., Pereira, A.B.D., Soder, K.J., & Ross, S. (2015). Interactions of corn meal or molasses with a soybean-sunflower meal mix or flaxseed meal on production, milk fatty acid composition, and nutrient utilization in dairy cows fed grass hay-based diets. *Journal of Dairy Science*, *98*, 443–457. <https://doi.org/10.3168/jds.2014-8353>
- Buttar, H.S., Kumar, H., Chandran, D., Tuli, H.S., & Dhama, K. (2022). Potential health benefits of using aloe vera as a feed additive in Livestock: A mini-review. *The Indian Veterinary Journal*, *99*(01), 09–18.
- Caroprese, M., Marzano, A., Marino, R., Gliatta, G., Muscio, A., & Sevi, A. (2010). Flaxseed supplementation improves fatty acid profile of cow milk. *Journal of Dairy Science*, *93*, 2580–2588. <https://doi.org/10.3168/jds.2008-2003>
- Chandran, D. (2021). Veterinary phytomedicine in India: A review. *International Journal of Scientific Research in Science, Engineering and Technology*, *8*(3), 598–605. <https://doi.org/10.32628/IJSRST2183135>
- Chandran, D., Emran, T.B., Nainu, F., Sharun, K., Kumar, M., Mitra, S., Chakraborty, S., Mohapatra, R.K., Tuli, H.S., & Dhama, K. (2022). Beneficial effects of dietary *Allium sativum* (garlic) supplementation on health and production of poultry: A mini-review. *The Indian Veterinary Journal*, *9*, 821–824.
- Cherian, G., & Quezada, N. (2016). Egg quality, fatty acid composition and immunoglobulin Y content in eggs from laying hens fed full fat camelina or flax seed. *Journal of Animal Science and Biotechnology*, *7*, 15. <https://doi.org/10.1186/s40104-016-0075-y>
- Cowieson, A.J., Acamovic, T., & Bedford, M.R. (2004). The effects of phytase and phytic acid on the loss of endogenous amino acids and minerals from broiler chickens. *British Poultry Science*, *45*, 101–108. <https://doi.org/10.1080/00071660410001668923>
- Cui, Z., Yan, B., Gao, Y., Wu, B., Wang, Y., Wang, H., Xu, P., Zhao, B., Cao, Z., & Zhang, Y. (2022). Agronomic cultivation measures on productivity of oilseed flax: A review. *Oil Crop Science*, *7*, 53–62. <https://doi.org/10.1016/j.ocsci.2022.02.006>
- Do Prado, R.M., Palin, M.F., do Prado, I.N., Dos Santos, G.T., Benchaar, C., & Petit, H.V. (2016). Milk yield, milk composition, and hepatic lipid metabolism in transition dairy cows fed flaxseed or linola. *Journal of Dairy Science*, *99*, 8831–8846.
- Deepak, C., Rani, K.J., Shyama, K., & Ally, K. (2020) Effect of dietary incorporation of Ksheerabala residue on growth performance in Wistar rats. *Journal of Veterinary & Animal Sciences*, *51*(2), 179–183.
- Đordević, V., Đor dević, J., Baltić Ž, M., Laudanović, M., Teodorović, V., Bošković, M., Peuraća, M., & Marković, R. (2016). Effect of sunflower, linseed and soybean meal in pig diet on chemical composition, fatty acid profile of meat and backfat, and its oxidative stability. *Acta Veterinaria*, *66*, 359–372.
- Dzuovor, C.K.O., Taylor, J.T., Acquah, C., Pan, S., & Agyei, D. (2018). Bioprocessing of functional ingredients from flaxseed. *Molecules*, *23*, 2444. <https://doi.org/10.3390/molecules23102444>
- Eastwood, L., Kish, P.R., Beaulieu, A.D., & Leterme, P. (2009). Nutritional value of flaxseed meal for swine and its effects on the fatty acid profile of the carcass. *Journal of Animal Science*, *87*, 3607–3619.
- Enneking, D., & Wink, M. (2000). Towards the elimination of anti-nutritional factors in grains legumes. In: Knight, R. (eds) Linking Research and Marketing Opportunities for Pulses in the 21st Century. Current Plant Science and Biotechnology in Agriculture, vol 34. Springer, Dordrecht. http://dx.doi.org/10.1007/978-94-011-4385-1_65
- Lan, Y., Ohm, J.B., Chen, B.C., & Rao, J.J. (2020). Physicochemical properties and aroma profiles of flaxseed proteins extracted from whole flaxseed and flaxseed meal. *Food Hydrocolloid*, *104*, 105731. <https://doi.org/10.1016/j.foodhyd.2020.105731>
- Li, L., Schoenhals, K.E., Brady, P.A., Estill, C.T., Perumbakkam, S., & Craig, A.M. (2012). Flaxseed supplementation decreases methanogenic gene abundance in the rumen of dairy cows. *Animal*, *6*(11), 1784–1787. <https://doi.org/10.1017/S175173111200078X>
- Gagnon, N., Côrtes, C., da Silva, D., Kazama, R., Benchaar, C., dos Santos, G., Zeoula, L., & Petit, H.V. (2009). Ruminant metabolism of flaxseed (*Linum usitatissimum*) lignans to the mammalian lignan enterolactone and its concentration in ruminal fluid, plasma, urine and milk of dairy cow. *British Journal of Nutrition*, *102*(7), 1015–1023. <https://doi.org/10.1017/s0007114509344104>

- Gandra, J.R., Barletta, R.V., Mingoti, R.D., Verdurico, L.C., Freitas, J.E., Oliveira, L.J., Takiya, C.S., Kfoury, J.R., Wiltbank, M.C., & Renno, F.P. (2016). Effects of whole flaxseed, raw soybeans, and calcium salts of fatty acids on measures of cellular immune function of transition dairy cows. *Journal of Dairy Science*, *99*, 4590–4606. <https://doi.org/10.3168/jds.2015-9974>
- Gholami, H., Chamani, M., Towhidi, A., & Fazeli, M.H. (2010). Effect of feeding a docosahexaenoic acid-enriched nutraceutical on the quality of fresh and frozen-thawed semen in Holstein bulls. *Theriogenology*, *74*, 1548–1558. <https://doi.org/10.1016/j.theriogenology.2010.06.025>
- Goodridge, J., Ingalls, J.R., & Crow, G.H. (2001). Transfer of omega-3 linolenic acid and linoleic acid to milk fat from flaxseed or Linola protected with formaldehyde. *Canadian Journal of Animal Science*, *81*, 525–532. <https://doi.org/10.4141/A01-024>
- Goyal, A., Sharma, V., Upadhyay, N., Gill, S., & Sihag, M. (2014). Flax and flaxseed oil: an ancient medicine & modern functional food. *Journal of Food Science and Technology*, *51*, 1633–1653. <https://doi.org/10.1007/s13197-013-1247-9>
- Gregory, M.K., Geier, M.S., Gibson, R.A., & James, M.J. (2013). Functional characterization of the chicken fatty acid elongases. *Journal of Nutrition*, *143*(1), 12–16. <https://doi.org/10.3945/jn.112.170290>
- Gul, K., Tak, A., Singh, A.K., Singh, P., Yousuf, B., & Wani, AA (2015). Chemistry, encapsulation, and health benefits of β -carotene-A review. *Cogent Food & Agriculture*, *1*(1), 1018696. <https://doi.org/10.1080/23311932.2015.1018696>
- Gutiérrez, C., Rubilar, M., Jara, C., Verdugo, M., Sineiro, J., & Shene, C. (2010). Flaxseed and flaxseed cake as a source of compounds for food industry. *Journal of Soil Science and Plant Nutrition*, *10*(4), 454–463. <http://dx.doi.org/10.4067/S0718-95162010000200006>
- Hao, X.Y., Yu, S.C., Mu, C.T., Wu, X.D., Zhang, C.X., Zhao, J.X., & Zhang, J.X. (2020). Replacing soybean meal with flax seed meal: effects on nutrient digestibility, rumen microbial protein synthesis and growth performance in sheep. *Animal*, *14*(9), 1841–1848. <https://doi.org/10.1017/S1751731120000397>
- Herchi, W., Sakouhi, F., Boukhchina, S., Kallel, H., & Pepe, C. (2011). Changes in fatty acids, tocopherols, carotenoids and chlorophylls content during flaxseed development. *Journal of the American Oil Chemists' Society*, *88*, 1011–1017. <https://doi.org/10.1007/s11746-010-1750-3>
- Hernandez, F.I.L. (2013). Performance and fatty acid composition of adipose tissue, breast and thigh in broilers fed flaxseed: A review. *Current Research in Nutrition and Food Science Journal*, *1*(2), 103–114. <http://dx.doi.org/10.12944/CRNFSJ.1.2.01>
- Huang, S., Baurhoo, B., & Mustafa, A. (2018). Effects of extruded flaxseed on layer performance, nutrient retention and yolk fatty acid composition. *British Poultry Science*, *59*(4), 463–469. <https://doi.org/10.1080/00071668.2018.1476676>
- Huang, G., Wang, J., Liu, K., Wang, F., Zheng, N., Zhao, S., Qu, X., Yu, J., Zhang, Y., & Wang, J. (2022a). Effect of flaxseed supplementation on milk and plasma fatty acid composition and plasma parameters of Holstein dairy cows. *Animals*, *12*(15), 1898. <https://doi.org/10.3390/ani12151898>
- Huang, G., Li, N., Liu, K., Yang, J., Zhao, S., Zheng, N., Zhou, J., Zhang, Y., & Wang, J. (2022b). Effect of flaxseed supplementation in diet of dairy cow on the volatile organic compounds of raw milk by HS-GC-IMS. *Frontiers in Nutrition*, *9*, 831178. <https://doi.org/10.3389/fnut.2022.831178>
- Isenberg, B.J., Soder, K.J., Pereira, A.B.D., Standish, R., & Brito, A.F. (2019). Production, milk fatty acid profile, and nutrient utilization in grazing dairy cows supplemented with ground flaxseed. *Journal of Dairy Science*, *102*, 1294–311. <https://doi.org/10.3168/jds.2018-15376>
- Ishag, O.A.O., Khalid, A.A., Abdi, A., Erwa, I.Y., Omer, A.B., & Nour, A.H. (2019). Proximate composition, physicochemical properties and antioxidant activity of flaxseed. *Annual Research and Reviews in Biology*, *34*, 1–10. <https://doi.org/10.9734/arrb/2019/v34i230148>
- Jahani-Moghadam, M., Mahjoubi, E., & Dirandeh, E. (2015). Effect of linseed feeding on blood metabolites, incidence of cystic follicles, and productive and reproductive performance in fresh Holstein dairy cows. *Journal of Dairy Science*, *98*, 1828–1835. <https://doi.org/10.3168/jds.2014-8789>
- Kaur, S., Singh, A.K., Honparkhe, M., Kumar, A., Singh, P., & Singh, U. (2021). Effect of flaxseed supplementation on metabolic state, endocrine profiles, body composition and reproductive performance of sows. *Asian Pacific Journal of Reproduction*, *10*(3), 127. <https://doi.org/10.4103/2305-0500.316625>
- Kajla, P., Sharma, A., & Sood, D.R. (2014). Flaxseed-a potential functional food source. *Journal of Food Science & Technology*, *52*(4), 1857–1871. <https://doi.org/10.1007/s13197-014-1293-y>
- Khan, S.A. (2019). Inclusion of pyridoxine to flaxseed cake in poultry feed improves productivity of omega-3 enriched eggs. *Bioinformation*, *15*(5), 333–341. <https://doi.org/10.6026/97320630015333>

- Khan, H.K., Qureshi, M.S., Khan, I., Rehman, S., Mehsud, T., Ullah, I., Aftab, M., & Rehman, F. (2015). Dietary flaxseed oil supplementation effect on bovine semen quality parameters. *Veterinary Journal*, *3*, 9–13.
- Konovalov, D.A., Cáceres, E.A., Shcherbakova, E.A., Herrera-Bravo, J., Chandran, D., Martorell, M., Hasan, M., Kumar, M., Bakrim, S., Bouyahya, A., & Cho, W.C. (2022). *Eryngium caeruleum*: an update on ethnobotany, phytochemistry and biomedical applications. *Chinese Medicine*, *17*(1), 1–17. <https://doi.org/10.1186/s13020-022-00672-x>
- Kouba, M., Enser, M., Whittington, F.M., Nute, G.R., & Wood, J.D. (2003). Effect of a high-linolenic acid diet on lipogenic enzyme activities, fatty acid composition, and meat quality in the growing pigs. *Journal of Animal Science*, *81*, 1967–1979.
- Kumar, F., Tyagi, P.K., Mir, N.A., Tyagi, P.K., Dev, K., Bera, I., Biswas, A.K., Sharma, D., Mandal, A.B., & Deo, C. (2019). Role of flaxseed meal feeding for different durations in the lipid deposition and meat quality in broiler chickens. *Journal of American Oil Chemists Society*, *96*, 261–271.
- Kumar, M., Tomar, M., Punia, S., Dhakane-Lad, J., Dhumal, S., Changan, S., Senapathy, M., Berwal, M.K., Sampathrajan, V., Sayed, A.A., & Chandran, D. (2022). Plant-based proteins and their multifaceted industrial applications. *Lebensmittel-Wissenschaft & Technologie*, *154*, 112620. <https://doi.org/10.1016/j.lwt.2021.112620>
- Kumari, N., Kumar, M., Mekhemar, M., Lorenzo, J.M., Pundir, A., Devi, K.B., Prakash, S., Puri, S., Thakur, M., Rathour, S., & Rais, N. (2022). Therapeutic uses of wild plant species used by rural inhabitants of Kangra in the western Himalayan region. *South African Journal of Botany*, *148*, 415–436. <https://doi.org/10.3390/horticulturae7100343>
- Liu, J., Shim, Y.Y., Timothy, J.T., Wang, Y., & Reaney, M.J. (2018). Flaxseed gum a versatile natural hydrocolloid for food and non-food applications. *Trends in Food Science and Technology*, *75*, 146–157. <https://doi.org/10.1016/j.tifs.2018.01.011>
- Mach, N., Devant, M., Díaz, I., Font-Furnols, M., Oliver, M.A., García, J.A., & Bach, A. (2006). Increasing the amount of n-3 fatty acid in meat from young Holstein bulls through nutrition. *Journal of Animal Science*, *84*(11), 3039–3048. <https://doi.org/10.2527/jas.2005-632>
- Madhusudhan, K.T., & Singh, N.P. (1985). Isolation and characterization of a small molecular weight protein of linseed meal. *Phytochemistry*, *24*, 2507–2509.
- Mahmut, O., & Ayhan, I. S. (2002). The use of tannins from turkish Acorns (valonia) in water treatment as a coagulant and coagulant aid. *Turkish Journal of Engineering and Environmental Sciences*, *26*, 255–263.
- Mattioli, S., Ruggeri, S., Sebastiani, B., Brecchia, G., Dal Bosco, A., Cartoni Mancinelli, A., & Castellini, C. (2017). Performance and egg quality of laying hens fed flaxseed: Highlights on n-3 fatty acids, cholesterol, lignans and isoflavones. *Animal*, *11*, 705–712. <https://doi.org/10.1017/S175173111600207X>
- Mitra, S., da Silva, L.E., Tuli, H.S., & Dhama, K. (2022). Potential health benefits of dietary *Curcuma longa* (turmeric) supplementation on health and production of poultry: A Mini-review. *Indian Veterinary Journal*, *99*(2), 7–13.
- Mridula, D., Kaur, D., Nagra, S.S., Barnwal, P., Gurumayum, S., & Singh, K.K. (2011). Growth performance, carcass traits and meat quality in broilers, fed flaxseed meal. *Asian Australian Journal of Animal Sciences*, *24*, 1729–1735. <http://dx.doi.org/10.5713/ajas.2011.11141>
- Mueed, A., Shibli, S., Korma, S.A., Madjirebaye, P., Esatbeyoglu, T., & Deng, Z. (2022). Flaxseed bioactive compounds: Chemical composition, functional properties, food applications and health benefits-related gut microbes. *Foods*, *11*(20), 307. <https://doi.org/10.3390/foods11203307>
- Ndou, S.P., Kiarie, E., Walsh, M.C., & Nyachoti, C.M. (2018). Nutritive value of flaxseed meal fed to growing pigs. *Animal Feed Science and Technology*, *238*, 123–129.
- Oomah, B.D., Kenaschuk, E.O., & Mazza, G. (1996). Phytic acid content of flaxseed as influenced by cultivar, growing season, and location. *Journal of Agriculture and Food Chemistry*, *44*, 2663–2666. <https://doi.org/10.1021/jf9601527>
- Palaniswamy, U.R., Bible, B.B., & McAvoy, R.J. (2002). Effect of nitrate: ammonium nitrogen ratio on oxalate levels of purslane. *Trends in New Crops and New Uses*, *11*(5), 453–455.
- Park, E., Hong, J., Lee, D., Han, S., & Lee, K. B. (2005). Analysis and decrease of cynogenic glycosides in flaxseed. *Journal of Korean Society Food Science and Nutrition*, *34*, 875879. <https://doi.org/10.1007%2Fs13197-013-1247-9>
- Petit, H.V., & Côrtes, C. (2010). Milk production and composition, milk fatty acid profile, and blood composition of dairy cows fed whole or ground flaxseed in the first half of lactation. *Animal Feed Science and Technology*, *158*, 36–43. <https://doi.org/10.1016/j.anifeedsci.2010.03.013>

- Pliego, A.B., Tavakoli, M., Khusro, A., Seidavi, A., Elghandour, M.M., Salem, A.Z., Márquez-Molina, O., & Rene Rivas-Caceres, R. (2022). Beneficial and adverse effects of medicinal plants as feed supplements in poultry nutrition: A review. *Animal Biotechnology*, 33(2), 369-391. <https://doi.org/10.1080/10495398.2020.1798973>
- Popescu, R.G., Voicu, S.N., Gradisteanu Pircalabioru, G., Gharbia, S., Hermenean, A., Georgescu, S.E., Panaite, T.D., Turcu, R.P., & Dinischiotu, A. (2021). Impact of dietary supplementation of flaxseed meal on intestinal morphology, specific enzymatic activity, and cecal microbiome in broiler chickens. *Applied Sciences*, 11, 6714. <https://doi.org/10.3390/app11156714>
- Prakash, P., Kumar, M., Pundir, A., Puri, S., Prakash, S., Kumari, N., Thakur, M., Rathour, S., Jamwal, R., Janjua, S., & Ali, M. (2021a) Documentation of commonly used ethnoveterinary medicines from wild plants of the high mountains in Shimla District, Himachal Pradesh, India. *Horticulturae*, 7(10), 351. <https://doi.org/10.3390/horticulturae7100351>
- Prakash, P., Kumar, M., Kumari, N., Prakash, S., Rathour, S., Thakur, M., Jamwal, R., Janjua, S., Ali, M., Pundir, A., & Puri, S. (2021b) Therapeutic uses of wild plants by rural inhabitants of Maraog region in district Shimla, Himachal Pradesh, India. *Horticulturae*, 7(10), 343. <https://doi.org/10.3390/horticulturae7100343>
- Prieto, N., Dugan, M.E.R., Larsen, I.L., Vahmani, P., & Aalhus, J.L. (2017). Palatability of beef from cattle fed extruded flaxseed before hay or mixed with hay. *Meat and Muscle Biology*, 1(1).
- Scheideler, S.E., & Froning, G.W. (1996). The combined influence of dietary flaxseed variety, level, form, and storage conditions on egg production and composition among vitamin E-supplemented hens. *Poultry Science*, 75(10), 1221-1226. <https://doi.org/10.3382/ps.0751221>
- Scollan, N., Hocquette, J.F., Nuernberg, K., Dannenberger, D., Richardson, I., & Moloney, A. (2006). Innovations in beef production systems that enhance the nutritional and health value of beef lipids and their relationship with meat quality. *Meat science*, 74(1), pp.17-33. <https://doi.org/10.1016/j.meatsci.2006.05.002>
- Shim, Y.Y., Song, Z., Jadhav, P.D., & Reaney, M.J. (2019). Orbitides from flaxseed (*Linum usitatissimum* L.): A comprehensive review. *Trends in Food Science & Technology*, 93, 197-211. <https://doi.org/10.1016/j.tifs.2019.09.007>
- Singh, K.K., Mridula, D., Rehal, J., & Barnwal, P. (2011). Flaxseed: a potential source of food, feed and fiber. *Critical Reviews in Food Science and Nutrition*, 51(3), 210-222. <https://doi.org/10.1080/10408390903537241>
- Sun, H.Y., & Kim, I.H. (2020). Coated omega-3 fatty acid from linseed oil positively affects sow immunoglobulin G concentration and pre-weaning performance of piglet. *Animal Feed Science & Technology*, 269, 114676.
- Tvrzicka, E., Kremmyda, L. S., Stankova, B., & Zak, A. (2011). Fatty acids as biocompounds: their role in human metabolism, health and disease--a review. Part 1: classification, dietary sources and biological functions. *Biomedical papers of the Medical Faculty of the University Palacky, Olomouc, Czechoslovakia*, 155(2), 117-130. <https://doi.org/10.5507/bp.2011.038>
- Vahmani, P., Rolland, D.C., McAllister, T.A., Block, H.C., Proctor, S.D., Guan, L.L., Prieto, N., López-Campos, Ó., Aalhus, J.L., & Dugan, M.E.R. (2017). Effects of feeding steers extruded flaxseed on its own before hay or mixed with hay on animal performance, carcass quality, and meat and hamburger fatty acid composition. *Meat Science*, 131, pp.9-17. <https://doi.org/10.1016/j.meatsci.2017.04.008>
- Vetter, J. (2000). Plant cyanogenic glycosides. *Toxicon*, 38(1), 11-36. [https://doi.org/10.1016/S0041-0101\(99\)00128-2](https://doi.org/10.1016/S0041-0101(99)00128-2)
- Ward, A.T., Wittenberg, K.M., & Przybylski, R. (2002). Bovine milk fatty acid profiles produced by feeding diets containing solin, flax and canola. *Journal of Dairy Science*, 85, 1191-1196. [https://doi.org/10.3168/jds.S0022-0302\(02\)74182-9](https://doi.org/10.3168/jds.S0022-0302(02)74182-9)
- Woyengo, T.A., Weihrauch, D., & Nyachoti, C.M. (2012). Effect of dietary phytic acid on performance and nutrient uptake in the small intestine of piglets. *Journal of Animal Science*, 90, 543-549. <https://doi.org/10.2527/jas.2011-4001>
- Wu, S., Wang, X., Qi, W., & Guo, Q. (2019). Bioactive Protein/Peptides of Flaxseed: A review. *Trends in Food Science & Technology*, 92, 184-193. <https://doi.org/10.1016/j.tifs.2019.08.017>
- Xu, L., Wei, Z., Guo, B., Bai, R., Liu, J., Li, Y., Sun, W., Jiang, X., Li, X., & Pi, Y. (2022). Flaxseed meal and its application in animal husbandry: A 4eview. *Agriculture*, 12, 2027. <https://doi.org/10.3390/agriculture12122027>
- Yang, J., Wen, C., Duan, Y., Deng, Q., Peng, D., Zhang, H., & Ma, H. (2021). The composition, extraction, analysis, bioactivities, bioavailability and applications in food system of flaxseed (*Linum usitatissimum* L.) oil: A review. *Trends in Food Science and Technology*, 118, 252-260.
- Yaqoob, N., Bhatti, I.A., Anwar, F., Mushtaq, M., & Artz, W.E. (2016). Variation in physico-chemical/analytical characteristics of oil among different flaxseed (*Linum usitatissimum* L.) cultivars. *Italian Journal of Food Science*, 28(1), 83-89. <https://doi.org/10.14674/1120-1770/ijfs.v461>

- Ye, X.P., XU, M.F., Tang, Z.X., Chen, H.J., Wu, D.T., Wang, Z.Y., Songzhen, Y.X., Hao, J., Wu, L.M., & Shi, L.E. (2022). Flaxseed protein: extraction, functionalities and applications. *Food Science and Technology*, 42. <https://doi.org/10.1590/fst.22021>
- Yonekura, L., & Nagao, A. (2007). Intestinal Absorption of dietary carotenoids. *Molecular Nutrition & Food Research*, 51(1), 107-115. <https://doi.org/10.1002/mnfr.200600145>
- Zachut, M., Arieli, A., Lehrer, H., Livshitz, L., Yakoby, S., & Moallem, U. (2010). Effects of increased supplementation of n-3 fatty acids to transition dairy cows on performance and fatty acid profile in plasma, adipose tissue, and milk fat. *Journal of Dairy Science*, 93(12), 5877-5889. <https://doi.org/10.3168/jds.2010-3427>
- Zajac, M., Kiczorowska, B., Samolińska, W., & Klebaniuk, R. (2020). Inclusion of camelina, flax, and sunflower seeds in the diets for broiler chickens: Apparent digestibility of nutrients, growth performance, health status, and carcass and meat quality traits. *Animals*, 10(2), 321. <https://doi.org/10.3390/ani10020321>
- Zhai, S.S., Zhou, T., Li, M.M., Zhu, Y.W., Li, M.C., Feng, P.S., Zhang, X.F., Ye, H., Wang, W.C., & Yang, L. (2019). Fermentation of flaxseed cake increases its nutritional value and utilization in ducklings. *Poultry Science*, 98(11), 5636-5647. <https://doi.org/10.3382/ps/pez326>



Journal of Experimental Biology and Agricultural Sciences

<http://www.jebas.org>

ISSN No. 2320 – 8694

Influence of biofertilizer produced using drumstick (*Moringa oleifera* L.) unused parts on the growth performance of two leafy vegetables

Hatsadong Chanthanousone¹ , Thao Thu Phan² , Co Quang Nguyen¹ ,
The Dieu Thi Nguyen¹, Hien Thao Thi Pham³ , Hai Thi Hong Truong^{1*} 

¹Institute of Biotechnology, Hue University, Road 10, Phu Thuong, Hue, Thua Thien Hue, Vietnam

²Tay Nguyen Institute of Agriculture and Rural Development, Dong A University, 33 Xo Viet Nghe Tinh, Da Nang, Vietnam

³University of Agriculture and Forestry, Hue University 102 Phung Hung, Dong Ba, Hue, Thua Thien Hue, Vietnam

Received – November 09, 2022; Revision – February 18, 2023; Accepted – March 03, 2023

Available Online – April 30, 2023

DOI: [http://dx.doi.org/10.18006/2023.11\(2\).280.289](http://dx.doi.org/10.18006/2023.11(2).280.289)

KEYWORDS

Lettuce

Moringa organic fertilizer

Mustard spinach

Organic farming

Rate of fertilizer

ABSTRACT

The non-edible parts of *Moringa oleifera*, such as stems, branches or leaf petioles, have often been discarded while the leaves are consumed as a vegetable or are used to produce organic fertilizer. This study aimed to determine the optimal conditions for producing *Moringa* organic fertilizer (MOF) from previously unused parts and to compare these fertilizers with cow manure and bio-organic fertilizer. Seventy kilograms of the unused *Moringa* parts were blended with fifty kilograms of manure, 0.2 kilogram of Trichoderma-based product and two kilograms of superphosphate. The mixture was incubated at different intervals, including 5, 7 or 9 weeks. Next, the effects of MOF on the growth, yield, ascorbic acid content and Brix of lettuce and mustard spinach were also determined and compared with other organic fertilizers (cow manure and bio-organic fertilizer). Results of the study revealed that 25 tons per ha of MOF were significantly superior to those treated with cow manure and bio-organic fertilizer in the case of vegetable yields. Further, 7 weeks of MOF incubation was found suitable to produce an optimal yield during the various incubation period. These results suggested that the *Moringa* non-edible parts can make organic fertilizer and enhance growth, yield, and leafy vegetable production.

* Corresponding author

E-mail: tthhai@hueuni.edu.vn (H.T.H. Truong)

Peer review under responsibility of Journal of Experimental Biology and Agricultural Sciences.

Production and Hosting by Horizon Publisher India [HPI]
(<http://www.horizonpublisherindia.in/>).
All rights reserved.

All the articles published by [Journal of Experimental Biology and Agricultural Sciences](#) are licensed under a [Creative Commons Attribution-NonCommercial 4.0 International License](#) Based on a work at www.jebas.org.



1 Introduction

Leafy vegetables such as lettuce (*Lactuca sativa* L.) and mustard spinach (*Brassica juncea*) are important sources of nutrients, fibre, minerals and vitamins. Lettuce also contains the most common types of vitamins, such as E, A, C and B9 (Wang et al. 2013), and bioactive compounds, such as polyphenols, carotenoids and chlorophyll (Coria–Cayupán et al. 2009). Similarly, mustard spinach is a good source of vitamins (A, C, K, B1, B2, B6 and B9) and mineral nutrients (Van Wyk 2005). Furthermore, its oil is used in traditional medicine and cosmetics (Yu et al. 2003; Kumar et al. 2011). Recently, the consumption of leafy vegetables in Vietnam has decreased due to food safety issues (Ha et al. 2020). Further, large amounts of nitrate residues have also been found in vegetable samples (Dang et al. 2018). The excessive use of nitrogen fertilizer causes nitrate accumulation in soil, water and leafy vegetables, which poses a risk to human health (Ahmed et al. 2017; Zhao et al. 2019).

Using organic fertilizer helps to enrich soil fertility and soil organic matter, leading to enhanced carbon sequestration (Verma et al. 2019). When soil organic matter is low, vegetable yields decline even if sufficient nutrients are supplied via synthetic fertilizers (Bauer and Black 1994). Therefore, organic fertilizers are needed to achieve optimal vegetable yields. Although organic fertilizers can be produced from agricultural wastes, animal manure, and compost, the organic fertilizer supply is limited and does not meet the demand in organic farming.

Moringa oleifera, a species from the family Moringaceae, grows well in tropical and subtropical regions. It is a vegetable crop with vast nutritional benefits. Various parts of *Moringa* trees are found to be enriched with nutrients. However, this tree is considered underutilized due to the lack of awareness (Faizi et al. 1994; Padulosi et al. 2011). The extract products derived from *Moringa* leaves help promote crops' growth and yield (Culver et al. 2012; Matthew 2016; Chanthanousone et al. 2020). Supplement of *M. oleifera* residues as soil conditioner increases available nitrogen in sandy and calcareous soil and polluted soil (Taiwo et al. 2022) and enhances grain yields (Merwad and Khalil 2018). Composts are necessary to produce safe agricultural products on a large scale (Paulin and O'Malley 2008).

Except for the leaf, most *M. oleifera* parts are still unused and have been discarded as waste. These materials can be utilized to generate *Moringa* organic fertilizer. Previous studies indicated that applying *Moringa* foliar biofertilizer produced from non-edible parts promotes the growth, yield, ascorbic acid content and Brix of lettuce (Chanthanousone et al. 2022). This study aimed to evaluate the effect of the incubation period on the *Moringa* residual organic fertilizer and its impact on the growth of lettuce and mustard spinach in Thua Thien Hue province,

Vietnam. Finally, *Moringa* residual organic fertilizer was compared to other organic fertilizers.

2 Materials and methods

2.1 Experimental site and plant materials

The experiments were conducted at the experimental field of the Institute of Biotechnology, Hue University (Thua Thien Hue province, Vietnam) from December 2020 to May 2021. During the study period, the daily temperature varied from 26 and 35°C. Plant materials included in the study are a lettuce variety (*Lactuca sativa* L.) obtained from Phu Nong Seeds Company and a mustard spinach variety (*Brassica juncea*) obtained from Ha Noi Xanh Company.

2.2 Moringa organic fertilizer (MOF) preparation

MOF was prepared from *Moringa* non-edible parts, including stems, branches and leaf petioles, at the Institute of Biotechnology, Hue University. The fertilizer was prepared with the following materials in the predetermined quantities, including 70 kilograms of ground moringa residues, 50 kilograms of manure, 0.2 kilograms of Tricho-compost (Trichoderma-based product) and 2.0 kilograms of superphosphate (Lam Thao Fertilizers and Chemicals JSC). First, *Moringa* residues were chopped into small parts and mixed with water and Tricho-compost until the mixture humidity reached 70%. For this, the mixture was fully covered by a dark plastic sheet. After three weeks (the mixture's temperature increased to 30–40°C), water was supplemented, and the mixture was stirred and incubated for another 5, 7 or 9 weeks.

2.3 Nutrient contents of MOF following different incubation periods

In this experiment, MOF was incubated for 5 weeks (I1), 7 weeks (I2) and 9 weeks (I3). Physicochemical properties of the MOF included the percentages of N, P, available P, available K, organic matter and pH were investigated. For each incubation period, three samples were taken for physicochemical analyses.

2.4 Effect of MOF amounts on the growth, yield and quality of leafy vegetables

The field experiment was conducted from January to March 2021 with two planting times. The investigation was conducted in a completely randomized design (CRD) following four treatments with different amounts of MOF applied (15 (R1), 20 (R2), 25 (R3) and 30 (R4) tons per ha). The plot size of each treatment was 10 m². Before planting, the soil was ploughed, and MOF was applied as basal dressing. The seedlings at the 3–4 leaf stage were planted with a density of 33 plants per m².

2.5 Effect of various organic fertilizers on growth, yield and quality of leafy vegetables

The field experiment was carried out from March to May 2021 with two planting times to compare the effects of MOF and other organic fertilizers on the growth, yield and quality of leafy vegetables (lettuce and mustard spinach). The experiment was conducted in a completely randomized design (CRD) with four treatments: F1 (25 tons of MOF per ha), F2 (Cow manure), F3 (Bio-organic fertilizer) and control (without fertilization). The plot size of each treatment was 10 m². The seedlings at 3-4 leaf stage were planted with a density of 33 plants/m² and all fertilizers were applied as basal dressing before planting.

2.6 Data collection and analysis

Growth time (day) was defined from sowing to harvesting. Growth parameters, including plant height (cm), canopy diameter (cm), number of leaves and leaf area index (leaf area/ground area), were observed. Plant height was measured from the ground to the highest point of the leaves. The leaf area index (LAI) is the sum of the leaf area from all plants divided by the ground area. Yield

components included: (i) fresh mass per plant (g/plant) (including the stems, leaves and roots); (ii) theoretical yield (tons per ha) (average fresh mass/plant × plant density); (iii) actual yield (tons per ha) was also estimated (Chanthanosone et al. 2022). Statistical analysis was performed by one-way analysis of variance (ANOVA), followed by Tukey's test, using the SPSS statistic 20.0 software (SPSS Inc., Chicago, IL, USA). Data represented significant differences as $p < 0.05$.

3 Results

3.1 Nutrient contents of MOF at different incubation periods

The results presented in Table 1 indicated that the nitrogen contents changed during the incubation period. MOF prepared with seven-week incubation had the highest nitrogen content (3.57%). On the other hand, phosphorus contents increased with the incubation period. While in the case of potassium content, it ranged from 20.63% (7 weeks) to 25.58% (5 weeks), while organic matter ranged from 6.58% (5 weeks) to 11.49% (7 weeks), but the differences were not significant. Further, the pH values for different incubation periods ranged from 5.88 (9 weeks) to 6.27 (5 weeks), suitable for planting vegetables.

Table 1 Effect of incubation periods on the quality of *Moringa* organic fertilizer (MOF)

Treatment	N (%)	P (%)	P ₂ O ₅ (%)	K ₂ O (%)	Organic matter (%)	pH
I1	0.82±0.01 ^c	2.02±0.19 ^b	4.62±2.05 ^b	25.58±4.41 ^a	6.58±1.42 ^c	6.27±0.03 ^a
I2	3.57±0.11 ^a	3.50±0.64 ^a	8.00±1.90 ^a	20.63±5.84 ^b	11.49±4.12 ^a	6.13±0.02 ^a
I3	2.29±0.17 ^b	3.76±1.39 ^a	8.61±2.42 ^a	26.24±4.63 ^a	8.12±0.75 ^b	5.88±0.17 ^b
LSD _{0.05}	0.21	1.75	4.05	8.30	5.09	0.22

The means with similar lower-case letters within columns did not differ significantly at a 5% probability. I1: 5 weeks, I2: 7 weeks, I3: 9 weeks. LSD: Least significant difference.

Table 2 Effect of MOF amounts on the growth of lettuce

Treatment	Growth time (day)	Plant height (cm)	Number of leaves (leaves per plant)	Canopy diameter (cm)	Leaf area index
First planting					
R1	30	19.2±1.83 ^{ab}	10.7±1.01 ^{ab}	28.3±1.66 ^{ab}	47.6±0.82 ^{ab}
R2	29	20.4±1.27 ^a	11.6±0.12 ^a	28.7±1.34 ^a	48.3±2.52 ^a
R3	30	19.5±1.17 ^{ab}	11.1±0.53 ^{ab}	26.7±0.61 ^{ab}	48.2±2.43 ^a
R4	30	17.3±2.01 ^b	9.6±1.28 ^b	25.3±0.42 ^b	45.3±1.15 ^b
LSD _{0.05}		2.95	1.62	3.2	2.6
Second planting					
R1	28	24.5±1.56 ^b	12.1±1.83 ^b	24.8±1.41 ^b	41.1±4.32 ^c
R2	28	25.6±0.64 ^{ab}	14.0±1.83 ^a	28.6±0.70 ^a	49.2±2.23 ^a
R3	29	26.7±0.92 ^a	14.4±1.83 ^a	29.2±0.57 ^a	50.9±3.71 ^a
R4	28	26.5±1.96 ^{ab}	13.6±1.83 ^{ab}	29.3±0.69 ^a	44.8±2.08 ^b
LSD _{0.05}		2.2	2.9	3.7	6.3

The means with similar lower-case letters within columns did not differ significantly at a 5% probability. R1: 15 tons per ha, R2: 20 tons per ha, R3: 25 tons per ha, R4: 30 tons per ha. LSD: Least significant difference.

3.2 Effect of MOF on the growth, yield and quality of leafy vegetables

3.2.1 Lettuce

In the first planting, 15 to 25 tons of MOF per ha seemed to promote various plant growth parameters of lettuce, including plant height (19.2–20.4 cm), number of leaves (10.7–11.6), canopy diameter (26.7–28.7 cm) and leaf area index (47.6–48.3). In the second planting, the plant growth parameters were similar when MOF application varied from 20 to 30 tons per ha. The canopy diameter of lettuce was lower in 15 tons per ha treatment than the others. At both planting times, fresh mass, theoretical yield, and actual yield of lettuce grown with 25 tons of MOF per

ha were significantly higher than those grown with 15 and 20 tons of MOF per ha (Table 2). Increasing the amount of MOF from 25 to 30 tons per ha did not affect the theoretical yield, actual yield, ascorbic acid content and Brix of lettuce. When 25 tons of MOF per ha were applied, lettuce yields peaked at 23.7 tons per ha and 25.6 tons/ha in the first and second planting times, respectively. These yields were higher than when 15 tons of MOF per ha were applied. Regarding ascorbic acid contents (Table 3), the values remained constant across treatments in the first planting, but in the second planting, the treatment with 15 tons of MOF per ha resulted in the lowest ascorbic content. Furthermore, the lowest amount of MOF (15 tons per ha) yielded the lowest values of fresh mass, yields and Brix in the second planting.

Table 3 Effect of MOF amounts on the yield and quality of lettuce

Treatment	Fresh mass (g per plant)	Theoretical yield (ton per ha)	Actual yield (ton per ha)	Ascorbic acid (%)	Brix (%)
First planting					
R1	100.3±6.66 ^b	26.7±0.63 ^b	19.0±1.67 ^c	2.767±0.11 ^a	4.93±0.31 ^{ab}
R2	101.7±4.23 ^b	27.0±1.78 ^b	20.3±2.01 ^{bc}	2.730±0.14 ^a	4.76±0.46 ^{ab}
R3	123.3±5.04 ^a	32.7±0.53 ^a	23.7±1.30 ^a	2.741±0.30 ^a	5.17±0.25 ^a
R4	125.4±6.50 ^a	33.0±1.34 ^a	22.7±1.71 ^{ab}	2.693±0.15 ^a	4.90±0.32 ^a
LSD _{0.05}	7.89	3.12	2.56	0.41	0.39
Second planting					
R1	99.9±2.01 ^c	25.7±0.54 ^c	20.8±0.42 ^c	2.607±0.11 ^b	4.40±0.26 ^b
R2	110.0±5.29 ^{bc}	29.3±1.42 ^b	22.9±1.10 ^{bc}	2.770±0.23 ^{ab}	4.76±0.33 ^{ab}
R3	122.7±4.73 ^a	31.7±0.67 ^a	25.6±0.98 ^a	2.863±0.05 ^a	5.10±0.36 ^a
R4	117.8±9.62 ^b	30.0±0.85 ^{ab}	24.5±2.00 ^{ab}	2.874±0.07 ^a	4.86±0.29 ^{ab}
LSD _{0.05}	12.0	2.1	2.5	0.2	0.4

The means with similar lower-case letters within columns did not differ significantly at a 5% probability. R1: 15 tons per ha, R2: 20 tons per ha, R3: 25 tons per ha, R4: 30 tons per ha. LSD: Least significant difference.

Table 4 Effect of MOF amounts on the growth of mustard spinach

Treatment	Growth time (day)	Plant height (cm)	Number of leaves (leaves/plant)	Canopy diameter (cm)	Leaf area index
First planting					
R1	31	23.2±1.36 ^b	11.0±0.64 ^a	25.8±1.51 ^b	39.8±1.79 ^b
R2	32	27.2±2.98 ^{ab}	11.9±1.63 ^a	26.9±0.64 ^b	43.5±1.13 ^{ab}
R3	33	28.8±2.65 ^a	12.1±0.99 ^a	29.3±2.09 ^a	44.6±0.86 ^a
R4	31	27.9±1.10 ^{ab}	11.3±0.91 ^a	28.1±1.33 ^{ab}	43.8±0.92 ^{ab}
LSD _{0.05}		2.50	1.80	3.34	4.03
Second planting					
R1	30	24.0±1.35 ^c	11.9±0.12 ^b	27.9±1.51 ^a	39.1±0.97 ^b
R2	32	26.6±1.04 ^b	12.5±0.50 ^{ab}	29.0±0.64 ^a	43.2±0.94 ^a
R3	31	29.6±0.50 ^a	13.3±0.84 ^a	29.4±1.39 ^a	43.3±0.97 ^a
R4	32	29.1±0.59 ^a	13.2±0.48 ^a	29.2±0.41 ^a	44.7±1.62 ^a
LSD _{0.05}		1.9	1.0	1.9	2.4

The means with similar lower-case letters within columns did not differ significantly at a 5% probability. R1: 15 tons per ha, R2: 20 tons per ha, R3: 25 tons per ha, R4: 30 tons per ha. LSD: Least significant difference.

3.2.2 Mustard spinach

The plant treated with 20 to 30 tons of MOF per ha showed a significant increase in plant height compared to those treated with 15 tons of MOF per ha (Table 4). The number of leaves did not change significantly according to MOF amounts in the first planting but was lower in those treated with 15 tons of MOF per ha in the second planting. The canopy diameter and LAI seemed to increase with the amount of MOF in the first planting, while in the second planting, no significant difference was observed in plants treated with 20 to 30 tons of MOF per ha. In addition, the yields were the highest when 25 tons of MOF per ha were used in both planting times (Table 5).

Mustard spinach grown with 25 tons of MOF per ha produced a higher yield (7 tons/ha) than those grown with 15 tons of MOF per

ha (Table 5). The ascorbic acid content of mustard spinach grown with 20–25 tons of MOF per ha was significantly higher than those grown with 15 tons of MOF per ha. Brix of mustard spinach ranged from 3.5 to 4.5 in the first planting while it was reported from 3.9 to 5.4 in the second planting. Brix was higher when applying 25 and 30 tons/ha of MOF.

3.3 Effect of various organic fertilizers on the growth, yield and quality of leafy vegetables

3.3.1 Lettuce

Applying organic fertilizers, including MOF, cow manure and bio-organic fertilizer, enhanced the lettuce's performance compared to the control (Table 6). Applying organic fertilizers did not affect the

Table 5 Effect of MOF amounts on the yield and quality of mustard spinach

Treatment	Fresh mass (g/plant)	Theoretical yield (ton/ha)	Actual yield (ton/ha)	Ascorbic acid (%)	Brix (%)
First planting					
R1	111.0±4.17 ^b	29.7±1.21 ^b	19.3±0.54 ^b	4.1±0.66 ^b	3.5±0.32 ^a
R2	121.3±5.42 ^b	32.0±2.12 ^b	21.0±0.67 ^b	5.4±0.35 ^a	3.4±0.17 ^a
R3	149.3±8.15 ^a	39.3±0.69 ^a	25.7±0.47 ^a	5.7±0.44 ^a	4.5±0.51 ^a
R4	146.0±3.67 ^a	38.7±0.47 ^a	25.3±0.36 ^a	5.3±0.51 ^a	4.4±0.46 ^a
LSD _{0.05}	13.68	2.92	2.49	1.18	1.16
Second planting					
R1	108.7±2.89 ^b	28.7±0.96 ^d	18.7±0.50 ^c	4.5±0.36 ^b	3.9±0.33 ^b
R2	115.3±9.18 ^b	32.1±0.70 ^c	19.6±1.51 ^c	5.4±0.51 ^a	4.3±0.58 ^b
R3	146.1±4.78 ^a	38.0±0.81 ^a	25.7±0.94 ^a	5.7±0.57 ^a	5.4±0.16 ^a
R4	136.7±2.35 ^a	35.3±1.05 ^b	23.0±0.58 ^b	5.4±0.39 ^{ab}	5.2±0.29 ^a
LSD _{0.05}	11.7	1.9	2.2	0.9	0.6

The means with similar lower-case letters within columns did not differ significantly at a 5% probability. R1: 15 tons per ha, R2: 20 tons per ha, R3: 25 tons per ha, R4: 30 tons per ha. LSD: Least significant difference.

Table 6 Effect of various organic fertilizers on the growth of lettuce

Treatment	Growth time (day)	Plant height (cm)	Number of leaves (leaves /plant)	Canopy diameter (cm)	Leaf area index
First planting					
F1	31	26.4±1.21 ^a	13.1±0.31 ^a	23.5±3.52 ^a	43.4±0.77 ^a
F2	32	24.2±2.00 ^b	12.5±0.91 ^a	24.1±2.33 ^a	41.8±2.24 ^a
F3	31	25.3±3.03 ^{ab}	13.2±0.69 ^a	24.9±1.68 ^a	42.4±1.08 ^a
Control	33	22.1±2.08 ^c	11.7±1.02 ^b	24.2±1.94 ^a	31.5±4.44 ^b
LSD _{0.05}		1.87	1.71	6.26	2.83
Second planting					
F1	33	25.5±2.12 ^a	13.4±0.25 ^a	28.6±0.92 ^a	41.8±10.64 ^a
F2	32	24.2±2.07 ^a	12.3±0.86 ^a	25.3±1.47 ^b	41.1±0.97 ^a
F3	33	25.9±1.16 ^a	13.0±0.62 ^a	24.8±1.69 ^{bc}	40.3±1.54 ^a
Control	34	19.8±1.35 ^b	10.1±0.56 ^b	23.2±2.62 ^c	28.9±3.08 ^b
LSD _{0.05}		2.7	1.7	1.8	2.2

The means with similar lower-case letters within columns did not differ significantly at 5% probability; F1: Moringa organic fertilizer (MOF); F2: Cow manure; F3: Bio-organic fertilizer; Control: without fertilization; LSD: Least significant difference.

Table 7 Effect of various organic fertilizers on the yield and quality of lettuce

Treatment	Fresh mass (g/plant)	Theoretical yield (ton/ha)	Actual yield (ton/ha)	Ascorbic acid (%)	Brix (%)
First planting					
F1	150.0±3.05 ^a	38.7±0.81 ^a	25.6±1.22 ^a	5.2±0.22 ^a	5.0±0.43 ^a
F2	133.7±2.57 ^b	35.6±0.39 ^b	23.1±0.76 ^b	5.2±0.31 ^a	4.7±0.49 ^{ab}
F3	128.3±6.02 ^b	33.5±2.11 ^b	22.1±1.18 ^b	5.3±0.16 ^a	5.0±0.47 ^a
Control	105.0±3.78 ^c	28.0±1.18 ^c	18.0±1.34 ^c	4.3±0.56 ^b	3.6±0.26 ^b
LSD _{0.05}	12.31	2.30	1.40	0.6	0.6
Second planting					
F1	145.7±3.52 ^a	37.4±0.53 ^a	25.5±0.34 ^a	5.6±0.30 ^a	5.1±0.10 ^a
F2	129.6±4.04 ^b	34.0±0.59 ^b	22.8±0.73 ^b	5.7±0.23 ^a	5.0±0.26 ^a
F3	123.5±4.92 ^c	33.5±1.67 ^b	21.7±1.42 ^b	5.7±0.29 ^a	5.1±0.15 ^a
Control	101.7±5.44 ^d	26.2±1.26 ^c	18.1±0.95 ^c	4.7±0.27 ^b	3.9±0.49 ^b
LSD _{0.05}	5.99	2.12	1.55	0.3	0.2

The means with similar lower-case letters within columns did not differ significantly at 5% probability; F1: Moringa organic fertilizer (MOF); F2: Cow manure; F3: Bioorganic fertilizer; Control: without fertilization; LSD: Least significant difference

lettuce's number of leaves and canopy diameter in the first planting. However, the canopy diameter increased when MOF was applied in the second planting. The height of lettuce was also significantly higher when MOF was applied in the first planting, but this observation was not reproducible in the second planting. LAI was larger when organic fertilizers were applied at both planting times.

Similarly, fresh mass, theoretical yield and actual yield were higher in MOF treatment than in other treatments (Table 7). The fresh mass of lettuce treated with MOF was 150 g per plant in the first planting and 146 g per plant in the second planting. Lettuce grown with cow manure and bio-organic fertilizer exhibited lower fresh mass (134 and 130 g per plant for cow manure and 128 and

124 g for bio-organic fertilizer in the first and second planting seasons, respectively). The yield of lettuce grown with MOF was 7.4–7.6 tons per ha higher than control plants.

3.3.2 Mustard spinach

Like lettuce, organic fertilizers enhanced the growth of mustard spinach compared to the control (Table 8). In the first planting, there were no significant differences in plant height, number of leaves, canopy diameter and LAI between MOF and other organic fertilizers. However, in the second planting, plant height and LAI were the highest with the application of MOF (28.2 cm and 43.1, respectively).

Table 8 Effect of various organic fertilizers on the growth of mustard spinach

Treatment	Plant height (cm)	Number of leaves (leaves/plant)	Canopy diameter (cm)	Leaf area index
First planting				
F1	26.7±2.44 ^a	12.2±0.42 ^a	32.1±1.50 ^a	42.8±3.28 ^a
F2	27.1±1.55 ^a	11.9±0.35 ^a	33.0±0.95 ^a	42.3±3.57 ^a
F3	27.4±5.63 ^a	12.0±0.30 ^a	30.3±2.61 ^{ab}	41.7±3.73 ^a
Control	21.6±3.21 ^b	11.6±0.87 ^a	27.4±1.54 ^b	32.0±4.52 ^b
LSD _{0.05}	3.6	1.8	3.6	7.1
Second planting				
F1	28.2 ^a ±1.63	12.8 ^a ±0.69	33.3 ^a ±1.25	43.1 ^a ±0.96
F2	25.7 ^b ±1.06	12.5 ^a ±0.62	33.4 ^a ±1.06	40.3 ^b ±0.84
F3	27.2 ^{ab} ±0.53	13.1 ^a ±0.53	31.6 ^a ±4.60	40.1 ^b ±1.17
Control	22.5 ^c ±1.47	11.7 ^a ±0.93	27.1 ^b ±0.68	30.2 ^c ±2.06
LSD _{0.05}	1.7	1.5	1.9	2.3

The means with similar lower-case letters within columns did not differ significantly at 5% probability; F1: Moringa organic fertilizer (MOF); F2: Cow manure; F3: Bio-organic fertilizer; Control: without fertilization; LSD: Least significant difference.

Table 9 Effect of various organic fertilizers on the yield and quality of mustard spinach

Treatment	Fresh mass (g/plant)	Theoretical yield (ton/ha)	Actual yield (ton/ha)	Ascorbic acid (%)	Brix (%)
First planting					
F1	158.0±8.93 ^a	38.7±0.38 ^a	25.9±0.51 ^a	5.7±0.38 ^a	4.5±1.01 ^a
F2	140.3±9.14 ^b	37.3±1.55 ^a	23.3±1.35 ^b	5.6±0.56 ^a	4.4±0.76 ^a
F3	136.7±7.70 ^b	37.0±1.97 ^a	24.3±1.42 ^{ab}	5.7±0.63 ^a	4.5±0.95 ^a
Control	111.3±7.26 ^c	28.2±1.70 ^b	18.4±0.98 ^c	4.2±0.74 ^b	3.6±2.14 ^b
LSD _{0.05}	14.4	2.4	1.8	1.2	1.2
Second planting					
F1	155.0±6.39 ^a	37.4±0.66 ^a	26.8±0.66 ^a	5.5±0.19 ^a	5.9±0.28 ^a
F2	138.1±4.55 ^b	35.3±1.87 ^b	23.9±1.24 ^b	5.2±0.84 ^a	4.7±0.74 ^b
F3	130.3±8.95 ^b	34.8±1.16 ^b	24.1±1.28 ^{ab}	5.3±0.58 ^a	5.5±0.32 ^a
Control	110.4±8.04 ^c	27.3±1.81 ^c	19.9±0.93 ^c	4.4±0.60 ^b	4.0±1.01 ^b
LSD _{0.05}	9.4	1.9	1.1	0.7	0.7

The means with similar lower-case letters within columns did not differ significantly at 5% probability; F1: Moringa organic fertilizer (MOF); F2: Cow manure; F3: Bioorganic fertilizer; Control: without fertilization; LSD: Least significant difference.

At harvest time, fresh mass and yields of mustard spinach were significantly different across organic fertilizer treatments (Table 9). Mustard spinach treated with MOF had more fresh mass than other organic fertilizers during both planting times. The MOF treatment also produced 2.6 to 2.9 tons per ha (actual yield) more than the cow manure treatment. On the other hand, cow manure and bio-organic fertilizer treatments resulted in similar yields and quality of mustard spinach. The ascorbic acid contents were similar among the organic fertilizer treatments. Finally, the Brix of mustard spinach was significantly higher in the MOF and bio-organic fertilizer treatments compared to the other two in the second planting.

4 Discussion

Using plant materials to produce organic fertilizers is an area of active research. These fertilizers contain various amino acids, vitamins and growth regulators, which will help to improve plant growth and the quality of agricultural products even if plants grow under stress or in hydroponic systems (Nofal et al. 2020; Khan et al. 2021; Jagathy and Lavanya 2021; Upendri and Karunarathna 2021). Research on the production of bio-extract or organic fertilizer derived from *M. oleifera* has demonstrated their effects in enhancing the performance of crops (Culver et al. 2012; Matthew 2016; Merwad 2018; Chanthanousone et al. 2020). Works from Fahey (2005) and Chanthanousone et al. (2020) demonstrated that *Moringa* leaves should be utilized as food rather than to produce fertilizers due to their high nutritional values. This work aimed to produce organic fertilizer from *Moringa* non-edible parts like the stems, branches and leaf petioles. Here, a more detailed method for producing moringa organic fertilizer (MOF) derived from *Moringa* non-edible parts was described, and its usefulness for growing leafy vegetables was characterized.

The length of the incubation period changed the quality of MOF. Nitrogen content was the highest during incubation for seven weeks. Nitrogen is an essential element that determines crop yield. The contents of nitrogen and organic matter kept in soil and fertilizer help to promote plant growth. Thus, the incubation period produced with the higher nitrogen content should be considered optimal for MOF production. Furthermore, seven-week incubation yielded the highest amount of organic matter, although the difference was insignificant. The phosphorus and phosphorus pentoxide contents did not change much between seven and nine weeks of incubation. In another report, *Moringa*-fortified compost made with poultry manure and sawdust achieved a higher level of total nitrogen after an eight-week incubation period, resulting in a pH similar to those reported in this study (Taiwo et al. 2022). In summary, a seven-week incubation period was optimal for producing organic fertilizer from unused moringa parts.

MOF doses affected the performance of leafy vegetables grown in both planting times. Plant height, number of leaves, canopy diameter and leaf area index of lettuce and these parameters were recorded highest when 20–25 tons of MOF per ha were applied at the first planting, and these values were similar to the second planting between 20–30 tons of MOF per ha. Meanwhile, for mustard spinach, these parameters were not significantly different (between 20–30 tons of MOF per ha) at both planting times, except for plant height. With increasing amounts of MOF up to 25 tons per ha, fresh mass, theoretical yield and actual yield were increased in lettuce and mustard spinach. In a previous report, Akther et al. (2019) found that the yield of Indian spinach increased with increasing amounts of vermicompost, and it was higher than 35 tons per ha in the combination of fertilizer and insect netting. Also, increasing levels of organic fertilizer prepared from meat and bone

greatly influenced the weight and size of *Brassicaceae* vegetables (Fracchiolla et al. 2020). Different amounts of MOF seemed not to change the ascorbic acid content in lettuce, although the lowest ascorbic acid content was observed in the 15 tons of MOF per ha treatment. The difference in Brix in both leafy vegetables was negligible across MOF amounts. The highest Brix at both planting times was recorded with the 25 tons of MOF per ha treatment.

Moringa organic fertilizer positively affected plant growth and lettuce and mustard spinach yield. Overall, the highest leaf area index, fresh mass, theoretical yield and actual yield were observed with the MOF treatment. The application of vegetable residues helps improve soil moisture content, water holding capacity and soil basal respiration and promotes lettuce growth and quality (Cavalheiro et al. 2021). The growth of vegetables was enhanced with organic fertilizers, compared to the non-fertilized vegetable. Among organic fertilizers, the growth, ascorbic acid content and Brix were comparable between MOF and other fertilizer treatments. Although the actual yield of lettuce increased with organic fertilizers, MOF treatment still yielded 2.5–3.5 tons per ha and 2.7–3.8 tons per ha more than the other fertilizer treatments in the first and second planting. The results of this study are consistent with earlier reports, using compost or vermicompost-based organic fertilizers (Coria-Cayupán et al. 2009; Masarirambi et al. 2010). Vitamin C is an essential antioxidant because it contributes 24.5% to the overall antioxidant activity in lettuce (Nicolle et al. 2004). This study found the highest ascorbic acid content in plants treated with MOF. The actual yield of mustard spinach grown in the first and second planting under treatment MOF reached 25.9 tons per ha and 26.8 tons per ha, respectively. However, the plants of this treatment yielded lower than those treated with *Moringa* foliar fertilizer (Chanthanosone et al. 2020). In another study, organic amendments such as green manure, poultry, cow, pig and rabbit manure, when being applied at 120 kg per ha, significantly increased the organic matter, Ca and Mg in soil and further enhanced okra yield, protein and mucilage contents (Adekiya et al. 2020). However, the effect of cow manure on the cultivation of leafy vegetables was less profound than that of MOF in this study. Therefore, *Moringa* organic fertilizer derived from non-edible moringa parts is promising for sustainable organic farming.

Conclusion

In conclusion, the moringa non-edible parts, such as stems, branches and leaf petioles, were promising materials to produce organic fertilizers. Optimal moringa organic fertilizer (MOF) was obtained after a seven-week incubation period. Furthermore, applying 25 tons of MOF per ha enhanced the yield and quality of leafy vegetables. MOF is a promising alternative to cow manure and other commercial bio-organic fertilizers to ensure safe and sustainable vegetable farming.

Acknowledgement

Hue University partially supported this work under project number DHH 2019-15-16. The authors also acknowledge the partial support of Hue University under the Core Research Program (Grant No. NCM.DHH.2019.01) and Dr. Han Ngoc Ho for English editing.

Declaration of Competing Interest

The authors declare no competing interests.

References

- Adekiya, A. O., Ejue, W. S., Olayanju, A., Dunsin, O., et al. (2020). Different organic manure sources and NPK fertilizer on soil chemical properties, growth, yield and quality of okra. *Scientific Reports*, 10(1), 1–9. DOI:<https://doi.org/10.1038/s41598-020-73291-x>
- Ahmed, M., Rauf, M., Mukhtar, Z., & Saeed, N. A. (2017). Excessive use of nitrogenous fertilizers: an unawareness causing serious threats to environment and human health. *Environmental Science and Pollution Research*, 24(35), 26983–26987. DOI: <https://doi.org/10.1007/s11356-017-0589-7>
- Akther, M. M., Islam, M. A., Rahman, M. S., Rahman, M. H., & Nandwani, D. (2019). Effect of Organic and Inorganic Fertilizer on the Growth and Yield of Indian spinach (*Basella alba* L.). *Archives of Agriculture and Environmental Science*, 4(3), 268–272. DOI: <https://doi.org/10.26832/24566632.2019.040302>
- Bauer, A., & Black, A. L. (1994). Soil Science Society of America. *Soil Science Society of America Journal*, 58(1), 185–193. <https://doi.org/10.2136/sssaj1940.036159950004000c0132x>
- Cavalheiro, T. R. T., Alcoforado, R. de O., Silva, V. S. de A., Coimbra, P. P. S., et al. (2021). The impact of organic fertilizer produced with vegetable residues in lettuce (*Lactuca sativa* L.) cultivation and antioxidant activity. *Sustainability (Switzerland)*, 13(1), 1–11. <https://doi.org/10.3390/su13010128>
- Chanthanosone, H., Hai, T. T. H., Phuc, L. K., The, N. T. D., Long, D. T., Cuc, N. T. K., & Thao, T. T. B. (2020). Influence of moringa organic foliar fertilizer on leafy vegetables in spring crop 2019. *Hue University Journal of Science: Agriculture and Rural Development*, 129(3B), 2–10. <https://doi.org/10.26459/hueuni-jard.v129i3b.5468>
- Chanthanosone, H., Thao, P. T., Co, N. Q., The, N. T. D., Long, D. T., Nhi, H. T. H., Bao, N. Q. L., & Hai, T. T. H. (2022). Influence of foliar application with *Moringa oleifera* residue fertilizer on growth and yield quality of leafy vegetables. *Journal of*

- Experimental Biology and Agricultural Sciences*, 10(6), 1453–1461. [https://dx.doi.org/10.18006/2022.10\(6\).1453.1461](https://dx.doi.org/10.18006/2022.10(6).1453.1461)
- Coria-Cayupán, Y. S., De Pinto, M. I. S., & Nazareno, M. A. (2009). Variations in bioactive substance contents and crop yields of lettuce (*Lactuca sativa* L.) cultivated in soils with different fertilization treatments. *Journal of Agricultural and Food Chemistry*, 57(21), 10122–10129. <https://doi.org/10.1021/jf903019d>
- Culver, M., Fanuel, T., & Chiteka, A. Z. (2012). Effect of Moringa extract on growth and yield of tomato. *Greener Journal of Agricultural Sciences*, 2(5), 207–211. <https://doi.org/10.5281/zenodo.3372890>
- Dang, T. T., Nguyen, T. Q., & Do, D. T. (2018). Evaluation of nitrate residue in some kinds of vegetables cultivated in Bac Ninh province. *Vietnam Journal Agriculture Science*, 16(1), 1–8. (in Vietnamese)
- Fahey, J. (2005). *Moringa oleifera*: A Review of The Medical Evidence for Its Nutritional, Therapeutic, and Prophylactic Properties. Part 1. *Trees for Life Journal*, 1(5), 1–15.
- Fracchiolla, M., Renna, M., D’Imperio, M., Lasorella, C., Santamaria, P., & Cazzato, E. (2020). Living mulch and organic fertilization to improve weed management, yield and quality of broccoli raab in organic farming. *Plants*, 9(2). <https://doi.org/10.3390/plants9020177>
- Ha, T. M., Shakur, S., & Pham Do, K. H. (2020). Risk perception and its impact on vegetable consumption: A case study from Hanoi, Vietnam. *Journal of Cleaner Production*, 271, 122793. <https://doi.org/10.1016/j.jclepro.2020.122793>
- Jagathy, K., & Lavanya, K. (2021). Comparative study on Synergistic effect of plant growth promoting microalgae and Panchagavya in reclaiming the wasteland and growth induction of *Vigna radiata*. *Indian Journal of Science and Technology*, 14(31), 2504–2510. <https://doi.org/10.17485/ijst/v14i30.855>
- Khan, A. U., Ullah, F., Khan, N., Mehmood, S., et al. (2021). Production of organic fertilizers from rocket seed (*Eruca sativa* L.), chicken peat and *Moringa oleifera* leaves for growing linseed under water deficit stress. *Sustainability (Switzerland)*, 13(1), 1–20. <https://doi.org/10.3390/su13010059>
- Kumar, V., Thakur, A. K., Barothia, N. D. & Chatterjee, S. S. (2011). Therapeutic potentials of *Brassica juncea*: an overview. *Cellmed Orthocellular Medicine and Pharmaceutical Association*, 1 (1), 1–16. <https://doi.org/10.5667/tang.2011.0005>
- Masarirambi, M., Hlawe, M., Oseni, O., & Sibiya, T. (2010). Effects of organic fertilizers on growth, yield, quality and sensory evaluation of red lettuce (*Lactuca sativa* L.) 'Veneza Roxa.' *Agriculture and Biology Journal of North America*, 1(6), 1319–1324. <https://doi.org/10.5251/abjna.2010.1.6.1319.1324>
- Matthew, A. (2016). Moringa leaf extract on the growth and yield of pepper (*Capsicum annum* L.). *ARPN Journal of Agricultural and Biological Science*, 11(3), 107–109.
- Merwad, A. R. M. A. (2018). Using *Moringa oleifera* extract as biostimulant enhancing the growth, yield and nutrients accumulation of pea plants. *Journal of Plant Nutrition*, 41(4), 425–431. <https://doi.org/10.1080/01904167.2017.1384012>
- Merwad, A. R., & Khalil, M. (2018). Effect of Moringa residues on nutrients availability and wheat production in sandy and calcareous soils. *Journal of Soil Sciences and Agricultural Engineering*, 9(1), 55–62. <https://doi.org/10.21608/JSSAE.2018.35530>
- Nicolle, C., Carnat, A., Fraisse, D., Lamaison, J. L., et al. (2004). Characterization and variation of antioxidant micronutrients in lettuce (*Lactuca sativa folium*). *Science of Food and Agriculture*, 84(15), 2061–2069. <https://doi.org/10.1002/jsfa.1916>
- Nofal, O. A., Rezk, A.I., & Abbas, M. M. (2020). The role of different fertilization strategies on the yield and quality of different flax varieties in the new lands. *Science Archives*, 01(03), 84–88. <https://doi.org/10.47587/sa.2020.1302>
- Faizi, S., Siddiqui, B. S., Saleem, R., Siddiqui, S., Aftab, K., & Gilani, A. H. (1994). Isolation and structure elucidation of new nitrile and mustard oil glycosides from *Moringa oleifera* and their effect on blood pressure. *Journal of Natural Products*, 57(9), 1256–1261. <https://doi.org/10.1021/np50111a011>
- Padulosi, S., Heywood, V., Hunter, D. & Jarvis, A. (2011). *Underutilized species and climate change: Current status and outlook* (1st ed.). In S. S. Yadav, R. J. Redden, J. L. Hatfield, H. Lotze-Campen, A. E. Hall (eds) *Crop Adaptation to Climate* (pp. 507-521), John Wiley & Sons, Inc. DOI: 10.1002/9780470960929.ch35
- Paulin, B. & O'Malley, P. (2008). *Compost production and use in horticulture*. Department of agricultural and food: Government of Western Australia.
- Taiwo, A. M., Oladotun, O. R., Gbadebo, A. M., Alegbeleye, W. O. & Hassan, T. M. (2022). Nutrient enhancement potentials of Moringa (*Moringa oleifera*), neem (*Azadirachta indica*), and pawpaw (*Carica papaya*) fortified composts in contaminated soils. *Environmental Monitoring and Assessment*, 194(3), 237. <https://doi.org/10.1007/s10661-022-10053-4>
- Upendri, H. F. L., & Karunarathna, B. (2021). Organic nutrient solution for hydroponic system. *Academia Letters*, (Article 1893). <https://doi.org/10.20935/al1893>

- Van Wyk, B.E. (2005). Food plants of the world, identification, culinary uses and nutritional value. 1st ed. Briza Publication, Pretoria, South Africa, 48 pp. DOI: 10.15159/AR.20.010 revise as per APA citations pattern.
- Verma, B. C., Pramanik, P., & Bhaduri, D. (2019). Organic fertilizers for sustainable soil and environmental management. In: Meena, R. (ed.) *Nutrient Dynamics for Sustainable Crop Production* (pp. 289-313). Springer, Singapore. https://doi.org/10.1007/978-981-13-8660-2_10
- Wang, C., Riedl, K. M., & Schwartz, S. J. (2013). Fate of folates during vegetable juice processing - Deglutamylation and interconversion. *Food Research International*, 53(1), 440-448. <https://doi.org/10.1016/j.foodres.2013.05.011>
- Yu, J. C., Jiang, Z., Li, R., & Chan, S. M. (2003). Chemical composition of the essential oils of *Brassica juncea* (L.) cross. Grown in different regions, Hebei, Shaanxi and Shandong, of China. *Journal of Food and Drug Analysis*, 11(1), 22-26. <https://doi.org/10.38212/2224-6614.2729>
- Zhao, H., Li, X., & Jiang, Y. (2019). Response of nitrogen losses to excessive nitrogen fertilizer application in intensive greenhouse vegetable production. *Sustainability*, 11(6), 1513. <https://doi.org/10.3390/su11061513>






Journal of Experimental Biology and Agricultural Sciences

<http://www.jebas.org>

ISSN No. 2320 – 8694

Optimization of protein extraction from "Cam" rice bran by response surface methodology

Le Thi Kim Loan¹, Quoc Ha Minh^{2,3}, Thuy Nguyen Minh⁴ , Nguyen Thanh Nhung⁵,
Tran Dang Xuan⁶ , Vu Xuan Duong⁷, Khuat Huu Trung⁵, Le Hoang Nhat Minh⁸,
Tran Dang Khanh^{5,9*} , Tran Thi Thu Ha^{10*}

¹Department of Agriculture and Food Technology, Tien Giang University, Tien Giang, VietNam

²National Food Institute, Technical University of Denmark, 2800 Kongens Lyngby, Denmark

³Department of Agricultural, Food and Environmental Sciences, Marche Polytechnic University, 60131 Ancona, Italy

⁴Department of Food Technology, College of Agriculture, Can Tho University, Can Tho, Vietnam

⁵Agricultural Genetics Institute, Hanoi, Vietnam

⁶Department of Development Technology, Graduate School for International Development and Cooperation, Hiroshima University, Hiroshima 739-8529, Japan

⁷Institute of Applied Research and Development, Hung Vuong University, Phu Tho 290000, Vietnam

⁸Department of Life Sciences, University of Science and Technology of Hanoi, Hanoi, Vietnam

⁹Vietnam National University of Agriculture, Trau Quy, Gia Lam, Hanoi, Vietnam

¹⁰Institute of Forestry and Sustainable Development (IFS), Thai Nguyen University of Agriculture and Forestry, Vietnam

Received – March 06, 2023; Revision – April 15, 2023; Accepted – April 24, 2023

Available Online – April 30, 2023

DOI: [http://dx.doi.org/10.18006/2023.11\(2\).290.296](http://dx.doi.org/10.18006/2023.11(2).290.296)

KEYWORDS

Rice bran

Protein content

Optimization

Nutritional value

ABSTRACT

"Cam" rice bran was considered a waste product from rice, which is rich in natural compounds and protein owing to its outstanding nutritional value. This study aimed to establish an optimization model for extracting protein from rice bran, with two responses: extraction yield (%) and protein content (%). The variable parameters included were pH (8.5-9.5), stirring time (3.5-4.5 h), and enzyme incubation temperature (85-95°C). The coefficient of determination for both models were above 0.95, indicating a high correlation between the actual and estimated values. The maximum extraction yield and protein content were achieved when the conditions were set at pH of 9.02, stirring time of 4.02 h, and extraction temperature of 90.6°C. Under these optimum conditions, the predicted protein extracted from rice bran was 43.03% (moisture <13.0%), with an extraction yield of 15.9%. The findings of this study suggested that this protocol can enhance the utilization of rice bran and might be employed on a large scale in the food industry to exploit the nutritional source.

* Corresponding author

E-mail: tdkhanh@vaas.vn (Tran Dang Khanh);

ha.tran2007@gmail.com (Tran Thi Thu Ha)

Peer review under responsibility of Journal of Experimental Biology and Agricultural Sciences.

Production and Hosting by Horizon Publisher India [HPI]
(<http://www.horizonpublisherindia.in/>).
All rights reserved.

All the articles published by [Journal of Experimental Biology and Agricultural Sciences](#) are licensed under a [Creative Commons Attribution-NonCommercial 4.0 International License](#) Based on a work at www.jebas.org.



1 Introduction

Rice (*Oryza sativa* L.) is a staple food consumed daily in almost Asia countries. Numerous rice varieties differ in nutritional value and natural compounds (Kushwaha 2016), especially in pigmented rice varieties such as black, brown, purple, and red rice, containing exceptionally high levels of natural compounds (Veni 2019; Hue et al. 2018). Further, the rice bran layer and endosperm contain many compounds of high nutritional value (Pengkumsri et al. 2015; Eng and Mohd Rozalli 2022), making rice bran a rich source of these compounds that can be optimized for use in food products (Majzoobi et al. 2013). Rice bran has a higher lysine content (approximately 3-4%) than rice endosperm, other grains, or legumes. Further, lysine with a molecular weight greater than 0.5 kDa derived from alkaline-assisted extraction can exhibit anti-cancer activity without affecting normal cells. Rice bran protein (RBP) contains a significant amount of hydrolysate, including bioactive peptides (Boonla et al. 2015), which are highly digestible (> 90%) (Wang et al. 2015). Additionally, rice bran is gluten-free and does not generally contain allergens (Ngoc et al. 2019; Kaur et al. 2022). These properties make it suitable for manufacturing instant food formulas, gluten-free products, and cosmetics. Moreover, RBPs with a molecular weight of 57 kDa have been reported to exhibit cell-adhesion activity against lung carcinoma cells in Lewis mice (Shoji et al. 2001). However, rice bran is often considered a by-product of the milling process or agricultural waste (Chiou et al. 2013).

"Cam" rice is a popular Vietnamese native cultivar grown in the Cai Lay district of Tien Giang province. This cultivar is a nourishing staple food, containing more nutrients than other rice cultivars (Loan and Thuy 2019), and is especially rich in protein content. It is essential to extract protein from this rice to remove redundant starch content using amylase for a higher yield and purity (Acton 2013). Additionally, the extraction protocols should be adequate to obtain the best possible product. For the apparent reason of having various controlling factors, using the response surface methodology seems to be the most feasible way to examine the variables and predict the optimal response with a limited number of trials (Phongthai et al. 2017; Van Tai et al. 2021; Thuy et al. 2022a). However, very few comprehensive studies on the optimization of protein extraction under alkaline and enzyme-assisted environment concerning various factors are available. Therefore, this study aimed to optimize the rice bran's protein extraction protocol by investigating three parameters, including pH, stirring time (h), and incubation temperature (°C). This

protocol may enhance the quantity and quality of protein extraction to use rice bran effectively for food products.

2 Materials and Methods

2.1 Materials and procedures

"Cam" rice is conventionally cultivated under conventional conditions in the Cai Lay district, Tien Giang province (10°29'49.5"N 106°03'11.0"E). After harvesting, the rice bran was collected after milling at a local company (Tien Giang Food Company). The bran was then dried at 40°C until its moisture content was less than 13% and then vacuum-packed and stored at 4°C until use. The "Cam" rice bran contained 14.1% protein, 20.5% starch, 10.1% ash, and 7.6% moisture, which were analyzed by AOAC (2005) method. After that, 25 g of rice bran was mixed with distilled water at a ratio of 1:7 (w/v). The pH of the suspension was adjusted to a range of 8.5 to 9.5 using 1N NaOH. The mixture was continuously stirred for 3.5 to 4.5 hrs with a magnetic stirrer at 500 rpm to dissolve the protein.

To hydrolyze the starch of rice bran, the pH of the solution was adjusted to 7.0 using (NH₄)₂SO₄. Next, 0.25% α-amylase was added to the mixture and heated for 20 min at 85°C to 95°C. Afterwards, the mixture was centrifuged at 3000 g to remove any remaining residues and collect the soluble protein fraction. The protein precipitation process was carried out at pH 3.5-4.5 by 1N HCl. The mixture was recentrifuged at 3000 g to yield the precipitated protein, which was then washed with sterile distilled water (2 times). Finally, the precipitated protein was dried until its moisture content was less than 13% and stored in vacuum-sealed PA packaging for later use. The enzyme Termamyl (Termamyl 120L, liquid endo-alpha amylase-1 gallon/3.785 liters) was purchased from Novozyme company. It had a pH range of 5.5 – 7.0, 120 KNU-T/g (Kilo Novo α-amylase unit), and was resistant to heat, retaining its activity even at 105 °C.

2.2 Optimization design

The extraction process optimization was designed using the Box-Behnken model with 15 experimental units, which included three central experiments and three replicates with selected variables. Each factor was surveyed with three levels (-1, 0, and +1), including the bran fluid pH (8.5 - 9.5), stirring time (3.5 to 4.5 h) for dissolving proteins, and suitable temperature (85 °C to 95 °C)

Table 1 Range and levels of the independent variables' experiments

Variables (extraction parameter)	Levels of code		
	-1	0	1
A: pH	8.5	9.0	9.5
B: Stirring time (h)	3.5	4.0	4.5
C: Incubation temperature (°C)	85	90	95

for amylase enzyme activity to hydrolyze starch, as shown in Table 1. The general equation of a response surface Y that depends on factors A , B , and C , is indicated below (Thuy et al. 2022b; Thuy et al. 2022c):

$$Y = b_0 + b_1A + b_2B + b_3C + b_4AB + b_5AC + b_6BC + b_7A^2 + b_8B^2 + b_9C^2 \quad (1)$$

Where A , B , C are independent variables, while b_{0-9} represent model term effects. The selection criteria of the model was based on the regression's R^2 value.

2.3 Determination of protein content

The protein content of rice bran extract (%) was determined by the Kjeldahl method (AOAC 2005). The protein extraction yield was calculated as the below formula (Eze et al. 2022):

$$\text{Protein extraction yield (Y1)(\%)} = \frac{\text{Total protein (rice bran + enzyme)} - \text{residual protein (in meal)}}{\text{Total protein (rice bran + enzyme)}}$$

2.4 Statistical analysis

The optimum levels of the components in the formulation for protein extraction from "Cam" rice bran were determined with RSM using Statgraphics Centurion 16. The data obtained were statistically treated by analysis of variance (ANOVA), and the means were compared by the Fisher LSD test at a significance level of 0.05. Data were presented as the mean of sample sets. Statistical analysis of the results to assess significant differences among samples was performed

3 Results and Discussion

3.1 Impact of single factors on protein extraction yield and protein content

This study focused on three factors that directly affect the rice bran's protein extraction process: pH, stirring time, and temperature to protein extraction yield (%) and protein content (%) (Figure 1). Cell disruption is critical for maximum protein acquisition since the rice bran is deep inside plant cells. The

stirring motion aids in cell breakdown (Mittal and Ranade 2023). Hence, we applied a mixing time of 3.5 to 4.5 h for further investigation. Tang et al. (2002) stated that stirring is a crucial agitated factor commonly used to disrupt cell structure. Temperature also affects protein extraction efficiency, as it determines enzyme activity, including that of α -amylase. Since rice grain contains numerous carbohydrates, removing these redundant residues is necessary for the highest and purest possible protein content, and the enzyme α -amylase performs this procedure.

It can be inferred that pH is the most impactful factor as long as the ideal value is maintained. The high protein extraction yield was under alkaline conditions (Ahlström et al. 2022). Furthermore, increasing pH, stirring time, or working temperature can gradually decrease protein extraction productivity. The findings of this study agree with the previous research by Chich et al. (2014), which reported that the optimal temperature range for the enzyme termamyl of seaweed is between 80-95°C.

The alkaline medium is the most effective for protein extraction as it breaks the hydrogen and peptide bonds between proteins. In contrast, an acidic environment is not optimal for protein collection as the protein isoelectric point is within this pH range. This study estimated the optimal pH range for protein extraction was from 8.5 to 9.5. Additionally, a more basic environment did not correlate with increased protein extraction efficiency, and a higher pH only decreased yield, consistent with findings by Silventoinen et al. (2019).

3.2 Regression equation of yield (%) and extracted protein content (%)

Table 2 presents the statistical analysis results for the studied factors, including pH, stirring time, and temperature, and their effects on extract yield and protein content. Most factors showed a statistically significant difference at a 95% confidence level with a p-value less than 0.05, except for the quadratic function of temperature in the regression equation of extract yield. The coefficients for determined and adjusted yield (%) were 95.3% and 94.1%, respectively, and for protein content, the coefficients were 94.4% and 94.0%. A high coefficient of determination value

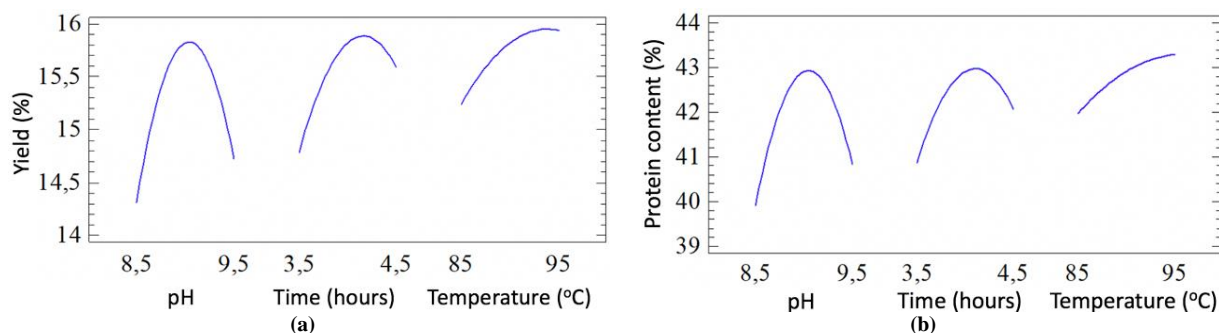


Figure 1 The effects of pH, stirring time, and temperature for α -amylase activity on the yield (%) and obtained protein content (%)

Table 2 Analysis results of the impact of coefficients on the regression equation of yield (%) and obtained protein content (%)

Model term	Protein content (%)		Yield (%)	
	P-value	Significant difference	P-value	Significant difference
A: pH	0.0001	Significant	0.0000	Significant
B: Stirring time (hour)	0.0000	Significant	0.0000	Significant
C: Temperature (°C)	0.0000	Significant	0.0000	Significant
A ²	0.0000	Significant	0.0000	Significant
AB	0.0000	Significant	0.0000	Significant
AC	0.0047	Significant	0.0108	Significant
B ²	0.0000	Significant	0.0000	Significant
BC	0.0017	Significant	0.0003	Significant
C ²	0.0019	Significant	0.0552	Insignificant
		R ² = 95.3%; R ² _{adjusted} = 94.1%	R ² = 94.4%; R ² _{adjusted} = 94.0%	

indicates the best fit between actual and predicted data considered. The determined coefficients indicate the effects of variables on the model and are sequentially converted into the adjusted values. Overall, the results suggest that the studied parameters apply to protein production.

After excluding the insignificant factor, we acquire formulas that show the correlation between recovery yield (%) and protein content (%):

$$\text{Yield (\%)} = -717.6 + 111.1A + 50.1B + 2.8C - 5.2A^2 - 2.3AB - 0.1AC - 2.5B^2 - 0.1BC$$

$$\text{Protein (\%)} = -1267.5 + 206.8A + 90.4B + 4.4C - 10.1A^2 - 2.6AB - 0.2AC - 5.6B^2 - 0.2BC - 0.01C^2$$

3.3 The optimization results of two response surfaces of yield and protein content (%)

Table 3 describes the optimization results of two response surfaces regarding each factor being considered with the other ones sequentially. It was found that a high recovery yield (16.0%) can be obtained by setting the pH at 9.0, stirring time at 4.12 h, and

temperature at 93.2°C. On the other hand, the maximum protein content (43.3%) can be achieved by setting the pH at 9.01, stirring time at 4.01 h, and temperature at 95°C. Simultaneous optimization for maximum recovery yield and protein content can be achieved by setting the pH at 9.02, stirring time at 4.02 h, and temperature at 90.6°C. It was also observed that the temperature was the most significant factor that varied the most among the three optimization factors.

Figures 2a and 2b illustrate the interactions between pH and two additional factors, stirring time and temperature, and their impact on protein extraction efficiency. The data indicates that as the pH increased from 8.5 to 9.0, protein extraction efficiency increased, with the maximum efficiency observed at pH 9.0. This finding is consistent with research by Hou et al. (2017), who reported a positive correlation between protein solubility and pH. This suggests that higher pH levels can lead to greater protein solubility, which may explain the increased extraction efficiency (Zhang et al. 2023).

In addition, Wang et al. (2015) have further elucidated that protein has a negative charge at a pH of 9.0, which increases its

Table 3 The optimal pH value, stirring time, and temperature for α -amylase to achieve the highest yield (%) and obtained protein content (%)

Factors	Optimization on each surface		Optimum condition of both surfaces
	Protein content (%)	Yield (%)	
pH	9.01	9.00	9.02
Stirring time (hour)	4.01	4.12	4.02
Temperature (°C)	95.0	93.2	90.6
Optimal results for each surface (%)	43.3	16.0	
Optimal results for both surfaces (%)	43.02	15.9	

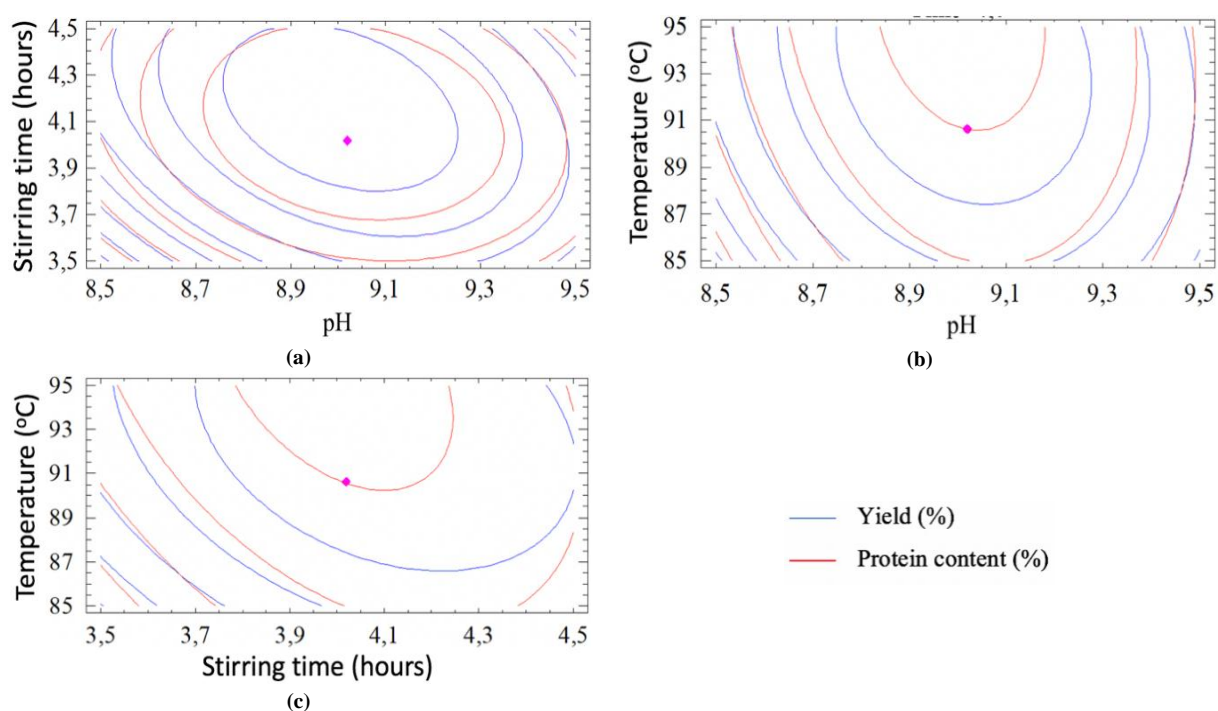


Figure 2 The response surface of each pair of factors investigated pH, stirring time, and temperature affecting the yield (%) and obtained protein content (%); (a) pH and stirring time (Temperature: 90°C); (b) pH and temperature (stirring time: 4 h); (c) Stirring time and temperature (pH: 4.0)

interaction with water molecules and enhances solubility. However, this relationship is not linear; solubility rises to a certain point and gradually decreases. Guan et al. (2017) proposed that this may be because proteins interact more with other raw materials than water, reducing the amount of protein available for extraction. This idea is supported by Theerakulkait et al. (2006), who found that pH 9.0 was more effective for protein extraction than pH 9.5. However, it is important to note that alkaline environments can cause protein degradation, leading to the formation of toxins in organisms. This degradation process can convert cysteine and serine residues into dehydroalanine and lysinoalanine, which alters their original conformation. Thus, selecting pH 9.0 may be an ideal condition for protein extraction while minimizing the risk of degradation and toxin formation. It also agreed with the study of Wang et al. (2022) on extracting protein from edible oil.

Figures 2a and 2c correlate stirring time and two other variables. The effectiveness of protein extraction generally improved as the stirring time increased from 3.5 to 4.0 h, reaching its peak at 4.0 h. According to Shen et al. (2008), extraction productivity rose sharply in the first 2.0 h, peaked at 4.0 h, and no significant growth was observed beyond 4 h. Stirring motions that occur in less than 4.0 h were necessary to break the bonds between phytic acids and proteins, which hinder protein extraction (Canan et al. 2011; Nourmohammadi et al. 2023). Surprisingly, stirring for

more than 4.5 h does not yield better results than stirring for 4.0 h since proteins are partially oxidized due to prolonged immersion in the water.

Figures 2b and 2c present temperature in the relationship with the two remaining factors and prove that raising the temperature from 85 to 90°C, increased the effectiveness of protein extraction. However, this conclusion must be considered that the temperature range must be within the tolerance of the enzyme under the denaturation point (Luong 2014). If inapplicable, as soon as the temperature exceeds the limit, the enzyme activity will gradually decrease and finally disappear (Jouanneau et al. 2010). Amylase cannot function properly, leading to the high remaining amount of carbohydrates in the rice bran, causing difficulty in extracting protein (Phuong et al. 2015). As a result, attained, 90°C acts as an upper limit since exceeding this temperature will decrease the efficiency of the process.

Conclusion

In conclusion, the working pH, stirring time, and temperature affected the protein extraction protocol used with "Cam" rice bran. The optimal parameters to achieve the highest extraction efficiency were pH 9.02, a stirring time of 4.02 hrs, and a temperature of 90.6°C. These conditions yielded an extraction efficiency of 15.9% with a protein content of 43.03% (moisture <13%).

Funding

This research received no external funding

Conflicts of Interest

The authors declare no conflict of interest

References

- Acton, Q.A. (2013). Amylases – Advances in Research and Application. Scholarly Editions, Atlanta, Georgia.
- Ahlström, C., Thuvander, J., Rayner, M., Matos, M., Gutiérrez, G., & Östbring, K. (2022). The Effect of Precipitation pH on Protein Recovery Yield and Emulsifying Properties in the Extraction of Protein from Cold-Pressed Rapeseed Press Cake. *Molecules*, 27(9), 2957
- AOAC. (2005). Protein (crude) in animal feed and pet food (Copper Catalyst), Method AOAC 2001.11. In: Official methods of analysis, 18th Edition, AOAC International Publisher Inc. Gaithersburg.
- Boonla, O., Kukongviriyapan, U., Pakdeechote, P., Kukongviriyapan, V., Pannangpetch, P., & Thawornchinsombut, S. (2015). Peptides derived from Thai rice bran improves endothelial function in 2K-1C renovascular hypertensive rats. *Nutrients*, 7(7), 5783-5799.
- Canan, C., Cruz, F.T.L., Delarozza, F., Casagrande, R., Sarmento, C.P.M., Shimokomaki, M., & Ida, E.I. (2011). Studies on the extraction and purification of phytic acid from rice bran. *Journal of Food Composition Analysis*, 24(7), 1057-1063.
- Chich, B.H., Ninh, D.V., & Boi, V.N. (2014). Investigation of Termamyl 120L properties on carrageenan substrate from *Kappaphycus alvarezii* (Doty). *Journal of Fisheries-Science & Technology, Nha Trang University*, 3, 16-20.
- Chiou, T.Y., Kobayashi, T., & Adachi, S. (2013). Characteristics and antioxidative activity of the acetone-soluble and-insoluble fractions of a defatted rice bran extract obtained by using an aqueous organic solvent under subcritical conditions. *Bioscience, Biotechnology, and Biochemistry*, 77(3), 624-630.
- Eng, H. Y., & Mohd Rozalli, N. H. (2022). Rice bran and its constituents: Introduction and potential food uses. *International Journal of Food Science & Technology*, 57(7), 4041-4051.
- Eze, O. F., Chatzifragkou, A., & Charalampopoulos, D. (2022). Properties of protein isolates extracted by ultrasonication from soybean residue (okara). *Food Chemistry*, 368, 130837.
- Guan, J., Takai, R., Toraya, K., Ogawa, T., Muramoto, K., Mohri, S., Ishikawa, D., Fujii, T., Chi, H., & Cho, S.J. (2017). Effects of alkaline deamidation on the chemical properties of rice bran protein. *Food Science and Technology Research*, 23(5), 697-704.
- Hou, F., Ding, W., Qu, W., Oladejo, A.O., Xiong, F., Zhang, W., He, R., & Ma, H. (2017). Alkali solution extraction of rice residue protein isolates: Influence of alkali concentration on protein functional, structural properties and lysinoalanine formation. *Food Chemistry*, 218, 207-15.
- Hue, H.T., Nghia, L.T., Minh, H.T., Anh, L.H., Trang, L.T.T., & Khanh, T.D. (2018). Evaluation of Genetic Diversity of Local-Colored Rice Landraces Using SSR Markers. *International Letters of Natural Science*, 67, 24–34.
- Jouanneau, D., Boulenguer, P., Mazoyer, J., & Helbert, W. (2010). Enzymatic degradation of hybrid ι - ν -carrageenan by *Alteromonas fortis* ι -carrageenase. *Carbohydrate Research*, 345(7), 934-40.
- Kaur, S., Kumar, K., Singh, L., Sharanagat, V. S., Nema, P. K., Mishra, V., & Bhushan, B. (2022). Gluten-free grains: Importance, processing and its effect on quality of gluten-free products. *Critical Reviews in Food Science and Nutrition*, 1-28.
- Kushwaha, U.K. (2016). Black Rice: Research, history and development. Springer. DOI: <https://doi.org/10.1007/978-3-319-30153-2>
- Loan, L.T.K., & Thuy, N.M. (2019). Optimization of germination process of "Cam" brown rice by response surface methodology and evaluation of germinated rice quality. *Food Research*, 4(2), 1-9.
- Luong, N.D. (2014). Enzyme technology. *Ho Chi Minh National University Publisher*.
- Majzoobi, M., Sharifi, S., Imani, B., & Farahnaky, A. (2013). The effect of particle size and level of rice bran on the batter and sponge cake properties. *Journal of Agricultural Science and Technology*, 15(6), 1175- 1184.
- Mittal, R., & Ranade, V. V. (2023). Intensifying extraction of biomolecules from macroalgae using vortex based hydrodynamic cavitation device. *Ultrasonics Sonochemistry*, 94, 106347
- Ngoc, N.T.L., Duy, L.N.D., & Ha, N.C. (2019). Study on the enzymatic hydrolysis of rice bran protein used in bacterial culture *Bacillus subtilis*. *Science Journal of Can Tho University*, 55(2), 267-275.
- Nourmohammadi, N., Austin, L., & Chen, D. (2023). Protein-based fat replacers: a focus on fabrication methods and fat-mimic mechanisms. *Foods*, 12(5), 957.

- Pengkumsri, N., Chaiyasut, C., Saenjum, C., Sirilun, S., Peerajan, S., Suwannalert, P., Sirisattha, S. (2015). Physicochemical and antioxidative properties of black, brown and red rice varieties of northern Thailand. *Food Science and Technology*, 35, 331-338.
- Phongthai, S., Lim, S.T., & Rawdkuen, S. (2017). Ultrasonic - assisted extraction of rice bran protein using response surface methodology. *Journal of Food Biochemistry*, 41(2), e12314.
- Phuong, N.T.M., Bac, V.H., Nhung, T.T., & Hiep, D.H. (2015). Research on protein recovery from rice bran. *Biology Journal*, 37(4), 479-486.
- Shen, L., Wang, X., Wang, Z., Wu, Y., & Chen, J (2008). Studies on tea protein extraction using alkaline and enzyme methods. *Food Chemistry*, 107(2), 929-38.
- Shoji, Y., Mita, T., Isemura, M., Mega, T., Hase, S., Isemura, S., & Aoyagi, Y. (2001). A fibronectin-binding protein from rice bran with cell adhesion activity for animal tumor cells. *Bioscience, Biotechnology, and Biochemistry*, 65(5), 1181-1186.
- Silventoinen, P., Rommi, K., Holopainen-Mantila, U., Poutanen, K., & Nordlund, E. (2019). Biochemical and techno-functional properties of protein-and fibre-rich hybrid ingredients produced by dry fractionation from rice bran. *Food Bioprocess Technology*, 12(9), 1487-99.
- Tang, S., Hettiarachchy, N.S., & Shellhammer, T.H. (2002). Protein extraction from heat-stabilized defatted rice bran. 1. Physical processing and enzyme treatments. *Journal of Agricultural and Food Chemistry*, 50(25), 7444-7448.
- Theerakulkait, C., Chaiseri, S. & Mongkolkanchanasiri, S. (2006). Extraction and Some Functional Properties of Protein Extract from Rice Bran. *Kasetsart Journal : Natural Science*, 40, 209-214.
- Thuy, N. M., Nhu, P. H., Tai, N. V., & Minh, V. Q. (2022c). Extraction Optimization of Crocin from Gardenia (*Gardenia jasminoides* Ellis) Fruits Using Response Surface Methodology and Quality Evaluation of Foam-Mat Dried Powder. *Horticulturae*, 8(12), 1199.
- Thuy, N. M., Tan, H. M., & Van Tai, N. (2022b). Optimization of ingredient levels of reduced-calorie blackberry jam using response surface methodology. *Journal of Applied Biology and Biotechnology*, 10(1), 68-75.
- Thuy, N. M., Tien, V. Q., Tuyen, N. N., Giao, T. N., Minh, V. Q., & Tai, N. V. (2022a). Optimization of Mulberry Extract Foam-Mat Drying Process Parameters. *Molecules*, 27(23), 8570.
- Van Tai, N., Linh, M. N., & Thuy, N. M. (2021). Optimization of extraction conditions of phytochemical compounds in "Xiem" banana peel powder using response surface methodology. *Journal of Applied Biology and Biotechnology*, 9(6), 56-62.
- Veni, B.K. (2019). Nutrition profiles of different colored rice: A review. *Journal of Pharmacognosy and Phytochemistry*, 2, 303-305.
- Wang, L., Wang, Y., Qin, Y., Liu, B., & Zhou, Y. (2022). Extraction and determination of protein from edible oil using aqueous biphasic systems of ionic liquids and salts. *Food and Bioprocess Technology*, 15, 190-202.
- Wang, T., Zhang, H., Wang, L., Wang, R., & Chen, Z. (2015). Mechanistic insights into solubilization of rice protein isolates by freeze-milling combined with alkali pretreatment. *Food Chemistry*, 178, 82-88.
- Zhang, J., Ström, A., Bordes, R., Alming, M., Undeland, I., & Abdollahi, M. (2023). Radial discharge high shear homogenization and ultrasonication assisted pH-shift processing of herring co-products with antioxidant-rich materials for maximum protein yield and functionality. *Food Chemistry*, 400, 133986.



Journal of Experimental Biology and Agricultural Sciences

<http://www.jebas.org>

ISSN No. 2320 – 8694

Effect of AM fungi during salt stress on biochemical content in Ginger (*Zingiber officinale* Rosc.)

Kishor Bhosale^{1#*}, Bharat Shinde²

¹Department of Botany, Nowrosjee Wadia College, 19, V. K. Joag Road Pune 411001, Pune (Maharashtra) India 411001

²V.P.A.S.C. College, Baramati District Pune, (Maharashtra) India

#Present Address: Survey No 48/2, Ceratec Greens, Wing A, Flat No 602, Jadhavnagar (Katraj), Pune 411046 (Maharashtra state) India

Received – December 23, 2022; Revision – April 04, 2023; Accepted – April 15, 2023

Available Online – April 30, 2023

DOI: [http://dx.doi.org/10.18006/2023.11\(2\).297.305](http://dx.doi.org/10.18006/2023.11(2).297.305)

KEYWORDS

AM fungi

Chlorophyll

Nucleic acids

Proteins

Proline

Reducing sugars

Total soluble carbohydrates

ABSTRACT

Ginger (*Zingiber officinale* Rosc.) is a highly-grown spice crop; its aromatic rhizomes are commercially important due to its high importance in the diet as a spice and some medicinal values. Irrigation methods in India increase salt content in the soil. Arbuscular Mycorrhizal (AM) fungi assist plants under salt stress. However, the vital role of mycorrhizal fungi in ginger salt tolerance has not been evaluated yet and needs to emphasize on its evaluation. The present investigation was conducted to assess the efficacy of AM fungi on ginger plants grown under different salt concentrations. In the current investigation level of Chlorophyll, nucleic acids like DNA and RNA, Proteins, Proline, reducing sugars, and total soluble carbohydrates contents have been evaluated to estimate the Growth and biochemical parameters. The study revealed that AM fungi significantly contributed to the salt stress tolerance of Ginger plants. Statistical analysis found an enormously significant correlation between growth parameters and salt tolerance. Pearson correlation coefficient has been used as testimony, resulting in a positive correlation of the use of AM fungi on ginger plant's Growth and biochemical contents.

* Corresponding author

E-mail: ksbhosale@gmail.com (Kishor Bhosale)

Peer review under responsibility of Journal of Experimental Biology and Agricultural Sciences.

Production and Hosting by Horizon Publisher India [HPI]
(<http://www.horizonpublisherindia.in/>).
All rights reserved.

All the articles published by [Journal of Experimental Biology and Agricultural Sciences](#) are licensed under a [Creative Commons Attribution-NonCommercial 4.0 International License](#) Based on a work at www.jebas.org.



1 Introduction

Ginger (*Zingiber officinale* Rosc.), a perennial herbaceous crop from the family Zingiberaceae, originated in South East Asia. It is being cultivated as a spice and condiment which enhance the flavour of the food (Park and Pezzuto 2002). Ginger is mainly grown in the countries like India, China, Nigeria, Australia, Jamaica etc. Among the ginger-cultivating countries, China and India are reported as leading ginger producers in the world (Blumenthal et al. 2000). Ginger rhizomes are used in the treatment of various ailments such as headache, cold, nausea and emesis (Blumenthal et al. 2000). The antioxidant (Nile and Park 2015), and anticancer activities of the ginger rhizome have also been well reported (Citronberg et al. 2013).

Now in these days, soil salinity is a significant issue, and according to Ruiz-Lozano et al. (2001), saline soils occupy near about 7 % surface of the land, and this percentage continuously increases and lead to almost half of the cultivable land loss till 2050 (Wang et al. 2003). Around 15 million hectares of cultivable fields worldwide and approximately 7.7 billion hectares of total land are likely unnatural due to excessive salt (Sheng et al. 2008). Yamato et al. (2008) recorded the presence of AM Fungi in saline environments and reported that the association of AM fungi with plant enhance the Growth and biomass of the host plant. Generally, salt concentration decreases plant growth and yield, specifically in dry regions. Rabie (2005) also testified that AM fungi augment the survival capacity of plants during salinity stress and improve the nutrient absorption and water uptake capacity. Most recent studies noted that AM-colonized plants are more vigorous than non-colonized plants underneath salinity (Al-Karaki 2000). Previous research on the efficacy of AM during salinity stress showed that symbiosis of AM fungi positively affected nutrients uptake and signifies that the effect of salinity stress is controlled by AM fungi (Dastogeer et al. 2020; Liu et al. 2023; Aziz et al. 2023). AM fungi effectively boost the availability of different macro and micro-nutrients, which improves photosynthetic efficiency and plant biomass (Chen et al. 2017; Mitra et al. 2020).

The effects of salt stress on the photosynthetic compound like Chlorophyll in Ginger have not been evaluated yet. Similarly, reports on the salt stress effect on Ginger's nucleic acid content are also unavailable. Ginger is an essential component of the human diet, and its assessment concerning nutritional value is highly needed. Protein, reducing sugars, and total soluble carbohydrates are essential content as far as diet is concerned, so the effect of salt stress on the analysis of these contents is also very important. During the stress conditions, proline acts as an osmolyte, and its content can help to conclude the intensity of salt stress on Ginger (Singh et al. 2017; El Moukhtari et al. 2020; Spormann et al. 2023). The present investigation is primarily being undertaken for two aspects; one is to assess biochemical content in the Ginger

rhizome during different concentrations of salt stress, and the other is to evaluate the influence of AM Fungi during salt stress with the help of measuring Chlorophyll and Proline content. The nucleic acid content in Ginger has not been evaluated yet; this is the first research attempt in this area. These studies would help know Ginger's food value in diet and AM fungi's value when plants are under salt stress.

2 Materials and methods

2.1 Set up of pot for experiment

The pot matrix to carry out this work was prepared by Soil, FYM and coarse sand in a ratio of 3:1:1, respectively. This mixture was autoclaved at 15 lbs for about 60 min. It was then added to selected pots, per Doganlar et al. (2010).

2.2 Ginger rhizomes cultivations

Fresh Ginger rhizomes of Satara variety procured from Satara, Maharashtra state, India. Rhizomes having buds were cut in pieces of 25-30g and treated for half an hour with 0.1% of the laboratory grade $HgCl_2$; this was followed by the washing of rhizomes with sterile water. Later, a soil-AM combination was prepared using 0.2 kg of autoclaved soil mixture and an assortment of five selected AM species, i.e. *Acaulospora appendiculata*, *A. gerdemanni*, *Glomus convolutum*, *G. fasciculatum* and *Scutellospora calospora*.

2.3 Salt stress treatment

The surface sterilized rhizomes were grown in each pot. All pots were kept inside the net house in a completely randomized block design with a sufficient water supply generally for 30 days at every five days interval. These rhizomes germinated within 2 to 3 weeks. The salinity treatment started one month later, growing it. Sodium chloride (NaCl) was used to give salt stress treatment. Four different concentrations, i.e., 25 mM, 50 mM, 75 mM and 100 mM of sodium chloride, were made using distilled water as per Dhanapackiam and Iliyas (2010) and have been used for treatment. For every concentration, three replicates were made along with control pots to evaluate the effect of salt concentration on the various growth parameters of Ginger under AM-supplemented soil. Consequent usages of different salt concentrations were administered with a gap of 5 days for the next three months. Every time 500 ml of NaCl of various intensities is introduced at each pot. Initially, salinity was escaped to escape plants from stress jolt. Ninety days after salinity treatment, plants were used for testing biochemical contents.

2.4 Isolation and quantification of Chlorophyll

Chlorophyll pigments were isolated from leaves of salinity-stressed Ginger treated with AM fungi (experimental) and without AM fungi (control). The estimation of pigments was carried out

using Arnon's (1949) method. Leaves are used from both mycorrhizal and control plants. The absorbance of the blank and leaf extract was recorded at 645 nm and 663 nm with a UV-visible spectrophotometer.

2.5 Isolation and Estimation of DNA

DNA isolation was carried out using ginger rhizomes by Dellaporta et al. (1983) method and estimated by Burton's (1956) method. Absorbance for the developed blue solution and blank was noted at 600 nm. DNA content in plant samples was calculated by using a standard graph.

2.6 Isolation and Estimation of RNA

RNA isolation is performed as per Brawerman's (1974) method and estimated by Bial's (1902) method. Absorbance noted with 660 nm range versus blank. The standard graph was used to estimate the RNA amount in plant samples.

2.7 Estimation of Protein

Protein estimation was performed using the method of Lowry et al. (1951). The reaction was carried out to quantify protein as per Lowry's method. At the end of the reactions, the mixture's changed colour was measured at 660 nm. The protein content in the sample was estimated by comparing it with a standard graph.

2.8 Estimation of Proline

Proline estimation was done with the Bates et al. (1973) method. Salt and water-stressed plant parts like rhizomes and leaves were used to estimate proline. For this, 0.5 g. samples were used for the estimation of proline. The absorbance of the mixture was noted at 520 nm. Standard proline was used to plot standard graphs and calculate proline content in plant samples.

2.9 Estimation of reducing sugars

Dinitrosalicylic acid (DNSA) reagent was used to estimate reducing sugars, as Miller (1959) described. At the end of the reaction, the mixture was cooled. D-glucose was used to plot a

standard graph and calculate different amounts of reducing sugars in plant samples.

2.10 Estimation of total soluble carbohydrates

Hedge et al. (1962) method was used to estimate total soluble carbohydrates. 1 g of rhizomes was used for estimation purposes. An absorbance read at 630 nm, and standard graph was used to estimate total soluble carbohydrates in plant samples.

2.11 Statistical Analysis

Data obtained were analyzed with MS Excel 2016. The variance between the control and experimental plants was calculated using a t-test. A comparison of the data was made using Pearson's correlation coefficient.

3 Results and Discussion

3.1 Estimation of Chlorophyll

Chlorophyll was extracted using ginger leaves as per Arnon's (1949) method. Among the tested salt concentrations, the highest concentration for all types of Chlorophyll (Chlorophyll a, chlorophyll b and total chlorophylls) was reported at a salt concentration of 25 mM, while the lowest was at 100 mM salt concentration. Further, all chlorophyll concentrations for 25 mM saline treatment are at par with the control. Chlorophyll content decreased as the concentration of saline solution increased (Table 1). Further, the concentration of all types of Chlorophyll in AM-treated plants was higher than in non-mycorrhizal plants, and this might be due to the higher photosynthetic efficacy of AM-treated plants. Results of the study show that the chlorophyll contents were reduced distinctly with elevated salinity. Further t-test for all chlorophyll contents in all experimental plants was significant at $P < 0.05$ level. Pearson's correlation test showed a negative correlation between chlorophyll content and to increase in salt concentration Table 1.

Salt stress significantly affects genetic potential, leading to several growth limitations (Gama et al. 2007). The amount of Chlorophyll lessens due to either slow formation or quick collapse, showing

Table 1 Effect of salt concentration and mycorrhiza treatment on chlorophyll content of Ginger

Salt Concentration	Chlorophyll a (mg/g)		Chlorophyll b (mg/g)		Total Chlorophylls (mg/g)	
	Control (Only Salt)	Experimental (Salt + AM)	Control (Only Salt)	Experimental (Salt + AM)	Control (Only Salt)	Experimental (Salt + AM)
25 mM	1.312 ± 0.002	1.466 ± 0.02***	1.354 ± 0.003	1.474 ± 0.09*	2.666 ± 0.09	2.940 ± 0.003**
50 mM	1.107 ± 0.002	1.251 ± 0.01***	1.217 ± 0.001	1.430 ± 0.001***	2.324 ± 0.01	2.680 ± 0.002***
75 mM	0.970 ± 0.003	1.132 ± 0.002***	1.068 ± 0.003	1.327 ± 0.001***	2.038 ± 0.002	2.459 ± 0.001***
100 mM	0.634 ± 0.004	0.743 ± 0.001***	0.846 ± 0.002	0.906 ± 0.001***	1.480 ± 0.002	1.710 ± 0.002***

Results are given as mean ± SD, based on the measurement of individual samples; t-tests with significant differences ($P < 0.05$) between means are indicated by different * signs (*significant at <0.05 level, ** significant at <0.001 level and *** significant at <0.0001 level).

that there was a mechanism of photoprotection through the reducing absorbance of light, which has resulted in decreasing chlorophyll contents (Elsheery and Cao 2008). Smirnov (1996) opined that salt stress might initiate the symptoms of oxidative stress, which has resulted in the inhibition of chlorophyll synthesis. Inoculation of plants with AM fungi activates different enzymatic activities, including Phosphoenolpyruvate carboxylase (PEPC) and rubisco, which enhances the rate of photosynthesis (Kaddes et al. 2019). These findings are contested with the various other plants such as maize (Rahmaty and Khara 2011), *Ocimum* (Heidari 2012), Barley (Meddich et al. 2021) and grapes (Ye et al. 2022). These researchers noted a decrease in chlorophyll content with increased salt concentration.

3.2 Estimation of DNA and RNA

Contradictory to chlorophyll content, the lowest DNA was isolated from the 25 mM salt concentration controlled plants, while it was highest in the 100 mM salt concentration. Similarly, the experimental plants' lowest DNA concentration was isolated from the 25mM and the highest at 100 mM saline concentrations. The DNA in non-treated plants was higher than in experimental ginger plants (Table 2). Similar trends have been recorded for the RNA content, and the lowest and highest salt concentrations were recorded at 25mM and 100mM for both control and experimental plants, respectively. Furthermore, DNA content was higher as compared to RNA in both sets. DNA and RNA were elevated as the concentration of salt increased in both experimental and controlled plants. The DNA and RNA within the AM-treated plants were noted to be lower than non-treated plants in all concentrations of salt. Further, RNA among control plants was reported to be higher than experimental ginger plants. Statistically, the t-test for both nucleic acid contents showed substantial differences at $P < 0.05$. Pearson's correlation test showed a positive correlation between DNA and RNA content with an elevation in salt concentration (Table 2).

The salinity stress might have resulted in a decrease in cell size. The smaller size of the cell increases its number per gram

of tissue. Thus, the amount of high DNA ultimately results in the elevation of RNA content per gram. In experimental plants, AM made nutrients available to roots and mobilized soil nutrients, specifically phosphate and abetted roots, to absorb other soil nutrients. This occasioned in the healthy and vigorous Growth of experimental plants. Due to robust Growth, the number of cells per gram of plant tissue decreased. The decreased number of cells affected nucleic acid content in plant cells. Thus, a smaller number of cells per gram of plant tissue resulted in less DNA and RNA in experimental plants. Similar outcomes were documented by Gomathi and Vasantha (2006) in sugarcane. Studies on nucleic acid contents in rhizomatous crops concerning salt stress have not been done, and it is the first report on the effect of salt stress on nucleic acid contents in Ginger.

3.3 Estimation of Proteins

Protein content was elevated with the intensity of salt in both sets of experiments. The lowest and highest protein content was reported at 25 mM and 100 mM salinity in both sets of experiments. Further, protein content in treated plants was recorded as lower than those of the non-treated plants for all the salinity concentrations. Additionally, plants with higher salinity have higher protein requirements (Table 2). Plants accumulate and use stored proteins to survive under stress conditions to protect cells from various stresses (Wang et al. 2003). Further, it was also reported that plants accumulated proteins during salt stress conditions which can be utilized in future in physiological processes. These results agree with the findings of Doganlar et al. (2010) in tomato cultivars. Sibole et al. (2003) also noted the salt stress among clover (*Medicago citrana* L.) and augmented the soluble proteins in seedlings compared to control plants. Similarly, Chao et al. (1999) noted an increase in tomato protein content in response to salinity stress. A similar type of protein content improvement was reported in *Asparagus* (Matsubara et al. 2014), clover plants (Xie et al. 2020) and Onion plants (Metwally et al. 2021). Saboor et al. (2021) noted that AM fungi assist the maize plant during salt stresses.

Table 2 Effect of salt concentration and mycorrhiza on DNA, RNA and Protein content of Ginger

Salt Concentration	DNA ($\mu\text{g/g}$)		RNA ($\mu\text{g/g}$)		Proteins (mg/g)	
	Control (Only Salt)	Experimental (Salt + AM)	Control (Only Salt)	Experimental (Salt + AM)	Control (Only Salt)	Experimental (Salt + AM)
25 mM	361.68 \pm 0.24	341.24 \pm 0.32***	320.61 \pm 0.45	312.20 \pm 0.42***	3.196 \pm 0.01	3.032 \pm 0.04**
50 mM	381.30 \pm 0.11	372.83 \pm 0.24***	350.15 \pm 0.28	341.94 \pm 0.20***	3.304 \pm 0.05	3.076 \pm 0.01**
75 mM	436.44 \pm 0.09	418.99 \pm 0.11***	388.30 \pm 0.11	379.07 \pm 0.11***	3.576 \pm 0.01	3.365 \pm 0.01***
100 mM	496.26 \pm 0.05	483.48 \pm 0.09***	422.15 \pm 0.15	413.74 \pm 0.07***	3.676 \pm 0.01	3.445 \pm 0.01***

Results are given as mean \pm SD, based on measurement on individual samples; Significant differences ($P < 0.05$) between means are indicated by Asterix (*significant at <0.05 level, ** significant at <0.001 level)

Table 3 Effect of salt concentration and mycorrhiza on Proline content in leaves and rhizome of Ginger

Salt Concentration	Proline leaves		Proline Rhizome	
	Control (Only Salt)	Experimental (Salt + AM)	Control (Only Salt)	Experimental (Salt + AM)
25 mM	0.65 ± 0.04	0.54 ± 0.03**	0.38 ± 0.03	0.32 ± 0.04 ^{ns}
50 mM	0.80 ± 0.05	0.69 ± 0.02**	0.67 ± 0.04	0.58 ± 0.05*
75 mM	1.63 ± 0.07	1.47 ± 0.05*	1.26 ± 0.05	1.19 ± 0.04 ^{ns}
100 mM	2.32 ± 0.05	2.25 ± 0.06 ^{ns}	2.19 ± 0.04	2.12 ± 0.04 ^{ns}

Results are given as mean ± SD, based on the measurement of individual samples. Significant differences ($p < 0.05$) between means are indicated by different letters (^{ns} not significant at >0.05 level *significant at <0.05 level, ** significant at <0.001 level)

3.4 Estimation of Proline

Proline content was also elevated with the upliftment in the salt concentration in both sets of experiments and the lowest proline content was noted at 25 mM of salinity, while the highest was noted at 100 mM salinity. Like protein, the proline content in AM-treated plants was recorded as lower than those of the non-treated plants among all the salt concentrations (Table 3). Further t-tests for leaf proline contents showed significant differences at $P < 0.05$ levels for 25 mM, 50 mM and 75 mM salt concentration in leaves and 50 mM salinity in the rhizome. Pearson's correlation test showed a positive correlation of proline content with respect to increased salt concentration in both leaves and rhizome (Table 3).

The buildup of proline has a vital role in osmotic balance and salt defence mechanism and generally accumulates in plants facing salinity stress. A defence response of proline in maintaining the osmotic pressure in a cell was observed by de Lacerda et al. (2003). Osmoregulation under water scarcity and salinity is essential for protein stabilization and preventing enzymes from heat denaturation. Lower osmotic potential might cause proline accumulation within plant tissues (Buhl and Stewart 1983). AMF improves the plant defence mechanism and produces low-molecular-weight compounds like proline (Bhosale and Shinde 2011; Vergara et al. 2018; Pirzadah et al. 2019). Among halophytes and glycophytes accumulation of proline is done as a non-toxic and protective osmolyte. Apart from osmolyte, proline also contributes to scavenging reactive oxygen species (ROS) and stabilizes subcellular structures (Fougere et al. 1991; Torabi and

Halim 2010; Bhosale and Shinde 2011). Liu et al. (2022) have reported that AM fungi have a significant role in the secretion of osmolyte-like proline in Rice plants.

3.5 Reducing sugars

A significant improvement in the concentration of reducing sugars was recorded with the progress of salt concentration, and the lowest amount of reducing sugars was recorded at 25 mM salinity. In comparison, the highest was recorded at 100 mM salinity in both sets of experiments (Table 4).

Level of reducing sugars within the AM treated Ginger was lower than the non-treated Ginger at various salt concentrations. During salt stress along with other essential solutes, sugars accumulate for adjustments in plants (Baki et al. 2000). Excessive amounts of sugars in the cytoplasm block the expression of Rubisco (Sewada et al. 1992). Therefore, the rate of glucose synthesis and alternations in metabolic processes might contribute to salt sensitivity in plants. The results recorded in the present investigation match with the results obtained by Kerepesi and Galiba (2000) in wheat plants, Amirjani (2011) in rice plants and Meng et al. (2021) in trifoliolate orange. The t-test for reducing sugars content showed a significant difference at $P < 0.05$ (Table 4).

3.6 Total soluble carbohydrates

The increased salinity at both experimental sets elevated the total soluble carbohydrate content. The lowest amount of total soluble carbohydrates was noted in 25 mM salinity, whereas the highest

Table 4 Effect of salt concentration and mycorrhiza on reducing sugars and total soluble carbohydrates content of Ginger

Salt Concentration	Reducing Sugars		Total soluble carbohydrates	
	Control (Only Salt)	Experimental (Salt + AM)	Control (Only Salt)	Experimental (Salt + AM)
25 mM	75.81 ± 0.07	63.09 ± 0.07***	203.01 ± 0.08	223.32 ± 0.04***
50 mM	91.42 ± 0.07	74.76 ± 0.06***	262.66 ± 0.09	281.77 ± 0.06***
75 mM	176.42 ± 0.07	130.94 ± 0.09***	356.36 ± 0.08	393.33 ± 0.04***
100 mM	200.71 ± 0.02	187.51 ± 0.05***	452.66 ± 0.09	528.77 ± 0.07***

Results are given as mean ± SD, based on the measurement of individual samples; Significant differences ($p < 0.05$) between means are indicated by different letters (*** significant at <0.0001 level)

amount of carbohydrate was noted at 100 mM salinity of AM-treated and non-treated sets of treatments. Further, a remarkable increase in the total soluble carbohydrates was recorded in the AM-treated plant as compared to the non-treated plants (Table 4). Preferential partitioning of carbohydrates is generally facilitated by salinity (Schellenbaum et al. 1998). Plants, facing sodium salt stress, always store more starch (Rathert, 1984). Total soluble carbohydrates act as a solute which is synthesized and accumulated in the cytosol under salinity stress. Due to the association of AM, all treated plants absorbed more nutrients, resulting in enhanced total soluble carbohydrate contents among treated plants as there was an increase in salt stress; the amount of carbohydrates was alleviated because plants store more carbohydrates due to stress for utilization in coming adverse conditions. Similar results were reported by Munns and Weir (1981) in wheat, where the amount of total soluble carbohydrates elevated with stress. Increases in total soluble carbohydrates have also been recorded in various crops such as *Sesbania grandiflora* (Dhanapackiam and Iliyas 2010), Onion (Metwally 2020), Wheat (Gupta et al. 2021) and *Cicer arietinum* plants (Garg and Cheema 2021).

Conclusions

The study results show that applying Arbuscular Mycorrhiza helps overcome the adverse effect of salinity stress and enhances photosynthesis efficiency and nutrient storage. Further, the impact of salinity stress was also recorded on the nucleic acid, protein and proline contents and increasing the salinity level enhances the nucleic acid, protein and proline content. The AM-treated plants showed fewer amounts of nutrient, protein and proline content. Reducing sugars and total soluble carbohydrate content due to the treatment of AM fungi indicates an accumulation of sugars for osmotic adjustments in plants during salt stress.

Acknowledgement

I thank Principal Bharat Shinde for allowing all laboratory facilities to accomplish the present investigation. Thanks to Dr Abhijit Kulkarni for helping with the statistical analysis work.

Conflicts of interest and financial disclosures

As the authors, I, Dr Kishor S. Bhosale, declare that no financial, academic, commercial or political interest could have influenced the findings noted in this article.

References

Al-Karaki, G. N. (2000). Growth of mycorrhizal tomato and mineral acquisition under salt stress. *Mycorrhiza*, 10 (2), 51-54.

Amirjani, M. R. (2011). Pigments and Enzyme Activity of Rice. *International Journal of Botany*, 7 (1), 73-81.

Anon, D. I. (1949). Copper enzymes in isolated chloroplasts. Polyphenoloxidase in *Beta vulgaris*. *Plant physiology*, 24 (1), 1.

Aziz, M. A., Islam, S., Gani, G., Dar, Z. M., Masood, A., & Baligah, S. H. (2023). AM Fungi as a Potential Biofertilizer for Abiotic Stress Management. Intech Open. doi: 10.5772/intechopen.108537.

Baki, G. A. E., Siefritz, F., Man, H. M., Weiner, H., Kaldenhoff, R., & Kaiser, W. M. (2000). Nitrate reductase in *Zea mays* L. under salinity. *Plant, Cell & Environment*, 23 (5), 515-521.

Bates, L. S., Waldren, R. P., & Teare, I. D. (1973). Rapid determination of free proline for water-stress studies. *Plant and soil*, 39 (1), 205-207.

Bial, M. (1902). Estimation of RNA nucleic acid. *Den Med Woch*, 28, 253.

Bhosale, K. S., & Shinde, B. P. (2011). Influence of arbuscular mycorrhizal fungi on proline and chlorophyll content in *Zingiber officinale* Rosc grown under water stress. *Indian Journal of Fundamental and Applied Life Sciences*, 1(3), 172-176.

Blumenthal, M., Goldberg, A., & Brinckmann, J. (2000). Ginger root. In *Herbal medicine: Expanded commission E monographs* (pp. 153–159). Newton, Massachusetts: Integrative Medicine Communications, Lippincott Williams & Wilkins

Brawerman, G. (1974). In- *Methods in Enzymology*. 30 (Eds. Moldave and Grossman, L.) Academic Press. New York, p. 605.

Buhl, M. B., & Stewart, C. R. (1983). Effects of NaCl on proline synthesis and utilization in excised barley leaves. *Plant physiology*, 72 (3), 664-667.

Burton, K. (1956). A study of the conditions and mechanism of the diphenylamine reaction for the colorimetric estimation of deoxyribonucleic acid. *Biochemical journal*, 62 (2), 315.

Chao, W. S., Gu, Y. Q., Pautot, V., Bray, E. A., & Walling, L. L. (1999). Leucine aminopeptidase RNAs, proteins, and activities increase in response to water deficit, salinity, and the wound signals systemin, methyl jasmonate, and abscisic acid. *Plant Physiology*, 120 (4), 979-992.

Chen, S., Zhao, H., Zou, C., Li, Y., Chen, Y., Wang, Z., et al. (2017). Combined Inoculation with multiple arbuscular mycorrhizal fungi improves Growth, nutrient uptake and photosynthesis in cucumber seedlings. *Frontiers in Microbiology*, 8, 25–16. doi: 10.3389/fmicb.2017.02516.

Citronberg, J., Bostick, R., Ahearn, T., Turgeon, D. K., Ruffin, M. T., Djuric, Z., & Zick, S. M. (2013). Effects of ginger

- supplementation on cell-cycle biomarkers in the normal-appearing colonic mucosa of patients at increased risk for colorectal cancer: results from a pilot, randomized, and controlled trial. *Cancer Prevention Research*, 6 (4), 271-281.
- Dastogeer, K. M., Zahan, M. I., Tahjib-Ul-Arif, M., Akter, M. A., & Okazaki, S. (2020). Plant salinity tolerance conferred by arbuscular mycorrhizal fungi and associated mechanisms: a meta-analysis. *Frontiers in plant science*, 11, 588550.
- de Lacerda, C. F., Cambraia, J., Oliva, M. A., Ruiz, H. A., & Prisco, J. T. (2003). Solute accumulation and distribution during shoot and leaf development in two sorghum genotypes under salt stress. *Environmental and Experimental Botany*, 49 (2), 107-120.
- Dellaporta, S. L., Wood, J., & Hicks, J. B. (1983). A plant DNA miniprep: version II. *Plant molecular biology reporter*, 1 (4), 19-21.
- Dhanapackiam, S., & Ilyas, M. (2010). Effect of salinity on chlorophyll and carbohydrate contents of *Sesbania grandiflora* seedlings. *Indian Journal of Science and technology*, 3 (1), 64-66.
- Doganlar, Z. B., Demir, K., Basak, H., & Gul, I. (2010). Effects of salt stress on pigment and total soluble protein contents of three different tomato cultivars. *African Journal of Agricultural Research*, 5 (15), 2056-2065.
- El Moukhtari, A., Cabassa-Hourton, C., Farissi, M., & Savouré, A. (2020). How does proline treatment promote salt stress tolerance during crop plant development? *Frontiers in plant science*, 11, 1127.
- Elsheery, N. I., & Cao, K. F. (2008). Gas exchange, chlorophyll fluorescence, and osmotic adjustment in two mango cultivars under drought stress. *Acta Physiologiae Plantarum*, 30 (6), 769-777.
- Fougere, F., Le Rudulier, D., & Streeter, J. G. (1991). Effects of salt stress on amino acid, organic acid, and carbohydrate composition of roots, bacteroids, and cytosol of alfalfa (*Medicago sativa* L.). *Plant physiology*, 96 (4), 1228-1236.
- Gama, P. B. S., Inanaga, S., Tanaka, K., & Nakazawa, R. (2007). Physiological response of common bean (*Phaseolus vulgaris* L.) seedlings to salinity stress. *African Journal of biotechnology*, 6 (2), 079-088.
- Garg, N., & Cheema, A. (2021). Relative roles of Arbuscular Mycorrhizae in establishing a correlation between soil properties, carbohydrate utilization and yield in *Cicer arietinum* L. under As stress. *Ecotoxicology and Environmental Safety*, 207, 111196.
- Gomathi, R., & Vasantha, S. (2006). Change in nucleic acid content and expression of salt shock proteins in relation to salt tolerance in sugarcane. *Sugar Tech*, 8(2-3), 124-127.
- Gupta, S., Thokchom, S. D., & Kapoor, R. (2021). Arbuscular mycorrhiza improves photosynthesis and restores alteration in sugar metabolism in *Triticum aestivum* L. grown in arsenic contaminated soil. *Frontiers in Plant Science*, 12, 640379.
- Hedge, J. E., Hofreiter, B. T., & Whistler, R. L. (1962). *Carbohydrate chemistry*. Academic Press, New York, pp.17.
- Heidari, M. (2012). Effects of salinity stress on growth, chlorophyll content and osmotic components of two basil (*Ocimum basilicum* L.) genotypes. *African Journal of Biotechnology*, 11 (2), 379.
- Kaddes, A., Fauconnier, M. L., Sassi, K., Nasraoui, B., & Jijakli, M. H. (2019). Endophytic fungal volatile compounds as solution for sustainable agriculture. *Molecules*, 24(6), 1065.
- Kerepesi, I., & Galiba, G. (2000). Osmotic and salt stress-induced alteration in soluble carbohydrate content in wheat seedlings. *Crop Science*, 40 (2), 482-487.
- Liu, Z., Bi, S., Meng, J., Liu, T., Li, P., Yu, C., & Peng, X. (2022). Arbuscular mycorrhizal fungi enhanced rice proline metabolism under low temperature with nitric oxide involvement. *Frontiers in Plant Science*, 13. <https://doi.org/10.3389/fpls.2022.962460>
- Liu, M. Y., Li, Q. S., Ding, W. Y., Dong, L. W., et al. (2023). Arbuscular mycorrhizal fungi inoculation impacts expression of aquaporins and salt overly sensitive genes and enhances tolerance of salt stress in tomato. *Chemical and Biological Technologies in Agriculture*, 10(1), 5.
- Lowry, O. H., Rosebrough, N. J., Farr, A. L., & Randall, R. J. (1951). Protein measurement with the Folin phenol reagent. *Journal of biological chemistry*, 193, 265-275.
- Matsubara, Y. I., Okada, T., & Liu, J. (2014). Suppression of *Fusarium* crown rot and increase in several free amino acids in mycorrhizal asparagus. *American Journal of Plant Sciences*, <http://dx.doi.org/10.4236/ajps.2014.52031>
- Meddich, A., Ouhaddou, R., Anli, M., & Boutasknit, A. (2021). Role of phosphorus and arbuscular mycorrhizal fungi in the growth performances and tolerance of barley to water stress. *Plant cell biotechnology and molecular biology*, 22(71-72), 45-67.
- Meng, L. L., Liu, R. C., Yang, L., Zou, Y. N., Srivastava, A. K., Kuča, K., & Wu, Q. S. (2021). The change in fatty acids and sugars reveals the association between trifoliate orange and endophytic fungi. *Journal of Fungi*, 7(9), 716.
- Metwally R. A. (2020). Arbuscular mycorrhizal fungi and *Trichoderma viride* cooperative effect on biochemical, mineral content, and protein pattern of onion plants. *Journal of basic*

- microbiology*, 60(8), 712–721. <https://doi.org/10.1002/jobm.202000087>
- Metwally, R. A., Soliman, S. A., Abdel Latef, A. A. H., & Abdelhameed, R. E. (2021). The individual and interactive role of arbuscular mycorrhizal fungi and *Trichoderma viride* on Growth, protein content, amino acids fractionation, and phosphatases enzyme activities of onion plants amended with fish waste. *Ecotoxicology and environmental safety*, 214, 112072. <https://doi.org/10.1016/j.ecoenv.2021.112072>
- Miller, G. L. (1959). Use of dinitrosalicylic acid reagent for determination of reducing sugar. *Analytical chemistry*, 31 (3), 426-428.
- Mitra, D., Uniyal, N., Panneerselvam, P., Senapati, A., & Ganeshamurthy, A. N. (2020). Role of mycorrhiza and its associated bacteria on plant growth promotion and nutrient management in sustainable agriculture. *International journal of life sciences and applied sciences*, 1(1), 1-1.
- Munns, R., & Weir, R. (1981). Contribution of sugars to osmotic adjustment in elongating and expanded zones of wheat leaves during moderate water deficits at two light levels. *Functional Plant Biology*, 8 (1), 93-105.
- Nile, S. H., & Park, S. W. (2015). Chromatographic analysis, antioxidant, anti-inflammatory, and xanthine oxidase inhibitory activities of ginger extracts and its reference compounds. *Industrial Crops and Products*, 70, 238-244.
- Park, E. J., & Pezzuto, J. M. (2002). Botanicals in cancer chemoprevention. *Cancer and Metastasis Reviews*, 21 (3-4), 231-255.
- Pirzadah, T. B., Malik, B., Tahir, I., Rehman, R. U., Hakeem, K. R., & Alharby, H. F. (2019). Aluminium stress modulates the osmolytes and enzyme defense system in *Fagopyrum* species. *Plant Physiology and Biochemistry*, 144, 178-186.
- Rabie, G. H. (2005). Influence of arbuscular mycorrhizal fungi and kinetin on the response of mungbean plants to irrigation with seawater. *Mycorrhiza*, 15 (3), 225-230.
- Rahmaty, R., & Khara, J. (2011). Effects of vesicular arbuscular mycorrhiza *Glomus intraradices* on photosynthetic pigments, antioxidant enzymes, lipid peroxidation, and chromium accumulation in maize plants treated with chromium. *Turkish Journal of Biology*, 35(1), 51-58.
- Rathert, G. (1984). Sucrose and starch content of plant parts as a possible indicator for salt tolerance. *Functional Plant Biology*, 11 (6), 491-495.
- Ruiz-Lozano, J. M., Collados, C., Barea, J. M., & Azcón, R. (2001). Arbuscular mycorrhizal symbiosis can alleviate drought-induced nodule senescence in soybean plants. *New Phytologist*, 151 (2), 493-502.
- Saboor, A., Ali, M. A., Danish, S., Ahmed, N., et al. (2021). Effect of arbuscular mycorrhizal fungi on the physiological functioning of maize under zinc-deficient soils. *Scientific reports*, 11(1), 18468. <https://doi.org/10.1038/s41598-021-97742-1>
- Schellenbaum, L., Müller, J., Boller, T., Wiemken, A., & Schüepp, H. (1998). Effects of drought on non-mycorrhizal and mycorrhizal maize: changes in the pools of non-structural carbohydrates, in the activities of invertase and trehalase, and in the pools of amino acids and imino acids. *The New Phytologist*, 138 (1), 59-66.
- Sewada, S., Usuda, H., & Tsukui, T. (1992). Participation of inorganic orthophosphate in regulation of the ribulose-1, 5-bisphosphate carboxylase activity in response to changes in the photosynthetic source-sink balance. *Plant and cell physiology*, 33 (7), 943-949.
- Sheng, M., Tang, M., Chen, H., Yang, B., Zhang, F., & Huang, Y. (2008). Influence of arbuscular mycorrhizae on photosynthesis and water status of maize plants under salt stress. *Mycorrhiza*, 18(6-7), 287-296.
- Sibole, J. V., Cabot, C., Poschenrieder, C., & Barceló, J. (2003). Efficient leaf ion partitioning, an overriding condition for abscisic acid-controlled stomatal and leaf growth responses to NaCl salinization in two legumes. *Journal of Experimental Botany*, 54(390), 2111-2119.
- Singh, A., Sharma, M. K., & Sengar, R. S. (2017). Osmolytes: Proline metabolism in plants as sensors of abiotic stress. *Journal of Applied and Natural Science*, 9(4), 2079-2092.
- Smirnoff, N. (1996). Botanical briefing: the function and metabolism of ascorbic acid in plants. *Annals of botany*, 78 (6), 661-669.
- Spormann, S., Nadais, P., Sousa, F., Pinto, M., et al. (2023). Accumulation of Proline in Plants under Contaminated Soils - Are We on the Same Page? *Antioxidants*, 12(3), 666.
- Torabi, M., & Halim, M. R. A. (2010). Variation of root and shoot Growth and free proline accumulation in Iranian alfalfa ecotypes under salt stress. *Journal of Food Agriculture and Environment*, 8 (3), 323-327.
- Vergara, C., Araujo, K. E. C., Souza, S. R. D., Schultz, N., et al. (2018). Plant-mycorrhizal fungi interaction and response to inoculation with different growth-promoting fungi. *Pesquisa Agropecuária Brasileira*, 54.

- Wang, W., Vinocur, B., & Altman, A. (2003). Plant responses to drought, salinity and extreme temperatures: towards genetic engineering for stress tolerance. *Planta*, *218* (1), 1-14.
- Xie, M. M., Zou, Y. N., Wu, Q. S., Zhang, Z. Z., & Kuča, K. (2020). Single or dual inoculation of arbuscular mycorrhizal fungi and rhizobia regulates plant growth and nitrogen acquisition in white clover. *Plant, Soil and Environment*, *66*(6), 287-294.
- Yamato, M., Ikeda, S., & Iwase, K. (2008). Community of arbuscular mycorrhizal fungi in a coastal vegetation on Okinawa island and effect of the isolated fungi on Growth of sorghum under salt-treated conditions. *Mycorrhiza*, *18* (5), 241-249.
- Ye, Q., Wang, H., & Li, H. (2022). Arbuscular Mycorrhizal Fungi Improve Growth, Photosynthetic Activity, and Chlorophyll Fluorescence of *Vitis vinifera* L. cv. Ecolly under Drought Stress. *Agronomy*, *12*(7), 1563. <https://doi.org/10.3390/agronomy12071563>



Journal of Experimental Biology and Agricultural Sciences

<http://www.jebas.org>

ISSN No. 2320 – 8694

An Integrative Approach Towards Recommending Farming Solutions for Sustainable Agriculture

Veena Ghuriani^{*#} , Jyotsna Talreja Wassan^{*} , Pragya Deolal ,
Vidushi Sharma , Dimpy Dalal , Aditi Goyal 

Department of Computer Science, Maitreyi College, University of Delhi, Delhi, India

Received – December 10, 2022; Revision – March 23, 2023; Accepted – April 10, 2023
Available Online – April 30, 2023

DOI: [http://dx.doi.org/10.18006/2023.11\(2\).306.315](http://dx.doi.org/10.18006/2023.11(2).306.315)

KEYWORDS

Sustainable agriculture
Precision Farming (PF)
Zero Budget Natural Farming (ZBNF)
Machine Learning (ML)
Classification

ABSTRACT

Sustainable Agriculture is rapidly emerging as an important discipline to meet societal needs for food and other resources by adopting paradigms of conserving natural resources while maximizing productivity benefits. This paper proposes an integrative methodological approach for critically analyzing Precision Farming (PF) paradigms and Zero Budget Natural Farming (ZBNF), providing sustainable farming solutions and achieving productivity and profitability. This paper analyses the productivity of crops in PF using various machine learning (ML) algorithms based on different soil and climatic factors to identify sustainable agricultural practices for maximizing crop production and generating recommendations for the farmers. When implemented on the collected dataset from various Indian states, the Random Forest (RF) model produced the best results with an AUC-ROC of 95.7%. The Juxtaposition of ZBNF and non-ZBNF is evinced. ZBNF is statistically ($p < 0.05$) observed to be a cost-efficient and more profitable alternative. The impact of ZBNF on soil microbial diversity and micro-nutrients is also discussed.

* Corresponding author

E-mail: vghuriani@maitreyi.du.ac.in (Veena Ghuriani);
jtwassan@maitreyi.du.ac.in (Jyotsna Talreja Wassan)

Peer review under responsibility of Journal of Experimental Biology and Agricultural Sciences.

Production and Hosting by Horizon Publisher India [HPI]
(<http://www.horizonpublisherindia.in/>).
All rights reserved.

All the articles published by [Journal of Experimental Biology and Agricultural Sciences](#) are licensed under a [Creative Commons Attribution-NonCommercial 4.0 International License](#) Based on a work at www.jebas.org.



1 Introduction

Agriculture is a magnanimous source of livelihood for a majority of people in the world. It promotes economically viable, socially supportive, ecologically sound farming practices that help the environment replenish. The need to accommodate production without keeping sustainability at stake has paved the way to adapt and integrate new technologies into current practices. The extent and rate of change in information technology have enabled better decision-making, and shifting towards technology-driven agriculture has improved economic efficiency (National Research Council, U.S. 1997). Using sophisticated technologies such as robots, and temperature sensors, allows agriculture to be more profitable and efficient. This can be achieved by applying statistical methods and machine learning (ML) algorithms to efficiently plan experiments and interpret experimental data. Precision Farming (PF) seems to be a vision for a sustainable future in this context. It amalgamates information technology and agronomic sciences (Beluhova-Uzunova and Dunchev 2019). PF centres on data collection and analysis of measurable features to improve crop yield and quality. It reduces production costs and wastage to ensure profitability, efficiency, and sustainability (D'Antoni et al. 2012). Computer applications and technology can be used to optimize field-level management, from creating farm plans to yield maps.

The need to preserve our environment escorts us to zero-budget natural farming (ZBNF). 'Zero Budget' implies no need for credit (Bishnoi and Bhati 2017). It is thought to dramatically reduce production costs by substituting commercial fertilizers and pesticides with home-grown products such as Jeevamritha, Beejamritha, Neemastra, and others, as well as using intercropping and mulching. Currently, it is being adopted in different forms by the farmers in most of the states in India, namely, Andhra Pradesh, Himachal Pradesh, Haryana, Karnataka, Kerala, Madhya Pradesh, and Telangana (Bishnoi and Bhati 2017).

The current research proposes an integrative analysis of the profitability and usability of ZBNF coupled with the PF dealing with the soil productivity of different districts in India. A framework to generate recommendations to farmers to implement both farming methods, having known the prolificity of the soil, is proposed.

Until 1960 India was going through a massive crisis as it didn't have enough food grains to feed its growing population. But the advancement of the green revolution in 1960 changed the Indian agriculture trajectory forever. The arrival of HYV seeds, chemical fertilizers, pesticides, and tractors produced abundant food grains, making India a prominent exporter. The major catalyzing factor was chemical fertilizers. The Green Revolution may have saved the day but didn't guarantee the future because degraded land,

eutrophication, expensive farm inputs, and farmers in vicious debt cycles followed. Studies found that chemical fertilizers contain heavy metals (e.g. cadmium and chromium) and high concentrations of radionuclides which lead to the accumulation of inorganic pollutants in the plants (Savcı 2012). Nitrate compounds in these fertilizers highly contaminate the surface and groundwater and cause various health issues like 'blue baby syndrome', which is fatal to infants, causes diabetes and is a precursor of carcinogens (Kostraba et al. 1992). The permissible limit of nitrate ions is 50 mg/l (Rahman et al. 2021). A study showed that from all the samples taken, nitrate concentration was between 1 and 415 mg/l, and 37% of the samples exceeded the safe limit (Jayarajan and Kuriachan 2021). They are toxic to farmers and lead to casualties. Recently, an expert committee set up by the agriculture ministry found that 66 insecticides/pesticides banned abroad are still used in India, and 27 are perilous to humans and animals (NABARD 2018). These chemical inputs are expensive and put a financial burden, especially on marginal farmers. This calls for natural alternatives. ZBNF seems perfectly tailored for such a system (Duddigan et al. 2023). It uses natural inputs and discourages deep plowing and extensive irrigation. As a result, pollution is kept to a minimum, soil fertility is restored, and the environment is preserved (FAO 2016). Four major aspects are integral to ZBNF-Bijamrita, Jeevamrutham, Mulching, and Waaphasa (Kumar et al. 2020). In 2016, the Government of Andhra Pradesh implemented ZBNF, aiming to achieve 100% chemical-free agriculture by 2024. As per the 2017-18 data, there were 17491 ZBNF farmers spread over 1000 villages across the 13 districts of Andhra Pradesh (Galab et al. 2018). The ZBNF market is further expected to grow at 20.5% in the forecast period of 2021 and 2026, to reach a value of about USD 2601 million by 2026 (Harini et al. 2021). Precision Farming (PF), on the other hand, is based on the applicability of technologies to analyze the dataset and derive "precise" results from it (Shafi et al. 2019). PF aims to instruct farmers in various perspectives, like foreseeing illness in cutting edge so that they can make moves and prevent the loss, suggesting crops reasonable for their field based on the climate and soil data, water system, and utilization of pesticides (Pierpaoli et al. 2013). Even though the adoption of PF technologies in farm management has been relatively new, the intrinsic simplicity of the crop recommendation models makes it more acquiescent. For a country like India, where agriculture is yet a prevailing occupation, accurate estimation/assessment of both the region and yield are similarly significant in guaranteeing the precise assurance of their products (Bakthavathchalam et al. 2022). The conventional cultivation techniques consequently give restricted crop yields compared to the inputs provided. Thus, to amplify the effects for a given number of inputs, various algorithms and recommender models have proven valuable in fostering a "precise" framework for smart farming (D'Antoni et al. 2012). Following PF, "recommender systems try to identify the needs and preferences of users, filter the

huge collection of data accordingly and present the best-suited option before the users by using some well-defined mechanism" (Fayyaz et al. 2020). A study by Mokarrama and Arefin (2017) built a recommendation model based on factors such as physiography, crop growing period, and crop production rate. The recent advances in PF using machine learning (ML) models have allowed these models to be integrated into recommender systems with better results (Bakthavatchalam et al. 2022). This makes it possible to include ML models which can recognize favourable patterns for enhancing agricultural productivity. Thus, an integrative research framework that uses Machine Learning (ML) models for monitoring agricultural productivity and generating recommendations to farmers while adopting PF and ZBNF is proposed.

2 Materials and Methods

The dataset for this study was assorted from Indian government websites related to agriculture in different states of India. The dataset comprising the soil and climate attributes was accumulated for various districts in India for a comprehensive analysis. The dataset was homogenized for predicting crop productivity, depending on factors such as pH, temperature, rainfall, humidity, N-P-K and organic carbon (OC), and crop type (Table 1). The dataset consists of 9 variables and 764 observations across five years from 2015 to 2020.

The soil's acidity or alkalinity (pH) affects the amount of nutrients and chemicals soluble in soil water, thus making the nutrients available to crops. Humidity is a measure of moisture that influences stomata-related processes like evaporation and transpiration. Likewise, temperature influences most processes like transpiration and germination, directly affecting crop growth. The N-P-K levels in the soil are considered essential for optimal plant growth. Nitrogen and Phosphorus are important components of proteins and nucleic acids, and Potassium, an inorganic plant component, plays a vital role in regulating enzyme-related processes and osmosis. The N-P-K content optimizes crop growth, production and yield. The productivity matrix was derived from the crop and yield data set. Productivity as yield per hectare was classified into "High" and "Low" classes keeping the median value as a threshold. Crop types considered for the study are wheat, areca

nut, bajra, banana, barley, cotton, dry chillies, garlic, ginger, jute, maize, onion, potato, rice and sugarcane.

2.1 Conduction of Study

An integrative analysis was conducted on the dataset repository generated by compiling information from various resources (Table 1). The workflow has been divided into two segments. The first segment analyses the productivity of crops for different districts in India. It aims to make predictions based on various factors like the soil, crop type and climate parameters influencing crop fecundity. This is done by implementing multiple ML classification algorithms to determine which is more suitable. The second segment analyses the profitability and usability of ZBNF using the statistical software STATA (Kohler and Kreuter 2005).

2.1.1 Precision Farming (PF)

For PF workflow (Figure 1), firstly, the data undergoes pre-processing and is cleaned and scrutinized. Then it is processed in classification algorithms using k-folds cross-validation to predict crop productivity. Secondly, associations between these attributes using association rule mining by targeting the commonality between the parameters are explored. After that, deriving predictions and results are developed by the analysis.

Popular classification algorithms, viz Naive Bayes (NB), Support Vector Machines (SVM) and Random Forest (RF) have been compared on the compiled dataset to determine crop productivity (High or low). A comparison between Kappa statistics (McHugh 2012), AUC-ROC (Calster et al. 2008), and RMSE (Chai and Draxler 2014) values have been the selection criteria for determining the best out of these models. The RMSE measures the average error between predicted values and observations in appropriate units. A lower RMSE is preferred. The R-squared explains how much variation in the response is defined by the model. Kappa statistics measure inter-rater reliability or precision. It varies from 0 to 1, with 1 being a perfect agreement. AUC-ROC value is a performance measurement for the classifier, which determines how much the model can distinguish between classes. The higher the AUC-ROC value, the better the model is at predicting.

Table 1 Varied sources referred to attain soil and climate parameters across different Indian States

Parameters	Source
Average pH	https://soilhealth7/gov.in/
Average Temperature	https://climateknowledgeportal.worldbank.org/country/india
N-P-K, OC	https://soilhealth7/gov.in/
Rainfall	https://mausam.imd.gov.in/imd_latest/contents/cs_anomaly_timeseries_temp_rainfall.php
Humidity	https://www.indiawaterportal.org/articles/district-wise-monthly-rainfall-data-2004-2010-list-india-meterological
Crops and Productivity	https://aps.dac.gov.in/APY/Public_Report1.aspx

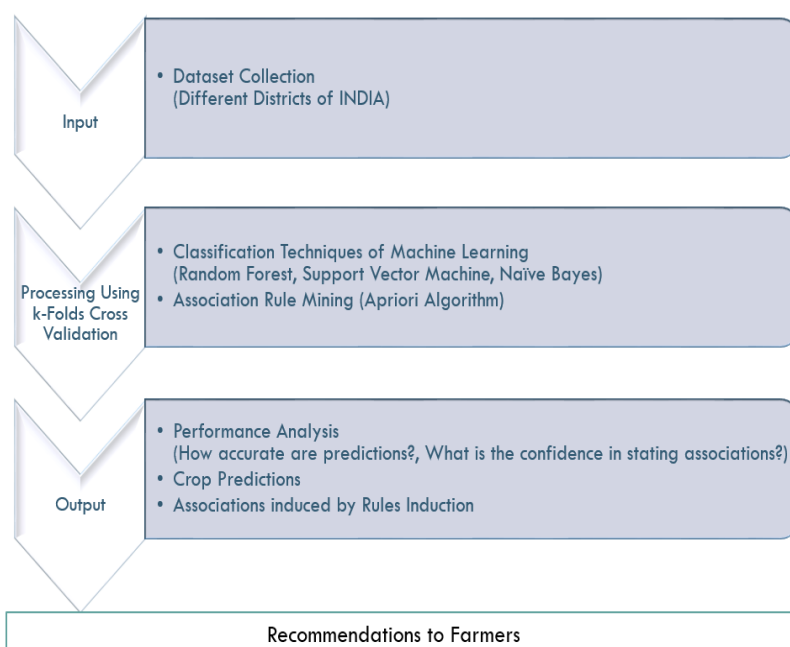


Figure 1 Workflow of Precision Farming

2.1.2 Naïve Bayes (NB)

NB Classifier is a simple probabilistic classifier that works based on Bayes' Theorem (Friedman et al. 1997), assuming that each input variable is independent or is unrelated to the presence of any other feature. Bayes' Theorem is used for calculating conditional probabilities, i.e., the probability of an event occurring given that another event has (assumption or assertion) occurred. According to the Theorem (Eq.1),

$$P(A|B) = P(B|A) * P(A) / P(B) \quad (1)$$

Here, B is the evidence or event, and A is the hypothesis or assumption that the predictors/features are independent. The naive Bayes Classifier calculates the posterior probability for each class (Friedman et al. 1997). It learns from training data the conditional probability of each attribute for a given class label - productivity matrix. The type with the highest posterior probability is the outcome of the prediction.

2.1.3 Support Vector Machine (SVM)

SVM is another ML classification algorithm used for two-group classification problems. The most straightforward formulation of SVM is the linear (Evgeniou and Pontil 2001), where the hyperplane lies in the space of the input data x (Eq.2).

$$f(x) = w \cdot x + b \quad (2)$$

In 2D, the discriminant is a line, where w is normal to the line known as the weight vector, and b is the bias. In 3D, a discriminant

is a plane, and in n-dimensional space, it finds a hyperplane to classify the data points from a subset of training points, called support vectors, where n is the number of features

2.1.4 Random Forest (RF)

RF classifier can be described as the collection of tree-structured classifiers (Breiman 2001). It fits separate decision trees on a predefined number of bootstrapped data sets to improve the predictive accuracy and control over-fitting. RF classifier was built using the above climate and soil attributes and productivity data from 2017-19 as a class, bagging with 100 iterations. In each iteration, 10% of the data was split off as a test set.

2.1.5 Apriori algorithm

Association rule mining is used to identify underlying relations between different items. The Apriori algorithm is one of the approaches to finding all the association rules with the condition of minimum support and minimum confidence (Angeline 2013). The Apriori considers all the non-empty subsets of the dataset and targets the frequency of repetition and commonality of an item set. It is a bottom-up approach. The subset test starts from the bottom-most item set and is performed at each stage. The item sets with inconsistent or infrequent subsets are pruned, and the process is iterated until no more than all the successful item sets are derived. Confidence derived from the test measures how often items appear in transactions, i.e., the likelihood of a particular item appearing, provided other factors are known.

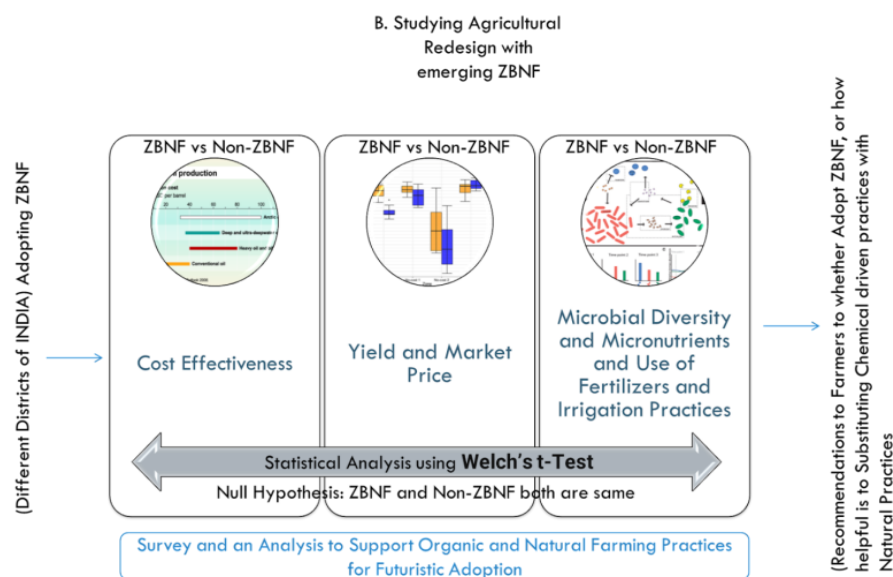


Figure 2 Analysis with ZBNF

2.2 ZBNF

ZBNF emerges as the beacon of hope to facilitate sustainability in an agriculture-based economy like India. The pilot experiments for ZBNF for the Indian districts have been compiled to draw statistical conclusions regarding the profitability and usability of ZBNF in real life (Figure 2).

In tandem, it is observed that medical and scientific experiments often have a small study group to prevent and minimize the extent of the inverse effects of the technology under consideration. In such situations, to record the difference in the samples before and after the experiment, different than usual statistical methods are used (Morgan 2017). In the following analysis as well since the sample size is small, Welch's t-test is used to give statistically significant results. Numerous economists have used this test in the past for similar situations. Since the sample size was small, it was suspected that the variance between the ZBNF and non-ZBNF groups was not equal; hence a Welch's t-test was conducted. Welch's t-test is the nonparametric equivalent of the conventional two-sample t-test (West 2021).

The ZBNF is explored to determine its cost-benefit, the scope of profit, and its effect on the soil's micronutrients and microbial diversity content. Welch's t-test was performed with a 95% confidence interval, under which the results are considered statistically significant if the p-value is less than 0.05. The test was conducted through the statistical software STATA.

The data for the same was collected and compiled district (Table 2) and factor-wise to interpret the results (Galab et al. 2018) efficiently. Furthermore, factors such as canals and tanks, irrigated

and rainfed agricultural lands and other irrigation sources were considered to present a holistic and inclusive comparative study of the ZBNF.

The data for Cost is in rupees per acre. The net returns per acre are also measured in the same metric. The data for both Cost and net returns are taken for the states of Andhra Pradesh, Karnataka, and Maharashtra for crops, namely paddy, sugarcane, black gram, finger millet, soybean, cotton, turmeric, and chickpea. The data for micronutrients is written as mg per Kg of soil. The yield per acre is presented in Quintals.

Table 2 ZBNF adopted across various districts in Andhra Pradesh

Mandya	Srikakulam	Visakhapatnam
Godavari	Guntur	Nellore
Prakarsa	Parbhani	Vizianagaram
Hingoli	Kurmool	Kadapa
Ananthapuramu	Chittoor	Krishna

3 Results

3.1 PF

Machine learning algorithms RF, NB, and SVM were applied to the crop dataset and ZBNF dataset. The input parameters considered for the model were the average pH, average temperature, rainfall, humidity, N-P-K, organic carbon, crop type, and productivity matrix classified in "High" and "Low" distributions keeping the median value as the threshold. The productivity matrix was used as the label or target for the entire model.

The crop prediction accuracy of the RF model accounts for 89.14% with a 0.96 AUC-ROC value. The range values for Kappa statistics lie in the range [1,-1], with 1 presenting complete agreement and 0 meaning independence. Kappa statistics for RF is 0.78, which shows substantial agreement. The RMSE value of RF is lesser than that of NB and SVM, and hence RF model is better than other classifiers, as in Table 3.

The crop prediction model gave 96.79% accuracy for the dataset, including ZBNF. It can be inferred from Table 4 that RF was determined to be the best among the three classifiers.

Following the RF model, Association Rule Mining was applied to the dataset to put forward the predictions obtained based on

support and confidence associative using the Apriori classification algorithm. The analysis gave around 96% confidence with minimum support of 0.55. After the Apriori algorithm was executed, several association rules were obtained. Out of the best rules found using the Apriori Algorithm, some of the recommendations derived are shown in Table 5.

3.2 ZBNF

3.2.1 The cost, yield, and net returns analysis

A Welch's test is performed to determine whether there is a statistically significant difference in Cost between districts and factors, yield per acre (in quintal) for farmers that received ZBNF

Table 3 ML Classifiers for Crop Productivity

Parameters	RF	NB	SVM
Accuracy	89.14%	84.32%	84.99%
Kappa Statistics	0.78	0.69	0.70
RMSE	0.28	0.33	0.39
Weighted AUC-ROC	0.96	0.92	0.85

Table 4 ML classifiers for ZBNF

Parameters	RF	NB	SVM
Accuracy	96.79%	91.29%	94.77%
Kappa Statistics	0.83	0.62	0.71
RMSE	0.15	0.27	0.23
Weighted AUC-ROC	0.99	0.93	0.83

Table 5 Instances for crop recommendation using Apriori Algorithm

pH	Temperature	Rainfall	NPK	Soil Type	Preferred Districts	Crop Recommended
Acidic	Hot	Low	Low to Medium	Alluvial	Panchkula, Mewat, Faridabad	Garlic
Acidic	Hot	Low	Low	Alluvial	Chirag, Kamrup, Nalbari, Baksa, Udalguri	Jute
Acidic	Hot	Low	Medium		Bandipora, Ganderbal	Dry Chillies
Acidic	Hot	High	Low	Alluvial	Barnala, Pathankot, Fazilla, Haridwar	Rice
Acidic	Cold/Hot	Low	Very Low to Low	Alluvial	Kurukshetra, Sirsa, Jhajjar, Banka, Patna, Arwal, Tawang, Sonapur	Potato
Alkaline	Hot	Low	Medium	Alluvium, Colluvium	Tamenglore, Goalpara	Arecanut
Acidic/Alkaline	Hot	Low	Low to Medium	Sandy Loam, Alluvial, Mountain Meadow	Muktsar, Bikaner, Jaipur, Banka, Patna, Aurangabad, Faridkot, Mansa, Jodhpur, Ajmer	Banana
Acidic	Hot	Low	Medium	Mountain Meadow	Kupwara, Rajauri, Samba	Garlic
Alkaline	Cold	Low	Low to Medium	Sandy Loam, Alluvial	Kulgam, Una, Almora, Sirsa, Sonipat	Onion
Acidic	Cold to slightly warm	Low	Medium to High	Alluvial	Shimla, Lohit, Aizwal, Champai, Una, West Siang, Hamirpur	Sugarcane



Figure 3 Boxplot of cost comparison of ZBNF and non-ZBNF

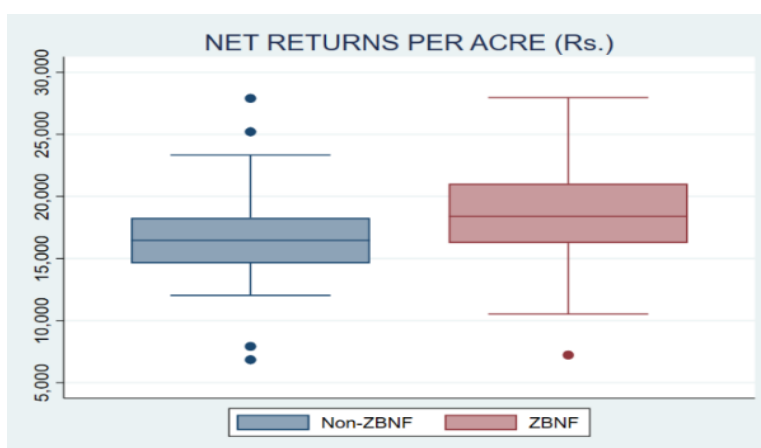


Figure 4 Boxplot of net returns per acre comparison of ZBNF and non-ZBNF

and the group that didn't. The sample size was small. Figure 3 displays two outliers, and the same reflects fitting the inefficiency in the farmer market structures, inconsistent information set, mediators, etc., which can be the possible causes for the same in the Indian context. Figure 3 showcases that ZBNF costs less than non-ZBNF and is more cost-efficient. No statistically significant difference could be recorded in the yield per acre recorded by farmers who used ZBNF for cultivation and the ones who did not, and hence is not deteriorating for them.

Additionally, Figure 4 showcases that ZBNF has slightly higher net returns per acre than the non-ZBNF alternative, which benefits the farmers. The difference in the span of boxes is evident. The ZBNF box's whiskers are longer than the non-ZBNF box.

3.2.2 Microbial Diversity

The natural factors also require a more extended period to show significant results. More profound research can broaden the outlook of the same. Additionally, the boxplot (Figure 5) of non-ZBNF is comparatively shorter; this implies the levels of microbial diversity

are moreover uniform, whereas the ZBNF is relatively tall, which implies different levels of microbial diversity. It is shown through various studies that ZBNF enriches the soil, and hence the same is observed; more exploratory research can add more valuable insights.

3.2.3 Micronutrients

Similarly, a Welch's test was performed to determine whether there is a statistically significant difference in micronutrients between districts that used ZBNF and those that didn't. There is no statistically significant difference in mean values between the two groups. The mean of group ZBNF is approximately the same as that of the non-ZBNF.

Hence, usage of ZBNF does not reduce or deteriorate the micronutrient content of the soil. Without the use of supplementary nutrients in the form of fertilizers after a complete agriculture cycle, the micronutrient content of the soil is retained in the ZBNF paradigm (Figure 6). This saves the variable Cost that would have been incurred on fertilizer consumption, thus reducing the Cost of production and increasing profits.

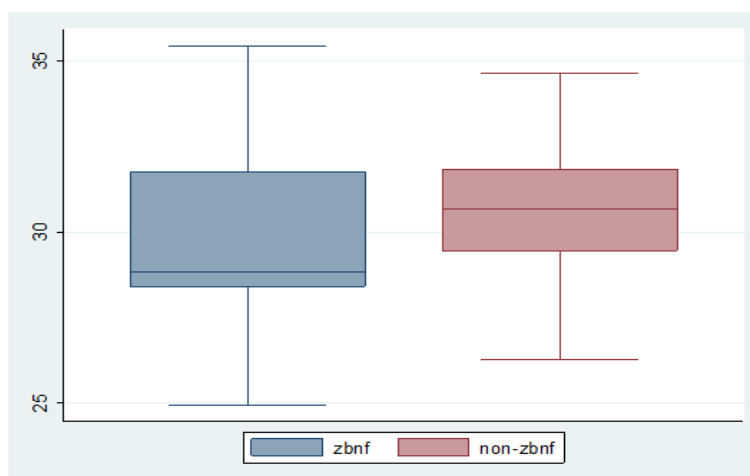


Figure 5 Boxplot of Microbial diversity comparison of ZBNF and non-ZBNF

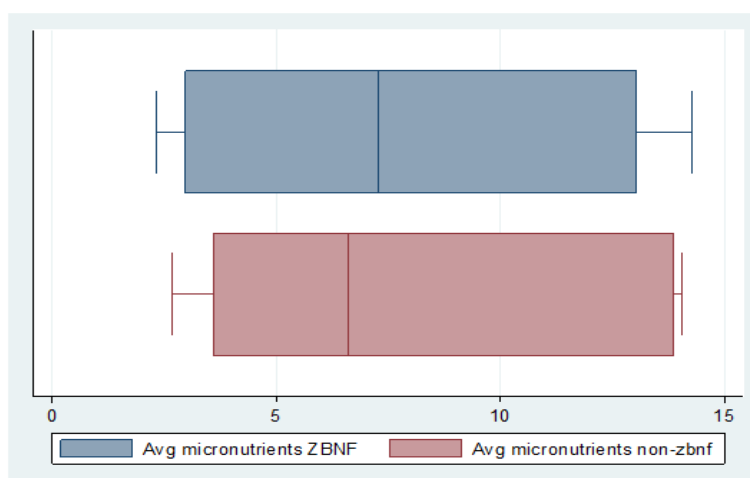


Figure 6 Boxplot of micronutrients comparison of ZBNF and non-ZBNF

4 Discussion

Precision farming is an evolving practice developing rapidly in the past two decades. Precision farming could be a solution to many challenges arising due to climate change. This technique could lead to an increase in agricultural output with less input. The current crop yield prediction is performed by state-of-the-art models, RF, NB, and SVM algorithms. Using ML in crop yield prediction has advantages as it provides faster and more accurate predictions. The crop yield depends on many parameters, like climatic factors, soil quality, air parameters, etc. ML-based prediction systems handle the dependency of the parameters efficiently. The Apriori algorithm produced results showing decent relations among the parameters with substantial confidence and generating recommendations to farmers. The crop recommendations are generated based on pH, rainfall, temperature, and districts. These predictions showed adequate results (> 80 % accuracy) and thus can be incorporated soon.

Welch's test provided statistically significant conclusions supporting ZBNF as an alternative to chemical-based farming. It showcased that ZBNF is more cost-efficient than non-ZBNF and gives slightly higher net returns per acre than the non-ZBNF. The research showed that ZBNF enriches the soil as the results show different levels of microbial diversity.

There was no significant statistical difference in the yield per acre recorded by farmers who opted for chemical-based farming instead of ZBNF. ZBNF does not deplete the soil of its natural content of micronutrients also. After the completion of an agricultural cycle, there is no need to rejuvenate the soil with fertilizers and supplements as the same micronutrients are retained. Hence, further decreasing the variable costs. ZBNF emerges as a more cost-efficient and profitable alternative for farmers. The advantages of using ML in integrative Agricultural Systems are (i) ML offers accurate detection of crop productivity with an accuracy of > 80%, which is better compared to manual/classical techniques, (ii) Prediction of crop

productivity based on environmental factors using ML exhibit low error indices such as RMSE measuring the model accuracy for statistical analysis (iii) ZBNF is a natural alternative and enhances productivity over non-ZBNF techniques and (iv) Accurately labelled dataset was designed for implementing an ML-based agricultural system which the research community could further use.

Though ZBNF is a beneficial technique, however few of the challenges and limitations in the prediction of crop yield were identified, and these are (i) varying parameters while analyzing datasets pose a challenge to the design of the prediction model, (ii) dataset selection is critical due to the complexity; as an improper selection of data may result in underfit/overfit problem, and (iv) Accurate classification through ML seems complicated in varying geographical conditions.

Based on the results of the study, some valuable recommendations to farmers have been generated, and these are (i) Garlic crop was recommended for Hot and Acidic Climates, (ii) Sugarcane was recommended to be grown in Alluvial soils in cold and slightly warm regions such as Shimla, Lohit, Aizwal, Champai, Una, West Siang, Hamirpur, (iii) Onions were recommended in Alkaline soil Regions, and (iv) Potatoes were recommended to be grown in Acidic Soil regions

The amalgamation of two approaches, i.e., integration of the recommender model and ZBNF, can be propelled towards agriculture sustainability.

Conclusion

The research paper delves into the concept of an integrative model amalgamating PF and ZBNF. PF includes analysis of soil, weather, crop, and other needs to increase agricultural productivity and improve its quality. In this paper, we empirically examine the application of ML in crop productivity within Indian farming systems. Using preliminary information from varied crop growers across Indian states, classification and regression models estimated a) the differences between high and low crop production and b) the differences between ZBNF and non-ZBNF approaches. This study used three established ML supervised models - RF, NB, and SVM- and a construct of ZBNF adoption perception to analyze these agriculture tools' adoption. Holistic and intricate datasets have been generated by compiling information from various online resources available, highlighting multiple external factors influencing crop productivity in Indian states/districts and the pilot surveys. The research primarily predicts crop productivity based on various factors like the soil, crop type, and climate parameters influencing crop productivity and making beneficial recommendations for the most suitable crop.

Additionally, exploratory research has been done to ascertain the profitability and usability of ZBNF using the statistical software

STATA. The study suggests that ZBNF costs less than non-ZBNF. Also, the study indicates that the micronutrient content of the soil is retained in the ZBNF paradigm even without using fertilizers. The pilot statistical experiments for ZBNF for the Indian districts have been compiled in this research to draw statistical conclusions regarding the profitability and usability of ZBNF. This article also concluded positively in favour of the integrative model with statistically significant results regarding PF and ZBNF. The article makes recommendations to farmers for an efficient and sustainable agricultural outlook.

In future work, digital platforms and chatbots can be built for farmers, and more ML algorithms can be explored in the sustainable agriculture industry.

Acknowledgments

The authors would like to express their gratitude towards the Centre for Research, Maitreyi College, University of Delhi, for providing the opportunity to take up this research. We highly appreciate the support provided by them throughout the research.

Conflict of Interest

The authors declare that the research was conducted without any commercial or financial relationships that could be constructed as a potential conflict of interest.

Authors Contribution

Dr. Veena Ghuriani and Dr. Jyotsna Talreja Wassan were involved in conceptualization, preparing the original draft and project administration. Pragya Deolal, Vidushi Sharma, Dimpay Dalal and Aditi Goyal worked on experimentation and writing. All authors have read and agreed to the published version of the manuscript.

References

- Angeline D. M. D. (2013). Association Rule Generation for Student Performance Analysis using Apriori Algorithm, *The SIJ Transactions on Computer Science Engineering & its Applications*, 1(1), 12-16.
- Bakthavatchalam, K., Karthik, B., Thiruvengadam, V., Muthal, S., Jose, D., Kotecha, K., & Varadarajan, V. (2022). IoT Framework for Measurement and Precision Agriculture: Predicting the Crop Using Machine Learning Algorithms. *Technologies*, 10, 13.
- Beluhova-Uzunova, R. P., & Dunchev, D. M. (2019). Precision Farming - Concepts and perspectives. *Problems of Agricultural Economics*, 360(3), 142-155.
- Bishnoi, R., & Bhati, A. (2017). An overview: Zero budget natural farming. *Trends in Biosciences*, 10(46), 9314-9316.

- Breiman, L. (2001). Random Forests. *Machine Learning*, 45, 5–32.
- Calster, B.V., Van Belle, V., Condous, G., Bourne, T., Timmerman, D., & Van Huffel, S. (2008). Multi-class AUC metrics and weighted alternatives. In *2008 IEEE International Joint Conference on Neural Networks (IEEE World Congress on Computational Intelligence)*, 1390–1396.
- Chai, T., & Draxler, R. R. (2014). Root mean square error (RMSE) or mean absolute error (MAE)? – Arguments against avoiding RMSE in the literature. *Geoscientific Model Development*, 7, 1247–1250.
- D'Antoni, J. M., Mishra, A. K., & Joo, H. (2012). Farmers' perception of precision technology: The case of autosteer adoption by cotton farmers. *Computers and Electronics in Agriculture*, 87, 121–128.
- Duddigan, S., Shaw, L. J., Sizmur, T., Gogu, D., et al. (2023). Natural farming improves crop yield in SE India when compared to conventional or organic systems by enhancing soil quality. *Agronomy for Sustainable Development*, 43(2), 31.
- Evgeniou, T., & Pontil, M. (2001). Support Vector Machines: Theory and Applications. *Machine Learning and Its Applications*, 249–257. DOI:10.1007/3-540-44673-7_12
- FAO (2016). Zero Budget Natural Farming in India. Retrieved from Web-Link <http://www.fao.org/3/a-bl990e.pdf>
- Fayyaz Z., Ebrahimian M., Nawara D., Ibrahim A. & Kashef R. (2020). Recommendation Systems: Algorithms, Challenges, Metrics, and Business Opportunities. *Applied Science*, 10(21), 7748.
- Friedman, N., Geiger, D. & Goldszmidt, M. (1997). Bayesian Network Classifiers. *Machine Learning*, 29, 131–163.
- Galab S., Prudhvikar Reddy, P., Sree Rama Raju, D., Ravi, C., & Rajani, A. (2018). Impact Assessment of Zero Budget Natural Farming in Andhra Pradesh – Kharif 2018-19. Retrieved from Web-Link: <https://www.scribd.com/document/468784250/CESS-FINAL-KHARIF-REPORT-ZBNF-19-8-19-pdf>.
- Harini, N., Veni, C. P., Sailaja, A., & Lata, A. M. (2021). Zero budget natural farming (ZBNF): A critical analysis on crop wise practices, ZBNF models and cropping systems. *The Pharma Innovation Journal*, 10(8S), 105–109.
- Jayarajan, S.K.P., & Kuriachan, L. (2021). Exposure and health risk assessment of nitrate contamination in groundwater in Coimbatore and Tirupur districts in Tamil Nadu, South India. *Environmental Science and Pollution Research International*, 28, 10248 - 10261.
- Kohler, U., & Kreuter, F. (2005). *Data analysis using Stata*. Stata press.
- Kostraba, J. N., Gay, E. C., Rewers, M., & Hamman, R. F. (1992). Nitrate levels in community drinking waters and risk of IDDM. An ecological analysis. *Diabetes care*, 15(11), 1505–1508.
- Kumar, R., Kumar, S., Yashavanth, B.S., Meena, P.C., et al. (2020). Adoption of Natural Farming and its Effect on Crop Yield and Farmers' Livelihood in India. *ICAR-National Academy of Agricultural Research Management, Hyderabad, India*. Retrieved from web link : <http://www.niti.gov.in/sites/default/files/2021-03/NaturalFarmingProjectReport-ICAR-NAARM.pdf>
- McHugh, M. (2012). Interrater reliability: The kappa statistic. *Biochemia medica : časopis Hrvatskoga društva medicinskih biokemičara*, 22(3), 276–282.
- Mokarrama, M.J., & Arefin, M.S. (2017). RSF: A recommendation system for farmers. *2017 IEEE Region 10 Humanitarian Technology Conference (R10-HTC)*, 843–850.
- Morgan C. J. (2017). Use of proper statistical techniques for research studies with small samples. *American journal of physiology, Lung cellular and molecular physiology*, 313(5), 873–877.
- NABARD. (2018). Agriculture Credit to Farmers. Retrieved from Web-Link <https://nabard.org/news-article.aspx?id= 25&cid= 552 &NID=160>
- National Research Council. (1997). *Precision Agriculture in the 21st Century: Geospatial and Information Technologies in Crop Management*. Washington, DC: The National Academies Press.
- Pierpaoli, E., Carli, G., Pignatti, E., & Canavari, M. (2013). Drivers of precision agriculture technologies adoption: A literature review. *Procedia Technology*, 8, 61–69.
- Rahman, A., Mondal, N.C. & Tiwari, K.K. (2021). Anthropogenic nitrate in groundwater and its health risks in the view of background concentration in a semi arid area of Rajasthan, India. *Scientific Reports*, 11(1), 9279
- Savcı, S. (2012). An Agricultural Pollutant: Chemical Fertilizer, *International Journal of Environmental Science and Development*, 3(1), 77–80.
- Shafi, U., Mumtaz, R., García-Nieto, J., Hassan, S. A., Zaidi, S. A. R., & Iqbal, N. (2019). Precision agriculture techniques and practices: From considerations to applications. *Sensors*, 19(17), 3796.
- West R. M. (2021). Best practice in statistics: Use the Welch *t*-test when testing the difference between two groups. *Annals of clinical biochemistry*, 58(4), 267–269.



Journal of Experimental Biology and Agricultural Sciences

<http://www.jebas.org>

ISSN No. 2320 – 8694

Usage of iron foliar spray in enhancing the growth and yield of the flax plant (*Linum usitatissimum* L)

Aqarab Husnain Gondal^{*1}, Franklin Ore Areche², Liliana Asunción Sumarriva-Bustinza³,
Nadia Lys Chávez-Sumarriva⁴, Nelly Olga Zela-Payí⁵, Jesús Manuel More López⁶,
José Yovera Saldarriaga⁶, Bertila Liduvina García-Díaz⁷, María Soledad Porras-Roque⁸,
Jose Carlos Ayuque-Rojas², Salomón Vivanco Aguilar², David Ruiz Vilchez²,
Russbelt Yaulilahua-Huacho², Rafael Julian Malpartida Yapias⁹, Abdul Jabbar¹⁰

¹Institute of Soil and Environmental Sciences, University of Agriculture, 38000, Faisalabad, Pakistan

²National University of Huancavelica, Huancavelica, Peru

³National University of Education Enrique Guzmán y Valle, Lima – Peru

⁴Universidad Científica del Sur, Lima, Perú

⁵National University of the Altiplano, Puno - Peru

⁶Santiago Antunez of Mayolo National University, Huaraz – Peru

⁷National University of Callao, Lima – Peru

⁸Jorge Basadre Grohmann National University, Tacna – Peru

⁹Autonomous University of Tarma, Tarma – Peru

¹⁰Fodder Research Farm Sargodha, Sargodha Punjab, Pakistan

Received – December 18, 2022; Revision – March 31, 2023; Accepted – April 18, 2023

Available Online – April 30, 2023

DOI: [http://dx.doi.org/10.18006/2023.11\(2\).316.324](http://dx.doi.org/10.18006/2023.11(2).316.324)

KEYWORDS

Seed oil contents

Growth enhancement

Yield

Application rate

Application method

ABSTRACT

The ideal growth and development of linseed plants depend on receiving the necessary nutrients during the growing season when they are grown. Flax's yield and oil content increase using a foliar spray containing micronutrients. This study aimed to determine how foliar iron (Fe) treatment affected flax yield and its constituents. The experiment was set up at the adoptive research farm Sargodha in a randomized block design and three replicates. At the capsule filling stages and bud initiation of the flax crop, foliar sprays with varying concentrations of Fe (5.5%, 4.5%, 3.5%, 2.5%, 1.5%) and without Fe (control) were administered. Sulphate of iron (Fe) was used as the source of Fe. All treatments resulted in notable enhancements in agronomic characteristics such as grain oil contents, harvest index, biological yield, number of capsule formations, technical stem length, plant height, as well as physiological

* Corresponding author

E-mail: aqarabhusnain944@gmail.com (Aqarab Husnain Gondal)

Peer review under responsibility of Journal of Experimental Biology and Agricultural Sciences.

Production and Hosting by Horizon Publisher India [HPI]
(<http://www.horizonpublisherindia.in/>).
All rights reserved.

All the articles published by [Journal of Experimental Biology and Agricultural Sciences](#) are licensed under a [Creative Commons Attribution-NonCommercial 4.0 International License](#) Based on a work at www.jebas.org.



parameters including fluorescence yield (Ft), quantum yield (YII), photosynthetically active radiation (PAR), electron transport rate (ETR), and chlorophyll contents. The results of this study suggested that the application of 3.5% to flax during the bud initiation and capsule filling stages increases the seed yield, yield attributes, and oil contents. In conclusion, foliar spray of Fe could enhance the yield of linseed crops.

1 Introduction

Linseed (*Linum usitatissimum* L.) is a highly profitable crop producing oil and fibre (Arslanoglu et al. 2022). It has higher nutritional value because it contains fat (41%), protein (20%), dietary fibres (28%), linoleic and omega-3 fatty acids, which regulate blood flow, lower cholesterol, prevent coronary complications and provides the body with anti-carcinogenic properties (Biswas and Ansari 2023). Linseed oil has a higher fatty acids rate and is used in paints, varnishes, printed inks, coating oils, and soaps due to its quick-drying properties (Hubmann et al. 2021). Pakistan's average linseed yield is meager compared to other countries, with a yield gap of up to 73 percent (Sangmesh et al. 2023). Low production is caused by cultivation on low-fertility marginal lands, inferior crop management methods, and insufficient application of micro and macronutrients (Eleni 2022). Furthermore, sandy soil, calcareous soils, Zn deficient soils and lower micro and macronutrient levels in Pakistani soils lead to severe yield losses due to deteriorating soil fertility (Sohail et al. 2021; Bisma et al. 2021; Gondal et al. 2022; 2021b;). Linseed yield can be improved in two ways, i.e., by growing the area under cultivation (horizontal production) or by applying balanced fertilizers. However, with the current land availability, expanding the breadth of agriculture is challenging. Therefore, keeping fertility high is the only option for increasing linseed output. This might be achieved by introducing higher-yielding variety crops and providing optimal crop fertilization (Jha et al. 2023).

Even though micronutrients are needed in trace amounts, these micronutrients play a significant role in improving crop growth. As evolution indicates, the consumption of micronutrients enhances the absorption of other micro and macronutrients by altering cellular physiology (Gondal et al. 2021g). Fe supplements aid in forming proteins and cell walls, promote photosynthesis and respiration, and suppress the production of auxins (Gondal et al. 2021f). Further, Fe micronutrients help maintain the chloroplast structure, enhance the rate of respiration and photosynthesis, and minimize nitrate and sulphate reductions. Besides, better micronutrient uptake also increases plants' micronutrient concentration. Both Fe and Zn serve essential roles in plant metabolism, without which plants would not be able to grow appropriately (Gondal et al. 2021a). These two micronutrients stimulate the plants' various metabolic, physiological and cellular processes (Alvarez et al. 2022). Such transition metals have unpaired electrons that facilitate their inclusion in oxidation-

reduction responses (Zeng et al. 2022). Plants uptake these two transition metals in small concentrations. Still, they perform a critical role in nitrogen fixation, reactive oxygen species scavenging, photosynthesis, chlorophyll synthesis, electron transport chain in chloroplast and mitochondria, DNA replication and act as a cofactor for proteins. These enzymes are also involved in the metabolic processes of mitochondria and chloroplast (Palmieri et al. 2022).

Thirty percent of the world's arable land is too alkaline for optimum crop development (Tayyiba et al. 2021; Gondal and Tayyiba, 2022). This makes low Fe availability due to high soil pH one of global agriculture's most pervasive abiotic stresses. In contrast, Fe deficiency is observed almost all over the world. Further, this Fe deficiency is most prominent in alkaline/calcareous soil with naturally lower organic carbon and highly limed, salt resistant and waterlogged soils (Gondal et al. 2021b; Gondal et al. 2021a). Soil fertility also declines as a result of growing high-yield crop cultivars that demand maximal levels of macro (N, P) and micronutrients (Fe, Zn, Mg, Mn) (Zhao et al. 2011). Fe fertilization is the practical approach to fix the problems mentioned earlier and achieve good production potential. The main objective of this study is to evaluate the (a) effect of Fe on the growth and yield of linseed and (b) to determine the appropriate level of Fe concentration towards linseed crops.

2 Materials and Methods

Sargodha, where the experiment occurred, is home to an adaptable research farm. It has a semiarid climate and is located at 32°07' N, 72°68' E, an elevation of 189 m. During the study, average temperatures ranged from 10 to 42.8 degrees Celsius.

2.1 Experimental setup

The randomized complete block design (RCBD) was used for this research. The plot's net size was 5 m × 1.2 m. The pre-analysis of soil was done before sowing the crop to determine the soil fertility status (Chapman and Pratt 1978). The description of the imposed treatment is given in Table 1.

Seedbed was prepared before sowing by four ploughings and one planking (breakage of large clods into the smooth surface). After that, the soil was levelled using a laser and a leveler. The flax crop seed was spread on the second fortnight of November using drill sowing, and keeping the spacing between plants and rows at 30 cm

Table 1 Detail of treatments used in this study

Treatment	Descriptions
Ctrl	Control
F1.5	Fe application of 1.5%
F2.5	Fe application of 2.5%
F3.5	Fe application of 3.5%
F4.5	Fe application of 4.5%
F5.5	Fe application of 5.5%

and 10 cm, respectively, allowed for a seeding rate of 15 kg/ha. The recommended doses of nitrogen (N), potassium (K) and phosphorus (P) fertilizers (58-58-30 kg NPK/ha) were applied for the maximum growth and improvement of plants, and the sources of fertilizer were urea, muriate of potash (MOP), and single super phosphate (SSP). The N dose is split into three parts: the first part is applied before sowing, and the remaining two are applied after the first and second irrigation. Three irrigations were used during the vegetative growth period to capsule formation. The experiment consists of 6 treatments in triplicates. The treatments include control, 1.5%, 2.5%, 3.5%, 4.5%, and 5.5%, application of Fe (Table 1), and the source of Fe foliar spray was Fe sulphate. Treatments were sprayed by hand sprayer during flowering and post-capsule formation stages. The crop was harvested after 150 days after sowing. The physicochemical properties of the study are soil have been given in Table 2.

Table 2 Physicochemical properties of soil used in this study

Parameters	Values
Sand (%)	53.8 ± 0.01
Silt (%)	25.4 ± 0.02
Clay (%)	20.8 ± 0.01
pH	8.48 ± 0.12
EC (dS m ⁻¹)	1.91 ± 0.01
Ca ²⁺ +Mg ²⁺ (mmolc L ⁻¹)	11.8 ± 0.73
Organic matter (%)	0.68 ± 0.01
Total organic carbon (%)	0.21 ± 0.07
Available N (mg kg ⁻¹)	6.70 ± 0.01
Available K (mg kg ⁻¹)	150 ± 9.11
Available P (mg kg ⁻¹)	0.36 ± 0.01

EC; Electrical Conductivity, Available P; Phosphorus, Available N; Nitrogen

2.2 Estimation of plant growth

Twenty plant samples were collected randomly from each plot to estimate agronomic parameters and oil contents. All the morphological parameters were determined by adopting the same

procedure used by Nofal et al. (2011). At the same time, seed oil contents were determined by following the AOAC (1980), in which Soxhlet apparatus and petroleum ether were used for extraction. The physiological parameters such as chlorophyll contents were determined by using the SPAD meter (SPAD-502 Konica, Minolta)(Pérez-Patricio et al. 2018) while electron transport reaction (ETR), quantum yield (YII), active photosynthetic radiation (PAR), fluorescence yield (Ft) were noted by using instrument MINI-PAM-II (ALZ Mess und Regeltechnik, Effeltrich, Germany).

2.3 Statistical analysis

Using Statistics 8.1, one-way factorial ANOVA was conducted on the provided data. Comparison among treatment means was made using the least significant difference test at 0.05% probability (Snedecor and Cochran 1990).

3 Results

The effects of various Fe concentrations on the linseed plant were shown to be statistically significant (P 0.05). All the foliar concentrations of Fe significantly improved the agronomic and physiological attributes of the linseed crop. Among the tested various concentrations, maximum plant height (30.3%) and technical stem length (32.4%) of linseed plants were observed in 3.5% Fe application, and the 2.5 and 1.5% followed this compared to control. Further, applications of F4.5 and F5.5 increased the 16.7% and 16.6% plant height and 11.1% and 11.3% technical stem length, respectively, compared to the control (Figure 1).

The maximum number of branches per plant (33.3%) and the number of capsules per plant (40.0%) were also recorded from the same dose of Fe (3.5%) treatment, and the Fe 2.5% followed this. The rest of the treatments are below the given decreasing order, and it was Fe 1.5% (14.3% and 30.7%) > Fe 4.5% (14.2% and 25.1%) > Fe 5.5% (7.70% and 17.2%) as shown in Figure 2.

Similarly, Fe (3.5%) application showed the best results in terms of the number of seeds per capsule (32.0%) and 1000-grain weight (38.0%) of linseed plants, followed by Fe 2.5%, Fe 1.5%, Fe 4.5% and Fe 5.5% and showing 22.7% and 23.1%, 19.0% and 18.0%, 15.0% and 15.7%, 10.5% and 11.3% higher number of seeds per capsule and 1000-grain weight respectively than the control (Figure 3).

The highest biological yield and seed yield were observed in Fe 3.5% application (31.2% and 38.1%), followed by Fe (2.5%), Fe (1.5%), Fe (4.5%) and Fe (5.5%), showing 28.7% and 34.6%, 26.9% and 26.4%, 16.7% and 20.8%, 13.2% and 18.7% higher biological yield and seed yield respectively than the control (Figure 4).

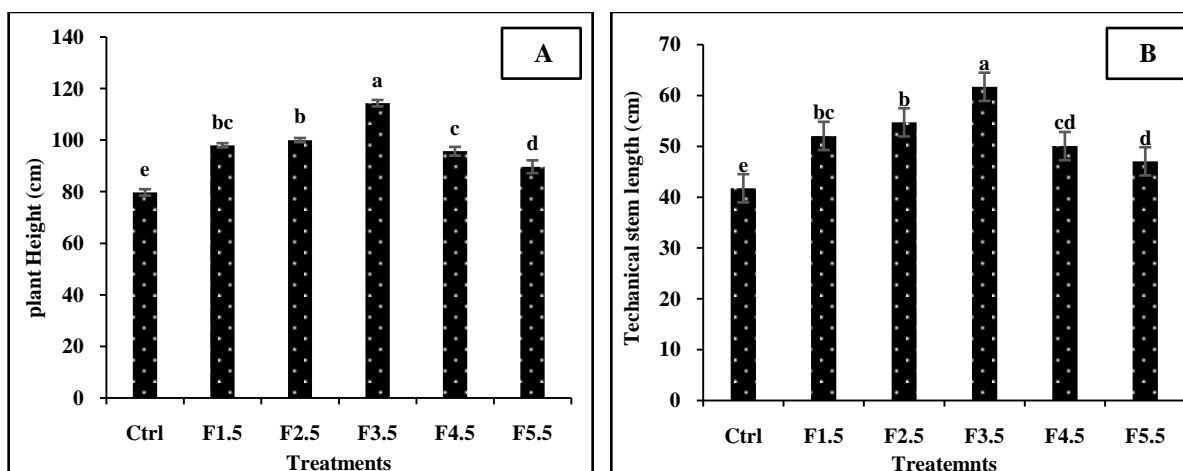


Figure 1 Impact of foliar application of Fe on (A) plant height and (B) technical stem length of linseed crop (means \pm STD, n = 3); Ctrl – Control

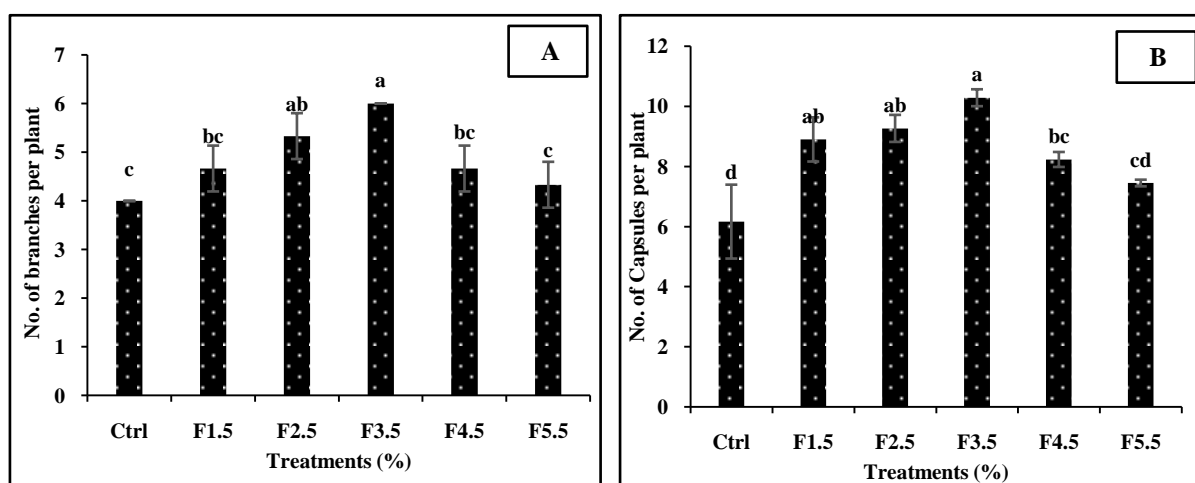


Figure 2 Impact of foliar application of Fe on (A) number of branches and (B) number of capsules per plant of linseed crop (means \pm STD, n = 3); Ctrl – Control

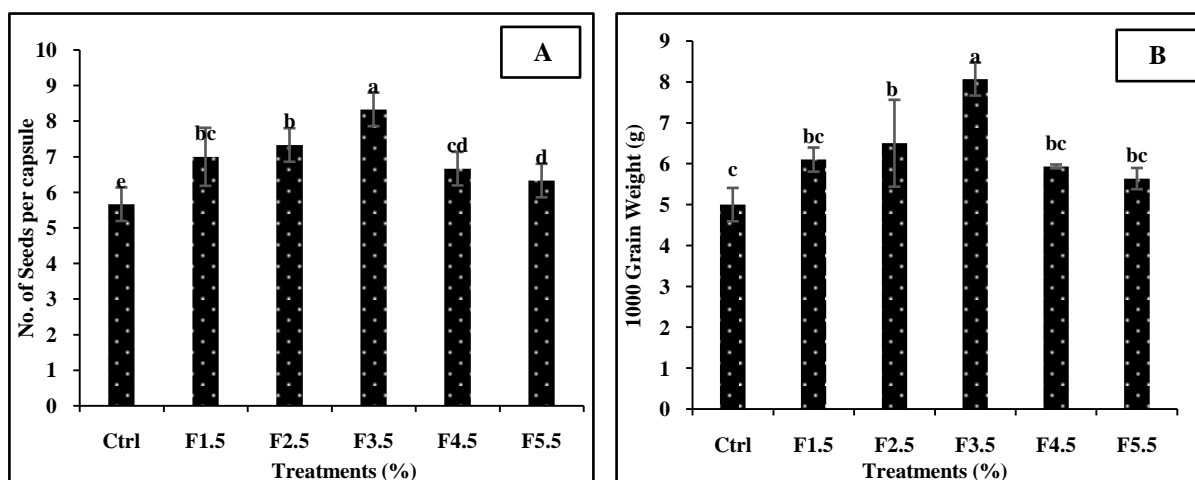


Figure 3 Impact of foliar application of Fe on (A) number of seeds per capsule and (B) 1000 grain weight of linseed crop (means \pm STD, n = 3); Ctrl -Control

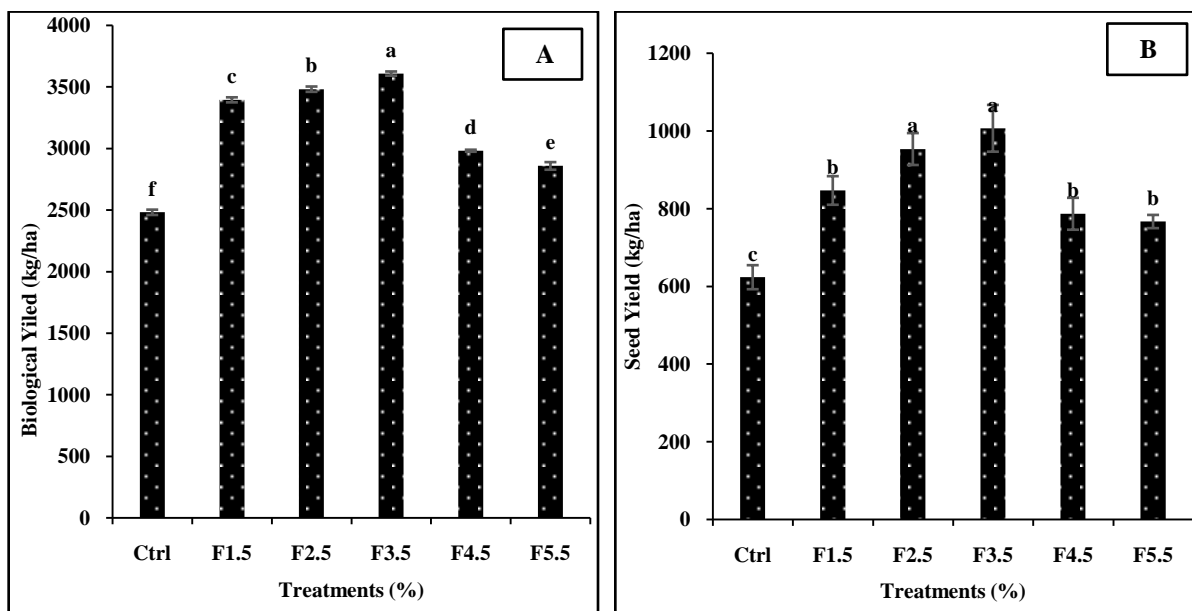


Figure 4 Impact of foliar application of Fe on (A) biological yield and (B) seed yield of linseed crop (means \pm STD, n = 3); Ctrl - Control; F

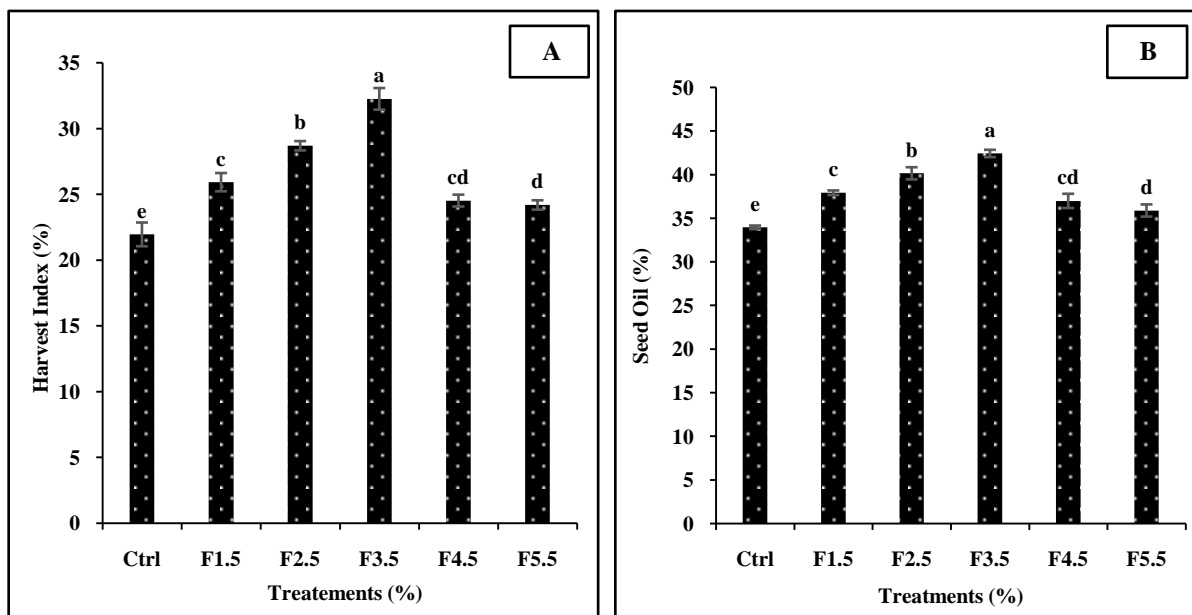


Figure 5 Impact of foliar application of Fe on (A) harvest index and (B) seed oil content of linseed crop (means \pm STD, n = 3); Ctrl - Control

In the case of harvest index also, similar trends were observed, and the decreasing order in harvest index of the linseed crop was Fe 3.5% (31.9%) > Fe 2.5% (23.5%) > Fe 1.5% (15.3%) > Fe 4.5% (10.5%) > Fe 5.5% (9.24%) as shown in Figure 5. Similarly, the Fe application significantly improved the seed oil contents of the linseed crop. The results of the study revealed that the application of Fe 3.5% showed the highest seed oil content (19.9%) followed by Fe 2.5%, Fe 1.5%, Fe 4.5% and Fe 5.5% and showing 15.4%, 10.5%, 8.20% and 5.40% seed oil content respectively than the control (Figure 5).

Like other parameters, the highest fluorescence yield (28.7%) and quantum yield (37.7%) were observed in the Fe 3.5% foliar application treatment, and this was followed by Fe 2.5%, Fe 1.5%, Fe 4.5% and Fe 5.5% and showing 23.4% and 30.3%, 17.4% and 26.1%, 14.2% and 19.5%, 10.8% and 15.8% higher fluorescence yield and quantum yield respectively as compared the control (Figure 6).

The maximum photosynthesis active radiation (43.7%) and electron transport rate (39.6%) were observed in Fe 3.5%

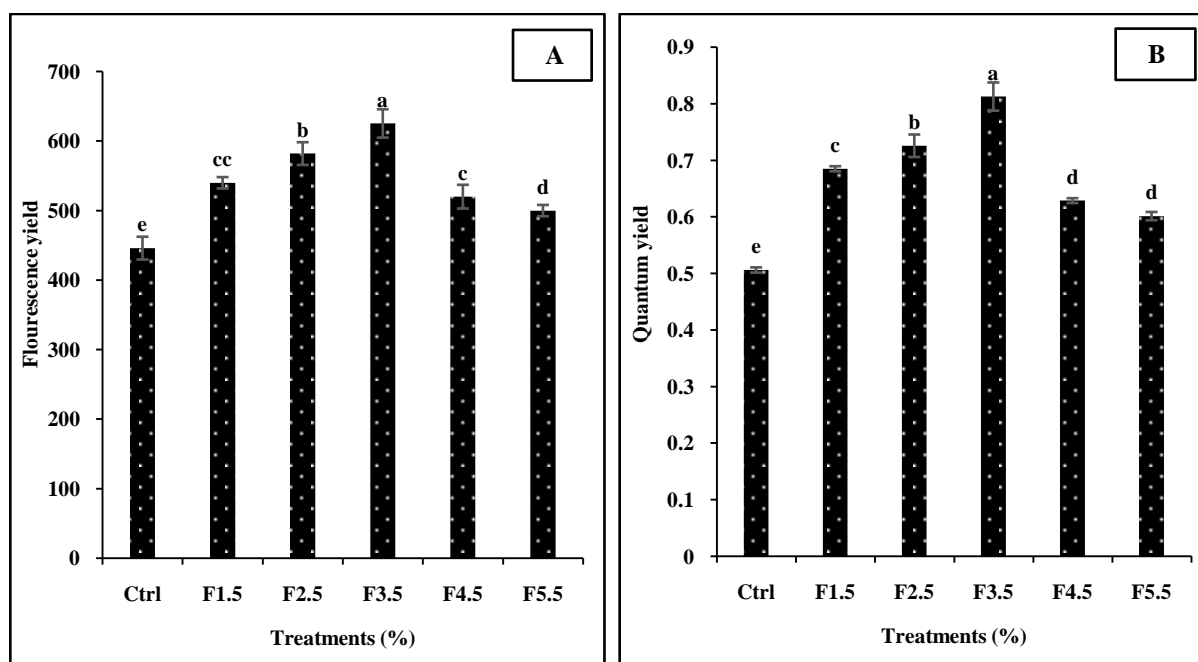


Figure 6 Impact of foliar application of Fe on (A) fluorescence yield and (B) quantum yield of linseed crop (means \pm STD, n = 3); the fluorescence yield and quantum yield were taken after 70 days of sowing; Ctrl – Control

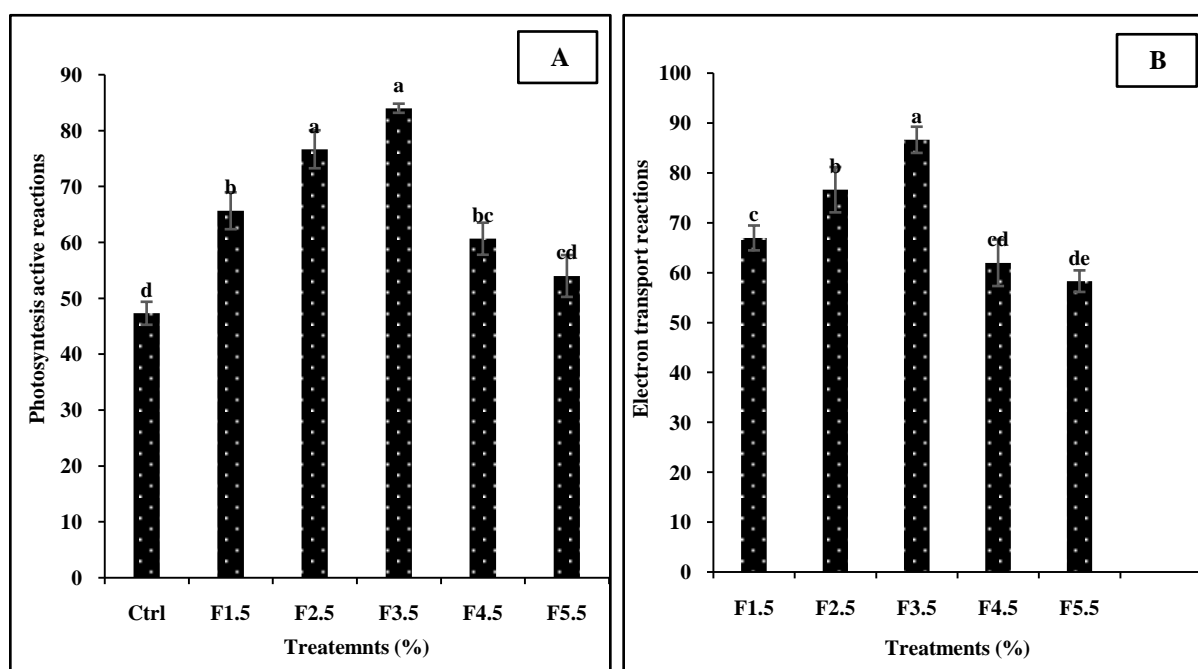


Figure 7 Impact of foliar application of Fe on (A) photosynthesis active radiation and (B) electron transport rate of linseed crop (means \pm STD, n = 3). The photosynthesis active radiation and electron transport rate were taken after 70 days of sowing; Ctrl - Control; F

application treatment, followed by Fe 2.5%, Fe 1.5%, Fe 4.5%, and Fe 5.5%, which showed 38.3% and 31.7%, 27.9% and 22.0%, 22.0% and 15.6%, 12.3% and 10.3% higher photosynthesis active radiation and electron transport rate respectively than the control (Figure 7).

The maximum chlorophyll content (30.3%) of linseed plants was observed in the Fe3.5% application, followed by Fe 2.5%, Fe 1.5%, Fe 4.5% and Fe 5.5% and showing 20.3%, 18.7% 16.7% and 11.1% higher chlorophyll content as compared to the control (Figure 8).

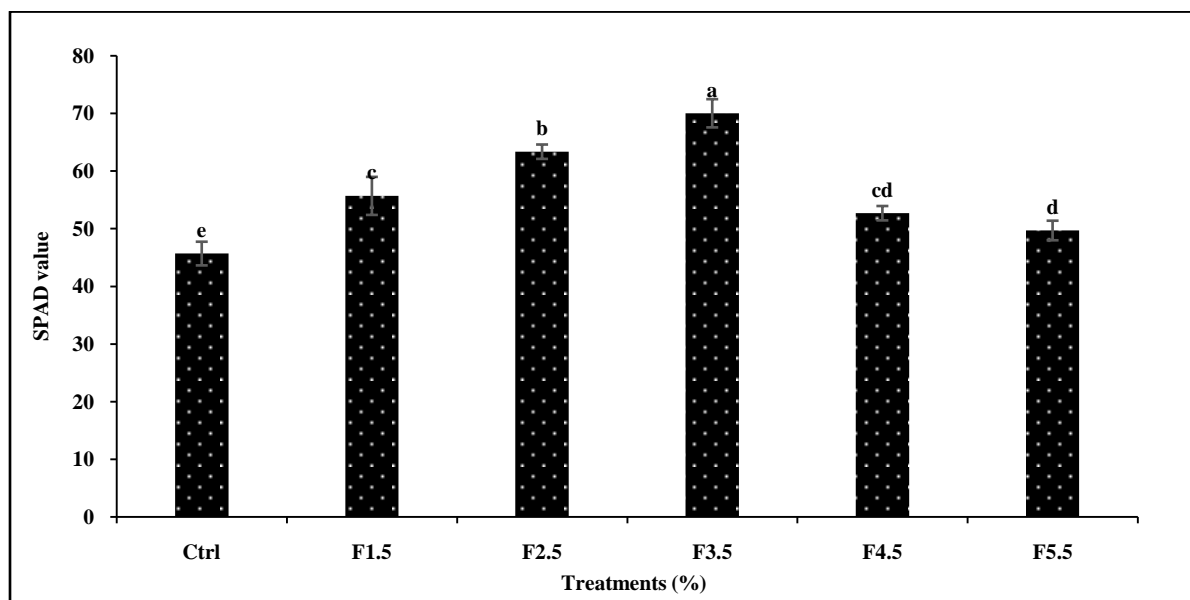


Figure 8 Impact of foliar application of Fe on chlorophyll content (SPAD value) of linseed crop (means \pm STD, n = 3). The SPAD value was taken after 70 days of sowing; Ctrl – Control

4 Discussion

The current study's findings showed that the foliar application of Fe significantly improved all flax plants' physiological and agronomic attributes. It may be due to the critical role of Fe's in chlorophyll synthesis that stimulates the plant structure, improves the functions of chloroplast and enhance the rate of photosynthesis (Rout and Sahoo 2015). Furthermore, the foliar application of Fe also improves the microbial and enzymatic activities that might help enhance the physiological and agronomic attributes of linseed plant (Gondal et al. 2021c; 2021d; 2021e; 2021f; Bisma et al. 2021; Kumar et al. 2021). The results of Esmail et al. (2014) supported this study. Cynthia et al. (2004) also suggested the role of Fe and zinc-like micronutrients in activating many essential enzymes and regulatory cofactors that help plant growth and yield improvement. Similarly, Rezaei-Chiyaneh (2016) suggested that applying Fe and chelated zinc increased flax and bean growth. According to Majeed et al. (2020), Fe enhances the economic returns, yield and yield components in the mungbean; in this manner, these results agree with the present study's findings. The Khalifa et al. (2011) results corroborated our findings and suggested that seed nutrient content, yield components, yield and oil percentage all exhibited significant interactions between cultivars and micronutrient foliar treatment.

Similarly, biological yield, harvest index, and grain oil contents were also improved due to the synthesis of pigments that increase the seed index (Mengel et al. 2001). These results are consistent with the results achieved by other researchers. Straw yield and its components vary greatly between flax genotypes. These findings revealed substantial variation between cultivars of flax when

grown in newly reclaimed sandy soil. These variations are likely attributable to differences in origin, growth habit, genetic diversity, and environmental variables among studied cultivars. Foliar spray of zinc, manganese, and iron increased oil and fibre production in flax plants (Grant et al. 2000; Ali et al. 2009; Bakry et al. 2012). Also, all the physiological parameters, including chlorophyll contents, were improved because Fe application creates better conditions for plant growth (Mengel et al. 2001). According to Nofal et al. (2011), applying micronutrients even in salt-affected soils enhanced the physiological parameters of flax plants. A similar finding was reported by Emam (2020). However, the foliar administration of micronutrients did not improve the seed oil content. Results of the study revealed that the best foliar application level of Fe was 3.5%. Khalifa et al. (2011) suggested that foliar spray of micronutrients has been exposed to an upsurge in seed oil and nutrient content.

Conclusions

Micronutrients are essential for increased flax growth and output but are only required in trace amounts. As much as 30 percent of the world's arable land is excessively alkaline for crop yield, making low Fe availability, and this is one of the most common abiotic stresses in global agriculture. The results suggested that Fe supplementation to the crop plant at various stages boosted plant growth, and it was successfully established with even a modest amount of Fe foliar application (1.5%), which improves the plant growth features compared to the control. The Fe supplementation at the rate of 3.5% improves flax yield and growth and can be established as a recommended dose for flax plants after more similar research.

References

- Ali, S., Shah, Arif, M., Miraj, G., Ali, I., et al. (2009). Enhancement of wheat grain yield and yield components through foliar application of zinc and boron. *Sarhad Journal of Agriculture*, 25(1): 15-19.
- Alvarez, M. E., Savouré, A., & Szabados, L. (2022). Proline metabolism as regulatory hub. *Trends in plant science*, 27(1), 39–55. <https://doi.org/10.1016/j.tplants.2021.07.009>.
- AOAC. (1980). Methods of the association of analytical chemists. 11thedn. Association of analytical Washington DC USA
- Arslanoglu, Ş. F., Sert, S., Şahin, H. A., Aytac, S., & El Sabagh, A. (2022). Yield and Yield Criteria of Flax Fiber (*Linum usitatissimum* L.) as Influenced by Different Plant Densities. *Sustainability*, 14(8), 4710.
- Bakry, B.A., Tawfik, M.M., Mekki, B.B., & Zeidan, M. (2012). Yield and Yield Components of Three Flax Cultivars (*Linum usitatissimum* L.) In Response to Foliar Application with Zn, Mn and Fe under Newly Reclaimed Sandy Soil Conditions. *American-Eurasian Journal of Agricultural and Environmental Science*, 12, 1075-1080.
- Bisma, I. C., Aqarab, H.G., Hooria, Z., Hasnain, U., Muhammad, D.T., et al. (2021). A brief correspondence on glyphosate remediation using microbes and mineral sources. *Annals of Reviews and Research*, 6(4), 555693.
- Biswas, S., & Ansari, M. J. (2023). Health-Endorsing Properties of Cereal Grains. In *Cereal Grains*: DOI:10.1201/9781003252023-5.
- Chapman, H.D., & Pratt, R.F. (1978). Methods analysis for soil, plant and water. University of California Division of Agricultural Science, pp. 16-38.
- Cynthia, G., Monreal, M., Irvine, B., McLaren, D., & Mohr R. (2004). The role of phosphorus fertility and mycorrhiza in flax production. Agriculture and Agri-Food Canada, Brandon Research Center, Brandon.
- Eleni, G. B. (2022). Effects of integrated use of inorganic and organic fertilizers on selected soil physico-chemical properties and yield of durum wheat (*Triticum turgidum* L.) on vertisols of ada'a district, east shewa zone, PhD thesis submitted to the Ambo University, Ambo, Oromia Region, Ethiopia.
- Emam, S. (2020). Estimation of Straw, Seed and Oil Yields for Flax Plants (*Linum usitatissimum* L.) Cultivars of Foliar Application of Mn, Fe and Zn under Dry Environment. *Egyptian Journal of Agronomy*, 42(1): 35-46.
- Esmail, A. O., Yasin, H. S., & Mahmood, B. J. (2014). Effect of levels of phosphorus and iron on growth, yield and quality of flax. *Journal of Agriculture and Veterinary Science*, 7, 7-11.
- Gondal, A. H., & Tayyiba, L. (2022). Prospects of Using Nanotechnology in Agricultural Growth, Environment and Industrial Food Products. *Reviews in Agricultural Science*, 10, 68-81.
- Gondal, A. H., Farooq, Q., Hussain, I., & Toor, M. D. (2021e). Role of Microbes in Plant Growth and Food Preservation. *Agrinula: Jurnal Agroteknologi Dan Perkebunan*, 4(2), 106-121.
- Gondal, A. H., Farooq, Q., Sohail, S., Kumar, S. S., Toor, M. D., Zafar, A., & Rehman, B. (2021c). Adaptability of soil pH through innovative microbial approach. *Current Research in Agricultural Sciences*, 8(2), 71-79.
- Gondal, A. H., Hussain, I., Ijaz, A.B., Zafar, A., et al. (2021d). Influence of Soil Ph and Microbes on Mineral Solubility and Plant Nutrition: A Review. *International Journal of Agriculture and Biological Sciences*, 5(1), 71-81.
- Gondal, A. H., Tampubolon, K., Toor, M. D., & Ali, M. (2021b). Pragmatic and Fragile Effects of Wastewater on a Soil-Plant-Air Continuum and Its Remediation Measures: A Perspective. *Reviews in Agricultural Science*, 9, 249-259.
- Gondal, A. H., Zafar, A. Toor, M.D., Ijaz, A.B., et al. (2021a). Alleviation of zinc deficiency from humans through plants by organic sources: A powerful tonic. *International Journal of Applied Research*, 7(4): 240-24
- Gondal, A. H., Zafar, A., Zainab, D., Toor, M. D., Sohail, S., et al. (2021g). A detailed review study of zinc involvement in animal, plant and human nutrition. *Indian Journal of Pure & Applied Biosciences*, 9(2), 262-271.
- Gondal, A. H., Zafar, H., Yousaf, H., Farooq, Q., Imran, B., et al. (2021f). Impacts of tillage technologies on soil, plant, environment and its management: A short communication. *Indian Journal of Pure and Applied Biosciences*, 9(3), 76-83.
- Grant, C.A., Dribnenki, J.C.O., & Bailey, L.D. (2000). Cadmium and zinc concentrations and ratios in seed and tissue of solin (cv LinolaTM 947) and flax (cvs McGregor and Vimy) as affected by nitrogen and phosphorus fertilizer and Provide (*Penicillium bilaji*). *Journal of Science of Food and Agriculture*, 80(12): 1735-1743.
- Hubmann, M., von Gunten, K., Alessi, D. S., & Curtis, J. M. (2021). Epoxidized linseed lipids as a durable and fast-curing alternative to drying oils. *Progress in Organic Coatings*, 159, 106406.

- Jha, N., Singha, S., & Borah, M. (2023). Indigenous Soybean Cultivars of North-East India: Source of Protein and Product Development for Climate-Smart Foods. In *Agro and Food Processing Technologies: Proceedings of NERC 2022* (pp. 17-32). Singapore: Springer Nature Singapore.
- Khalifa, R., Manal, F., Bakry, A., & Zeidan, M. (2011). Response of some flax varieties to micronutrients foliar application under newly reclaimed sandy soil. *Australian Journal of Basic and Applied Science*, 5(8): 1328-1334.
- Kumar, S. S., Gondal, A. H., Hayat, F., Mahale, A. G., Farooq, Q., & Umer, H. (2021). Weed and disease eradication in crops through genetically modified microbes and soil microorganisms: A promising treatment. *Journal of Agriculture and Allied Fields*, 3(1), 37-51.
- Majeed, A., Minhas, W. A., Mehboob, N., Farooq, S., Hussain, M., Alam, S., & Rizwan, M. S. (2020). Iron application improves yield, economic returns and grain-Fe concentration of mungbean. *PLoS one*, 15(3), e0230720. <https://doi.org/10.1371/journal.pone.0230720> (Retraction published PLoS One. 2022 Nov 16;17(11):e0277622).
- Mengel, K., Kirkby, E.A., Kosegarten, H., Appel, T. (2001). Soil Copper. In: K., Mengel, E.A., Kirkby, H., Kosegarten, & T., Appel, (Eds) *Principles of Plant Nutrition* (pp 599-611). Springer, Dordrecht. https://doi.org/10.1007/978-94-010-1009-2_16.
- Nofal, O., Zedean, M., & Bakry, B. A. (2011). Flax yield and quality traits as affected by zinc foliar application under newly reclaimed sandy soils. *Journal of Applied Sciences Research*, 7 (9), 1361-1367.
- Palmieri, F., Monné, M., Fiermonte, G., & Palmieri, L. (2022). Mitochondrial transport and metabolism of the vitamin B-derived cofactors thiamine pyrophosphate, coenzyme A, FAD and NAD⁺, and related diseases: A review. *IUBMB life*, 74(7), 592–617. <https://doi.org/10.1002/iub.2612>.
- Pérez-Patricio, M., Camas-Anzueto, J., Sanchez-Alegría, A., Aguilar-González, A., Gutiérrez-Miceli, F., Escobar-Gómez, E., & Grajales-Coutiño, R. (2018). Optical method for estimating the chlorophyll contents in plant leaves. *Sensors*, 18(2): 650.
- Rezaei-Chiyaneh, E. (2016). Intercropping of flax seed (*Linum usitatissimum L.*) and pinto bean (*Phaseolus vulgaris L.*) under foliar application of iron nano chelated and zinc. *Journal of Agricultural Science and Sustainable Production*, 26(1): 39-56.
- Rout, G. R., & Sahoo, S. (2015). Role of iron in plant growth and metabolism. *Reviews in Agricultural Science*, 3, 1-24.
- Sangmesh, B., Patil, N., Jaiswal, K. K., Gowrishankar, T. P., Selvakumar, K. K., Jyothi, M. S., Jyothilakshmi, R., & Kumar, S. (2023). Development of sustainable alternative materials for the construction of green buildings using agricultural residues: A review. *Construction and Building Materials*, 368, 130457.
- Snedecor, G.W., & Cochran, W.G. (1990). *Statistical Methods*. 8th Edition, Iowa State University Press, Ames.
- Sohail, S., Husnain Gondal, A., Farooq, Q., Tayyaba, L., et al. (2022). Organic Vegetable Farming; A Valuable Way to Ensure Sustainability and Profitability. *IntechOpen*, doi: 10.5772/intechopen.101095
- Tayyiba, L., Zafar, H., Gondal, A. H., Farooq, Q., Mukhtar, M. M., et al. (2021). Efficiency of Zinc in Plants, its Deficiency and Sensitivity for Different Crops. *Current Research in Agricultural Sciences*, 8(2), 128-134.
- Zeng, A., Chen, W., Rasmussen, K. D., Zhu, X., Lundhaug, M., Müller, D. B., Tan, J., Keiding, J. K., Liu, L., Dai, T., Wang, A., & Liu, G. (2022). Battery technology and recycling alone will not save the electric mobility transition from future cobalt shortages. *Nature communications*, 13(1), 1341. <https://doi.org/10.1038/s41467-022-29022-z>.
- Zhao, A.Q. Bao, Q. Tian, X. H. Lu, X., & William, J. W. (2011). Combined effect of iron and zinc on micronutrient levels in wheat (*Triticum aestivum L.*). *Journal of Environmental Biology*, 32(2):235-239.



Journal of Experimental Biology and Agricultural Sciences

<http://www.jebas.org>

ISSN No. 2320 – 8694

Growth and development patterns in Mustard (*Brassica* spp.) as influenced by sowing time

Sushan Chowhan^{1+*} , Majharul Islam² , Md. Shohel Rana³ , Nazmul Alam Khan⁴ ,
 Md. Khan Jahan Ali⁵ , Nasir Uddin Ahmed⁶, Md. Moshir Rahman⁷ 

¹Adaptive Research and Extension Division, Bangladesh Institute of Nuclear Agriculture (BINA), Sub-station, Ishurdi, Pabna-6620, Bangladesh²Soil Science Division, BINA, BAU campus, Mymensingh-2202, Bangladesh³Plant Breeding Division, BINA, BAU campus, Mymensingh-2202, Bangladesh⁴Biotechnology Division, BINA, BAU campus, Mymensingh-2202, Bangladesh⁵Plant Breeding Division, BINA Sub-station, Ishurdi, Pabna-6620, Bangladesh⁶Advanta Seeds International, Dhaka, Bangladesh⁷Plant Breeding Division, BINA Sub-station, Satkhira-9400, Bangladesh⁺Graduate School of Science and Engineering, Saitama University, Saitama, Japan

Received – February 20, 2023; Revision – April 07, 2023; Accepted – April 28, 2023

Available Online – April 30, 2023

DOI: [http://dx.doi.org/10.18006/2023.11\(2\).325.338](http://dx.doi.org/10.18006/2023.11(2).325.338)

KEYWORDS

Planting date

Binasarisha

BARI Sarisha

Magura

Growth rate

ABSTRACT

Mustard is Bangladesh's leading oil crop, produced only during the winter (*rabi*) season. The sowing date is a key factor determining mustard's optimum growth and development. Because of global warming, gradual changes in season and weather parameters over time is creating a challenge in mustard cultivation. Thus, the present investigation assessed the role of different planting dates on several modern mustard varieties to disclose the optimum growth indicators necessary for elevated biological yield (BY) and harvest index (HI). Three planting times, viz. 31st October (D₁), 10th November (D₂), 20th November (D₃) and six varieties viz. Binasarisha-4 (V₁), Binasarisha-9 (V₂), Binasarisha-10 (V₃), BARI Sarisha-14 (V₄), BARI Sarisha-16 (V₅), BARI Sarisha-17 (V₆) were put on a replicated factorial randomized complete block design (RCBD) during *rabi* 2019 at BINA Sub-station farm, Magura. At the final harvest stage, outcomes depicted that highest and lowest total dry mass (g/plant) was produced by treatment D₃ × V₅ (64.03) and D₁ × V₁ (15.34), maximum and minimum absolute growth rate (mg/plant/day) by D₁ × V₅ (2389.10) and D₂ × V₁ (184.50), most and least relative growth rate (mg/g/day) in D₁ × V₄ (53.34) and D₂ × V₁ (3.55), maximum and least crop growth rate (g/m²/day) with D₁ × V₃ (55.60) and D₃ × V₄ (20.04). BY was the peak (8.13, 8.71, 8.77 t/ha) under all plantings (D₁, D₂, D₃) with V₅

* Corresponding author

E-mail: sushan04@yahoo.com (Sushan Chowhan)

Peer review under responsibility of Journal of Experimental Biology and Agricultural Sciences.

Production and Hosting by Horizon Publisher India [HPI]
 (<http://www.horizonpublisherindia.in/>).
 All rights reserved.

All the articles published by [Journal of Experimental Biology and Agricultural Sciences](#) are licensed under a [Creative Commons Attribution-NonCommercial 4.0 International License](#) Based on a work at www.jebas.org.



variety, but HI (44.96%) was most in variety V₄ with D₂ sowing. Therefore, correlation studies showed a significant positive relationship between biological yield and harvest index. Overall, BARI Sarisha-16 performed well in all three sowing times, and remarkably, BY was rising with delayed planting in the case of Binasarisha-9, Binasarisha-10, and BARI Sarisha-14. This implies that delayed planting might not hamper yield but boost yield to some extent.

1 Introduction

Mustard (*Brassica spp.*) is a major edible oilseed crop grown worldwide, including Bangladesh. It is produced in cool temperatures during winter with or without irrigation (Chowhan and Islam 2022a). It is a photo and thermosensitive crop (Ghosh and Chatterjee 1988), and a temperature between 12°C to 25°C is an ideal growth temperature, but low temperatures may hamper the growth of this plant (Wahhab et al. 2002). Hence this crop needs to be sowed within a specific time. In Bangladesh, Mustard is the time window for planting in mid-October to mid-November (Alam et al. 2014). Due to seasonal inundation driven by climate change, the mustard sowing date does not remain constant. Rather it depends on the location and weather of a particular region. However, the planting date has been delayed for the past few years due to sudden rainfall in mid-October. So, farmers are facing a big challenge to cope with this situation. Though productivity drops owing to the shortening of the vegetative and reproductive phases under late-seeded conditions. During the reproductive period, late-sown Mustard is subjected to high temperatures combined with high evaporative demand of the atmosphere, resulting in forced maturity, increased senescence, and reduced yield (Porter 2005). Therefore, crop plants consider a single-degree temperature rise over the threshold level as heat stress (Hasanuzzaman et al. 2013). Mustard prefers cool weather throughout the vegetative growth and slightly warm (>25°C) during the reproductive period. So, planting time is a vital factor in determining a cultivar's growth development, yield and quality.

Accumulation of total dry mass is an essential criterion for gaining improved morpho-physical and yield quality properties which are also influenced by sowing dates (Singh and Yeshpal 2011). It is notable in Mustard that, during the reproductive stage, the flowering, fruiting and vegetative growth coincide until physiological maturity (Mondal et al. 2013). Thus, developing reproductive sinks are competing for assimilates with vegetative sinks. It was evident that seeds per unit area are related to canopy photosynthesis during flowering and pod set. Furthermore, the canopy photosynthesis rate determines through the leaf area index (LAI) and crop growth rate (CGR). Main physiological properties, for example, absolute growth rate (AGR), CGR, relative growth rate (RGR), net assimilation rate (NAR) and total dry mass (TDM), vary, and these depend on

crop variety and environmental factors. Thus, these parameters can address various constraints for increasing productivity (Tandale and Ubale 2007).

Up to date, BARI (Bangladesh agricultural research institute) and BINA (Bangladesh Institute of nuclear agriculture) have developed more than 25 rapeseed mustard varieties (BINA 2022; Azad et al. 2020); most of them have satisfactory levels of growth and better yield capacity. Considering the above factors, we tested some popular BINA and BARI mustard varieties concerning various planting dates to disclose the optimum sowing date and varieties with better growth, development, biological yield and harvest index.

2 Materials and methods

2.1 Experimental site

BINA, Sub-station farm, Magura was the experimental site under the Agro-Ecological Zone 11 (AEZ); this area was characterized by a high Ganges river flood plain with high to medium land type. Soils were calcareous dark grey to brown floodplain soils. Organic matter content in brown ridge soils is low but higher in dark grey soils. Soils were slightly alkaline with a deficit in fertility (FRG 2012). Details of the weather parameters during the experimental period are expressed in Figure 1.

2.2 Crop Establishment and Cultural Practices

The experiment was established on the farm during *rabi* (winter) 2019. Tillage was followed as per methods stated by Chowhan and Nahar (2022); Chowhan and Islam (2022b). Considering the low soil fertility level, yield goal (2±0.2 t/ha) fertilizers were applied following the procedures described by Chowhan et al. (2023) and Ahmed et al. (2018). A full dose of P, K, S, Zn, B and half N was given on soil as the basal. The rest of the N was top-dressed at 22 days of seedling age, comprising light irrigation. Line-to-line and plot-to-plot distances were each 30 cm, and the unit plot measured 1.5 m by 2.0 m. In the three planting dates (31 October, 10 November and 20 November), seeds were line sown (broadcast method) at a 7.5 kg/ha rate. To maintain the target plant population, surplus plants were thinned and mulched 20 days after sowing (DAS) (BINA 2014). Seeds were harvested when the siliques gained 75% maturity and appeared brownish to straw colour

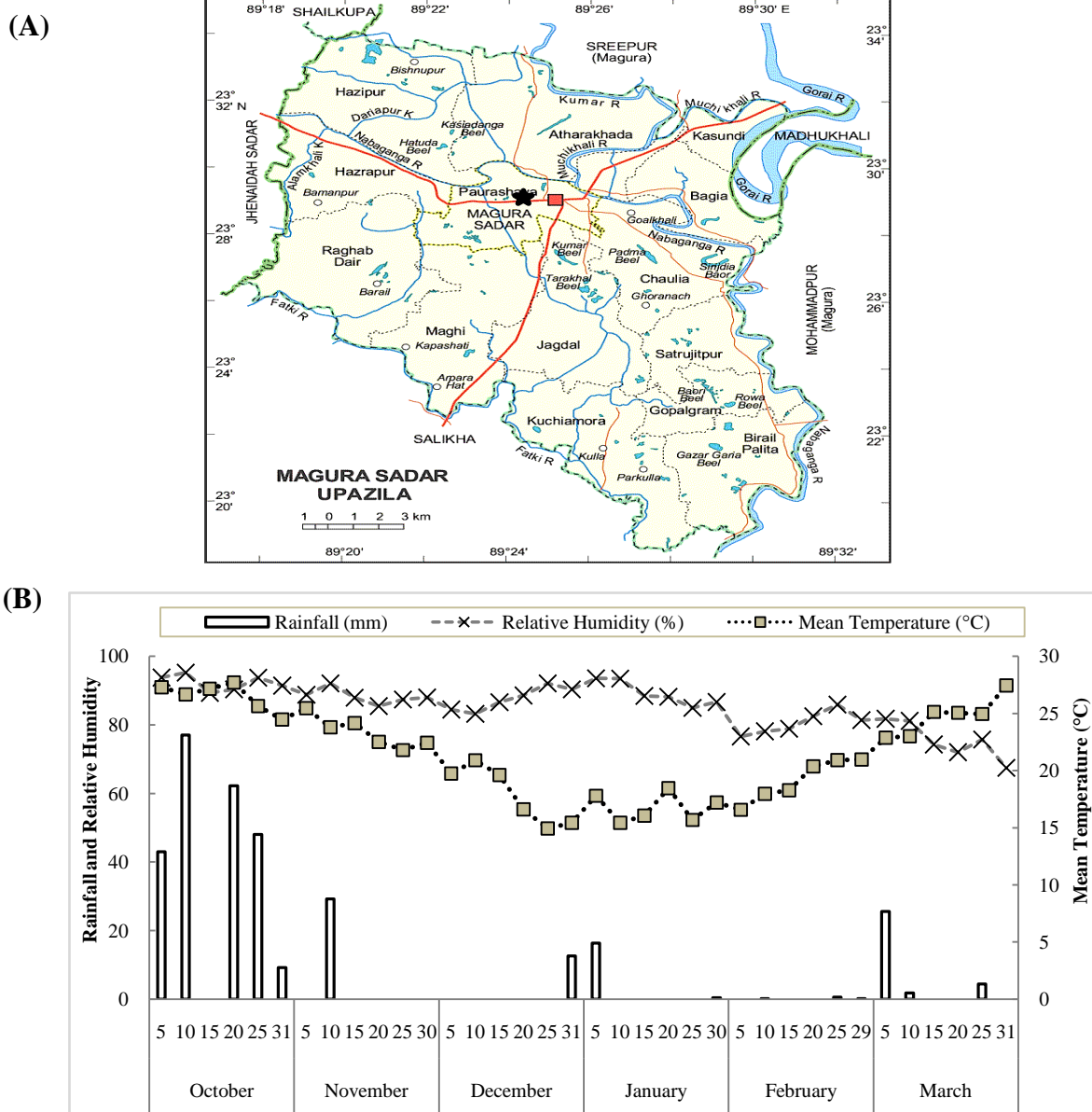


Figure 1 Experimental location and weather status of Magura sadar upazila (A) Black star indicates the experimental site; (B) Mean weather parameters of the experimental area from October 2019 to March 2020 (BINA 2020)

2.3 Experimental design

The experiment followed a factorial Randomized complete block design (RCBD) with three replications. Replication to replication gap was 1m. There were two factors (variety and sowing date) in the experiment. Three sowing dates were assigned as factor A, and six varieties were considered factor B. Details of the factors and treatment are pointed below

Factor A: Sowing dates (3)

$D_1 = 31-10-2019$, $D_2 = 10-11-2019$, $D_3 = 20-11-2019$.

Factor B: Variety (6)

$V_1 = \text{Binasarisha-4}$, $V_2 = \text{Binasarisha-9}$, $V_3 = \text{Binasarisha-10}$,
 $V_4 = \text{BARI Sarisha-14}$, $V_5 = \text{BARI Sarisha-16}$, $V_6 = \text{BARI Sarisha-17}$

2.4 Data Collection and Analysis

Five plants were randomly sampled for growth parameters from 30 DAS and continued at an interval of 10 days up to harvest. Plants were separated into roots, stems, leaves and silique and

the corresponding dry weights were recorded after oven drying at $80 \pm 2^\circ\text{C}$ for 72 hours. The following physiological parameters were noted according to Hunt et al. (2002) and Sarkar et al. (2016)

Total dry mass (TDM) = $W_1 - W_2$ (g/plant)

Absolute growth rate (AGR) = $\frac{W_f - W_i}{t_2 - t_1}$ (mg/plant/day)

Relative growth rate (RGR) = $\frac{\ln W_f - \ln W_i}{t_2 - t_1}$ (mg/g/day)

Crop growth rate (CGR) = $\frac{1}{A} \times \frac{W_f - W_i}{t_2 - t_1}$ (g/m²/day)

Where,

W_1 = Fresh weight of the plant (g)

W_2 = Oven dry weight of the plant (g)

W_i = Total plant dry matter at initial time t_1 (g)

W_f = Total plant dry matter at final time t_2 (g)

t_2 = final time (day)

t_1 = initial time (day)

$t_2 > t_1$

A = Ground area (m²)

ln = Natural logarithm

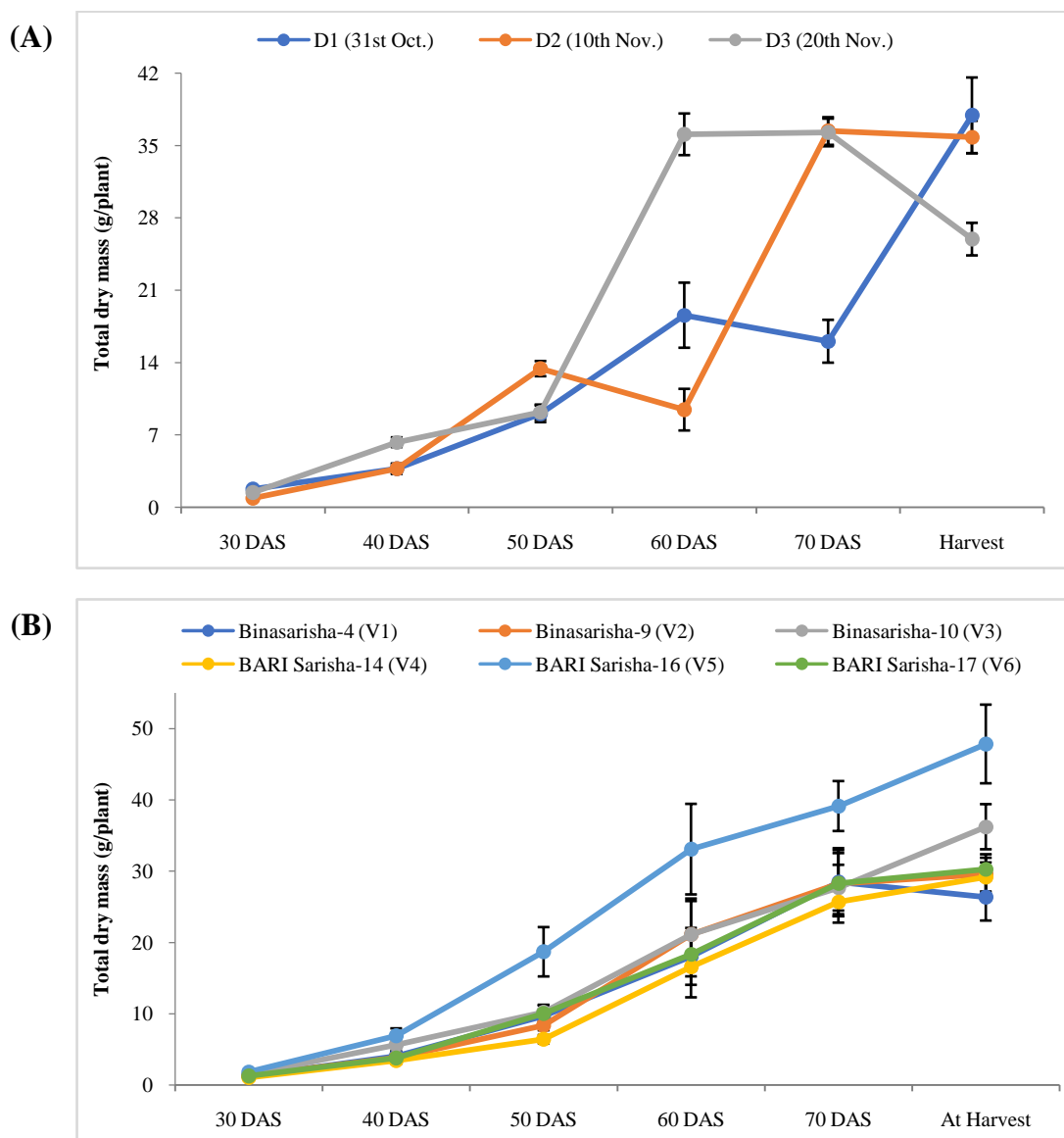


Figure 2 Total dry mass (TDM) under three planting times of six mustard varieties (A) Individual lines show the mean TDM of the defined planting time on different days after sowing (DAS) up to harvest (B) Indicates the average TDM of the cultivars at various intervals (DAS) until harvest (Each data point represents the mean of 5 plant samples; Error bars are the standard error values)

Harvest index (HI) (%) (Chowhan et al. 2018) and biological yield (Chowhan et al. 2017) was recorded using the following formulae

- $HI (\%) = \{Economic \text{ (grain) yield} \div biological \text{ yield}\} \times 100$
- $Biological \text{ yield (t/ha)} = seed \text{ yield} + straw \text{ yield}$

Data taken on the parameters were analyzed statistically by Statistix 10 (Statistix 2022) subject to LSD (least significant difference) test at a 5% level of probability was used for average distinctions (Russel 1986) among the treatments.

3 Results and discussion

3.1 Total dry mass

Dry matter accumulation was more or less alike up to 50 DAS (Figure 2A). Later from 60 DAS, dry mass deposition followed a zigzag pattern for all the sowing dates. However, at the harvest

time, D1 and D2 treatments produced statistically identical dry mass; the lowest was found with the D₃ treatment. All the varieties followed a similar lift of dry mass increase except BARI Sarisha-16 (V₅); the total dry mass of this variety was significantly higher than others (Figure 2B).

The interaction effect of the treatments implied that D₃ × V₅ had the maximum and D₁ × V₁ had the minimum amount of total dry mass at the maturity stage of the crop (Table 1). The sowing date may have played a significant role in dry matter production; thus, late sowing showed a lesser dry mass. A contrary varietal trait is another important criterion that is also responsible for the dry matter content. So, BARI Sarisha-16 (V₅) gained abundant dry mass. The combined effect indicated that early sowing always favours more dry mass than late sowing, as plants get enough time for adequate growth. However, dry matter content may also depend on variety as some may be suitable for early sowing and others not. These findings are consistent with those of Sharif et al. (2017).

Table 1 Collective effect of sowing time, varieties on total dry mass (g/plant)

Treatments	30 DAS	40 DAS	50 DAS	60 DAS	70 DAS	Harvest
D ₁ × V ₁	0.71 ^f	3.18 ^{c-f}	6.55 ^{de}	7.37 ^e	10.43 ^d	15.34 ^f
D ₁ × V ₂	0.97 ^{def}	1.85 ^f	9.21 ^{b-e}	8.99 ^e	12.76 ^d	21.98 ^{ef}
D ₁ × V ₃	1.10 ^{c-f}	5.70 ^{bcd}	7.39 ^{b-e}	6.95 ^e	16.46 ^d	29.94 ^{de}
D ₁ × V ₄	0.71 ^f	2.95 ^{def}	6.11 ^e	7.78 ^e	16.67 ^d	27.46 ^{de}
D ₁ × V ₅	1.10 ^{c-f}	5.77 ^{bcd}	13.99 ^b	14.83 ^e	29.23 ^c	30.02 ^{de}
D ₁ × V ₆	0.78 ^{ef}	3.02 ^{def}	11.03 ^{b-e}	10.82 ^e	10.88 ^d	30.98 ^{de}
D ₂ × V ₁	1.26 ^{b-f}	4.00 ^{c-f}	8.68 ^{b-e}	14.08 ^e	37.44 ^{abc}	36.39 ^{cd}
D ₂ × V ₂	1.44 ^{b-e}	3.54 ^{c-f}	8.74 ^{b-e}	19.49 ^{cde}	33.73 ^{bc}	37.25 ^{cd}
D ₂ × V ₃	1.49 ^{b-e}	3.97 ^{c-f}	10.66 ^{b-e}	16.38 ^{de}	32.56 ^{bc}	35.48 ^{cd}
D ₂ × V ₄	1.23 ^{b-f}	2.26 ^{ef}	6.699 ^{cde}	8.83 ^e	30.07 ^c	27.51 ^{de}
D ₂ × V ₅	1.92 ^{ab}	5.28 ^{bcd}	13.72 ^{bcd}	37.42 ^{ab}	47.63 ^a	49.48 ^b
D ₂ × V ₆	1.19 ^{b-f}	3.35 ^{c-f}	6.76 ^{cde}	15.34 ^e	37.05 ^{bc}	28.86 ^{de}
D ₃ × V ₁	1.73 ^{bc}	4.91 ^{b-e}	13.81 ^{bc}	32.67 ^{bc}	37.49 ^{abc}	27.30 ^{de}
D ₃ × V ₂	1.54 ^{bcd}	6.08 ^{bc}	7.09 ^{b-e}	34.86 ^{ab}	38.23 ^{abc}	29.45 ^{de}
D ₃ × V ₃	1.90 ^{ab}	7.16 ^{ab}	12.59 ^{b-e}	39.96 ^{ab}	33.99 ^{bc}	43.26 ^{bc}
D ₃ × V ₄	1.14 ^{c-f}	5.05 ^{b-e}	6.43 ^e	33.16 ^b	30.40 ^{bc}	32.53 ^{cde}
D ₃ × V ₅	2.52 ^a	9.66 ^a	28.32 ^a	46.98 ^a	40.51 ^{ab}	64.03 ^a
D ₃ × V ₆	1.77 ^{bc}	4.92 ^{b-e}	12.26 ^{b-e}	28.93 ^{bcd}	36.97 ^{bc}	31.03 ^{de}
LSD _{0.05}	0.72	2.96	7.19	13.35	10.28	11.16
SEm	0.35	1.45	3.53	6.56	5.05	5.49
CV	32.02%	38.84%	41.05%	37.62%	20.95%	20.23%

Figures in a column with a different letter (s) differ significantly at a 5% probability level, according to LSD; n=5, P < 0.05; by analysis of variance with factorial randomized complete block design; SEm - Standard error mean; CV - Coefficient of variation

3.2 Absolute growth rate (AGR)

Sowing dates caused differential AGR. At 70-80 DAS highest AGR was obtained from D₁, and the lowest was observed in the D₂ treatment (Figure 3A). Only BARI Sarisha-16 (V₅) among the tested varieties reached the ultimate AGR. Rest five varieties showed similar AGR at 70-80 DAS (Figure 3B). The combined effect demonstrated that treatment D₁ × V₅ had the highest AGR; contrary, the lowest was noted with D₂ × V₁ at 70-80 DAS (Table

2). Interestingly combined effect illustrates that varietal interaction with D₂ sowing lessens the AGR, but when combined with D₃ sowing, again, the AGR rises; the same phenomenon is also spotted with the sole effect of planting time. This may be due to the variable weather parameters during the experimental period. BARI Sarisha-16 (V₅) followed a different pattern of AGR, which might be of its inherent attributes. Mondal et al. (2018) ascertained variable AGR of mutants/variety at different growth stages of *Brassica juncea*.

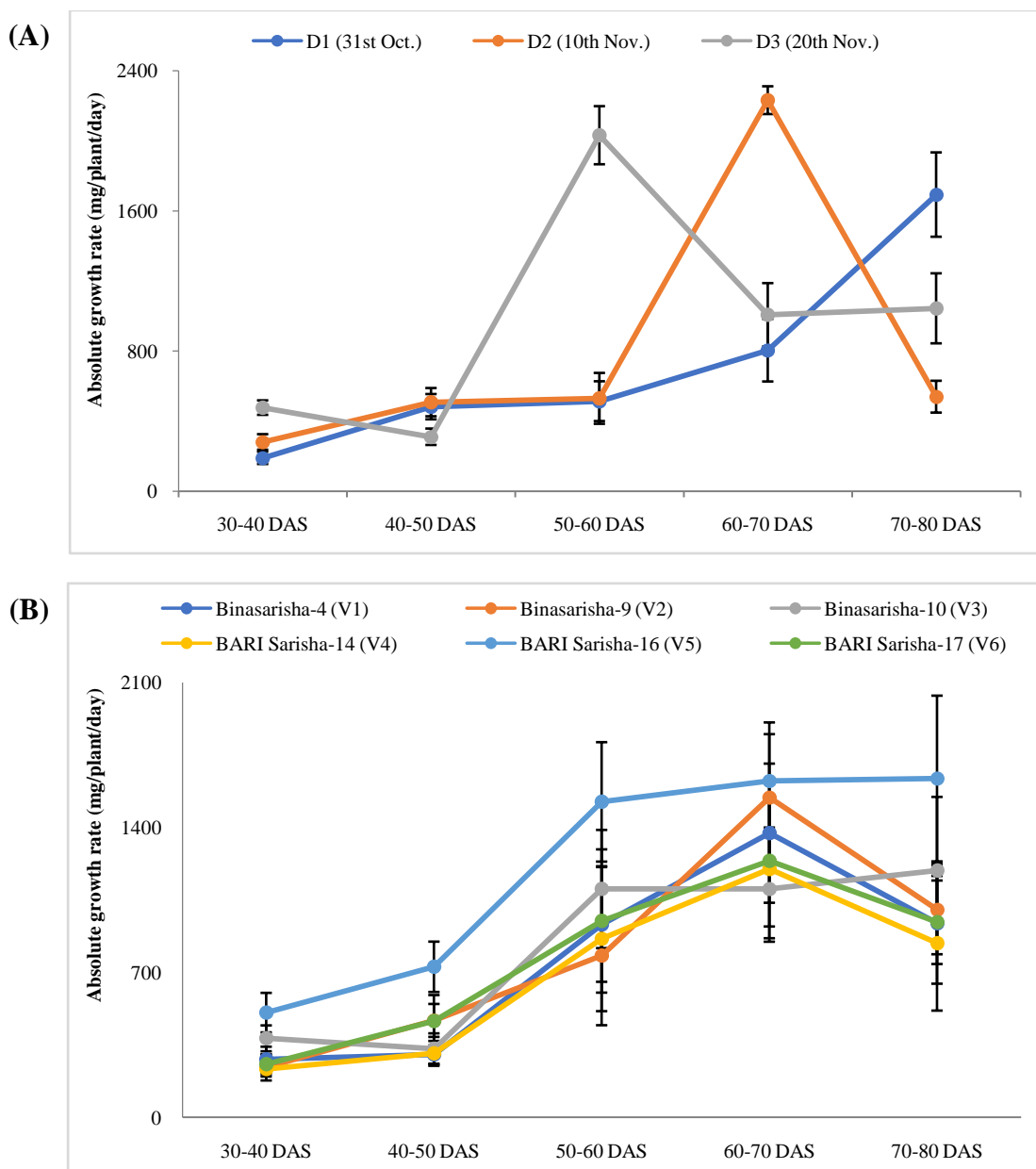


Figure 3 Absolute growth rate (AGR) under three sowing dates of six mustard varieties (A) Individual lines show the mean AGR of the three planting time at different sowing intervals (DAS) up to harvest (B) Indicates the average AGR of six mustard cultivars at different durations (DAS) until harvest (Each data point represents the mean of 5 plant samples; Error bars are the standard error values)

Table 2 Absolute growth rate (mg/plant/day) of mustard affected by sowing time and varieties

Treatment combinations	30-40 DAS	40-50 DAS	50-60 DAS	60-70 DAS	70-80 DAS
D ₁ × V ₁	145.10 ^{ef}	198.75 ^e	527.50 ^{cde}	499.20 ^f	1186.30 ^{b-e}
D ₁ × V ₂	33.07 ^f	732.88 ^{abc}	219.80 ^e	948.90 ^{def}	1070.40 ^{cde}
D ₁ × V ₃	322.17 ^{b-e}	284.67 ^{de}	528.80 ^{cde}	632.30 ^f	2368.10 ^{ab}
D ₁ × V ₄	180.53 ^{def}	316.30 ^{de}	226.00 ^e	875.90 ^{def}	1733.10 ^{abc}
D ₁ × V ₅	325.70 ^{b-e}	822.12 ^{ab}	1252.00 ^{a-d}	1362.60 ^{a-f}	2389.10 ^a
D ₁ × V ₆	137.90 ^{ef}	541.40 ^{b-e}	331.50 ^{de}	510.50 ^f	1410.30 ^{a-d}
D ₂ × V ₁	329.53 ^{b-e}	336.42 ^{cde}	643.90 ^{b-e}	2363.60 ^{abc}	184.50 ^e
D ₂ × V ₂	257.12 ^{c-f}	346.77 ^{cde}	206.70 ^e	2465.70 ^a	543.20 ^{cde}
D ₂ × V ₃	272.40 ^{c-f}	327.50 ^{cde}	549.30 ^{cde}	1997.10 ^{a-d}	291.80 ^{de}
D ₂ × V ₄	154.78 ^{ef}	416.82 ^{b-e}	134.90 ^e	2228.90 ^{abc}	324.00 ^{de}
D ₂ × V ₅	417.95 ^{bcd}	955.18 ^a	1348.10 ^{abc}	1931.60 ^{a-e}	1076.20 ^{cde}
D ₂ × V ₆	257.62 ^{c-f}	668.68 ^{a-d}	298.50 ^{de}	2402.20 ^{ab}	819.20 ^{cde}
D ₃ × V ₁	365.43 ^{b-e}	376.33 ^{cde}	1624.90 ^{ab}	1256.10 ^{b-f}	1440.60 ^{a-d}
D ₃ × V ₂	434.30 ^{bc}	325.83 ^{cde}	1916.00 ^a	1221.80 ^{c-f}	1395.90 ^{a-d}
D ₃ × V ₃	551.27 ^{ab}	380.97 ^{cde}	2231.70 ^a	682.90 ^f	916.30 ^{cde}
D ₃ × V ₄	366.60 ^{b-e}	194.80 ^e	2228.90 ^a	494.20 ^f	466.40 ^{de}
D ₃ × V ₅	774.75 ^a	405.12 ^{cde}	1972.00 ^a	1582.90 ^{a-f}	1445.80 ^{a-d}
D ₃ × V ₆	372.68 ^{b-e}	183.78 ^e	2216.30 ^a	804.10 ^{ef}	598.30 ^{cde}
LSD _{0.05}	252.60	409.14	1002.50	1148.80	1197.80
SEm	124.30	201.22	493.32	565.29	589.42
CV	48.08%	56.80%	58.92%	51.37%	66.10%

Figures in a column having a different letter (s) differ significantly at a 5% level of probability according to LSD; n=5, P < 0.05; by analysis of variance with factorial randomized complete block design; SEM, Standard error mean; CV - Coefficient of variation

3.3 Relative growth rate (RGR)

An up-down trend of RGR was seen during the planting times. But, early sowing, i.e. D₁ had the greatest RGR over the other planting times at 70-80 DAS (Figure 4A). A varietal consequence of RGR was nonsignificant for all sowing intervals except 40-50 DAS, where Binasarisha-9 (V₂) had the utmost RGR. But at the final time (70-80 DAS) all the varieties had a centered RGR level (Figure 4B). The combined effect exhibited a zigzag pattern of RGR at different DAS. However, at 70-80 DAS, extreme RGR was marked with treatment D₁ × V₄ and the minimum was recorded with D₂ × V₁ (Table 3). Sowing dates had a significant influence on the RGR. But the varietal effect was not prominent on RGR. With the advancement of time, RGR declined for all varieties, as per the findings of Uddin et al. (2012). Interaction of the two factors perceived that advance planting (D₁) with Binasarisha-10 (V₃) and BARI Sarisha-14 (V₄) might be better for obtaining the best RGR. Maurya et al. (2022) noted RGR of two

Indian mustard varieties declined upon the progress of crop duration. But our results show different findings, possibly due to varietal and weather factors.

3.4 Crop growth rate (CGR)

Initially, the CGR was slow up to 50-60 DAS for all sowing dates and varieties; but after that, it had a sharp increase from 60-70 DAS; Thus, at 70-80 DAS, the CGR value drastically rose about two to five times than 60-70 DAS (Figure 5A, 5B). At the final stage (70-80 DAS), CGR was unaffected by planting times. Interaction effects depicted that, at 70-80 DAS, significantly higher CGR was obtained from D₁ × V₃ and the lowest was identified with D₃ × V₄ treatment combination, which differed from the other treatments (Table 4). Though there was variation in CGR from 30-40 DAS to 60-70 DAS, but at 70-80 DAS, both sowing dates and varieties didn't significantly affect CGR value. Initial variation might be due to cultural practice. But after the flowering stage, no major

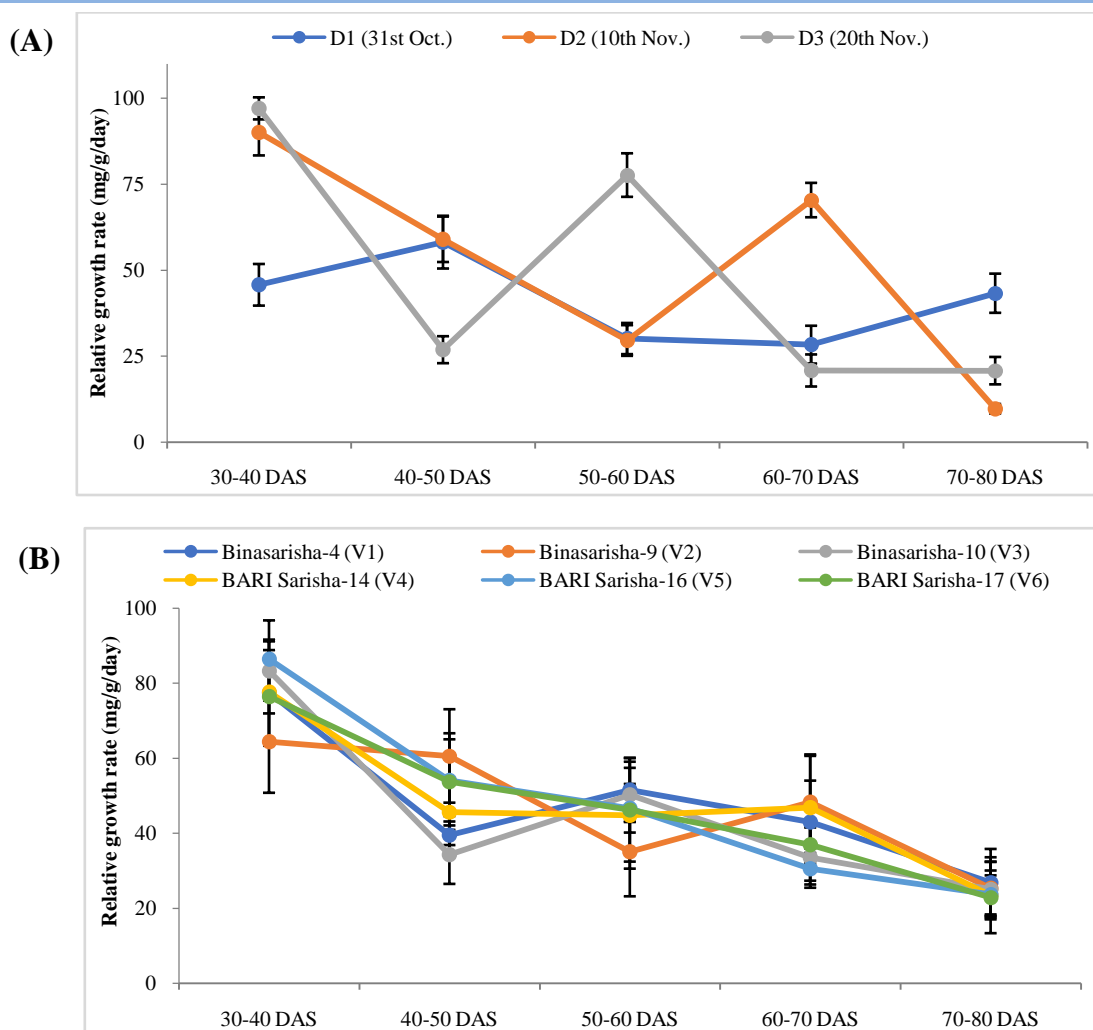


Figure 4 Relative growth rate (RGR) under three sowing dates of six mustard varieties (A) Individual lines show the mean RGR of the three planting time at different sowing intervals (DAS) up to harvest (B) Indicates the average RGR of six mustard cultivars at different durations (DAS) until harvest (Each data point represents the mean of 5 plant samples; Error bars are the standard error values)

Table 3 Effect of sowing time, varieties and their interaction on RGR (mg/g/day)

Treatment combinations	30-40 DAS	40-50 DAS	50-60 DAS	60-70 DAS	70-80 DAS
$D_1 \times V_1$	39.58 ^{de}	33.69 ^{c-f}	45.99 ^{c-f}	24.05 ^d	41.42 ^{abc}
$D_1 \times V_2$	14.22 ^c	88.49 ^a	13.27 ^f	29.77 ^{cd}	37.77 ^{a-e}
$D_1 \times V_3$	62.57 ^{bcd}	31.80 ^{c-f}	36.01 ^{ef}	24.94 ^d	52.47 ^{ab}
$D_1 \times V_4$	63.06 ^{bcd}	47.32 ^{b-f}	22.04 ^f	41.19 ^{bcd}	53.34 ^a
$D_1 \times V_5$	56.52 ^{cd}	60.86 ^{b-e}	40.12 ^{def}	26.88 ^d	34.15 ^{a-f}
$D_1 \times V_6$	38.42 ^{de}	68.58 ^{a-d}	23.18 ^f	23.18 ^d	40.52 ^{a-d}
$D_2 \times V_1$	102.43 ^{ab}	46.05 ^{b-f}	45.82 ^{c-f}	70.38 ^{ab}	3.55 ^g
$D_2 \times V_2$	86.09 ^{abc}	47.47 ^{b-f}	17.38 ^f	88.27 ^a	9.99 ^{d-g}
$D_2 \times V_3$	84.47 ^{abc}	41.61 ^{b-f}	39.10 ^{ef}	63.34 ^{abc}	5.86 ^{fg}
$D_2 \times V_4$	76.91 ^{a-d}	68.89 ^{a-d}	14.44 ^f	90.92 ^a	7.54 ^{efg}
$D_2 \times V_5$	94.01 ^{abc}	78.32 ^{ab}	40.95 ^{c-f}	38.80 ^{bcd}	14.72 ^{c-g}

Treatment combinations	30-40 DAS	40-50 DAS	50-60 DAS	60-70 DAS	70-80 DAS
D ₂ × V ₆	96.32 ^{abc}	71.42 ^{abc}	19.56 ^f	70.41 ^{ab}	16.41 ^{c-g}
D ₃ × V ₁	90.39 ^{abc}	38.71 ^{b-f}	62.75 ^{b-e}	34.51 ^{cd}	35.70 ^{a-f}
D ₃ × V ₂	92.92 ^{abc}	27.83 ^{ef}	74.49 ^{a-d}	26.82 ^d	28.26 ^{a-g}
D ₃ × V ₃	102.75 ^{ab}	29.44 ^{def}	75.57 ^{abc}	12.23 ^d	17.04 ^{c-g}
D ₃ × V ₄	92.82 ^{abc}	20.83 ^f	97.94 ^a	8.28 ^d	9.54 ^{efg}
D ₃ × V ₅	108.77 ^a	23.07 ^{ef}	58.92 ^{cde}	25.90 ^d	22.32 ^{b-g}
D ₃ × V ₆	94.46 ^{abc}	21.30 ^{ef}	96.10 ^{ab}	17.20 ^d	11.76 ^{c-g}
LSD _{0.05}	40.82	39.65	34.83	35.67	30.56
SEm	20.09	19.51	17.14	17.55	15.04
CV	31.70%	49.80%	45.87%	53.97%	74.95%

Figures in a column with a different letter (s) differ significantly at a 5% probability level according to LSD; n=5, P < 0.05; by analysis of variance with factorial randomized complete block design; SEm - Standard error mean; CV - Coefficient of variation

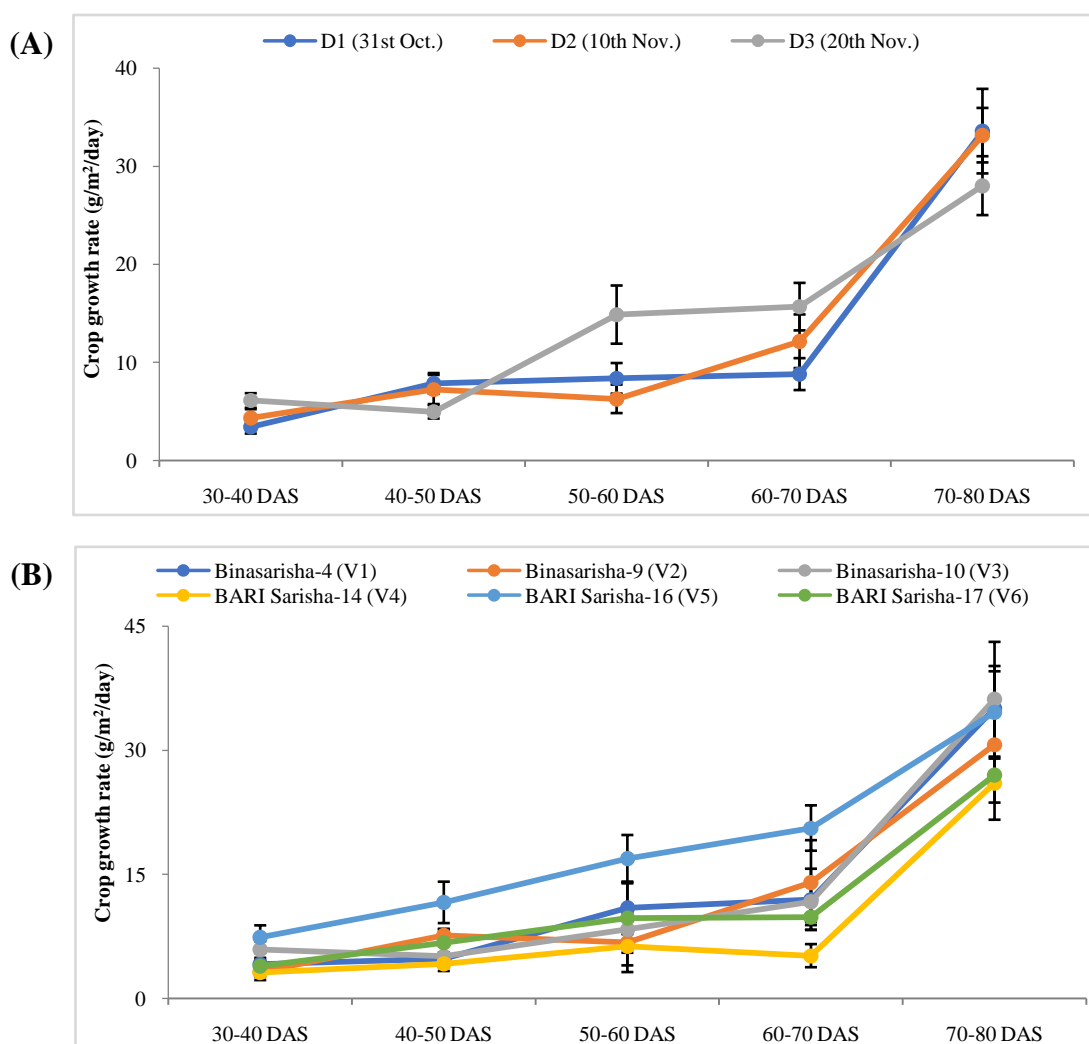


Figure 5 Crop growth rate under three sowing dates of six mustard varieties (A) Individual lines show the mean CGR of the three planting time at different sowing intervals (DAS) up to harvest (B) Indicates the average CGR of six mustard cultivars at different durations (DAS) until harvest (Each data point represents the mean of 5 plant samples; Error bars are the standard error values)

Table 4 Crop growth rate (g/m²/day) with the interaction effect of sowing time and varieties

Treatment combinations	30-40 DAS	40-50 DAS	50-60 DAS	60-70 DAS	70-80 DAS
D ₁ × V ₁	2.54 ^{bcd}	3.20 ^d	7.43 ^{ab}	6.31 ^{bcd}	21.04 ^d
D ₁ × V ₂	0.48 ^d	10.34 ^b	3.16 ^{ab}	3.63 ^d	24.81 ^{cd}
D ₁ × V ₃	7.23 ^{ab}	6.82 ^{bcd}	12.31 ^{ab}	14.91 ^{a-d}	55.60 ^a
D ₁ × V ₄	3.09 ^{bcd}	5.60 ^{bcd}	3.69 ^{ab}	5.42 ^{cd}	36.35 ^{a-d}
D ₁ × V ₅	4.26 ^{bcd}	11.18 ^b	16.56 ^{ab}	16.16 ^{a-d}	33.59 ^{bcd}
D ₁ × V ₆	2.94 ^{bcd}	10.04 ^{bc}	7.09 ^{ab}	6.39 ^{bcd}	30.11 ^{bcd}
D ₂ × V ₁	5.76 ^{abc}	4.08 ^{cd}	8.62 ^{ab}	11.76 ^{a-d}	46.87 ^{ab}
D ₂ × V ₂	5.02 ^{bcd}	6.65 ^{bcd}	3.86 ^{ab}	21.85 ^{ab}	35.72 ^{a-d}
D ₂ × V ₃	3.29 ^{bcd}	3.24 ^d	4.63 ^{ab}	6.36 ^{b-d}	23.43 ^{cd}
D ₂ × V ₄	1.53 ^{cd}	4.04 ^{cd}	1.31 ^b	3.05 ^d	21.77 ^{cd}
D ₂ × V ₅	7.32 ^{ab}	18.03 ^a	15.68 ^{ab}	20.64 ^{abc}	42.98 ^{abc}
D ₂ × V ₆	3.10 ^{bcd}	7.36 ^{bcd}	3.59 ^{ab}	9.22 ^{bcd}	28.25 ^{bcd}
D ₃ × V ₁	4.13 ^{bcd}	7.08 ^{bcd}	16.80 ^{ab}	17.86 ^{a-d}	37.22 ^{a-d}
D ₃ × V ₂	4.16 ^{bcd}	5.91 ^{bcd}	13.27 ^{ab}	16.52 ^{a-d}	31.57 ^{bcd}
D ₃ × V ₃	7.24 ^{ab}	5.32 ^{bcd}	8.20 ^{ab}	13.76 ^{a-d}	29.47 ^{bcd}
D ₃ × V ₄	4.84 ^{bcd}	2.94 ^d	14.00 ^{ab}	7.06 ^{bcd}	20.04 ^d
D ₃ × V ₅	10.61 ^a	5.61 ^{bcd}	18.46 ^a	24.98 ^a	27.18 ^{bcd}
D ₃ × V ₆	5.66 ^{bc}	2.82 ^d	18.06 ^a	13.87 ^{a-d}	22.65 ^{cd}
LSD _{0.05}	4.94	6.14	15.66	15.60	21.84
SEm	2.43	3.02	7.70	7.67	10.74
CV	64.43%	55.46%	95.88%	77.01%	41.65%

Figures in a column with a different letter (s) differ significantly at a 5% probability level according to LSD; n=5, P < 0.05; by analysis of variance with factorial randomized complete block design; SEm - Standard error mean; CV - Coefficient of variation

cultural operations were done, so all the varieties attained closer CGR values. The combined effect implies that certain varieties acquire better CGR when planted earlier than late sowing. Thus Binasarisha-10 (V₃), when plated early, may give better CGR, but BARI Sarisha-14 (V₄), if late planted, may give inferior CGR. CGR was; therefore, variety and time sowing depended. Chowhan and Islam (2022c) reported a similar trend of CGR progress in seven Bangladeshi lentil cultivars.

3.5 Biological yield

Peak and significantly higher biological yield were seen with D₂ and D₃ planting, but D₁ showed significantly least yield; contrary, BARI Sarisha-16 (V₅) showed a significantly top biological yield accompanied by Binasarisha-4 (V₁) and Binasarisha-9 (V₂). The statistically lowest yield was observed in BARI Sarisha-14 (V₄) (Figure 6A). Treatment amalgamations noted that Binasarisha-10 (V₃) and BARI Sarisha-14 (V₄) produced significantly least biological yield in D₁ planting, while BARI Sarisha-16 (V₅)

showed the best yield in all plantings (D₁, D₂ and D₃). Additionally, Binasarisha-4 (V₁) and Binasarisha-9 (V₂) delivered better yields in D₂ planting over the treatment combinations (Figure 6B). Current results do not align with the findings of Bala et al. (2011), who investigated the biological yield of Mustard under seven planting times and reported a decline of yield over time (late sowing). This may be due to the shift of weather over time and some areas' late start of winter.

3.6 Harvest index

Late planting (D₃) induced a significantly maximum harvest index (HI) over D₁ and D₂ planting. Whereas, BARI Sarisha-17 (V₆) together with BARI Sarisha-14 (V₄) rendered statistically peak HI; conversely, the lowest was produced by BARI Sarisha-16 (V₅) accompanied by Binasarisha-10 (V₃) (Figure 6A). Interaction effects denoted the highest HI of treatment combination was in D₂ × V₄ followed by D₂ × V₄, and the least was acquired by D₃ × V₅ (Figure 6B).

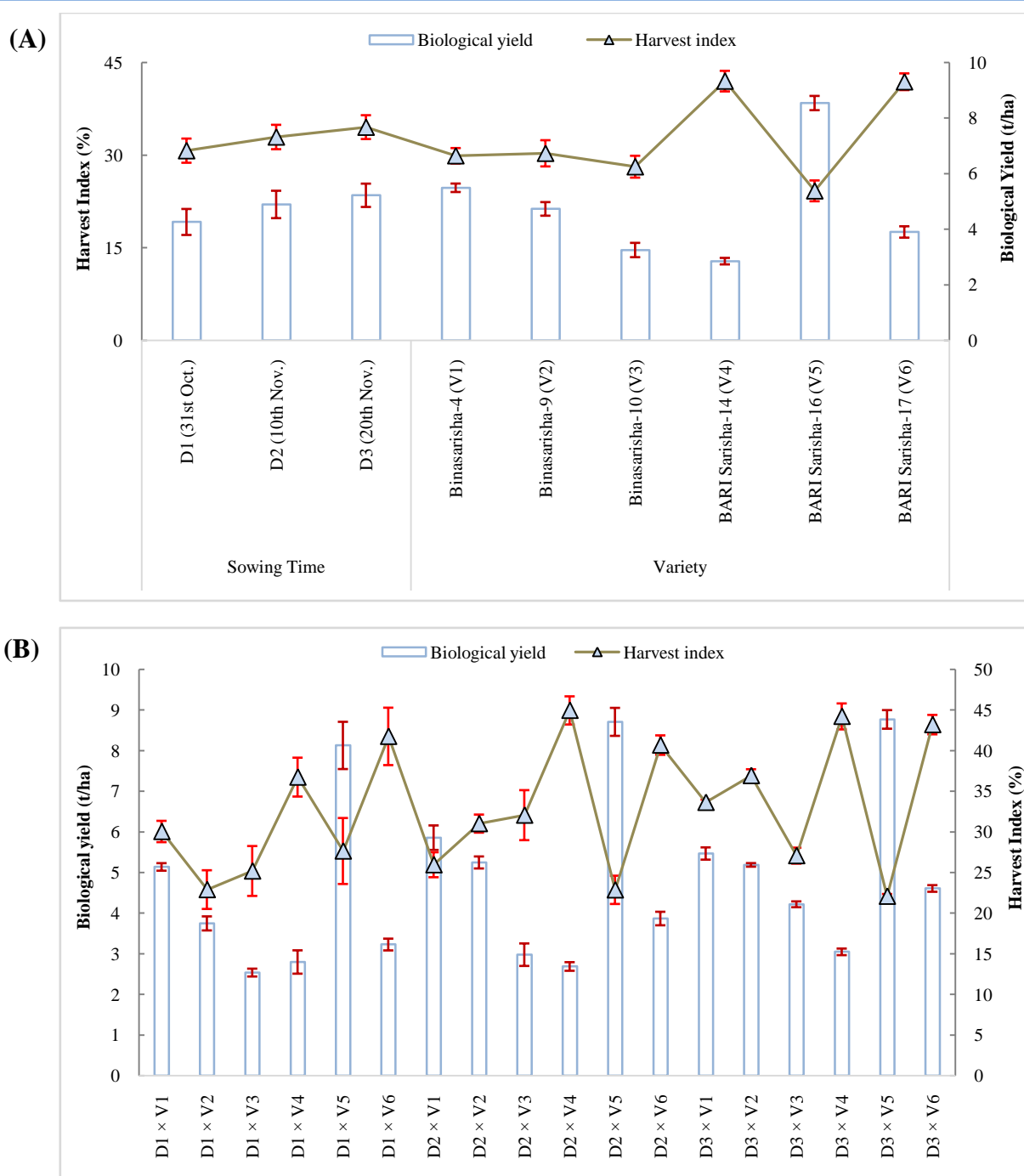


Figure 6 Biological yield (BY) and harvest index (HI) of six mustard varieties at three planting dates after harvest (A) Exhibits the individual influence of sowing times and varieties on HI and BY, (B) Presents the combined effect of sowing times and varieties on HI and BY (Here BY and HI were calculated using whole plot, i.e., 3m² harvesting; Error bars are the standard error values)

Kumar et al. (2018) studied the yield attributes of six Indian mustard genotypes (*Brassica juncea* L.) at three sowing times on 23 September, 16 October, 21 November and concluded that later planting (21 November) gives the least harvest index (%). These results are in agreement with the findings of the present.

3.7 Relationship between growth and yield at different sowing times

Results figured that plant height was significantly and positively correlated with days to maturity, which means plant height would

Table 5 Relationship between growth and yield parameters of mustard varieties

Attribute(s)	Plant height	Primary branch	Secondary branch	Total dry matter	Biological yield (t/ha)	HI (%)	Days to maturity
Plant height	1	0.87 ^{NS}	0.98 ^{NS}	0.85 ^{NS}	0.93 ^{NS}	0.96 ^{NS}	0.99*
Primary Branch		1	0.95 ^{NS}	0.99*	0.99*	0.97 ^{NS}	0.83 ^{NS}
Secondary Branch			1	0.93 ^{NS}	0.98 ^{NS}	0.99*	0.97 ^{NS}
Total dry matter				1	0.98 ^{NS}	0.96 ^{NS}	0.81 ^{NS}
Biological yield (t/ha)					1	0.99*	0.90 ^{NS}
HI (%)						1	0.94 ^{NS}
Days to maturity							1

* indicates 5% level of significance; NS - not significant.

increase with the increase in days to maturity of mustard varieties. Mostofa et al. (2016) established similar results. It was also reported by Aytac and Kınacı (2009). But it had a positive, nonsignificant correlation with primary branches, secondary branches, biological yield, total dry matter, and harvest index. Primary branches showed a significant and positive relationship with total dry matter and biological yield but a nonsignificant and positive relationship with secondary branches, harvest index and days to maturity. Secondary branches had a significant and positive relationship with harvest index but a nonsignificant and positive relationship with total dry matter, biological yield and days to maturity. Total dry matter showed a nonsignificant and positive relationship with biological yield, harvest index and days to maturity. Similar outcomes were also observed by Sharif et al. (2017). The biological yield had a significant and positive relationship with the harvest index but a nonsignificant and positive relationship with days to maturity. Alike findings were also obtained by Mostofa et al. (2016). The harvest index showed a nonsignificant but positive relationship with days to maturity (Table 5).

Conclusion

Mid of October is considered the best sowing time for Mustard, but this timing is shifting behind due to seasonal and weather changes. Our results show that most growth parameters were peak under 31st October planting, but varieties showed a different trend. BARI Sarisha-16 seemed to have a wide range of adaptation over the planting times, thus attaining top biological yield with all sowing times and retaining maximum TDM and AGR at harvest. However, the yield of popular cultivars like Binasarisha-9, Binasarisha-10 and BARI Sarisha-14 increased in the late sowing condition. Findings revealed that even if sowing is delayed about three weeks from the optimum time, the yield might not reduce, and it was positively significantly correlated to the harvest index. So, farmers can sow mustard seeds up to 20 November without sacrificing any significant biological yield from Magura's perspective.

Acknowledgements

We would like to express our heartfelt gratitude to Md. Abu Sayed, Farm Manager, Mrinal Kumar Shil, Junior Experimental Officer, ASM Mushfiqur Rahman, SA-1, Outsourcing staffs- Akash, Shohan, Jahangir, Shahin, and labours of BINA sub-station, Magura for their solid cooperation during the research period. We also want to thank the same station's Scientific Officers, Mst. Rokeya Sultana, Md. FoyzalAhmed, Shampa Rani Ghosh, and Fam Superintendent Hossain Md. Ferdous, for their assistance in collecting field data. Finally, we would like to sincerely thank the Bangladesh Institute of Nuclear Agriculture for its logistical support in executing this time-driven research study.

References

- Ahmed, S., Jahiruddin, M., Razia, S., Begum, R.A., et al. (2018). *Fertilizer recommendation guide-2018*. Bangladesh Agricultural Research Council (BARC), Farmgate, Dhaka 1215, pp. 1-223. ISBN: 984-500-029-1.
- Alam, M.M., Begum, F., & Roy, P. (2014). Yield and yield attributes of rapeseed mustard (*Brassica*) genotypes grown under late sown condition. *Bangladesh Journal of Agricultural Research*, 39 (2), 311-336. doi.org/10.3329/bjar.v39i2.20434
- Aytac, Z., & Kınacı, G. (2009). Genetic variability and association studies of some quantitative characters in winter rapeseed (*Brassica napus* L). *African Journal of Biotechnology*, 8(15), 3547-3554.
- Azad, A.K., Miaruddin, M., Ohab, M.A., Sheikh, H.R., Nag, B.L., & Rahman, H.H. (2020). *Krishi projuktihatboi (Handbook on Agro-Technology)*, 9th edition Bangladesh Agricultural Research Institute, Gazipur-1701, Bangladesh, pp.93-102. Retrieved from https://drive.google.com/file/d/1h81CIRy3vHF_iuAwY3kyPcl6T2x-tlvY/view?usp=sharing

- Bala, P., Azad, A.K., & Hossain, M.F. (2011). Yield response of Mustard to sowing date. *Libyan Agriculture Research Center Journal International*, 2 (3), 112-117.
- BINA (2014). *Leaflet of Binasarisha-9 and Binasarisha-10* (In Bengali). Retrieved from http://bina.portal.gov.bd/sites/default/files/files/bina.portal.gov.bd/page/e598357f_0ebb_46a4_ad26_3b0bbfc4f815/Binasarisha-9%20%26%2010.pdf
- BINA (2022). Bangladesh institute of nuclear agriculture. Released varieties (Mustard). Retrieved from [http://www.bina.gov.bd/site/page/92a41b28-908c-43a9-8fdc-8950d686806a/\[front](http://www.bina.gov.bd/site/page/92a41b28-908c-43a9-8fdc-8950d686806a/[front)
- Chowhan, S., & Islam, M. (2022a). Boron regulates growth and morpho physical properties of mustard in no-till farming. *International Journal of Agricultural and Applied Sciences*, 3(1), 47-53. doi.org/10.52804/ijaas2022.318
- Chowhan, S., & Islam, M. (2022b). Alterations in the yield features of mustard varieties under various planting dates. *International Conference on System of Crop Intensification (ICSCI 2022) for Climate Smart Livelihood and Nutritional Security*. 12-14 December 2022, Society for the Advancement of Rice Research, ICAR-Indian Institute of Rice Research, Hyderabad, Telangana, India. pp. 442-444.
- Chowhan, S., & Islam, M. (2022c). Varietal roles on morpho-physiological and yield attributes of lentil (*Lens culinaris* Medik). *Legume Research [Online first]*, doi.org/10.18805/LR-4913.
- Chowhan, S., & Nahar, K. (2022). Evaluating the role of fertilizer and seed soaking on direct seeded aus rice varieties. *Acta Scientific Agriculture*, 6(2), 02-17. doi.org/10.31080/ASAG.2022.06.1093
- Chowhan, S., Gupta, R., Islam, M.M., & Begum, S.N. (2018). Evaluation of NERICA rice mutant in Jhum cultivation. *International Journal of Agronomy and Agricultural Research*, 12(2), 24-31.
- Chowhan, S., Haider, M. R., Hasan, A. F. M. F., Hoque, M. I., Kamruzzaman, M., & Gupta, R. (2017). Comparative on farm performance of five modern rice varieties with two local cultivars. *Journal of Bioscience and Agriculture Research*, 13(1), 1074-1086. doi.org/10.18801/jbar.130117.131
- Chowhan, S., Islam, M., Rana, M. S., Sultana, M. R., et al. (2023). Optimum and late sowing of mustard varieties show similar seed yield. *Plant Science Today*, 10(2), 382-392. doi.org/10.14719/pst.2246
- FRG (2012). *Fertilization Recommendation Guide*. Bangladesh Agricultural Research Council (BARC), Farmgate, Dhaka 1215, pp. 01-258. ISBN: 978-984-500-000-0.
- Ghosh, R.K., & Chatterjee, B.N. (1988). Effect of dates of sowing on oil content and fatty acid profiles of Indian Mustard. *Indian Journal of Oil Seed Research*, 5, 144-149.
- Hasanuzzaman, M., Nahar, K., Alam, M. M., Roychowdhury, R., & Fujita, M. (2013). Physiological, biochemical, and molecular mechanisms of heat stress tolerance in plants. *International Journal of Molecular Sciences*, 14, 9643-9684. doi.org/10.3390/ijms14059643
- Hunt, R., Causton, D.R., Shipley, B., & Askew, A. (2002). A modern tool for classical plant growth analysis. *Annals of Botany*, 90(4), 485-488. doi.org/10.1093/aob/mcf214.
- Kumar, A., Lal, M., Mohan, N., Kumar, M., & Kumar, N. (2018). Effect of different sowing dates on yield and yield attributes of Indian mustard (*Brassica juncea* L.) genotypes. *International Journal of Pure and Applied Bioscience*, 6(2), 848-853. doi.org/10.18782/2320-7051.6264
- Maurya, S. K., Kalhapure, A., Singh, N., Kumar, A., Yadav, P., Kumar, M., et al. (2022). Growth and yield response of different Indian Mustard [*Brassica juncea* (L.)] varieties to irrigation scheduling. *Biological Forum- An International Journal*, 14(3), 434-439.
- Mondal, M. M. A., Malek, M. A., & Bhuiyan, M. S. H. (2018). The role of morpho-physiological attributes on the seed yield of *Brassica juncea*. *Acta Scientific Agriculture*, 2(5), 22-26.
- Mondal, M.M.A., Puteh, A.B., Malek, M.A., Roy, S., & Yusop, M.R. (2013). Contribution of morpho-physiological traits on yield of lentil (*Lens culinaris* Medik). *Australian Journal of Crop Science*, 7(8), 1167-1172.
- Mostofa, U. H. M., Nazrul, I. M., Kadir, M., & Miah, N. H. (2016). Performance of rapeseed and Mustard (*Brassica* sp.) varieties/lines in north-east region (sylhet) of Bangladesh. *Advances in Plants and Agriculture Research*, 5(1), 457-462. doi.org/10.15406/apar.2016.05.00168
- Porter, J. R. (2005). Rising temperatures are likely to reduce crop yields. *Nature*, 436, 174. doi.org/10.1038/436174b
- Russell, D.F. (1986). MSTAT-C computer package programme. Crop and Soil Science Department, Michigan State University, US.
- Sarkar, S.C., Akter, M., Islam, M. R., & Haque, M.M. (2016). Performance of five selected hybrid rice varieties in aman season. *Journal of Plant Sciences*, 4(2), 72-79. doi.org/10.11648/j.jps.20160404.13.
- Sharif, M., Haque, M., Howlader, M., & Hossain, M. (2017). Effect of sowing time on growth and yield attributes of three

- mustard cultivars grown in Tidal Floodplain of Bangladesh. *Journal of the Bangladesh Agricultural University*, 14(2), 155–160.
- Singh, A.K., & Yeshpal, R.P. (2011). Performance of mustard hybrids under different sowing dates and spacings. *Pantnagar Journal of Research*, 9(1), 16-19.
- Statistix (2022). Data analysis software for researchers (Version 10.0). Analytical Software, 2105 Miller Landing Rd, Tallahassee Florida 32312, USA.
- Tandale, M. D., & Ubale, S. S. (2007). Evaluation of effect of growth parameters, leaf area index, leaf area duration, crop growth rate on seed yield of soybean during Kharif season. *International Journal of Agricultural Sciences*, 3(1), 119-123.
- Uddin, M.A., Sultana, F., Ullah, M.A., Rahman, K.M., & Mashra, M.M. (2012). Evaluation of some rapeseed mutants based on growth attributes. *Journal of Agroforestry and Environment*, 6(1), 117-120.
- Wahhab, M. A., Mondal, M. R. I, Akbar, M. A., Alam, M. S., Ahmed, M. U., & Begum, F. (2002). Status of oil crop production in Bangladesh. Oil seed Research Centre Bangladesh Agricultural Research Institute, Joydebpur, Gazipur pp. 4-62.




Journal of Experimental Biology and Agricultural Sciences

<http://www.jebas.org>

ISSN No. 2320 – 8694

Determination of carbendazim residues in Moroccan tomato samples using local enzyme-linked immunosorbent assay and comparison with liquid chromatography

Najwa Bellemjid^{1,2}, Ahmed Moussaif¹, Mohammed El Mzibri¹ ,
Abdelhalim Mesfioui², Abdelghani Iddar^{1*} 

¹Biotechnology and Engineering of Biomolecules Unit, National Centre for Nuclear Energy, Science and Technology (CNESTEN-Morocco), Rabat, Morocco
²Biology and Health Laboratory, Faculty of Sciences, Ibn Tofail University, Kenitra, Morocco

Received – November 17, 2022; Revision – March 14, 2023; Accepted – April 27, 2023
Available Online – April 30, 2023

DOI: [http://dx.doi.org/10.18006/2023.11\(2\).339.350](http://dx.doi.org/10.18006/2023.11(2).339.350)

KEYWORDS

Carbendazim
Moroccan tomato
HPLC-UV
ELISA
Extraction

ABSTRACT

The fungicide carbendazim (CBZ) is not approved for agricultural uses in some countries but is still used by many farmers due to its effectiveness. For this reason, in previous work of the same authors, they developed a competitive enzyme immunoassay (ELISA) using rabbit polyclonal antibodies to detect CBZ. This study aimed to validate this in-house ELISA after extraction with methanol for CBZ analysis in tomato samples, and the results were compared with the conventional high-performance liquid chromatography (HPLC) method after QuEChERS extraction. The results showed that both ELISA and HPLC methods have good repeatability, reproducibility and high precision with a good variation verified by principal components analysis (PCA). ANOVA tested the detection limit (LOD), and quantification limit (LOQ), and the values for ELISA (LOD = 0.026 ± 0.001 $\mu\text{g/L}$ and LOQ = 0.083 ± 0.003 $\mu\text{g/L}$) were significantly lower than those obtained by HPLC (LOD = 0.61 ± 0.02 $\mu\text{g/L}$ and LOQ = 1.85 ± 0.07 $\mu\text{g/L}$). ELISA and HPLC were used for analyzing CBZ in 100 Moroccan tomato samples. These two methods detected the presence of CBZ above the Maximum Residue Limit (MRL) level in 9 samples. However, the presence of the CBZ was detected in the 79 samples by ELISA and quantified in 66 samples. In contrast, the presence of CBZ was detected in 57 and quantified in 35 samples by HPLC. These results showed that the ELISA system coupled with a simple methanol extraction is much more sensitive than HPLC after QuEChERS extraction.

* Corresponding author

E-mail: abdeliddar@gmail.com (Abdelghani Iddar)

Peer review under responsibility of Journal of Experimental Biology and Agricultural Sciences.

Production and Hosting by Horizon Publisher India [HPI]
(<http://www.horizonpublisherindia.in/>).
All rights reserved.

All the articles published by [Journal of Experimental Biology and Agricultural Sciences](#) are licensed under a [Creative Commons Attribution-NonCommercial 4.0 International License](#) Based on a work at www.jebas.org.



1 Introduction

Pesticides play an important role in the development of agriculture by reducing agricultural product losses, improving productivity, controlling vector diseases and contributing to the diversification of food (Patibanda and Ranganathswamy 2018). In 2019, global pesticides used in agriculture crop protection was around 4.2 million tons of active ingredients, and worldwide pesticide application was 2.7 kg/ha per cropland area (FAO 2021). Morocco is an agricultural economy country and produces various crops every year, requiring large quantities of pesticides. Due to the absence of a national phytopharmaceutical industry, Morocco imported around 22,000 tonnes of pesticides in 2019 (Bouterfas et al. 2022).

Some pesticides are potentially hazardous and can cause harm to animal and human health and the ecosystem when they persist in the environment (Sharma et al. 2019; Sarkar et al. 2021). Different concentrations of pesticides have been found in various food samples (Moussaif et al. 2021), and it has been shown that the dietary intake containing pesticides represents the primary source of exposure in humans leading to neurological and developmental disorders (Sakali et al. 2021). Several works have shown possible links between pesticide consumption and various health effects such as cardiovascular disease, reproductive disorders, Parkinson's disease, etc. (Nicolopoulou-Stamati et al. 2016). In addition, these chemicals are suspected to have neurotoxic, cytotoxic, genetic mutation, chromosomal and DNA damage effects (Barron Cuenca et al. 2022).

According to the Food and Agriculture Organisation statistics (FAOSTAT), fungicides are the second most used pesticides, with 31% of world consumption after insecticides (FAOSTAT 2022). Fungicides protect crops against harmful fungi that cause several plant diseases. They also protect agricultural products during storage (Magunga and Malebo 2023). Methyl 2-benzimidazole carbamate or carbendazim (CBZ) is a benzimidazole fungicide that has been widely used to treat soils and protect many crops such as cereals, fruits and vegetables against fungal pathogens (Wang et al. 2023). However, CBZ is known to be hazardous for humans, animals and the environment (Kasaeinasab et al. 2023). It has been banned in Australia, USA, and most European Union countries (Elshafey et al. 2022). In Morocco, CBZ was registered and approved by ONSSA (National Office of Food Safety) for eight crops, including onion, tomato, apricot, peach, pear, apple, vine and rose before 2017. The fungicide has been banned by ONSSA since 2017, but farmers are still using formulations containing carbendazim, accounting for approximately 40% of all pesticide formulations used in agriculture in 2021 (Ben Khadda et al. 2021).

Solanum lycopersicum L. (tomato) is a trendy vegetable crop, and it is widely consumed worldwide. Along with many beneficial

nutrients, tomatoes are also known to reduce the effects of chronic diseases, cancer, cardiovascular diseases, osteoporosis etc. (Kumar et al. 2020). In Morocco, tomatoes are economically important crops and rank second in the position of exported crops after citrus. In 2018, Morocco became the world's 15th tomato producer, producing more than 1,409.44 million fresh tomatoes and a yield of 8.83 kilos per metre of cultivated land (FAOSTAT 2022). Improving this productivity has often been associated with the action of pesticides (Benaboud et al. 2021). It should be noted that CBZ is applied by spraying in the field or by dipping produce after harvest. It is used in high doses and often repeated as per the target disease (Wang et al. 2012). Recently, its residues have been detected in various Moroccan tomato samples (Choubbane et al. 2022).

Many analytical techniques, such as high-performance liquid chromatography (HPLC), liquid chromatography-mass spectrometry (LC-MS), gas chromatography (GC), etc., are used for the analysis of carbendazim residue (Lesueur et al. 2008; Phansawan et al. 2015). However, conventional methods are slow, expensive and require several solvents, especially when analyzing many samples (Aylaz et al. 2021). Therefore, other techniques like immunoassays could be exciting alternatives to chromatography. These techniques often detect single analytes with high specificity (Liu et al. 2007). Enzyme-linked immunosorbent assay (ELISA) has been used to analyze several pesticides (Maftouh et al. 2020). In a previous work by Bellemjid et al. (2018), indirect competitive ELISA was developed for CBZ detection.

This study aimed to validate the in-house ELISA system for CBZ analysis in tomatoes after a simple extraction procedure and to apply this system to detect the fungicide in 100 tomato samples purchased from local Moroccan markets. The results were compared with the well-established HPLC method after QuEChERS extraction.

2 Material and methods

2.1 Sampling methodology and preparation

One hundred tomato samples with an average weight of 80 to 100g were collected from the market in the province of Rabat, Morocco, from January to June 2022. An organic tomato sample from the bio-market was used for extraction optimization and control. A representative portion of each tomato sample was blended, and aliquots of 10 g were stored at -20 °C.

2.2 Extraction of CBZ

Figure 1 illustrates the schematic flowchart of extractions methods used for HPLC and ELISA analysis. For HPLC analysis, the extraction of CBZ from blended tomato samples was made according to the QuEChERS method (Quick, Easy, Cheap, Effective, Rugged and Safe method) (Kim et al. 2019). A

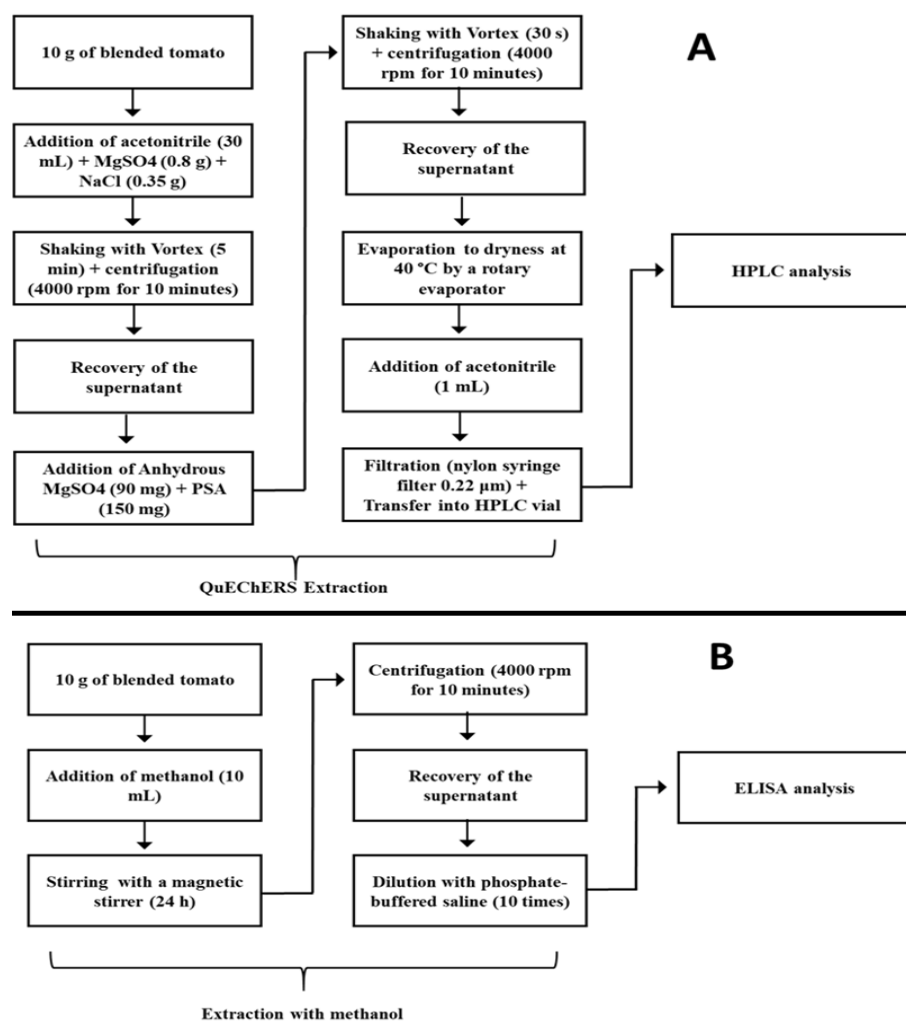


Figure 1 Schematic presentation of CBZ extractions methods in tomato samples. A: QuEChERS method used for HPLC analysis. B: methanol extraction used for ELISA analysis.

total of 10 g of blended tomato was mixed with 0.8 g of MgSO_4 and 0.35 g of NaCl in 30 mL of acetonitrile (ACN), and the mixture was shaken for 5 minutes. This was followed by centrifuging the mixture for 10 minutes at 4000 rpm at 4°C. Anhydrous MgSO_4 (90 mg) and PSA (150 mg) were added to the supernatant. After shaking for 30 seconds, the mixture was centrifuged at 4000 rpm for 5 minutes. A rotary evaporator evaporated the supernatant to dry at below 40 °C. After that, 1 mL of acetonitrile was added to the dry extract, and the mixture was vortexed and transferred to an HPLC vial after filtration with a 0.22 μm nylon syringe filter.

For ELISA analysis, tomato extracts were prepared by mixing 10 g of tomato samples with 10 ml of methanol and shaking for 24 hours. After centrifugation at 4000 rpm for 10 minutes, the supernatant was collected and diluted 10-fold with phosphate-buffered saline (PBS).

2.3 ELISA development and analysis

A rabbit polyclonal antibody ELISA test for the detection of CBZ was developed as described in previous work by the same authors (Bellemjid et al. 2018). Figure 2 illustrates the development phases of the ELISA test.

Briefly, 2 CBZ haptens with 4 or 5 carbon spacer arms were synthesized. A hapten with four carbon spacer arms has been conjugated to bovine serum albumin (BSA) and used for antibody production in rabbits. The 5-carbon Hapten is conjugated to human albumin (HAS) and coated in well plates. After that, the coating antigen, antibody dilution and standard concentration were optimized. For the indirect ELISA test, CBZ was 100 ng/well hapten HSA as coating, 1/2000 of antiserum anti-CBZ as a diluent and 0.01 to 1000 $\mu\text{g/L}$ CBZ as standard curve (Bellemjid et al. 2018).

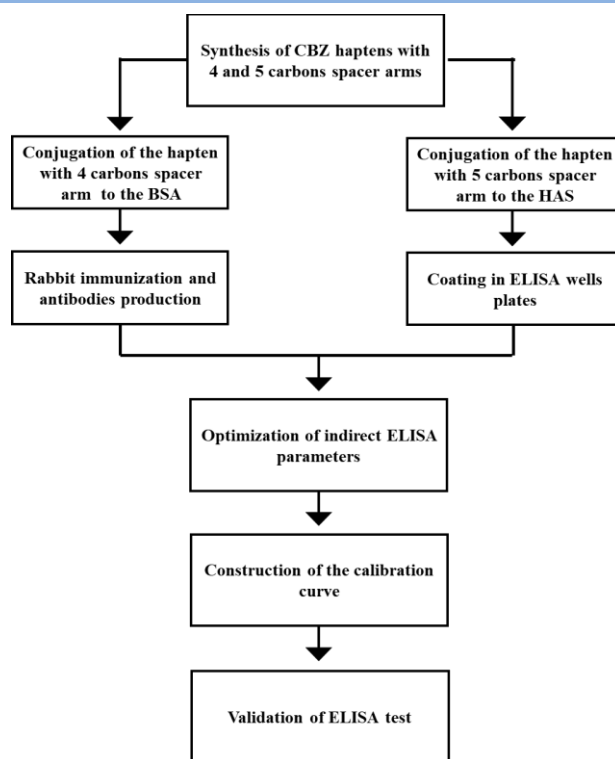


Figure 2 Schematic presentation of ELISA development.

For the immunoassay test, hapten-HSA was coated on microtiter plates using 50 mM carbonate-bicarbonate at pH 9.6 for 12 hours at 4°C. After washing with PBS, the wells were blocked with 300 µl of 3% skim milk in PBS for 12 hours at 4°C. Wells were washed twice with PBS, and 50 µl of CBZ standards in PBS containing 10% methanol were added to each well, followed by 50 µl of 1/2000 v/v antiserum in PBS. After incubation at 28°C for 2 hours, the plate was washed 5 times with PBS (PBST) containing 0.05% Tween 20, then 100 µl of peroxidase-conjugated anti-rabbit IgG was added to each well and incubated at 28°C for 1 hour. The plate was re-washed 5 times with PBST and 100 µl/well OPD (1mg/mL of O-phenylenediamine dihydro-chloride in citrate-acetate buffer pH 5.5 and containing 0.1% of H₂O₂). The reaction was stopped by adding 50 µl of 3 M HCl, and the absorbance was measured at 492 nm. The following formula allows the calculation of relative binding (Maftouh et al. 2020):

$$\% \frac{B}{B_0} = \frac{A - A_{XS}}{A_0 - A_{XS}} \times 100$$

A: the absorbance. A₀: the zero-dose absorbance of the CBZ. A_{XS}: the absorbance to an excess of the CBZ.

A standard curve that looks like a sigmoid was constructed by plotting the B/B₀ value (%) versus the logarithm of the analyte concentration (Raab 1983). SigmaPlot® 14.0 software (Systat Software, San Jose, CA, USA) was used to plot the ELISA

competition curve for CBZ. The IC₅₀ value (50% inhibition of antigen/antibody binding) was calculated using the following function (Rodbard 1981):

$$y = D + \frac{A - D}{1 + 10^{B(X - \log C)}}$$

A: the minimum percentage of B/B₀ (representing an infinite concentration of CBZ), D: %B/B₀ at the maximum (zero concentration of CBZ), Log C: the logarithm of the IC₅₀ corresponding to the inflexion point of the curve, B: the Hill's slope at C, X: the concentration of free CBZ

For CBZ analysis in samples, 50 µL/well of diluted methanol extract was used in the immunoassay system (as described above). The concentration values were obtained by fitting the sigmoidal curves. The fungicide concentrations were reported to mg/kg of fresh tomato, considering the extraction dilutions.

2.4 Cross-reactivity in ELISA analysis

The ELISA system was prepared with a standard curve of the studied compounds to evaluate the percentage of cross-reactivity (CR) with other pesticides structurally related to CBZ. The CR is the ratio of the CBZ IC₅₀ to the IC₅₀ of the tested compound and is expressed as a percentage CR. Benzimidazole (benomyl, Thiabendazole and fuberidazole) and carbamate (Carbaryl and carbofuran) pesticides were tested in the developed ELISA system.

2.5 HPLC analysis

The stock solution of the certified CBZ (Honeywell Fluka analytical standards Munich, Germany) was prepared at 1 mg/mL in acetonitrile and stocked in the dark at 4 °C until use. Standard solutions of CBZ (0.0001, 0.001, 0.025, 0.05, 0.1 and 1 mg/L) were prepared independently in acetonitrile from the stock solution. HPLC analysis was performed by Alliance Waters 2695 system. The column was a Sunfire C18 column (4.6 mm x 250 mm, 5 µm, 100Å). The mobile phase consisted of acetonitrile/acidified water containing 0.1% phosphoric acid (20/80, v/v), with a 1.0 mL/min flow rate and 10 µL injection volume. The detection wavelength was 285 nm, and analyses were performed at 25°C. The calibration curve has been plotted and corresponds to the peak area versus CBZ concentration. Its linearity was verified by the correlation coefficient (r^2).

2.6 Evaluation of recovery percentages

Recovery studies were evaluated by adding known concentrations of CBZ (0.05, 0.1, 0.2, 0.3, 0.4 and 0.5 mg/kg) to mixed organic tomatoes. The mixture was shaken at room temperature for one hour. Methanol extracts and QuEChERS extracts were analyzed using the developed immunoassay and HPLC, respectively. The accuracy of the method was determined by analyzing a blank (organic tomato) and a spiked blank. The percent recovery of CBZ was calculated using the following formula (Moussaif et al. 2021):

$$\% \text{ Recovery} = \frac{\text{Amount of pesticide after spiking}}{\text{Original pesticide content} + \text{Spiked amount}} \times 100$$

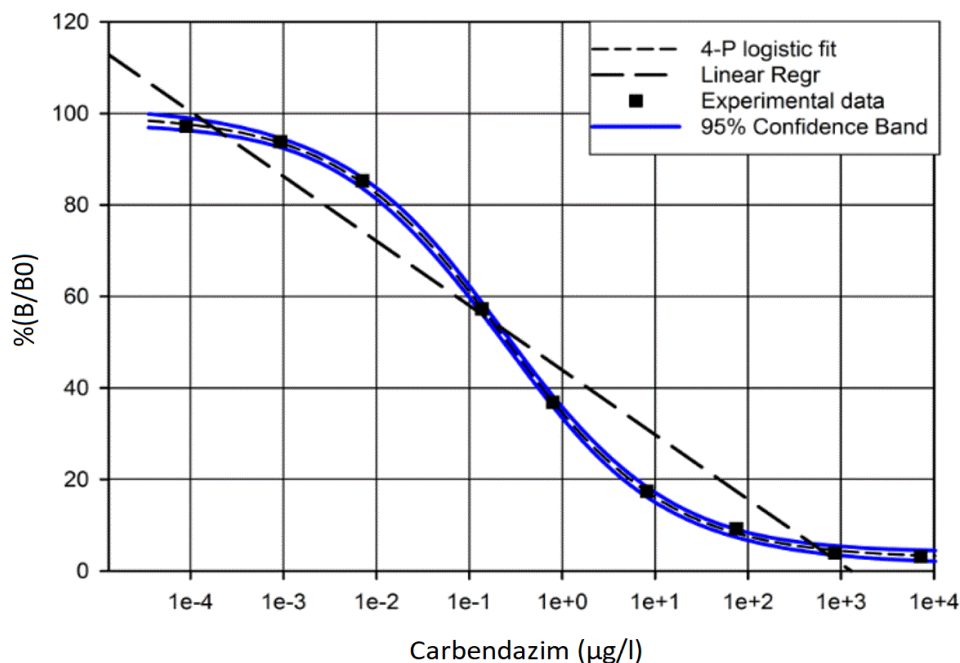


Figure 3 Indirect immunoassay standard carbendazim (CBZ) curves using 100 ng of CBZ-HAS for coating and anti-CBZ at 1/2000. Serial dilutions of the CBZ (0.01 to 1000 µg/L) were used as standards

2.7 Statistical data analysis

Limits of detection (LOD), limits of quantitation (LOQ), precision and repeatability parameters were determined according to Boscolo et al. (2013) LOD is the lowest concentration that gives a response equal to 3 times the baseline noise, and it was determined from the analysis of the 0 standards. The LOQ is the lowest fungicide concentration that gives a response 10 times the baseline noise. The precision of the analytical method was assessed by repeating and reporting the relative standard deviation (RSD%). Data were analyzed using IBM SPSS statistics software, version 27.0. The validation parameters of ELISA and HPLC methods are subjected to principal components analysis (PCA) to evaluate the variation. Values were expressed as mean ± standard deviation (SD) of 5 independent assays. The comparison was carried out by the analysis of variance (ANOVA), and significant mean differences were separated using the Tukey test at the 5% probability level.

3 Results

3.1 Optimisation Indirect ELISA for CBZ analysis and performances

The indirect ELISA was developed using 100 ng/well of antigen coating and 1/2000 antibodies dilution. These antibodies were used for competition between the free CBZ and the corresponding coated CBZ-hapten conjugate. A typical standard curve of CBZ immunoassay is shown in Figure 3. The IC_{50} was recorded at $0.63 \pm 0.024 \mu\text{g/L}$ during this study.

The characteristics of the designed ELISA system are regrouped in Table 1. The results showed good repeatability (RSD = 4.35 %) and reproducibility (RSD = 1.22 %). LOD and LOQ values were recorded $0.026 \pm 0.001 \mu\text{g/L}$ and $0.083 \pm 0.003 \mu\text{g/L}$ respectively. Higher accuracy was obtained with a percentage recovery from 88.1 ± 4.3 to 96.9 ± 1.9 % (Table 1). It should be noted that the

resistance of the ELISA to methanol used to dissolve CBZ was tested, and the results showed that the inhibition of reactivity by more than 10% methanol in PBS increases with increasing solvent concentration (for example, when methanol concentrations were 15 and 20%, the IC_{50} values increased by 1.5 and 1.9 fold respectively).

Table 1 Validation of CBZ analysis using ELISA and HPLC-UV

Validation parameters	ELISA	HPLC
Correlation coefficient (r^2)	-	0.998
Detection limit (LOD) ($\mu\text{g/L}$)	0.026 ± 0.001^a	0.61 ± 0.02^b
Quantification limit (LOQ) ($\mu\text{g/L}$)	0.083 ± 0.003^c	1.85 ± 0.07^d
Repeatability (RSD%)	4.35	3.18
Reproducibility (RSD%)	1.22	0.19
Accuracy at 0.05 mg/kg (% recovery)	95.6 ± 2.5	96.2 ± 2.2
Accuracy at 0.1 mg/kg (% recovery)	96.9 ± 1.9	91.3 ± 3.6
Accuracy at 0.2 mg/kg (% recovery)	88.1 ± 4.3	97.4 ± 1.2
Accuracy at 0.3 mg/kg (% recovery)	89.5 ± 3.2	98.1 ± 1.3
Accuracy at 0.4 mg/kg (% recovery)	91.7 ± 4.5	85.7 ± 4.2
Accuracy at 0.5 mg/kg (% recovery)	95.2 ± 2.8	89.1 ± 4.6

Given values are the average of five replicates; values followed by \pm are SD (Standard Deviation); Different superscript letters indicate significant differences in LOD and LOQ between ELISA and HPLC

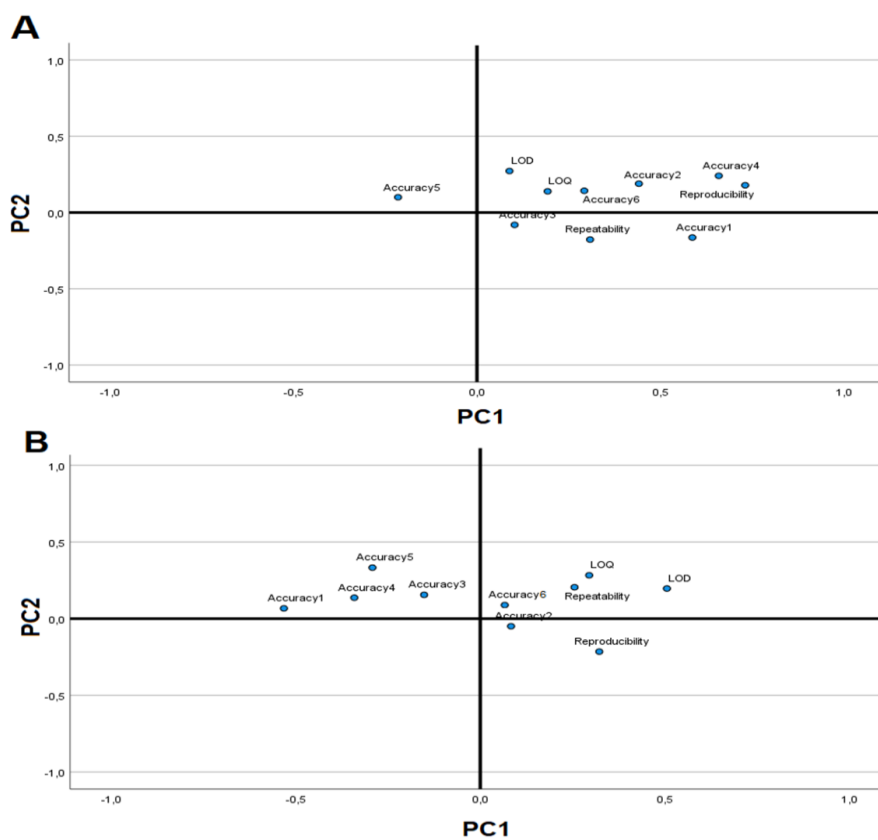


Figure 4 Principal component analysis (PCA) for validation parameters of ELISA (A) and HPLC (B) analytical methods

Principal component analysis (PCA) was used to understand the variability of the validation parameters in five different assays. The validation parameters (LOD, LOQ, repeatability, reproducibility, accuracy 1 at 0.05 mg/kg, accuracy 2 at 0.1 mg/kg, accuracy 3 at 0.2 mg/kg, accuracy 4 at 0.3 mg/kg, and accuracy 5 at 0.4 mg/kg and accuracy 5 at 0.5 mg/kg) collection points were the variables, and number of tests (5 tests) were the matrix lines. The two principal components explained 99.63 % and 98.84 % of variability for all variables in the data for ELISA and HPLC, respectively. The data set was visualized in the component shown in Figure 4.

The percentage CR of different compounds in the developed ELISA system was compared to CBZ and are reported in Table 2. Except for benomyl, the interference between CBZ and all tested compounds was negligible. The benomyl fungicide represented a high cross-reactivity, which CR percentage was around 83.1% (Table 2).

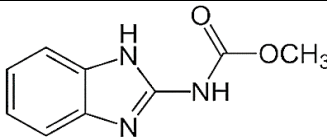
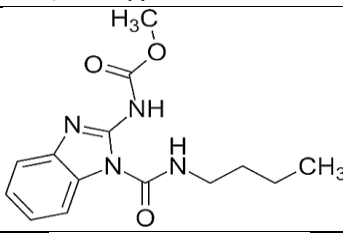
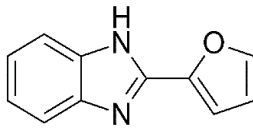
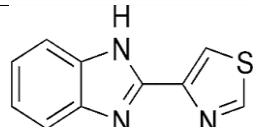
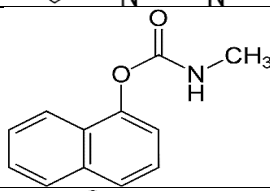
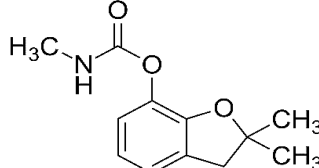
3.2 Validation of HPLC-UV method

Analytical data from the CBZ standards allowed statistical assessment of the accuracy and precision of the HPLC analysis. Validation parameters showed that the HPLC method could detect $0.61 \pm 0.02 \mu\text{g/L}$ CBZ with a limit of quantitation (LOQ) of $1.85 \pm 0.07 \mu\text{g/L}$ (Table 1). The correlation coefficient is 0.998, and the corresponding curve has good linearity and high accuracy (85.7 ± 4.2 to 98.1 ± 1.3 % recovery rate).

3.3 Correlation between ELISA and HPLC

Until the analysis of samples, analytical results for ELISA and HPLC using spiked organic tomatoes with CBZ (0.05, 0.1, 0.2, 0.3, 0.4 and 0.5 mg/kg) were compared. The enriched samples estimated by ELISA and HPLC were close to the theoretical values. A good correlation was found between the two techniques, with a correlation coefficient (r_2) of 0.994 (Figure 5).

Table 2 Cross-reactivity (CR) related to CBZ in the ELISA system

Compounds	Structure	%CR
CBZ		100
Benomyl		83.1
Fuberidazole		2.05
Thiabendazole		1.22
Carbaryl		0.63
Carbofuran		0.34

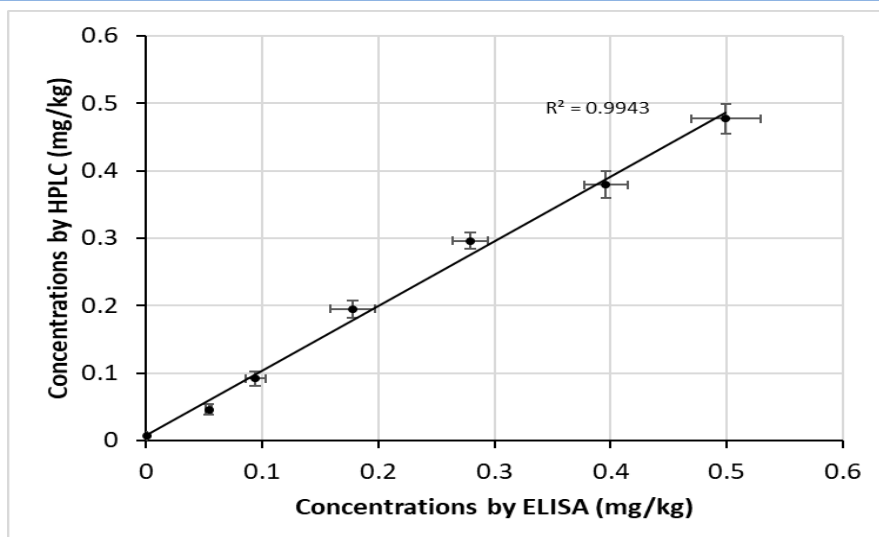


Figure 5 Comparisons of analytical results obtained for ELISA and HPLC using spiked organic tomato

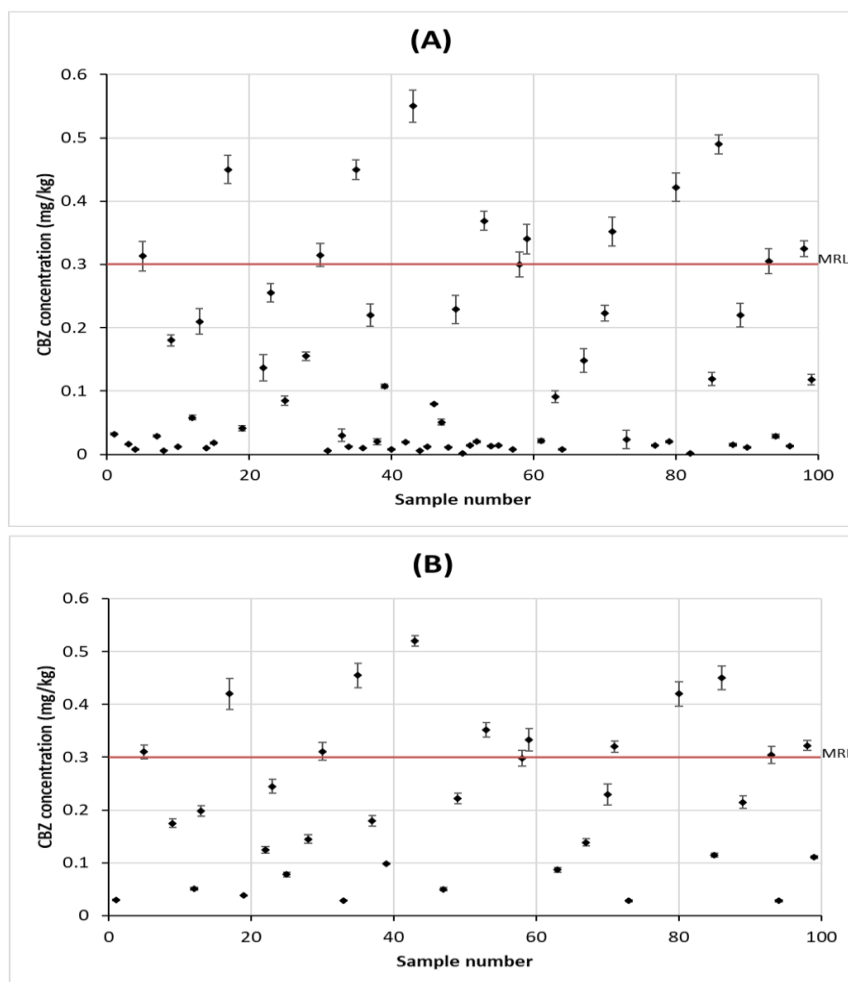


Figure 6 CBZ levels found in Moroccan tomato sample extracts (A) ELISA analysis, (B) HPLC analysis; Only quantified concentrations are represented. MRL (Maximum Residue Limit) are represented in the Figure, according to ONSSA 2014

Table 3 Parameters for the analyzed tomato samples

	ELISA	HPLC
Total samples	100	100
Total quantified	66	35
Total detected	79	57
Not detected	21	43
> MRL	9	9

3.4 CBZ analysis in tomato samples

The ELISA and HPLC systems were used to quantify the fungicide (CBZ) in 100 actual tomato samples. Figure 6 represents CBZ concentrations in samples that are statistically above the limit of quantification. The HPLC made quantifying about 34 among the 100 analyzed samples possible. These concentrations are approximately the same as found by the ELISA method (Figure 6). However, the developed ELISA quantified about 66 samples.

The results of both HPLC–UV and ELISA methods were compared, and the main parameters are included in Table 3. Based on three independent assays, both data sets show a statistical difference. In 100 analyzed samples, CBZ was detected in 57 by HPLC (> LOD), with 35 quantified samples (>LOQ) and 43 samples where CBZ was not detected. However, the developed ELISA detected the presence of CBZ in 79 samples, and it was quantified in 66 samples, and only 21 samples were without fungicide. Both methods detected the presence of CBZ above the maximum residue limit (MRL) in 9 samples (Figure 6 and Table 3). This determination of MRL was established by ONSSA (2014).

4 Discussion

Carbendazim (CBZ) has been used as a pre-and post-harvest treatment to control fungal diseases of various vegetables and fruits such as tomatoes (Liu et al. 2023). Because of its hazardous effects on humans, animals and the environment, the usage of CBZ in agricultural practices has been banned in Europe, Australia, USA and other countries, however, it is still used in some developing countries (Elshafey et al. 2022). For this reason, developing a rapid, sensitive assay to detect traces of CBZ in food is necessary. Immunoassays can meet these requirements, and several ELISA systems were used for detecting CBZ in different matrices (Yan et al. 2015; Liu et al. 2021). The characteristic of each ELISA is determined by the specificity and sensitivity of antibodies used to capture the target molecule.

Consequently, antibodies production strategy is essential for the immunoassay (Wu et al. 2022). In the previous work of Bellemjid et al. (2018), the production strategy of anti-CBZ was described. Hapten (4 carbons) of CBZ have been synthesized, coupled to

BSA, and used to produce polyclonal antibodies in rabbits. On the other hand, Hapten(5 carbons) associated with HAS have been used for wells plates coating. For the indirect ELISA development, the antigen coating concentration and the antibodies dilution were optimized (100 ng/well for the antigen concentration and 1/2000 for the antibodies dilution). Antibodies were used for competition between standards (free CBZ) and the coated CBZ-hapten conjugate. A standard curve of CBZ immunoassay showed that IC_{50} , LOD and LOQ were 0.63 ± 0.024 , 0.026 ± 0.001 and 0.083 ± 0.003 $\mu\text{g/L}$ respectively, with good repeatability (RSD = 4.35 %) and reproducibility (RSD = 1.22 %). In comparison, the direct ELISA system for detecting CBZ was performed by Song et al. (2019), with an IC_{50} value of 2.7 ± 0.3 $\mu\text{g/L}$ and a LOD of 0.3 ± 0.15 $\mu\text{g/L}$. ELISA tests for CBZ using monoclonal antibodies were developed by Yan et al. (2015) with an IC_{50} value of 0.45 $\mu\text{g/L}$. This study validated the developed ELISA for CBZ analysis in tomatoes. Using ELISA to detect pesticides in food samples requires a prior extraction with organic solvents; generally, a simple extraction method is coupled to ELISA for the analysis (Verdini and Pecorelli 2022). In this study, a simple extraction with methanol was used to extract CBZ from tomato samples. The methanol extract was used for ELISA after 10 times dilution because beyond 10% of the reactivity of the antibodies decreased (Maftouh et al. 2020). In addition, the quality of the immunoassay is generally affected by interference and cross-reactions (CRs) (Maftouh et al. 2020). So, various pesticides were tested for CR in the developed ELISA. A higher CR of 83.1 % with benomyl was observed. Because of the tremendous structural similarity of benomyl with CBZ, the antibody has good reactivity. It should be noted that the degradation of benomyl obtains CBZ (Sebastian et al. 2022). The developed ELISA was used to detect CBZ in tomato samples collected from the market in the province of Rabat, Morocco. The results obtained by ELISA were compared with HPLC. After the QuEChERS extraction method, the HPLC analysis has been widely used for the CBZ analysis in water, soil, vegetables, etc. (Scheel and Tarley 2020). The QuEChERS method has been used intensely to extract various environmental pollutants and pesticides from different matrices (Kim et al. 2019). The HPLC method was validated for CBZ analysis with LOD and LOQ of 0.61 ± 0.02 and 1.85 ± 0.07 $\mu\text{g/L}$, respectively. These values are comparable with those found in the literature (Kim et al. 2019).

Nevertheless, ANOVA tested the LOD and LOQ for ELISA and HPLC, and the values obtained by HPLC were significantly higher than those obtained for ELISA. Several ELISAs developed for determining pesticides have shown lower LOD and LOQ values than HPLC (Zhai et al. 2023). The recovery of CBZ using methanol extraction followed by ELISA or QuEChERS extraction followed by HPLC analysis ranged from 85.7 to 98.1 % in the spiked tomato samples. These two selected methods presented a reasonable accuracy. The variability of all validation parameters was verified by principal component analysis (PCA).

ELISA and HPLC were used to analyze 100 tomato samples. HPLC and ELISA gave the same analytical results when CBZ was detectable and quantifiable. The two methods detected the presence of CBZ above the MRL level (0.3 mg/kg of tomato) in 9 samples. This MLR was recommended by the ONSSA in Morocco (ONSSA 2014). On the other hand, ELISA could quantify CBZ in 66 samples compared to HPLC (35 samples). In addition, ELISA's detection limit (LOD) was lower, allowing the detection of CBZ in 79 samples compared to HPLC (57 samples). These results showed an outstanding sensitivity of ELISA compared to HPLC for detecting CBZ in tomatoes. Maftouh et al. (2020) have already reported a better sensitivity of the ELISA system than HPLC for pesticide analysis. In many countries where CBZ is banned, the CBZ MRL has been defined as the limit of detection (LOD) using typical analytical methods (Elshafey et al. 2022). An interesting fact is that the high sensitivity of ELISA could help to detect traces of the banned fungicide CBZ, but also the presence of benomyl was reported in the food samples.

Conclusion

A polyclonal antibody in-house ELISA for detecting CBZ in tomatoes using a one-step extraction method was developed. A comparison of the ELISA and HPLC results showed that the agreement between the two techniques was perfect, and the sensitivity of the ELISA was higher. The developed ELISA is handy for the rapid analysis of many samples. This technology can also reduce the MRL of banned pesticides such as carbendazim. In the long term, we aimed to validate the developed ELISA system for determining CBZ in other environmental matrices.

Conflicts of interest

The authors reported no potential conflict of interest.

References

Aylaz, G., Kuhn, J., Lau, E. C., Yeung, C., et al. (2021). Recent developments on magnetic molecular imprinted polymers (MMIPs) for sensing, capturing, and monitoring pharmaceutical and agricultural pollutants. *Journal of Chemical Technology & Biotechnology*, 96(5), 1151-1160. <https://doi.org/10.1002/jctb.6681>.

Barron Cuenca, J., de Oliveira Galvão, M. F., Ünlü Endirlik, B., Tirado, N., et al. (2022). In vitro cytotoxicity and genotoxicity of single and combined pesticides used by Bolivian farmers. *Environmental and Molecular Mutagenesis*, 63(1), 4-17. <https://doi.org/10.1002/em.22468>.

Bellemjid, N., Iddar, A., Moussaif, A., Abbadi, N. E., et al. (2018). Analysis of carbamates pesticides: immunological technique by local development of enzyme-linked immuno-sorbent assay. *Journal of Pharmacy and Pharmacology*, 6, 395-402. <https://doi.org/10.17265/2328-2150/2018.04.010>.

Ben Khadda, Z., Fagroud, M., El Karmoudi, Y., Ezrari, S., et al. (2021). Farmers' Knowledge, Attitudes, and Perceptions Regarding Carcinogenic Pesticides in Fez Meknes Region (Morocco). *International journal of environmental research and public health*, 18(20), 10879. <https://doi.org/10.3390/ijerph182010879>.

Benaboud, J., Elachour, M., Oujidi, J., & Chafi, A. (2021). Pesticides used by Moroccan's farmer in oriental Morocco: Case of Berkane region. *Academia Journal of Environmental Sciences*, 2(4), 052-058. <https://doi.org/10.15413/ajes.2014.0101>.

Boscolo, S., Pelin, M., De Bortoli, M., Fontanive, G., et al. (2013). Sandwich ELISA assay for the quantitation of palytoxin and its analogs in natural samples. *Environmental science & technology*, 47(4), 2034-2042. <https://doi.org/10.1021/es304222t>.

Bouterfas, M., Soufiane, F., Zouheir, C., Elhalouani, H., et al. (2020). Evaluation of farmers' phytosanitary practices in the plain of triffa (astern morocco), identification and evaluation of sanitary and environmental risks. *Moroccan Journal of Chemistry*, 8(2), 8-2. <https://doi.org/10.48317/IMIST.PRSM/morjchem-v8i2.19573>.

Choubbane, H., Ouakhssase, A., Chahid, A., Taourirte, M., et al. (2022). Pesticides in fruits and vegetables from the Souss Massa region, Morocco. *Food Additives & Contaminants: Part B*, 1-10. <https://doi.org/10.1080/19393210.2022.2028196>.

Elshafey, R., Abo-Sobehy, G. F., & Radi, A. E. (2022). Imprinted polypyrrole recognition film cobalt oxide/electrochemically reduced graphene oxide nanocomposite for carbendazim sensing. *Journal of Applied Electrochemistry*, 52, 45-53.

FAO. (2021). Pesticides Use, Pesticides Trade and Pesticides Indicators. Global, Regional and Country Trends, 1990–2019. Analytical Brief Series No. 29. Retrieved from <https://www.fao.org/3/cb6034en/cb6034en.pdf>

FAOSTAT. (2022). Statistical Databases. Retrieved from <http://www.fao.org/faostat/en/#data/RT/visualize/>

Kasaeinasab, A., Mahabadi, H. A., Shahtaheri, S. J., Faridbod, F., et al. (2023). Carbendazim trace analysis in different samples by

- using nanostructured modified carbon paste electrode as voltametric sensor. *PLoS one*, 18(1), e0279816. <https://doi.org/10.1371/journal.pone.0279816>.
- Kim, L., Lee, D., Cho, H. K., & Choi, S. D. (2019). Review of the QuEChERS method for the analysis of organic pollutants: Persistent organic pollutants, polycyclic aromatic hydrocarbons, and pharmaceuticals. *Trends in Environmental Analytical Chemistry*, 22, e00063. <https://doi.org/10.1016/j.teac.2019.e00063>.
- Kumar, A., Kumar, V., Gull, A., & Nayik, G.A. (2020). Tomato (*Solanum Lycopersicon*). In: G.A. Nayik, & A. Gull (eds) *Antioxidants in Vegetables and Nuts - Properties and Health Benefits* (pp 191-207). Springer, Singapore. https://doi.org/10.1007/978-981-15-7470-2_10.
- Lesueur, C., Gartner, M., Mentler, A., & Fuerhacker, M. (2008). Comparison of four extraction methods for the analysis of 24 pesticides in soil samples with gas chromatography–mass spectrometry and liquid chromatography–ion trap–mass spectrometry. *Talanta*, 75(1), 284-293. <https://doi.org/10.1016/j.talanta.2007.11.031>.
- Liu, D., Gong, Q., Xu, X., Meng, S., et al. (2023). Photoelectrochemical aptasensor based on cascade dual Z-scheme CdTe-polyaniline@ MoS₂ heterostructure for the sensitive carbendazim detection. *Journal of Electroanalytical Chemistry*, 117143. <https://doi.org/10.1007/s10800-021-01613-6>.
- Liu, H., Wang, Y., Fu, R., Zhou, J., et al. (2021). A multicolor enzyme-linked immunoassay method for visual readout of carbendazim. *Analytical Methods*, 13(37), 4256-4265. <https://doi.org/10.1039/D1AY01028J>.
- Liu, Y. H., Jin, M. J., Gui, W. J., Cheng, J. L., et al. (2007). Hapten design and indirect competitive immunoassay for parathion determination: Correlation with molecular modeling and principal component analysis. *Analytica chimica acta*, 591(2), 173-182. <https://doi.org/10.1016/j.aca.2007.03.071>.
- Maftouh, I., Iddar, A., Moussaif, A., El Abbadi, N., et al. (2020). Development of an enzyme-linked immunosorbent assay for detection of Chlorpyrifos-ethyl and its metabolites 3, 5, 6-Trichloro-2-Pyridinol and Diethylthiophosphate. *International Journal of Environmental Analytical Chemistry*, 100 (12), 1336-1349. <https://doi.org/10.1080/03067319.2019.1653456>.
- Magunga, B. T., & Malebo, N. J. (2023). In-vitro assessment of Thyme oil (*Thymus vulgaris*) as antifungal agent against *Phyllosticta citricarpa*. *Access Microbiology*, 000591-v1. <https://doi.org/10.1099/acmi.0.000591.v1>.
- Moussaif, A., El Yahyaoui, A., Saghdani, N., El Kazzouli, S., et al. (2021). Assessment of pesticide residues, exogenous heavy metals and essential minerals in spinach after cleaning with traditional methodologies. *International Journal of Environmental Analytical Chemistry*, 1-14. <https://doi.org/10.1080/03067319.2021.1931857>.
- Nicolopoulou-Stamati, P., Maipas, S., Kotampasi, C., Stamatis, P., et al. (2016). Chemical pesticides and human health: the urgent need for a new concept in agriculture. *Frontiers in public health*, 4, 148. <https://doi.org/10.3389/fpubh.2016.00148>.
- ONSSA. (2014). National Food Safety Office/Plant Protection service, Morocco BO n°6322bis. Retrieved from <http://eservice.onssa.gov.ma/Docs/arr.156-14.fr.pdf/>
- Patibanda, A. K., & Ranganathswamy, M. (2018). Effect of agrichemicals on biocontrol agents of plant disease control. In: D. Panpatte, Y. Jhala, H. Shelat, & R. Vyas (eds) *Microorganisms for green revolution: Volume 2: Microbes for Sustainable Agro-ecosystem* (pp.1-21), Springer, Singapore.
- Phansawan, B., Prapamontol, T., Thavornnyutikarn, P., Chantara, S., et al. (2015). A sensitive method for determination of carbendazim residue in vegetable samples using HPLC-UV and its application in health risk assessment. *Chiang Mai Journal of Science*, 42, 681-690.
- Raab, G. M. (1983). Comparison of a logistic and a mass-action curve for radioimmunoassay data. *Clinical chemistry*, 29(10), 1757-1761. <https://doi.org/10.1093/clinchem/29.10.1757>.
- Rodbard, D. (1981). Mathematics and statistics of ligand assays: An illustrated guide. In J. Langan & J. J. Clapp (Eds.), *Ligand Assay: analysis of international developments on isotopic and nonisotopic immunoassay*, (pp. 45-99). New York: Masson Publishing.
- Sakali, A. K., Bargiota, A., Fatouros, I. G., Jamurtas, A., et al. (2021). Effects on Puberty of Nutrition-Mediated Endocrine Disruptors Employed in Agriculture. *Nutrients*, 13(11), 4184. <https://doi.org/10.3390/Nu13114184>.
- Sarkar, S., Gil, J. D. B., Keeley, J., & Jansen, K. (2021). The use of pesticides in developing countries and their impact on health and the right to food. *European Parliament's Committee on Development*, PE 653.622. <https://doi.org/10.2861/28995>.
- Scheel, G. L., & Tarley, C. R. T. (2020). Simultaneous microextraction of carbendazim, fipronil and picoxystrobin in naturally and artificial occurring water bodies by water-induced supramolecular solvent and determination by HPLC-DAD. *Journal of Molecular Liquids*, 297, 111897. <https://doi.org/10.1016/j.molliq.2019.111897>.
- Sebastian, N., Yu, W. C., Balram, D., Al-Mubaddel, F. S., & Noman, M. T. (2022). Functionalization of CNFs surface with β -cyclodextrin

- and decoration of hematite nanoparticles for detection and degradation of toxic fungicide carbendazim. *Applied Surface Science*, 586, 152666. <https://doi.org/10.1016/j.apsusc.2022.152666>.
- Sharma, A., Kumar, V., Shahzad, B., Tanveer, M., et al. (2019). Worldwide Pesticide Usage and its Impacts on Ecosystem. *SN Applied Sciences*, 1, 1446. <https://doi.org/10.1007/S42452-019-1485-1>.
- Song, Y., Xie, C. H., Wang, M. S., Liu, S., et al. (2019). Rapid Determination of Carbendazim Residues in Mushrooms by Immunosorbent Assay. *E3S Web of Conferences*, 78, 02018. <https://doi.org/10.1051/e3sconf/20197802018>.
- Verdini, E., & Pecorelli, I. (2022). The current status of analytical methods applied to the determination of polar pesticides in food of animal origin: a brief review. *Foods*, 11(10), 1527. <https://doi.org/10.3390/foods11101527>.
- Wang, J., Xing, C., Xia, J., Chen, H., et al. (2023). Degradation of carbendazim in aqueous solution by dielectric barrier discharge cold plasma: Identification and toxicity of degradation products. *Food Chemistry*, 403, 134329. <https://doi.org/10.1016/j.foodchem.2022.134329>.
- Wang, X., Song, M., Wang, Y., Gao, C., et al. (2012). Response of soil bacterial community to repeated applications of carbendazim. *Ecotoxicology and environmental safety*, 75, 33-39. <https://doi.org/10.1016/j.ecoenv.2011.08.014>.
- Wu, W., Li, C., Liu, D., Ji, J., et al. (2022). Ultrasensitive antibody production strategy based on hapten property for simultaneous immunoassay. *Food Chemistry*, 395, 133565. <https://doi.org/10.1016/j.foodchem.2022.133565>.
- Yan, H., Liu, L., Xu, N., Kuang, H., et al. (2015). Development of an immunoassay for carbendazim based on a class-selective monoclonal antibody. *Food and Agricultural Immunology*, 26(5), 659-670. <https://doi.org/10.1080/09540105.2015.1007446>.
- Zhai, R., Chen, G., Liu, G., Huang, X., et al. (2023). Comparison of Chemiluminescence Enzyme Immunoassay (Cl-ELISA) with Colorimetric Enzyme Immunoassay (Co-ELISA) for Imidacloprid Detection in Vegetables. *Foods*, 12(1), 196. <https://doi.org/10.3390/foods12010196>.







Journal of Experimental Biology and Agricultural Sciences

<http://www.jebas.org>

ISSN No. 2320 – 8694

Isolation and production of polyhydroxybutyrate (PHB) from *Bacillus pumilus* NMG5 strain for bioplastic production and treatment of wastewater from paper factories

Ho Ky Quang Minh¹ , Ngo Duy Thai² , Tran Vu Anh Khoa² ,
Nguyen Thi Ngoc Thao¹ , Jirapast Sichaem^{3,*} 

¹Faculty of Environmental Science, Saigon University, 273 An Duong Vuong, Dist.5, Ho Chi Minh City, Vietnam

²Saigon University Institute of Environment – Energy Technology, Saigon University, 20 Ngo Thoi Nhiem, Dist. 3, Ho Chi Minh City, Vietnam

³Research Unit in Natural Products Chemistry and Bioactivities, Faculty of Science and Technology, Thammasat University Lampang Campus, Lampang 52190, Thailand

Received – November 25, 2022; Revision – March 19, 2023; Accepted – April 03, 2023

Available Online – April 30, 2023

DOI: [http://dx.doi.org/10.18006/2023.11\(2\).351.358](http://dx.doi.org/10.18006/2023.11(2).351.358)

KEYWORDS

Bacillus pumilus

Polyhydroxybutyrate (PHB)

Activated sludge

Wastewater

16S rRNA

ABSTRACT

Polyhydroxybutyrate (PHB) has the potential to replace traditional plastics and limit environmental pollution caused by plastic waste. This study combined wastewater treatment with PHB production to reduce costs. Bacteria capable of synthesizing PHB were isolated from paper mill wastewater and identified using Matrix Assisted Laser Desorption/Ionization–Time of Flight (MALDI-TOF) mass spectrometry and 16S rRNA gene analysis. *Bacillus pumilus* NMG5 strain was found to have a good yield in modified Nutrient Broth culture, reaching 42.28% of dry biomass. The PHB product was analyzed using FTIR spectroscopy and ¹H NMR spectroscopy. The bacterial strain was also tested for its ability to treat paper mill wastewater, and it showed impressive results in terms of biochemical oxygen demand (COD), total nitrogen, and total phosphorus, with efficiencies of 95.93%, 79.36%, and 83.55%, respectively. The study found that wastewater treatment combined with PHB production was a promising solution to reduce costs and limit environmental pollution. The bacterial strain *B. pumilus* NMG5 had a high yield of PHB, and the PHB product was of high quality, as confirmed by FTIR and ¹H NMR spectroscopy. Furthermore, the bacterial strain showed impressive results in treating paper mill wastewater with high COD, total nitrogen, and total phosphorus efficiencies. These results suggest that this harmless bacterium could be used in paper mill wastewater treatment systems to produce PHB, providing a sustainable and environmentally friendly solution.

* Corresponding author

E-mail: jirapast@tu.ac.th (Jirapast Sichaem)

Peer review under responsibility of Journal of Experimental Biology and Agricultural Sciences.

Production and Hosting by Horizon Publisher India [HPI]
(<http://www.horizonpublisherindia.in/>).
All rights reserved.

All the articles published by [Journal of Experimental Biology and Agricultural Sciences](#) are licensed under a [Creative Commons Attribution-NonCommercial 4.0 International License](#) Based on a work at www.jebas.org.



1 Introduction

Environmental pollution is a pressing issue, notably pollution caused by industrial wastewater and plastic waste, which directly harms human health and ecosystems and negatively impacts many countries' sustainable development. Industrial wastewater, mainly pulp and paper factory wastewater, contains many highly toxic compounds, with over 250 identified substances, such as dioxins, phenols, and furans (Ali and Sreerishnan 2001). Therefore, it is crucial and necessary to address thoroughly the problem of water pollution caused by the paper industry's wastewater.

Plastic has become an essential material widely used in daily human life and has been produced on an industrial scale since the 1940s (Ncube et al. 2021). It is a valuable and durable material that is difficult to decompose in the natural environment, and after use, plastic has become one of the significant causes of environmental pollution. Only 9% of the world's nine billion tons of plastic waste is recycled yearly (Obebe and Adamu 2020). In the United States, plastic waste accounts for approximately 12% of total municipal waste, estimated at 30 million tons per year (United State Environmental Protection Agency [EPA], n.d). This figure is predicted to increase as the population and per capita consumption of plastic products rise. In Vietnam, this is equivalent to about 3.1 million tons (The World Bank 2022). These figures show that urgent measures are necessary to manage and solve the problem of plastic waste to minimize adverse environmental impacts. One current solution is to replace traditional plastics that are difficult to decompose with bioplastics that can decompose quickly in a natural environment (Moshood et al. 2022).

Bioplastics are polymers that can decompose into simple molecules such as CO₂, water, CH₄, inorganic compounds, or biomass under the activities of many microorganisms under natural conditions. One bioplastic evaluated with great potential is polyhydroxyalkanoate (PHA), extracted from bacterial cells. PHAs are a group of polymers produced by bacteria that ferment sugars and fats, composed of 10³ -10⁴ monomers, existing as distinct particles within a cell, with sizes ranging from 0.2 to 0.5 μm. After being extracted from the cell, they exhibit properties similar to conventional resins but are biodegradable, insoluble in water, and non-toxic (Bosco and Chiampo 2010). PHA plastic is, therefore, considered suitable for producing disposable items such as food packaging, packaging film, containers, etc.

To simultaneously address the problems related to wastewater from the paper industry and plastic replacement by bioplastic production, this research was carried out to isolate PHAs synthesized bacterial strains from paper factories' wastewater. This is intended to enhance the survivability of isolated bacteria when putting them into practical applications. These isolated bacterial strains were also screened for their ability to treat

wastewater, their biosynthesis of PHAs and the characteristics of the obtained PHA products.

2 Material and Methods

2.1 Screening for bacteria isolation

Wastewater samples having a higher concentration of carbohydrates were collected from three paper factories, including Minh Hung (Minh Hung 3 industrial park, Binh Phuoc province, Vietnam), Saigon (Tan Thanh District, Ba Ria Vung Tau Province, Vietnam), and Lee & Man (Chau Thanh District, Hau Giang Province, Vietnam) paper factories. After diluting to the appropriate concentration (10⁻⁴), the sample was spread on the solid medium surface to activate synthetic PHAs, which are low in nutrients but high in carbohydrates. In this study, ½ concentration of Nutrient Agar medium was used as per the manufacturer's recommendation (agar 7.5 g/L; meat extract 0.5 g/L; peptone 2.5 g/L; sodium chloride 2.5 g/L; yeast extract 1 g/L) and supplemented with glucose (4g/L) and Nile Blue A dye. Bacterial strains capable of biosynthesized PHAs will fluoresce from pale yellow to orange and pink under UV light (Li et al. 2018; Kung et al. 2007).

2.2 Bacterial identification

All the isolated bacterial strains were quickly identified by MALDI-TOF (Matrix Assisted Laser Desorption/Ionization– Time of Flight) mass spectrometry (Schulthess et al. 2014), using a Bruker Daltonik MALDI Biotyper (Germany) system at the Center of Science and Biotechnology, University of Natural Sciences, Ho Chi Minh City, Vietnam. After identification, bacterial strains causing diseases to humans, animals, plants, etc., will be removed from the collections. The remaining non-pathogenic strains will be further confirmed by analyzing the gene sequence encoding for 16S rRNA with primer pairs 16sF 5'- AGA GTT TGA TCC TGG CTC AG -3' and 16sR 5'- ACG GCT ACC TTG TTA CGA CTT- 3' (Thirumala et al. 2010). The products obtained after amplification by polymerase chain reaction (PCR) were sequenced at the Biotechnology Center of Ho Chi Minh City, Vietnam and blasted to compare with the US GenBank (NCBI) database for confirmation.

2.3 Enrichment and growth rate determination

Bacterial strains that could biosynthesize PHA were cultured media enriched on 100 mL Luria-Bertani Broth medium (LB) at 37° C, shaken at 100 rounds per minute (rpm) for 72 hours. The density of cells was checked every 2 hours to determine the growth rate by optical density (OD) measurement at 600 nm. The dried biomass was tested by centrifuging it for 15 minutes at 10,000 rpm and then drying it at 55°C until it reached a constant weight (Hungund et al. 2013). The strains with significant development

Table 1 Synthetic wastewater and minor solution compositions

Synthetic wastewater		Minor solution	
Composition	Content (mg/L)	Composition	Content (mg/L)
Glucose	165	H ₃ BO ₃	50
NaHCO ₃	270	ZnCl ₂	50
NH ₄ Cl	127	CuCl ₂	30
K ₂ HPO ₄	53	MnSO ₄ ·H ₂ O	50
CaCl ₂ ·2H ₂ O	30	(NH ₄) ₆ Mo ₇ O ₂₄ ·4H ₂ O	50
MgSO ₄ ·7H ₂ O	12	AlCl ₃	50
FeCl ₃	3.5	CoCl ₂ ·6H ₂ O	50
		NiCl ₂	50

and high biomass yield would be additionally grown in a modified ½ strength (w/v) Nutrient Broth medium supplemented by 4g/L of glucose to produce PHAs.

2.4 Wastewater treatment capabilities of isolated strains

After the strains were selected and enriched, activated sludge would be produced using these strains. The activated sludge would then be used to evaluate the wastewater treatment ability. In a 12-hour retention time, 30 L of synthetic wastewater was applied to the sequencing batch reactors (SBRs), and the treated wastewater was used as a substrate. The composition of synthetic wastewater was prepared with a C:N ratio of around 20:1 (Johnson et al. 2010), and then 1 mL of minor solution (Wang and Yu 2006) was added, as shown in Table 1. Dissolved oxygen (DO) in the system was maintained at around 4 mg/L by a 58-watt air blower.

Furthermore, the culturing of activated sludge was carried out until the stabilization phase was reached and the mixed liquor suspended solids (MLSS) value was greater than 2.5 g/L. At the end of each of the ten experimental days following the stabilization phase, total COD, nitrogen, and phosphorus parameters were analyzed to determine treatment efficiency. The process of testing and evaluating the treatment efficiency was continued with actual wastewater collected from the Minh Hung paper factory. To prepare the system, we used 2 L of activated sludge for every 20 L of wastewater and allowed it to acclimate for 24 hours. The output wastewater was collected daily and retained for 12 hours before analysis. Simultaneously, activated sludge samples were collected to perform extraction and evaluate the PHAs' synthesizing ability.

2.5 PHA extraction and analysis

To evaluate the synthesis ability as well as product characteristics of the polymerized PHAs product, the selected strain was cultured

in 4 g/L Nutrient Broth (Merck 105443) supplemented with glucose (4 g/L). The biomass was collected after 48 hours. After sampling, PHAs were extracted based on the modified method of Singh et al. (2011). The biomass sample was washed and dried using distilled water and then sent to the centrifuge to remove excess water. The 5g of dried biomass was then incubated in 500 mL of NaClO (4,7%) at 85°C for 1 hour. A continuous shaking force was applied throughout the incubation to break down the cells. After 1 hour, the sample was sent to the centrifuge again for 15 minutes at 5,500 rpm to collect pellets. Then, the pellets were washed using distilled water and dried by centrifuge at 5,500 rpm. Afterwards, the pellets were incubated in 0.13 M of ammonium laurate solution for 3 hours at 75 °C (Mannina et al. 2019). Pellets were then collected using the centrifuge for 15 minutes at 5,500 rpm. Finally, the collected pellets were washed by running them through distilled water and ethanol and then centrifuged and dried overnight at 60°C to collect PHAs.

Continually, the extracted and purified polymer (5 mg) was thoroughly mixed with spectroscopic grade KBr (100 mg) and pelletized. Fourier Transform Infrared (FTIR) spectroscopy analyzed the functional groups of the isolated polymer using a Bruker FTIR spectrophotometer in the range of 4000 to 400 cm⁻¹. Based on proton nuclear magnetic resonance (¹H NMR) spectroscopic analysis, the chemical structure of the isolated polymer was interpreted. The polymer samples (5 mg) were dissolved in 0.5 mL of DMSO-*d*₆ and analyzed with a Bruker ¹H NMR (600 MHz) spectrophotometer. The chemical shifts were represented on the δ_H scale [parts per million (ppm)], and TMS (tetramethylsilane) was used as the internal standard.

The PHAs polymer product's thermal stability was tested by the thermogravimetric analyzer (TGA) by Q500, TA Instruments, USA, and the PHAs yield was estimated by conversion to crotonic acid with concentrated H₂SO₄ then measured by absorbance at 235 nm (Law and Slepecky 1961).

Table 2 Identification results by the MALDI-TOF method

No.	Sample name	Species	Pathogen	Source
1	LM2	<i>Bacillus cereus</i>	×	Lee & Man Paper Manufacturing LTD.
2	LM5	<i>Citrobacter braakii</i>	×	
3	LM3	<i>Neisseria gonorrhoeae</i>	×	
4	NMG3	<i>Bacillus cereus</i>	×	Saigon Paper Company
5	NMG4	<i>Bacillus flexus</i>		
6	NMG5	<i>Bacillus pumilus</i>		
7	NMG9	<i>Bacillus cereus</i>	×	
8	NMG2-L	<i>Bacillus cereus</i>	×	Minh Hung Paper Joint Stock Company
9	BP1	<i>Rhizobiumradiobacter</i>	×	
10	BP3	<i>Bacillus weihenstephanensis</i>	×	
11	BP5	<i>Bacillus megaterium</i>		
12	BP7	<i>Pseudacidovorax intermedius</i>		
13	BP8	<i>Delftiaacidovorax</i>	×	

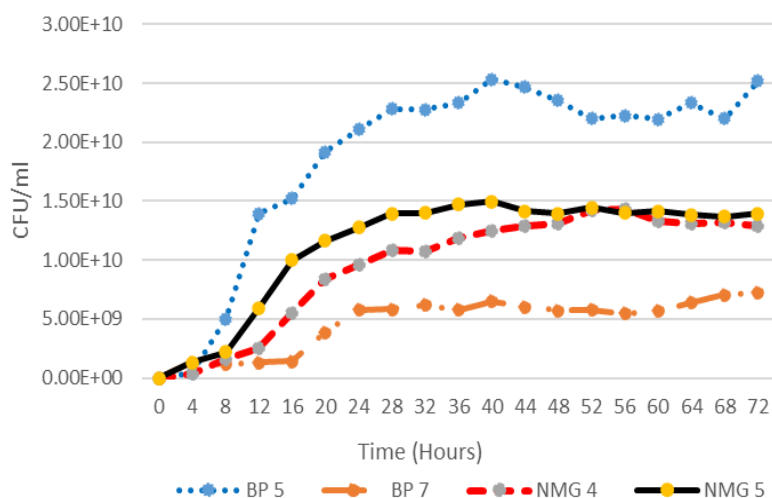


Figure 1 The growth rates of BP5, BP7, NMG4, and NMG5 strains

3 Results and Discussion

3.1 Bacterial Isolation and growth rate

As a result of the screening, 13 bacterial strains capable of synthesizing PHAs were obtained, including three from Lee and Man, four from Saigon, and six from Minh Hung paper factories. From the results shown in Table 2, strains suspected to be pathogenic to humans, livestock, or plants were removed. Growth rate surveys were continued on four remaining strains, including NMG4, NMG5, BP5, and BP7.

The results indicate the presence of beneficial bacteria, particularly those capable of synthesizing polyhydroxyalkanoates (PHAs), even

in the toxic conditions found in paper industry wastewater. This finding supports our research team's original aim of coordinating the wastewater treatment and PHA synthesis processes. Furthermore, these bacteria are better suited to adapting and growing in paper mill wastewater than those collected from other sources, making them a promising candidate for PHA synthesis.

The results presented in Figure 1 revealed that all tested strains are approximately at their maximum growth rate after 24 hours. These results are similar to the findings of Seo et al. (2013). Among the four studied strains, the BP5 strain had the highest cell density, reaching 2.5×10^{10} CFU/mL, while the BP7 strain had the lowest cell density at 3×10^9 CFU/mL. However, the dried biomass result of BP5 was so low (0.38 g/L) compared to NMG5 (2.66 g/L).

These results were not as good as those of a previous study by Getachew and Woldesenbet (2016), which studied optimal conditions for *Bacillus* sp. and obtained biomass ranging from 8.37 to 15.49 g/L. However, because our study focused on using microorganisms in wastewater treatment systems, we could not control certain conditions such as temperature and carbon source, as was done in the study by the authors mentioned above. As a result, we chose to proceed with further trials using strain NMG5.

The sequence of the 16S ribosomal RNA gene segment of strain NMG5 was 1412 nucleotides long and matched 99.72% with the 16S ribosomal RNA fragment of *B. pumilus* DFs 1420 (NCBI Reference Sequence: NR_043242.1). This allows us to confirm that the strain NMG5 has the correct *B. pumilus* identifier. This beneficial aerobic bacterium is being utilized broadly in many industrial and agricultural fields, so it is safe and very suitable to direct PHA production in wastewater treatment systems (Maliehe et al. 2016).

3.2 Wastewater treatment capacities

After culturing in the Nutrient Broth medium, the *B. pumilus* NMG5 strain was cultured with synthetic wastewater, and the

activated sludge began to appear on the sixth culture day. By the 22nd culture day, the amount of activated sludge in the system had reached the steady phase, around 2.5 g/L of mixed liquor suspended solids (MLSS). The wastewater was stopped from providing oxygen and left to settle for the next 10 days (from the 23rd to the 32nd day), the sludge was separated, and the effluent water was collected to analyze and evaluate the treatment efficiency. The study results show that COD removal efficiency was over 94.5%, tended to increase slightly, and peaked on the 29th day with a treatment efficiency of 97.71%. Similarly, the nitrogen and phosphorus treatment capacities of *B. pumilus* NMG5 achieved the highest treatment efficiencies of 84.6% and 86.5% on the 29th day, respectively (Table 3).

On the 33rd day, real wastewater collected from the Minh Hung paper factory was used. After one day of acclimatization, the results showed that the treatment efficiency for all three parameters was slightly decreased, at 95.93%, 79.36%, and 83.55% for COD, total nitrogen, and total phosphorus, respectively (Table 4).

This lower treatment efficiency can be explained by some microbial inhibitors in the paper mill industry's wastewater. Even so, with such treatment efficiency as *B. pumilus* NMG5 strain, the

Table 3 Treatment efficiency when using analyzed wastewater

Day	COD			Total nitrogen			Total phosphorus		
	Input (mg/L)	Output (mg/L)	Treatment efficiency (%)	Input (mg/L)	Output (mg/L)	Treatment efficiency (%)	Input (mg/L)	Output (mg/L)	Treatment efficiency (%)
23		77	94.50		4.72	72.40		3.65	78.33
24		75	94.64		4.47	73.86		3.47	79.39
25		57	95.93		3.58	79.06		2.77	83.55
26		64	95.43		3.8	77.78		3.02	82.07
27	1400	57	95.93	17.10	3.53	79.36	16.84	2.9	82.78
28		48	96.57		3.37	80.29		2.52	85.04
29		32	97.71		2.63	84.62		2.27	86.52
30		38	97.29		2.67	84.39		2.32	86.22
31		34	97.57		2.65	84.50		2.28	86.46
32		33	97.64		2.63	84.62		2.28	86.46

Table 4 Treatment efficiency when using real wastewater from Minh Hung paper factory

Day	COD			Total nitrogen			Total phosphorus		
	Input (mg/L)	Output (mg/L)	Treatment efficiency (%)	Input (mg/L)	Output (mg/L)	Treatment efficiency (%)	Input (mg/L)	Output (mg/L)	Treatment efficiency (%)
34		77	94.50		4.72	72.40		3.65	78.33
35		75	94.64		4.47	73.86		3.47	79.39
36	680	57	95.93	12.8	3.58	79.06	1.44	2.77	83.55
37		64	95.43		3.8	77.78		3.02	82.07
38		57	95.93		3.53	79.36		2.9	82.78

output wastewater still meets the A standard, according to Vietnam's regulations on industrial wastewater (National Technical Regulation on Industrial Wastewater QCVN 40:2011/BTNMT).

3.3 Polymer production capacity

The quantitative results of the PHA polymer obtained were 2.1g/5g of dry biomass, equivalent to 42.28%. The FTIR spectra of this PHAs polymer (Figure 2) revealed distinct absorption spectrum for esters: -OH bending at 3436 cm^{-1} , C-H stretching at 2933 cm^{-1} , the absorption band of aliphatic carbonyl C=O at 1723 cm^{-1} and the -CH group of the aliphatic compound at $1228\text{--}1381\text{ cm}^{-1}$. This

result revealed that the PHA's polymer chain structure consists of hydroxybutyrate (HB) monomers.

The polyhydroxybutyrate (PHB) structure was confirmed by ^1H NMR spectroscopy. ^1H NMR spectrum of the polymer (Figure 3) displayed three signals characteristic of PHB, including a doublet at $\delta_{\text{H}} 1.20\text{ ppm}$ ($J = 12.0\text{ Hz}$), which was attributed to the methyl group (-CH₃), a multiplet at $\delta_{\text{H}} 2.55\text{ ppm}$, which was assigned to the methylene group (-CH₂), and a multiplet at $\delta_{\text{H}} 5.11\text{ ppm}$, which was characterized as the methine group (-CH). The NMR spectrum obtained followed the data reported in the literature (Shamala et al. 2009; Das et al. 2022), which confirmed that the polymer was made from the *B. pumilus* NMG5 strain PHB.

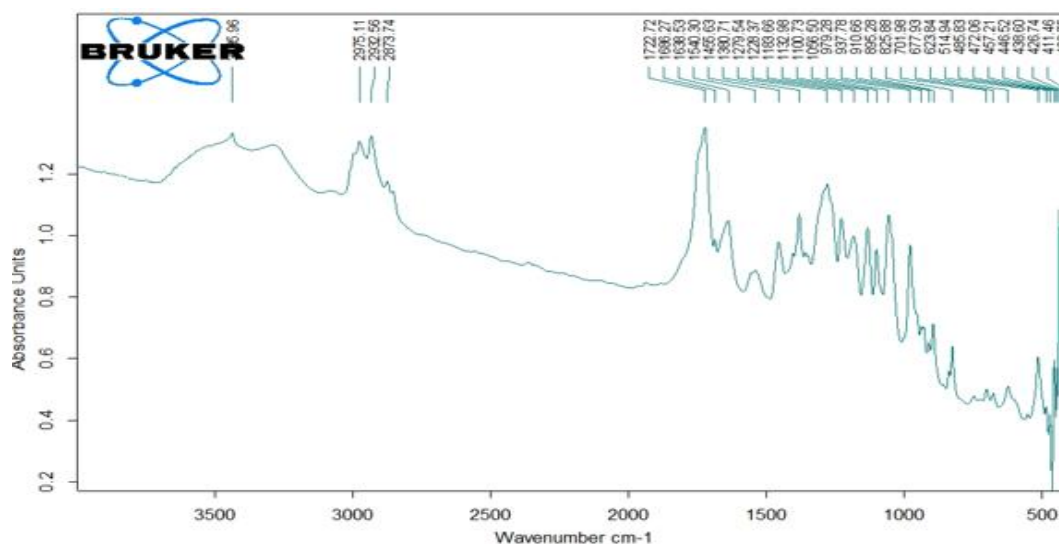


Figure 2 FTIR spectrum of PHA polymer product

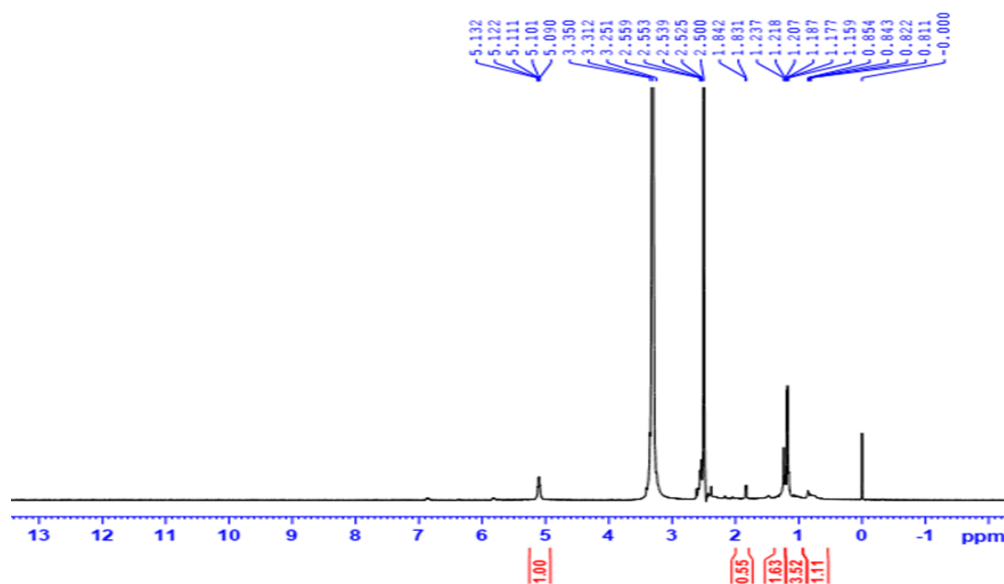


Figure 3 ^1H NMR spectral analysis of PHB polymer product in $\text{DMSO-}d_6$

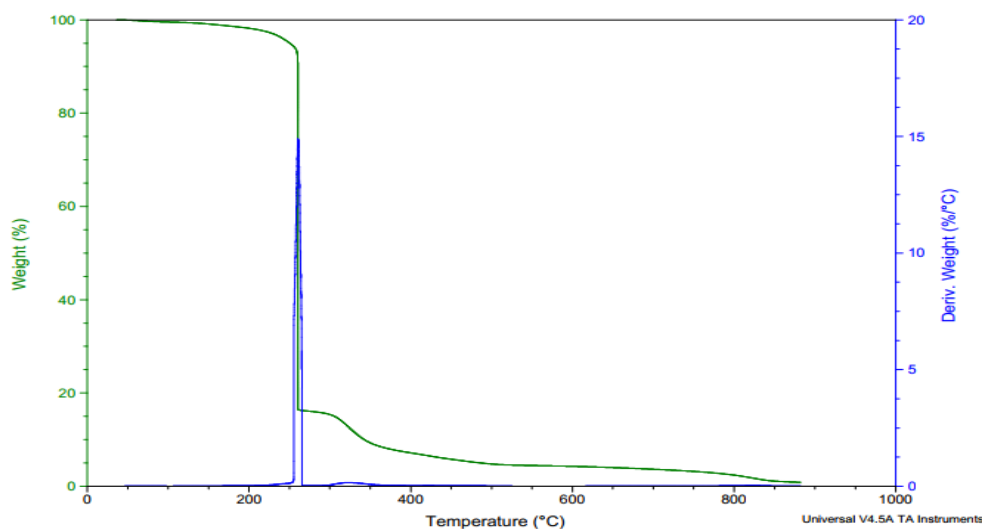


Figure 4 Thermogravimetric (TGA) spectrum of PHB from *B. pumilus* NMG5 strain

Figure 4 depicts PHB TGA test results, demonstrating the material's good stability and the most significant weight loss at 260°C. This outcome is comparable to those reported by Pradhan et al. (2018) and Vahabi et al. (2019) investigations. In which PHB samples that were synthesized from bacteria, as well as standard PHB, were degraded at a temperature between 250°C and 300°C.

Conclusion

The results of this study suggested that the *B. pumilus* NMG5 strain, which was isolated from paper mill wastewater, is safe and capable of synthesizing PHB with a quite good yield of 42.28 %/dry biomass weight. Additionally, this strain has a high ability to adapt and treat paper mill wastewater. However, to integrate PHB production with wastewater treatment in actual practice, a variety set of bacteria should be used to ensure safety and treatment effectiveness. Therefore, we recommend continuing to search, isolate, and evaluate for more bacterial strains capable of biosynthesizing PHB and highly adapted to wastewater environments.

Conflict of Interest

The authors declare that they do not have any conflict of interest.

References

Ali, M., & Sreerishnan, T. R. (2001). Aquatic toxicity from pulp and paper mill effluents: a review. *Advances in Environmental Research*, 5(2), 175-196. [https://doi.org/10.1016/S1093-0191\(00\)00055-1](https://doi.org/10.1016/S1093-0191(00)00055-1).

Bosco, F., & Chiampo, F. (2010). Production of polyhydroxyalkanoates (PHAs) using milk whey and dairy wastewater activated sludge: production of bioplastics using dairy

residues. *Journal of Bioscience and Bioengineering*, 109(4), 418-421. <https://doi.org/10.1016/j.jbiosc.2009.10.012>.

Das, R., Pal, A., & Paul, A. K. (2022). Optimization of process parameters for production of poly (3-hydroxybutyrate) by *Bacillus pumilus* AHSD 04, a seed borne Endophyte of oleaginous plant *Arachis hypogaea* L. *Biointerface Research in Applied Chemistry*, 12(4), 5280-5295. <https://doi.org/10.33263/BRIAC124.52805295>.

Getachew, A., & Woldesenbet, F. (2016). Production of biodegradable plastic by polyhydroxybutyrate (PHB) accumulating bacteria using low cost agricultural waste material. *BMC Research Notes*, 9(1), 1-9. <https://doi.org/10.1186/s13104-016-2321-y>.

Hungund, B., Shyama, V. S., Patwardhan, P., & Saleh, A. M. (2013). Production of polyhydroxyalkanoate from *Paenibacillus durus* BV-1 isolated from oil mill soil. *Journal of Microbial and Biochemical Technology*, 5, 013-017. <http://dx.doi.org/10.4172/1948-5948.1000092>.

Johnson, K., Kleerebezem, R., & van Loosdrecht, M. C. (2010). Influence of the C/N ratio on the performance of polyhydroxybutyrate (PHB) producing sequencing batch reactors at short SRTs. *Water Research*, 44(7), 2141-2152. <https://doi.org/10.1016/j.watres.2009.12.031>.

Kung, S. S., Chuang, Y. C., Chen, C. H., & Chien, C. C. (2007). Isolation of polyhydroxyalkanoates producing bacteria using a combination of phenotypic and genotypic approach. *Letters in Applied Microbiology*, 44(4), 364-371. <https://doi.org/10.1111/j.1472-765X.2006.02090.x>.

Law, J. H., & Slepecky, R. A. (1961). Assay of poly-β-hydroxybutyric acid. *Journal of Bacteriology*, 82 (1), 33-36. <https://doi.org/10.1128/jb.82.1.33-36.1961>.

- Li, R., Gu, P., Fan, X., Shen, J., Wu, Y., Huang, L., & Li, Q. (2018). Isolation and characterization of PHA-producing bacteria from propylene oxide saponification wastewater residual sludge. *Applied Biochemistry and Biotechnology*, 186(1), 233-244. <https://doi.org/10.1007/s12010-018-2731-5>.
- Maliehe, T. S., Simonis, J., Basson, A. K., Reve, M., Ngema, S., & Xaba, P. S. (2016). Production, characterization and flocculation mechanism of bioflocculant TMT-1 from marine *Bacillus pumilus* JX860616. *African Journal of Biotechnology*, 15, 2352-2367.
- Mannina, G., Presti, D., Montiel-Jarillo, G., & Suárez-Ojeda, M. E. (2019). Bioplastic recovery from wastewater: A new protocol for polyhydroxyalkanoates (PHA) extraction from mixed microbial cultures. *Bioresource Technology*, 282, 361-369. <https://doi.org/10.1016/j.biortech.2019.03.037>.
- Moshood, T.D., Nawanir, G., Mahmud, F., Mohamad, F., Ahmad, M.H., Ghani, A.A. (2022). Sustainability of biodegradable plastics: New problem or solution to solve the global plastic pollution?. *Current Research in Green and Sustainable Chemistry*, 5, 100273. <https://doi.org/10.1016/j.crgsc.2022.100273>
- National Technical Regulation on Industrial Wastewater. (2011). QCVN 40:2011/BTNMT. Retrieved from <https://emas.tdtu.edu.vn/sites/emas/files/EMAS/V%C4%83n%20b%E1%BA%A3n%20ph%C3%A1p%20lu%E1%BA%ADt/qcvn-40-n%C6%B0%E1%BB%9Bc-th%E1%BA%A3i-cn.pdf>
- Ncube, L. K., Ude, A. U., Ogunmuyiwa, E. N., Zulkifli, R., & Beas, I. N. (2021). An overview of plastic waste generation and management in food packaging industries. *Recycling*, 6(1), 12. <https://doi.org/10.3390/recycling6010012>.
- Nwodo U.U., Makapela B., Okaiyeto K., Ntozonke N., Green E., Mabinya L.V., and Okoh A.I. (2016). Assessment of *Bacillus pumilus* isolated from freshwater milieu for bioflocculant production. *Applied Sciences*, 6, 211-231.
- Obebe, S. B., & Adamu, A. A. (2020). Plastic pollution: causes, effects and preventions. *International Journal of Engineering Applied Sciences and Technology*, 4(12), 85-95.
- Pradhan, S., Dikshit, P. K., & Moholkar, V. S. (2018). Production, ultrasonic extraction, and characterization of poly (3-hydroxybutyrate) (PHB) using *Bacillus megaterium* and *Cupriavidus necator*. *Polymers for Advanced Technologies*, 29 (8), 2392-2400. <https://doi.org/10.1002/pat.4351>.
- Schulthess, B., Ledermann, R., Mouttet, F., Zbinden, A., Bloemberg, G. V., Böttger, E. C., & Hombach, M. (2014). Use of the Bruker MALDI Biotyper for identification of molds in the clinical mycology laboratory. *Journal of Clinical Microbiology*, 52(8), 2797-2803. <https://doi.org/10.1128/JCM.00049-14>.
- Seo, J. K., Park, T. S., Kwon, I. H., Piao, M. Y., Lee, C. H., & Ha, J. K. (2013). Characterization of cellulolytic and xylanolytic enzymes of *Bacillus licheniformis* JK7 Isolated from the Rumen of a Native Korean Goat. *Asian-Australasian Journal of Animal Sciences*, 26 (1), 50-58. <https://doi.org/10.5713/ajas.2012.12506>
- Shamala, T. R., Divyashree, M. S., Davis, R., Kumari, K. S., Vijayendra, S. V. N., & Raj, B. (2009). Production and characterization of bacterial polyhydroxyalkanoate copolymers and evaluation of their blends by fourier transform infrared spectroscopy and scanning electron microscopy. *Indian Journal of Microbiology*, 49(3), 251-258. <https://doi.org/10.1007/s12088-009-0031-z>.
- Singh, G., Mittal, A., Kumari, A., Goel, V., Aggarwal, N. K., & Yadav, A. (2011). Optimization of poly-β-hydroxybutyrate production from *Bacillus* species. *European Journal of Biological Sciences*, 3(4), 112-116.
- The World Bank. (2022). Towards a national single use plastics roadmap in Vietnam: strategies and options for reducing priority single-use plastics. Retrieved from <https://www.worldbank.org/en/country/vietnam/publication/towards-a-national-single-use-plastics-roadmap-in-vietnam-strategies-and-options-for-reducing-priority-single-use-plasti>
- Thirumala, M., Reddy, S. V., & Mahmood, S. K. (2010). Production and characterization of PHB from two novel strains of *Bacillus* spp. isolated from soil and activated sludge. *Journal of Industrial Microbiology and Biotechnology*, 37(3), 271-278. <https://doi.org/10.1007/s10295-009-0670-4>.
- Vahabi, H., Michely, L., Moradkhani, G., Akbari, V., Cochez, M., Vagner, C., Renard E., Saeb R. M., & Langlois, V. (2019). Thermal stability and flammability behavior of poly (3-hydroxybutyrate) (PHB) based composites. *Materials*, 12(14), 2239. <https://doi.org/10.3390/ma12142239>.
- Wang, J., & Yu, H. Q. (2006). Cultivation of polyhydroxybutyrate-rich aerobic granular sludge in a sequencing batch reactor. *Water Science and Technology: Water Supply*, 6(6), 81-87. <https://doi.org/10.2166/ws.2006.966>.



Journal of Experimental Biology and Agricultural Sciences

<http://www.jebas.org>

ISSN No. 2320 – 8694

Contraceptive efficacy and antioxidant potential of *Leptadenia reticulata* bark extracts in male albino rats

Nisha Kanwar¹ , Ravindra Singh Thakur² , Ram Prakash Saran^{1*} , Ashok Purohit¹ 

¹Department of Zoology, Faculty of Science, Jai Narain Vyas University, Jodhpur, Rajasthan, India, Pin code-342005

²Department of Forensic Science, Teerthanker Mahaveer University, Moradabad, Uttar Pradesh, India, Pin Code-244001

Received – November 12, 2022; Revision – March 12, 2023; Accepted – March 27, 2023

Available Online – April 30, 2023

DOI: [http://dx.doi.org/10.18006/2023.11\(2\).359.370](http://dx.doi.org/10.18006/2023.11(2).359.370)

KEYWORDS

Antioxidant

Contraceptive

Leptadenia reticulata (jivanti)

Testosterone

Spermatozoa

ABSTRACT

Birth control measures available are primarily for women which are hormonal supplements that are increasing cancer risks and reproductive health issues. Male contraceptive options are effective and available, i.e. barrier methods and vasectomy. Condoms are failure-prone and single-use, while a vasectomy is a permanent sterilization method done surgically, and reversion is not always successful and expensive. A promising oral male contraceptive drug candidate is yet to be discovered. This study investigated the contraceptive efficacy and antioxidant potential of various extracts of *Leptadenia reticulata* bark in male rats. To study the effects of various extracts (ethanolic and petroleum ether) of *L. reticulata* bark in male rats, oral administration at the dose level of 250 mg/kg body weight/ day was done for 60 days. Observations were made for body and organ weight, hematology, serum biochemical chemistry, testosterone and antioxidants, lipid profile, sperm parameters (density and motility) and histological changes (reproductive organs). As compared to control in treated groups (TP and bark petroleum ether extract), a significant reduction ($P \leq 0.001$) was perceived in sperm motility and density, as well as reproductive organ weight, serum testosterone, and serum antioxidant parameters like SOD. Histological observations revealed arrest in spermatogenesis and reduced seminiferous tubule diameter, mature Leydig cells, secondary spermatogonia, and spermatids which caused a substantial increase in LPO and GSH. From the research findings, it can be concluded that bark petroleum ether extract of *L. reticulata* possesses contraceptive potential in male albino rats and can serve as a safe and reversible oral contraceptive for males.

* Corresponding author

E-mail: saranrp@live.com (Ram Prakash Saran)

Peer review under responsibility of Journal of Experimental Biology and Agricultural Sciences.

Production and Hosting by Horizon Publisher India [HPI]
(<http://www.horizonpublisherindia.in/>).
All rights reserved.

All the articles published by [Journal of Experimental Biology and Agricultural Sciences](#) are licensed under a [Creative Commons Attribution-NonCommercial 4.0 International License](#) Based on a work at www.jebas.org.



1 Introduction

The present hunt or pursuit for safe oral contraception for the male is continued since ancient times (Jain et al. 2013). In family planning programs, the first choice is female contraceptive measures which are harmful. Furthermore, all of the methods tested to use for males as spermicides entering the cervix or infertility inducers, were also ineffective and unsafe. As a result, several scientists are evaluating alternative and complementary medicine to lower these adverse effects (Hifnawy et al. 2021). Male contraceptives are relatively less used and are few as compared to females. Primary contraceptive methods are classified into two groups, i.e. Traditional and Modern. Traditional male contraceptive methods include withdrawal and periodic abstinence. Modern techniques involve sterilization (vasectomy) and barrier methods (condoms). These methods account for 8.9% (United Nations, World Contraceptive Use 2009). Till date in market not a single oral male contraceptive is brought, despite of continuous efforts and experimental trials are done to introduce pharmacological agents and hormonal chemicals.

Due to side effects, irreversibility and incomplete efficacy of the results in most cases total arrest in spermatogenesis was observed (Kogan and Wald 2014). Present contraceptive methods for males have numerous adverse effects and unwanted pregnancies, which are rising at an unacceptable rate (Montaserti et al. 2007; Mishra et al. 2009). Many chemicals used in agriculture, such as pesticides, insecticides, herbicides and fertilizers, negatively affect fertility. They tend to have total arrest in the spermatogenesis process which is irreversible (El-Kashoury et al. 2009). Male contraception due to these adverse effects remains unacceptable worldwide (Beckman and Harvey 1996; Moore et al. 1996). Thus, the challenge is to search for a safe, reversible, and effective male contraceptive drug with the least negative impact. Due to the great benefit of health, plants and folk medicines have consistently been acclaimed. Nowadays, plants are safe sources of medications. Many plant extracts have been accessed concerning both the male and female antifertility potential. Various plant extracts exert different effects like reduction in sperm counts, altering mobility of sperm and bringing spermicidal reaction (Singh and Singh 2009). Some others can produce changes in hormonal levels, and some can make changes in the testis (Reddy et al. 1997). Many plant metabolites such as saponins, phenolic acids, steroids, flavonoids and alkaloids showed antifertility activity (Siddiqui et al. 1978; Chakravarty et al. 2003; Russo and Borrelli 2005; Manthri et al. 2011). Developing fertility control methods for males can achieve immense social and health benefits. Worldwide numerous medicinal plants with antifertility activities are reported. Still, hardly any contraception has been processed from extracts of plants, which is due to an inaccurate determination of their activities, and insufficient knowledge of the extract's active fraction and mode of action (Ghosh et al. 2002).

Leptadenia reticulata belonging to the family Apocynaceae, is one of the desert plants which might have antifertility potential but has still not been evaluated. Species of *Leptadenia* are mostly economically valued as they have therapeutic properties. According to Sivarajan and Balachandran (1994), this plant possesses lactogenic, rejuvenating and revitalizing properties. Chemical components reported in *L. reticulata* include terpenoids, phenolics, flavonoids, and esters. Qualitative tests revealed that the aerial part of the plant has terpenoids, alkaloids, sterols, tannin, saponins, flavonoids, carbohydrates and glycosides (Verma and Agarwal 1962; Pal et al. 2012; Hewageegana et al. 2014). *L. reticulata* has been reported to have Antianaphylactic, Antiasthmatic, Antimicrobial, Antioxidant, Anti proliferative, Hepatoprotective Potential, Anticancerous, Anti-Implantation, Antidepressant, Antiulcer, Antimalarial, Antiabortifacient, Anti-Implantation, Aphrodisiac and Anti-Inflammatory activities (Mohanty et al. 2017). It has been claimed that this plant has anti-implantation and anti-abortifacient properties in females. However, despite its use in herbal remedies for boosting fertility with other herbal plants, which lacks scientific support, its antifertility activity for males is yet to be evaluated. This study aimed to determine the antifertility capacity of *L. reticulata* bark extract, which might help find novel male oral contraceptives.

2 Materials and Methods

2.1 Collection of plant sample, identification and authentication

Bark of *L. reticulata* was collected from AFRI (Arid Forest Research Institute), Jodhpur, Rajasthan, India and was identified and verified by an expert at the Botanical Survey of India, Jodhpur with authentication number BSI/ AZRC/ I.12012/ Tech./ 2021-22 (PI-Id.). Samples were preserved in the BSI department for future reference.

2.2 Extract preparation

The bark of *L. reticulata* was air-dried in the shade to reduce the moisture content. Dried bark was finely ground to powder using a grinder, and 200 g of bark powder was mixed with 800 ml of ethanol (99.9%) and petroleum ether (40-60%) each. These mixtures were subjected to soxhlet extraction apparatus separately for 32 hours. To avoid sticking material in the flask bottom intermittent shaking was done. After 32 hours, the solution was filtrated using a muslin cloth, and the obtained filtrate was subjected to evaporation under reduced pressure to get a semi-solid paste of extracts. The extracted materials were weighed and stored at -4°C in sterile, airtight containers. These extracts were used to treat male albino rats. To prepare extracts for phytochemical assessment, sheets of Whatman No. 1 filter paper or extraction thimbles were used. The extraction apparatus' sample tube was inserted with a thimble filled with the bark powder. The bottom flask of the apparatus was filled with the solvent, and the unit was

then operated at the solvent's boiling temperature. The device was run until colourless solvent entered the syphon tube. To obtain the crude extract, the solvent was evaporated at reduced pressure (Sasikala and Kannikaparameswari 2023).

2.3 Phytochemical screening

Freshly prepared ethanolic and petroleum ether bark extract samples were sent to CDRI, Lucknow, for quantitative analytical analyses to identify various phytochemical components.

2.4 Maintenance of experimental animals

For the current investigation, albino rats, both male and female, weighing 150 - 200 g, were used. The experimental animals were kept in standard temperature conditions of 23 ± 2 °C with 12-hour cycles of light and darkness. Before the onset of experiments, the animals were acclimated for seven days. For this, these experimental animals were kept inside animal houses in sanitized polypropylene cages that contained water bottles. Standard pellets and unrestricted access to water were available as a base diet. The Institutional ethical committee (IAEC) Reg. No. JNVU/IAEC/2020/03 approved all the experimental work conducted for this research, and guidelines from CPCSEA (Committee for the Purpose of Control and Supervision of Experiments on Animals), The Government of India, were followed for animal handling. The veterinary advisor regularly supervised animals.

2.5 Physiological dose determination

Using the fixed-dose method described by Walum (1998), the LD50 (Lethal dose) was calculated. The dosage given was 250 mg/kg body weight for 60 days. Different bark extracts of *L. reticulata* were given by an oral route in the morning before 11 A.M. every day, and at the dose level of 0.01 mg/day, intramuscular injections of TP were given for 30 days to male albino rats.

2.6 Fertility test of male albino rats

Before administering extracts, rats were subjected to a fertility test that involved pairing up healthy male and female rats in a 3:1 ratio in individual cages for 5–6 days, i.e., 1 adult male with 3 adult females in a cage. Every female underwent a vaginal smear test for 5–6 days to check for the presence of sperm. Fertile males were identified by this test and used for this experiment.

2.7 Treatment protocol

Fertile and healthy albino male rats weighing 150 - 200 grams were used as model organisms. Five groups of animals were made; each group had five animals in duplicate. Group I

(Control): Animals were fed a regular diet and given 2ml distilled water/day for 30 days. Group II: Testosterone propionate (TP) at 0.01 mg/day intramuscularly was given for 30 days. Group III: *L. reticulata* ethanolic extract of bark was orally administered to male albino rats at a dose level of 250 mg/Kg body weight/day dissolved in 2ml distilled for 60 days. Group IV: Petroleum ether extract of *L. reticulata* bark was orally administered for 60 days at the dose level of 250 mg/Kg body weight/day dissolved in 2ml distilled water to male albino rats. Group V: Petroleum Ether extract of bark was orally given at the dose level of 250 mg/Kg body weight/day dissolved in 2ml distilled water for 30 days and intra-muscular injections of TP at a dose level of 0.01 mg/day for 30 days were given to male albino rats. A standard diet was fed in all experimental groups throughout the experimental period.

2.8 Scheduling autopsy

Overnight fasted animals under mild anaesthesia were autopsied after completion of the experiment on the 30th and 60th day of treatments. Blood samples were collected using a clean and dry syringe via puncturing left ventricle and kept in both regular and EDTA-coated test tubes for the haematological, serum biochemistry, lipid profile, and antioxidant studies. For the separation of serum, centrifugation of blood for 15 minutes was done at 3000 rpm. For histological examination, all the vital organs (heart, kidney and liver) and reproductive organs (testes, cauda, caput, ventral prostate, vas deference and seminal vesicle) were dissected out, normal saline was used to clean the dissected organs, and 10% formalin was used to fix the tissues. It was further processed for histological slide preparations.

2.9 Body and reproductive organ weight determination

The initial and final body weight was weighed and recorded for all experimental animals. All vital and reproductive organs' weights were recorded after dissecting organs, removing extra tissues adhered to organs and cleaning them with saline.

2.10 Sperm motility and density

For this study, testes and epididymides were taken. After blood collection, epididymides immediately was separated, and cauda was taken for sperm motility and density (Prasad et al.1972).

2.11 Serum biochemistry

Serum total protein, globulin, albumin, urea, uric acid, creatinine, bilirubin and liver marker enzymes like SGOT (serum glutamic oxaloacetic transaminase), SGPT (serum glutamic pyruvic transaminase) and ALP (alkaline phosphatase) were estimated by using standard commercial kits.

2.12 Hematological parameters

Hematological parameters such as HB (Hemoglobin), HCT (hematocrit), TRBC (total red blood cells), MCV (mean corpuscular volume), MCHC (mean corpuscular hemoglobin concentration), PLT (platelet (thrombocyte) count), TLC (total leukocytes count), PCT (procalcitonin test), MPV (mean platelet volume), RDW (red cell distribution width) and PDW (platelet distribution width) of blood samples were determined by using standard kits.

2.13 Lipid profile

Standard commercial kits were used for total serum cholesterol, VLDL (Very-low-density lipoprotein), HDL (high-density lipoprotein), LDL (low-density lipoprotein) and triglyceride estimation

2.14 Estimation of hormonal level

The Enzyme Immuno Assay method (EIA) was used for the determination of serum testosterone levels by using a commercial kit available.

2.15 Organ Histopathology

The vital (liver, kidney, heart) and reproductive organs (testes, cauda, caput, ventral prostate, vas deference and seminal vesicle), after fixation in 10% formalin, were dehydrated in successive grades of alcohol and then rinsed with xylene. Molten paraffin wax was used for embedding tissues. Microtome was used for cutting sections at a thickness of 5 μm , and for staining sections, hematoxylin and eosin were used. The slides were observed under a light microscope at 200 and 400 X magnifications for histopathological changes, especially in the reproductive organs. ImageJ software was used for testicular cell population counting or histometry of histological slides with the help of protocol given by Abercrombie (1946) and Dixon and Massey (1957).

2.16 Estimation of Antioxidant

2.16.1 SOD (Superoxide Dismutase)

SOD assay was carried out by the pyrogallol autoxidation protocol described by Marklund and Marklund (1974).

2.16.2 Catalase

In the presence of Catalase, the decomposition of H_2O_2 was estimated by Aebi (1984).

2.16.3 LPO (Lipid Peroxidation)

LPO was carried out following the procedure outlined by Ohkawa et al. (1979).

2.16.4 FRAP (ferric reducing antioxidant power assay or the ferric reducing ability of plasma)

FRAP assay was executed using a modified approach of Benzie and Strain (1996).

2.16.5 GSH (Glutathione)

GSH levels in serum were estimated based on the method given by Beutler et al. (1963).

2.17 Statistical analysis

One-way analysis of variance (ANOVA) was used to assess the data, after which Tukey's multiple comparison tests were conducted. Data analysis was done statistically using a graph pad prism.

3 Results and Discussions

The challenge is to search for a safe, effective, reversible oral contraceptive for the male. Humans use plants to improve health because of their lengthy folk uses, ensuring their safe use. Also, plant-based products are readily assessable, cost-friendly, and have negligible side effects. Recently, plant research for their medicinal use and properties, i.e., ethnobotanical information, has gained attention (Heinrich 2000). The present study assessed the antifertility activity of *L. reticulata* bark extract in male albino rats.

3.1 Extraction

Soxhlet extraction was carried out using ethanol and petroleum ether as solvents, and the percentage extraction yield for bark was 2.33% in ethanolic and 2.02% in petroleum ether. *Boerhaavia diffusa* and *Achyranthes aspera* root powder was used for the soxhlet extraction procedure with different solvents by Sasikala and Kannikaparameswari (2023) and recorded a 24 % yield from the *A. aspera* root ethanolic extract while in case of petroleum ether extract, it was recorded 17 %. Further, in the case of *B. diffusa*, the yield of ethanolic root extract was recorded at 26 %, while it was recorded at 13% in the case of petroleum ether extract. This yield is relatively high than the yield of *L. reticulata* bark extract.

3.2 Phytochemical screening

Bark extracts disclosed the presence of carbohydrates, starch, glycosides, protein, phytosterols, flavonoids, terpenoids, tannins, phenolic compounds and alkaloids. Three species of the family Asclepiadaceae (*Peruglaria tomentosa* L., *Pentatropis spiralis* (Forsk.) and *Calotropis procera* L.) were examined for phytochemistry from their crude extracts. Glycosides, alkaloids, saponins, tannins, terpenoids and flavonoids were found in the extracts after the phytochemical screening (Al-Dalalmeh et al.

2022). These constituents are quite similar to the reports of the present study.

3.3 Effect on body weight and reproductive organs weight

Rats administered with *L. reticulata* bark extract showed no noticeable changes in body weights. However, a noticeable reduction ($P \leq 0.05$) was noticed in the weight of the treated group's reproductive organs, such as testes, seminal vesicles, and epididymides, in comparison to the control (Table 1). A highly significant reduction was observed in groups II and IV. Results agree with the findings of Sharma et al. (2022) those, who recorded the antispermatogenic activity of *Momordica dioica* methanolic root extract. The weight of the testes significantly decreased after oral administration of the *M. dioica* methanolic root extract at a dose level of 50 mg/kg body weight/day ($p < 0.05$), although there was no discernible alteration in body weight or epididymis weight.

3.4 Effect on serum biochemistry and hematological parameters

Hematology and biochemical indicators showed no difference between the treated and the control groups after the oral administration of *L. reticulata* bark extracts. All results were found in the normal range. The non-toxic effect of the orally administered extract on the body's general metabolism is reflected

by non-significant changes in serum biochemistry and haematology (Sripriya et al. 2011).

3.5 Effect on lipid profile

The orally fed bark extract of *L. reticulata* caused a marginal increase in lipid profile components like LDL, VLDL, HDL triglyceride and total cholesterol of control and treated groups. However, the increase remains statically insignificant in the amount of these components. Impairing in spermatogenesis results due to low androgen concentration. Increased cholesterol levels interfere with steroidogenesis in the testes (Agarwal et al. 2009). Steroidogenesis is affected by the increased cholesterol, while the increase observed was marginal, which may not have negatively impacted the androgen synthesis.

3.6 Effect on sperm motility and density

L. reticulata bark extract-fed rats showed decreased sperm parameters (testes and epididymides). Highly convincing ($P \leq 0.001$) falls in sperm motility and density (Table 2) were observed in group II and group IV as compared to the control group, and a significant increase in group V as compared to group II. It is a general fact that the fertilization capability of sperm is influenced by sperm motility (Amelar et al. 1980). A significant reduction in sperm motility and density of *L. reticulata* bark extract treated

Table 1 Body and Reproductive organ weight of various Bark extracts of *Leptadenia reticulata* treated male albino rats

TREATMENT GROUPS	Body Weight (gm)		Reproductive Organ Weight (gm/100gm Body Weight)			
	Initial	Final	Testes	Seminal Vesicle	Epididymis	Ventral prostate
Group I (Intact Control)	195.74±3.45	200.03±1.87	1198.36±4.95	698.32±3.24	480.18±4.03	256.83±6.98
Group II (TP)	163.91±5.57	186.13±3.42	828.24±2.49 ^c	460.57±7.29 ^c	372.24±2.83 ^c	169.86±2.19 ^c
Group-III (Bark Ethanolic)	197.66±11.15	207±7.93	1051.39±44.30 ^{h,g}	557.43±37.50 ^{c,f}	430.01±33.50 ^{a,e}	206.92±16.23 ^{b,f}
Group-IV (Bark Petroleum Ether)	176±8.54	196.66±6.11	811.14±19.24 ^{c,h}	410.87±39.52 ^{c,e}	360.08±31.46 ^{c,h}	165.15±9.64 ^{c,h}
Group-V (Bark Petroleum Ether + TP)	224.48±11.68	244.92±13.97	990.10±72.99 ^{b,f}	422.84±28.91 ^{c,e}	460.09±20.53 ^{d,g}	238.20±20.70 ^{d,f}

Gr. II to IV compared with Gr. I: $P \leq 0.05 = a$, $P \leq 0.01 = b$, $P \leq 0.001 = c$, Non-significant = d; Gr. III & IV compared with Gr. II: $P \leq 0.05 = e$, $P \leq 0.01 = f$, $P \leq 0.001 = g$ Non-significant = h

Table 2 Sperm dynamics of various Bark extracts of *Leptadenia reticulata* treated male albino rats

TREATMENT GROUPS	SPERM MOTILITY (%)	SPERM DENSITY	
		CAUDA (million/ml)	TESTES (million/ml)
Group I (Intact Control)	86.06±3.24	68.01±0.97	4.6±0.32
Group II (TP)	15.12±0.91 ^c	14.72±1.41 ^c	1.16±0.30 ^c
Group-III (Bark Ethanolic)	79.35±1.62 ^{a,g}	42.13±2.50 ^{ca,g}	4.83±0.67 ^{d,g}
Group-IV (Bark Petroleum Ether)	10.32±0.99 ^{c,h}	4.44±0.40 ^{c,g}	0.78±0.02 ^{c,h}
Group-V (Bark Petroleum Ether + TP)	68.68±3.22 ^{b,g}	54.46±4.82 ^{b,g}	3.30±0.43 ^{a,g}

Gr. II to IV compared with Gr. I: $P \leq 0.05 = a$, $P \leq 0.01 = b$, $P \leq 0.001 = c$, Non-significant = d; Gr. III & IV compared with Gr. II: $P \leq 0.05 = e$, $P \leq 0.01 = f$, $P \leq 0.001 = g$ Non-significant = h

Table 3 Histometrical Parameters of Testes and Epididymides of various Bark extracts of *Leptadenia reticulata* treated male albino rats

TREATMENT GROUPS	Seminiferous Tubule Diameter (μm)	Epithelial Cell Height (μm)	
		Caput	Cauda
Group I (Intact Control)	260.93 \pm 10.31	39.20 \pm 3.64	29.58 \pm 0.61
Group II (TP)	150.45 \pm 4.93 ^c	30.34 \pm 0.88 ^a	21.03 \pm 1.48 ^c
Group-III (Bark Ethanolic)	206.59 \pm 16.64 ^{b,f}	33.93 \pm 3.32 ^{d,h}	27.48 \pm 2.08 ^{d,e}
Group-IV (Bark Petroleum Ether)	144.96 \pm 8.37 ^{c,h}	26.39 \pm 2.44 ^{b,e}	19.93 \pm 1.56 ^{c,h}
Group-V (Bark Petroleum Ether + TP)	245.50 \pm 16.94 ^{d,g}	30.85 \pm 2.21 ^{a,h}	23.90 \pm 1.84 ^{b,h}

Gr. II to IV compared with Gr. I: $P \leq 0.05 = a$, $P \leq 0.01 = b$, $P \leq 0.001 = c$, Non-significant = d; Gr. III & IV compared with Gr. II: $P \leq 0.05 = e$, $P \leq 0.01 = f$, $P \leq 0.001 = g$ Non-significant = h

groups was observed. A highly significant decrease was observed in bark petroleum ether extract, and reversibility of this reduction was observed in the combinational treatment of this extract with TP (Testosterone propionate). Reduction in male rat sperm motility after the extract administration may be due to the reduction in ATPase and succinate dehydrogenase levels (Rao 1987). Or it may be due to increased membrane fluidity and destruction of sperm membrane by lipid peroxidation, which results in cell apoptosis by damaging DNA by inactivating the membrane channels, proteins and enzymes (Oborna et al. 2009).

3.7 Effect on histopathology

After treatment with *L. reticulata* bark extracts, the main effect on histology was observed in reproductive organs. Seminiferous tubules were observed with degenerative changes such as arrest in spermatogenesis, highly convincing ($P \leq 0.001$) reduction in seminiferous tubule diameter and a denoting reduction in the secretion of ventral prostate and seminal vesicle (Table 3). The reduction was highly significant ($P \leq 0.001$) in correlation to control, especially in groups II and IV, while a notable increase in

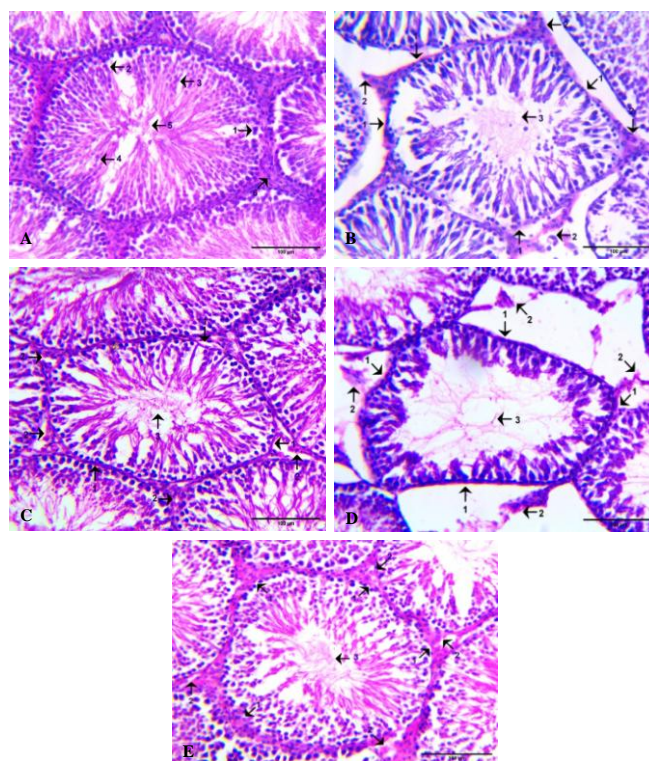


Figure 1 Microphotographs of different groups Testes; A. Control male albino rat Testes labeling showing various spermatogenesis stages used for histometry 1. Spermatogonia; 2. Primary Spermatocyte; 3. Secondary Spermatocyte; 4. Spermatid; 5. Lumen filled with spermatozoa; 6. Leydig Cells; HE, 200 \times ; B. TP- Testosterone propionate, C. Bark Ethanolic and D. Bark Petroleum Ether Extract treated male albino rat testes labeling showing: 1. Reduction in diameter of seminiferous tubule; 2. Reduction in leydig cells; 3. Leumen with reduced spermatozoa; HE, 200 \times . E. TP + Bark Petroleum Ether Extract treated male albino rat Testes labeling showing 1. Recovering diameter of seminiferous tubule; 2. Regenerating leydig cells; 3. Leumen with increased spermatozoa (HE, 200 \times)

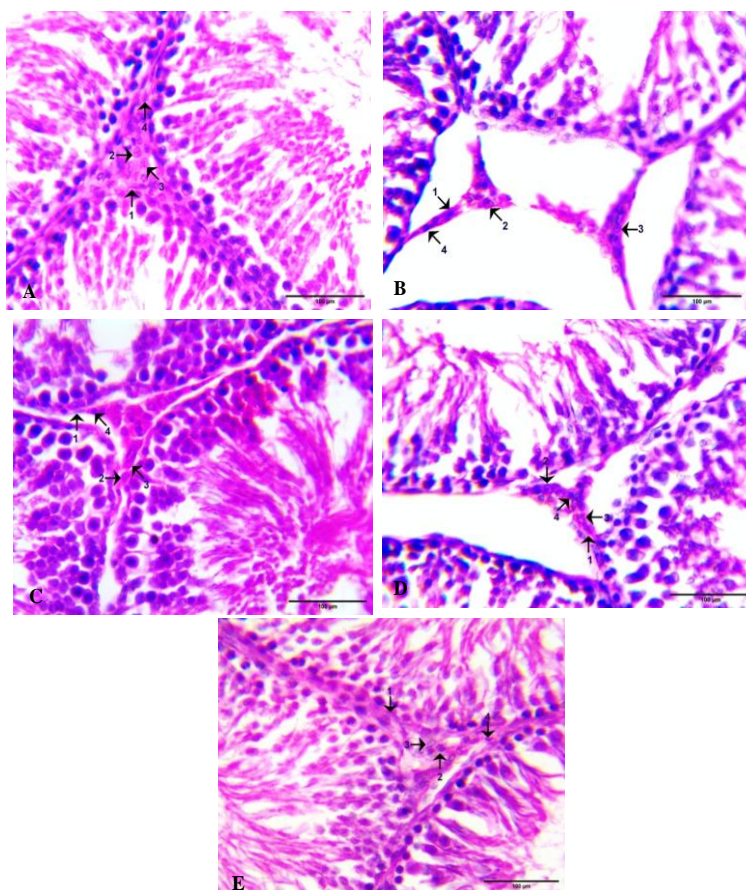


Figure 2 Microphotographs of interstitial cells of different groups: A. Control (Group I), B. TP-Testosterone propionate (Group II), C. Bark Ethanolic Extract (Group III), D. Bark Petroleum Ether Extract (Group IV) & E. TP + Bark Petroleum Ether Extract (Group V) labeling showing: 1. Fibroblast Cells; 2. Immature Leydig Cells; 3. Mature Leydig Cells; 4. Degenerating Cells (HE, 400 \times)

these parameters of group V as compared to group II was observed (Figures 1 and 2). In the present investigation, orally administered bark extract of *L. reticulata* reduced the weight of reproductive organs. Reduction in testes and seminiferous tubule diameter reflects damage or degenerative changes in these organs. In assessing spermatogenesis, the first way is to assess the testicular size because approximately 98% of testis mass comprises tubules and germinal cells (Keel and Abney 1980). Degenerative changes in the testis, epididymis, vas deferens and disintegration of Leydig cells reflect anti-androgenic activity (Rajan et al. 2013).

3.8 Effect on testicular cell population

The bark extract of *L. reticulata* treatment significantly ($P \leq 0.001$) reduced the secondary spermatogonia, spermatids, and mature Leydig cells and significantly ($P \leq 0.001$) increased in degenerative cells (Table 4). Compared to the control, the reduction in groups II and IV was highly significant, while a significant increase was noticed in these parameters in group V

(Figures 1 and 2). The diameter of the seminiferous tubule, testicular and Leydig cell population dynamics were significantly reduced by *L. reticulata* bark extract. Compared to an ethanolic extract of bark, reduction in testicular and Leydig cell population was more significant in petroleum ether extract of bark. The reduction was more prominent in the secondary spermatocytes, spermatids and mature leydig cells. Reduction in diameter and surface area of the seminiferous tubule is attributed to steroids (De Souza et al. 2017). Atrophy of seminiferous tubules might be caused due to reduction in FSH and testosterone levels, which is a causative agent in surface area and the reduction of seminiferous tubule diameter. The number of germ cells in the testes is affected by spermatogenesis disruption. Increased lumen surface area and reduction in spermatogenic cells in seminiferous tubules lead to morphological changes (Yama et al. 2011). The primary source for androgens or steroidogenesis is leydig cells in the interstitial area of seminiferous tubules (Shima et al. 2013). Degenerative changes in leydig cells may be due to a decline in LH secretion (Nair et al. 1995).

Table 4 Testicular Cell Population Dynamics of various Bark extracts of *Leptadenia reticulata* treated male albino rats

TREATMENT GROUPS	Germinal Cell Type					Interstitial Cell Type		
	Spermatogonia	Primary Spermatoocytes	Secondary Spermatoocytes	Spermatids	Fibroblast Cells	Immature Leydig Cells	Mature Leydig Cells	Degenerating Cells
Group I (Intact Control)	46.19±1.52	35.21±3.51	86.67±4.50	148.26±2.15	60.65±3.21	50.43±1.52	72.36±2.51	17.29±1.52
Group II (TP)	36.36±2.51 ^b	33.28±1.52 ^d	41.38±3.51 ^c	29.97±2.51 ^c	54.66±3.05 ^d	40.53±4.50 ^a	41.71±1.52 ^c	64.47±2.51 ^c
Group-III (Bark Ethanolic)	41.92±2.32 ^{a,e}	29.52±0.84 ^{a,h}	78.77±1.75 ^{d,g}	138.86±4.16 ^{a,g}	62.85±3.33 ^{d,e}	46.28±1.49 ^{a,h}	59.67±3.25 ^{b,g}	32.14±2.41 ^{c,g}
Group-IV (Bark Petroleum Ether)	32.93±1.70 ^{c,h}	29.93±2.14 ^{a,h}	38.91±0.46 ^{c,h}	25.98±1.49 ^{c,h}	55.5±2.42 ^{d,h}	43.16±1.83 ^{b,h}	39.8±3.54 ^{c,h}	61.83±3.31 ^{c,h}
Group-V (Bark Petroleum Ether + TP)	41.89±1.86 ^{a,e}	32.96±2.11 ^{d,h}	78.61±3.49 ^{d,g}	139.33±4.75 ^{a,g}	60.30±1.96 ^{d,e}	49.39±2.06 ^{d,e}	65.98±2.32 ^{d,g}	25.66±1.95 ^{c,g}

Gr. II to IV compared with Gr. I: P ≤ 0.05= a, P ≤ 0.01= b, P ≤ 0.001 = c, Non-significant = d; Gr. III & IV compared with Gr. II: P ≤ 0.05= e, P ≤ 0.01 = f, P ≤ 0.001= g Non- significant = h

3.9 Effect on serum testosterone level

Compared to the control, *L. reticulata* bark extract significantly (P 0.001) decreased serum testosterone levels in all treated groups (Figure 3). This reduction was highly significant in groups II and IV. However, group V showed a considerable increase as compared to group II. A primary and representative androgen that controls the progression of spermatogenesis is testosterone (Turner et al. 1984).

Decreased testosterone levels may cause alteration in cell signalling, DNA repair, apoptosis, metabolism, RNA processing and meiosis; this might result from testosterone requirement in male germ cells development and maturation (Stanton et al. 2012). Significant reduction in serum testosterone was noticed in bark extract administered groups, possibly due to decreased mature leydig cells (Gupta et al. 2011), and the restoration of serum testosterone was observed in TP combined with the extract.

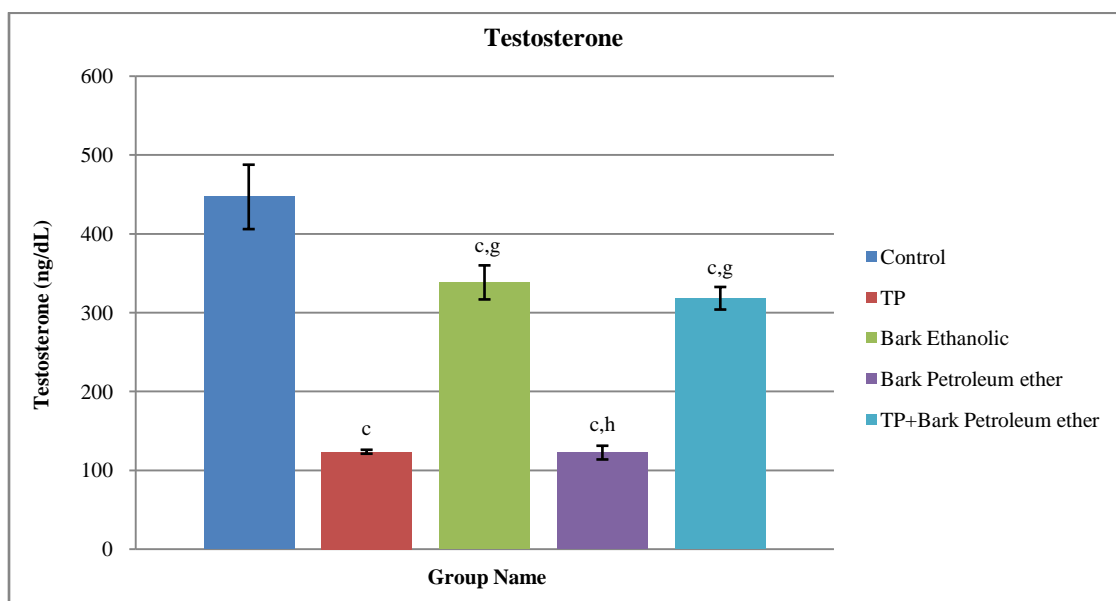


Figure 3 Effect on serum testosterone level in male albino rats after oral administration of bark extracts of *L. reticulata*. Data was expressed in Mean ± SD. Error bars are representing SD of Mean and superscripts denoting significance level.

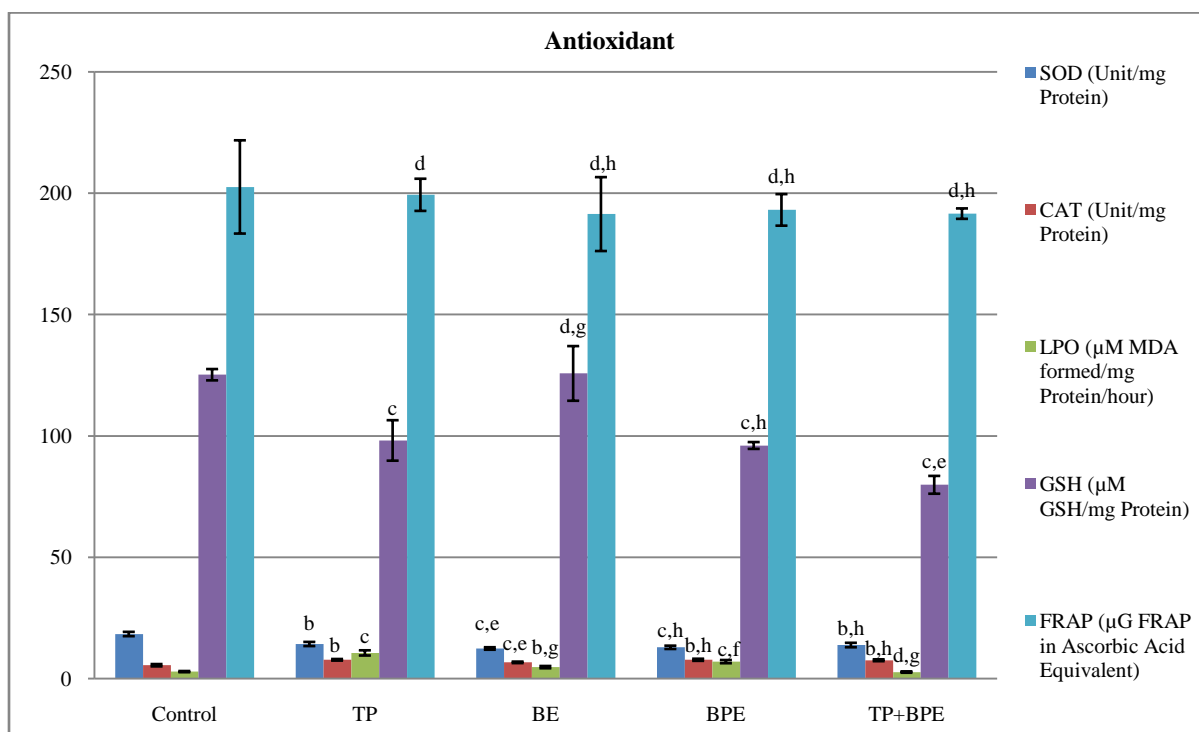


Figure 4 Effect on serum antioxidant assay in male albino rat after oral administration of *Leptadenia reticulata* bark extracts (Sod, Catalase, LPO, GSH and FRAP). Data was expressed in Mean \pm SD. Error bars are representing SD of Mean and superscripts denoting significance level. TP- Testosterone Propionate, BE- Bark Ethanolic extract, BPE- Bark Petroleum Ether extract and TP+BPE- Testosterone Propionate + Bark Petroleum Ether extract.

3.10 Effect on serum antioxidant level

Like other parameters, *L. reticulata* bark extract treatment significantly reduced ($P \leq 0.001$) SOD and GSH and significantly increased Catalase ($P < 0.01$) and LPO concentration ($P \leq 0.001$) in all groups except group III which resulted in no significant change as compared to control. While the FRAP assay produced negligible differences from the control (Figure 4). Low oxygen conditions in reproductive organs may scavenge the free radical-mediated damages as oxidative stress is one of the barriers in leydig cell steroidogenesis and spermatogenesis (Smith et al. 2007). Prevention of lipid peroxidation of plasma membrane involves Catalase, GSH and superoxide dismutase (SOD), which is involved in scavenging superoxide ions (Jeulin et al. 1989) and converts them into (H_2O_2) and molecular oxygen (O_2), which in turn are converted to H_2O and O_2 Catalase and GSH. These help in maintaining decreased levels of LPO.

Increased serum LPO levels were observed after the administration of *Cynoglossum zeylanicum* extracts. This may be due to a decreased antioxidant potential of extract as it has reduced SOD, Catalase and GSH levels (Anitha et al. 2013). In contrast, the present findings showed a significant decline in SOD but a marginal rise in Catalase, a significant decline in GSH, and an elevation in the serum status of LPO. Additionally, non-significant

change in the FRAP assay was seen in the treated groups of bark extracts, and serum antioxidant activity was restored in the treated group that had a combination of TP and bark petroleum ether extract. The increased levels of SOD, and Catalase, significant decreases in LPO and GSH, and non-significant changes in FRAP demonstrate the reversibility of the extract's effect on fertility. SOD, Catalase and GSH levels increase in serum, maintain antioxidant potential and decrease reactive oxygen species, which is reflected in LPO levels (Mruk et al. 2002). This contraceptive potential of bark extract is possible because of the different flavonoids, saponins and phenolic compounds in the extract.

It may be inferred that *L. reticulata* bark petroleum ether extract has an antifertility effect, most likely due to the degeneration of leydig cells responsible for maintaining testosterone levels in the blood. A possible mechanism for this contraceptive potential can be concluded that the drug (Extract) might have either blocked the maturation of leydig cells, i.e., the pathway of leydig cell development from immature leydig cell to mature leydig cell or the oxidative stress may have interfered with the leydig cell to produce testosterone level. Low testosterone level in the blood has affected the sertoli cells and spermatogenesis arrest, or the extract might have disturbed the testosterone synthesis pathway. Further investigation regarding *in silico* targeting the receptor and enzyme involved in testosterone synthesis is underway.

Conclusion

Bark petroleum ether extract of *L. reticulata* has significantly reduced the sperm motility, density, and testicular cell population dynamics, especially seminiferous tubule diameter, secondary spermatocytes, spermatids and mature leydig cells. Testosterone level was also significantly decreased after the extract administration. These parameters were recovered when the extract was provided in combination with TP, which shows reversibility of the extract's effect. It is obvious from the observations and results of the above research findings that the bark petroleum ether extract has contraceptive activity and can be used as a potent reversible herbal male oral contraceptive to regulate fertility without any side effects after extensive clinical trials.

Acknowledgement

The authors are grateful to the Head, Department of Zoology, Jai Narain Vyas University, Jodhpur, Rajasthan, India, for providing resources and amenities for the aforementioned research work. The authors are grateful to UGC (UGC-Ref. No.: 940/(CSIR-UGC NET DEC.2017) for financial support for our research work. We would like to express our gratitude to Dr. Heera Ram for his advice and assistance.

Conflict of Interest

No conflicts.

References

Abercrombie, M. (1946). Estimation of nuclear population from microtome section. *The anatomical record*, 94(2), 239-247.

Aebi, H. (1984). Catalase in Vitro. *Methods in enzymology*, 105, 121-126.

Agarwal, M., Chauhan, A., & Gehani, T. (2009). Investigation of the effects of *Myristica fragrans* oil on the reproductive organs of male albino rats (*Rattus norvegicus*). *Pharmaceutical Biology*, 47(6), 509-515.

Al-Dalahmeh, Y., Al-Bataineh, N., Al-Balawi, S. S., Lahham, J. N., et al. (2022). LC-MS/MS screening, total phenolic, flavonoid and antioxidant contents of crude extracts from three Asclepiadaceae species growing in Jordan. *Molecules*, 27(3), 859.

Amelar, R. D., Dubin, L., & Schoenfeld, C. (1980). Sperm motility. *Fertility and Sterility*, 34(3), 197-215.

Anitha, M., Sakthidevi, G., Muthukumarasamy, S., & Mohan, V. R. (2013). Evaluation of antifertility activity of ethanol extract of *Cynoglossum zeylanicum* (vehl ex hornem) thumb. ex lehm (boraginaceae) whole plant on male albino rats. *Journal of Current Chemical and Pharmaceutical Sciences*, 3(2), 135-145.

Beckman, L. J., & Harvey, S. M. (1996). Factors affecting the consistent use of barrier methods of contraception. *Obstetrics & Gynecology*, 88(3), 65S-71S.

Benzie, I., & Strain, J. (1996). The Ferric Reducing Ability of Plasma (FRAP) as a Measure of Antioxidant Power: The FRAP Assay. *Analytical biochemistry*, 239(1), 70-76.

Beutler, E., Duron, O., & Kelly, B. M. (1963). Improved method for the determination of blood glutathione. *Journal of Laboratory and Clinical Medicine*, 61, 882-888.

Chakravarty, A. K., Garai, S., Masuda, K., Nakane, T., & Kawahara, N. (2003). Bacopasides III-V: three new triterpenoid glycosides from *Bacopa monniera*. *Chemical and Pharmaceutical Bulletin*, 51(2), 215-217.

De Souza, B. R., Mathias, L. S., De Souza, T. L. M., & Camargo, I. C. C. (2017). Histopathological and morphometric evaluation in the testis and epididymis of adult rats submitted to a recovery period after treatment with anabolic steroid, alcohol, and/or nicotine. *Journal of Interdisciplinary Histopathology*, 5(3), 92-98.

Dixon, W., & Massey, F. J. (1957). *Introduction of statistical analysis*. New York, US: 2nd ed. McGraw Hill Book Co. Ubc.

El-Kashoury, A. A., Salama, A. F., Selim, A. I., & Mohamed, R. A. (2009). Animal Model Study of Reproductive Toxicity of the Chronic Exposure of Dicofol. *Life Science Journal*, 6(3), 1-18.

Ghosh, D., Jana, D., & Debnath, J. M. (2002). Effects of leaf extract of *Stephania hernandifolia* on testicular gametogenesis and androgenesis in albino rats: a dose-dependent response study. *Contraception*, 65(5), 379-84.

Gupta, R., Kachhawa, J. B., Gupta, R. S., Sharma, A. K., et al. (2011). Phytochemical evaluation and antispermatogenic activity of *Thevetia peruviana* methanol extract in male albino rats. *Human Fertility*, 14(1), 53-59.

Heinrich, M. (2000). Ethnobotany and its role in drug development. *Phytotherapy Research*, 14(7), 479-488.

Hewageegana, S. P., Arawwawala, M., Dhammaratana, I., Ariyawansa, H., & Tisser, A. (2014). Proximate analysis and standardization of leaves: *Leptadenia reticulata* (Retz) Wight and Arn (Jeevanti). *World Journal of Pharmaceutical Research*, 3(10), 1603-1612.

Hifnawy, M. S., Aboseada, M. A., Hassan, H. M., Tohamy, A. F., Naggar, E. I., & Abdelmohsen, U. R. (2021). Nature-inspired male contraceptive and spermicidal products. *Phytochemistry Reviews*, 20(4), 797-843.

- Jain, S., Choudhary, G. P., & Jain, D. K. (2013). Pharmacological Evaluation and Antifertility Activity of *Jatropha gossypifolia* in Rats. *BioMed Research International*, 2013. <https://doi.org/10.1155/2013/125980>
- Jeulin, C., Soufir, J. C., Weber, P., Laval-Martin, D., & Calvayrac, R. (1989). Catalase activity in human spermatozoa and seminal plasma. *Gamete research*, 24(2), 185-196.
- Keel, A. B., & Abney, T. O. (1980). Influence of Bilateral Cryptorchidism in the Mature Rat: Alterations in Testicular Function and Serum Hormone Levels. *Endocrinology*, 107(4), 1226-1233.
- Kogan, P., & Wald, M. (2014). Male contraception: history and development. *Urologic Clinics*, 41(1), 145-161.
- Manthri, S., Kota, C. S., & Talluri, M. (2011). Phytochemical and pharmacological review of *Dendrophthoe falcata*. *Journal of Phytology*, 3(3), 18-25.
- Marklund, S., & Marklund, G. (1974). Involvement of superoxide anion in autooxidation of pyrogallol and a convenient assay of superoxide dismutase. *European journal of biochemistry*, 47(3), 469-474.
- Mishra, N., Joshi, S., Tondon, V. L., & Munjal, A. (2009). Evaluation of Antifertility potential of aqueous extract of *Bougainvillea spectabilis* leaves in Swiss albino mice. *International Journal of Pharmaceutical Sciences and Drug Research*, 1(1), 19-23.
- Mohanty, S. K., Swamy, M. K., Sinniah, U. R., & Anuradha, M. (2017). *Leptadenia reticulata* (Retz.) Wight & Arn. (jivanti): Botanical, Agronomical, Pharmacological and Biotechnological Aspects. *Molecules*, 22(6), 1019.
- Montaserti, A., Pourheydar, M., Khazaei, M., & Ghorbani, R. (2007). Antifertility effects of *Physalis alkekengi* alcoholic extract in female rat. *Iranian Journal of Reproductive Medicine*, 5(1), 13-16.
- Moore, P. J., Adler, N. E., & Kegeles, S. M. (1996). Adolescents and the contraceptive pill: the impact of beliefs on intentions and use. *Obstetrics & Gynecology*, 88(3), 48S-56S.
- Mruk, D. D., Silvestrini, B., Mo, M. Y., & Cheng, C. Y. (2002). Antioxidant superoxide dismutase-a review: its function, regulation in the testis, and role in male fertility. *Contraception*, 65(4), 305-311.
- Nair, N., Bedwal, R. S., & Mathur, R. S. (1995). Effect of adrenalectomy and adrenalectomy + hydrocortisone treatment on histopathological, biochemical and zinc and copper profiles in rat testes. *Indian Journal of Experimental Biology*, 33(9), 655-663.
- Oborna, I., Wojewodka, G., De Sanctis, J., Fingerova, H., et al. (2009). Increased lipid peroxidation and abnormal fatty acid profiles in seminal and blood plasma of normozoospermic males from infertile couples. *Human reproduction*, 25(2), 308-316.
- Ohkawa, H., Ohishi, N., & Yagi, K. (1979). Assay for lipid peroxidation in animal tissues by thiobarbituric acid reaction. *Analytical biochemistry*, 95(2), 351-358.
- Pal, A., Sharma, P. P., Pandya, T. N., Acharya, R., et al. (2012). Phytochemical evaluation of aqueous extract of Jivanti (*L. reticulata*). *Ayu*, 33(4), 557-560.
- Prasad, M. R. N., Chinoy, N. J., & Kadam, K. M. (1972). Changes in succinate dehydrogenase levels in the rat epididymis under normal and altered physiological conditions. *Fertility and Sterility*, 23(3), 186-190.
- Rajan, T. S., Sarathchandiran, I., & Kadalmani, B. (2013). Evaluation of antifertility activity of herbal oral contraceptive suspension on male Wistar albino rats. *Journal of pharmacy research*, 7(4), 342-346.
- Rao, M. V. (1987). Antifertility effects of alcoholic seed extracts of *Abrus precatorious* linn. In male albino rats. *Acta europaea fertilitatis*, 18(3), 217-220.
- Reddy, C. M., Murthy, D. R., & Patil, S. B. (1997). Antispermatic and androgenic activities of various extracts of *Hibiscus rosa sinesis* in albino mice. *Indian Journal of Experimental Biology*, 35(11), 1170-1174.
- Russo, A., & Borrelli, F. (2005). *Bacopa monniera*, a reputed nootropic plant: an overview. *Phytomedicine*, 12(4), 305-317.
- Sasikala, S., & Kannikapameswari, N. A. (2023). Comparative Study on Phytochemical and *in Vitro* Antioxidant Activity of Herbal Formulation of *Achyranthes aspera* and *Boerhavia diffusa* Ethanolic Extracts. *Journal of University of Shanghai for Science and Technology*, 25(02), 102-117.
- Sharma, R., Lakhne, R., & Gupta, R. S. (2022). Antispermatic Activity of *Momordica Dioica* Methanolic Root Extract. *International Journal of Innovative Science and Research Technology*, 7(10), 1940-1945.
- Shima, Y., Miyabayashi, K., Haraguchi, S., Arakawa, T., et al. (2013). Contribution of Leydig and Sertoli cells to testosterone production in mouse fetal testes. *Molecular endocrinology*, 27(1), 63-73.
- Siddiqui, A., Naim, Z., & Siddiqui, B. A. (1978). Studies in the steroidal constituents of *Abrus precatorious* Linn. (scarlet variety). *Pakistan Journal of Scientific and Industrial Research*, 21(5-6), 158-161.

- Singh, A., & Singh S. K. (2009). Evaluation of antifertility potential of Brahmi in male mouse. *Contraception*, 79(1), 71–79.
- Sivarajan, V. V., & Balachandran, I. (1994). *Ayurvedic Drugs and Their Plant Sources*. Delhi, India: Oxford IBH Co. Pvt. Ltd.
- Smith, R., Kaune, H., Parodi, D., Madariaga, M., et al. (2007). Extent of sperm DNA damage in spermatozoa from men examined for infertility. Relationship with oxidative stress. *Revista medica de Chile*, 135(3), 279-286.
- Sripriya, S., Yuvaraj, G., Nema, R. K., Kumar, V. M., & Deecaraman, M. (2011). Evaluation of Antifertility activity from Stem Part of *Ocimum gratissimum* in Acetone extracts. *International Journal of Pharmaceutical and Clinical Research*, 3(2), 41-44.
- Stanton, P. G., Sluka, P., Foo, C. F. H., Stephens, A. N., et al. (2012). Proteomic changes in rat spermatogenesis in response to in vivo androgen manipulation; impact on meiotic cells. *PLoS One*, 7(7):e41718.
- Turner, T. T., Jones, C. E., Howards, S. S., Ewing, L. L., Zegeye, B., & Gunsalus, G. L. (1984). On the androgen microenvironment of maturing spermatozoa. *Endocrinology*, 115(5), 1925–1932.
- United Nations (UN). Department of Economic and Social Affairs. Population Division (New York). (2009). *World contraceptive use 2009*. UN.
- Verma, S. C. I., & Agarwal, S. L. (1962). Studies on *Leptadenia reticulata* (part II). Preliminary chemical investigations. *The Indian journal of medical research*, 50, 439–445.
- Walum, E. (1998). Acute Oral Toxicity. *Environmental health perspectives*, 106(2), 497-503.
- Yama, O. E., Duru, F. I., Oremosu, A. A., Osinubi, A. A., Noronha, C. C., & Okanlawon, A. O. (2011). Sperm quotient in Sprague–Dawley rats fed graded doses of seed extract of *Momordica charantia*. *Middle East Fertility Society Journal*, 16(2), 154-158.



Journal of Experimental Biology and Agricultural Sciences

<http://www.jebas.org>

ISSN No. 2320 – 8694

Antibacterial activity of Libyan *Juniperus phoenicea* L. leaves extracts against common nosocomial pathogens

Aml O. Alhadad , Galal S. Salem * , Suliman M. Hussein , Sarah M. Elshareef 

Department of Botany, Faculty of Science, University of Benghazi, Libya

Received – November 14, 2022; Revision – February 19, 2023; Accepted – March 17, 2023

Available Online – April 30, 2023

DOI: [http://dx.doi.org/10.18006/2023.11\(2\).371.379](http://dx.doi.org/10.18006/2023.11(2).371.379)

KEYWORDS

Juniperus phoenicea

Antibacterial activity

Infectious diseases

Plant extract

ABSTRACT

In ancient times, botanical extracts were essential complementary method for microbial control. This study has been carried out to assess the antibacterial activities of methanol, acetone, and aqueous leaf extracts of Libyan *Juniperus phoenicea* L. against multidrug-resistant (MDR) clinical isolates (*Staphylococcus aureus*, *S. haemolyticus*, *Pseudomonas aeruginosa*, and *Proteus mirabilis*) using the agar well diffusion method. Based on the inhibition zone's diameter or appearance, the tested MDR bacteria were identified as susceptible, intermediate, or resistant using the standard criteria. The current study's findings showed that the concentration, type of solvent and bacterial species had a significant impact on the effectiveness of the plant extracts. Results of the study revealed that the methanol and acetone extracts demonstrated moderate to excellent antibacterial properties against all tested bacteria at all predefined concentrations (25, 50, 75, and 100%), with the zone of inhibition ranging from 15.66 to 27.66 mm. Among the tested solvents, the aqueous extract of *J. phoenicea* was the least effective against the clinical bacterial isolates. Further, the plant's leaf extracts were more effective against Gram-positive bacteria than Gram-negative bacterial pathogens. Most importantly, neither the aqueous extract nor the standard antibiotics inhibited *P. aeruginosa*, while the methanol and acetone extracts displayed remarkable inhibition zones against all tested bacteria. Consequently, the plant extracts (acetone and methanol) in this study may provide insightful information about the potential use of *J. phoenicea* leaves as a natural antibacterial agent, which could be used to combat antibiotic-resistant bacteria.

* Corresponding author

E-mail: galalsalem@uob.edu.ly (Galal Salem)

Peer review under responsibility of Journal of Experimental Biology and Agricultural Sciences.

Production and Hosting by Horizon Publisher India [HPI]
(<http://www.horizonpublisherindia.in/>).
All rights reserved.

All the articles published by [Journal of Experimental Biology and Agricultural Sciences](#) are licensed under a [Creative Commons Attribution-NonCommercial 4.0 International License](#) Based on a work at www.jebas.org.



1 Introduction

In recent decades, the prevalence of infections caused by multidrug-resistant (MDR) microbes has become a problem for global health. Among the most common MDR bacteria, *Staphylococcus aureus*, *S. haemolyticus*, *Pseudomonas aeruginosa*, and *Proteus mirabilis* are some fundamentally pathogenic bacteria that cause many nosocomial infectious diseases (Mehta and Kumari 1997; De Champs et al. 2000; EL-Mahmood 2009; Hoseini Alfatemi et al. 2014; Amenu 2014; Czekaj et al. 2015). Plant products exhibit strong antimicrobial properties, making them a compelling alternative route for treating and preventing infections caused by bacteria, especially in cases where traditional chemical antibiotics are ineffective or unavailable. Additionally, plant-based therapies may have fewer side effects and lower toxicity, making them much more reliable and promising avenues for future research and development than synthetic drugs (Akinduti et al. 2022; Akinyemi et al. 2005). In addition, plant products are widely available and affordable, making them accessible to a large population in developed and developing countries. Thereby, the use of plant products as therapeutic agents has the potential to provide a cost-effective and sustainable solutions to combat infectious diseases.

Juniperus phoenicea L., also known as Phoenician juniper, belongs to the family Cupressaceae and is an evergreen plant usually grown as a shrub or a tree in the Mediterranean basin (Fouad et al. 2011; Abu-Darwish et al. 2014). This plant species abundantly grows in the eastern part of Libya and is widely used in traditional medicine by Libyan people to treat various ailments (Aljaiyash et al. 2014; Al Groshi et al. 2018). Aqueous extracts of *J. phoenicea* leaves are used to treat diarrhea, gout, and anorexia in Libya (Qnais et al. 2005), nephrotoxicity and hepatotoxicity in Egypt (Ali et al. 2010). The aqueous extract also improves liver and kidney functions. The traditional Moroccan healers used *J. phoenicea* leaves powder to treat diuretics, diabetes, diarrhea, rheumatism, and hypoglycemia

(Abu-Darwish et al. 2014). These researchers have also reported that the leaves of this plant are the fundamental source of various active ingredients like phenolic, lipid and mineral compounds. Radical scavenging activity of ethyl acetate and methanolic extracts of *J. phoenicea* leaves has been reported by Medini et al. (2013) in Tunisia. Although many previous studies have established the various medicinal and antimicrobial properties of *J. phoenicea*, the antibacterial activity of plant leaves collected from the Sidi Emhamad forest (Alabyar, Libya) against MDR bacteria has not yet been studied. Therefore, the current study has been conducted to assess the antibacterial efficacy of the *J. phoenicea* leaf extract against four multidrug-resistant bacteria (*Staphylococcus aureus*, *S. haemolyticus*, *Pseudomonas aeruginosa*, and *Proteus mirabilis*), which pose a high threat to human health. The findings of this investigation could potentially lead to the development of new and effective antibacterial agents which could be used to combat antibiotic-resistant bacteria.

2 Materials and Methods

2.1 Plant Material

The leaves of *J. phoenicea* have been collected from one individual tree located in SidiEmhamad forest (Al-abyar city), which is roughly 60 km from the city of Benghazi (Libya) with geographical coordinates of 32° 11' 20" N, 20° 35' 48" E (Figure 1a & 1b). The collected plant samples were taxonomically identified by the expert taxonomist of the Department of Botany, Faculty of Science, University of Benghazi, Libya. The identified plant specimen was assigned voucher specimen no. 1-20582 and preserved in the herbarium of the Botany Department, Faculty of Science, University of Benghazi, Libya.

2.2 Preparation of Plants Extract

The collected plant leaves were gently washed with running tap water, rinsed with distilled water, and then allowed to dry in the shade for two weeks at room temperature. The home mixture and



Figure 1 (a) leaves of *J. phoenicea* and (b) *J. phoenicea* trees at SidiEmhamad forest, Alabyar city, Libya.

grinder ground dried leaves and thirty grams of plant powder was mixed with 300 mL of methanol, acetone, and aqueous solutions separately overnight and then filtered through Whatman No.1 filter paper. The filtrated samples were then evaporated and dried under reduced pressure using a rotatory evaporator with a water bath temperature of 40°C for methanol and acetone, while the aqueous solvent was extracted at 100°C for 30 min. Four concentrations of each extract, i.e. 25, 50, 75, and 100% (v/v), were used to test their antibacterial activities. The obtained extract was stored at 4°C in the refrigerator until the antibacterial test. All experiments were repeated in triplicate.

2.3 Collection of bacterial strains

The antibacterial activity of three leaves extracts of *J. phoenicea* was tested against the two Gram-positive (*Staphylococcus aureus* "SA" and *S. haemolyticus* "SH") and two Gram-negative bacteria (*Pseudomonas aeruginosa* "PA", and *Proteus mirabilis* "PM"). Selected bacterial isolates were obtained from the Benghazi Children's Hospital, Libya and were identified by standard methods in El-Jala Teaching Hospital and confirmed by Phoenix (Alhadad et al. 2021).

2.4 Determination of Antibacterial Activity

The antibacterial assay was performed on Muller-Hinton agar (MHA) using the agar well diffusion method according to Debalke et al. (2018) with some required modifications. Each bacterial suspension was calibrated to a turbidity standard of 0.5 McFarland (10^8 CFU/mL). The MHA plates were inoculated by spreading the bacterial inoculum across the agar surface using a sterile swab. After that, five wells with a diameter of 8 mm were cut using a sterile cork borer. Four predefined concentrations of particular plant extract solutions (25, 50, 75, and 100% v/v) and 100 μ L of each solvent was filled in the prepared wells. The negative control was placed at the centre of each plate with absolute methanol, dimethylsulfoxide (DMSO), and distilled water for methanol, acetone, and aqueous solutions, respectively. While the reference antibiotic discs of levofloxacin (5 μ g), amoxicillin (25 μ g), and ampicillin (10 μ g) were used as positive controls and put in separate plates. The plates were allowed to diffuse for 20 min at room temperature and then incubated for 24 h at 37°C. The inhibition zone formed around each well (including the well's diameter) was measured in millimetres using a ruler and compared with the standard discs and negative controls.

The sizes of the inhibitory zones for the plant extracts and the tested antibiotics were classified as susceptible, intermediate or resistant based on the criteria outlined in the Clinical and Laboratory Standards Institute (CLSI) breakpoint system (CLSI 2020).

2.5 Statistical Analysis

The statistical analysis was conducted using an ANOVA followed by a *post-hoc* Tukey HSD test in GraphPad Prism version 9.4.1 (681). Differences between means were considered statistically significant at a *p*-value < 0.05. All obtained results were presented as mean \pm standard error (SEM) in triplicate.

3 Results and Discussion

Due to the lack of new antimicrobial agents being discovered and developed, MDR bacteria are currently the most significant threat to human health and are typically associated with nosocomial infections (van Duin and Paterson 2020). In this investigation, the antibacterial efficacy of Libyan *J. phoenicea* leaf extracts was assessed against the four MDR bacteria, i.e. *Staphylococcus aureus*, *S. haemolyticus*, *Pseudomonas aeruginosa*, and *Proteus mirabilis* by using methanol, acetone, and aqueous extracts. To ensure higher accuracy and improved antimicrobial susceptibility performance, the Clinical Laboratory Standards Institute (CLSI 2020) testing was used to interpret the findings of the current research (susceptible, intermediate, or resistant).

Results presented in Table 1 and Figure 2 revealed the inhibitory effects of three plant extracts and selected common antibiotics against the four selected clinical MDR isolates. Concerning the negative controls, the results of this study exhibited that none of the tested bacteria had any inhibition zones (Figure 2). All the studied extracts exhibited concentration-dependent antibacterial activity against all tested clinical bacterial isolates.

Findings of the present study showed that methanol and acetone extracts of *J. phoenicea* had demonstrated moderate to high antibacterial activity against all tested clinical isolates (zones of inhibition ranging from 15.66 to 27.66 mm) at all studied concentrations and *S. aureus* and *S. haemolyticus* were found most susceptible to these extracts (Table 1 and Figure 3a-c). These results are in agreement with previous investigations, which illustrated that methanol and acetone extracts showed moderate to high antibacterial activities toward the growth of pathogenic bacteria when compared to aqueous extracts (El-mahmood et al. 2008; Dewangan et al. 2010; Al-Daihan et al. 2013; Atwaa et al. 2022; Borges et al. 2020; Prakash 2023).

The inhibition efficiency of the aqueous extract was also observed against the selected clinical bacterial isolates, but it varied from moderate to less or no inhibition. At the higher concentrations (50-100%), the aqueous extract exhibited moderate antibacterial activity, with the inhibition zones ranging from 15.66 to 17.00 mm against *S. aureus*, 15.33 to 15.66 mm towards *S. haemolyticus*, and 15.00 mm against *P. mirabilis* at a concentration of 100% only. However, at the lowest concentration (25%), all the

Table 1 Antibacterial activity of *J. phoenicea* leaves extracts and standard drugs against clinical bacterial isolates

Extract/ Antibiotic	Concentration (%)	Diameter of inhibition zone (mm)			
		Gram-positive bacteria		Gram-negative bacteria	
		SA	SH	PA	PM
Aqueous	25	14.66±0.88 (R)	13.33±0.33 (R)	-	10.33±0.33 (R)
	50	15.66±0.33 (I)	15.33±0.33 (I)	-	12.33±0.33 (R)
	75	17.00±0.00 (I)	15.66±0.33 (I)	-	13.66±0.33 (R)
	100	17.00±0.00 (I)	15.66±0.33 (I)	-	15.00±0.00 (I)
Acetone	25	21.66±0.33 (S)	23.00±0.57 (S)	17.00±0.00 (I)	16.33±0.33 (I)
	50	23.66±0.33 (S)	23.33±0.66 (S)	18.33±0.66 (I)	17.00±0.57 (I)
	75	24.66±0.33 (S)	24.33±0.33 (S)	19.33±0.33 (I)	18.33±0.66 (I)
	100	25.66±0.66 (S)	27.00±0.57 (S)	20.33±0.88 (S)	19.66±0.33 (I)
Methanol	25	23.33±0.88 (S)	19.33±1.20 (I)	16.66±0.33 (I)	15.66±0.66 (I)
	50	25.00±0.00 (S)	21.33±0.66 (S)	19.66±0.33 (I)	18.00±1.00 (I)
	75	26.33±0.88 (S)	23.33±0.33 (S)	22.33±0.33 (S)	19.00±0.57 (I)
	100	27.66±0.66 (S)	24.00±0.00 (S)	23.66±0.33 (S)	19.66±1.20 (I)
Levofloxacin (5µg)		34.33±0.33 (S)	33.00±0.57 (S)	-	36.33±0.33 (S)
Ampicillin (10µg)		15.33±0.33 (R)	23.00±0.00 (R)	-	-
Amoxicillin (25µg)		15.67±1.85 (R)	11.00±0.57 (R)	-	-

Here - = No zone of inhibition detected; results are presented as mean values ± standard error (SE) (N=3); Clinical breakpoints, as recommended by CLSI guideline, are denoted by the susceptible (S), intermediate (I), and resistant (R); SA; *Staphylococcus aureus*, SM; *Staphylococcus haemolyticus*, PA; *Pseudomonas aeruginosa*, and PM; *Proteus mirabilis*

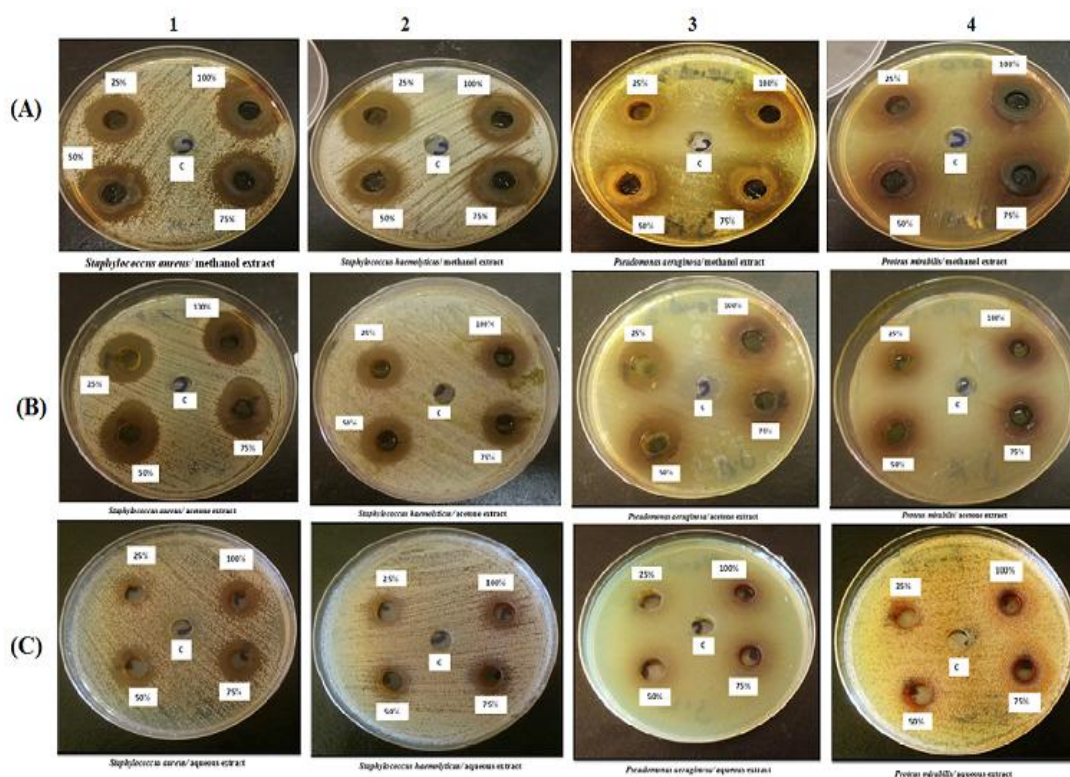


Figure 2 Antibacterial activity of three leaves extracts of *J. phoenicea* by agar well diffusion method against four pathogenic bacteria; A (methanol extract), B (acetone extract), and C (aqueous extract); 1 *S. aureus*, 2 *S. haemolyticus*, 3 *P. aeruginosa*, and 4 *P. mirabilis*

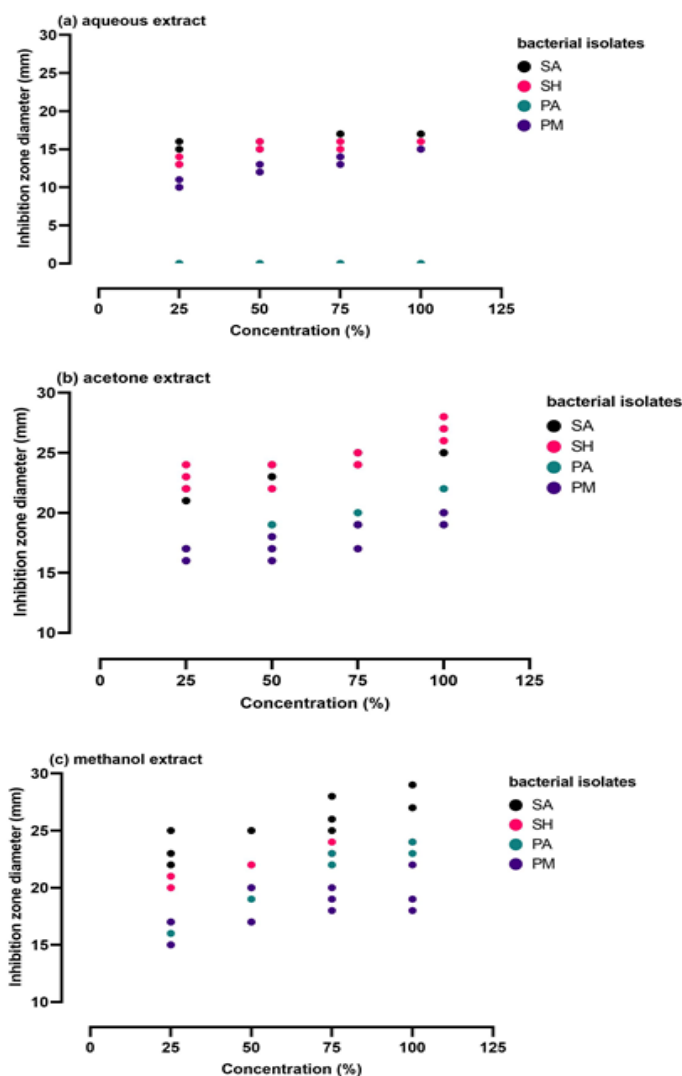


Figure 3 Effect of *J. phoenicea* plant aqueous extract, (a) acetone extract, (b) methanol extract, (c) on the growth of pathogenic bacteria; SA - *S. aureus*, SH - *S. haemolyticus*, PA - *P. aeruginosa*, and PM - *P. mirabilis*

studied bacterial isolates were shown to be resistant to the aqueous extract, with a zone of inhibition diameter ranging between 0.00 to 14.66 mm. These findings are consistent with a previous study, which demonstrated that the antibacterial efficiency of an aqueous leaf extract of *Bidens pilosa* was detected against different bacterial pathogens, such as *P. aeruginosa* and *S. aureus* at the highest concentrations only (Omotanwa et al. 2023).

On the other hand, Mohammed and Aziz (2023) have reported that the aqueous extract of *Peganum harmala* had the highest antibacterial activity against *Proteus mirabilis* at a concentration of 10%. However, the aqueous extract of *Cinnamomum zeylanicum* was ineffective against *Proteus mirabilis*. Prakash (2023) recently demonstrated that the aqueous extract of *Baccharoides anthelmintica* seed displayed potent activity against *Yersinia pestis*

and *Listeria monocytogenes* and exhibited no inhibition against the bacterial species *B. cereus*, *E. coli*, *P. aeruginosa*, and *S. aureus*. These variations might be attributed to the concentration of the plant extracts, the kind of used plant material and species, as well as dependent on the bacterial strains.

Overall the results of the current study also revealed that the aqueous extract had the lowest antibacterial efficacy against all clinical isolates of bacteria. This could be because the aqueous extract was subjected to high temperatures (boiling), which can affect the bioactive components. The findings of this investigation were similar to the previous study, which reported that the chemical compositions of the aqueous extract of *Ocimum gratissimum* were significantly reduced under extraction temperature (100° C). Still, these compounds increased at a

temperature of 110°C (Onyebuchi and Kavaz 2020). Shehadi et al. (2014) revealed that the effect of high temperature (100°C) on the activity of bioactive compounds (terpenoids, flavonoids, and phenolics) was not observed in the extractions of cloves and rosemary, but these components were not found in mint.

Conversely, El-mahmood et al. (2008) illustrated the antibacterial efficiency of the stem, bark, and leaf extracts of *Vitellaria paradoxa* was not affected by increasing the temperature (boiled water). Furthermore, other studies also demonstrated that the aqueous extracts of various plant species showed the highest activity against different strains of pathogenic bacteria, even at the heat temperature of 100°C (Saeed and Tariq 2008; Atwaa et al. 2022). These results suggest that the effect of the extraction temperature (100°C) on the bioactive compounds is significantly dependent upon the species of the plant.

The standard drug (Levofloxacin) was active against all the selected clinical bacterial isolates except for *P. aeruginosa*, with the inhibition zones ranging between 33.00-36.33 mm in diameter. In contrast, all the tested bacteria were resistant to Ampicillin and Amoxicillin (Table 1). Various previous studies have reported that *P. aeruginosa* displayed resistance to a wide variety of antimicrobials (Breidenstein et al. 2011; Mishra and Padhy 2013; Cole et al. 2014; Pang et al. 2019; Zgurskaya and Rybenkov 2020; Ahmed et al. 2021; Atwaa et al. 2022; Tabcheh et al. 2023). Interestingly, methanol and acetone extracts showed the highest remarkable inhibition of antibacterial activity against all the tested clinical bacterial isolates, including *P. aeruginosa*, while no inhibition was reported by either the antibiotic

standards or aqueous extract on this bacterium. These results are supported by the findings of a previous study conducted by Alhadad et al. (2022).

In contrast, Rukundo et al. (2023) investigated and found that the aqueous extract of ginger was effective against *P. aeruginosa* at a higher concentration (2g/ml). The current investigation revealed that Gram-negative bacteria (*P. aeruginosa* and *P. mirabilis*) were comparatively less susceptible to antibacterial agents than Gram-positive bacteria (*S. aureus* and *S. haemolyticus*). By contrast, Karuppiah and Mustaffa (2013) have demonstrated that the antibacterial activity of the leaves of *Musa* species was more efficient against the Gram-negative bacteria than the Gram-positive bacteria. On the other hand, many previous studies have revealed that juniper essential oils or extracts were less sensitive against Gram-negative bacteria than Gram-positive ones (Ennajar et al. 2009; EL-Mahmood 2009; Elmhdwi et al. 2015; Guedri et al. 2020). Hence, despite the presence of an outer membrane in Gram-negative bacteria, which acts as a permeability barrier for impeding the passage of drugs and preventing the antibiotic from reaching its binding site in the bacterial cell, the antibacterial activity was mainly dependent on the extraction method and the plant species (Ghai and Ghai 2018; Zgurskaya and Rybenkov 2020).

According to ANOVA results, the means of inhibition zones for all the concentrations of the plant extracts were significantly different compared to the negative control. Figure 4 showed that all tested concentrations showed no significant differences between the mean growth inhibition zones of methanol and acetone extracts. The reference antibiotic disc (Levofloxacin) had the highest mean

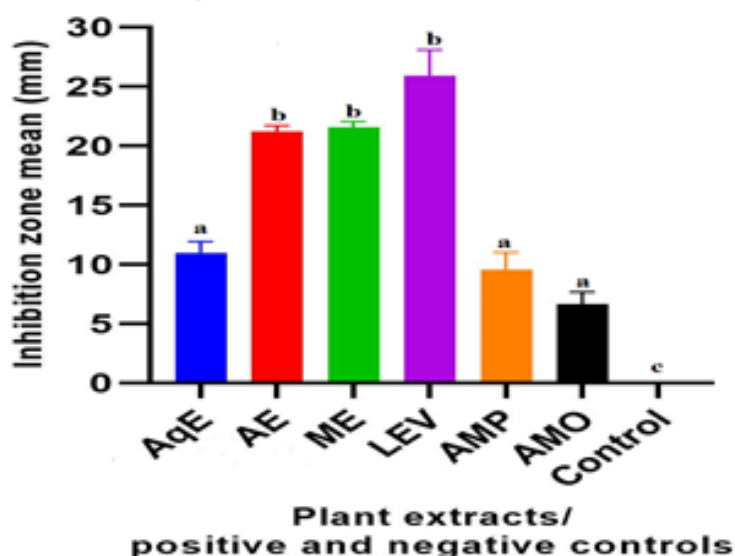


Figure 4 The average of inhibition zones of triplicates ($n=3$) \pm standard error (SEM); AqE; aqueous extract, AE; acetone extract, ME; methanol extract; LEV; levofloxacin, AMP; ampicillin, AMO; amoxicillin (positive controls); Different letters indicate significant differences ($p < 0.01$) between mean values of inhibition zones for all the concentrations of the plant extracts compared with the positive and negative controls according to ANOVA followed by Tukey's HSD test

antibacterial activity. Hence, in this investigation, to prove and support the results of the plant extracts, further minimal inhibitory concentration (MIC) and minimal bactericidal concentration (MBC) assays should be performed for their antibacterial activity against the susceptible bacterial isolates.

Conclusion

The present study illustrated that the methanol and acetone extracts could be potential sources of antibacterial agents for developing novel drugs to combat infectious diseases. Further research is required to detect the active substances responsible for the observed antibacterial activity and to evaluate their potential as alternative remedies for bacterial infections. In addition, investigating the cytotoxicity of these extracts on human cells is necessary before considering their use in clinical settings.

Conflicts of interest

All authors declare no conflicts of interest.

Acknowledgements

None

References

- Abu-Darwish, M. S., Cabral, C., & Salgueiro, L. (2014). *Juniperus phoenicea* from Jordan. *Medicinal and Aromatic Plants of the Middle-East*, 5, 241-252.
- Ahmed, O., Mohamed, H., Salem, W., Afifi, M., & Song, Y. (2021). Efficacy of Ethanolic Extract of *Syzygium aromaticum* in the Treatment of Multidrug-Resistant *Pseudomonas aeruginosa* Clinical Isolates Associated with Urinary Tract Infections. *Evidence-based complementary and alternative medicine : eCAM*, 2021, 6612058. <https://doi.org/10.1155/2021/6612058>
- Akinduti, P. A., Emoh-Robinson, V., Obamoh-Triumphant, H. F., Obafemi, Y. D., & Banjo, T. T. (2022). Antibacterial activities of plant leaf extracts against multi-antibiotic resistant *Staphylococcus aureus* associated with skin and soft tissue infections. *BMC complementary medicine and therapies*, 22(1), 1-11.
- Akinyemi, K. O., Oladapo, O., Okwara, C. E., Ibe, C. C., & Fasare, K. A. (2005). Screening of crude extracts of six medicinal plants used in South-West Nigerian unorthodox medicine for anti-methicillin resistant *Staphylococcus aureus* activity. *BMC complementary and alternative medicine*, 5(1), 1-7.
- Al Groshi, A., Evans, A. R., Ismail, F. M., Nahar, L., & Sarker, S. D. (2018). Cytotoxicity of Libyan *Juniperus phoenicea* against human cancer cell lines A549, EJ138, HepG2 and MCF7. *Pharmaceutical Sciences*, 24(1), 3-7.
- Al-Daihan, S., Al-Faham, M., Al-shawi, N., Almayman, R., Brnawi, A., & Shafi Bhat, R. (2013). Antibacterial activity and phytochemical screening of some medicinal plants commonly used in Saudi Arabia against selected pathogenic microorganisms. *Journal of King Saud University-Science*, 25(2), 115-120.
- Alhadad, A. O., Elmhdwi, M. F., Salem, G. S., & Elshareef, S. M. (2021). Evaluation the in vitro antibacterial activity of acetone leaf extracts from *Pistacia lentiscus* against multidrug resistant *Pseudomonas aeruginosa* and *Staphylococcus aureus*. *Journal of Medicinal Plants*, 9(4), 100-105.
- Alhadad, A. O., Salem, G. S., Elmhdwi, M. F., Hussein, S. M., & Elshareef, S. M. (2022). Assessments of Antibacterial and Antioxidant Properties in the Methanolic and Aqueous Leaf Extracts of *Pistacia lentiscus* against Different Antibiotic Resistance Pathogenic Bacteria. *Advances in Bioscience and Biotechnology*, 13(3), 113-133.
- Ali, S. A., Rizk, M. Z., Ibrahim, N. A., Abdallah, M. S., Sharara, H. M., & Moustafa, M. M. (2010). Protective role of *Juniperus phoenicea* and *Cupressus sempervirens* against CCl₄. *World Journal of Gastrointestinal Pharmacology and Therapeutics*, 1(6), 123.
- Aljaiyash, A. A., Gonaïd, M. H., Islam, M., & Chaouch, A. (2014). Antibacterial and cytotoxic activities of some Libyan medicinal plants. *Journal of Natural Product and Plant Resources*, 4(2), 43-51.
- Amenu, D. (2014). Antimicrobial activity of medicinal plant extracts and their synergistic effect on some selected pathogens. *American Journal of Ethnomedicine*, 1(1), 18-29.
- Atwaa, E. S. H., Shahein, M. R., Radwan, H. A., Mohammed, N. S., Aloraini, M. A., Albezrah, N. K. A., & Elmahallawy, E. K. (2022). Antimicrobial Activity of Some Plant Extracts and Their Applications in Homemade Tomato Paste and Pasteurized Cow Milk as Natural Preservatives. *Fermentation*, 8(9), 1-16.
- Borges, A., José, H., Homem, V., & Simões, M. (2020). Comparison of Techniques and Solvents on the Antimicrobial and Antioxidant Potential of Extracts from *Acacia dealbata* and *Olea europaea*. *Antibiotics*, 9(2), 48.
- Breidenstein, E. B., de la Fuente-Núñez, C., & Hancock, R. E. (2011). *Pseudomonas aeruginosa*: all roads lead to resistance. *Trends in microbiology*, 19(8), 419-426.
- CLSI. Performance Standards for Antimicrobial Susceptibility Testing. (2020). 30th ed. supplement M100. Wayne, PA: Clinical and Laboratory Standards Institute. Retrieved from

- file:///C:/Users/user/Downloads/Attachment%20D%20CRE%20Instrument%20Attachment%20Laboratory%20Guidelines.pdf
- Cole, S. J., Records, A. R., Orr, M. W., Linden, S. B., & Lee, V. T. (2014). Catheter-associated urinary tract infection by *Pseudomonas aeruginosa* is mediated by exopolysaccharide-independent biofilms. *Infection and immunity*, 82(5), 2048–2058. <https://doi.org/10.1128/IAI.01652-14>
- Czekaj, T., Ciszewski, M., & Szewczyk, E. M. (2015). *Staphylococcus haemolyticus*—an emerging threat in the twilight of the antibiotics age. *Microbiology*, 161(11), 2061–2068.
- De Champs, C., Bonnet, R., Sirot, D., Chanal, C., & Sirot, J. (2000). Clinical relevance of *Proteus mirabilis* in hospital patients: a two year survey. *Journal of Antimicrobial Chemotherapy*, 45(4), 537–539.
- Debalke, D., Birhan, M., Kinubeh, A., & Yayeh, M. (2018). Assessments of antibacterial effects of aqueous-ethanolic extracts of *Sida rhombifolia*'s aerial part. *The Scientific World Journal*, 2018, 1-8. DOI: 10.1155/2018/8429809.
- Dewangan, G., Koley, K. M., Vadlamudi, V. P., Mishra, A., Poddar, A., & Hirpurkar, S. D. (2010). Antibacterial activity of *Moringa oleifera* (drumstick) root bark. *Journal of Chemical and Pharmaceutical Research*, 2(6), 424–428.
- El-Mahmood, A. M., Doughari, J. H., & Ladan, N. (2008). Antimicrobial screening of stem bark extracts of *Vitellaria paradoxa* against some enteric pathogenic microorganisms. *African Journal of Pharmacy and Pharmacology*, 2(5), 089–094.
- EL-mahmood, M. A. (2009). Efficacy of crude extracts of garlic (*Allium sativum* Linn.) against nosocomial *Escherichia coli*, *Staphylococcus aureus*, *Streptococcus pneumoniae* and *Pseudomonas aeruginosa*. *Journal of Medicinal Plants Research*, 3(4), 179–185.
- Elmhawi, M. F., Attitalla, I. H., & Khan, B. A. (2015). Evaluation of antibacterial activity and antioxidant potential of different extracts from the leaves of *Juniperus phoenicea*. *Journal of Plant Pathology and Microbiology*, 6(9), 300.
- Ennajar, M., Bouajila, J., Lebrihi, A., Mathieu, F., Abderraba, M., Raies, A., & Romdhane, M. (2009). Chemical composition and antimicrobial and antioxidant activities of essential oils and various extracts of *Juniperus phoenicea* L. (Cupressaceae). *Journal of food science*, 74(7), M364–M371.
- Fouad, B., Abderrahmane, R., Youssef, A., Rajae, H., & Fels, M. A. E. A. E. (2011). Chemical composition and antibacterial activity of the essential oil of Moroccan *Juniperus phoenicea*. *Natural product communications*, 6(10), 1515–1518.
- Ghai, I., & Ghai, S. (2018). Understanding antibiotic resistance via outer membrane permeability. *Infection and drug resistance*, 11, 523–530.
- Guedri, M. M., Romdhane, M., Lebrihi, A., Mathieu, F., & Bouajila, J. (2020). Chemical composition and antimicrobial and antioxidant activities of Tunisian, France and Austrian *Laurus nobilis* (Lauraceae) essential oils. *Notulae Botanicae HortiAgrobotanici Cluj-Napoca*, 48(4), 1929.
- Hoseini Alfatemi, S. M., Motamedifar, M., Hadi, N., & Sedigh Ebrahim Saraie, H. (2014). Analysis of Virulence Genes Among Methicillin Resistant *Staphylococcus aureus* (MRSA) Strains. *Jundishapur journal of microbiology*, 7(6), e10741. <https://doi.org/10.5812/jjm.10741>
- Karuppiah, P., & Mustafa, M. (2013). Antibacterial and antioxidant activities of Musa sp. leaf extracts against multidrug resistant clinical pathogens causing nosocomial infection. *Asian Pacific journal of tropical biomedicine*, 3(9), 737–742. [https://doi.org/10.1016/S2221-1691\(13\)60148-3](https://doi.org/10.1016/S2221-1691(13)60148-3)
- Medini, H., Elaissi, A., Khouja, M. L., & Chemli, R. (2013). Phytochemical screening and antioxidant activity of *Juniperus phoenicea* ssp. *phoenicea* L. extracts from two Tunisian locations. *Journal of Experimental Biology and Agricultural Sciences*, 1(2), 78–82.
- Mehta, G., & Kumari, S. (1997). Multi-resistant *Staphylococcus haemolyticus* in a neonatal unit in New Delhi. *Annals of tropical paediatrics*, 17(1), 15–20.
- Mishra, M. P., & Padhy, R. N. (2013). In vitro antibacterial efficacy of 21 Indian timber-yielding plants against multidrug-resistant bacteria causing urinary tract infection. *Osong public health and research perspectives*, 4(6), 347–357.
- Mohammed, R. M., & Aziz, N. F. (2023). Antibacterial activity of some plants extracts against proteus mirabilis bacteria. *3c Empresa: investigación y pensamiento crítico*, 12(1), 301–309.
- Omotanwa, A. N., Kenneth, E. I., Owuna, J. E., Stella, O. S., Anne, D. N., & Obiekezie, S. O. (2023). Antibacterial activity and phytochemical screening of some medicinal plant extracts against bacteria isolated from food materials sold in Keffi, Nasarawa State, Nigeria. *GSC Biological and Pharmaceutical Sciences*, 22(1), 321–329.
- Onyebuchi, C., & Kavaz, D. (2020). Effect of extraction temperature and solvent type on the bioactive potential of *Ocimum gratissimum* L. extracts. *Scientific reports*, 10(1), 21760.

- Pang, Z., Raudonis, R., Glick, B. R., Lin, T. J., & Cheng, Z. (2019). Antibiotic resistance in *Pseudomonas aeruginosa*: mechanisms and alternative therapeutic strategies. *Biotechnology advances*, 37(1), 177-192.
- Prakash, V. (2023). An investigation of *Baccharoides anthelmintica* (L.) Moench seed extract for antibacterial and antioxidant activities. *Journal of Drug Delivery and Therapeutics*, 13(1), 29-32.
- Qnais, E. Y., Abdulla, F. A., & Abu Ghalyun, Y. Y. (2005). Antidiarrheal effects of *Juniperus phoenicia* L. leaves extract in rats. *Pakistan Journal of Biological Sciences*, 8(6), 867-71.
- Rukundo, A., Omara, D., Majalija, S., Odur, S., Alafi, S., & Okech, S. G. (2023). Antibacterial activity of ethanolic and aqueous extracts of *Zingiber officinale* on *Streptococcus pneumoniae* and *Pseudomonas aeruginosa*. *bioRxiv*, 2023-01.
- Saeed, S., & Tariq, P. (2008). In vitro antibacterial activity of clove against Gram negative bacteria. *Pakistan Journal of Botany*, 40(5), 2157-2160.
- Shehadi, M., Awada, F., Oleik, R., Chokr, A., Hamze, K., Abou Hamdan, H., & Kobaissi, A. (2014). Comparative analysis of the antibacterial activity of four plant extracts. *International Journal of Current Research and Academic Review*, 2(6), 83-94.
- Tabcheh, J., Vergalli, J., Davin-Réglé, A., Ghanem, N., Al-Bayssari, C., & Brunel, J. M. (2023). Rejuvenating the Activity of Usual Antibiotics on Resistant Gram-Negative Bacteria: Recent Issues and Perspectives. *International Journal of Molecular Sciences*, 24(2), 1515.
- van Duin, D., & Paterson, D. L. (2020). Multidrug-resistant bacteria in the community: an update. *Infectious Disease Clinics*, 34(4), 709-722.
- Zgurskaya, H. I., & Rybenkov, V. V. (2020). Permeability barriers of Gram-negative pathogens. *Annals of the New York Academy of Sciences*, 1459(1), 5-18.















Journal of Experimental Biology and Agricultural Sciences

<http://www.jebas.org>

ISSN No. 2320 – 8694

Phytochemical investigations, *in-vitro* antioxidant, antimicrobial potential, and *in-silico* computational docking analysis of *Euphorbia milii* Des Moul

Md Sohel Ahmed¹ , Israt Jahan Khan¹ , Shahbaz Aman^{2*} , Samrat Chauhan^{3*} ,
 Narinder Kaur² , Shalini Shrivastav² , Kirti Goel¹ , Monika Saini¹ ,
 Sanchit Dhankhar^{3,4} , Thakur Gurjeet Singh³ , Jai Dev² , Somdutt Mujwar³ 

¹M. M. College of Pharmacy, Maharishi Markandeshwar (Deemed to be University), Mullana, Ambala, Haryana, India, 133207²Department of Microbiology, M. M. Institute of Medical Science and Research, Maharishi Markandeshwar (Deemed to be University), Mullana, Ambala, Haryana, India 133207³Chitkara College of Pharmacy, Chitkara University, Rajpura, Punjab, India, 140401⁴Ganpati Institute of Pharmacy, Bilaspur, Yamunanagar, Haryana, India-135102

Received – December 22, 2022; Revision – March 26, 2023; Accepted – April 07, 2023

Available Online – April 30, 2023

DOI: [http://dx.doi.org/10.18006/2023.11\(2\).380.393](http://dx.doi.org/10.18006/2023.11(2).380.393)

KEYWORDS

Euphorbia milii

Antioxidants

Antimicrobial

Molecular docking

Medicinal plants

ABSTRACT

Euphorbia milii Des Moul is a deciduous bush indigenous to Madagascar. The present study aims to investigate the presence of the phytochemical, *in-vitro* antioxidant and antimicrobial potency, and *in-silico* computational analysis of ethanolic and aqueous preparations of *E. milii* leaves and flowers. The ethanolic and aqueous extracts were tested for *in-vitro* antioxidant activity by DPPH, H₂O₂, TAC, and FRAP assay. In addition, antimicrobial potentials were assayed by agar well diffusion technique against *Escherichia coli*, *Pseudomonas aeruginosa*, *Klebsiella pneumoniae*, *Staphylococcus aureus*, and *Candida albicans* for various clinical isolates. The qualitative phytochemical analysis results confirmed the existence of alkaloids, flavonoids, phenolics, and tannins. The quantitative analysis elicits the availability of a magnificent number of alkaloids, flavonoids, phenolics, flavonols, and tannins. Among all the extracts, aqueous extracts of leaves exhibited potent antioxidant activity in DPPH, FRAP, and H₂O₂ assay with the IC₅₀ value of 30.70, 60.05, and 82.92 μg/mL, respectively. In agar well diffusion assay, all extracts displayed zone of inhibition varies from 2-24mm at different concentrations ranging from 10-320 mg/mL, whereas no activity was observed against *Candida albicans*. Furthermore, docking-based computational analysis has revealed that beta-sitosterol and taraxerol are the plant's active

* Corresponding author

E-mail: samrat.chauhan11@gmail.com (Samrat Chauhan);
shahbazaman095@gmail.com (Shahbaz Aman)

Peer review under responsibility of Journal of Experimental Biology and Agricultural Sciences.

Production and Hosting by Horizon Publisher India [HPI]
(<http://www.horizonpublisherindia.in/>).
All rights reserved.All the articles published by [Journal of Experimental Biology and Agricultural Sciences](#) are licensed under a [Creative Commons Attribution-NonCommercial 4.0 International License](#) Based on a work at www.jebas.org.

constituents responsible for their antimicrobial and antioxidant activities. Research findings suggest that the *E. milii* plant has an excellent prospect for further study for its extended antioxidative and antimicrobial potential. It could be a natural source of various ailments and can be utilized to develop new drugs.

1 Introduction

The instability that occurs at the cellular level between the generation and buildup of reactive oxygen species (ROS) and the capacity of organisms to neutralize them is what causes oxidative stress. ROS can seriously damage body tissues and cells (Aman et al. 2022, 2023). ROS is crucial in the aetiology of many common physiological conditions. In addition to cellular damage, cancer, hepatic, ageing, neurological, cardiovascular, and renal illnesses are strongly influenced by reactive oxygen species (Migdal and Serres 2011). Endogenous antioxidants might not be sufficient to face the overwhelming oxidative stress to ensure regular cellular activity, and to overcome this problem, dietary antioxidants are required (Aryal et al. 2019).

In addition, the development of microbial resistance to conventional antibiotics has occurred, which poses a significant risk to the efficiency of the antimicrobial treatments that are currently in use. Therefore, identifying new antimicrobial drugs to combat antibiotic resistance is a major medical issue of the 21st century (Chauhan et al. 2022). Since there is no effective therapy for cancer, tumours, and antimicrobial resistance in modern medicine, synthetic or semi-synthetic drugs have more severe adverse effects and are cytotoxic to humans, scientists are looking for a potent bioactive drug with non-cytotoxic qualities (Shriwastav et al. 2023). A significant foundation of possible

antioxidants and antimicrobials has been found in natural sources, which may defend against the toxicity of ROS by preventing ROS generation and interfering with bacteria by inhibiting or destroying their cell walls. Antioxidants have a potent antimicrobial impact because they create a scavenging environment that inhibits bacteria. In addition, the antioxidant activity of the constituents minimizes the number of free radicals, which also boosts antibacterial activity (Singh and Sharma 2020). These activities have demonstrated a correlation between antioxidant and antimicrobial characteristics (Sagayaraj et al. 2020). The present emphasis on discovering and characterizing bioactive components responsible for radical scavenging and the ethnopharmacological effects of these components may open up possibilities for focused drug development (Habu and Ibeh 2015). Plants have an impressive potential for developing new therapeutics of immense benefit to humanity. Several epidemiological studies have demonstrated that antioxidant-rich plants benefit health and disease prevention, and their intake reduces the danger of cancer, heart disease, and hypertension (Rehni et al. 2008; Muanda et al. 2011)

Euphorbia milii is a deciduous shrub widely distributed in India and China and native to Madagascar, belonging to the Euphorbiaceae family (Figure 1)(Sreenika et al. 2015). Leaves, flowers, stems, roots, and thorns of *E.milii* were traditionally used in Chinese and Indian medicinal systems for various therapeutic purposes. In the conventional medicine approach, *E. milii* was used



Figure 1 The aerial part of *Euphorbia milii* Des Moul

to treat warts, cancer, and hepatitis in southern Brazil and China (Aleksandrov et al. 2019). On top of that, the seeds serve as a laxative for kids, the petals are applied to cure dermatitis and snake bites, and the entire shrub paste is applied to treat broken animal bones (Ajanaku et al. 2017). According to recent studies, more than 5% of the Euphorbia species are mainly used therapeutically (Sagar and Bisht 2021).

Phytochemical investigations of *E. milii* revealed the existence of subordinate metabolites like alkaloids, polyphenols, glycosides, and saponins (Narendra et al. 2015; Haleshappa et al. 2019). Furthermore, in this regard, several extracts of the *E. milii* aerial part were reported for their antioxidant (Gapuz and Besagas 2018; Mutalib et al. 2020) and antimicrobial potentials (Rauf et al. 2014; Pradyutha et al. 2015; Narendra et al. 2015). Also, methanol & chloroform extracts correspondingly testified for antiviral and anticancer activities (Chaman et al. 2019). Therefore, present research work has been deliberate in evaluating the antioxidant and antimicrobial potentials of ethanol and aqueous extract of leaves and flowers of *E. milii*, followed by the docking-based computational screening of various chemical constituents of the concerned plant to find the most active constituent in the plant accountable for its antimicrobial as well as antioxidant potential and to predict the most probable mechanism involved in it.

2 Materials and Methods

2.1 Collection and identification of the plant

Plants of *E. milii* were gathered from the botanical garden of Maharishi Markandeshwar (Deemed to be) University, Ambala, Haryana, India, in January 2022. The collected plant samples were identified by experienced plant taxonomist (IAAT: 337), Dr. K. Madhava Chetty and a voucher specimen (Number-0978) has been deposited in the herbarium of the Department of Botany, Sri Venkateswara University Tirupati, India (Rao et al. 2003).

2.2 Preparation of plant extracts

Fresh leaves and flowers were shade dried for 21 days and crushed to a coarse powder (Dobriyal et al. 2021). Based on their polarity, the powdered materials were weighed and extracted by Soxhlation with different solvents (ethanol and distilled water). The temperature was set based on the boiling point of the particular solvents. A rotary flash evaporator operating at decreased pressure concentrated the solvent extract separately. After that, each solvent extract was measured before being stored at a temperature of between 4 and 5 degrees Celsius in an airtight container. The percentage yield of the extracts was determined by using the formula given by Moges et al. (2021):

$$(\% \text{ Yield}) = \frac{\text{amount of preparation}}{\text{amount of powdered drug}} \times 100$$

2.3 Phytochemical screening

Qualitative & quantitative phytochemical investigation of leaves and flowers of *E. milii* was carried out according to the established protocol and quantified the secondary phytoconstituents as designated by Sofowara (1993), Kokate et al. (2003), Trease and Evans (2009) and Harborne (2020).

2.3.1 Total alkaloids content (TAC)

Total alkaloids were quantified using the Harborne (2020) protocol with some modifications. First, 5 g of the sample plant extracts were poured into a beaker after being measured out, and a mixture of 200 mL of 10% acetic acid in ethanol was added. After that, the beaker was covered with a lid and set aside for four hours to rest. Next, the above mixture was drained, and the extracts were condensed to 1/4 of their original volume in a water bath. Next, the preparation was treated with drops of concentrated NH₄OH till the residue was obtained. When the mixture was settled, it was washed by the weak NH₄OH and filtered. Finally, the filtrate is desiccated and weighed to determine the total alkaloid (Abifarin et al. 2019).

2.3.2 Total phenol content (TPC)

The Folin-Ciocalteu method was used to determine the phenolic content of plant extracts (Jahan et al. 2012). First, 1 mL of the plant extract (1 mg/mL) and 1 mL of standard gallic acid consisting of a wide range of concentrations, starting from 10–2560 µg/mL, were added with 2.5 ml of Folin-Ciocalteu reagent. After 30 minutes, 2.0 mL of Na₂CO₃ (7.5%) was incorporated into the blend solutions, which was then nurtured (Al-zoreky and Al-Taher 2015) for 2.5 hours at 25°C with periodic stirring. The spectrum was then checked at 765 nm compared to a blank without extract (Gülçin 2005). Three copies of each test sample extract were run. The Absorbance against concentration data was used to plot the gallic acid calibration curve. The total phenol content was determined by mg GAE/g fw (Rajesh and Perumal 2014).

2.3.3 Total flavonoid content (TFC)

The Dowd assay was employed to check the presence of flavonoids in various solvents of *E. milii* (Arvouet-Grand et al. 1994). A mixture of 0.6mL of sterile water, 0.2mL of 10%(w/v) ethanolic AlCl₃ solution, and 1mL of potassium acetate was used to treat a portion of 1mL of sample solution (1Mg/mL) and 1mL of standard quercetin (10–320 g/mL). UV-spectrophotometer was utilized to determine the Absorbance at 415nm after the above mixture had been placed at 25°C for 30 min. The outcomes were given in mg QE/g (Godara 2022).

2.3.4 Total tannin content (TTC)

Total tannin content was identified using vanillin and p-dimethyl amino cinnamaldehyde method (Stavrou et al. 2018). The resulting

combination comprised 3mL of 50% sodium acetate solution, 2mL of ethanolic AlCl₃, and 2mL of plant preparation. The above blend was placed at 20°C for 2.5 hours before the wavelength at 440 nm was determined. Then, total flavonol was calculated using the calibration curve produced at different concentrations (10–1249 g/mL).

2.4 *In-vitro* antioxidant test

In-vitro evaluations of the antioxidant potential of ethanolic and aqueous extracts of flowers and leaves were carried out using the standard procedure to determine the antioxidant potentials of crude plant extracts at various concentrations (10–320 µg/mL).

2.4.1 Total Antioxidant Capacity (TAC)

The TAC was investigated using the phosphomolybdate method with some alterations (Prieto et al. 1999). First, a 0.3 mL plant sample (1 mg/mL) was mixed with 3 mL of phosphomolybdate and placed for 10 minutes at 95 °C. The Absorbance was then determined at 695 nm. Then, using the ascorbic acid calibration curve (10–320 g/mL), the TAC was defined as mg AAE/g raw weight of the sample.

2.4.2 DPPH assay

The radical scavenging activity (RSA) of isolated compounds has been utilized to determine antioxidant capacity as per the DPPH method with minor changes (Yan-Hwa et al. 2000). In this study, 0.1 mm DPPH solution and 2 mL of extracts (10–320 g/mL) in ethanol were mixed. The mixes were kept in an incubator at 25° C for half an hour, and the wavelength was obtained at 517 nm against a blank consisting of an equal quantity of DPPH and ethanol (Yao et al. 2022). The percentage was calculated by the formula given below.

$$\text{Percentage radical scavenging activity (\%)} = \left[\frac{(A_0 - A_1)}{A_0} \right] \times 100 \quad (1)$$

Where A₀ = Absorbance of the control and A₁ = Absorbance of the samples.

2.4.3 Hydrogen peroxide (H₂O₂) assay

The measurement of the H₂O₂ scavenging activity was carried out by employing Ruch et al. (1989) method with certain modifications. In this experiment, 1 mL extracts (10–320 µg/mL), 2.4 mL phosphate buffer (0.1M, pH 7.4), and 0.6 mL H₂O₂ (40 mM) were energetically mixed and placed at 27° C for 10 minutes. The wavelength was evaluated at 230 nm. To determine the percentage of H₂O₂ that was scavenged was estimated by the following equation:

$$\text{Percentage scavenging activity (\%)} = \left[1 - \frac{(A_1 - A_2)}{A_0} \right] \times 100 \quad (2)$$

Where A₀ = Absorbance of the control, A₁ = Absorbance of the samples, and A₂ = Absorbance of the sample only (phosphate buffer with sample)(Yan et al. 2018).

2.4.4 FRAP assay

The modified Fe³⁺ to Fe²⁺ reduction assay was utilized to determine the reducing power of the crude extracts (Oyaizu 1986). First, the response was carried out in a blend with 2.5 mL of sample (10–320 µg/mL) added with 2.5 mL of 0.1M sodium phosphate buffer (pH: 6.6) and 2.5mL of potassium ferrocyanide and kept at 50 °C for 20 min. Then, 2.5 mL of trichloroacetic acid (10% w/v) was put into the mixture. After that, 5 ml of the above mixture was diluted with 0.5 ml of fresh FeCl₃ (0.1%), and the intensity of the blue colour was measured at 700 nm against a blank. Finally, the percentage of radical scavenging activity was calculated using the following formula (1).

2.5 *In-vitro* antimicrobial activity

There has been rising attention to investigating and developing novel antibacterial substances derived from various natural resources to combat microbial resistance. This research focused on the *in-vitro* antimicrobial investigation of leaves and flower extracts of *E.milii* as a potential antimicrobial agent. The agar well diffusion method was used to test the antibacterial activity of the ethanol and aqueous extracts of *E. milii* on several different clinical isolates (Bonev et al. 2008; Sheela and Rajkumar 2013).

2.5.1 Collection and identification of microbial isolates

Clinical isolates of microbial strains (*Escherichia coli*, *Pseudomonas aeruginosa*, *Klebsiella pneumoniae*, *Staphylococcus aureus*, and *Candida albicans*) were collected from M. M. Institute of Medical Science and Research (MMMSR), India and Central Research Laboratory of Microbiology; Maharishi Markandeshwar University was used to perform the experiments. These microbes were isolated from clinical specimens after being cultured on blood and MacConkey agar. Microbial colonies were then exposed to a biochemical test to determine their phenotype, and the Vitek–2 automated system validated further bacterial identification (Pincus 2010). *S. aureus* and *E. coli* were used as the taxonomic key for bacterial identification.

2.5.2 Preparation and maintenance of bacterial Suspension

A pure microbial inoculum was taken, and 1–3 colonies were moved to a sterile tube having 500µl of standard saline solution and carefully mixed to generate a microbial suspension with turbidity equivalent to 0.5 McFarland's standard solution (1.5x10⁸ CFU/mL) using a McFarland optic densitometer. A sterile Mueller-Hinton Agar (MHA) medium was inoculated with a microbial solution using

Table 1 Percentage extractive yields of *E. milii* leaves and flowers with various solvents

Parts of plants	Solvents	Wt. of dry powder	% Yields of dry extracts	Total % yields of dry extracts
Leaves	Ethanol	39.060 gm	35.671%	69.642%
	Aqueous		33.970%	
Flowers	Ethanol	18.621 gm	43.311%	64.702%
	Aqueous		21.391%	

a sterilized cotton swab. All microbial strains were grown by incubating MHA plates at 37°C for 24 hours.

2.5.3 Agar well diffusion assay

The microbial suspension (0.5 McFarland's) was engaged, and with the help of a sterile cotton swab, lawn culture was prepared on MHA. A6-8mm well was punched aseptically using a sterilized cork borer. The extract solution volume (10–200 µL) at the required concentration (10-320 Mg/mL) was put into the well to analyze its antimicrobial properties by agar well diffusion technique (Balouiri et al. 2016). The examined bacteria are cultured on the agar plates for 18–24 hrs at 35°C. Following incubation, the mean \pm SD of the clear zone's diameter around the hole was measured to determine the levels of the antimicrobial activity of the plant extract against the organism being tested (Usman et al. 2009). All the experimental tests were accomplished in triplicates.

2.6 In-silico computational docking analysis

Antibacterial, antifungal, and antioxidant drug targets were selected based on their physiological involvement in the pathogenic life cycle and the oxidative metabolic processes inside the human body. The structural model of each pharmacological target utilized and considered for this investigation was retrieved from the protein databank (Berman et al. 2000). By employing the Chimera apparatus, the complex reference ligand was dissociated from the macromolecular complex associated with each target receptor. The separated receptor for all the macromolecular targets were prepared by adding hydrogens and Gasteiger charge, followed by its equal distribution among the macromolecular residues for docking analysis (Pradhan et al. 2015; Kaur et al. 2016). Covering the receptor's active binding site and creating an artificial grid box was the first step in the preparation process. Then the docking protocol for each macromolecular target is validated by redocking the reference ligand from the crystallized complex. In the next step, docking-based screening of the plant chemical components of the *E. milii* plant against different antimicrobial and antioxidant drug targets (Agrawal et al. 2021; Mujwar et al. 2022; Fidan et al. 2022; Shinu et al. 2022; Mujwar and Tripathi 2022).

3 Result and Discussion

3.1 Percentage extractive yields

The extraction of dry powdered leaves and flowers yielded an excellent quantity of crude dry extract. The percentage extractive yields of leaves and flowers of *E. milii* crude fractions were 69.64% and 64.70%, respectively. Furthermore, Table 1 illustrates the extraction percentage yield of dry fractions of leaves and flowers with various solvents based on their polarity (Et and Aq). The ethanolic fraction of flowers and leaves showed the highest extraction yield (43.312% and 35.671%, respectively), followed by aqueous fractions of leaves and flowers, which demonstrated relatively lower yields than Chohan et al. (2020).

3.2 Phytochemical investigation

The phytochemical analysis is essential to identify a new source of therapeutically valuable compounds. Medicinal plants have lately piqued the interest of researchers due to their immense therapeutic properties with no or minimal side effects. These medicinal plants contain various secondary metabolites, including alkaloids, flavonoids, flavonols, phenol, coumarins, terpenoids, essential oils, and tannins. Although they are utilized as defensive chemicals, they are also a vital source of phytomedicines due to their vast potential to battle bacterial, fungal, protozoal, and viral infections (Kabir et al. 2016). As a result, they represent a significant source of physiologically active chemicals, which are responsible for a vast number of medications employed in modern treatments. Thus far, natural products have played a critical role in ensuring human wellness and have been the medications of choice because of their safety and efficacy (Rauf et al. 2014). Phytochemical investigation of leaves and flowers reveals the existence of alkaloids, flavonoids, tannins, saponins, phenolics, glycosides, etc. (Table 2) (Pradyutha et al. 2015; Ogah et al. 2020).

According to the comprehensive literature review conducted for this study, plant phenolics are one of the essential classes of chemicals that operate as principal antioxidants (Roghini and Vijayalakshmi 2018). These compounds have various biochemical functions and scavenging capabilities for scavenging both active oxygen species and electrophiles. In addition, they have been correlated to multiple biological belongings with health-promoting qualities (Lelono et al. 2009), such as anticancer, antimicrobial,

Table 2 Qualitative phytochemical screening of *E. milii* leaves and flowers extracts

S. No	Phytochemical constituents	Leaves		Flowers	
		Ethanol	Aqueous	Ethanol	Aqueous
1	Alkaloids	+	+	+	+
2	Flavonoids	+	+	+	+
3	Carbohydrates	-	+	-	+
4	Reducing sugar	-	+	-	+
5	Cardiac glycosides	+	+	+	+
6	Protein & amino acids	-	+	-	+
7	Glycosides	+	-	+	-
8	Phenolic compounds	+	+	+	+
9	Tannins	-	+	-	+
10	Phlobatannins	+	+	+	+
11	Saponins	+	+	+	+
12	Coumarin	+	+	-	+
13	Anthocyanins	+	+	-	+
14	Quinones	+	+	+	+
15	Phytosterols	+	-	+	-
16	Triterpenoids	+	-	+	-
17	Steroids	+	-	+	-

Key: Positive result (+), Negative result (-)

Table 3 Quantitative phytochemical tests of leaves and flowers extracts of *E. milii* (mg/g)

Parts of plant	Extract	TAC	TFC	TPC	TTC
Leaf	Ethanol	5.58±0.43	38± 0.25	89.81± 0.43	38.25± 0.33
	Aqueous	11.24±0.31	133.94±0.38	252.41±0.56	14.42± 0.31
Flower	Ethanol	3.84±0.37	30.03± 0.73	76.29±0.42	21.46± 0.32
	Aqueous	8.39±0.47	62.93± 0.38	155.56±0.42	7.75± 0.32

TAC- Total alkaloid content, TFC- Total flavonoid content, TPC- Total phenol content, TTC- Total tannins content

anti-inflammation, and antiviral properties. Current investigations showed that the quantitative phytochemical analysis indicates sufficient alkaloids, flavonoids, phenolics, and tannins content in each extract (Table 3). Leaf aqueous and flower aqueous showed potentially higher amounts of alkaloids, flavonoids, and phenolic contents, while the maximum amount of tannins was confirmed in leaf ethanol and flower ethanol extracts (Ghagane et al. 2017). Overall, aqueous extracts of leaves and flowers exhibited the highest amount of total alkaloid (11.24±0.31 and 8.39±0.47mg/g), total flavonoid (133.94±0.38 and 62.93±0.38mg/g) and total phenol content (252.41±0.56 and 155.46±0.42 mg/g) respectively, compared to the ethanolic extracts except total tannins. For tannins, ethanolic extracts of leaves and

flowers exhibited the highest total tannin content, 38.25±0.33 and 21.46±0.32mg/g, respectively, compared to the aqueous extracts of leaves and flowers. According to the findings of this study, tested plant extracts can be employed as antioxidants and antimicrobial agents (Saleem et al. 2019).

3.3 Antioxidant assay

The antioxidant properties of polyphenols, including flavonoids, are primarily due to their redox characteristics, which can contribute to the absorption and neutralization of reactive oxygen species, quenching of singlet and triplet oxygen, and peroxide breakdown (Kabir et al. 2016). Antioxidants defend our bodies

from many illnesses by scavenging ROS or safeguarding the antioxidant defence systems (Jayathilakan et al. 2007). Natural antioxidants are found in medicinal plants with significant antioxidant properties. Antioxidant activity is present in many secondary metabolites classified as polyphenols, terpenes, and alkaloids (Lee et al. 2003). The major portion of plant antioxidant activity may be derived from phenolic molecules such as flavonoids, isoflavones, flavones, etc. Although their exact activities in this study were not studied, it has been reported that the most active components in these species include flavonoids, steroids, glycosides, and alkaloids (Ogah et al. 2020). Leaves aqueous extracts of *E. milii* showed the maximum inhibition on antioxidant capacity, DPPH, H₂O₂, and FRAP assay, as reflected in their IC₅₀ values tested for antioxidant activity. Results of the antioxidant activity revealed that *E. milii* plants with relatively high flavonoid and phenolic content might be a substantial natural antioxidant source. Quantifying these active ingredients might be a foundation for this species to treat ROS-related conditions. The effectiveness of this species can be credited to the commonality and mix of subordinate metabolites found in each extract.

3.3.1 Total antioxidant capacity

All the extracts showed potential antioxidant capacity as compared to standard ascorbic acid. However, Aqueous extracts of leaves & flowers exhibited the highest total antioxidant capacity, 318.96±0.8 and 254.74±0.66mg/g, respectively, as compared to the ethanolic extracts of leaves and flowers. Table 4 demonstrates the results of the total antioxidant capacity in different *E. milii* leaves and flower extracts (Ogah et al. 2020).

3.3.2 DPPH assay

The results demonstrated a promising antioxidant effect in the DPPH experiment. The aqueous extracts of leaves and flowers showed maximum 90.31% and 87.22% inhibition with IC₅₀ values of 30.70 and 36.34µg/ml, respectively, associated with the standard ascorbic acid of 27.9µg/ml with a maximum inhibition of 95.99±0.43% followed by the ethanolic leaves and flowers extracts (Chohan et al. 2020). Table 4 illustrates the results of various extracts of *E. milii* for the DPPH assay.

3.3.3 H₂O₂ assay

In the H₂O₂ scavenging assay, all the preparations demonstrated a dose-dependent scavenging activity. The aqueous leaves and flowers extracts showed the maximum inhibition of 91.79% and 84.62% with IC₅₀ values of 82.92 and 89.16µg/ml, respectively, which is significant compared to the IC₅₀ of standard ascorbic acid 71.73 µg/ml with a maximum inhibition of 86.92% (Chohan et al. 2020). Table 4 demonstrates the results of the H₂O₂ scavenging assay in various extracts of *E. milii*.

3.3.4 FRAP assay

The results revealed a proportionate increase in reduction power with increasing extract concentration. The reducing power results suggest the maximum reducing power of leaves aqueous and ethanolic extracts with EC₅₀ values of 60.05 and 70.59µg/ml, respectively, compared to the EC₅₀ of standard ascorbic acid 33.95µg/ml (Chohan et al. 2020). Table 4 demonstrates the results of the FRAP assay in various extracts of *E. milii*.

3.4 Antimicrobial assay

3.4.1 Agar well diffusion assay

Due to the emergence of microbial drug resistance, the indiscriminate and irrational use of antimicrobial medicines has posed an unprecedented threat to human civilization. The rise of multidrug-resistant pathogens has recently gained international attention and is now a significant concern for the future of humanity. Additionally, the adverse side effects of modern synthetic medications like antibiotics, fungicides, and antioxidants have driven researchers to develop new medicines without adverse effects on the human body. People are again looking to biodiversity for health care management, as natural resources have traditionally benefited people (Tollefson and Miller 2000). Since plants have a rich structural diversity of chemical compounds, utilizing this vast resource to develop novel medications to treat various infectious illnesses is crucial. As a result, there has been a renaissance in interest in investigating novel plants as a source of possible medication candidates in recent years. Isolated microbial

Table 4 Results of antioxidant assay of ethanol and aqueous extracts of *E. milii*

Parts of plants	Extracts	TAC (mg AA/g)	DPPH		H ₂ O ₂		FRAP
			% RSA	IC ₅₀	% RSA	IC ₅₀	EC ₅₀
Standard	Ascorbic A	-	95.99±0.43	27.95	86.92±0.36	71.73	33.95
Flowers	Ethanol	108.58±0.79	78.19±0.09	78.19	82.31±0.12	95.93	85.04
	Aqueous	254.74±0.66	87.22±0.26	36.34	84.62±0.29	89.16	75.56
Leaves	Ethanol	179.60±0.46	82.96±0.14	46.17	83.33±0.16	93.38	70.59
	Aqueous	318.96±0.8	90.31±0.21	30.70	91.79±0.27	82.92	60.05

strains were resistant to some modern medicines, so further investigation is required if an extract of *E. milii* could control these pathogens. The agar-well diffusion technique was used to examine the antibacterial activities. Zones of inhibition were seen in all isolates tested using the agar well diffusion technique ranging from 2-24mm at 10-320mg/mL concentrations (Tables 5 and 6). Both gram(+ve) *S. aureus* and gram(-ve) *K. pneumonia* bacterial isolates were discovered to be susceptible to flower ethanol extracts. Leaf ethanol and aqueous extracts showed broad-spectrum efficacy against gram -ve *E. coli*, and *P. aeruginosa* isolates. Except for *C. albicans*, all other species were shown to be effective against the tested isolates (Tables 5 and 6). This study's data on antifungal activity showed that *E. milii* was less effective in antifungal action. *E. milii* was shown to have a substantial inhibitory effect on both gram +ve and -ve bacteria tested. Several authors have well-documented the efficacy of *E. milii* as an antioxidant, antibacterial, and antifungal. The results of this experiment indicate that ethanolic extracts of the tested species were shown to be more effective when compared to aqueous extracts (Nayak et al. 2015).

3.5 Computational docking analysis

The structural model of the dihydrofolate reductase (DHFR) enzyme of *E. coli* (pdb id: 6cqa), DNA gyrase of *P. aeruginosa* (pdb id: 6mlj), DHFR of *S. aureus* (pdb id: 2w9s), acetolactate synthase of *K. pneumoniae* (pdb id: 5d6r), DHFR of *C. albicans* (pdb id: 1ai9), and cytochrome P450 reductase of *H. sapiens* (pdb id: 3qfs) was used in the current study (Berman et al. 2000). Prepared macromolecular receptors were saved in the default Auto dock format (*. Pdb qt). The imaginary grid-box was prepared for each target receptor by covering the extended conformations of the utilized ligands and the macromolecular binding residues for each target protein. Molecular docking analysis revealed that the taraxerol and beta-sitosterol were the active ingredients in the *E. milii* plant responsible for executing antimicrobial, antifungal, and antioxidant effects. The taraxerol is found to be interacting with the DHFR enzyme of *E. coli* and *C. albicans* for antimicrobial and antifungal effects. In contrast, the beta-sitosterol was found to be interacting with the acetolactate synthetase enzyme of *K. pneumoniae* for

Table 5 Zone of inhibition at various concentrations of *E. milii* extracts against several MDR isolates afterwards 24 hrs

Plant extracts	MDR isolates	Zone of inhibition (mm) at various concentrations (mg/ml)						Colistin (10µg)
		10mg	20mg	40mg	80mg	160mg	320mg	
Flower ethanol	<i>E. coli</i>	3.92±0.38	8.5 ±0.5	10.58±0.52	14.58±0.63	17.84±0.76	20.08±0.38	17.5 ±0.5
	<i>P. aeruginosa</i>	2.42 ±0.38	5.42 ±0.52	7.5 ±0.5	11.58 ±0.63	15.59 ±0.52	19 ±0.25	17.92 ±0.38
	<i>K. pneumoniae</i>	5.42 ±0.52	9.5 ±0.5	12.83 ±0.62	17.16 ±0.29	19.33 ±0.38	22.92 ±0.38	19.5 ±0.5
	<i>S. aureus</i>	3.5 ±0.5	7.75 ±0.25	14.25 ±0.25	17.25 ±0.25	19.75 ±0.25	24 ±0.25	19.83 ±0.29
	<i>C. albicans</i>	-	-	-	-	-	-	-
Flower aqueous	<i>E. coli</i>	2.33 ±0.58	5.25 ±0.66	7.5 ±0.5	10.73 ±0.75	14.58 ±0.52	18.08 ±0.38	17.08 ±0.38
	<i>P. aeruginosa</i>	2.25 ±0.5	5.08 ±0.35	8.42 ±0.52	10.92 ±0.38	14.42 ±0.38	18.58 ±0.52	17.41 ±0.38
	<i>K. pneumoniae</i>	2.25 ±0.25	6.58 ±0.62	10.42±0.38	16.5 ±0.5	18.33 ±0.38	20.25 ±0.25	18.42 ±0.38
	<i>S. aureus</i>	-	5.42 ±0.52	8.25 ±0.25	13.5 ±0.5	15.57 ±0.52	19.33 ±0.29	18.25 ±0.25
	<i>C. albicans</i>	-	-	-	-	-	-	-
Leaf ethanol	<i>E. coli</i>	5.33 ±0.57	7.5 ±0.5	10.75±0.66	13.5 ±0.5	18.08 ±0.38	20.75 ±0.25	17.58±0.52
	<i>P. aeruginosa</i>	3.75 ±0.25	7.83 ±1.04	12.75±1.08	15.58±0.8	19.42 ±0.62	21.58±0.52	19.16±0.29
	<i>K. pneumoniae</i>	2.25 ±0.25	7.08 ±0.15	11.5±0.5	14.5±0.5	17.25±0.43	20.92±0.38	18.92±0.38
	<i>S. aureus</i>	-	6.25±0.25	10.42±0.38	13.42±0.38	17.5±0.5	20.42±0.38	17.42±0.38
	<i>C. albicans</i>	-	-	-	-	-	-	-
Leaf aqueous	<i>E. coli</i>	-	1.33±0.38	3.5±0.5	7.48±0.5	12.75±0.66	18.42±0.52	18±0.25
	<i>P. aeruginosa</i>	2.5 ±0.5	7.42±0.94	10.08±0.88	12.58±0.8	18.17±0.76	23.58±0.36	17.5±0.5
	<i>K. pneumoniae</i>	-	3.33 ±0.38	6.67±0.62	10.5±0.5	16.5±0.66	19.58±0.52	17.58±0.63
	<i>S. aureus</i>	-	2.5±0.5	8.25±0.43	11.58±0.52	14.42±0.38	17.5±0.5	17.42±0.38
	<i>C. albicans</i>	-	-	-	-	-	-	-

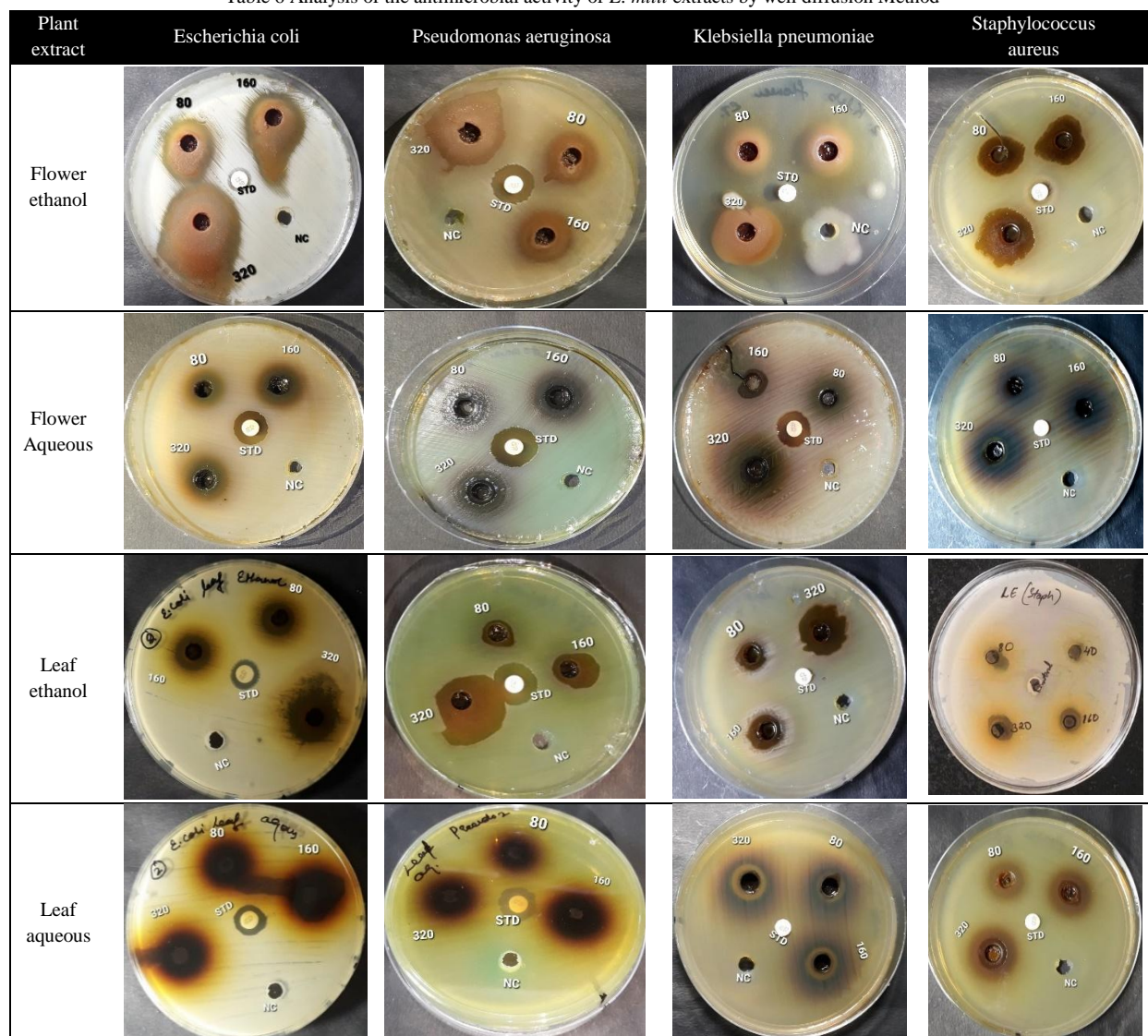
Table 6 Analysis of the antimicrobial activity of *E. milii* extracts by well diffusion Method

Table 7 Coordinates are used to prepare a grid box for various macromolecular targets in the current computational paradigm

PDB Id	x-axis	y-axis	z-axis	Spacing (Å)	x centre	y centre	z centre
6cqa	40	40	40	0.386	14.844	26.998	6.265
6m1j	40	40	40	0.397	21.478	58.663	41.43
2w9s	40	40	40	0.369	5.984	-0.45	40.784
5d6r	40	40	40	0.375	-7.403	36.502	-12.131
1ai9	52	52	52	0.403	29.081	-6.919	11.8
3qfs	40	40	40	0.564	42.794	24.08	21.506

antimicrobial effect, with DHFR of *C. albicans* for antifungal effect and cytochrome P450 reductase enzyme for executing antioxidant effect. The grid parameters used in the current study were tabulated in Table 7. Docking results for the screened

ligand, standard drug, and reference ligand were tabulated in Table 8. The three-dimensional binding mode of the taraxerol and beta-sitosterol against various macromolecular targets is shown in Figure 2.

Table 8 Binding energy obtained for chemical constituents from *E. milii* plant against different drug targets considered in the current study

S.N	Name	Antibacterial				Antifungal	Antioxidant
		<i>E. coli</i> DHFR (6cqa)	<i>P. aeruginosa</i> DNA Gyrase (6mlj)	<i>S. aureus</i> DHFR (2w9s)	<i>K. pneumoniae</i> AcetoA synthetase (5d6r)	<i>C. albicans</i> DHFR (1ai9)	<i>H. Sapiens</i> cP450 reductase (3qis)
1	Taraxerol	-9.36	-7.95	-8.81	-8.66	-10.64	-8.48
2	2,8-hydroxyfriedelan-1,3-dione-29- oic acid						
3	Quercetin 3-O-(2"-O-galloyl)-a-Larabinofuranoside	-6.22	-5.52	-8.05	-6.06	-6.86	-6.15
4	7 7'- dihydroxy, 8, 6'-bicumarin	-8.14	-7.45	-8.19	-7.61	-7.61	-8.36
5	9-acetyl-3'4'-dimethoxy dehydroconiferyl-3-alcohol	-7.49	-6.66	-6.24	-7.78	-7.13	-6.60
6	Beta-sitosterol	-9.00	-9.31	-9.42	-9.81	-8.95	-8.37
7	1-octacosanol	-3.35	-1.72	-4.82	-2.04	-4.13	-1.18
8	1-triacontanol	-2.31	-1.83	-4.49	-3.20	-2.34	-1.41
9	Cyclobarbital	-7.67	-6.40	-8.21	-7.06	-6.41	-5.96
10	Mephobarbital	-7.16	-5.78	-7.53	-5.89	-6.30	-6.46
11	N-methyl-N-acetyl-3,4 methylenedioxybenzylamine	-5.63		-5.95	-6.10	-6.27	-6.04
12	Palmitic acid	-4.90	-4.29	-4.45	-4.31	-4.87	-4.77
13	Butanoic acid	-2.97	-2.94	-3.14	-3.45	-4.51	-3.99
14	3-amino-1-phenylbutane acetyl derivative	-7.08	-6.53	-6.86	-7.39	-5.36	-5.93
15	Stearic acid	-5.11	-3.49	-4.63	-4.26	-5.12	-3.43
16	Standard	-5.78	-6.14	-6.08	-5.57	-5.85	-5.12

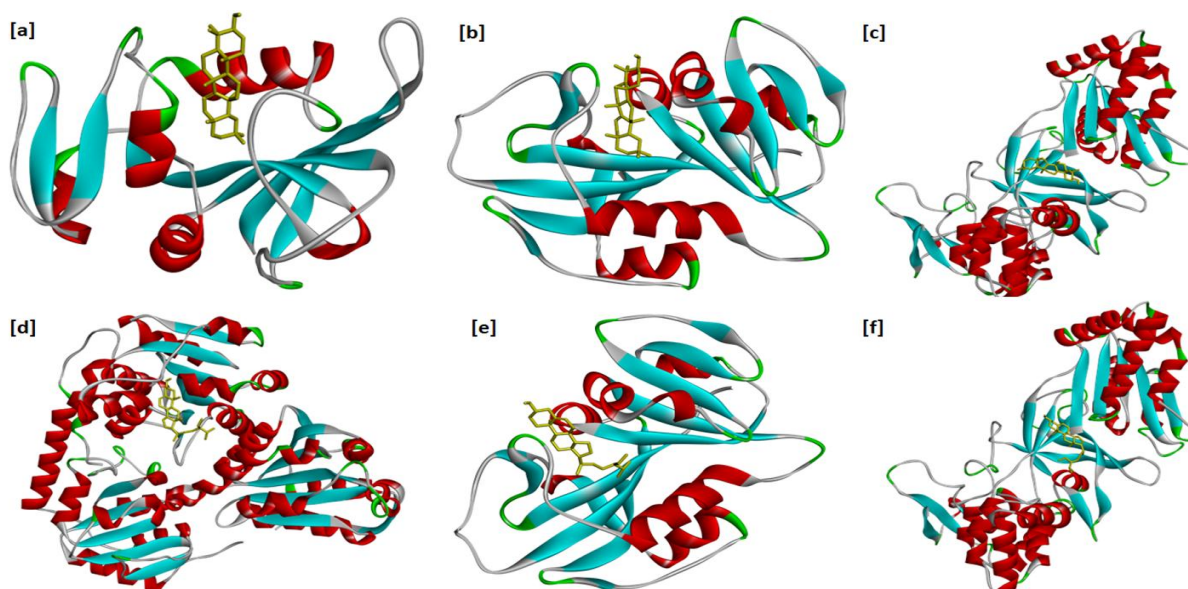


Figure 2 Three-dimensional binding conformation obtained after molecular docking for taraxerol against (a) DHFR enzyme of *E.coli*, (b) DHFR enzyme of *C. albicans*, (c) cytochrome P450 reductase enzyme of *H. sapiens*, (d) Beta-sitosterol against acetolactate synthetase enzyme of *K. pneumoniae*, (e) DHFR enzyme of *C. albicans*, (f) cytochrome P450 reductase enzyme of *H. sapiens*

Conclusions

In current findings, the quantitative phytochemical analysis indicates the existence of alkaloids, flavonoids, phenolics, and tannins content in the extract. Leaf and flower extracts exhibited antioxidant activity, likely due to their high flavonoid and phenolic content. Furthermore, *E. milii* showed impressive antibacterial potency against clinically isolated multidrug-resistant bacteria, while the extract does not exhibit antifungal activity against *Candida albicans*. Docking-based in-silico screening of the chemical constituents of the *E. milii* concerned has revealed that the taraxerol and beta-sitosterol are the active constituents that are supposed to be responsible for antimicrobial and antioxidant potential. Further research is required to clarify the mechanistic aspect of the antimicrobial & antioxidant traits of *E. milii*. This plant has the prospect of being a prodigious source of novel chemical compounds for appropriate new drug developments.

Abbreviations

E. milii: *Euphorbia milii*; EE: Ethanolic extract; AE: Aqueous extract; DPPH: α , α -Diphenyl- ρ -picryl hydrazyl; FRAP: Ferric reducing antioxidant potential; TAC: Total antioxidant capacity; IC₅₀: 50% Inhibitory concentration; TPC: Total polyphenol content; TFC: Total flavonoid content; TAC: Total alkaloid content; TTC: Total tannins content; GAE: Gallic acid equivalent; RE: Rutin equivalent; DHFR; Dihydrofolate reductase, cP450; Cytochrome P450 inhibitors

Acknowledgments

The authors are thankful to Maharishi Markandeshwar (Deemed to be University) for providing a research facility.

Conflict of interest

All the authors declare no conflict of interest regarding this work.

Author contributions

All authors have combinedly contributed to complete the work. Therefore, we ensure and hereby declare that all authors have read and approved the final manuscript to submit to the selected journal.

References

- Abifarín, T. O., Afolayan, A. J., & Otunola, G. A. (2019). Phytochemical and Antioxidant Activities of *Cucumis africanus* L.f.: A Wild Vegetable of South Africa. *Journal of Evidence-Based Integrative Medicine*, 24, 1–8. <https://doi.org/10.1177/2515690X19836391>
- Agrawal, N., Mujwar, S., Goyal, A., & Gupta, J. K. (2021). Phytoestrogens as Potential Antiandrogenic Agents Against

Prostate Cancer: An In Silico Analysis. *Letters in Drug Design & Discovery*, 19(1), 69–78. <https://doi.org/10.2174/1570180818666210813121431>

Ajanaku, C.O., Echeme, J.O., Mordi, R.C., Ajani, O.O., J.A.O., O., Owoeye, T.F., Taiwo, O., & Ataboh, J.U. (2017). Phytochemical Screening and Antimicrobial Studies of *Crateva adansonii* Leaf Extract. *Covenant Journal of Physical and Life Sciences*, 4(2), 35–41. <http://journals.covenantuniversity.edu.ng/index.php/cjpls/article/view/408/291>

Aleksandrov, M., Maksimova, V., & Koleva Gudeva, L. (2019). Review of the anticancer and cytotoxic activity of some species from genus *Euphorbia*. *Agriculturae Conspectus Scientificus*, 84(1), 1–5.

Al-zoreky, N. S., & Al-Taher, A. Y. (2015). Antibacterial activity of spathe from *Phoenix dactylifera* L. against some food-borne pathogens. *Industrial Crops and Products*, 65, 241–246. <https://doi.org/10.1016/j.indcrop.2014.12.014>

Aman S, Mittal D, Shrivastav S, Tuli HS, Chauhan S, Singh P, Sharma S, Saini RV, Kaur N, Saini AK. (2022) Prevalence of multidrug-resistant strains in device associated nosocomial infection and their in vitro killing by nanocomposites. *Annals of Medicine and Surgery*, 78:103687. <https://doi.org/10.1016/j.amsu.2022.103687>

Aman, S., Kaur, N., Mittal, D., Sharma, D., Shukla, K.K., Singh, B., Sharma, A., Siwal, S.S., Thakur, V.K., Joshi, H., Gupta, R., Saini, R.V., & Saini, A.K. (2023). Novel Biocompatible Green Silver Nanoparticles Efficiently Eliminates Multidrug Resistant Nosocomial Pathogens and Mycobacterium Species. *Indian Journal of Microbiology*. <https://doi.org/10.1007/s12088-023-01061-0>

Arvouet-Grand, A., Vennat, B., Pourrat, A., & Legret, P. (1994). Standardization of propolis extract and identification of principal constituents. *Journal de Pharmacie de Belgique*, 49(6), 462–468.

Aryal, S., Baniya, M. K., Danekhu, K., Kunwar, P., Gurung, R., & Koirala, N. (2019). Total Phenolic content, Flavonoid content and antioxidant potential of wild vegetables from western Nepal. *Plants*, 8(4), 1–12. <https://doi.org/10.3390/plants8040096>

Balouiri, M., Sadiki, M., & Ibnsouda, S. K. (2016). Methods for in vitro evaluating antimicrobial activity: A review. *Journal of Pharmaceutical Analysis*, 6(2), 71–79. Xi'an Jiaotong University. <https://doi.org/10.1016/j.jpha.2015.11.005>

Berman, H. M., Westbrook, J., Feng, Z., Gilliland, G., Bhat, T. N., Weissig, H., Shindyalov, I. N., & Bourne, P. E. (2000). The Protein Data Bank. *Nucleic Acids Research*, 28(1), 235–242. <https://doi.org/10.1093/nar/28.1.235>

- Bonev, B., Hooper, J., & Parisot, J. (2008). Principles of assessing bacterial susceptibility to antibiotics using the agar diffusion method. *Journal of Antimicrobial Chemotherapy*, 61(6), 1295–1301. <https://doi.org/10.1093/jac/dkn090>
- Chaman, S., Khan, F. Z., Khokhar, R., Maab, H., Qamar, S., Zahid, S., Ahmad, M., & Hussain, K. (2019). Cytotoxic and antiviral potentials of *Euphorbia milii* var. Splendens leaf against peste des petits ruminant virus. *Tropical Journal of Pharmaceutical Research*, 18(7), 1507–1511. <https://doi.org/10.4314/tjpr.v18i7.21>
- Chauhan S, Kaur Narinder, Saini A.K., Aman S, Chauhan J, Kumar Harit. (2022) Colistin Resistant Gram-Negative Bacteria Isolated from Various Clinical Samples in North Indian Tertiary Care Center. *International Journal of Pharmaceutical Quality Assurance*, 13(3), 324-329. <https://doi.org/10.25258/ijpqa.13.3.18>
- Chohan, T. A., Sarfraz, M., Rehman, K., Muhammad, T., Ghori, M. U., Khan, K. M., Afzal, I., Akash, M. S. H., Alamgeer, Malik, A., & Chohan, T. A. (2020). Phytochemical profiling, antioxidant and antiproliferation potential of *Euphorbia milii* var.: Experimental analysis and in-silico validation. *Saudi Journal of Biological Sciences*, 27(11), 3025–3034. <https://doi.org/10.1016/j.sjbs.2020.08.003>
- Dobriyal, V., Guleri, S., & Singh, M. (2021). Morphological, anatomical and preliminary phytochemical characterization of *Buddleja madagascariensis* Lam. *Current Botany*, 12, 53-61. <https://doi.org/10.25081/cb.2021.v12.6242>.
- Fidan, O., Mujwar, S., & Kciuk, M. (2022). Discovery of adapalene and dihydrotachysterol as antiviral agents for the Omicron variant of SARS-CoV-2 through computational drug repurposing. *Molecular Diversity*, 27(1), 463-475. <https://doi.org/10.1007/s11030-022-10440-6>
- Gapuz, M., & Besagas, R. (2018). Phytochemical profiles and antioxidant activities of leaf extracts of *Euphorbia* species. *Journal of Biodiversity and Environmental Sciences*, 12(4), 59–65. <http://www.innspub.net>
- Ghagane, S. C., Puranik, S. I., Kumbar, V. M., Nerli, R. B., Jalalpure, S. S., Hiremath, M. B., Neelagund, S., & Aladakatti, R. (2017). In vitro antioxidant and anticancer activity of *Leea indica* leaf extracts on human prostate cancer cell lines. *Integrative Medicine Research*, 6(1), 79–87. <https://doi.org/10.1016/j.imr.2017.01.004>
- Godara, A. (2022). Preliminary Phytochemical Screening and Determination of Total Phenols and Flavonoids in Aerial Parts of *Viola Tricolor*. *ECS Transactions*, 107(1), 8219–8227. <https://doi.org/10.1149/10701.8219ecst>
- Gülçin, I. (2005). The antioxidant and radical scavenging activities of black pepper (*Piper nigrum*) seeds. *International Journal of Food Sciences and Nutrition*, 56(7), 491–499. <https://doi.org/10.1080/09637480500450248>
- Habu, J. B., & Ibeh, B. O. (2015). In vitro antioxidant capacity and free radical scavenging evaluation of active metabolite constituents of *Newbouldia laevis* ethanolic leaf extract. *Biological Research*, 48(16), 1–10. <https://doi.org/10.1186/s40659-015-0007-x>
- Haleshappa, R., Keshamma, E., Girija, C. R., Thanmayi, M., Nagesh, C. G., Fahmeen, G. H. L., Lavanya, M., & Patil, S. J. (2019). Phytochemical Study and Antioxidant Properties of Ethanolic Extracts of *Euphorbia milii*. *Asian Journal of Biological Sciences*, 13(1), 77–82. <https://doi.org/10.3923/ajbs.2020.77.82>
- Harborne, J. B. (2020). Phytochemical Methods. *Ethnoveterinary Botanical Medicine* (11th ed.). Springer Netherlands. <https://doi.org/10.1201/ebk1420045604-8>
- Jahan, I. A., Hossain, M. H., Nimmi, I., Islam, S., Kawsar, M. H., & Islam, M. A. (2012). Evaluation of anti-inflammatory and antioxidant potential of the kernel root of *Xylocarpus mekongensis* (Lamk.) M. Roem. *Oriental Pharmacy and Experimental Medicine*, 12(3), 181–188. <https://doi.org/10.1007/s13596-012-0068-0>
- Jayathilakan, K., Sharma, G. K., Radhakrishna, K., & Bawa, A. S. (2007). Antioxidant potential of synthetic and natural antioxidants and its effect on warmed-over-flavour in different species of meat. *Food Chemistry*, 105(3), 908–916. <https://doi.org/10.1016/j.foodchem.2007.04.068>
- Kabir, M. S. H., Hossain, M. M., Kabir, M. I., Ahmad, S., Chakrabarty, N., Rahman, M. A., & Rahman, M. M. (2016). Antioxidant, antidiarrheal, hypoglycemic and thrombolytic activities of organic and aqueous extracts of *Hopea odorata* leaves and in silico PASS prediction of its isolated compounds. *BMC Complementary and Alternative Medicine*, 16(1), 1–13. <https://doi.org/10.1186/s12906-016-1461-x>
- Kaur, A., Mujwar, S., & Adlakha, N. (2016). In-silico analysis of riboswitch of *Nocardia farcinica* for design of its inhibitors and pharmacophores. *International Journal of Computational Biology and Drug Design*, 9(3), 261–276. <https://doi.org/10.1504/IJCBD.2016.078278>
- Kokate, C. K., Purohit, A. P., & Gokhale, S. B. (2003). *A Text Book of Practical Pharmacognosy* (Vol. 22). Nirali Prakashan, Educational publishers.
- Lee, S. E., Hwang, H. J., Ha, J. S., Jeong, H. S., & Kim, J. H. (2003). Screening of medicinal plant extracts for antioxidant activity. *Life Sciences*, 73(2), 167–179. [https://doi.org/10.1016/S0024-3205\(03\)00259-5](https://doi.org/10.1016/S0024-3205(03)00259-5)

- Lelono, R. A. A., Tachibana, S., & Itoh, K. (2009). In vitro antioxidative activities and polyphenol content of *Eugenia polyantha* wight grown in Indonesia. *Pakistan Journal of Biological Sciences*, 12(24), 1564–1570. <https://doi.org/10.3923/pjbs.2009.1564.1570>
- Migdal, C., & Serres, M. (2011). Reactive oxygen species and oxidative stress. *Medecine Sciences*, 27(4), 405–412. <https://doi.org/10.1051/MEDSCI/2011274017>
- Moges, A., Barik, C. R., Purohit, S., & Goud, V. V. (2021). Dietary and bioactive properties of the berries and leaves from the underutilized *Hippophae salicifolia* D. Don grown in Northeast India. *Food Science and Biotechnology*, 30(12), 1555–1569. <https://doi.org/10.1007/s10068-021-00988-8>
- Muanda, F., Koné, D., Dicko, A., Soulimani, R., & Younos, C. (2011). Phytochemical composition and antioxidant capacity of three malian medicinal plant parts. *Evidence-based complementary and alternative medicine*, 2011, 674320. <https://doi.org/10.1093/ecam/nep109>
- Mujwar, S., & Tripathi, A. (2022). Repurposing benzbromarone as antifolate to develop novel antifungal therapy for *Candida albicans*. *Journal of Molecular Modeling*, 28(7), 1–9. <https://doi.org/10.1007/s00894-022-05185-w>
- Mujwar, S., Sun, L., & Fidan, O. (2022). In silico evaluation of food-derived carotenoids against SARS-CoV-2 drug targets: Crocin is a promising dietary supplement candidate for COVID-19. *Journal of Food Biochemistry*, 46(9). <https://doi.org/10.1111/jfbc.14219>
- Mutalib, N. S. A. A., Yusuf, N., Asari, A., Aziz, A. N., & Wahab, N. H. A. (2020). Qualitative and quantitative of phytochemical analysis of Malaysian *Euphorbia milii* (Euphorbiaceae) and its antioxidant activities. *Malaysian Applied Biology*, 49(4), 233–239. <https://doi.org/10.55230/mabjournal.v49i4.1626>
- Narendra, D., Mounisha, A., Bhavani, B., Sireesha, G., Vijaya Kamari, K., & Sri Ramavenkata Reddy, M. (2015). Antimicrobial studies on flowers of *Euphorbia milii*. *Der Pharmacia Lettre*, 7(3), 196–204.
- Nayak, D., Pradhan, S., Ashe, S., Rauta, P. R., & Nayak, B. (2015). Biologically synthesized silver nanoparticles from three diverse family of plant extracts and their anticancer activity against epidermoid A431 carcinoma. *Journal of Colloid and Interface Science*, 457, 329–338. <https://doi.org/10.1016/j.jcis.2015.07.012>
- Ogah, C., Igbokwe, N., Owolabi, M., & Alabi, F. (2020). Antimicrobial Evaluation of the Leaf Extract of *Euphorbia milii*.var *splendens*. *African Journal of Pharmaceutical Research & Development*, 12(2), 199–207.
- Oyaizu, M. (1986). Studies on products of browning reaction. Antioxidative activities of products of browning reaction prepared from glucosamine. *The Japanese Journal of Nutrition and Dietetics*, 44(6), 307–315. <https://doi.org/10.5264/eyogakuzashi.44.307>
- Pincus, D. H. (2010). Microbial identification using the bioMérieux VITEK® 2 system. In *Encyclopedia of Rapid Microbiological Methods*. chrome-extension://efaidnbmnnnibpcajpcglclefindmkaj/https://store.pda.org/TableOfContents/ERMM_V2_Ch01.pdf
- Pradhan, P., Soni, N. K., Chaudhary, L., Mujwar, S., & Pardasani, K. R. (2015). In-silico prediction of riboswitches and design of their potent inhibitors for H1N1, H2N2 and H3N2 strains of influenza virus. *Biosciences Biotechnology Research Asia*, 12(3), 2173–2186. <https://doi.org/10.13005/bbra/1889>
- Pradyutha, C.A., Maheswara Rao, U. V, Uma Maheswara Rao, V., District, G., & Pradesh, A. (2015). Phytochemical screening and antimicrobial evaluation of *Euphorbia milii* leaf extracts. *World Journal of Pharmaceutical Research World Journal of Pharmaceutical Research*, 5, 4(8), 1626–1633.
- Prieto, P., Pineda, M., & Aguilar, M. (1999). Spectrophotometric quantitation of antioxidant capacity through the formation of a phosphomolybdenum complex: Specific application to the determination of vitamin E. *Analytical Biochemistry*, 269(2), 337–341. <https://doi.org/10.1006/abio.1999.4019>
- Rajesh, V., & Perumal, P. (2014). In vivo assessment of antidiabetic and antioxidant activities of methanol extract of *Smilax zeylanica* leaves in wistar rats. *Oriental Pharmacy and Experimental Medicine*, 14(2), 127–144. <https://doi.org/10.1007/s13596-013-0137-z>
- Rao, Y. K., Damu, A. G., Rao, A. J., Venkatesan, S., Kuo, P. C., Rao, C. V., & Wu, T. S. (2003). Flavonoids from *Andrographis viscosula*. *Chemical and Pharmaceutical Bulletin*, 51(12), 1374–1376. <https://doi.org/10.1248/cpb.51.1374>
- Rauf, A., Khan, A., Uddin, N., Akram, M., Arfan, M., Uddin, G., & Qaisar, M. (2014). Preliminary phytochemical screening, antimicrobial and antioxidant activities of *Euphorbia milli*. *Pakistan Journal of Pharmaceutical Sciences*, 27(4), 947–951.
- Rehni, A. K., Singh, T. G., Jaggi, A. S., & Singh, N. (2008). Pharmacological preconditioning of the brain: A possible interplay between opioid and calcitonin gene related peptide transduction systems. *Pharmacological Reports*, 60(6), 904–913. <http://europepmc.org/abstract/MED/19211983>
- Roghini, R., & Vijayalakshmi, K. (2018). Phytochemical Screening, Quantitative Analysis of Flavonoids and Minerals in

- Ethanol Extract of *Citrus Paradisi*. *International Journal of Pharmaceutical Sciences and Research*, 9(11), 48-59. [https://doi.org/10.13040/IJPSR.0975-8232.9\(11\).4859-64](https://doi.org/10.13040/IJPSR.0975-8232.9(11).4859-64)
- Ruch, R. J., Cheng, S. jun, & Klaunig, J. E. (1989). Prevention of cytotoxicity and inhibition of intercellular communication by antioxidant catechins isolated from Chinese green tea. *Carcinogenesis*, 10(6), 1003–1008. <https://doi.org/10.1093/carcin/10.6.1003>
- Sagar, S., & Bisht, M. (2021). A Review on Phytopharmacology of Medicinal Plant: *Euphorbia milii* Des Moul. *International Research Journal Of Pharmacy*, 12(6), 67–74. <https://doi.org/10.7897/2230-8407.1206146>
- Sagayaraj, R., Dhineshkumar, T., Prakash, A., Aravazhi, S., Chandrasekaran, G., Jayarajan, D., & Sebastian, S. (2020). Fabrication, microstructure, morphological and magnetic properties of W-type ferrite by co-precipitation method: Antibacterial activity. *Chemical Physics Letters*, 759. <https://doi.org/10.1016/j.cplett.2020.137944>
- Saleem, H., Zengin, G., Locatelli, M., Mollica, A., Ahmad, I., Mahomoodally, F. M., Zainal Abidin, S. A., & Ahemad, N. (2019). In vitro biological propensities and chemical profiling of *Euphorbia milii* Des Moul (Euphorbiaceae): A novel source for bioactive agents. *Industrial Crops and Products*, 130, 9–15. <https://doi.org/10.1016/j.indcrop.2018.12.062>
- Sheela Devi, A., & Rajkumar, J. (2013). In vitro antibacterial activity and stability of *Avicennia marina* against urinary tract infection pathogens at different parameters. *Pakistan Journal of Biological Sciences*, 16(19), 1034–1039. <https://doi.org/10.3923/pjbs.2013.1034.1039>
- Shinu, P., Sharma, M., Gupta, G. L., Mujwar, S., Kandeel, M., Kumar, M., Nair, A. B., Goyal, M., Singh, P., Attimarad, M., Venugopala, K. N., Nagaraja, S., Telsang, M., Aldhubiab, B. E., & Morsy, M. A. (2022). Computational Design, Synthesis, and Pharmacological Evaluation of Naproxen-Guaiacol Chimera for Gastro-Sparing Anti-Inflammatory Response by Selective COX2 Inhibition. *Molecules*, 27(20), 6905. <https://doi.org/10.3390/molecules27206905>
- Shriwastav S, Kaur N, Bala R, et al. (2023) In vitro Antibacterial Potency of Leaf Extract of *Moringa oleifera* against NFGNB Isolated from UTI Patients and their Plasmid Profiling. *Journal of Pure and Applied Microbiology*, 17(1), 222-230. <https://doi.org/10.22207/JPAM.17.1.11>
- Singh, B., & Sharma, R. A. (2020). Secondary metabolites of medicinal plants: Ethnopharmacological properties, biological activity and production strategies. In *Secondary Metabolites of Medicinal Plants: Ethnopharmacological Properties, Biological Activity and Production Strategies*. Wiley Blackwell. <https://doi.org/10.1002/9783527825578>
- Sofowora, A. (1993). Medicinal Plants and Traditional Medicine in Africa. In *Spectrum Books*. John Wiley and Sons.
- Sreenika, G., K, N. S., Bvs, L., Thulja, P., & Sudhakar, M. (2015). Antioxidant and Antitumor Activity of *Euphorbia milii* Flower Extract Against *in-vivo* Breast Cancer and Colon Cancer in Mice . *World Journal of Pharmacy and Pharmaceutical Sciences*, 4(06), 912–934.
- Stavrou, I. J., Christou, A., & Kapnissi-Christodoulou, C. P. (2018). Polyphenols in carobs: A review on their composition, antioxidant capacity and cytotoxic effects, and health impact. *Food Chemistry*, 269, 355–374. Elsevier. <https://doi.org/10.1016/j.foodchem.2018.06.152>
- Tollefson, L., & Miller, M. A. (2000). Antibiotic use in food animals: controlling the human health impact. *Journal of AOAC International*, 83(2), 245–254.
- Trease, E. C., & Evans, W. C. (2009). *Pharmacognosy*, (16th ed.). Macmillan Publisher.
- Usman, A., Abdulrahman, F. I., & Usman, A. (2009). Qualitative phytochemical screening and in vitro antimicrobial effects of methanol stem bark extract of *Ficus thonningii* (Moraceae). *African Journal of Traditional, Complementary and Alternative Medicines*, 6(3), 289–295. <https://doi.org/10.4314/ajtcam.v6i3.57178>
- Yan, S., Shao, H., Zhou, Z., Wang, Q., Zhao, L., & Yang, X. (2018). Non-extractable polyphenols of green tea and their antioxidant, anti- α -glucosidase capacity, and release during in vitro digestion. *Journal of Functional Foods*, 42, 129–136. <https://doi.org/10.1016/j.jff.2018.01.006>
- Yan-Hwa, C., Chang, C. L., & Hsu, H. F. (2000). Flavonoid content of several vegetables and their antioxidant activity. *Journal of the Science of Food and Agriculture*, 80(5), 561–566. [https://doi.org/10.1002/\(SICI\)1097-0010\(200004\)80](https://doi.org/10.1002/(SICI)1097-0010(200004)80)
- Yao, L., Sun, J., Liang, Y., Feng, T., Wang, H., Sun, M., & Yu, W. (2022). Volatile fingerprints of *Torreya grandis* hydrosols under different downstream processes using HS-GC-IMS and the enhanced stability and bioactivity of hydrosols by high pressure homogenization. *Food Control*, 139, 109058. <https://doi.org/10.1016/j.foodcont.2022.109058>



Journal of Experimental Biology and Agricultural Sciences

<http://www.jebas.org>

ISSN No. 2320 – 8694

A Study of the Photodegradation Carbofuran and its Metabolites in Paddy Water Samples

Nurul Syuhada Haji Baharudin , Harlina Ahmad* 

Environmental Technology Division, School of Industrial Technology, Universiti Sains Malaysia, 11800 Penang, Malaysia

Received – December 25, 2022; Revision – April 10, 2023; Accepted – April 18, 2023

Available Online – April 30, 2023

DOI: [http://dx.doi.org/10.18006/2023.11\(2\).394.404](http://dx.doi.org/10.18006/2023.11(2).394.404)

KEYWORDS

Carbofuran

Carbofuran-phenol

3-keto carbofuran

Degradation

Metabolites

Paddy water

Photodegradation

ABSTRACT

Rice fields are one of the agricultural sectors in Malaysia that are heavily pesticide-treated. This study aimed to determine how carbofuran degrades in paddy water and how carbofuran metabolites such as carbofuran-phenol and 3-keto carbofuran reacted during the degradation. The experiment was conducted in two distinct conditions: the first water sample was exposed to sunlight, while the second water sample remained in the dark. During the 56 days of observation, the study discovered carbofuran decomposed slowly in both conditions. The water sample exposed to sunlight showed a faster degradation rate (0.04/day carbofuran) than the water kept in the dark (0.0186/day). The results also demonstrated that photolysis and hydrolysis enhanced the carbofuran degradation in the water. Both 3-keto carbofuran and carbofuran-phenol were detected as metabolites with low concentration levels, ranging from 0.03 ± 0.301 to 0.23 ± 0.142 ppm. These metabolites are considered 'emerging pollutants' as they can be detected in the environment and may post-treat as much as the parent compounds themselves. Hence, this study is trying to fill the research gap to assess the route and rate of carbofuran and its transformation products.

* Corresponding author

E-mail: harlinaa@usm.my (Harlina Ahmad)

Peer review under responsibility of Journal of Experimental Biology and Agricultural Sciences.

Production and Hosting by Horizon Publisher India [HPI]
(<http://www.horizonpublisherindia.in/>).
All rights reserved.

All the articles published by [Journal of Experimental Biology and Agricultural Sciences](#) are licensed under a [Creative Commons Attribution-NonCommercial 4.0 International License](#) Based on a work at www.jebas.org.



1 Introduction

Pesticides are chemical substances that are highly diverse. These are hazardous and non-biodegradable and have the potential to pollute our ecosystems. Pesticides are chemicals that prevent, eliminate, destroy, or minimize various pests such as insects, animals, fungi, and parasite plants (Hijosa-Valsero et al. 2016; Khalid et al. 2020). Among the total agricultural chemical expenditures in Malaysia, herbicides accounted for 70% (Tey et al. 2014; Foguesatto and Machado 2022; López-Felices et al. 2023), followed by insecticides (19%), fungicides (7%) and rodenticides (5%) (Shamsudin et al. 2010; Srivastava 2020). Malaysia's primary food crop is rice, and around 70% of pesticides are exclusively used in paddy fields (Bhattacharjee et al. 2012; Wang et al. 2021).

Carbofuran (2,3-dihydro-2,2-dimethyl benzofuran-7-yl-N-methyl carbamate) is a systemic acaricide, insecticide, and nematicide that belongs to the carbamate derivative pesticide family (Vithanage et al. 2016; Ćwieląg-Piasecka et al. 2021). In Malaysia, rats in rice fields and the rhinoceros beetle in oil palm plantations are controlled by using insecticides. Carbofuran is believed to be more long-lasting than other carbamate or organophosphate insecticides. Additionally, carbofuran's secondary metabolites, notably 3-keto carbofuran and 3-hydroxy carbofuran, are also fatal to human beings (Ferrari et al. 2023; Goh et al. 2021).

Pesticide mobility and degradation are determined by several indicators, including the country's climate and soil conditions, pH, humidity, soil type, organic matter, and clay content (Rasool et al. 2022). Furthermore, the environmental conditions under which pesticides were applied to plants and the physical-chemical characteristics of the pesticides also influence the pesticides movement and their environmental degradation (Arias-Estévez et al. 2008; Sharma et al. 2020). Pesticides can degrade and form metabolites in water, soil, and air. Degradation can occur through hydrolysis, photolysis, surface runoff, leaching, volatilization, oxidation or reduction, and microbial degradation (Lewis et al. 2016; Nieder et al. 2018).

Most studies agree that hydrolysis and photolysis are the most effective pathways for pollutant degradation. Further, transformation mechanisms are essential to understanding the pesticide's fate in water. Pesticide hydrolysis is a secondary reaction that involves nucleophilic substitution and follows the first-order reaction kinetics model (Chen et al. 2018). Furthermore, photolysis and hydrolysis of pesticides yield secondary pesticide compounds that are more polar and stable than the parent pesticides. Some pesticides remained for several months, contaminating the ecosystem (Sim et al. 2020; Tien et al. 2017). Besides pesticide degradation, reaction pathways are

also crucial in determining the process, type of reactive intermediates, and end-products; all of these contribute to pesticide distribution in the environment (Chaudhari et al. 2023; Riyaz et al. 2023). The primary carbofuran metabolites discovered in different samples were 3-hydroxy carbofuran and 3-keto carbofuran. Both by-products are more polar but somewhat hazardous to specific and non-specific species (Osesua et al. 2017; Mishra et al. 2020).

However, there are limited studies on carbofuran degradation and its transformation products in tropical paddy water, particularly in Malaysia, where the level of ultraviolet radiation (UV) and the existence of microorganisms may result in faster deterioration. Therefore, the purpose of this study is (i) to determine the degradation rate of carbofuran spiked into paddy water, (ii) to consider the potential pathways of degradation of carbofuran, and (iii) to determine the half-life of carbofuran and its by-products carbofuran-phenol and 3-keto carbofuran in paddy water samples. This study estimates the carbofuran degradation rate over 56 days in paddy field water in two environments, with and without sunlight.

2 Materials and Methods

2.1 Sampling site

Water samples were collected from a paddy field at Padang Tembusu Village in Penaga Mukim 5, Seberang Perai Utara, and Pulau Pinang, Malaysia. The study area has an annual average temperature of approximately 27°C to 32°C, a rainfall range of 100mm to 400mm, and a relative humidity range of 60 to 75%. The site of Padang Tembusu Village is portrayed in Figure 1.

2.2 Experimental Setup for the degradation study

100mL of paddy water was collected and placed in a glass container for the degradation study. The sample bottle is wrapped in aluminium foil and stored in the refrigerator before use in the batch study to slow down the reaction in the samples. From this, each 100mL of water was spiked with 0.1g of carbofuran, and the samples were stored in two conditions, including outdoors at ambient temperature which, exposed to sunlight (open location), and in the dark (in a drying cabinet set to 28°C and 60% humidity). The bottles stored under dark conditions were wrapped in aluminium foil to protect the samples from sunlight. The degradation study was conducted for 56 days, and data were collected every seven days (0 - 56 days). The standard methodology estimated various physicochemical parameters, including pH, temperature, turbidity, BOD, COD, and TSS of collected paddy water samples. Samples were extracted using solid-phase extraction and analyzed using GC-ECD to determine carbofuran and its by-product concentrations (Figure 2).

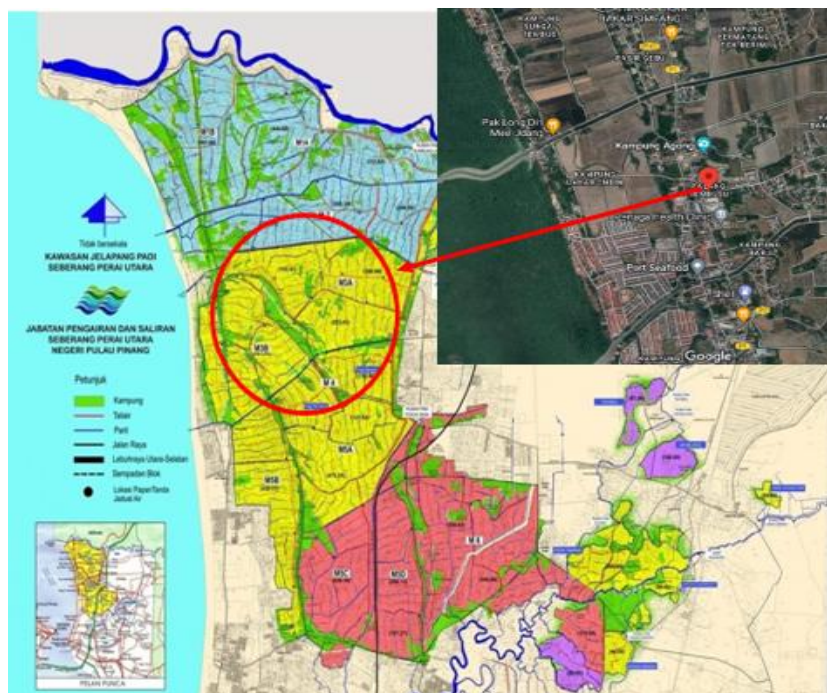


Figure 1 Padang Tembusu Village, Penaga Mukim 5, SPU, and Pulau Pinang, Malaysia (jps.penang.gov.my)

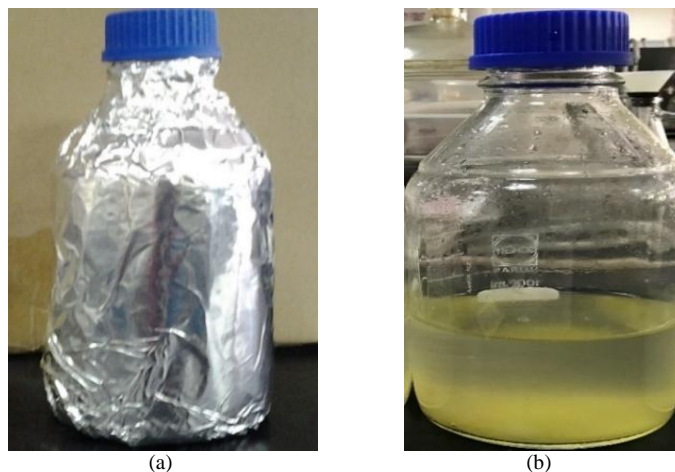


Figure 2 Experimental setup for (a) a sample kept in the dark and (b) a sample exposed to sunlight

2.3 Solid-phase extraction of water samples

The carbofuran and its products were extracted from water samples using solid-phase extraction (SPE) as described by Ismail et al. (2012). Before the separation procedure, water samples were pre-filtered. Before being connected to the manifold, the SPE cartridge was pre-washed with 10 mL acetone, 3 mL acetonitrile, and 3 mL distilled water. The cartridge was loaded with 100 mL of water, and the water sample flow rate of the disc was controlled at 1.5 mL/min pressure. After extracting the insecticide from the cartridge, it was eluted with 6 mL of acetonitrile. The extract was then dried using a rotary evaporator before injection into the GC-ECD.

2.4 Gas chromatographic-electron capture detector (GC-ECD) analysis

The analysis was done via a gas chromatography-electron capture detector (Shimadzu GC-ECD QP2010). The carrier gas nitrogen was employed at a 1 mL/min rate at 250°C in splitless mode. The detector's temperature was maintained at 280 °C, and the oven temperature was increased from 100°C to 250–280°C at a rate of 10°C per minute, then by 3°C per minute. A capillary column of 5% phenyl polysilphenylene-siloxane, BPX-5 (30 m×0.25 mm id×0.25 mm thickness) was used for sample uploading.

2.5 Recovery Study

The method's accuracy was determined by calculating carbofuran, carbofuran-phenol, and 3-keto carbofuran recovery rates at a few fortification levels as per the Lee et al. (2020) and Ripp (1996) method. The procedures were repeated three times for each blank sample in the recovery study. The analytical method of limit detection is calculated by multiplying the sample standard deviation by the correct student's t-value. Spike tests were used to conduct the recovery experiments. The concentration of the chosen compound was determined using an external calibration curve. A set of carbofuran standard solutions was prepared to produce the external calibration curve (0.5–15 ppm; n = 3).

3 Results and Discussion

3.1 Water quality analysis

Six physicochemical parameters, i.e., pH, temperature, turbidity, BOD, COD, and TSS of collected paddy water samples, were estimated by the standard methodology and shown in Table 1. The temperature during the study period ranged between 26 - 33°C, and the test samples' pH value was 6 to 6.7, which is consistent with the pH of river water. These values are equivalent to what has been found in other rice fields in northern Malaysia. According to Aqmal-Naser and Ahmad (2018), the reasons that may affect the pH of the water are rainfall distribution, application of fertilizer, and decomposition of organic material like weeds and rice stalks.

The collected water samples' average BOD and COD values were 6 mg/L and 109.2 mg/L, respectively. Suratman et al. (2015) and

Wu et al. (2018) indicate that concentrations of BOD and COD will remain high in the presence of significant organic contamination in the water. Further, paddy water has a high content of organic materials, including crop waste, fertilizer discharge faeces, and other waste, and bacteria use more oxygen to break down the organic material during oxidation. Total suspended solids are also crucial indicators for assessing water quality since they define residential wastewater concentration and influence water turbidity. The collected paddy water sample shows the low concentration of TSS (17.3 mg/L), which might be due to the dilution of water samples (Kamarudina et al. 2020).

3.2 Degradation of carbofuran in paddy water samples

The presence of carbofuran and its transformation products in the water will be monitored under two conditions (with and without sunlight). Samples were taken, extracted, and the concentrations of the samples were measured with external standard solutions. Throughout the experiment, carbofuran degradation was observed faster for the first 28 days than the subsequent 28 to 56 days. Figure 3 illustrates the declining concentration of carbofuran in paddy water, implying that carbofuran rapidly disappeared in the first week and generally continued to decline slowly until day 56.

The intermediates products were also reviewed to understand the major degradation mechanisms involved in carbofuran photodegradation. Only two carbofuran by-products, i.e. 3-keto carbofuran and carbofuran-phenol, were recorded using GC-ECD analysis compared to genuine analytical standards. Degradation started on day 7 for both 3-keto carbofuran and carbofuran-phenol,

Table 1 Water quality of paddy water sample

pH	Temp (°C)	Turbidity (NTU)	BOD(mg/L)	COD(mg/L)	TSS(mg/L)
6.5	33.8	23.7	6	109.2	17.3

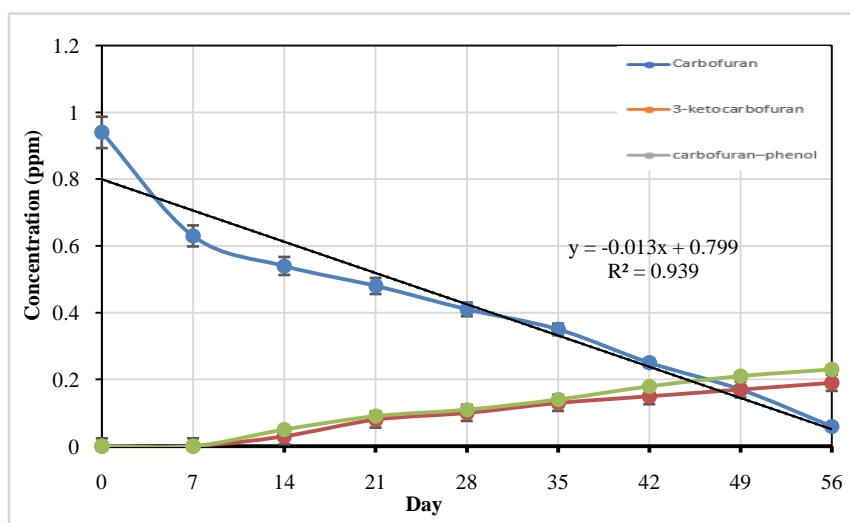


Figure 3 The concentrations of carbofuran and its transformation products in water samples exposed to sunlight

and their concentrations were increased from 0.03 ± 0.301 to 0.23 ± 0.142 ppm.

Similarly, Siddaramappa et al. (1978) recorded that carbofuran was rapidly hydrolyzed to carbofuran-phenol after five days of its application to paddy water. The turbidity of the sample began to decrease with time increased, which may lead to a faster rate in the first half of the study period. With fewer suspended solids, sunlight may permeate the solution more efficiently, allowing photodegradation to occur more rapidly (Seiber and Cahill, 2022). There is no evidence of algal growth in the collected water sample throughout the study period; it might be due to nutrient deficiency or pesticide toxicity.

Results presented in Figure 4 show the trends of carbofuran degradation in water without sunlight (dark). The study's results also revealed that carbofuran degradation began on day 1 and persisted until day 56. The trends of carbofuran degradation

showed a similar trend to the water samples exposed to sunlight. However, on day 56, the carbofuran concentrations in the dark remained significantly higher (0.32 ± 0.447 ppm) than the samples exposed to the light (0.03 ± 0.301 ppm).

The trends of carbofuran degradation decreased in both conditions and are shown in Figures 3 and 4, and it was recorded between R^2 0.9397 and 0.9572. The possible mechanism of carbofuran degradation was hydrolysis and oxidation in the water sample. Further, 3-keto carbofuran and carbofuran-phenol were detected in the water extract simultaneously. 3-keto carbofuran reached a maximal concentration after day 35 and was subsequently stable, whereas there was a slow increase in concentration for carbofuran-phenol between days 28 and 56.

Results presented in Table 2 revealed that most of the carbofuran exposed to sunlight was degraded up to 93.62%, whereas the percentage of carbofuran degradation was only 67.01% in the

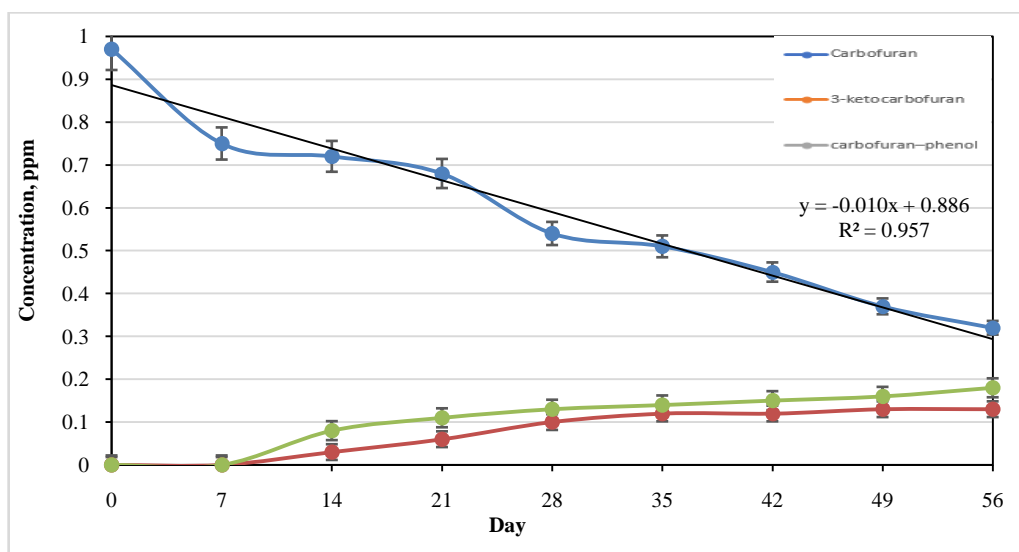


Figure 4 The concentrations of carbofuran and its transformation products in dark

Table 2 Percentage of carbofuran and its metabolites' degradation in collected paddy water sample

Day	Paddy water exposed to the sunlight			Paddy water in the dark		
	Carbofuran (%)	3-keto carbofuran (%)	Carbofuran phenol (%)	Carbofuran (%)	3-keto carbofuran (%)	Carbofuran-phenol (%)
7	32.98	0	0	22.68	0	0
14	42.55	3	5	25.77	3	8
21	48.94	8	9	29.90	6	11
28	56.38	10	11	44.33	10	13
35	62.77	13	14	47.42	12	14
42	73.40	15	18	53.61	12	15
49	81.91	17	21	61.86	13	16
56	93.62	19	23	67.01	13	18

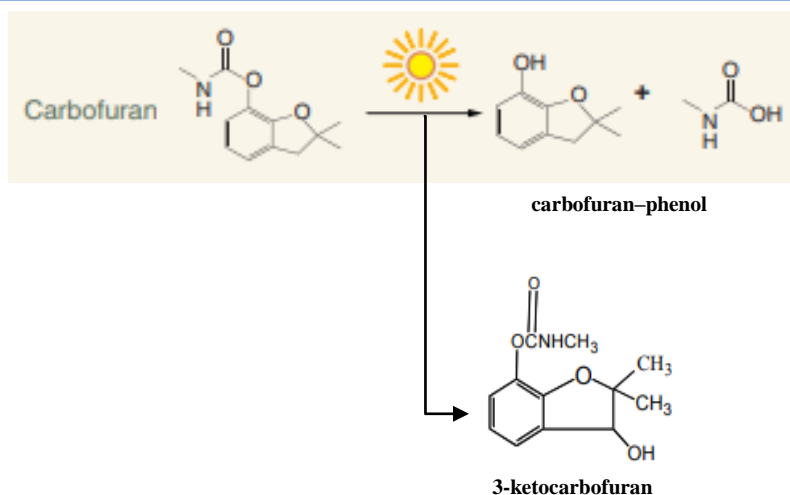


Figure 5 Reaction pathways of carbofuran (direct photodegradation)

paddy water samples kept in the dark. Here carbofuran degradation is slow, and it might be due to only two main degradation pathways, i.e., hydrolysis and oxidation. Throughout the experiment, 3-keto carbofuran and carbofuran-phenol were detected and varied greatly as per the time duration and storage conditions.

The results of the study showed that degradation of the carbofuran is faster in the first week. Similarly, Ecobichon (2019) also reported that carbofuran was degraded entirely in one week. Furthermore, the rate of carbofuran degradation in the dark was slightly slower than in the sunlight. Many pesticides are altered by 'oxidizers generated by sunlight' rather than directly absorbing sunlight (Field 2013; Temgoua et al. 2023). Carbofuran is a water-insoluble compound that accumulates in water over time, so many countries have prohibited its usage (Lan et al. 2020). Figure 5 shows the degradation mechanism (photodegradation) and reaction pathways of carbofuran and its metabolites, carbofuran-phenol and 3-keto carbofuran, in the water samples exposed to sunlight.

The study's results agree with the findings of Howard (2017) and Remual (2014), who suggested that sunlight directly degraded the carbofuran and its by-products. The pesticide's photodegradation rate is substantially faster in seawater, pond water, and humic acid solutions than in distilled water at the same pH values, implying that dissolved organic matter is indirectly sensitized in photodegradation, a critical loss mechanism. While carbofuran degrades more rapidly in river water than in seawater, adding humic acids has been shown to lower the carbofuran by direct photolysis (Campbell et al. 2004; Iwafune 2018; Atwan et al. 2020).

Insecticides are commonly applied to manage various insects and have a long residual effect on the environment (Gaur et al. 2018).

Hydrolysis of carbofuran produces less hazardous metabolite endosulfan diol in certain bacteria (*Pseudomonas aeruginosa*, *Burkholderia cepacia*). Carbofuran degradation was associated with the development of carbofuran-phenol, carbofuran hydrolysis product, and its formation in paddy water, and it can also be proven by thin-layer chromatography (Parte et al. 2017; Mudhoo et al. 2019; Seiber and Cahill 2022). The analysis of carbofuran by-products is essential because they might be more stable and prevalent than the parent pesticides. This is especially important in tropical environments, where carbofuran breakdown at the application site can be relatively fast (Aisha et al. 2022; Mustaffha and Sabran 2020).

3.3 Determination of rate of degradation, k, and half-life of carbofuran

According to Farahani et al. (2012), chemical degradation can be defined by a first-order degradation curve ($C = C_0 e^{-kt}$) or ($\ln C = \ln C_0 - kt$), where C is the compound's concentration at time t , C_0 is the compound's initial concentration, and k is the rate constant. A pesticide's half-life is described as the time it takes for the pesticide concentration to be half that of its initial concentration, as defined by $t_{1/2} = \ln 2/k$. A straight line may be formed by plotting the \ln of concentration vs. time, from which the rate constant (k) and half-life ($t_{1/2}$) can be calculated. Table 3 presents the degradation rate and different half-lives of carbofuran insecticide when exposed to sunlight and kept in the dark in the previous study.

Table 3 shows that this study's half-life of carbofuran was double that of most previous studies. This can be due to the low pH of paddy water as compared to other previous studies where the pH was higher and the soil was more alkaline. The ability of carbofuran to remain stable in water decreases gradually as the pH of the water increases (Howard 2017; Khan et al. 2020). During

Table 3 Rate constant of degradation (k) and half-life ($t_{1/2}$) of carbofuran in paddy water samples exposed to sunlight and kept in dark

Degradation of Carbofuran	This study		Farahani et al. 2012	Cromlab 2010	Kim and Kim 2002	Seiber et al. 1978; Campbell et al. 2004
	Rate constant (day^{-1})	Half-life (day)	Half-life (day)	Half-life (day)	Half-life (day)	Half-life (day)
Exposed to sunlight	0.040	17.33	6.6	6.25	9.7	7.2
Kept in the dark	0.0186	37.27	8.6	-	-	9.3

photolysis, rice plants take up carbon dioxide from the water and release oxygen, which can increase the pH of the water. As it occurs mainly during daylight hours, the pH of paddy water tends to increase during the day and decrease at night (Aisha et al. 2022; Mustaffha and Sabran 2020). Further, this degradation pattern is more prominent in the early growing season before the canopy blocks sunlight from reaching the paddy water. Additionally, colloidal matter in paddy soils may absorb ultraviolet light, drastically lowering the energy available for photodegradation. It shows that the fast dissipation seen in rice paddies is caused by hydrolysis at high pH (Katagi 2016; Davenport et al. 2022; Southwell et al. 2023).

Photolysis may enhance the degradation process in the water. The UV radiation from the sun, which makes up around 10% of the sun's overall electromagnetic radiation output, can break specific chemical bonds, creating transformation products. Bachman and Patterson (1999) developed a pathway for the UV degradation of carbofuran that involves the Fries' rearrangement, which produces a by-product consistent with the hydrolysis of the ethereal moiety of the 2,3-dihydrofuran ring. The results of this study were established by the findings of Elsheikh (2020) and Harmoko et al. (2023), who reported that carbofuran degradation was faster under sun exposure compared to the dark. From the results of this study, it can be concluded that the water sample exposed to sunlight had a faster rate of carbofuran degradation than the water sample kept in the dark (0.04/day with a correlation coefficient $R^2 = 0.8758$ compared to the water that was kept in the dark at 0.0186/day with a correlation coefficient $R^2 = 0.9771$). The half-life, $t_{1/2}$ period for the samples exposed to sunlight was 17.33 days, whereas it was reported to be 37.27 days for the samples stored in the dark. de-Azeredo Morgado et al. (2023) and Maqueda et al. (2017) suggested that the half-life of glyphosate in water is 10.0 days, less than the carbofuran, indicating that the carbofuran is more stable in water as compared the glyphosate. The half-life period of the carbofuran is approximately 30–120 days under natural conditions, and this degradation rate depends on location, temperature, soil types, water pH, and the surrounding medium's moisture content. The major routes of carbofuran degradation are hydrolysis and biodegradation (Vishnuganth et al. 2017; Cid et al. 2018). Carbofuran is more mobile in soil than other insecticides, and its degradation is faster in water than in soil (Matthies and Beulke 2017; Chae and An 2018; Jain 2021). Further, ions, organic

molecules, and chemical sensitizers may have facilitated carbamate pesticide photodegradation. The prolonged half-life of carbofuran observed when it is stored in the dark might be due to the slow photodegradation (Remucal 2014; Kaur et al. 2021). Since many pesticides do not absorb sunlight directly, they are transformed by 'oxidizers formed by sunlight'. Photochemical breakdown, as a rule, is not complete and leads to the formation of breakdown products (Peña et al. 2020). Many countries have prohibited its use due to its persistence in water and its transformation into other products, which allowed it to remain in the water longer.

Few studies have been conducted on identifying and analyzing the route of carbofuran degradation and its major degradation products, which can be long-lasting and toxic compared to their parent substances (Nollet and Rathore 2016). This study demonstrated that sunlight can enhance the photodegradation of carbofuran in water, and hydrolysis is the main route for carbofuran degradation in water. Findings of previous studies suggested that 3-keto carbofuran and 3-hydroxy carbofuran are the most stable carbofuran metabolites (Ramasubramanian and Paramasivam 2018; Mohamed et al. 2021; Boonkhao et al. 2022). In the current study, the recovery for carbofuran, 3-hydroxy carbofuran, and 3-keto carbofuran is within the acceptable range (83–94%). As previously reported by Martínez Vidal et al. (2000), the best recovery range for pesticides found in water samples is between 76% and 122%. The detection limits for all pesticides were in the range of 0.005 and 0.3 g/mL (Hladik et al. 2008; Masoner et al. 2019).

Conclusion

In conclusion, this study demonstrated that paddy water exposed to sunlight degraded approximately two times faster than water in the dark. The results also showed that sunlight helps in the faster degradation of carbofuran. Both 3-keto carbofuran and carbofuran-phenol were detected as metabolites as their concentration increased at low levels, ranging from 0.03 ± 0.301 to 0.23 ± 0.142 ppm. Therefore, with a rising number of pesticide by-products in diverse environmental media, a more thorough understanding of the ecological threat of pesticide by-products is required for future risk assessments and regulatory policy-making on pesticide restriction.

Acknowledgments

The authors acknowledge the Malaysian Ministry of Education and Universiti Sains Malaysia (USM) for awarding the Fundamental Research Grant Scheme (FRGS) to conduct this research (FRGS/1/2019/WAB05/USM/02/3).

Conflict of Interest

The authors declare that they have no conflict of interest concerning this work.

References

- Aisha, S. M., Thamrin, N. M., Ghazali, M. F., Ibrahim, N. N. L. N., & Ali, M. S. A. M. (2022). Non-Linear Autoregressive Dissolved Oxygen Prediction Model for Paddy Irrigation Channel. *Technology Education Management Journal*, 11(2), 842.
- Aqmal-Naser, M., & Ahmad, A. B. (2018). Ichthyofauna in rice agroecosystem at Seberang Perai Tengah, Pulau Pinang, Malaysia with notes on the introduced species. *Journal of Agrobiotechnology*, 9(1), 27–40.
- Arias-Estévez, M., López-Periogo, E., Martínez-Carballo, E., Simal-Gándara, J., Mejuto, J.C., & García-Río, L. (2008). The mobility and degradation of pesticides in soils and the pollution of groundwater resources. *Agriculture, Ecosystems & Environment*, 123(4), 247–260.
- Atwan, A. A., Elmehasseb, I. M., Talha, N., & El-Kemary, M. (2020). Parameters affecting carbofuran photocatalytic degradation in water using ZnO nanoparticles. *Journal of the Chinese Chemical Society*, 67(10), 1833–1842.
- Bachman, J., & Patterson, H.H. (1999). Photodecomposition of the Carbamate Pesticide Carbofuran: Kinetics and the Influence of Dissolved Organic Matter. *Environmental Science & Technology*, 33 (6), 874–881.
- Bhattacharjee, S., Fakhruddin, A. N. M., Chowdhury, M. A. Z., Rahman, M. A., & Alam, M. K. (2012). Monitoring of Selected Pesticides Residue Levels in Water Samples of Paddy Fields and Removal of Cypermethrin and Chlorpyrifos Residues from Water Using Rice Bran. *Bulletin of Environmental Contamination and Toxicology*, 89(2), 348–353. <https://doi.org/10.1007/s00128-012-0686-8>
- Boonkhao, L., Phonkaew, S., Kwonpongsagoon, S., & Rattanachaikunsopon, P. (2022). Carbofuran residues in soil and consumption risks among farmers growing vegetables in Ubon Ratchathani Province, Thailand. *AIMS Environmental Science*, 9(5), 593–602.
- Campbell, S., David, M. D., Woodward, L. A., & Li, Q. X. (2004). Persistence of carbofuran in marine sand and water. *Chemosphere*, 54(8), 1155–1161.
- Chae, Y., & An, YJ (2018). Current research trends on plastic pollution and ecological impacts on the soil ecosystem: A review. *Environmental Pollution*, 240, 387–395.
- Chaudhari, Y. S., Kumar, P., Soni, S., Gacem, A., Kumar, V., et al. (2023). An inclusive outlook on the fate and persistence of pesticides in the environment and integrated eco-technologies for their degradation. *Toxicology and applied pharmacology*, 466, 116449. <https://doi.org/10.1016/j.taap.2023.116449>.
- Chen, R., Yin, H., Zhang, C., Luo, X., & Liang, G. (2018). Hydrolysis of a neonicotinoid: a theoretical study on the reaction mechanism of dinotefuran. *Structural Chemistry*, 29, 315–325.
- Cid, A., Astray, G., Morales, J., Mejuto, J. C., & Simal-Gándara, J. (2018). Influence of b-Cyclodextrins upon the Degradation of Carbofuran Derivatives. *Journal of Pesticides and Biofertilizers*, 1, 1–4.
- Cromlab. (2010). *Carbofuran*. 3.
- Ćwieląg-Piasecka, I., Debicka, M., & Medyńska-Juraszek, A. (2021). Effectiveness of Carbaryl, Carbofuran and Metolachlor Retention in Soils under the Influence of Different Colloid. *Minerals*, 11(9), 924.
- Davenport, R., Curtis-Jackson, P., Dalkmann, P., Davies, J., Fenner, K., Hand, L., McDonough, K., Ott, A., Ortega-Calvo, J. J., & Parsons, J. R. (2022). Scientific concepts and methods for moving persistence assessments into the 21st century. *Integrated Environmental Assessment and Management*, 18(6), 1454–1487.
- De Azeredo Morgado, M. G., Passos, C. J. S., Garnier, J., de Lima, L. A., de Alcântara Mendes, R., Samson-Brais, É., & Lucotte, M. (2023). Large-scale agriculture and environmental pollution of ground and surface water and sediment by pesticides in the Brazilian Amazon: the case of the Santarém region. *Water, Air, & Soil Pollution*, 234(3), 150.
- Ecobichon, D. (2019). Carbamic Acid Ester Insecticides. In *Pesticides and Neurological Diseases* (pp. 263–302). CRC Press, Boca Raton.
- Elsheikh, M. A. A. (2020). Degradation kinetics Of carbofuran insecticide in tomato fruits. *European Chemical Bulletin*, 9(12), 355–359.
- Farahani, G. H. N., Zuriati, Z., Aini, K., & Ismail, B. S. (2012). Persistence of carbofuran in Malaysian waters. *American-Eurasian Journal of Agricultural & Environmental Sciences*, 12(5), 616–623.

- Ferrari, G. C. P., Rheingantz, M. L., Rajão, H., & Lorini, M. L. (2023). Wanted: A systematic review of the most trafficked songbirds in a Neotropical hotspot. *Frontiers in Forests and Global Change*, 6, :930668. <https://doi.org/10.3389/ffgc.2023.930668>.
- Field, J. A. (2013). Environmental Fate of Pesticides. *Oregon State University Department of Environmental and Molecular Toxicology, Non-Crop Vegetation Management Course*.
- Foguesatto, C. R., & Machado, J. A. D. (2022). Adoption of sustainable agricultural practices in Brazil: understanding the influence of socioeconomic and psychological factors. *Journal of Agribusiness in Developing and Emerging Economies*, 12(2), 204–222.
- Gaur, N., Narasimhulu, K., & PydiSetty, Y. (2018). Recent advances in the bio-remediation of persistent organic pollutants and its effect on environment. *Journal of Cleaner Production*, 198, 1602–1631.
- Goh, M. S., Lam, S. D., Yang, Y., Naquiddin, M., Addis, S. N. K., Yong, W. T. L., Luang-In, V., Sonne, C., & Ma, N. L. (2021). Omics technologies used in pesticide residue detection and mitigation in crop. *Journal of Hazardous Materials*, 420, 126624.
- Harmoko, H., Putra, G. K., Munawar, H., Lioe, H. N., & Andarwulan, N. (2023). Thermochemical degradation investigation of pesticide residues in banana homogenate. *Food Control*, 143, 109329.
- Hijosa-Valsero, M., Bécáres, E., Fernández-Aláez, C., Fernández-Aláez, M., Mayo, R., & Jiménez, J. J. (2016). Chemical pollution in inland shallow lakes in the Mediterranean region (NW Spain): PAHs, insecticides and herbicides in water and sediments. *Science of the Total Environment*, 544, 797–810.
- Hladik, M. L., Smalling, K. L., & Kuivila, K. M. (2008). A multi-residue method for the analysis of pesticides and pesticide degradates in water using HLB solid-phase extraction and gas chromatography-ion trap mass spectrometry. *Bulletin of Environmental Contamination and Toxicology*, 80(2), 139–144. <https://doi.org/10.1007/s00128-007-9332-2>
- Howard, P. H. (2017) Handbook of environmental fate and exposure data for organic chemicals. Routledge, United States.
- Ismail, B. S., Siti, H. H., & Talib, L. (2012). Pesticide residue levels in the surface water of the irrigation canals in The Muda Irrigation Scheme Kedah, Malaysia. *International Journal of Basic & Applied Sciences*, 12(6), 85–90.
- Iwafune T. (2018). Studies on the behavior and ecotoxicity of pesticides and their transformation products in a river. *Journal of pesticide science*, 43(4), 297–304. <https://doi.org/10.1584/jpestics.J18-01>.
- Jain, M. (2021). Current research trends on plastic pollution and ecological impacts on the soil ecosystem: A review. *South Asian Journal of Marketing & Management Research*, 11(11), 115–120.
- Kamarudina, M. K. A., Abd Wahabb, N., Samahc, M. A. A., Saudid, A. S. M., Ismailb, A., et al. (2020). Assessing of water quality and sedimentation problems in Lata Sungai Limau, Malaysia. *Environment*, 21, 22.
- Katagi T. (2016). Pesticide behavior in modified water-sediment systems. *Journal of pesticide science*, 41(4), 121–132. <https://doi.org/10.1584/jpestics.D16-060>.
- Kaur, R., Singh, D., Kumari, A., Sharma, G., Rajput, S., & Arora, S. (2021). Pesticide residues degradation strategies in soil and water: a review. *International Journal of Environmental Science and Technology*, 20(11), 1–24.
- Khalid, S., Shahid, M., Murtaza, B., Bibi, I., Naeem, M. A., & Niazi, N. K. (2020). A critical review of different factors governing the fate of pesticides in soil under biochar application. *Science of the Total Environment*, 711, 134645.
- Khan, M. A., Sharma, A., Yadav, S., & Sharma, S. (2020). Rhizospheric Microbes as Potential Tool for Remediation of Carbofuran: An Overview. In: S.K. Sharma, U.B. Singh, , PK Sahu, H.V. Singh, & P.K. Sharma, (eds) *Rhizosphere Microbes* (pp. 557–571). Springer, Singapore. https://doi.org/10.1007/978-981-15-9154-9_23
- Kim, K., & Kim, Y.-H. (2002). Aqueous Photolysis of the Organophosphorus Insecticide Carbofuran. *Korean Journal of Environmental Agriculture*, 21(3), 172–177.
- Lan, J., Sun, W., Chen, L., Zhou, H., Fan, Y., Diao, X., Wang, B., & Zhao, H. (2020). Simultaneous and rapid detection of carbofuran and 3-hydroxy-carbofuran in water samples and pesticide preparations using lateral-flow immunochromatographic assay. *Food and Agricultural Immunology*, 31(1), 165–175.
- Lee, H.J., Kim, C., Ryu, H.-D., Chung, E. G., Shin, D., & Lee, J. K. (2020). Simultaneous determination of pesticides and veterinary pharmaceuticals in environmental water samples by UHPLC–Quadrupole-Orbitrap HRMS combined with on-Line Solid-Phase Extraction. *Separations*, 7(1), 14.
- Lewis, S. E., Silburn, D. M., Kookana, R. S., & Shaw, M. (2016). Pesticide behavior, fate, and effects in the tropics: an overview of the current state of knowledge. *Journal of Agricultural and Food Chemistry*, 64(20), 3917–3924.

- López-Felices, B., Velasco-Muñoz, J. F., Aznar-Sánchez, J. A., & Román-Sánchez, I. M. (2023). Factors influencing the use of rainwater for agricultural irrigation: the case of greenhouse agriculture in southeast Spain. *AQUA-Water Infrastructure, Ecosystems and Society*, 72(2), 185–201.
- Maqueda, C., Undabeytia, T., Villaverde, J., & Morillo, E. (2017). Behaviour of glyphosate in a reservoir and the surrounding agricultural soils. *Science of the Total Environment*, 593, 787–795.
- Martínez Vidal, J. L., Espada, M. C., Frenich, A. G., & Arrebola, F. J. (2000). Pesticide trace analysis using solid-phase extraction and gas chromatography with electron-capture and tandem mass spectrometric detection in water samples. *Journal of chromatography. A*, 867(1-2), 235–245. [https://doi.org/10.1016/S0021-9673\(99\)01082-1](https://doi.org/10.1016/S0021-9673(99)01082-1).
- Masoner, J. R., Kolpin, D. W., Cozzarelli, I. M., Barber, L. B., Burden, D. S., Foreman, W. T., Forshay, K. J., Furlong, E. T., Groves, J. F., & Hladik, M. L. (2019). Urban stormwater: An overlooked pathway of extensive mixed contaminants to surface and groundwaters in the United States. *Environmental Science & Technology*, 53(17), 10070–10081.
- Matthies, M., & Beulke, S. (2017). Considerations of temperature in the context of the persistence classification in the EU. *Environmental Sciences Europe*, 29(1), 15. <https://doi.org/10.1186/s12302-017-0113-1>
- Mishra, S., Zhang, W., Lin, Z., Pang, S., Huang, Y., Bhatt, P., & Chen, S. (2020). Carbofuran toxicity and its microbial degradation in contaminated environments. *Chemosphere*, 127419.
- Mohamed, B., Rachid, M., & Amina, A. (2021). Study on Biodegradation and Dissipation of 14 C-Carbofuran in Clay Soil from Loukkos Perimeter, Northwestern Morocco. *New Ideas Concerning Science and Technology*, 7, 92–103.
- Mudhoo, A., Bhatnagar, A., Rantankila, M., Srivastava, V., & Sillanpää, M. (2019). Endosulfan removal through bioremediation, photocatalytic degradation, adsorption and membrane separation processes: a review. *Chemical Engineering Journal*, 360, 912–928.
- Mustaffha, S., & Sabran, M. S. (2020). River Water Quality Monitoring at Paddy Field in Merlimau, Melaka. *Advances in Agricultural and Food Research Journal*. <https://doi.org/10.36877/aafj.a0000286>,
- Nieder, R., Benbi, D.K., Reichl, F.X. (2018). Health Risks Associated with Pesticides in Soils. In: *Soil Components and Human Health*, (503-573). Springer, Dordrecht. https://doi.org/10.1007/978-94-024-1222-2_10
- Nollet, L. M. L., & Rathore, H. S. (2016). *Handbook of pesticides: methods of pesticide residues analysis*. CRC press.
- Osesua, B. A., Anyekema, M., Tsafe, A. I., & Malik, A. I. (2017). Distribution of pesticide residues in water and sediment samples collected from Lugu dam in Wurno irrigation area, Sokoto state, Nigeria. *International Journal of Chemistry and Chemical Processes*, 3(2), 2545–5265.
- Parte, S. G., Mohekar, A. D., & Kharat, A. S. (2017). Microbial degradation of pesticide: a review. *African Journal of Microbiology Research*, 11(24), 992–1012.
- Peña, A., Delgado-Moreno, L., & Rodríguez-Liébana, J. A. (2020). A review of the impact of wastewater on the fate of pesticides in soils: Effect of some soil and solution properties. *Science of the Total Environment*, 718, 134468.
- Ramasubramanian, T., & Paramasivam, M. (2018). Persistence and metabolism of carbofuran in the soil and sugarcane plant. *Environmental Monitoring and Assessment*, 190(9), 1–9.
- Rasool, S., Rasool, T., & Gani, K. M. (2022). A review of interactions of pesticides within various interfaces of intrinsic and organic residue amended soil environment. *Chemical Engineering Journal Advances*, 11, 100301. <https://doi.org/https://doi.org/10.1016/j.cej.2022.100301>
- Remucal, C. K. (2014). The role of indirect photochemical degradation in the environmental fate of pesticides: a review. *Environmental Science: Processes & Impacts*, 16(4), 628–653.
- Ripp, J. (1996). Analytical detection limit guidance & laboratory guide for determining method detection limits. [Madison, WI] : Wisconsin Dept. of Natural Resources, Laboratory Certification Program, [1996]. Retrieved from <https://search.library.wisc.edu/catalog/999788165802121>
- Riyaz, M., Mathew, P., Shah, R. A., Sivasankaran, K., & Zuber, S. M. (2023). Environmental Pesticide Degradation: Mechanisms and Sustainability. In *Bioremediation and Phytoremediation Technologies in Sustainable Soil Management* (pp. 3–51). Apple Academic Press.
- Seiber, J N, Catahan, M. P., & Barril, C. R. (1978). Loss of carbofuran from rice paddy water: Chemical and physical factors. *Journal of Environmental Science and Health, Part B*, 13(2), 131–148. <https://doi.org/10.1080/03601237809372083>
- Seiber, J. N., & Cahill, T. M. (2022). *Pesticides, Organic Contaminants, and Pathogens in Air: Chemodynamics, Health Effects, Sampling, and Analysis*. Taylor & Francis.

- Shamsudin, M. N., Amir, H. M., & Radam, A. (2010). Economic benefits of sustainable agricultural production: the case of integrated pest management in cabbage production. *Environment Asia*, 3, 168–174. <http://dx.doi.org/10.14456/ea.2010.57>.
- Sharma, A. K., Sharma, D., & Chopra, A. K. (2020). An overview of pesticides in the development of agriculture crops. *Journal of Applied and Natural Science*, 12(2), 101–109.
- Siddaramappa, R., Tirol, A. C., Seiber, J. N., Heinrichs, E. A., & Watanabe, I. (1978). The degradation of carbofuran in paddy water and flooded soil of untreated and retreated rice fields. *Journal of Environmental Science and Health, Part B*, 13(4), 369–380. <https://doi.org/10.1080/03601237809372103>
- Sim, S. F., Chung, L. Y., Jonip, J., & Chai, L. K. (2020). Uptake and Dissipation of Carbofuran and Its Metabolite in Chinese Kale and Brinjal Cultivated Under Humid Tropic Climate. *Advances in Agriculture*, 2019, 7937086 | <https://doi.org/10.1155/2019/7937086>.
- Southwell, R. V., Hilton, S. L., Pearson, J. M., Hand, L. H., & Bending, G. D. (2023). Water flow plays a key role in determining chemical biodegradation in water-sediment systems. *Science of The Total Environment*, 880, 163282.
- Srivastava, R. K. (2020). Influence of sustainable agricultural practices on healthy food cultivation. In K. Gothandam, S. Ranjan, N. Dasgupta, E. Lichtfouse (eds) *Environmental Biotechnology Vol. 2* (pp. 95–124). Springer.
- Suratman, S., Sailan, M. M., Hee, Y. Y., Bedurus, E. A., & Latif, M. T. (2015). A preliminary study of water quality index in Terengganu River basin, Malaysia. *Sains Malaysiana*, 44(1), 67–73.
- Temgoua, R. C. T., Tonlé, I. K., & Boujtita, M. (2023). Electrochemistry coupled with mass spectrometry for the prediction of the environmental fate and elucidation of the degradation mechanisms of pesticides: current status and future prospects. *Environmental Science: Processes & Impacts*, 25, 340–350. DOI <https://doi.org/10.1039/D2EM00451H>.
- Tey, Y. S., Li, E., Bruwer, J., Abdullah, A. M., Brindal, M., Radam, A., Ismail, M. M., & Darham, S. (2014). The relative importance of factors influencing the adoption of sustainable agricultural practices: A factor approach for Malaysian vegetable farmers. *Sustainability Science*, 9, 17–29.
- Tien, C., Huang, H., & Chen, C. S. (2017). Accessing the carbofuran degradation ability of cultures from natural river biofilms in different environments. *CLEAN–Soil, Air, Water*, 45(5), 1600380.
- Vishnuganth, M. A., Remya, N., Kumar, M., & Selvaraju, N. (2017). Carbofuran removal in continuous-photocatalytic reactor: Reactor optimization, rate-constant determination and carbofuran degradation pathway analysis. *Journal of Environmental Science and Health, Part B*, 52(5), 353–360. <https://doi.org/10.1080/03601234.2017.1283141>
- Vithanage, M., Mayakaduwa, S. S., Herath, I., Ok, Y. S., & Mohan, D. (2016). Kinetics, thermodynamics and mechanistic studies of carbofuran removal using biochars from tea waste and rice husks. *Chemosphere*, 150, 781–789.
- Wang, R., Bingner, R. L., Yuan, Y., Locke, M., Herring, G., Denton, D., & Zhang, M. (2021). Evaluation of thiobencarb runoff from rice farming practices in a California watershed using an integrated RiceWQ-AnnAGNPS system. *Science of The Total Environment*, 767, 144898.
- Wu, Z., Wang, X., Chen, Y., Cai, Y., & Deng, J. (2018). Assessing river water quality using water quality index in Lake Taihu Basin, China. *Science of the Total Environment*, 612, 914–922.








Journal of Experimental Biology and Agricultural Sciences

<http://www.jebas.org>

ISSN No. 2320 – 8694

Haberlea rhodopensis alcohol extract normalizes stress-responsive transcription of the human TP53 gene

Neli Dimitrova^{1§} , Dessislava Staneva^{2§} , Borislav Popov¹ , Albena Alexandrova³ ,
Milena Georgieva² , George Miloshev^{2*} 

¹Department of Molecular Biology, Immunology and Medical Genetics, Faculty of Medicine, Trakia University, Stara Zagora, Bulgaria

²Laboratory of Molecular Genetics, Epigenetics and Longevity, Institute of Molecular Biology "RoumenTsanev", Bulgarian Academy of Sciences, 1113 Sofia, Bulgaria

³Laboratory of Free Radical Processes, Institute of Neurobiology, Bulgarian Academy of Sciences, 23 Acad. G. Bonchev str, 1113 Sofia, Bulgaria

[§]These authors contributed equally

Received – December 01, 2022; Revision – March 22, 2023; Accepted – April 03, 2023

Available Online – April 30, 2023

DOI: [http://dx.doi.org/10.18006/2023.11\(2\).405.415](http://dx.doi.org/10.18006/2023.11(2).405.415)

KEYWORDS

Haberlea rhodopensis

HRE ethanol extracts

TP53 gene expression

Catalase activity

Gamma irradiation

Hydrogen peroxide

ABSTRACT

The Orpheus flower *Haberlea rhodopensis* (Friv.) of the family *Gesneriaceae* can go into anabiosis for long periods in an almost entirely desiccated state. It is an endemic relict from the Balkan Peninsula. Alcohol extracts from *H. rhodopensis* contain many biologically active substances with potent antioxidant, antigenotoxic, radioprotective, revitalizing and antiaging capabilities. However, regulating the gene networks responsible for these activities is vastly unknown. This study explores the cellular mechanisms underlying the protective effect of *H. rhodopensis* extracts (HRE). HeLa cells (human cervix epithelial carcinoma, HeLa ATCC® CCL-2™) were used as a model. We examined the changes in catalase activity and TP53 mRNA level shortly after oxidative (H₂O₂) and ionizing radiation (IR) induced stress with and without pre-incubation with HRE extracts. The dynamics in the activity of catalase, a main cellular antioxidant enzyme, and the expression of the stress-responsive gene TP53 were investigated by UV spectrophotometric assay and RT-qPCR, respectively. Under the applied stress conditions, H₂O₂ treatment and gamma radiation, catalase activity increased. This was a sign of induced ROS generation. In the first hours after treatment, the two stressors led to opposite changes in the levels of TP53 gene expression, which were alleviated by pre-incubation with HRE in a concentration-dependent manner. The broad biological activities of the studied extract, taking into account our results, show that ability of HRE to reduce the effect of stress is achieved through complex molecular mechanisms

* Corresponding author

E-mail: karamolbiol@gmail.com; gmlab@chromatinepigenetics.com (Prof. George Miloshev)

Peer review under responsibility of Journal of Experimental Biology and Agricultural Sciences.

Production and Hosting by Horizon Publisher India [HPI]
 (<http://www.horizonpublisherindia.in/>).
 All rights reserved.

All the articles published by [Journal of Experimental Biology and Agricultural Sciences](#) are licensed under a [Creative Commons Attribution-NonCommercial 4.0 International License](#) Based on a work at www.jebas.org.



aimed at preserving cellular homeostasis. Mechanisms include the normalization of antioxidant enzyme activity such as catalase and the activity of TP53, one of the genes responsive to stress, by up or down-regulation.

1 Introduction

In the family *Gesneriaceae*, the Orpheus flower, *H. rhodopensis* (Friv.), is a well-known but endangered endemic remnant from the Balkans. It grows in various rocky regions of the Rhodope and Balkan mountains, northern Greece, and the Bulgarian Sredna Gora. *H. rhodopensis* belongs to a group of highly resurrecting plants because of its prominent feature to survive long-lasting anabiosis in an almost fully desiccated state and to recover quickly in the availability of water (Gechev et al. 2013). This ability is provided through the continuous high-level expression of desiccation stress-responsive proteins, even in non-stress conditions (Gechev et al. 2013). The potential of resurrection plants to attenuate the oxidation caused by free radicals and to protect membranes from desiccation was also discovered. Resurrection plants also accumulated significant levels of carbohydrates and phenolic compounds, both of which are crucial for the survival of plants under harsh environments (Muller et al. 1997; Berkov et al. 2011).

A phytochemical study indicated the glucosides myconoside, paucifloside and flavone 8-C glycosides as the compounds present in alcohol extract from *H. rhodopensis* (Ebrahimi et al. 2011). Several research groups reported that *H. rhodopensis* contains lipids, disaccharides and polysaccharides, tannins, flavonoids, and free phenolic acids, of which syringic acid is most prevalent (Stefanov et al. 1992; Muller et al. 1997; Radev et al. 2009; Berkov et al. 2011). Evidence shows that among the components with biological activity found in *H. rhodopensis*, the myconoside has potent antioxidant and hepatoprotective effects (Kondeva-Burdina et al. 2013). Together with the phenolic content, these compounds significantly contribute to the antioxidant properties of *H. rhodopensis* extracts (Mihaylova et al. 2011). In particular, ethanolic extracts of *H. rhodopensis* leaves have been reported to exhibit vital antimicrobial and antioxidant activities, reduce the clastogenic effect of γ -irradiation, and exert *in vivo* anticlastogenic and antimutagenic potential against the anticancer drug cyclophosphamide (Popov et al. 2010a; Ebrahimi et al. 2011; Popov et al. 2011). Methanolic extracts of *in vitro* propagated *H. rhodopensis* plants also showed antioxidant properties, modulated genotoxic and inflammatory stress and improved yeast *Saccharomyces cerevisiae*'s cell viability during chronological ageing (Hayrabedian et al. 2013; Georgieva et al. 2015). Notably, it has been shown that *H. rhodopensis* possesses a more significant number of antioxidant genes than plant species whose genomes were sequenced at the time (Gechev et al. 2013).

The significant devastating effect of hydrogen peroxide and gamma radiation exposure is attributed to the reactive oxygen species (ROS) overgeneration and the subsequent oxidative destruction of DNA, lipids and proteins in the exposed biological samples (Giorgio et al. 2007; Valko et al. 2007; Gomes et al. 2018). The ionizing radiation (IR) can damage DNA directly (when electrons attack DNA) or indirectly by radiolysis of intracellular water, forming different types of ROS, e.g. hydroxyl ($\cdot\text{OH}$) and superoxide ($\cdot\text{O}_2^-$) radicals, hydrogen peroxide (H_2O_2), lipid hydroperoxides, etc. (O'Neill and Fielden 1993). IR is arguably one of the primary sources of genotoxic stress, causing various DNA lesions like bulky adducts, single-strand and double-strand DNA breaks, and intra-strand cross-linking (Hickman and Samson 1999). In addition, enzymes of the intracellular antioxidant system, catalase (CAT), superoxide dismutase (SOD), mitochondrial Mn-SOD, glutathione peroxidase (GPx), aldehyde dehydrogenase (ALDH), etc., play a crucial role in removing ROS and protecting cells from oxidation-induced damage. Cells respond to genotoxic stress by initiating a multistep process involving cell cycle arrest and maintenance of this arrest during DNA repair. Therefore, numerous crucial genes involved in DNA damage repair and cell cycle regulation exhibit altered expression following radiation exposure. This leads to reprogramming many biochemical and cellular processes to synchronize the adequate response to radioactive stress. Numerous studies reported interlinks between ROS content, p53 expression and antioxidant enzymes, including CAT, at transcript, protein and activity levels (Bai and Cederbaum 2003; Hussain et al. 2004; Liu et al. 2008; O'Connor et al. 2008; Popowich et al. 2010; Kang et al. 2013; Park and Kwak 2022). The transcriptional level of the TP53 gene was significant for cell cycle control, DNA repair mechanisms, and redox enzyme regulation (O'Connor et al. 2008; Kang et al. 2013; Stevenson 2016).

In the present study, changes in the CAT enzyme activity and the transcription of the TP53 gene in HeLa cells pre-incubated with *H. rhodopensis* extracts (HRE) and then treated with hydrogen peroxide or exposed to gamma ionizing radiation (γ -IR) have been studied to evaluate the molecular effects of HRE in a genotoxic stress context.

2 Materials and methods

2.1 Collection of *H. rhodopensis* plants and ethanol extracts preparation

After obtaining official permission from the Ministry of Environment and Water (MoEW), *H. rhodopensis* leaves were

taken from plants growing in their natural environment (a region close to the village of Bachkovo, Bulgaria, 41.9520 N, 24.8587 E). The botanical identification was made at the Department of Pharmacognosy, Faculty of Pharmacy, Sofia Medical University. To comply with the rule that the amount of active substances directly depends on the conditions under which medicinal plants grow, the samples were collected in the same season (May and June) and in the same place. The fresh leaves were cut and dried at room temperature for one month in the dark. The dry leaves were refined to 1 mm particles. Following the leaves grinding, the mixture was macerated in 70% ethyl alcohol for 48 hours (Bulgarian Pharmacopoeia Roll 3, p.218, $d^{20} = 0.887$), after which the ethanol was distilled in a vacuum vaporizer to a drug/liquid phase ratio of 5:1. Next, the primary extract was concentrated in a vacuum-distillation apparatus on Ulbricht at a residual pressure of 0.3 atmospheres and temperature to 50°C until an azeotropic mixture of 5% ethanol was obtained, the distillation being terminated at a volume ratio of 1:1 extract to drugs. The filter paper removed the emulsified non-polar chemicals, chlorophyll, etc., from the resulting extract, leaving a clear liquid phase with 5% ethanol. The extract was standardized by comparing the mass of a given volume of the extract to the mass of a comparable amount of water measured at 20°C using an analytical balance with an accuracy of 10^{-4} g. This was accomplished using the formula for determining the relative density, d^{20} . The differences in the relative densities of the extract and the water and the number of total extracts were determined in g/cm^3 . The extracted substances ranged between 9.8×10^{-3} and 11.3×10^{-3} g/cm^3 (average 10.5×10^{-3} g/cm^3). Stock extract with a 100 mg/mL concentration was diluted and used in the experiments.

2.2 Cell line culturing, treatment with HRE and exposure to gamma irradiation and H₂O₂

HeLa cells (human cervix epithelial carcinoma, HeLa ATCC® CCL-2™) were cultured in six-well plates with 2 mL growth medium (DMEM + 10% FBS) at an initial concentration of 4×10^5 cells/well. Incubation at 37°C, 5% CO₂ was allowed till reaching cell culture confluence (about 1.6×10^6 cells/mL). Three sets of cell samples were prepared (i) genotoxin-free, designated as HRE⁺ H₂O₂⁻ / 2 Gy⁻, (ii) cells preincubated with HRE and then treated with 10 mM H₂O₂ for 30 min, designated as HRE⁺ H₂O₂⁺, and (iii) cells incubated with HRE before exposure to 2 Gy γ -IR, named HRE⁺ 2 Gy⁺. We applied the HRE extract in five different concentrations, i.e. (i) no HRE, (ii) HRE at 10 $\mu\text{g}/\text{mL}$, (iii) HRE at 25 $\mu\text{g}/\text{mL}$, (iv) HRE at 50 $\mu\text{g}/\text{mL}$, and (v) HRE at 100 $\mu\text{g}/\text{mL}$ final concentrations (f.c.). For all HRE-treated samples, cells were cultured for 1 hour at 37°C with the respective HRE dose. In addition, each set of genotoxin-treated samples included a control not supplemented with HRE but exposed to H₂O₂ or γ -IR alone.

2.3 Analyzing the activity of catalase

The activity of catalase was determined by the UV spectrophotometric method, as described previously by Aebi (1984). In addition, the decrease of absorption at 240 nm caused by the enzymatic dissociation of H₂O₂ was assessed. Therefore, CAT activity was conveyed in units of $\Delta A_{240}/\text{min}/\text{mg}$ protein.

2.4 Total RNA preparation and cDNA synthesis

Following pre-incubation with HRE and exposure to genotoxic stress, cells were immediately scraped and collected for total RNA preparation in the case of hydrogen peroxide treatment or cultured at 37°C for 120 min before harvesting in the case of γ -irradiation.

Thermo Scientific's GeneJET™ RNA Purification Kit was used to prepare total RNA from control cells that had not been treated and cells that had been given HRE, H₂O₂, and/or 2 Gy IR, following the manufacturer's instructions. Using an ND-1000 spectrophotometer (NanoDrop Technologies, Inc., Wilmington, DE), the amount and purity of the isolated RNA were assessed at A₂₆₀ and A₂₈₀. To eliminate the remains of genomic DNA, isolated total RNAs were treated with RNase-free DNase I (Fisher Scientific) at a f.c. of 1 U/ μg RNA in the presence of 1 U/ μL ribonuclease inhibitor at 37°C for 35 min. Subsequently, EGTA to f.c. of 2 mM was added to the reactions, followed by incubation at 65°C for 10 min for endonuclease deactivation. Reactions for copy DNA (cDNA) synthesis contained oligo (dT)₁₈ primer, 450 ng total RNA and Revert Aid H Minus First Strand cDNA Synthesis Kit (Thermo Scientific). One microliter of the reverse transcriptase reaction was applied for the subsequent qPCR assay. Water replaced cDNA in the "no template controls" (NTC). The "reverse transcriptase minus" controls (RT-) contained all necessary reagents for the reverse transcription reaction except for the RT enzyme.

2.5 RT-qPCR analysis

To investigate the transcription of the TP53 gene, a reverse transcription quantitative PCR was performed (Carson et al. 2019) in Rotor-Gene™ 6000 Real-Time PCR cycler (Corbett Life Science, Qiagen) with 2X Maxima SYBR Green Master Mix (Thermo Scientific™) according to the protocol provided by the manufacturer (<https://www.thermofisher.com/order/catalog/product/K0221>). The optimized reaction contained 1 μL cDNA, 0.2 μM of the appropriate forward and reversed primer and 1 \times Maxima® SYBR Green qPCR Master Mix in a total volume of 20 μL . The conditions for PCR included initial heating at 95°C for 10 min and 45 cycles of 15 sec at 95°C and 60 sec at 60°C. For assessing TP53 gene transcription, the activity of the GAPDH (glyceraldehyde phosphate dehydrogenase) housekeeping gene served as a reference. Oligonucleotide primers are described in

Table 1 Nucleotide sequences of the oligonucleotide primers

Primer	Sequence	Amplicon, bp
TP53 forward	5'-AACAGCTTTGAGGTGCGTGTGGTGG-3'	144
TP53 reverse	5'-AGAGGAGCTGGTGTGGTGGGCA-3'	
GAPDH forward	5-ACCAGGTGGTCTCTCTGACTCAA-3'	136
GAPDH reverse	5'-ACCCTGTTGCTGTAGCCAAATTCG-3'	

Table 2 Effect of HRE on catalase activity (ΔA_{240} /min/mg protein) in HeLa cells

	HRE [$\mu\text{g/mL}$]				
	0	10	25	50	100
CAT activity	6.10 \pm 0.09	5.65 \pm 0.23 ^{&}	5.42 \pm 0.03 ^{&}	5.97 \pm 0.18 ^{&}	6.10 \pm 0.01 ^{&}

[&]p>0.05

Table 1 and were designed on target templates NCBI RefSeqs NM_000546.5 and NM_002046.7 for TP53 and GAPDH mRNAs, respectively.

The polymerase reaction's specificity and the amplified products' correct size were examined by melting curve (dF/dT) analysis and electrophoretic analysis of DNA fragments in agarose gel. Melting curves analyses were performed with ramping from 55 to 95°C, increasing by 1°C per step and waiting for 5 sec before acquiring fluorescence.

For analyses of RT-qPCR results, we used the Rotor-Gene 6000 Series Software 1.7. The CT values were used to calculate the samples' relative gene expression (ratio). To this end, two comparative quantification methods were applied: the two standard curves method and the DeltaDelta Ct ($2^{-\Delta\Delta Ct}$) method (Livak and Schmittgen 2001). Both methods gave similar results. In general, the gene expression in a sample of interest is considered to be changed (up- or down-regulated) if there is at least a two-fold difference compared to the calibrator.

2.6 Statistic evaluation of the obtained results

The IBM SPSS Statistics (Statistical Package for Social Sciences) version 19.0 software was used for the statistical analysis. Data were reported as mean \pm SD of three repeats. A paired Student t-test with a two-tailed distribution was applied to compare the experimental groups. Values of $p \leq 0.05$ were considered statistically significant, while those above 5% were denoted as insignificant.

3 Results and Discussion

3.1 HRE ameliorates the redox imbalance

The first step of the present study was to follow CAT activity, a main constituent of the cellular enzyme antioxidant system, as changes in CAT activity indicate redox imbalance caused by H_2O_2 excess. The model system was the HeLa cell line (HeLa (ATCC[®]

CCL-2[™]), derived from cervical adenocarcinoma cells. At standard conditions, in the absence of an exogenous stressor, treatment with HRE did not significantly affect the level of CAT activity (Table 2). Although incubation with 10 and 25 $\mu\text{g/ml}$ HRE slightly decreased enzymatic activity, the observed differences were insignificant ($p > 0.05$). The average CAT activity in HRE-administrated samples was 5.78 ± 0.28 U/mg protein.

Incubating HeLa cells with 10 mM H_2O_2 led to a statistically significant ($p < 0.05$) rise in CAT activity (Figure 1). However, enzymatic activity decreased (Figure 1A) when the cells were treated with various amounts of HRE and then exposed to H_2O_2 . The decrease was not so marked in cells pre-incubated with 10 and 25 $\mu\text{g/mL}$ HRE before adding hydrogen peroxide. The values were statistically distinguishable compared to the control HRE⁻ H_2O_2 ⁻ group and undistinguishable compared to cells treated only with H_2O_2 (without HRE).

Notably, a significant effect of HRE on the level of CAT activity was detected when cells were pre-incubated with 50 $\mu\text{g/mL}$ HRE before oxidative stress. At this concentration of HRE (Figure 1A), the enzyme activity was significantly different from that of the H_2O_2 treated group (HRE⁻ H_2O_2 ⁺) and most similar to that of the HRE⁻ H_2O_2 ⁻ control. Similar to this, the activity of CAT has elevated significantly after the treatment of HeLa cells with 2 Gy (HRE⁻ 2 Gy⁺) but pared down in the samples, being supplemented with HRE before exposure to IR, HRE⁺ 2 Gy⁺ (Figure 1B). Again, the increase in HRE amount resulted in a concentration-dependent decrease in enzyme activity. Specifically, HRE at 10 $\mu\text{g/mL}$ seemed insufficient as this concentration did not statistically attenuate CAT activity after 2 Gy IR exposure. However, after supplementing cells with higher concentrations of HRE, the enzyme activity decreased significantly compared to the control and irradiated groups (Figure 1B). Therefore, it can be deduced that the effective concentration of the extract needed to cope with 2 Gy of irradiation and to bring the activity of CAT to the average level would be higher than 10 but lower than 25 $\mu\text{g/mL}$ of HRE.

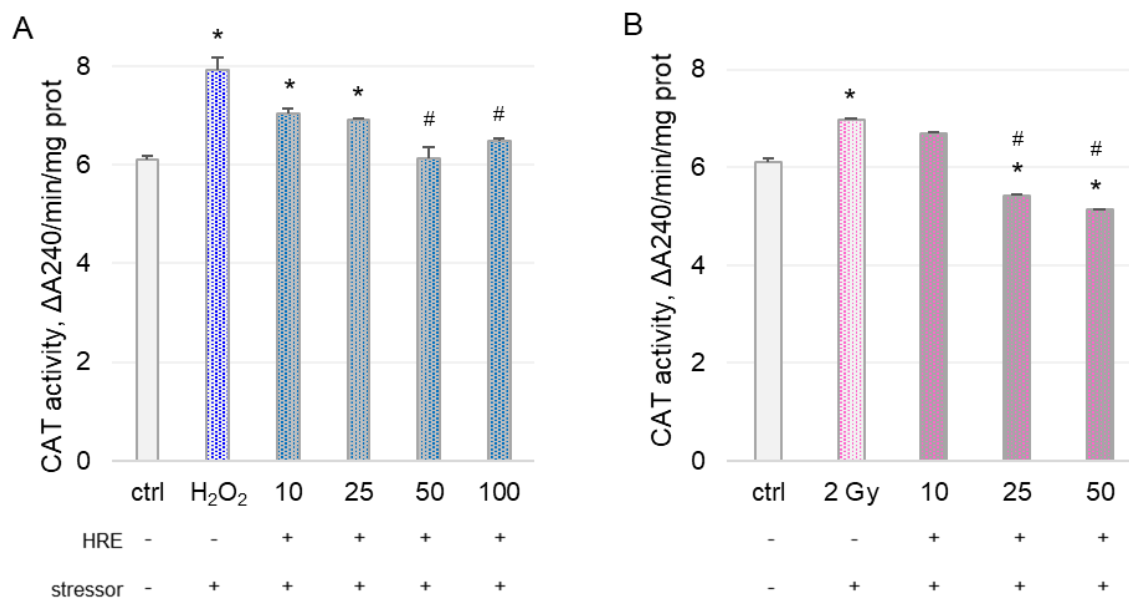


Figure 1 The activity of catalase in stressed HeLa cells, (A) 10 mM H₂O₂ and (B) 2 Gy irradiation, with or without HRE pre-incubation. *Haberlea* extract was administrated to cell cultures to f.c. of 10, 25, 50 or 100 μg/ml. The presence or absence of the specified therapy is shown by the + and - marks. Catalase activity varied statistically from that of the control HRE⁻ H₂O₂⁻ / 2 Gy⁻ group (*p<0.05 versus ctrl) or the stressor-treated HRE⁻ H₂O₂⁺ / 2 Gy⁺ groups (#p<0.05); values are provided as average ±SD.

Catalase (EC 1.11.1.6), one of the most abundant and essential cellular antioxidant enzymes, converts hydrogen peroxide (H₂O₂) into molecular oxygen (O) and water (H₂O). Its vital role is neutralizing excess ROS, which is involved in many physiological processes and pathological conditions, including cancer, atherosclerosis, cataract, diabetes, nutritional deficiency, inflammation, and ageing (Vendemiale et al. 1999; Checa and Aran, 2020). Previous reports showed that administration of H₂O₂ induces the intracellular generation of ROS, which is accompanied by alterations in the synthesis and activities of cellular antioxidant enzymes, e.g. CAT, glutathione peroxidase (GPX) and superoxide dismutase (SOD), as well as sestrin 1, sestrin 2, etc. (Valko et al. 2007; O'Connor et al. 2008; Zhang et al. 2020). For example, in Hep G2 cells treated with H₂O₂ for 4 h, the excess ROS reduced the activity of CAT, GPX and SOD and enhanced lipid peroxidation (Zhang et al. 2020). However, it was shown that the catalase gene in the gills of the crab *Macrophthalmus japonicus* linearly increased in response to exposure to persistent organic pollutants, which cause oxidative stress (Park and Kwak 2022). Furthermore, decreased ROS production and inhibited p53-mediated apoptosis were established in various systems upon overexpression or exogenous addition of CAT (Johnson et al. 1996; Bai and Cederbaum 2003; Hussain et al. 2004; Popowich et al. 2010). We identified that shortly (40 min) after the addition of H₂O₂ to the cells, the intracellular CAT activity increased by 30% relative to the control group (p<0.05). Pre-incubation with HRE abrogated this impact and restored the enzymatic activity to the basal level of

the controls. The observed effect is most likely due to the well-proven potential of HRE to scavenge ROS and thereby reduce the level of oxidants in cells.

3.2 HRE abrogates the alterations in TP53 gene transcription caused by stress conditions

One of the molecules studied extensively in stress-response research is p53 because of its critical role in the physiological stress response (Kasthuber and Lowe 2017). Logically, we continued our studies by assessing HRE's impact on the activity of the gene coding for the p53 protein – TP53 gene in human cells cultivated under normal conditions. It is worth noting that although the gene encoding the p53 protein is changed by numerous mutations in different cancerous cell lines, the TP53 sequence is not altered in HeLa cells (HeLa p53+/+) (Hoppeseyler and Butz 1993; Leroy et al. 2014). The levels of TP53 gene transcription upon incubation of HeLa cells with the studied concentrations of *Haberlea* extracts are shown in Table 3. The incubation with four increasing concentrations of HRE did not evoke dramatic alterations in the relative amount of mRNA transcribed from the TP53 gene compared with the non-HRE control (HRE⁺ vs HRE⁻). Although we have observed slight differences in the relative amount of the TP53 transcript, these variations were considered insignificant as they were below 2-fold change and p>0.05. This proves that at the concentrations tested, *H. rhodopensis* extract does not significantly affect the level of TP53 transcript in HeLa cells under non-stress conditions.

Table 3 Relative concentration of TP53 mRNA in HeLa cells after treatment with *H. rhodopensis* ethanol extract (HRE)

The relative concentration of TP53 mRNA	HRE [$\mu\text{g/mL}$]				
	0	10	25	50	100
	1.00	$1.43 \pm 0.54^{\&}$	$1.15 \pm 0.63^{\&}$	$0.78 \pm 0.72^{\&}$	$1.02 \pm 0.07^{\&}$

$\&p > 0.05$

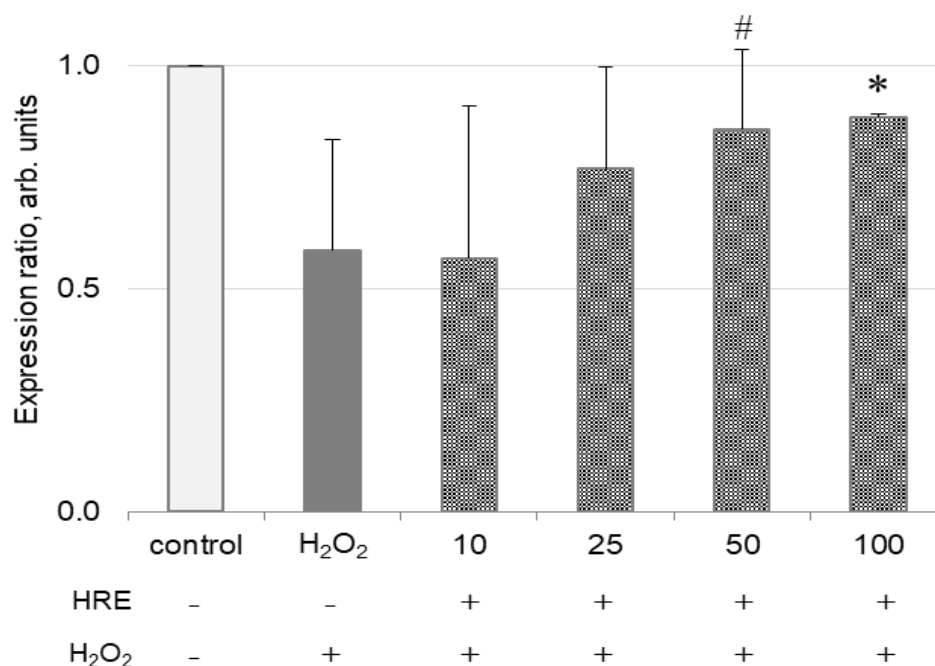


Figure 2 Relative expression of TP53 gene in cells incubated with different concentrations of HRE and exposed to 10 mM H₂O₂; the control sample has not been subjected to any treatment (HRE⁻ H₂O₂⁻); Value is presented as mean \pm SD; $\&p < 0.05$ compared to the control; # $p < 0.05$ vs the group treated with H₂O₂ alone (HRE⁻ H₂O₂⁺)

Hydrogen peroxide is essential for cell viability as one of the most reactive oxygen species. It is well evidenced that exogenous and endogenously present H₂O₂, especially in higher than physiological concentrations, can inflict various types of damage on cellular DNA. This study used hydrogen peroxide as a genotoxin with well-described genotoxic activity (Benhusein et al. 2010). After being exposed to the studied HRE doses for an hour, HeLa cultures were treated with 10 mM H₂O₂ to induce oxidative stress. The TP53 transcription levels were studied by RT²-PCR (Figure 2). To evaluate the combined effect of the stressor and pre-incubation with the extract, the level of TP53 transcript in non-treated control samples (HRE⁻ H₂O₂⁻) was used as a calibrator. The immediate response of HeLa cells to the direct H₂O₂-induced oxidative stress was a decrease in TP53 gene expression (Figure 2, compare HRE⁻ H₂O₂⁺ vs HRE⁻ H₂O₂⁻).

Interestingly, despite the hydrogen peroxide treatment, the amount of TP53 mRNA steadily raised in cells pre-incubated with HRE with the increment of extract concentration (Figure 2). The addition of 50 $\mu\text{g/mL}$ of HRE to the cells normalized the

expression of p53 transcript to the level close to that of non-treated control cells (HRE⁻ H₂O₂⁻) and the genotoxin-free (HRE⁺ H₂O₂⁻), i.e. HRE-only supplemented, cells (1.0 vs 0.86 ± 0.18 and 0.78 ± 0.72 vs 0.86 ± 0.18 ; Figure 2 and Table 3, respectively). Furthermore, the increase of TP53 transcription in cells pretreated with 50 $\mu\text{g/mL}$ HRE was statistically significant compared to those treated with H₂O₂ alone, HRE⁻ H₂O₂⁺. This demonstrates the beneficial effect of HRE supplementation. Therefore, the obtained results reveal that *H. rhodopensis* extracts modulate the expression of TP53 mRNA in HeLa cells under oxidative stress.

Next, we evaluated the levels of TP53 gene transcription in HeLa cell cultures incubated with increasing concentrations of HRE before γ -irradiation. The results indicated up to two-fold increased transcription from the TP53 gene two hours after exposure of HeLa cells to 2 Gy -IR (Figure 3, $p < 0.05$). Furthermore, we have observed that the expression of TP53 was in reverse order following the increase of HRE concentrations. Namely, the higher the extract concentration, the lower the expression of TP53 was (Figure 3).

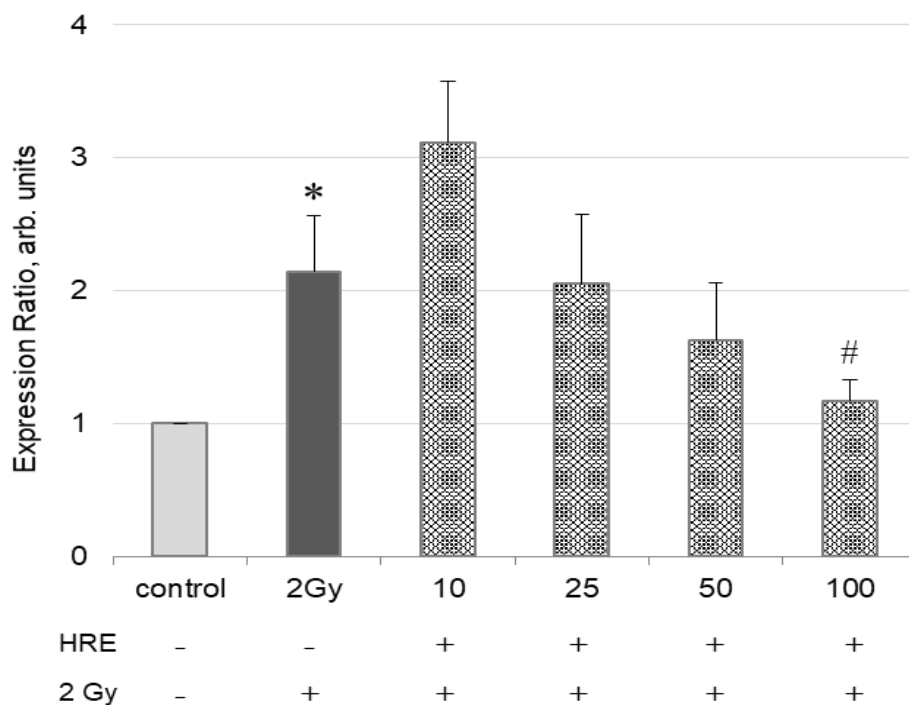


Figure 3 The average fold change of TP53 gene expression in HeLa cells incubated with HRE and exposed to 2 Gy γ -IR. The control cells were treated neither with the extract nor with γ -radiation (HRE⁻ 2Gy⁻) and used as a calibrator. Results are presented as mean \pm SD.

* $p < 0.05$ from the control group; # $p < 0.05$ relative to the 2 Gy γ -IR treated group (HRE⁻ 2 Gy⁺)

When cells were supplemented with 100 $\mu\text{g/mL}$ of HRE, TP53 transcription returned to the basal level, showing values close to those of the two control samples: the one without treatment (1.17 ± 0.16 vs 1.0, $p > 0.05$) and that with 100 $\mu\text{g/mL}$ HRE alone (1.17 ± 0.16 to 1.02 ± 0.07), $p > 0.05$. Compared to cells exposed to 2 Gy of radiation, pretreating the cells with 100 $\mu\text{g/mL}$ HRE caused a nearly two-fold reduction in the amount of TP53 mRNA, and this difference was significant ($p = 0.05$), as shown in Figure 3. Therefore, pre-supplementation of cells with ethanol HRE diminished the expression of the TP53 gene upon 2 Gy-induced genotoxic stress. The effect on TP53 transcription most probably resulted from reduced radiation/oxidation-induced DNA damage in HRE preincubated cells due to the potent antioxidant activities of HRE (Popov et al. 2010b; Georgieva et al. 2013; Popov et al. 2013).

Low physiological amounts of intracellularly produced ROS are not harmful because cells have an efficient system to maintain cellular redox equilibrium and prevent oxidative damage. However, exogenous factors such as ionizing radiation or artificial hydrogen peroxide generate excess ROS production and trigger oxidative stress. Moreover, these factors exhibit strong genotoxicity by causing further damage to the genomic DNA. They thus could direct cellular fate to proliferation, cell-cycle arrest, differentiation, transformation, senescence, autophagy or apoptosis (Campisi, 2013). All this could imperil organismal health, eventually leading to cancer or premature ageing.

The transcription factor p53 is a crucial regulator of cellular response to various stressors, e.g. ionizing radiation, ROS, genotoxins and carcinogens. By activating different downstream pathways, p53 could direct cellular fate to cell cycle arrest, senescence or apoptotic death (Liu et al. 2008; Santoro and Blandino 2010; Cao et al. 2014; Pflaum et al. 2014; Shi et al. 2021; Park and Kwak 2022). Here, we have demonstrated that while H_2O_2 down-regulates the transcription of the TP53 gene, the addition of *Haberlea* extract to the cells is helping the transcription machinery to increase its expression. Thus, concerning TP53 expression, pre-incubation of the cells with HRE at concentrations above 50 $\mu\text{g/mL}$ is efficient for maintaining the gene's activity at an average level and alleviating the attack of 10 mM H_2O_2 by increasing the TP53 transcription to the level of the non-treated control. This effect can be explained by the richness of the extracts with many biologically active compounds such as polyphenols, polysaccharides, vitamins etc. Previous studies demonstrated that the presence of *H. rhodopensis* extract (i) increased the transcription of collagen VI, collagen XVI and elastin genes in H_2O_2 -stressed human dermal fibroblasts (Dell'Acqua and Schweikert 2012), (ii) reduced the H_2O_2 -induced oxidative stress and (iii) prevented cells from apoptosis and cell death (Hayrabedyan et al. 2013). Therefore, it is unsurprising that HRE modulated the expression of a significant stress-responsive gene like TP53 under stress conditions.

3.3 Interlinks between p53 and redox enzymes, including CAT

Numerous investigations have demonstrated that *H. rhodopensis* alcohol extracts exhibit antigenotoxic and radiation-protective properties both *in vivo* and *in vitro*. The high concentration of physiologically active chemicals in HRE that have antioxidant, immunomodulating, antiaging, and anticancer activities can account for these characteristics (Popov et al. 2010b; Mihaylova et al. 2011; Popov et al. 2011; Hayrabedian et al. 2013; Kondeva-Burdina et al. 2013). It should be noted that to apply these extracts properly and successfully, the molecular mechanisms of their action must be thoroughly understood. However, the precise details of these mechanisms are yet unclear. To reveal the details of HRE effects at a molecular level, we have incubated HeLa cells with increasing concentrations of *H. rhodopensis* ethanol extracts and studied the activity of the antioxidant enzyme CAT and the expression of the TP53 stress-responsive gene under optimal and stress conditions.

Gamma radiation causes ionization which can disrupt macromolecules and cellular structures; that is why gamma rays pose a significant challenge to radiation protection, especially during radiotherapy. Data show that HRE pre-treatment could significantly decrease chromosome aberrations, micronuclei frequencies, and the level of blood plasma malondialdehyde and increase SOD and CAT activity in erythrocytes of *in vivo* irradiated rabbits (Georgieva et al. 2013). Previous studies reported that γ -IR did not affect TP53 protein levels but induced p53-serine 15 phosphorylation and increased transcriptional targets p21 and MDM2 (Siliciano et al. 1997; Cao et al. 2014). Conversely, it was shown that upon radiation exposure, the cells respond with increased p53 protein by inhibiting protein degradation and protein translation enhancement (MacCallum et al. 1996; Lee et al. 2013). However, the rationality of these effects regarding gene transcription regulation remained obscure. In line with the above data, we detected a statistically significant increase in CAT activity and two times increased transcription from the TP53 gene after irradiation of HeLa cells with 2 Gy gamma rays.

Here we demonstrated that supplementation with HRE in a concentration above 50 $\mu\text{g}/\text{mL}$ before radiation exposure normalized the TP53 mRNA synthesis to the control group level. It seems that 100 $\mu\text{g}/\text{mL}$ of the ethanol HRE can abolish the effect of radiation to trigger TP53 gene activation and keep its expression at the level of the non-irradiated cells. Thus, HRE's observed *in vivo* radioprotective property is associated with a change in the transcription of the essential stress-response modulator p53.

Interlinks between p53 and redox enzymes, including CAT, have been previously reported in regulating the cellular antioxidant response. It was demonstrated that p53 regulates the transcription of catalase and some other antioxidant enzymes encoding genes

(e.g. GPX1, ALDH4, MnSOD), and these genes are direct p53 targets. On the human MnSOD, GPX, and rat CAT promoters, consensus sequences for binding the p53 transcription factor have been found (Hussain et al. 2004; O'Connor et al. 2008). On the other hand, several authors have reported that upregulation of the CAT gene defends against apoptotic cell death induced by genotoxins (Johnson et al. 1996; Hussain et al. 2004; Popowich et al. 2010). This correlated with an increase in the protein degradation of p53 and a decrease in its phosphorylation (Bai and Cederbaum, 2003). A linear correlation between the expression patterns of p53 and catalase was detected in rat retinal ganglion and *Macrophthalmus japonicas* crab cells (O'Connor et al. 2008; Park and Kwak 2022). However, in human fibroblasts, CAT protein expression remained unaffected after p53 induction and consensus p53 binding elements were not identified on the CAT promoter (Hussain et al. 2004). Kang and co-authors have shown that the opposing roles of p53 in regulating intracellular ROS levels via tuning CAT activity, both up and down, depended on the type and degree of stress and the cellular environment (Kang et al. 2013). Under physiological conditions or mild stress, p53 functions as an antioxidant and upregulates catalase activity through its downstream target p53R2, thereby protecting against ROS. Upon activation following genotoxic stress, p53, in cooperation with PIG3 (another p53-inducible gene), inhibits CAT activity, disturbs intracellular redox homeostasis and could result in p53-mediated apoptosis (Kang et al. 2013). Following earlier findings, our results showed a linear association between p53 expression and CAT activity after cells were exposed to 2 Gy irradiation and an inverse correlation in the case of 10 mM H_2O_2 treatment. Thus, the different responsiveness of the stress-sensing TP53 gene and CAT activity that we observed could be explained by the diverse nature of the applied stressors, the short period after the stress in which the effect was examined and the activation of specific p53 downstream targets. Importantly, one-hour incubation of HeLa cells with HRE in a concentration range between 25-100 $\mu\text{g}/\text{mL}$ before stress conditions maintained TP53 gene expression and catalase activity at basal levels characteristics of untreated controls.

At first sight, the opposite effects of H_2O_2 and γ -IR on the TP53 gene activity can be startling. H_2O_2 and gamma rays can produce single and double-strand cuts in DNA and oxidize proteins and lipids. However, behind their similar effects, these two agents possess some very well-pronounced differences in action on the biological macromolecules. H_2O_2 , as one of the ROS, directly cuts DNA and oxidizes proteins, while gamma radiation ionizes cellular cytoplasm and produces ROS, but simultaneously can modify chemically macromolecules. For instance, the reductive stress brought on by IR causes protein methionine and cysteine residues to lose sulphur, and DNA-protein adducts are created as a result (Reisz et al. 2014).

Conclusions

Our findings unequivocally demonstrate that *H. rhodopensis* alcoholic extracts alter the TP53 gene transcription in a way that distinguishes the genotoxic effects of H₂O₂ and gamma rays. Shortly after being exposed to stress, these effects were discovered. One of the molecular mechanisms of the well-established radioprotective effects of HRE *in vivo* can be attributed to the observed alterations in the activity of catalase, a major cellular antioxidant enzyme, and the expression of TP53, a significant stress-responsive gene. More extensive future trials will reveal the specifics of the phenomena seen in the present investigation.

Acknowledgements

This work was supported by Trakia University, Bulgaria, under Fund grant №6/2018, and partially by the Bulgarian National Research Fund Grant number: DN 11/15 and NATO Science for Peace and Security program Grant number: NATO SPS MYP G5266.

Conflict of interest

The authors declare they have no competing interests.

References

- Aebi, H. (1984). Catalase in vitro. *Methods in Enzymology*, 105, 121-126. [https://doi.org/10.1016/s0076-6879\(84\)05016-3](https://doi.org/10.1016/s0076-6879(84)05016-3)
- Bai, J., & Cederbaum, A. I. (2003). Catalase protects HepG2 cells from apoptosis induced by DNA-damaging agents by accelerating the degradation of p53. *Journal of Biological Chemistry*, 278(7), 4660-4667. <https://doi.org/10.1074/jbc.M206273200>
- Benhusein, G. M., Mutch, E., Aburawi, S., & Williams, F. M. (2010). Genotoxic effect induced by hydrogen peroxide in human hepatoma cells using comet assay. *Libyan Journal of Medicine*, 5. <https://doi.org/10.3402/ljm.v5i0.4637>
- Berkov, S. H., Nikolova, M. T., Hristozova, N. I., Momekov, G. Z., Ionkova, I. I., & Djilianov, D. L. (2011). GC-MS profiling of bioactive extracts from *Haberlea rhodopensis*: an endemic resurrection plant. *Journal of the Serbian Chemical Society*, 76(2), 211-220. <https://doi.org/10.2298/Jsc100324024b>
- Campisi, J. (2013). Aging, Cellular Senescence, and Cancer. *Annual Review of Physiology*, 75, 685-705. <https://doi.org/10.1146/annurev-physiol-030212-183653>
- Cao, L. L., Kawai, H., Sasatani, M., Iizuka, D., Masuda, Y., et al. (2014). A Novel ATM/TP53/p21-Mediated Checkpoint Only Activated by Chronic gamma-Irradiation. *Plos One*, 9(8). <https://doi.org/ARTN e10427910.1371/journal.pone.0104279>
- Carson, S., Miller, H. B., Witherow, D. S., & Srougi, M. C. (2019). Molecular Biology Techniques: A Classroom Laboratory Manual. In S. Carson, H. B. Miller, D. S. Witherow, & M. C. Srougi (Eds.), *Molecular Biology Techniques (Fourth Edition)* (Fourth Edition ed.). Academic Press. <https://doi.org/https://doi.org/10.1016/B978-0-12-815774-9.00035-6>
- Checa, J., & Aran, J. M. (2020). Reactive Oxygen Species: Drivers of Physiological and Pathological Processes. *Journal of Inflammation Research*, 13, 1057-1073. <https://doi.org/10.2147/Jir.S275595>
- Dell'Acqua, G., & Schweikert, K. (2012). Skin benefits of a myconoside-rich extract from resurrection plant *Haberlea rhodopensis*. *International Journal of Cosmetic Science*, 34(2), 132-139. <https://doi.org/10.1111/j.1468-2494.2011.00692.x>
- Ebrahimi, S. N., Gafner, F., Dell'Acqua, G., Schweikert, K., & Hamburger, M. (2011). Flavone 8-C-Glycosides from *Haberlea rhodopensis* FRIV. (Gesneriaceae). *Helvetica Chimica Acta*, 94(1), 38-45. <https://doi.org/DOI 10.1002/hlca.201000378>
- Gechev, T. S., Benina, M., Obata, T., Tohge, T., Sujeeth, N., et al. (2013). Molecular mechanisms of desiccation tolerance in the resurrection glacial relic *Haberlea rhodopensis*. *Cellular and Molecular Life Sciences*, 70(4), 689-709. <https://doi.org/10.1007/s00018-012-1155-6>
- Georgieva, M., Moyankova, D., Djilianov, D., Uzunova, K., & Miloshev, G. (2015). Methanol extracts from the resurrection plant *Haberlea rhodopensis* ameliorate cellular vitality in chronologically ageing *Saccharomyces cerevisiae* cells. *Biogerontology*, 16(4), 461-472. <https://doi.org/10.1007/s10522-015-9566-z>
- Georgieva, S., Popov, B., & Bonev, G. (2013). Radioprotective effect of *Haberlea rhodopensis* (Friv.) leaf extract on gamma-radiation-induced DNA damage, lipid peroxidation and antioxidant levels in rabbit blood. *Indian Journal of Experimental Biology*, 51(1), 29-36.
- Giorgio, M., Trinei, M., Migliaccio, E., & Pelicci, P. G. (2007). Hydrogen peroxide: a metabolic by-product or a common mediator of ageing signals? *Nature Reviews Molecular Cell Biology*, 8(9), 722a-728.
- Gomes, T., Song, Y., Brede, D. A., Xie, L., Gutzkow, K. B., Salbu, B., & Tollefsen, K. E. (2018). Gamma radiation induces dose-dependent oxidative stress and transcriptional alterations in the freshwater crustacean *Daphnia magna*. *Science of the Total Environment*, 645, 1035-1045. <https://doi.org/10.1016/j.scitotenv.2018.07.103>

- Environment*, 628-629, 206-216. <https://doi.org/10.1016/j.scitotenv.2018.02.039>
- Hayrabyan, S., Todorova, K., Zasheva, D., Moyankova, D., Georgieva, D., Todorova, J., & Djilianov, D. (2013). *Haberlea rhodopensis* Has Potential as a New Drug Source Based on Its Broad Biological Modalities. *Biotechnology & Biotechnological Equipment*, 27(1), 3553-3560. <https://doi.org/10.5504/Bbeq.2012.0112a>
- Hickman, M. J., & Samson, L. D. (1999). Role of DNA mismatch repair and p53 in signaling induction of apoptosis by alkylating agents. *Proceedings of the National Academy of Sciences of the United States of America*, 96(19), 10764-10769. <https://doi.org/DOI 10.1073/pnas.96.19.10764>
- Hoppeseyler, F., & Butz, K. (1993). Repression of Endogenous P53 Transactivation Function in HeLa Cervical-Carcinoma Cells by Human Papillomavirus Type-16 E6, Human Mdm-2, and Mutant P53. *Journal of Virology*, 67(6), 3111-3117. <https://doi.org/Doi 10.1128/Jvi.67.6.3111-3117.1993>
- Hussain, S. P., Amstad, P., He, P. J., Robles, A., Lupold, S., et al. (2004). p53-induced up-regulation of MnSOD and GPx but not catalase increases oxidative stress and apoptosis. *Cancer Research*, 64(7), 2350-2356. <https://doi.org/Doi 10.1158/0008-5472.Can-2287-2>
- Johnson, T. M., Yu, Z. X., Ferrans, V. J., Lowenstein, R. A., & Finkel, T. (1996). Reactive oxygen species are downstream mediators of p53-dependent apoptosis. *Proceedings of the National Academy of Sciences of the United States of America*, 93(21), 11848-11852. <https://doi.org/DOI 10.1073/pnas.93.21.11848>
- Kang, M. Y., Kim, H. B., Piao, C., Lee, K. H., Hyun, J. W., Chang, I. Y., & You, H. J. (2013). The critical role of catalase in prooxidant and antioxidant function of p53. *Cell Death and Differentiation*, 20(1), 117-129. <https://doi.org/10.1038/cdd.2012.102>
- Kastenhuber, E. R., & Lowe, S. W. (2017). Putting p53 in Context. *Cell*, 170(6), 1062-1078. <https://doi.org/10.1016/j.cell.2017.08.028>
- Kondeva-Burdina, M., Zheleva-Dimitrova, D., Nedialkov, P., Girreser, U., & Mitcheva, M. (2013). Cytoprotective and antioxidant effects of phenolic compounds from *Haberlea rhodopensis* Friv. (Gesneriaceae). *Pharmacognosy Magazine*, 9(36), 294-301. <https://doi.org/10.4103/0973-1296.117822>
- Lee, C. L., Blum, J. M., & Kirsch, D. G. (2013). Role of p53 in regulating tissue response to radiation by mechanisms independent of apoptosis. *Translational Cancer Research*, 2(5), 412-421. <https://doi.org/10.3978/j.issn.2218-676X.2013.09.01>
- Leroy, B., Girard, L., Hollestelle, A., Minna, J. D., Gazdar, A. F., & Soussi, T. (2014). Analysis of TP53 Mutation Status in Human Cancer Cell Lines: A Reassessment. *Human Mutation*, 35(6), 756-765. <https://doi.org/10.1002/humu.22556>
- Liu, B., Chen, Y. M., & Clair, D. K. S. (2008). ROS and p53: A versatile partnership. *Free Radical Biology and Medicine*, 44(8), 1529-1535. <https://doi.org/10.1016/j.freeradbiomed.2008.01.011>
- Livak, K. J., & Schmittgen, T. D. (2001). Analysis of relative gene expression data using real-time quantitative PCR and the 2(-Delta Delta C(T)) Method. *Methods*, 25(4), 402-408. <https://doi.org/10.1006/meth.2001.1262>
- MacCallum, D. E., Hupp, T. R., Midgley, C. A., Stuart, D., Campbell, S. J., et al. (1996). The p53 response to ionizing radiation in adult and developing murine tissues. *Oncogene*, 13(12), 2575-2587.
- Mihaylova, D., Bahchevanska, S., & Toneva, V. (2011). Microwave-assisted extraction of flavonoid antioxidants from leaves of *Haberlea rhodopensis*. *Journal of International Scientific Publications: Materials, Methods & Technologies*, 5(1), 104-114.
- Muller, J., Sprenger, N., Bortlik, K., Boller, T., & Wiemken, A. (1997). Desiccation increases sucrose levels in *Ramonda* and *Haberlea*, two genera of resurrection plants in the Gesneriaceae. *Physiologia Plantarum*, 100(1), 153-158. <https://doi.org/DOI 10.1034/j.1399-3054.1997.1000117.x>
- O'Connor, J. C., Wallace, D. M., O'Brien, C. J., & Cotter, T. G. (2008). A novel antioxidant function for the tumor-suppressor gene p53 in the retinal ganglion cell. *Investigative Ophthalmology & Visual Science*, 49(10), 4237-4244. <https://doi.org/10.1167/iovs.08-1963>
- Oneill, P., & Fielden, E. M. (1993). Primary Free-Radical Processes in DNA. *Advances in Radiation Biology*, 17, 53-120.
- Park, K., & Kwak, I. S. (2022). Apoptotic p53 Gene Expression in the Regulation of Persistent Organic Pollutant (POP)-Induced Oxidative Stress in the Intertidal Crab *Macrophthalmus japonicus*. *Antioxidants*, 11(4). <https://doi.org/Artn 77110.3390/Antiox11040771>
- Pflaumf, J., Schlosser, S., & Muller, M. (2014). p53 family and cellular stress responses cancer. *Frontiers in Oncology*, 4. <https://doi.org/Artn 28510.3389/Fonc.2014.00285>
- Popov, B., Dobрева, Z. G., Georgieva, S., & Stanilova, S. A. (2010a). Enhancement of anti-KLH IgG antibody production in rabbits after treatment with *Haberlea rhodopensis* extracts. *Trakia Journal of Sciences*, 8(2), 92-97.

- Popov, B., Georgieva, S., Gadjeva, V., & Petrov, V. (2011). Radioprotective, anticlastogenic and antioxidant effects of total extract of *Haberlea rhodopensis* on rabbit blood samples exposed to gamma radiation in vitro. *Revue De Medecine Veterinaire*, *162*(1), 34-39.
- Popov, B., Georgieva, S., Oblakova, M., & Bonev, G. (2013). Effects of *Haberlea rhodopensis* Extract on Antioxidation and Lipid Peroxidation in Rabbits after Exposure to (Co)-C-60-Gamma-Rays. *Archives of Biological Sciences*, *65*(1), 91-97. <https://doi.org/10.2298/Abs1301091p>
- Popov, B., Radev, R., & Georgieva, S. (2010b). In vitro incidence of chromosome aberrations in gamma-irradiated rabbit lymphocytes, treated with *Haberlea rhodopensis* extract and vitamin C. *Bulgarian Journal of Veterinary Medicine*, *13*(3), 148-153.
- Popowich, D. A., Vavra, A. K., Walsh, C. P., Bhikapurwala, H. A., Rossi, N. B., et al. (2010). Regulation of reactive oxygen species by p53: implications for nitric oxide-mediated apoptosis. *American Journal of Physiology-Heart and Circulatory Physiology*, *298*(6), H2192-H2200. <https://doi.org/10.1152/ajpheart.00535.2009>
- Radev, R., Lazarova, G., Nedialkov, P., Sokolova, K., Rukanova, D., & Tsokeva, Z. (2009). Study on antibacterial activity of *Haberlea rhodopensis*. *Trakia Journal of Sciences*, *7*(1), 34-36.
- Reisz, J. A., Bansal, N., Qian, J., Zhao, W. L., & Furdai, C. M. (2014). Effects of Ionizing Radiation on Biological Molecules-Mechanisms of Damage and Emerging Methods of Detection. *Antioxidants & Redox Signaling*, *21*(2), 260-292. <https://doi.org/10.1089/ars.2013.5489>
- Santoro, R., & Blandino, G. (2010). p53: The pivot between cell cycle arrest and senescence. *Cell Cycle*, *9*(21), 4262-4263. <https://doi.org/10.4161/cc.9.21.13853>
- Shi, T., van Soest, D. M. K., Polderman, P. E., Burgering, B. M. T., & Dansen, T. B. (2021). DNA damage and oxidant stress activate p53 through differential upstream signaling pathways. *Free Radical Biology and Medicine*, *172*, 298-311. <https://doi.org/10.1016/j.freeradbiomed.2021.06.013>
- Siliciano, J. D., Canman, C. E., Taya, Y., Sakaguchi, K., Appella, E., & Kastan, M. B. (1997). DNA damage induces phosphorylation of the amino terminus of p53. *Genes & Development*, *11*(24), 3471-3481. <https://doi.org/DOI.10.1101/gad.11.24.3471>
- Stefanov, K., Markovska, Y., Kimenov, G., & Popov, S. (1992). Lipid and Sterol Changes in Leaves of *Haberlea-Rhodopensis* and *Ramonda-Serbica* at Transition from Biosis into Anabiosis and Vice-Versa Caused by Water-Stress. *Phytochemistry*, *31*(7), 2309-2314. [https://doi.org/Doi.10.1016/0031-9422\(92\)83270-9](https://doi.org/Doi.10.1016/0031-9422(92)83270-9)
- Stevenson MA, C. S. (2016). Molecular and cellular biology In T. J. Gunderson LL (Ed.), *Clinical Radiation Oncology* (pp. 14-50). Elsevier Inc. <https://doi.org/https://doi.org/10.1016/C2013-0-00648-2>
- Valko, M., Leibfritz, D., Moncol, J., Cronin, M. T. D., Mazur, M., & Telser, J. (2007). Free radicals and antioxidants in normal physiological functions and human disease. *International Journal of Biochemistry & Cell Biology*, *39*(1), 44-84. <https://doi.org/10.1016/j.biocel.2006.07.001>
- Vendemiale, G., Grattagliano, I., & Altomare, E. (1999). An update on the role of free radicals and antioxidant defense in human disease. *International Journal of Clinical & Laboratory Research*, *29*(2), 49-55. <https://doi.org/DOI.10.1007/s005990050063>
- Zhang, X. X., Wang, L., Lu, H., Zong, Z. Q., et al. (2020). Preservation of hydrogen peroxide-induced oxidative damage in HepG-2 cells by rice protein hydrolysates pretreated with electron beams. *Scientific Reports*, *10*(1). <https://doi.org/Artn.841510.1038/S41598-020-64814-7>







Journal of Experimental Biology and Agricultural Sciences

<http://www.jebas.org>

ISSN No. 2320 – 8694

The Effect of Titanium Dioxide Nanoparticles on *Haematococcus pluvialis* Biomass Concentration

Manishaa Sri Mahendran¹ , Ling Shing Wong² ,
 Anto Cordelia Tanislaus Antony Dhanapal^{1*} , Sinouvassane Djearamane^{3,4*} 

¹Department of Chemical Science, Faculty of Science, Universiti Tunku Abdul Rahman, Kampar, 31900 Malaysia²Life Science Division, Faculty of Health and Life Sciences, INTI International University, Nilai, 71800 Malaysia³Department of Allied Health Science, Faculty of Science, Universiti Tunku Abdul Rahman, Kampar, 31900 Malaysia⁴Biomedical Research Unit and Lab Animal Research Centre, Saveetha Dental College, Saveetha Institute of Medical and Technical Sciences, Saveetha University, Chennai 602 105, India

Received – February 06, 2023; Revision – April 14, 2023; Accepted – April 29, 2023

Available Online – April 30, 2023

DOI: [http://dx.doi.org/10.18006/2023.11\(2\).416.422](http://dx.doi.org/10.18006/2023.11(2).416.422)

KEYWORDS

Algal biomass

Biomass concentration

Growth pattern

H. pluvialis

Titanium dioxide nanoparticles

ABSTRACT

The increased release of Titanium dioxide nanoparticles (TiO₂ NPs) into the aquatic ecosystem is caused by the augmented utilization of nanoparticles in personal care and household products. This has resulted in the contamination of marine, aquatic, and ground water resources, causing adverse impacts on the biota and flora, both in vivo and in vitro. The main purpose of this research was to examine the negative impacts of TiO₂ NPs on the bioaccumulation of *Haematococcus pluvialis*. The interaction and buildup of TiO₂ NPs on *H. pluvialis* were studied using scanning electron microscopy (SEM). The exposure of *H. pluvialis* to TiO₂ NPs with increasing concentrations (5–100 µg/mL) and time intervals (24 h to 96 h) impacted the biomass concentration of the microalgae. The SEM images provided evidence of changes in characteristics and impairment of the exterior of exposed cells. The findings revealed that the exposure of *H. pluvialis* to TiO₂ NPs resulted in a decline in biomass, which was dependent on the concentration and duration of exposure. The most severe adverse effects were observed after 96 hours of exposure, with a reduction of 43.29 ± 2.02% of biomass concentration. This study has demonstrated that TiO₂ NPs harm *H. pluvialis*, as evidenced by the negative impact on algal biomass resulting from the binding and buildup of these particles on microalga *H. pluvialis*. To sum up, the decline in algal growth is caused by the accumulation and interaction of TiO₂ NPs on microalgae scoring the adverse effects on the growth of *H. pluvialis* by TiO₂ NPs. The findings of this study call for novel screening methods to detect and eliminate TiO₂ NPs contamination in aquatic sources used for the cultivation of microalgae which may otherwise pose delirious effects to the consumers.

* Corresponding author

E-mail: antoc@utar.edu.my (Anto Cordelia Tanislaus Antony Dhanapal);
 drsino31@gmail.com (Sinouvassane Djearamane)

Peer review under responsibility of Journal of Experimental Biology and Agricultural Sciences.

Production and Hosting by Horizon Publisher India [HPI]
 (<http://www.horizonpublisherindia.in/>).
 All rights reserved.

All the articles published by [Journal of Experimental Biology and Agricultural Sciences](#) are licensed under a [Creative Commons Attribution-NonCommercial 4.0 International License](#) Based on a work at www.jebas.org.



1 Introduction

Nanotechnology focuses on the understanding and application of atoms and molecules smaller than 100 nanometres (nm). The nanoparticles' wide applications and unique features clearly explain the huge market potential for nanoparticles (NPs) (Banerjee and Roychoudhury 2019). The nanoparticles have been used in the pharmaceutical industry, water treatment, cosmetics, engineering, as a colourant in white plastics, pigments for food, and many other consumers and industrial products (Iswarya et al. 2015; Ziental et al. 2020).

Zinc oxide nanoparticles (ZnO NPs) and titanium dioxide nanoparticles (TiO₂ NPs) are the most commonly manufactured nanomaterials, with an estimated global output ranging from 10,000 to 88,000 tons per year. TiO₂ NPs are used in numerous fields with annual production exceeding four million tons annually. The production of TiO₂ NPs is still an increasing trend because of their vast range of uses, so the nanoparticle's release into the aquatic environment is inevitable (Bameri et al. 2022). Therefore, studying how TiO₂ NPs affect the environment, particularly aquatic creatures, is crucial. Microalgae have previously been employed as exemplary organisms for investigating the harmfulness of metallic oxide nanoparticles in the atmosphere (Djearamane et al. 2019). Several parameters can be used to indicate the presence of metallic oxide nanoparticles, including biomass and photosynthetic activities.

Haematococcus pluvialis is an important microalga with high nutritional importance. This freshwater microalga contain carbohydrates (30–40%), proteins (20–30%), fatty acids (7–25%), astaxanthin (>1.5%), carotenoids (>1.75%), and minerals. It is also one of the lushest natural sources of astaxanthin- a natural substance with potent antioxidant, anticancer, and anti-inflammatory properties (Harker et al. 1996; Dong et al. 2014; Hong et al. 2016; Matos et al. 2017). Furthermore, *H. pluvialis* holds high agricultural value as this microalga give colour to trout, farmed salmon, ornamental fish, prawns, and sea bream (Dore and Cysewski 2003). Therefore, they have been fed to the farmed aquaculture feeds. Environmental stress makes *H. pluvialis* cells highly sensitive and changes their morphology in response to environmental factors (Djearamane et al. 2019). The investigation was carried out to explore the influence of TiO₂ NPs on the biomass concentration of *H. pluvialis*. Consumption of microalgae nutritional supplements contaminated with TiO₂ NPs could potentially compromise the nutritional value and pose adverse health effects to consumers. Therefore, understanding the consequence of TiO₂ NPs on *H. pluvialis* would be crucial in assessing the ecological implications of TiO₂ NPs in waterways. These findings will also aid in the development of screening methods for TiO₂ NPs contamination in microalgae, which may alternatively cause negative health impacts to the consumers.

2 Materials and Procedures

2.1 Microalgae Cultivation

The stock culture was provided by UTEX1926 (University of Texas Culture Collection, Austin, TX, USA). *H. pluvialis* stock culture of 4mL was added to 200 mL of Bold's basal medium and was kept at room temperature (21 to 23°C) with a cool white fluorescent bulb providing 1200 lux illumination for 16 hours of daylight and 8 hours of darkness (Djearamane et al. 2018)

2.2 Microalgae's Exposure to TiO₂ NPs

TiO₂ NPs with particle size (23-35nm) were procured from Chemical Solutions, Malaysia, and used in this experiment. TiO₂ NPs stock solution of 200 µg/mL concentration was prepared in the appropriate culture medium to produce a homogeneous NPs suspension. TiO₂ NPs stock solutions were diluted with the BBM to prepare the working concentrations. Then, *H. pluvialis* cells from the eighth day of growth (exponential phase) with the initial optical density (OD) of 0.4 were exposed to NP concentrations over 96 hours in a 250 mL Erlenmeyer flask alongside NP-free controls. The influence of NPs (5, 10, 25, 50, 100 µg/mL) on the nutritional values of *H. pluvialis* was examined by comparing the NP exposed algal cells with the control cells at 24, 48, 72, and 96 hours. This investigation allowed us to assess the influence of NPs on the algal cells and how their nutritional values varied with NPs' exposure time (Djearamane et al. 2018).

2.3 Cellular Interaction of TiO₂ NPs on Algal Cells via SEM-EDX Analysis

The adsorption and accumulation of TiO₂ NPs in *H. pluvialis* biomass were analyzed using SEM-EDX to understand how TiO₂ NPs affected cell morphology. The algal cells were spun upon exposure to TiO₂ NPs, and the pellet was obtained. It was then washed twice with distilled water and 0.1X PBS and freeze-dried for further analysis. SEM-EDX was performed for the freeze-dried algal cells (JSM-6701F, Joel, Japan).

2.4 Effects of TiO₂ NPs on Algal Biomass Concentration

The algal biomass concentration of the test and the control were assessed using a spectrophotometer at an optical density of 680 nm (Gynesys 10S UV-Vis, Thermo Scientific, United States of America). An additional control with just the TiO₂ NPs for each concentration was also recorded and adjusted from the test reading to exclude the interference from TiO₂ NPs. BBM served as the blank for both the test and the controls. The trial and control results were expressed as a percentage of change in biomass and were used to calculate the trend of algal growth following the treatment with various concentrations of TiO₂ NPs at different time intervals.

$$\text{OD of the culture at 680nm} = \text{OD}_1 - \text{OD}_0 \quad (\text{eq. 1})$$

$\text{OD}_0 = \text{OD of the medium with TiO}_2 \text{ NPs only}$

$\text{OD}_1 = \text{OD of cell culture with TiO}_2 \text{ NPs only}$

$$\% \text{ change in biomass} = \frac{(\text{OD 680 of negative control} - \text{OD 680 of test cell culture}) \times 100}{(\text{OD 680 of negative control})} \quad (\text{eq. 2})$$

2.5 Statistical Analysis

All challenge tests were performed in triplicates ($n = 3$), and the data were conferred as mean \pm standard error. The experimental results were tested for normality using the Shapiro-Wilk test. One-way analysis of variance (ANOVA) was used for all analyses with significant values set at $p < 0.05$. Tukey's post hoc test was used for multiple comparisons.

3 Results

3.1 SEM-EDX Analysis of Algal Cell Interactions with TiO₂ Nanoparticles

SEM image of *H. pluvialis* cells untreated and treated with TiO₂ NPs at 100 mg/mL is shown in Figure 1. The images demonstrate that cells in Figure 1A appeared as smooth cylindrical structures with undamaged cell membranes when they were not treated with TiO₂ NPs. The cells treated with TiO₂ NPs in Figure 1B show cell entrapment with NP clusters, aggregation of algal cells, and rupture of the cell membrane, which led to cell rupture and wrinkled cells of *H. pluvialis*. We have specifically reported the differences between the control and exposure at a concentration of 100 $\mu\text{g/mL}$ TiO₂ NPs due to the significant changes observed in this particular concentration.

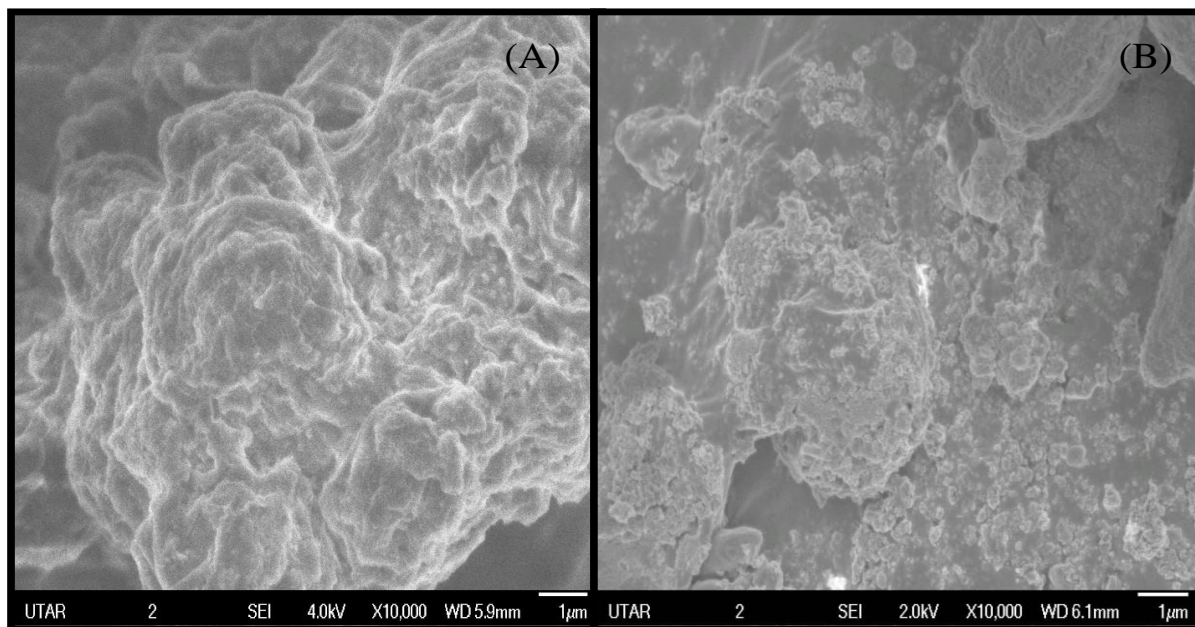


Figure 1 Scanning Electron Microscopy: (A) *H. pluvialis* cells without treating TiO₂ NPs at 96h with 10000X magnification; (B) *H. pluvialis* cells treated with 100 $\mu\text{g/mL}$ TiO₂ NPs at 96h with 10000X magnification.

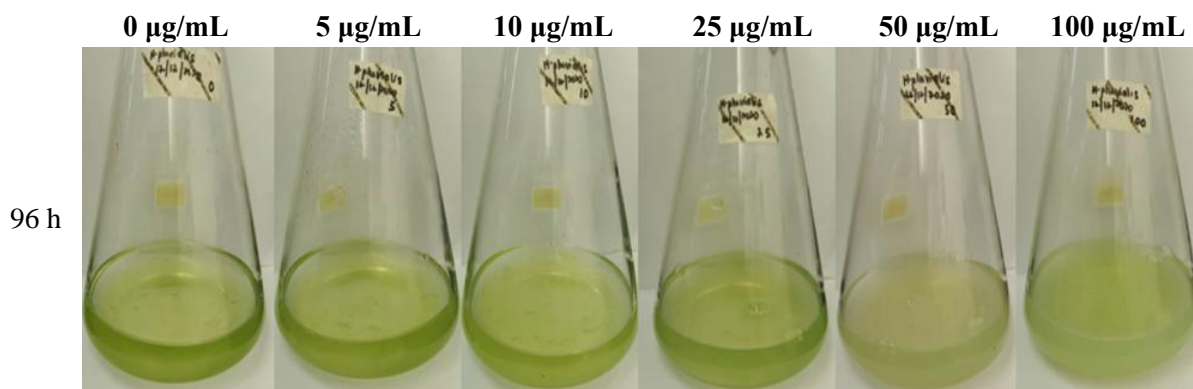


Figure 2 *H. pluvialis* cultures treated with different concentrations of TiO₂ NPs at 96 hrs

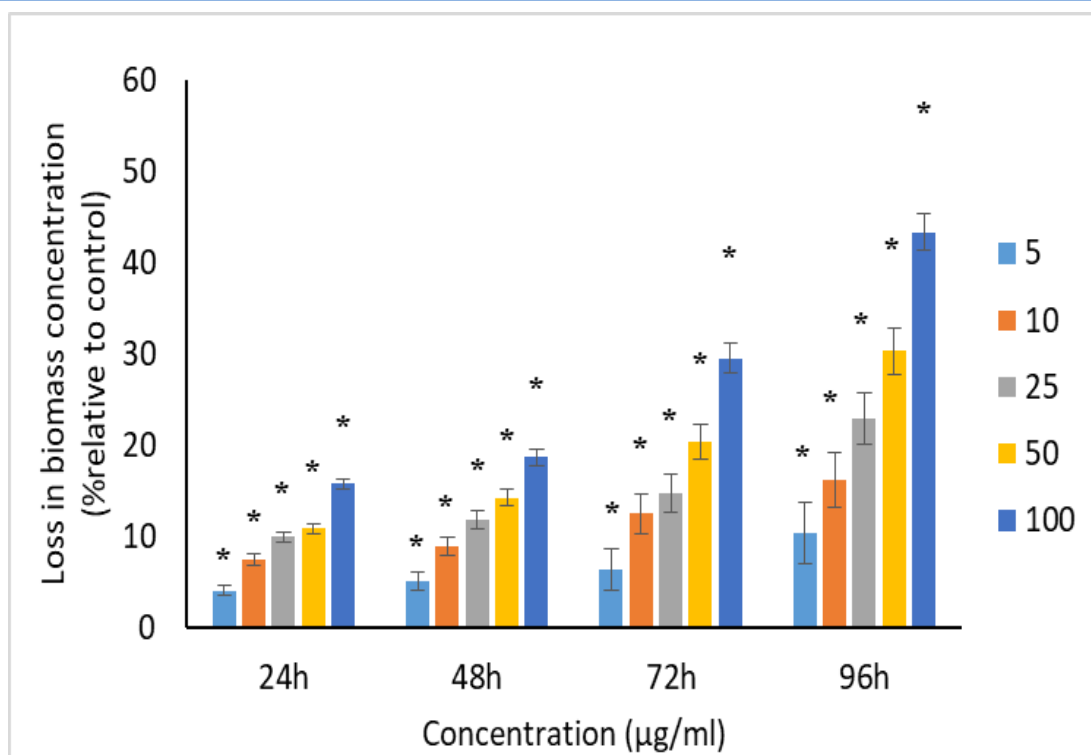


Figure 3 Plotted the mean values and standard deviation of the percentage loss in biomass concentration of *H. pluvialis* relative to the control after treatment with TiO₂ NPs from 24 to 96 h. The asterisk (*) indicates a significant difference at $p < 0.05$ between the control and TiO₂ NPs treated algal suspension for all the time intervals

3.2 Effects of TiO₂ NPs on Algal Biomass Concentration

When *H. pluvialis* culture was exposed to several TiO₂ NPs concentrations, as presented in Figure 2, a slight difference in the culture's colour was observed. As the concentration and exposure time increased, the intensity of the green colour decreased. This qualitative data indicates that the biomass concentration of *H. pluvialis* decreased with increased concentration and exposure time. Figure 3 depicts the percentage reduction of *H. pluvialis* biomass concentration relative to control when treated with different TiO₂ NPs concentrations ranging from 5 to 100 µg/mL for 24 to 96 hrs. A significant ($p < 0.05$) loss in biomass was detected for the tested concentrations of TiO₂ NPs between 24 and 96 hours. The highest loss in biomass occurred at 96 hours, with values reported as 10.42%, 16.15%, 22.87%, 30.29%, and 43.29% for 5, 10, 25, 50, and 100 µg/mL TiO₂ NPs respectively.

4 Discussion

SEM-EDX analysis was conducted on *H. pluvialis* cells exposed to TiO₂ NPs to determine the accumulation of the particles in the biomass and any resulting changes in cell morphology. Two pathways for metal ion uptake into algal cells were reported (Gupta et al. 2014). The initial step involved the adherence of metal ions onto the surface of the algae, after which the ions were taken up by

cytoplasmic organelles and transported through the cell membranes. The current investigation used SEM-EDX to determine TiO₂ NPs' accumulation in the algal biomass, according to the mechanisms outlined by Gupta et al. (2014). Many researchers validated similar results (Dmytryk et al. 2014; Djearmane et al. 2018), where EDX analysis was carried out to show the accumulation of ZnO NPs, zinc, and Se within cells of *Spirulina platensis*' algal biomass.

Multiple layers of NPs adhering to and building up on the cell surface might interfere with food uptake and put photosynthetic bacteria under physical stress (Metzler et al. 2011). The study revealed that the size of TiO₂ NPs used in this research was much smaller than the pore diameter (ranging from 5 to 20 nm) in the cell walls of the microalgae (Navarro et al. 2008). Furthermore, it is suggested that most TiO₂ NPs adhered to the surface of *H. pluvialis*. It was noted that the physical barrier created by the NPs' surface attachment to the cells prevented the development of microorganisms that use sunlight for photosynthesis. Hazeem et al.(2016) suggested that when NPs adhere to the surface of cells and cluster together, it could cause physical harm and lead to changes in the cellular metabolic processes. These changes may restrict growth, lower biomass concentration, and affect photosynthetic compound production (Metzler et al. 2011).

To explore TiO₂ NPs' influence on the biomass of *H. pluvialis*, the changes in the algal biomass of *H. pluvialis* before and after exposure to TiO₂ NPs over 96 hours were evaluated using spectrophotometric techniques. Contradictory to our results, a previous study reported lesser impact that *H. pluvialis* biomass decreased by 18.1% on day 9 after being exposed to 100 µg/mL TiO₂ NPs. This could be due to the small size of the nanoparticles used in our research (Comotto et al. 2014). The toxicity of nanoparticles increases as their size decreases. According to a study by Xia et al. (2015), both bulk and nano titanium particles limited the growth of *Nitzschia closterium*. The calculated EC₅₀ values were 88.78 ± 6.43 and 118.80 ± 12.78 mg/L for 21 and 60 nm TiO₂ NPs, respectively. That study also revealed that after exposing the cells for 96 hours, the 21nm TiO₂ NPs induced more toxicity than 60nm TiO₂ NPs and bulk particles of titanium. The cytotoxicity of TiO₂ NPs may also be influenced by their size, which is a factor in the study. The research conducted by Sendra et al. (2017) demonstrated that smaller Ag NPs had a greater inhibitory effect on the growth of *Chlamydomonas reinhardtii*. *C. reinhardtii* demonstrated over 50% growth suppression after 72 hours when subjected to 10 g/L of 4.5 and 16.7 nm Ag NPs, and the EC₅₀ for Ag NPs was determined to be 10 g/L. Conversely, Ag NPs sized at 46.7 nm had an EC₅₀ value of > 300 g/L. The growth of *H. pluvialis* is impeded by ZnO NPs, leading to declining algal biomass and cell viability. When *H. pluvialis* was exposed to different concentrations of ZnO NPs from 10 to 200 µg/mL for 72 hours, the microalgae's biomass concentration and cell viability reduced significantly. The extreme growth inhibition was seen at 96 hrs when 200 µg/mL of ZnO NPs resulted in a 49% drop in algal biomass and a 52% drop in cell viability compared to the control. Additionally, after 15 days of exposure, 100 µg/mL of 14 nm TiO₂ NPs reduced the biomass content of *S. platensis* by 74% (Comotto et al. 2014).

The form, shape, concentration, surface charge, and surface properties of nanoparticles exposed on microalgae may impact how quickly they grow (Cepoi et al. 2020). Many studies hypothesized that the formation of reactive oxygen species (ROS)(Djearmane et al. 2020; Suman et al. 2015; Xia et al. 2015) or mechanical damage to the cells produced by NPs was the cause of the reduction of cell development (Castro-Bugallo et al. 2014). Some factors cause the reduction in cell growth, for example, metal ion release (Lee and An 2013; Aravantinou et al. 2015; Suman et al. 2015), the effect of light shading (Sadiq et al. 2011), synergistic effects (Manzo et al. 2013) and also contact with the culture medium (Manier et al. 2013). One of the causes of growth inhibition is the degradation of cell membranes caused by exposure to NPs, which results in the unregulated release and absorption of electrolytes and consequently affect the photosynthetic system and the production of macronutrients (Anusha et al. 2017). The growth rate of microalgae *H. pluvialis*

was affected when the metal ions interacted with the functional group of the microalgae surface (Balaji et al. 2014).

4.1 Limitations and moving forward

The current study did not report on the influence of TiO₂ NPs on the nutritional properties of *H. pluvialis*, including macromolecules and pigments. In the future, research can be performed to ascertain the impact of TiO₂ NPs on the nutritional properties of *H. pluvialis*. Further in-depth analysis is deemed essential to enhance the knowledge about the adverse effects of MNPs in aquatic environments that are used for commercial growth and cultivation of microalgae. It is also necessary to further create public awareness of using nanotechnologies to regulate commercial products that include nanomaterials in their production, as they may impede the ecological imbalance, directly and indirectly deteriorating human wellness. Furthermore, genomic studies can be carried out to analyze the impact of NPs on the synthesis of macromolecules and pigments.

Conclusion

To conclude, exposure of *H. pluvialis* to TiO₂ NPs resulted in a concentration and time-dependent buildup of NPs in the microalgae cells, leading to detrimental effects on the algal cells and biomass and severely damaging the cell surfaces and interiors. The findings of this research can assist in developing methods to detect TiO₂ NP contamination in *H. pluvialis*, enabling the production of high-quality nutritional supplements with uncompromised nutritional properties. Failure to do so may result in the consumption of TiO₂ NP-contaminated *H. pluvialis* supplements, which may not provide the intended nutritional benefits and may even pose health risks.

Acknowledgement

The authors acknowledge the financial support provided through the UTAR Research Fund 2020, [Project no.:IPSR/RMC/UTARRF/2020-C1/A05], by Universiti Tunku Abdul Rahman, Malaysia.

Conflict of Interest

The authors declare that they have no conflicts of interest.

References

- Anusha, L., Chingambam, S.D., Sibi, G. (2017). Inhibition Effects of Cobalt Nano Particles Against Fresh Water Algal Blooms Caused by *Microcystis* and *Oscillatoria*. *American Journal of Applied Scientific Research*, 3 (4), 26-32.
- Aravantinou, A. F., Tsarpali, V., Dailianis, S., & Manariotis, I. D. (2015). Effect of cultivation media on the toxicity of ZnO

- nanoparticles to freshwater and marine microalgae. *Ecotoxicology and Environmental Safety*, 114, 109–116. <https://doi.org/10.1016/j.ecoenv.2015.01.016>
- Balaji, S., Kalaivani, T., & Rajasekaran, C. (2014). Biosorption of Zinc and Nickel and Its Effect on Growth of Different *Spirulina* Strains: Biosorption Potentials of *Spirulina* Strains. *CLEAN - Soil, Air, Water*, 42(4), 507–512. <https://doi.org/10.1002/clen.201200340>
- Bameri, L., Sourinejad, I., Ghasemi, Z., & Fazelian, N. (2022). Toxicity of TiO₂ nanoparticles to the marine microalga *Chaetoceros muelleri* Lemmermann, 1898 under long-term exposure. *Environmental Science and Pollution Research*, 29, 30427–30440. <https://doi.org/10.1007/s11356-021-17870-z>
- Banerjee, A., & Roychoudhury, A. (2019). Explicating the cross-talks between nanoparticles, signaling pathways and nutrient homeostasis during environmental stresses and xenobiotic toxicity for sustainable cultivation of cereals. *Chemosphere*, 286(3), 131827. <https://doi.org/10.1016/j.chemosphere.2021.131827>
- Castro-Bugallo, A., González-Fernández, Á., Guisande, C., & Barreiro, A. (2014). Comparative Responses to Metal Oxide Nanoparticles in Marine Phytoplankton. *Archives of Environmental Contamination and Toxicology*, 67(4), 483–493. <https://doi.org/10.1007/s00244-014-0044-4>
- Cepoi, L., Zinicovscaia, I., Rudi, L., Chiriac, T., Rotari, I., Turchenko, V., & Djur, S. (2020). Effects of PEG-Coated Silver and Gold Nanoparticles on *Spirulina platensis* Biomass during Its Growth in a Closed System. *Coatings*, 10(8), 717. <https://doi.org/10.3390/coatings10080717>
- Comotto, M., Casazza, A. A., Aliakbarian, B., Caratto, V., Ferretti, M., & Perego, P. (2014). Influence of TiO₂ nanoparticles on growth and phenolic compounds production in photosynthetic microorganisms. *The Scientific World Journal*, 2014, 961437. <https://doi.org/10.1155/2014/961437>
- Djearamane, S., Lim, Y. M., Wong, L. S., & Lee, P. F. (2018). Cytotoxic effects of zinc oxide nanoparticles on cyanobacterium *Spirulina (Arthrospira) platensis*. *Peer J*, 6, e4682. <https://doi.org/10.7717/peerj.4682>
- Djearamane, S., Lim, Y. M., Wong, L. S., & Lee, P. F. (2019). Cellular accumulation and cytotoxic effects of zinc oxide nanoparticles in microalga *Haematococcus pluvialis*. *PeerJ*, 7, e7582. <https://doi.org/10.7717/peerj.7582>
- Djearamane, S., Ling Shing, W., Yang Mooi, L., & Lee, P. F. (2020). Oxidative stress effects of zinc oxide nanoparticles on fresh water microalga *Haematococcus pluvialis*. *Ecology, Environment and Conservation*, 26, 2020–2663.
- Dmytryk, A., Saeid, A., & Chojnacka, K. (2014). Biosorption of microelements by *Spirulina*: towards technology of mineral feed supplements. *The Scientific World Journal*, 2014, 356328. <https://doi.org/10.1155/2014/356328>
- Dong, S., Huang, Y., Zhang, R., Wang, S., & Liu, Y. (2014). Four Different Methods Comparison for Extraction of Astaxanthin from Green Alga *Haematococcus pluvialis*. *The Scientific World Journal*, 2014, 1–7. <https://doi.org/10.1155/2014/694305>
- Dong, S., Huang, Y., Zhang, R., Wang, S., & Liu, Y. (2014). Four Different Methods Comparison for Extraction of Astaxanthin from Green Alga *Haematococcus pluvialis*. *The Scientific World Journal*, 2014, 1–7. <https://doi.org/10.1155/2014/694305>
- Dore J.E., Cysewski G.R. (2003) Cyanotech Corporation *Haematococcus* Algae Meal as a Source of Natural Astaxanthin for Aquaculture Feeds. Retrieved from <http://www.ruscom.com/cyan/web02/pdfs/naturrose/nrtl09.pdf>
- Gupta, A., Vidyarthi, S.R., & Sankaramakrishnan, N. (2014). Enhanced sorption of mercury from compact fluorescent bulbs and contaminated water streams using functionalized multiwalled carbon nanotubes. *Journal of Hazardous Materials*, 274, 132–144. DOI: 10.1016/j.jhazmat.2014.03.020
- Harker, M., Tsavalos, A. J., & Young, A. J. (1996). Factors responsible for astaxanthin formation in the Chlorophyte *Haematococcus pluvialis*. *Bioresource Technology*, 55(3), 207–214. [https://doi.org/10.1016/0960-8524\(95\)00002-X](https://doi.org/10.1016/0960-8524(95)00002-X)
- Harker, M., Tsavalos, A. J., & Young, A. J. (1996). Factors responsible for astaxanthin formation in the Chlorophyte *Haematococcus pluvialis*. *Bioresource Technology*, 55(3), 207–214. [https://doi.org/10.1016/0960-8524\(95\)00002-X](https://doi.org/10.1016/0960-8524(95)00002-X)
- Hazeem, L.J., Bououdina, M., Rashdan, S., Brunet, L., Slomianny, C., & Boukherroub, R. (2016). Cumulative effect of zinc oxide and titanium oxide nanoparticles on growth and chlorophyll a content of *Picochlorum* sp. *Environmental Science and Pollution Research*, 23(3), 2821–2830 DOI 10.1007/s11356-015-5493-4.
- Hong, M. E., Choi, Y. Y., & Sim, S. J. (2016). Effect of red cyst cell inoculation and iron(II) supplementation on autotrophic astaxanthin production by *Haematococcus pluvialis* under outdoor summer conditions. *Journal of biotechnology*, 218, 25–33. <https://doi.org/10.1016/j.jbiotec.2015.11.019>
- Iswarya, V., Bhuvaneshwari, M., Alex, S. A., Iyer, S., Chaudhuri, G., Chandrasekaran, P. T., Bhalerao, G. M., Chakravarty, S., Raichur, A. M., Chandrasekaran, N., & Mukherjee, A. (2015). Combined toxicity of two crystalline phases (anatase and rutile) of Titania nanoparticles towards freshwater microalgae: *Chlorella* sp.

- Aquatic Toxicology*, 161, 154–169. <https://doi.org/10.1016/j.aquatox.2015.02.006>
- Lee, W.M., & An, Y.J. (2013). Effects of zinc oxide and titanium dioxide nanoparticles on green algae under visible, UVA, and UVB irradiations: No evidence of enhanced algal toxicity under UV pre-irradiation. *Chemosphere*, 91(4), 536–544. <https://doi.org/10.1016/j.chemosphere.2012.12.033>
- Manier, N., Bado-Nilles, A., Delalain, P., Aguerre-Chariol, O., & Pandard, P. (2013). Ecotoxicity of non-aged and aged CeO₂ nanomaterials towards freshwater microalgae. *Environmental pollution (Barking, Essex : 1987)*, 180, 63–70. <https://doi.org/10.1016/j.envpol.2013.04.040>
- Manzo, S., Miglietta, M. L., Rametta, G., Buono, S., & Di Francia, G. (2013). Toxic effects of ZnO nanoparticles towards marine algae *Dunaliella tertiolecta*. *The Science of the total environment*, 445–446, 371–376. <https://doi.org/10.1016/j.scitotenv.2012.12.051>
- Matos, J., Cardoso, C., Bandarra, N. M., & Afonso, C. (2017). Microalgae as healthy ingredients for functional food: a review. *Food & function*, 8(8), 2672–2685. <https://doi.org/10.1039/c7fo00409e>
- Metzler, D.M., Li, M., Erdem, A., & Huang, C.P. (2011). Responses of algae to photocatalytic nano-TiO₂ particles with an emphasis on the effect of particle size. *Chemical Engineering Journal*, 170, 538–546.
- Navarro, E., Piccapietra, F., Wagner, B., Marconi, F., Kaegi, R., Odzak, N., Sigg, L., & Behra, R. (2008). Toxicity of silver nanoparticles to *Chlamydomonas reinhardtii*. *Environmental science & technology*, 42(23), 8959–8964. <https://doi.org/10.1021/es801785m>
- Sadiq, I. M., Pakrashi, S., Chandrasekaran, N., & Mukherjee, A. (2011). Studies on toxicity of aluminum oxide (Al₂O₃) nanoparticles to microalgae species: *Scenedesmus* sp. and *Chlorella* sp. *Journal of Nanoparticle Research*, 13(8), 3287–3299. <https://doi.org/10.1007/s11051-0110243-0>
- Sendra, M., Yeste, M. P., Gatica, J. M., Moreno-Garrido, I., & Blasco, J. (2017). Direct and indirect effects of silver nanoparticles on freshwater and marine microalgae (*Chlamydomonas reinhardtii* and *Phaeodactylum tricornutum*). *Chemosphere*, 179, 279–289. <https://doi.org/10.1016/j.chemosphere.2017.03.123>
- Suman, T. Y., Radhika Rajasree, S. R., & Kirubakaran, R. (2015). Evaluation of zinc oxide nanoparticles toxicity on marine algae *Chlorella vulgaris* through flow cytometric, cytotoxicity and oxidative stress analysis. *Ecotoxicology and Environmental Safety*, 113, 23–30. <https://doi.org/10.1016/j.ecoenv.2014.11.015>
- Xia, B., Chen, B., Sun, X., Qu, K., Ma, F., & Du, M. (2015). Interaction of TiO₂ nanoparticles with the marine microalga *Nitzschia closterium*: Growth inhibition, oxidative stress and internalization. *Science of The Total Environment*, 508, 525–533. <https://doi.org/10.1016/j.scitotenv.2014.11.066>
- Ziental, D., Czarczynska-Goslinska, B., Mlynarczyk, D. T., Glowacka-Sobotta, A., Stanis, B., Goslinski, T., & Sobotta, L. (2020). Titanium Dioxide Nanoparticles: Prospects and Applications in Medicine. *Nanomaterials*, 10(2), 387. <https://doi.org/10.3390/nano10020387>



Journal of Experimental Biology and Agricultural Sciences

<http://www.jebas.org>

ISSN No. 2320 – 8694

 Morphology and DNA marker for distinguishing *Paphiopedilum hangianum* and *Paphiopedilum emersonii* from Vietnam

 Yen Nguyen Thi Hai^{1*} , Quang Ngo Xuan^{2,4} , Trong Nguyen Dinh³ ,
 Phat Do Tien^{3,4} , Mau Chu Hoang⁵ 
¹TNU-University of Sciences, Tan Thinh Ward, Thai Nguyen City, Vietnam²VAST-Institute of Tropical Biology, 85, Tran Quoc Toan, Dist.3, Ho Chi Minh City, Vietnam³VAST-Institute of Biotechnology, 18, Hoang Quoc Viet, Cau Giay, Ha Noi, Vietnam⁴VAST - Graduate University of Sciences and Technology, 18 Hoang Quoc Viet, Cau Giay, Ha Noi, Vietnam⁵TNU - University of Education, Quang Trung Ward, Thai Nguyen City, Vietnam

Received – December 11, 2022; Revision – March 25, 2023; Accepted – April 17, 2023

Available Online – April 30, 2023

DOI: [http://dx.doi.org/10.18006/2023.11\(2\).423.435](http://dx.doi.org/10.18006/2023.11(2).423.435)

KEYWORDS

DNA barcoding

Identification

Molecular

Northern Vietnam

Orchidaceae

ABSTRACT

Genus *Paphiopedilum* has species having lovely flowers which are incredibly attractive to everyone. Their ornamental and commercial value caused over-collection and illegal poaching and trade. Due to these reasons, nowadays, the Venus slipper orchids are facing to deplete in nature. Therefore, it is important to consider these species conservation. Mainly, it is necessary to prioritize the identification and phylogenetic analysis methods of the genus *Paphiopedilum* which includes many species with similar morphological characteristics. Consequently, it isn't easy to distinguish the identical species of this genus when the plants are young or not yet fully flowering. Therefore, this study aimed to distinguish two *Paphiopedilum* species, i.e. *P. hangianum* and *P. emersonii*, which have similar morphological characteristics, through comparative morphological analysis and differences in DNA barcoding sequences. To solve the problem associated with species identifications, a morphological comparison table was created with the four DNA sequence markers *matK*, *rbcL*, *rpoC1* and *trnH-psbA*. The results of the morphological analysis showed that *P. hangianum* and *P. emersonii* are significantly different from each other in the flower's characteristics. While the difference in leaf morphology of both selected species is found very little, it is also distinguishable upon careful comparison. Moreover, the DNA barcoding indicator gave accurate and rapid distinctions between the two species, even when the plants are young or without flowers. Furthermore, this DNA barcoding can establish an evolutionary

* Corresponding author

E-mail: yennth@tus.edu.vn (Yen Nguyen Thi Hai)

Peer review under responsibility of Journal of Experimental Biology and Agricultural Sciences.

 Production and Hosting by Horizon Publisher India [HPI]
 (<http://www.horizonpublisherindia.in/>).
 All rights reserved.

 All the articles published by [Journal of Experimental Biology and Agricultural Sciences](#) are licensed under a [Creative Commons Attribution-NonCommercial 4.0 International License](#) Based on a work at www.jebas.org.


relationship between the two selected species and the other species of the genus *Paphiopedilum*. The results of this study also suggested that the indicator *trnH-psbA* is a suitable marker for distinguishing these two species and can be applied for the phylogenetic analysis of the genus *Paphiopedilum* in Vietnam.

1 Introduction

Genus *Paphiopedilum* Pfitzer (Venus's slipper) belongs to the family Orchidaceae, which can be easily recognized by its unique flower structure with a deformed, sac-like central petal called a com lips. Venus's Slipper orchids are a small but prominent branch of the Orchid family, representing one of the most specialized lines of insect-pollinated flowering plants. Genus *Paphiopedilum* is native to southeast Asia (Myanmar, Thailand), northern India, southern China and New Guinea, with more than 80 species distributed worldwide (Braem et al. 1998; Braem et al. 1999; Cribb 1998, Koopowitz 2008). Vietnam has the world's most considerable diversity of *Paphiopedilum* genera. Averyanov et al. (2004) listed 22 species of the *Paphiopedilum* genus, including four natural hybrids of Vietnam.

Based on the initial morphology, the genus *Paphiopedilum* has been divided into three subgenera *Parvisepalum*, *Brachypetalum*, and *Paphiopedilum*. Subgenus *Paphiopedilum* is a heterogeneous group with the highest number of species. Meanwhile, the subgenus *Paphiopedilum* is divided into five sections: *Paphiopedilum*, *Barbata*, *Pardalopetalum*, *Cochlopetalum* and *Coryopetalum* (Averyanov et al. 2004). Later, the species *P. canhii* was discovered and added to a section *Pygmaea* under subgenus *Paphiopedilum* due to the interbreeding characteristics between subgenus (Gorniak et al. 2014) or even a new subgenus *Megastaminodium* to contain this species (Braem and Gruss 2012).

Two species of genus *Paphiopedilum*, i.e., *P. hangianum* (Perner and Gruss 1999) and *P. emersonii* (Koop and Cribb 1986), are endemic to Vietnam and distributed only in some provincial mountainous areas such as Thai Nguyen, Bac Kan, Tuyen Quang, and Ha Giang (Averyanov et al. 2004). These species give the most beautiful flowers and are very popular not only in Vietnam but also in many countries around the world. Morphologically these two species could not be distinguished without flowers (Averyanov et al. 2004; Dang et al. 2017; Vu et al. 2019).

Traditional methods based on morphological characteristics are not found suitable for the identification of these two species before flowering; therefore, a combination of traditional and modern molecular markers-based techniques like DNA barcodes can be an alternative to this problem (Xu et al. 2014; Vu et al. 2019; Bui et al. 2022, Cahyaningsih et al. 2022, Worthy et al. 2022). DNA barcoding molecular identification method provides accurate and reliable data to identify target species with the help of selected

molecular markers by passing a specific DNA region. Further, the selection of appropriate marker gene sequences will increase the efficiency of species identification. The nuclear marker *ITS* is the most widely used molecular marker (Hollingsworth et al. 2009; Singh et al. 2012; Wu et al. 2012; Yukawa et al. 2013; Xu et al. 2015; Veldman et al. 2018; Tran et al. 2018). However, the chloroplast genome in plants has many features relevant for DNA markers, either in coding sequences (such as *rbcL* and *matK*) or intergenic regions (such as *trnH-psbA*). The molecular marker *trnH-psbA* has been widely used for identification purposes in previous studies, with species resolution up to 100% across a wide range of 72 plant genera (Kress and Erickson 2007) or over a small range of species within a genus (Parveen et al. 2012; Bolson et al. 2015). In addition, the combination of multiple loci of the *trnH-psbA*, *rpoB*, *rpoCl*, *rbcL*, and *matK* has been recommended for taxonomy and phylogenetic studies (Gorniak et al. 2014; Vu et al. 2019).

Furthermore, for the genus *Paphiopedilum*, the first barcode-based species identification study was conducted in India by Parveen et al. (2012). This study obtained excellent results with five barcodes gene *rpoB*, *rpoCl*, *rbcL*, *matK*, and *ITS*. Further, Gorniak et al. (2014) combined morphological characteristics, cytological analysis, and DNA barcode gene markers to identify species *P. canhii*, which was previously controversial in the taxonomic system because of its characteristics of interference between different genera. Additionally, studies on DNA barcoding with several markers such as *ITS*, *LEAFY*, *ACO*, *matK*, *trnL*, *rpoB*, *rpoCl*, and *trnH-psbA* to identify genus *Paphiopedilum* were conducted, especially in Vietnam (Trung et al. 2013; Vu et al. 2020).

Therefore, this study aims to observe, analyze and describe morphological characteristics of the stem, roots, leaves, and flowers to identify two orchid species, i.e., *P. hangianum* and *P. emersonii*. Our objectives are also to provide new insight into the molecular classification of these two species through the chloroplast and nuclear DNA barcode sequences and further to distinguish species *P. hangianum* from *P. emersonii* by using DNA barcode combined with morphological characterization.

2 Materials and Methods

2.1 Collection of plant materials

A total of 5 individuals of each species, i.e., *P. hangianum* and *P. emersonii*, were collected by a field trip in 2017 from four northern

provinces, i.e., Thai Nguyen, Bac Kan, Ha Giang and Tuyen Quang of Viet Nam (Table 1; Figure 1) and cultivated under the greenhouse of the Faculty of Biotechnology, Thai Nguyen University of Sciences, Viet Nam. So far, we have obtained three flower samples. The young leaves of each species were collected into Fancol tubes and preserved at a temperature of 4°C for DNA extraction.

Table 1 Codes, coordinates and addresses of samples collection in 4 provinces of Northern Vietnam

Species	Codes	Coordinates	Receiving place/coordinate	Characteristic
<i>P. ermesonii</i>	HH01	Lat: 21.75729 Long: 105.8877	Mo Ba, Tan Long, Dong Hy Thai Nguyen –Viet Nam	have flower
	HH02	Lat: 22.52493 Long: 105.6295	Cao Tan, Pac Nam, Bac Kan – Viet Nam	adulthood
	HH03	Lat: 22.52493 Long: 105.6400	Cao Tan, Pac Nam, Bac Kan – Viet Nam	have flower
	HH04	Lat: 21.75729 Long: 105.8999	Lan Quan, Tan long, Dong Hy, Thai nguyen – Viet Nam	have flower
	HH05	Lat: 21.76717 Long: 105.96411	Khuon Muc, Cuc Duong, Dong Hy, Thai Nguyen – Viet Nam	nurseling
<i>P. hangianum</i>	HA01	Lat: 21.966667 Long:106.05	Ban Buoc, Phuc Yen, Lam Binh, Tuyen Quang, Vietnam	nurseling
	HA02	Lat: 21.96666 Long: 106.045	Ban Buoc, Phuc Yen, Lam Binh, Tuyen Quang, Vietnam	have flower
	HA03	Lat: 21.9711 Long: 106.02	Ban Buoc, Phuc Yen, Lam Binh, Tuyen Quang, Vietnam	have flower
	HA04	Lat: 22.6935 Long: 105.0908	Linh Ho, Kim Thach, Vj Xuyên, Ha Giang, Vietnam	have flower
	HA05	Lat: 22.6826 Long: 105.2493	Thuong Tan, Bac Me, Ha Giang, Vietnam	adulthood

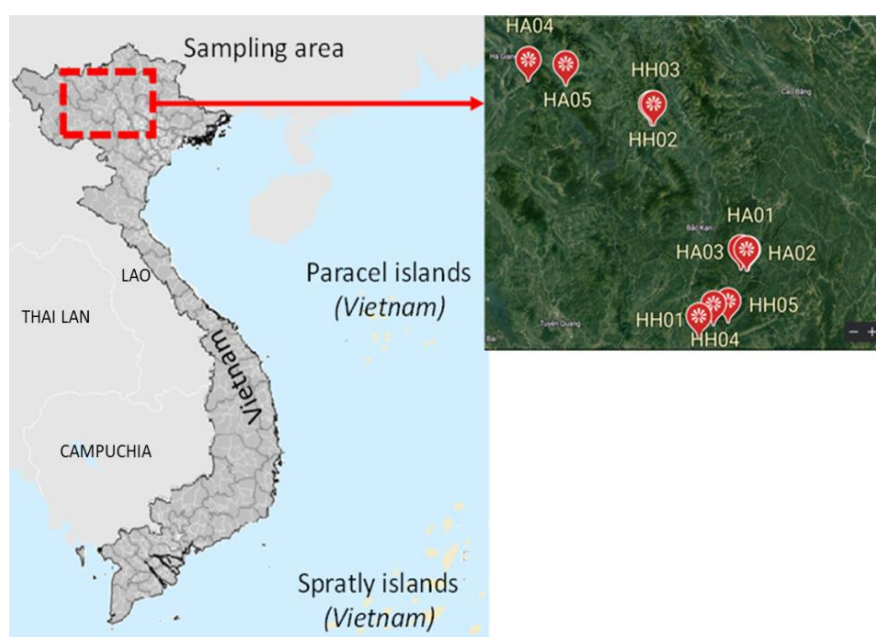


Figure 1 Sampling map in some provinces of Northern Vietnam

2.2 Morphological identification

The plant materials were directly observed, and the characteristics of each plant part were described in detail to compare with existing documents and identification keys (Koopowitz and Cribb 1986; Perner and Gruss 1999; Averyanov et al. 2004, Koopowitz 2008).

2.3 DNA extraction, amplification

Total DNA was extracted using the modified CTAB method to match the experimental conditions in Vietnam (Collins and Symons 1992). Leaf samples were ground in liquid nitrogen, supplemented with separation buffer and incubated at 65°C for two hours. A solution of chloroform: isoamyl alcohol (24:1) was added to the tube containing the separation buffer and the sample in a 1:1 volumetric ratio to separate the DNA. The sample was centrifuged

at 13000 Rpm/g for 10 min, the supernatant was transferred to a new tube, and isopropanol (1:1 v/v sample: isopropanol) was added to precipitate the DNA. Specific primer pairs were used to multiply the gene fragments. Primers used in PCR for the amplification: *matK*, *trnH-psbA*, *rpoCl*, *rbcL* (Tate and Simpson, 2003, Parveen et al. 2012). The detailed sequences of the used primers are shown in Table 2. The PCR reaction components and heat cycle multiplying genes are shown in Table 3 and 4.

2.4 Sequencing, alignment, and phylogenetic analyses

PCR products were purified for sequencing on an ABI PRISM 3100 Avant Genetic Analyzer automatic nucleotide sequencer. Sequences were blasted in NCBI and processed with Snapgene and BioEdit software, and gene sequence-based taxonomy was built with MEGA X software. DNA sequences were imported to MEGA

Table 2 Primer sequences for the DNA barcode gene

Primers	Nucleotide sequence	Annealing temperature	Expected sizes	Reference
<i>trnH-psbA</i>	F,5'-GTTATGCATGAACGTAATTGCTC-3'	52	600 bp	Tate and Simpson (2003)
	R,5'-CGCGCATGGTGGATTCACAATCC-3'			
<i>matK</i>	F,5'-CGATCTATTCATTCAATATTC-3'	52	900 bp	Parveen et al. (2012)
	R,5'-TCTAGCACACGAAAGTCGAAAGT-3'			
<i>rpoCl</i>	F,5'-GTGGATACACTTCTTGATAATGG-3'	52	600 bp	Parveen et al. (2012)
	R,5'-CCATAAGCATATCTTGAGTTGG-3'			
<i>rbcL</i>	F,5'-ATGTCACCACAAACAGAAAC-3'	52	750 bp	Parveen et al. (2012)
	R,5'-TCGCATGTACCTGCAGTAGC-3'			

Table 3 PCR reaction mixture volume and concentrations for all barcodes

Components	Barcode locus			
	<i>rbcL</i>	<i>MatK</i>	<i>rpoCl</i>	<i>trnH-psbA</i>
PCR Master Mix (2X)	12.5µL (×1)	12.5 µL (×1)	12.5 µL (×1)	12.5 µL (×1)
Forward & reverse primers	1 µL (10µM)	1 µL (10 µM)	1 µL (10µM)	1 µL (10µM)
Distilled water	4.5	4.5	4.5	4.5
DNA (50 µg/µl)	1 µL	1 µL	1 µL	1 µL

Table 4 PCR cycling profile for each barcode locus

Components	Barcode locus			
	<i>rbcL</i>	<i>MatK</i>	<i>rpoCl</i>	<i>trnH-psbA</i>
Initial denaturation	94°C, 5 min	94°C, 5 min	94°C, 5 min	94°C, 5 min
Denaturation	94°C, 45s	94°C, 45s	94°C, 45s	94°C, 45s
Annealing	54°C, 30s	52°C, 30s	54°C, 30s	52°C, 30s
Extension	72°C, 50s	72°C, 40s	72°C, 60s	72°C, 50s
Final extension	72°C, 7 min	72°C, 7 min	72°C, 7 min	72°C, 7 min

X for alignment with sequences from the GenBank database with the addition of the outgroup species *P.hangianum* and *P.emersonii*. Maximum Likelihood analyses with 1000 bootstrap replications and the Tamura-Nei model (1993) of sequence evolution were used to construct a phylogenetic tree (Tamura and Nei 1993).

3 Results

3.1 Morphological characteristics of two *Paphiopedilum* species

Botanical characteristics (stems, roots, flowers, etc.) of the collected orchid samples were recorded by direct observation and the results are presented in Table 5 and Figures 2 & 3. The results of the morphological analysis showed that both *P. hangianum* and *P. emersonii* were very similar in shape and size in the absence of

flowers. The leaves size, color and shape are very similar without much difference. Here are a few subtle differences that can help differentiate these two species even without flowers. Both *P. hangianum* and *P. emersonii* stems have stacked leaves; however, the leaves of *P. hangianum* are closely overlapping to form a regular V, and the leaves extend straight up. In contrast, *P. emersonii* leaves are somewhat looser; the leaf neck is wide when holding the plant straight in hand, and the leaves tend to hang horizontally. The *P. hangianum* leaves are dark green, while *P. emersonii* leaves are slightly lighter and more glossy. The *P. hangianum* leaf margins are somewhat wavy, making the leaves slightly warped above and below. However, these distinct characteristics were only observed when the plants matured and grew under the same conditions. These distinguishing characteristics are not apparent with young trees or trees collected from the forest. Flowers are the main identifying

Table 5 Diagnostic morphological characters of *P. hangianum* and its closest *P. emersonii*

Characters	<i>P. hangianum</i>	<i>P. emersonii</i>
Stem		
Height	Less than 10 cm	Less than 10 cm
Arrangement of Leaves	Two rows, overlapping close,	Two rows, overlapping loose,
Leaves		
Number per plant	6 to 8	6 to 8
Apex	Obtuse	Obtuse
Shape	Oblong	Oblong
Length (cm)	More than 20cm	More than 20cm
Width (cm)	Medium 3 to 6 cm	Medium 3 to 6 cm
Upper surface colour	Green, Light mixed (near uniform)	Light green, Light mixed (near uniform)
Lower surface colour	Green	Green
Inflorescence and flower		
Peduncle length	More than 20 cm	More than 20 cm
Floral bract	Green colour and broadly lanceolate	Green, white colour and broadly lanceolate
Flower width in front view	8-9 cm in average, horizontal egg shape	7-8 cm in average, circle shape
Dorsal sepal	6-6,5×4-4,2cm, dorsal sepal with oval shape, convex curvature, entire margin and yellow dominant	4-4, 5× 2, 8-3cm, dorsal sepal with oblong oval shape, light undulate curvature, undulate margin and white dominant
Synsepalum	5, 5-6× 5-5,5cm, synsepalum with sub-orbicular shape, obtuse apex and yellow dominant. Synsepalum yellow pattern inside	5-5, 2 × 4-4, 2cm, synsepalum with sub-orbicular shape, obtuse apex and yellow dominant. Synsepalum white with a yellow line on synsepalum length, absent pattern inside
Petal	7-7, 5×4, 2-4, 5cm, Petal with oval with slightly round tip shape, obtuse apex	5-5, 2×4-4,2cm, Petal with sub-orbicular shape, obtuse apex
Lip	4-4, 2×2-2.2 cm, pale yellow, glossy, the lower part is. The inside has many small dots about 1mm in size, reddish brown.	3, 2-3.5 ×1, 6-2 cm, the outer surface is not flat but rough, with two lobes. The inner surface has many prominent dark brown dots.
Staminode	1.2 × 0.8 cm, carried dark yellow anther with a brown border, about 2 mm in size. The stigma is large, glossy yellow, oval to ovoid-elliptical, about 6mm in size.	1.5× 0.8 cm, carried pale yellow anthers, about 2 mm in size. The stigma is large, glossy yellow, oval to ovoid-elliptic, about 6 mm in size.

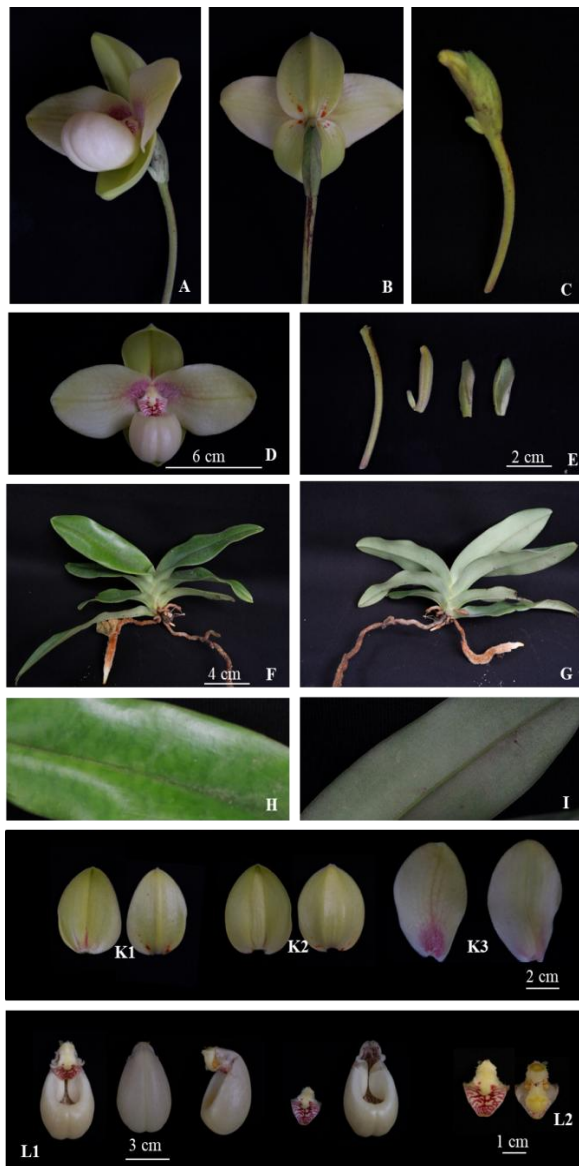


Figure 2 Morphology of stems, leaves and flower structure of *P. hangianum* A-D. Flower; E. Peduncle, ovary and Floral bract; F-I. Stem and leaves; K1. Dorsal sepal; K2. Synsepalum; K3. Petal; L1. Lip; L2. Staminode

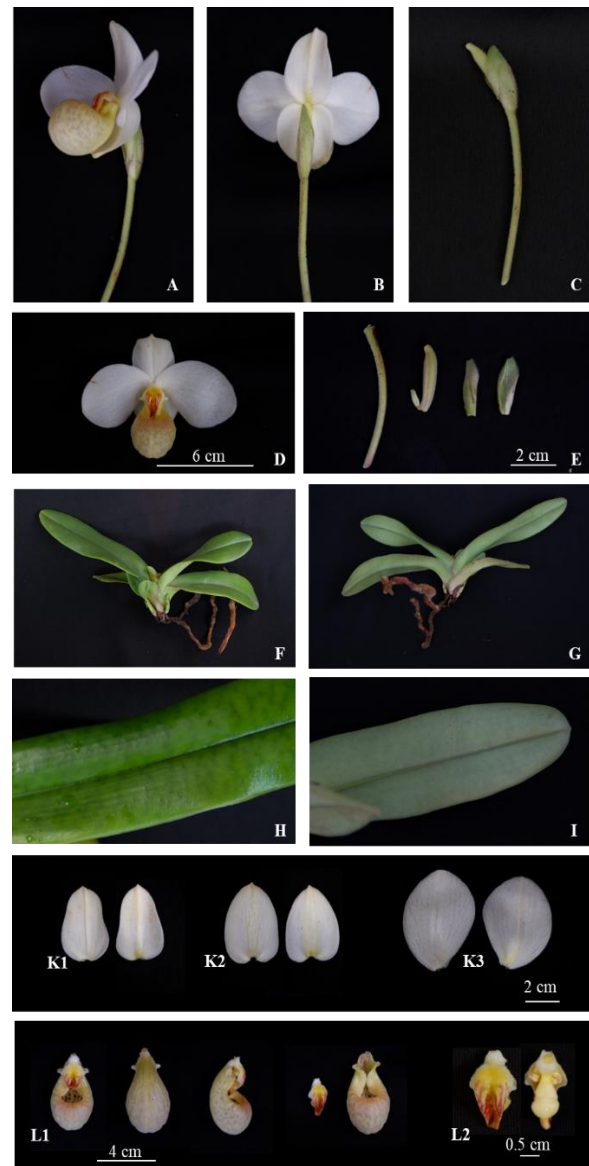


Figure 3 Morphology of stems, leaves and flower structure of *P. emersonii* A-D. Flower; E. Peduncle, ovary and Floral bract; F-I. Stermand leaves; K1. Dorsal sepal; K2. Synsepalum; K3. Petal; L1. Lip; L2. Staminode

feature of plants; although the leaf morphology of the two studied *Paphiopedilum* species are highly similar, their flowers are entirely different. The detailed descriptions of both species' morphological characteristics have been presented in Table 5 and Figures 2 & 3.

3.2 DNA barcode analysis results

Total DNA was extracted from the leaves of the two studied species. The obtained OD value of the isolated DNA was 260/280 which is within the allowable limits (no results expressed). The electrophoresis results of PCR products of *matK*, *rbcL*, *rpoC1* and

trnH-psbA genes obtained a specific DNA segment; the size is consistent with the theoretical calculation (do not represent the results). PCR products were used for sequencing by the Sanger method on the ABI PRISM®3100 Avant Genetic Analyzer. The gene sequences were analyzed by the BLAST tool. The tree classification scheme was built by comparing the DNA sequence of the study sample with the common species of the genus *Paphiopedilum* in Vietnam, which was published on GenBank using MegaX software. The maximum Likelihood Method was used for evolutionary analysis. Evolutionary history is based on the Maximum Likelihood method and the Tamura-Nei18 model. The

classification tree based on the most significant likelihood coefficient (-1102.40) is selected and presented.

3.2.1 Differentiation of two *Paphiopedilum* species based on DNA barcode sequence

The *rbcL* sequence obtained from two studied species has a length of 709 nucleotides, which is a highly conserved sequence. Blast results on NCBI coverage (query coverage value) showed 97 -

99% similarities with species of genus *Paphiopedilum* with a similarity coefficient of 99.15% - 99.85%, especially species *P. emersonii* (code NC_053544.1 on GenBank) has 99.86% similarity (99% coverage). Analysis of the *rbcL* sequence similarity of the two studied species with other species of genus *Paphiopedilum* showed that this indicator has a high degree of conservatism, and the selected two species have no genetic difference in the *rbcL* gene. In contrast, other species' differences range from 0.00 - 0.77 (Table 6).

Table 6 Code of gene sequences representing the genus *Paphiopedilum* used for genetic relationship analysis

	GenBank accessionnumber			
	<i>matK</i>	<i>rpoCl</i>	<i>rbcL</i>	<i>trnH-psbA</i>
Section <i>Paphiopedilum</i> – Subgenus <i>Paphiopedilum</i>				
<i>P. barbigerum</i>		MN153814.1		NC050870.1
<i>P. hirsutissimum</i>		NC050871.1	JN181466.1	NC050671.1
<i>P. gratrixianum</i>	MW284890.1			MW284890.1
<i>P. tranlienianum</i>	KX886262.1	MW794129.1		MW794129.1
<i>P. spicerianum</i>		NC052702.1	MT683624.1	
<i>P. henryum</i>	MK792666.1			
<i>P. helenae</i>	MK792663.1			
<i>P. coccineum</i>	MK792626.1			
Section <i>Pardalopetalum</i> Hallier f. & Pfitzer - Subgenus <i>Paphiopedilum</i>				
<i>P. dianthum</i>	MF983795.1	MF983795.1	MF983795.1	
<i>P. haynaldianum</i>			AB176547.1	
Section <i>Barbata</i> (Kraenzl.) V.A. Albert & Borge Pett. – Subgenus <i>Paphiopedilum</i>				
<i>P. purpuratum</i>		NC045279.1	NC045279.1	NC045279.1
<i>P. callosum</i>	KC692133.1			
<i>P. applotonianum</i>				JQ929367.1
Section <i>Parvisepalum</i> Aver. & Cribb – Subgenus <i>Parvisepalum</i> Karas. & Saito				
<i>P. micranthum</i>	NC045287.1	NC045276.1	NC045278.1	NC045278.1
<i>P. malipoense</i>	MK792675.1			JF796885.1
<i>P. delenatii</i>	NC045278.1	NC041309.1	NC041309.1	NC041309.1
<i>P. armeniacum</i>		LC085347.1	KT388109.1	LC085347.1
<i>P. vietnamense</i>	MK787425.1		JQ182212.1	EF156073.1
Section <i>Emersonianum</i> Aver. & Cribb - Subgenus <i>Parvisepalum</i> Karas. & Saito				
<i>P. emersonii</i>	MK792646.1			NC053544.1
	MK792647.1			
<i>P. hangianum</i>	KY966590.1			
	MK792652.1			
	MK792653.1			
	MK792656.1			
Subgenus <i>Brachypetalum</i> (Hallier) Pfitzer				
<i>P. concolor</i>	JQ929367.1			

The *rpoC1* sequence obtained from 2 studied species has a length of 586 nucleotides with high conservatism. Blast results on NCBI showed that the two studied species were closely related to 27 species of the genus *Paphiopedilum* (coverage reached over 97%), with similarity coefficients from 98.77% - 99.82%. The genetic similarity of the two studied species with other *Paphiopedilum* species in terms of the *rpoC1* sequence is also high. It is impossible to distinguish the two studied species by this indicator (Table 6).

The *matK* sequence obtained from the two studied species has a length of 857 nucleotides. The *matK-HaiHang* sequence blast obtained 100 sequences of species belonging to the *Paphiopedilum* genus. The highest similarity was 99.87% (MK792656.1 *P. hangianum*), and the lowest was 97.1% (NC_052702.1 *P. spicerianum*). Coverage reached 94 - 99%, the highest similarity was 100% (JQ182193.1 *P. delenatii*), and the lowest was 96.61% (MW528213.1 *P. parishii*). Analysis of the genetic similarity of the two studied species by *matK* indicator showed that the two species have high similarity (the coefficient of difference is only

0.006). The coefficient of difference for other species of the genus *Paphiopedilum* ranges from 0.006 - 1.04.

The *trnH-psbA* sequence obtained from the two studied species has a length of 608 nucleotides. Blast *trnH-psbA-HaiHang* obtained 100 sequences, including 91 sequences of species belonging to the genus *Paphiopedilum* (the remaining nine convergences belong to other genera, including seven species of *Phragmipedium*, one species of *Selenipedium* and one species of *Mixepedium*). Coverage ranged from 70 - 97%, the highest similarity was 99.32% (NC_045278.1 *P. micranthum*), and the lowest was 91.15% (FR851215.1 *M. xerophyticum*).

The result of Blast sequence *trnH-psbA - HaiHuong* is similar to the result of blast *trnH-psbA - HaiHang*; the Blast results were identical to 91 sequences of species belonging to the genus *Paphiopedilum* and nine sequences of species of other genera. Coverage reached 70% - 96%; the highest similarity was 99.83% (NC_053544.1 *P. emersonii*), and the lowest was 91.29% (FR851215.1 *M. xerophyticum*).

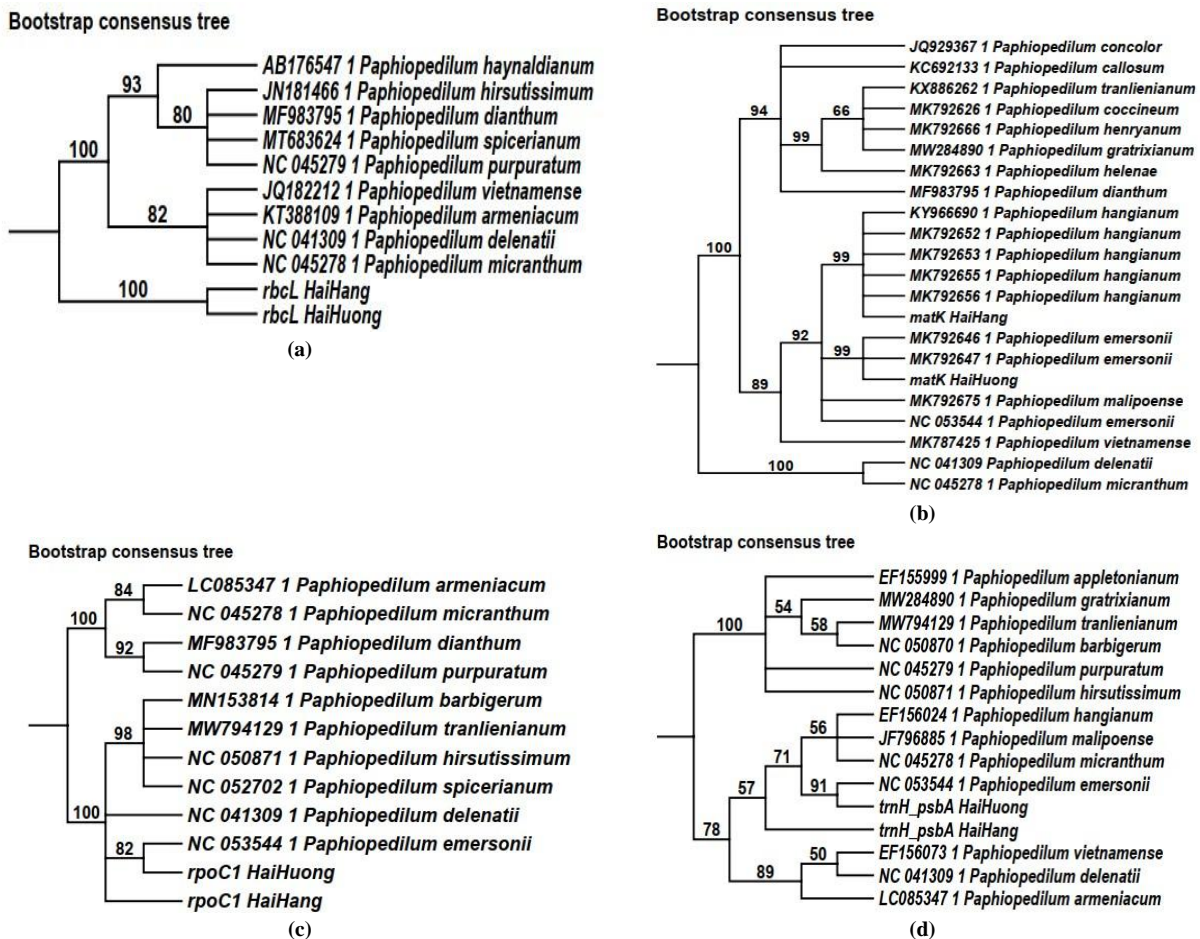


Figure 4 Molecular phylogenetic analysis of the (a) *rbcL*, (b) *matK*, (c) *rpoC1*, and (d) *trnH-psbA* marker. Bootstrap values are above the nodes of branches. The capital letters and numbers in parentheses are Accession numbers of *Paphiopedilum* species published on GenBank.

3.2.2 Phylogenetic analysis

The classification tree was established based on the *matK*, *rbcL*, *rpoC1*, and *trnH-psbA* markers showing that the two species *P. hangianum* and *P. emersonii* have a very high degree of closeness. Of the four sequence markers used, only the *trnH-psbA* marker could distinguish these two species. On the tree classification diagram, they are on different branches. The first clade contains only *trnH-psbA-HaiHang* while the second group has the sequence (*trnH-psbA-HaiHuong*, C_053544.1 *P. emersonii*, NC 045278.1 *P. micranthum*, and JF796885.1 *P. malipoense*) with a bootstrap coefficient of 81%. All remaining markers could not distinguish between the two studied species, although *matK* was proposed as the best barcode, with 100% resolution in the two previous *Paphiopedilum* studies (Cahyaningsih et al. 2022; Trung et al. 2013). In addition, *MatK* has been proposed as the standard barcode of many other plant species (Gruss et al. 2018).

Analysis of the taxonomic tree in ability to identify the species grouping found that the markers differed in correspondence with the morphological classification of the identified species. In markers *rbcL* and *rpoC1*, although the two studied species are separated from the other branches according to the morphological classification system, in the branches, there is a mix of species in different sections and subgenus. In the indicator *mat K* and *trnH-psbA*, the two studied species belong to the *Ermersonianum* section and the same clade as *P. malipoense* and *P. micranthum* belong to the *Parvisepalum* section. All remaining branches have species according to the correct section and subgenus as in the traditional taxonomy by morphology (Averyanov et al. 2004). *Matk* and *trnH-psbA* have good species resolution, which can be used as suitable indicators for the Differentiation and phylogenetic identification of the Venus slippers orchids.

The combination of DNA barcode markers is often used to identify plant species (Rajaram et al. 2019). Guo et al. (2016) recommend the combination of *matK* + *atpF-atpH* + ITS as a barcode for Venus slippers. However, the combination does not often bring the desired results. In this study, only *matK* and *trnH-psbA* markers could distinguish the selected two species (Figure 4).

4 Discussion

4.1 Morphological characteristics of two orchid species, *P. hangianum* and *P. emersonii*

Although classifying plants based on morphological characteristics is classical, but necessary and significantly supports the identification. Many plant identification keys have been successfully developed and used to identify various orchid species based on plant morphological structure. Most new species'

announcements for the Orchidaceae family are based on plant morphological descriptions, in which flower structure is the most objective criterion (Averyanov et al. 2010; Wang et al. 2017; Gruss et al. 2018, Zheng et al. 2020).

Paphiopedilum is the largest genus and most differentiated and studied in great detail in orchids. Averyanov et al. (2004) established a prominent taxonomic system for the *Paphiopedilum* in Vietnam. This classification system was later developed and used to recognize new species. In this taxonomy, *P. hangianum* and *P. emersonii* are grouped in a section that includes only these two species (Section *Emersonianum* Aver. & Cribb - Subgenus *Parvisepalum* Karas. & Saito). Vu et al. (2020) preliminary classified *Paphiopedilum* into two large groups based on leaf morphology. According to these authors, group 1 includes striated leaves, and Group 2 has leaf species without veins. Group 2 is again divided into group 2A, species with small, long soft leaves, and group 2B, which includes three large and stiff leaves. *P. hangianum* and *P. emersonii* belong to group 2B. After this detailed classification, these authors couldn't distinguish these two species and put them in the same group.

In this study, when directly and meticulously observing the two species over a long period of culture under the same growing conditions, we found that *P. hangianum* and *P. emersonii* have some small distinct features like leaf colour, the arrangement of leaves on the stem, the clarity of the veins on the leaves and the winding of the edges of the leaves, these features can be used to distinguish these two species including. These characteristics have not been described in the previous classification of *Paphiopedilum*. Therefore, these results are new milestones in identifying selected two species. In investigating the ecoregions of the two studied species, we found that, although they share many similarities, they are placed in the same subgenus and section in the taxonomic keys. Still, they are two species with different ecoregions in the wild and rarely encounter them in the same habitat. Similar findings were previously reported by Averyanov et al. (2004).

Although in the genus *Paphiopedilum*, many species are similar in leaf morphology (Averyanov et al. 2004; Vu et al. 2019), each species has distinct characteristics and flowers are used as the primary classification criterion. Venus orchids have a long growth cycle and short flowering time. Therefore, making it difficult to identify by normal morphology, good expertise is needed to distinguish similar species accurately. This makes it difficult to conserve and trade venus orchids, so developing an effective species identification method is necessary, in which a DNA barcode is a potential method. For a long time, using DNA barcodes to classify plants has gradually become a popular tool. Many studies on many plant species use different barcodes and recommend barcodes suitable for them.

Table 7 The distinguishes ability to distinguish two studied species

	<i>MatK</i>	<i>trnH-psbA</i>	<i>RpoC1</i>	<i>rbcL</i>	<i>trnH-psbA + matK</i>	<i>trnH-psbA + rpoC1</i>	<i>trnH-psbA + rbcL</i>	<i>trnH-psbA + matK + rpoC1</i>	<i>trnH-psbA + matK + rbcL</i>	<i>trnH-psbA + rbcL+rpoC1</i>	<i>matK + trnH-psbA+rpoC1 +rbcL</i>
Ability to distinguish	-	+	-	-	+	-	-	-	-	-	-

4.2 Insight into the molecular classification of *P. hangianum* and *P. emersonii*

For the genus Orchid, the study of species identification based on barcodes was first conducted by Parveen et al. (2012). Among the eight species of *Paphiopedilum* occurring in India, the study tested five potential barcodes (*rpoB*, *rpoC1*, *rbcL*, *matK*, and nrITS). The results showed that *matK*, with an average interspecies divergence value of 0.9%, yielded a species resolution of 100% of identified species, while ITS only reached 50%, so *matK* was recommended as a barcode to distinguish *Paphiopedilum* species (Table 7). So far, *matK* remains the proposed indicator in studying orchid subspecies. Worthy et al. (2022) also reported the excellent efficacy of the *matK* indicator (compared to the *rbcL* directive) in the barcode study of orchid sub-species and subgenus. In this study, *matK* proved effective in distinguishing two closely related species, *P. hangianum* and *P. emersonii*. Guo et al. (2016) used a database of 107 samples representing 77 *Paphiopedilum* species with eight chloroplast DNA markers and nrITS found; among the single-locus barcodes, nrITS was the most efficient for species identification of the genus (52.27%), while *matK + atpF-atpH* was the most efficient multi-locus combination (28.97%). Moreover, combining *matK + atpF-atpH + ITS* as a code to identify the genus *Paphiopedilum* is recommended. Rajaram et al. (2019) used four markers (*rbcL*, *matK*, ITS, *trnH-psbA*) to test the 17 samples of 4 endangered *Paphiopedilum* species on the Malixia peninsula. The results found that *matK* is the most potential barcode that has high sequence quality (100%), high accuracy in BLASTn (100%), and precise resolution of species in neighbouring phylogenetic trees (100%), different barcode spacing followed by ITS, are *trnH-psbA*, and *rbcL*. Multiple indicators and criteria are required for accurate classification in some exceptional cases. For example, in the case of the species *P. canhii*, it was pretty controversial about the taxonomy because of the mixed morphological features among the subgenus. To solve this problem, Górnai et al. (2014) used a combination of morphological data, cytology, and phylogenetic analysis based on DNA barcode (with chloroplast gene markers such as *Xdh*, *matK*, *trnH-psbA*, *trnQ-rps16*, nuclear genes such as

ITS), leaf adaxial epidermal studies, and gynostemium structures were obtained from Scanning Electron Microscopy (SEM) and Light Microscopy (L.M.). Vu et al. (2019) used a DNA barcode to classify 22 species of *Paphiopedilum* in Vietnam. According to the author, *trnH - psbA* is limited in amplification; ITS is the best single barcode, and the author recommends the *matK*+ITS combination as the most suitable for Vietnam's Venus orchid classification.

Many previous studies have used DNA barcodes to classify a group or a system of orchids in a country, but no published report has been available to distinguish these two closely related species. In this study, when assessing the species specificity of *P. hangianum* and *P. emersonii* by four single chloroplast makers (*rbcL*, *rpoC1*, *matK*, *trnH-psbA*) and seven maker combinations (*trnH-psbA + matK*, *trnH-psbA + rpoC1*, *trnH-psbA + rbcL*, *trnH-psbA + matK + rpoC1*, *trnH-psbA + matK + rbcL*, *trnH-psbA + rbcL + rpoC1*, *matK + trnH-psbA+rpoC1+rbcL*) we found *trnH-psbA* to be the single marker with the best distinction. The *trnH-psbA + matK* complex was the only combination that could distinguish two close species in the Vietnamese *Paphiopedilum* classification system. These are also the two most suitable markers for the Differentiation and phylogenetic determination of the Venus orchid in this study. The analyzed species were grouped according to previous studies' morphological classification. However, using a combination of two markers will be costly in terms of time and cost; therefore, we propose using *trnH-psbA* as an indicator to differentiate *P. hangianum* and *P. emersonii* and phylogenetic determination *Paphiopedilum* genus of Vietnam.

DNA barcoding is increasingly developing and has many applications; chloroplast genome (super barcodes) brings outstanding applications in taxonomic and phylogenetic research (Liu et al. 2022, Sun et al. 2022). They are overcoming the limitations of previous barcode studies, such as some unanswered phylogenetic questions in *Paphiopedilum*. For example, recent phylogenetic studies indicate widespread reticular evolution within

the genus and that earlier markers cannot address the deep phylogenetic relationship (Tsai et al. 2020). In addition, barcodes have been studied under the name in-silico on the phylogenetic framework associated with the characteristics of *Paphiopedilum* species distributed by a country to determine the species' passport characteristics (Siga et al. 2022). These results will guide future research related to the genus *Paphiopedilum* in Vietnam.

Conclusions

This study identified morphologically and DNA markers to distinguish *P. hangianum* and *P. emersonii* at the flowering and non-flowering stages. Some detailed characteristics of flowers, such as bracts, sepals, synaptic membranes, petals, lips, and stamens, can be used as indicators to distinguish the two species at the flowering stage. Four chloroplast DNA markers such as *rbcL*, *matK*, *rpoCl*, and *trnH-psbA*, were analyzed for the marker as a DNA barcode, and the indicator *trnH-psbA* was proposed as a DNA barcode to distinguish two species of *P. hangianum* and *P. emersonii* at the non-flowering stages. Identifying two similar species, *P. hangianum* and *P. emersonii*, of the genus *Paphiopedilum*, based on morphological characteristics in combination with the DNA barcoding method, solved the identification problems in the absence of flowers or young conditions.

Acknowledgements

This study was funded by the Project of Thai Nguyen University of Science under grant number CS2021-TN06-36

Conflicts of interest

All authors declare no conflicts of interest.

References

- Averyanov, L., Cribb, P., Phan, K.L., & Nguyen, T.H. (2004). Slipper Orchids of Vietnam, Bird Life. Royal Botanic Gardens KEW, World Bank: Ho Chi Minh City, Vietnam 100-120, 308,
- Averyanov, V.L., Gruss, O., Chu, X.C., Phan, K.L., Bui, X.D., & Nguyen, T.H. (2010). *Paphiopedilum canhii* - a new species from Northern Vietnam. *Orchids*, 79(5), 289-290.
- Bolson, M., Smidt, E.C., Brotto, M.L., & Silva-Pereira, V. (2015). ITS and trnH-psbA as efficient DNA Barcodes to identify threatened commercial woody angiosperms from southern Brazilian Atlantic rainforests. *PLoS ONE*, 10:e0143049.
- Braem, G.J., & Gruss, G.R. (2012). *Paphiopedilum* subgenus *Megastaminodium* Braem & Gruss, a new subgenus to accommodate *Paphiopedilum canhii*. *The 67th Santa Barbara International Orchid Show*, 3-164.
- Braem, G.J., Baker, C.O., & Baker, M.L. (1998). *The Genus Paphiopedilum, Natural History and Cultivation*, vol. 1. Botanical Publishers Inc., pp. 182.
- Braem, G.J., Baker, C.O., & Baker, M.L. (1999). *The Genus Paphiopedilum, Natural History and Cultivation*, vol. 2. Botanical Publishers Inc., pp. 363.
- Bui, T.T.H., Duong, X.A., Nguyen, H.C., Ngo, T.A., Dong, H.G., Ho, M.T., Chu, H.H., Tran, T.T.H., Khuat, H.T., & Tran, D.K. (2022). Morphological characteristics and DNA barcoding in bach hop (*Lilium poilanei* Gagnep) in Vietnam. *Australian Journal of Crop Science*, 16(04), 471-478.
- Cahyaningsih, R., Compton, L.J., Rahayu, S., Magos Brehm, J., & Macted, N. (2022). DNA Barcoding Medicinal Plant Species from Indonesia. *Plants*, 11(10), 1375.
- Collins, G.G. & Symons, R.H. (1992). Extraction of nuclear DNA from grape vine leaves by modified procedure. *Plant Molecular Biology Reporter*, 10, 233-235
- Cribb, P. (1998). The Genus *Paphiopedilum*. 2nd ed. *Natural History Publications (Borneo), Kinabalu & Kew*.
- Dang, V.K., Nguyen, T.N., & Vu, H.T. (2017). Screening, designing, pilot evaluation and application of some potential primers for molecular discrimination of *Paphiopedilum* species in Vietnam. Vietnam. *Journal of Agriculture and Rural Development in the Tropics and Subtropics*, 12, 113-118.
- Gorniak, M., Szlachetko, D.L., Kowalkowska, A.K., Bohdanowicz, J., & Canh, C.X. (2014). Taxonomic placement of *Paphiopedilum canhii* (Cypripedioideae; Orchidaceae) based on cytological, molecular and micromorphological evidence. *Molecular Phylogenetics and Evolution*, 70, 429-441.
- Gruss, O., Averyanov, V.L., Chu, X.C., & Nguyen, H.T. (2018). A new variety of a natural hybrid of the genus *Paphiopedilum* from Vietnam: *Paphiopedilum* × *aspersum* var. *Trantuanhii*. *Die Orchidee*, 4, 52-54.
- Guo, Y.Y., Huang, L.Q., Liu, Z.J., & Wang, X.Q. (2016). Promise and Challenge of DNA Barcoding in Venus Slipper (*Paphiopedilum*). *PLoS ONE*, 11(1), e0146880.
- Hollingsworth, P.M., Forrest, L.L. & Spouge, J.L. (2009). A DNA barcode for land plant. *Proceedings of the National Academy of Sciences of the United States of America*, 106, 12794-12797.

- Koopowitz, H. & Cribb, P.J. (1986) Original description of *Paphiopedilum emersonii*. *The Orchid Advocate*, 12(3): 84-86
- Koopowitz, H. (2008). *Tropical Slipper Orchids: Paphiopedilum and Phragmipedium Species and Hybrids*. Portland, Oregon: Timber Press
- Kress, W.J., & Erickson, D.L.(2007). A two-locus global DNA barcode for land plants: the coding *rbcL* gene complements the non-coding *trnH-psbA* spacer region. *PLoS ONE*, 2(6): e508.
- Liu, H., Ye, H., Zhang, N., Ma, J., Wang, J., Hu, G., Li, M., & Zhao, P. (2022) Comparative Analyses of Chloroplast Genomes Provide Comprehensive Insights into the Adaptive Evolution of *Paphiopedilum* (Orchidaceae). *Horticulturae*, 8, 391. <https://doi.org/10.3390/horticulturae8050391>
- Parveen, I., Singh, H. K., Raghuvanshi, S., Pradhan, U. C., & Babbar, S. B. (2012). DNA barcoding of endangered Indian *Paphiopedilum* species. *Molecular ecology resources*, 12(1), 82–90. <https://doi.org/10.1111/j.1755-0998.2011.03071.x>
- Perner, H. & Gruss, O. (1999). Original description of *Paphiopedilum hangia* num. 6.
- Rajaram, M.C., Yong, C.S.Y., Gansau, J.A., & Go, R. (2019). DNA Barcoding of Endangered *Paphiopedilum* species (Orchidaceae) of Peninsular Malaysia. *Phytotaxa*, 387(2), 94–104
- Siga, A., Sarkar, A., Konwar, P., Saikia, J., Saikia, S. P., & Banik, D. (2022). Trait-linked phylogenetic framework of *Paphiopedilum* distributed in India revealed species passport trait to prevent unethical trade through in-silico study. *South African Journal of Botany*, 150(11):420-430. DOI: 10.1016/j.sajb.2022.07.021
- Singh, H.K., Parveen, I., Raghuvanshi, S., & Babbar, S.B. (2012). The loci recommended as universal barcodes for plants on the basis of floristic studies may not work with congeneric species as exemplified by DNA barcoding of *Dendrobium* species. *BMC Research Notes*, 5, 42.
- Sun, Y., Zou, P., Jiang, N., Fang, Y. & Liu, G. (2022) Comparative Analysis of the Complete Chloroplast Genomes of Nine *Paphiopedilum* Species. *Frontiers in Genetics*, 12, 772415, 1:19. doi:10.3389/fgene.2021.772415
- Tamura, K. & Nei M. (1993). Estimation of the number of nucleotide substitutions in the control region of mitochondrial DNA in humans and chimpanzees. *Molecular Biology and Evolution*, 10, 512-526.
- Tate, J.A., & Simpson, B.B. (2003). Paraphyly of *Tarasa* (Malvaceae) and diverse origins of the polyploid species. *Systematic Botany*, 28,723–737.
- Tsai, C.C., Liao, P.C., Ko, Y.Z., Chen, C.H., & Chiang, Y.C. (2020). Phylogeny and Historical Biogeography of *Paphiopedilum* Pfitzer(Orchidaceae) Based on Nuclear and Plastid DNA. *Frontiers in Plant Science*, 11, 126. doi:10.3389/fpls.2020.00126
- Tran, D.D., Khuat, H.T., La, T.N., Nguyen, T.T.T., Pham, B.H., Nguyen, T.K., Tran, H.D., Do, M.T., & Tran, D.K. (2018). Identification of Vietnamese Native *Dendrobium* Species Based on Ribosomal DNA Internal Transcribed Spacer Sequence. *Advanced Studies in Biology*, 10, 1–12.
- Trung, K.H., Khanh, T.D., Ham, L.H., Duong, T.D., & Khoa ,T. (2013). Molecular Phylogeny of the Endangered Vietnamese *Paphiopedilum* Species Based on the Internal Transcribed Spacer of the Nuclear Ribosomal DNA. *Advanced Studies in Biology*, 5, 337–346
- Veldman, S., Kim, S.J., van Andel, T.R., Bello Font, M., Bone, R.E., Bytebier, B., Chuba, D., Gravendeel, B., Martos, F., Mpatwa,G., et al. (2018). Trade in Zambian Edible Orchids-DNA Barcoding Reveals the Use of Unexpected Orchid Taxa for Chikanda. *Genes*, 9, 595.
- Vu, H.T., Bui, M.H., Vu, Q.L., Nguyen, T.D., Tran, H., Khuat, H.T., & Le, L. (2019). Identification of Vietnamese *Paphiopedilum* Species Using Vegetative Morphology. *Annual Research & Review in Biology*, 34(1), 1-14.
- Vu, H.T., Vu, Q.L., Nguyen, T.D., Tran, N., Nguyen, T.C., Luu, P.N., Tran, D.D., Nguyen, T.K., & Le, L. (2020). Genetic Diversity and Identification of Vietnamese *Paphiopedilum* Species Using DNA Sequences. *Biology*, 9(1) 9, 2020.
- Wang, M., Lan, S.-R., & Liu, Z.J. (2017). *Paphiopedilum notatisepalum*, a new species of slipper orchid (Cyripedioideae, Orchidaceae) from China based on morphological and DNA evidence. *Phytotaxa*, 302(2), 156–164.
- Worthy, S. J., Bucalo, K., Perry, E., Reynolds, A., Cruse-Sanders, J., Pérez. A. J. & Burgess, K. S. (2022). Ability of *rbcL* and *matK* DNA barcodes to discriminate between montane forest orchids. *Plant Systematics and Evolution*, 308: 19. DOI: 10.1007/s00606-022-01809-z
- Wu, C.T., Gupta, S.K., Wang, A.Z.M., Lo, S.F., Kuo, C., Ko, Y.J., Chen, C., Hsieh, C.C., & Tsay, H.S. (2012). Internal Transcribed Spacer Sequence Based Identification and Phylogenetic Relationship of *Herba Dendrobii*. *Journal of Food and Drug Analysis*, 20, 143–151.
- Xu, Q., Zhang, G.Q., Liu, Z.J., & Luo, Y.B. (2014). Two new species of *Dendrobium* (Orchidaceae: Epidendroideae)from China: Evidence from morphology and DNA. *Phytotaxa*, 174(3), 129-143.

- Xu, S., Li, D., Li, J., Xiang, X., Jin, W., Huang, W., Jin, X., & Huang, L. (2015). Evaluation of the DNA Barcodes in *Dendrobium* (Orchidaceae) from Mainland Asia. *PLoS ONE*, *10*, e0115168.
- Yukawa, T., Kinoshita, A., & Tanaka, N. (2013). Molecular Identification Resolves Taxonomic Confusion in *Grammatophyllum speciosum* Complex (Orchidaceae). *Bulletin of the National Museum of Nature and Science*, *39*, 137–145.
- Zheng, B. Q., Zou, L.H., Wan, X., & Wang, Y. (2020). *Dendrobium jinghuanum*, a new orchid species from Yunnan, China: evidence from both morphology and DNA. *Phytotaxa*, *428*(1): 030–042.



Journal of Experimental Biology and Agricultural Sciences

<http://www.jebas.org>

ISSN No. 2320 – 8694

Effects of lipoperoxidation and mitochondrial state on milk yield of dairy cows under technological stress

A.V. Deryugina^{1*} , M.N. Ivashchenko¹ , V.B. Metelin^{2,3} ,
D.A. Danilova¹ , A.V. Polozova¹ , M.N. Talamanova¹ 

¹Department of Physiology and Anatomy, Lobachevsky State University, Nizhny Novgorod, Russia

²Vladimirsky Moscow Regional Clinical Research Institute, Moscow, Russia

³Russian State University named after AN Kosygin, Moscow, Russia

Received – November 22, 2022; Revision – March 16, 2023; Accepted – April 08, 2023

Available Online – April 30, 2023

DOI: [http://dx.doi.org/10.18006/2023.11\(2\).436.443](http://dx.doi.org/10.18006/2023.11(2).436.443)

KEYWORDS

Stress

Cows

Hematological parameters

Free-radical oxidation

Mitochondria

ABSTRACT

Evaluation of the physiological state of cattle is crucial in creating healthy, high-performing dairy cattle herds. Technological stress is one of the most critical factors determining the biological potential of higher-yielding cows. This work aimed to assess the effect of technological stress on various oxidative parameters and mitochondrial states in dairy cows' blood, milk yield and milk composition. The study was conducted on the black-and-white breed of healthy herds. Regrouping, changing service personnel, and carrying out veterinary and sanitary manipulations were considered technological stress factors. The concentration of cortisol in the blood serum was studied by the immunological method. The concentrations of malonic dialdehyde (MDA), diene conjugates (D.C.), Schiff bases (S.B.), reduced glutathione and catalase activity were measured spectrophotometrically. The mitochondrial state was estimated by laser interference microscopy. While the milk yield, protein and lipid composition of cow milk were studied using an ultrasound analyzer. The researched indicators were analyzed before and for 30 days after the effect of technological stress. Results of the study suggested that technological stress caused an increase in oxidative processes, along with a reduction of antioxidant activity of blood and milk at the initial stages of registration (1-7 days). The concentration of glutathione remained reduced for 30 days after technological stress. A decrease in mitochondrial refractoriness and disintegration accompanied these processes. The milk yield indicator decreased was not restored to the values of intact animals by 30 days after technological stress. Further, the protein and lipid composition also reduced.

* Corresponding author

E-mail: derugina69@yandex.ru (A.V. Deryugina)

Peer review under responsibility of Journal of Experimental Biology and Agricultural Sciences.

Production and Hosting by Horizon Publisher India [HPI]
(<http://www.horizonpublisherindia.in/>).
All rights reserved.

All the articles published by [Journal of Experimental Biology and Agricultural Sciences](#) are licensed under a [Creative Commons Attribution-NonCommercial 4.0 International License](#) Based on a work at www.jebas.org.



Thus, a decrease in the quantity and quality of milk under technological stress may be mediated by the development of oxidative stress, which the refractoriness and disintegration of mitochondria might trigger.

1 Introduction

Industrial technologies are widely used in modern agricultural enterprises; sometimes, these technologies show adverse impacts and might create stressful conditions for animals. New equipment, noise exposure, table size, maintenance method, and change of personnel care are the main factors of technological stress for cattle (Breuer et al. 2003; Gupta et al. 2007; Hernandez et al. 2014). The severity of the stress reaction depends on the duration and the type of stress factors, and these two factors causing the things to disturb the regulatory mechanisms of the animal body and a violation of physiological, behavioural and metabolic parameters (Mandal et al. 2021; Chikkagoudara et al. 2022). The sympathoadrenal and hypothalamus-pituitary-adrenal (HPA) axes are crucial in the implementation of the action of stress factors (Bagath et al. 2019). Recent studies have suggested that catecholamines alter the number and function of lymphocytes exerting an inflammatory effect, while cortisol causes a decrease in the immune system of animals (Ibrahim et al. 2023). It has been shown that stress worsens the immune response and causes immunosuppressive effects (Chen et al. 2018). In this regard, the consequences of stress are decreases in susceptibility to infections (Akinmoladun 2021). The effect of any stress factors is associated with the activation of oxidative stress and depletion of the antioxidant system.

Further, stress factors are also associated with the disturbance of the delicate balance between the lipid peroxidation processes and the antioxidant defence system, including the disruption of Mitochondria (Chauhan et al. 2014). Additionally, the acid-base status is also changed. Due to their wide-ranging impact, the development of acidosis and increased oxidative stress can lead to a deterioration of the physiological state of animals and a substantial diminution of milk yield (Raghubandan et al. 2022; Semsirboon et al. 2023).

Consequently, comprehending the stress reaction mechanisms and analyzing more accurate stress indicators give advanced opportunities to eliminate damaging factors, avoid animal diseases and increase milk yield. Therefore, this research aim was to evaluate the relationship between oxidative parameters and the mitochondria state in the blood serum, milk yield and milk quality under technological stress.

2 Materials and Methods

2.1 Experimental animals and design

This study was carried out on a clinically healthy dairy population of 2nd lactation (n=20) Black-and-White breed of Holstein cows under the conditions of the Nizhny Novgorod region industrial

complex. All the experimental conditions, like feeding and keeping animals were the same. The research was conducted as per the suggestions of the European Convention for the Protection of Vertebrate Animals used for Experimental or Scientific Purposes (ETS No. 123, Strasbourg, 1986) and the Ministry of Health of the Russian Federation No. 708 N dated August 28, 2010. Further, the Russian Academy of Agricultural Sciences norms were followed, and the experimental animals were kept tethered in standard barns throughout the year, taking food and water according to the standards.

As stress factors, regrouping, changing service personnel, and conducting veterinary and sanitary manipulations were employed in this study. The research was carried out in the winter season. After the morning feeding, the blood samples were collected from the jugular vein of animals before and after 1, 3, 14, and 30 days of selected stress exposure. This dynamic made it possible to analyze the role of stress in the short-term (up to 3 days) and long-term (up to 30 days) periods. Cortisol concentration, indicators of oxidative stress (concentration of MDA), diene conjugates (D.C.), Schiff bases, catalase activity, and reduced glutathione content in blood serum were recorded in the blood as per the standard methodology, as suggested in subsequent paragraphs.

2.2 Analysis of Blood samples

Serum cortisol level was determined using an automatic ELISA analyzer (Evolis Twin Plus, Russia) (Asuzu et al. 2023). The MDA concentration was determined by reaction with thiobarbituric acid to form a coloured trimethine complex, and the absorption of this complex was recorded with the help of spectrophotometrically at 530 nm (Deryugina et al. 2019a).

Further, the level of serum peroxide reduction was used to determine the catalase activity (Deryugina et al. 2018a).

A spectrophotometric assay (using a wavelength of 240nm) was implemented immediately after adding H₂O₂ into the serum and after 20 seconds. Catalase activity was calculated by the formula: $A = (\log E1/E2 \times 120000)/Hb$, where A is catalase activity, the E is molar extinction coefficient (E1 - immediately, E2 - after 20 sec); Hb is the amount of hemoglobin in the sample. Catalase activity was expressed in $\mu\text{M H}_2\text{O}_2 / 1 \text{ min } 10^3$.

The reduced glutathione level was determined using Ellman's method (1959) with 5,5'-di-thio-bis(-2-nitrobenzoic) acid. A sulfosalicylic acid solution was used for protein precipitation in the

studied samples to avoid the spontaneous transition of glutathione from the reduced to the oxidized form. The reduced glutathione concentration was expressed in mmol/l.

The intensity of oxidative damage was studied by the content of molecular products of lipid peroxidation (LPO) such as diene conjugates and Schiff's bases by the spectrophotometric method (Volchegorsky et al. 1989) using an SF-2000 spectrophotometer (St. Petersburg, Russian Federation).

The content of diene conjugates and Schiff bases were estimated by relative values of E232/E220 and E400/E220 and expressed in relative units. Diene conjugates (232 nm is absorption wavelengths) and Schiff bases (400 nm is absorption wavelengths) phase was measured in comparison with the corresponding control (220 nm is absorption wavelengths of isolated double bonds) by relative values of E232/E220, E400/E220 and expressed in relative units.

2.3 Isolation and estimation of mitochondria

60-100 ml of venous blood sample was mixed with 25 ml of medium containing 5% dextran, 0.12 M NaCl, 10 mM EDTA, pH 7.4, and centrifuged for 45 min at 4 °C for erythrocytes precipitation. Further, the precipitate was gathered and centrifuged at 5000 × g for 10 minutes. Then the sediment was suspended in the hypotonic medium (pH 7.6) containing sucrose (0.25 m) as an osmotic shock inhibitor. This suspension was centrifuged at 600 × g for 10 minutes; the received precipitate was exposed to a second osmotic shock and re-centrifuged. The supernatants were stored, combined and centrifuged at 12,000 × g for 20 min to precipitate the mitochondria. The mitochondrial precipitate was suspended in a medium containing 0.25 M sucrose, 2 mM EDTA, and pH 7.4 (Egorova and Afanasiev 2011).

Structural changes in mitochondria were studied using a laser interference microscope MIM-340 (Yekaterinburg, Russia) with a 30x objective (NA=0.65), λ laser=650 nm, and images were captured using high-resolution VS-415U CCD video camera, and a mirror substrate was used for the signal enhancement.

Consequently, a double-sideband phase shift of a coherent light source beam at each point of the object was recorded, and an extra wave from the same source was used to form an interference image of the organelle. Images of 10 sites with the one-layer placement of organelles in the interference channel were obtained for research. The mitochondrial state was evaluated by recording the optical path difference (OPD) mean relevance and diameter of the mitochondria's phase image. For reliability, the indices were measured using a minimum of 20 mitochondria from each sample (Deryugina et al. 2018b).

2.4 Methods of studying milk and milk productivity of cows

The control milking estimated the milk productivity of animals for a month from the start of the study. When investigating milk productivity, fat and protein content were also determined using an ultrasonic analyzer, "Lactan 1-4" (Russia). The lipoperoxidation intensity in animal milk samples was assessed by determining the primary and secondary lipoperoxidation products by Spectrophotometry of the lipid extract was performed at three wavelengths, i.e., 220, 232, and 278 nm, which allowed determining the content of primary oxidation products (diene conjugates "D.C."), the content of secondary oxidation products (ketodienes and conjugated trienes "CD/CT"). The final products of lipoperoxidation-Schiff bases were determined by the method of Lvovskaya et al. (1991). The content of free radical lipid oxidation products was expressed in units of the oxidation index.

2.5 Statistical analysis

The obtained data were processed using the Statistica program; subsequent analysis to determine statistically significant differences was carried out using the Student's T-test.

3 Results and Discussion

3.1 Cortisol concentration analysis

The development of a stress reaction is accompanied by an increase in the content of corticosterone in the blood, which increases the production of adrenocorticotropic hormone (Mormede et al. 2007; Deryugina et al. 2019b). Cortisol concentrations indicate the stress level in the cows. It was shown that before the technological stress, the cortisol levels were within the physiological parameters characteristic of cattle and amounted to 17.68 ± 0.79 nmol/l. A 2.5 times increase in the hormone cortisol concentration was recorded by 44.77 ± 5.61 mol/l on the first day. By days 7 and 14, the cortisol level was recorded as 29.43 ± 1.69 and 25.89 ± 2.19 , respectively. The amount of cortisol in the blood decreased after the 30th day of stress exposure, but this value also exceeded the values obtained before the technological stress (19.32 ± 0.60 nmol/l). The percentage changes in the cortisol level compared to the before treatment are represented in Figure 1.

3.2 Lipoperoxidation and blood antioxidant system

An integral part of the imbalance of internal homeostasis in animals under stress is a change in the concentration of free radicals and the development of oxidative stress against these technological stresses (Slimen et al. 2016). Considering the dynamics of the LPO products obtained a day after the onset of exposure, a 2-fold rising of the level of D.C. was recorded with the

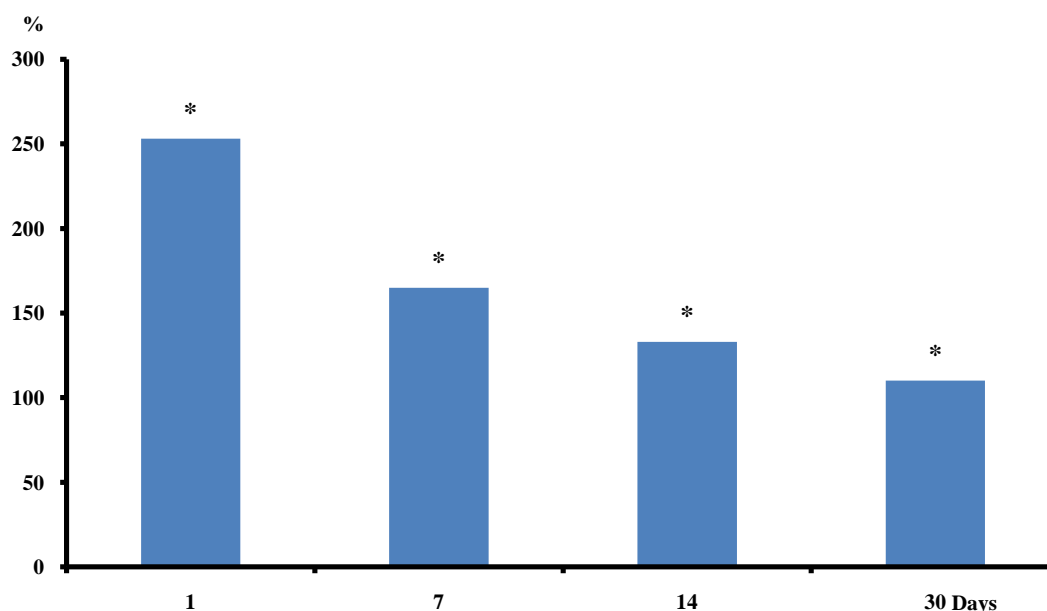


Figure 1 Dynamics of blood cortisol concentration after technological stress (Here 100 % represented the level of the indicator before technological stress, * mark on each bar represented the statistically significant differences concerning the indicators before technological stress at $p < 0.05$)

Table 1 The level of peroxidation products and indicators of the antioxidant capacity system in the blood of cows

Indicator	Initial value Before stress	Days After Technological Stress			
		1	3	14	30
D.C. (rel. units/ml serum)	0.34 ± 0.02	$0.70 \pm 0.01^*$	$0.73 \pm 0.03^*$	$0.62 \pm 0.02^*$	0.39 ± 0.02
MDA ($\mu\text{mol/l}$)	1.45 ± 0.03	$1.71 \pm 0.01^*$	$1.74 \pm 0.02^*$	$1.96 \pm 0.04^*$	$1.39 \pm 0.02^*$
S. B. (rel. units/ml serum)	0.33 ± 0.02	0.34 ± 0.02	$0.40 \pm 0.01^*$	$0.58 \pm 0.02^*$	0.34 ± 0.04
Catalase ($\mu\text{M H}_2\text{O}_2 / 1 \text{ min } 10^3$)	18.87 ± 1.29	$15.43 \pm 1.55^*$	$14.45 \pm 1.53^*$	$15.13 \pm 1.27^*$	17.88 ± 0.73
Glutathione reduced (mmol/l)	0.25 ± 0.02	$0.14 \pm 0.01^*$	$0.12 \pm 0.01^*$	$0.18 \pm 0.01^*$	$0.19 \pm 0.03^*$

Diene conjugates (D.C.); Schiff bases (S.B.), value followed by * showing statistically significant differences with indicators before technological stress ($p < 0.05$)

maintenance of elevated values during 14 days of observation relative to the indicator before stress. The concentration of malondialdehyde (MDH) increased from the first day; the peak of the increase in this product was found in blood samples obtained 14 days after the technological stress by 24% relative to the initial values. The same dynamic was observed for the concentration of fluorescent Schiff bases. Studies have shown that the level of Schiff bases was ultimate by day 14 relative to the data before stress (Table 1). The effect of stress also affected the antioxidant activity in the blood of cows (Table 1). In particular, the level of catalase was below the initial level for 14 days after technological stress. The amount of reduced glutathione during the experiment was reduced by 30-50% over 30 days, depending on the timing of exposure.

3.3 Mitochondrial analysis

The study of mitochondria by laser interference microscopy showed that the phase characteristics of the organelles changed under technological stress (figure 2). It was shown that the ratio of mitochondrial height to diameter allows for calculating mitochondrial refractoriness (Yaguzhinsky et al. 2008). Under technological stress, the refractoriness of individual mitochondria decreased, which may be related to the inhibition of the electron transport chain. The number of disintegrated mitochondria under technological stress increased 2-fold by day 1 compared to the indicators of the control group. Mitochondria are the primary source of reactive oxygen species (Long et al. 2009; Guevera et al. 2011), and the growth of disintegrated mitochondria with an

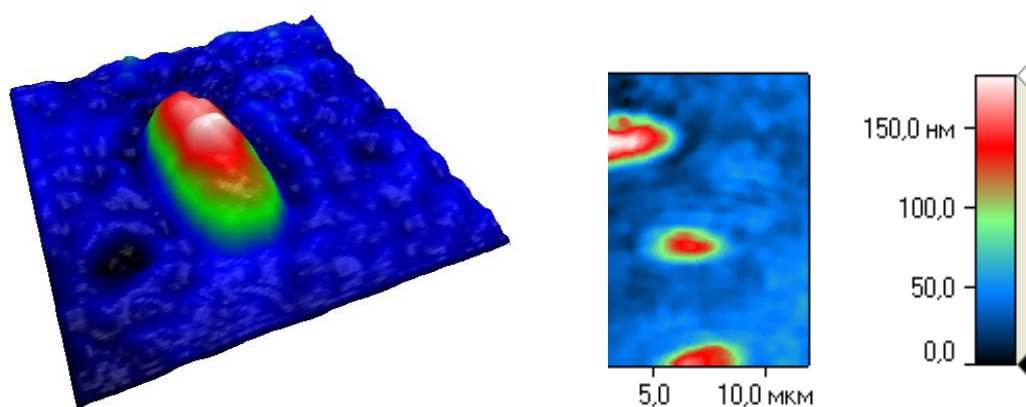


Figure 2 Phase portraits of mitochondria obtained by interference microscopy

Table 2 The effect of low-intensity laser radiation on dairy productivity of cows and the content of lipoperoxidation products of cow's milk

Indicator	Initial level before stress	after stress, hours	
		1	30
Milk productivity, kg	44.9±2.20	30.1±2.17*	32.3±2.13*
Mass fraction of fat, %	5.13±0.56	4.47±0.7	4.52±0.70
Mass fraction of protein, %	3.20±0.08	2.82±0.18*	3.06±0.24
Diene conjugates (c.u.)	0.94±0.16	1.32±0.17*	1.29±0.21
Kettani and related trienes (c.u.)	0.085±0.01	0.103±0.012*	0.104±0.014
Schiff base (c.u.)	0.015±0.001	0.023±0.01	0.022±0.013

Value followed by * showing statistically significant differences with indicators before technological stress ($p < 0.05$)

altered refractory level can enhance the development of oxidative stress in cows, which will have a negative effect on their productivity.

3.4 Milk analysis

The analysis of milk productivity in cows on day 1 after technological stress showed a decrease in milk productivity by 32% relative to the values of cows without technological stress and preservation of the reduced milk productivity indicator at day 30 of the study. Under technological stress, the amount of protein significantly decreased by 13% on day 1 after technological stress and recovered by day 30. The mass fraction of fat tended to decline. An increase in lipoperoxidation products in milk was recorded under technological stress. The number of diene conjugates, Kettani and related trienes increased significantly by day 1 of technological stress, while on day 30, the indices tended to decrease (Table 2).

Results of the study suggested that the cortisol level after 30 days of technological stress reached the initial values but, after this, also remained above the standard limit. Glucocorticoids function as

checkpoints for energy homeostasis and mediate many effects of stress on metabolism. A high cortisol level suppresses the animal immune system and increases the incidence of diseases (Fomichev et al. 2012).

Additionally, in most deviations of the diverse etiologies, lipid peroxidation activity enlarges, leading to pronounced changes in the physicochemical properties of lipids. The structure and, consequently, the main functions of membrane proteins are more regulated by the protein–lipid interaction (Hammerschmid et al. 2023). Violating lipid and protein components with increased lipid peroxidation leads to cellular dysfunction. A detrimental impact of lipid peroxidation is manifested by a violation of lipid and protein components of the membranes and leads to cellular dysfunction (Villalón-García et al. 2023).

Furthermore, it is assumed that cytotoxic free radical processes' activity reduces the SS-groups and raises the level of S.H. groups. The detrimental impact of various factors on thiol compounds arises explicitly due to their ability to instantly and, at the same time, convertible oxidize. Among the multiple antioxidant mechanisms that prevent cell damage, the critical

place is controlled by thiol–disulfide exchange, and glutathione is the essential component that maintains cell REDOX balance (Asanuma and Miyazaki 2021). Glutathione (γ -glutamyl-cysteinylglycine) is a thiol-tripeptide that exists in two interconvertible forms, reduced glutathione (GSH) and oxidized glutathione (GSSG). The reduced glutathione is the principal intracellular antioxidant buffer which is crucial for maintaining the level of cysteine in proteins. Additionally, glutathione controls the maintenance of the normal oxidation-antioxidant equilibrium states and scavenges the hydrogen and lipid peroxide (Kuhn et al. 2017; Ighodaro and Akinloye 2018; Bayir et al. 2020).

The study's results also demonstrated that the content of the GSH was reduced after technological stress. The reduced level of glutathione remained on the 30th day of registration, which indicates a decrease in the adaptation and resistance to oxidative stress. Oxidation of fatty acid esterified in membrane phospholipids leads to the primary mechanisms of cellular oxidative damage.

The primary substrates for free radical-induced damages are the double bonds of unsaturated fatty acids in phospholipids (Gaschler and Stockwell 2017). Mitochondrial membranes are particularly susceptible to reactive oxygen species (ROS) because cardiolipin is localized in the inner mitochondrial membrane (Schenkel and Bakovic 2014). Under technological stress, the functional activity of mitochondria decreases, which is caused by the disruption of the antioxidant system and the formation of non-selective mitochondrial pores. The opening of these pores leads to irreversible disruption of mitochondrial functions (Bernardi et al. 2015). At the same time, the enzyme glutathione peroxidase (GPx) is required to maintain the levels of ROS in mitochondria (Shimura et al. 2022).

Consequently, the decrease in glutathione during the study may negatively affect the efficiency of mitochondria. Meanwhile, mitochondrial dysfunction can be considered an oxidative stress trigger in cows. The separation of respiration and phosphorylation process in mitochondria leads to a superoxide anion radical production by the respiratory chain (Skulachev et al. 2012). Thus, under technological stress, it is necessary to consider its intensity so that a vicious circle does not develop, increasing free-radical oxidation, damage to mitochondria, and increasing oxidative stress.

Conclusion

The study shows that technological stress significantly affects the processes of lipid oxidation in blood serum and milk, which is accompanied by a decrease in milk productivity. The most pronounced changes were registered on the 1st day after the action of technological stress. The revealed disorders of oxidative

processes may be mediated by mitochondrial disintegration. It is shown that the index of the antioxidant system, i.e., reduced glutathione, was not restored to the initial values, which was combined with a decrease in milk productivity on day 30 of registration. Effects on mitochondrial energetics can significantly increase the efficacy of therapeutic drugs. However, the mechanisms of regulation of these processes are not fully understood. The answer to the extent to which cell energy modulation will contribute to the adaptation of the organism to stress is crucial for developing an effective direction of prevention and therapy.

Declaration of interest

The authors declare that there is no conflict of interest.

Financial support statement

The research was carried out at the expense of a grant from the Russian Science Foundation № 22-26-00311, <https://rscf.ru/project/№22-26-00311>

References

- Akinmoladun O. F. (2021). Stress amelioration potential of vitamin C in ruminants: a review. *Tropical animal health and production*, 54(1), 24. doi: 10.1007/s11250-021-03026-1
- Asanuma, M., & Miyazaki, I. (2021). Glutathione and Related Molecules in Parkinsonism. *International journal of molecular sciences*, 22(16), 8689. doi: 10.3390/ijms22168689
- Asuzu, D. T., Bhatt, S., Nwokoye, D., Hayes, C., et al. (2023). Cortisol and ACTH Measurements at Extubation From Pituitary Surgery Predicts Hypothalamic-Pituitary-Adrenal Axis Function. *Journal of the Endocrine Society*, 7(4), bvad025. doi.org/10.1210/jendso/bvad025
- Bagath, M., Krishnan, G., Devaraj, C., Rashamol, V. P., Pragna, P., Lees, A. M., & Sejian, V. (2019). The impact of heat stress on the immune system in dairy cattle: A review. *Research in veterinary science*, 126, 94–102. doi: 10.1016/j.rvsc.2019.08.011
- Bayir, H., Anthonymuthu, T. S., Tyurina, Y. Y., Patel, S. J., et al. (2020). Achieving Life through Death: Redox Biology of Lipid Peroxidation in Ferroptosis. *Cell chemical biology*, 27(4), 387–408. doi: 10.1016/j.chembiol.2020.03.014
- Bernardi, P., Rasola, A., Forte, M., & Lippe, G. (2015). The Mitochondrial Permeability Transition Pore: Channel Formation by F-ATP Synthase, Integration in Signal Transduction, and Role in Pathophysiology. *Physiological reviews*, 95(4), 1111–1155. doi: 10.1152/physrev.00001.2015

- Breuer, K., Hemsworth, P.H., & Coleman G.J. (2003). The effect of positive and negative handling on the behavioural and physiological responses of nonlactating heifers. *Applied Animal Behaviour Science*, 84, 3-22. doi:10.1016/S0168-1591(03)00146-1
- Chauhan, S. S., Celi, P., Leury, B. J., Clarke, I. J., & Dunshea, F. R. (2014). Dietary antioxidants at supranutritional doses improve oxidative status and reduce the negative effects of heat stress in sheep. *Journal of animal science*, 92(8), 3364–3374. doi: 10.2527/jas.2014-7714
- Chen, S., Wang, J., Peng, D., Li, G., Chen, J., & Gu, X. (2018). Exposure to heat-stress environment affects the physiology, circulation levels of cytokines, and microbiome in dairy cows. *Scientific reports*, 8(1), 14606. doi: 10.1038/s41598-018-32886-1
- Chikkagoudara, K. P., Singh, P., Bhatt, N., Barman, D., et al. (2022). Effect of heat stress mitigations on physiological, behavioural, and hormonal responses of Buffalo calves. *International journal of biometeorology*, 66(5), 995–1003. doi: 10.1007/s00484-022-02255-9
- Deryugina, A.V., Boyarinov, G.A., Simutis, I.S., Nikolskiy, V.O., Kuznetsov A.V., & Efimova T.S. (2018a). Correction of Metabolic Indicators of Erythrocytes and Myocardium Structure with Ozonized Red Blood-Cell Mass. *Cell and Tissue Biology*, 12, 207-212. doi: 10.1134/S1990519X18030033
- Deryugina, A.V., Ivashchenko, M.N., Ignatiev, P.S., Ice, M.S., & Samodelkin, A.G. (2019a). Changes in the phase portrait and electrophoretic mobility of erythrocytes in various types of diseases. *Modern Technologies in Medicine*, 11(2), 63-68. doi: 10.17691/stm2019.11.2.09
- Deryugina, A.V., Ivashchenko, M.N., Ignatiev, P.S., Talamanova, M.N., & Samodelkin, A.G. (2018b). The capabilities of interference microscopy in studying the in vitro state of erythrocytes exposed to low-intensity laser radiation for stress correction. *Modern Technologies in Medicine*, 10(4), 78-83. doi: 10.17691/stm2018.10.4.09
- Deryugina, A.V., Ivashchenko, M.N., Ignatyev, P.S., Samodelkin, A.G., Zolotova, M. V., Shabalin, M. A., & Gracheva, E.A. (2019b) Diagnostic capabilities of the electrophoretic mobility of red blood cells and buccal cells in stress. *International Journal of Physiology and Pathophysiology*, 63, 106 – 111. doi: 10.21103/Article8(4)_OA16
- Egorova, M.V. & Afanasiev, S.A. (2011). The isolation of mitochondria from cells and tissues of animals and humans. *Current methodological approaches Siberian Medical Journal*, 26(1), 22-28.
- Ellman, G.L. (1959). Tissue sulfhydryl groups. *Archives of biochemistry and biophysics*, 82(1), 70–77. doi: 10.1016/0003-9861(59)90090-6
- Fomichev, Y., Sulima, N., Sidorov, E. & Bardin, O. (2012). Heat stress in lactating dairy cows and methods for its prevention. *Dairy and beef cattle breeding*, 2, 30-32.
- Gaschler, M. M., & Stockwell, B. R. (2017). Lipid peroxidation in cell death. *Biochemical and biophysical research communications*, 482(3), 419–425. doi: 10.1016/j.bbrc.2016.10.086
- Guevara, R., Gianotti, M., Roca, P., & Oliver, J. (2011). Age and sex-related changes in rat brain mitochondrial function. *Cellular physiology and biochemistry: international journal of experimental cellular physiology, biochemistry, and pharmacology*, 27(3-4), 201–206. doi: 10.1159/000327945
- Gupta, S., Earley, B., & Crowe, M. A. (2007). Pituitary, adrenal, immune and performance responses of mature Holstein x Friesian bulls housed on slatted floors at various space allowances. *Veterinary journal*, 173(3), 594–604. doi: 10.1016/j.tvjl.2006.02.011.
- Hammerschmid, D., Calvaresi, V., Bailey, C., Russell Lewis, B., et al. (2023). Chromatographic Phospholipid Trapping for Automated H/D Exchange Mass Spectrometry of Membrane Protein-Lipid Assemblies. *Analytical chemistry*, 95(5), 3002–3011. doi: 10.1021/acs.analchem.2c04876
- Hernandez C. E., Thierfelder T., Svennersten-Sjaunja K., Berg C., Orihuela A., & Lidfors L. (2014). Time lag between peak concentrations of plasma and salivary cortisol following a stressful procedure in dairy cattle. *Acta Veterinaria Scandinavica*, 56(1), 61. doi: 10.1186/s13028-014-0061-3
- Ibrahim, S., Al-Sharif, M., Younis, F., Ateya, A., Abdo, M., & Fericean, L. (2023). Analysis of Potential Genes and Economic Parameters Associated with Growth and Heat Tolerance in Sheep (*Ovis aries*). *Animals*, 13(3), 353. doi.org/10.3390/ani13030353
- Ighodaro, O.M., & Akinloye O.A. (2018). First line defence antioxidants-superoxide dismutase (SOD), catalase (CAT) and glutathione peroxidase (GPX): Their fundamental role in the entire antioxidant defence grid. *Alexandria Journal of Medicine*, 54 (4), 287-293. doi:10.1016/j.ajme.2017.09.001
- Kuhn, V., Diederich, L., Keller, T. C. S., Kramer, C. M., et al. (2017). Red Blood Cell Function and Dysfunction: Redox Regulation, Nitric Oxide Metabolism, Anemia. *Antioxidants & redox signaling*, 26(13), 718–742. doi: 10.1089/ars.2016.6954

- Long, J., Gao, F., Tong, L., Cotman, C. W., Ames, B. N., & Liu, J. (2009). Mitochondrial decay in the brains of old rats: ameliorating effect of alpha-lipoic acid and acetyl-L-carnitine. *Neurochemical research*, *34*(4), 755–763. doi: 10.1089/ars.2016.6954
- Lvovskaya, I.E., Volchegorsky, I.A. Shemyakov, S.E., & Lifshits, R.I. (1991). Spectrophotometric determination of final products of lipid peroxidation. *Voprosi medical chemistries*, *4*, 92-93.
- Mandal, D.K., Bhakat, C., & Dutta, T.K. (2021). Impact of environmental factors on physiological adaptability, thermo-tolerance indices, and productivity in Jersey crossbred cows. *International journal of biometeorology*, *65*(12),1999-2009. doi: 10.1007/s00484-021-02157-2.
- Mormède, P., Andanson, S., Aupérin, B., Beerda, B., et al. (2007). Exploration of the hypothalamic-pituitary-adrenal function as a tool to evaluate animal welfare. *Physiology & behavior*, *92*(3), 317–339. <https://doi.org/10.1016/j.physbeh.2006.12.003>
- Raghunandan, T., Sultana, J.R., Chandra, A.S. Prakash, M.G., Venkateswarlu, M., & Ramana, D.B.V. (2022). Effect of dietary Chromium, vitamin E and Selenium supplementation on biochemical and physiological parameters of Holstein Friesian cows under heat stress. *The Indian Journal of Animal*, *92* (7). doi.org/10.56093/ijans.v92i7.109736
- Schenkel, L. C. & Bakovic, M. (2014). Formation and regulation of mitochondrial membranes. *International journal of cell biology*, *709828*. <https://doi.org/10.1155/2014/709828>
- Semsirboon, S., Do Nguyen, D.K., Chaiyabutr, N., Poonyachoti, S., Lutz, T.A., & Thammacharoen S. (2023). High Dietary Cation and Anion Difference and High-Dose Ascorbic Acid Modify Acid–Base and Antioxidant Balance in Dairy Goats Fed under Tropical Conditions. *Animals*, *13*(6), 970. doi.org/10.3390/ani13060970
- Shimura, T., Shiga, R., Sasatani, M., Kamiya, K., & Ushiyama, A. (2022). Melatonin and MitoEbselen-2 Are Radioprotective Agents to Mitochondria. *Genes*, *14*(1), 45. doi: 10.3390/genes14010045
- Skulachev, V.P., Bogachev, A.V., & Kasparinsky, F.O. (2012). Membrane bioenergetics. Moscow: Moscow University Press.
- Slimen, B.I., Najar, T., Ghram, A., & Abdrrabba, M. (2016). Heat stress effects on livestock: molecular, cellular and metabolic aspects, a review. *Journal of animal physiology and animal nutrition*, *100*(3), 401–412. doi: 10.1111/jpn.12379
- Villalón-García, I., Povea-Cabello, S., Álvarez-Córdoba, M., Talaverón-Rey, M., et al. (2023). Vicious cycle of lipid peroxidation and iron accumulation in neurodegeneration. *Neural regeneration research*, *18*(6), 1196–1202. doi: 10.4103/1673-5374.358614
- Volchegorsky, I.A., Nalimov, A.G., & Yarovinsky, B.G. (1989). Comparison of different approaches to the determination of lipid peroxidation products in heptane-isopropanol blood extracts. *Laboratornoe delo*, *4*, 127-31.
- Yaguzhinsky, L.S., Vyshenskaya, T.V., Kretushev, A.V., & Tychinsky, V.P. (2008). Identification of two discrete states of energized mitochondria: experiments on single mitochondria. *Biochemistry*, *2*(2), 144-149. doi:10.1134/S1990747808020086